

Artificial Intelligence

104th Scientific Assembly and Annual Meeting November 25–30 | McCormick Place, Chicago





AI021-EC-X

Methodology to Curate and Crowdsource Annotation of the ChestX-ray14 Dataset for the RSNA-STR Machine Learning Challenge: How We Did It

All Day Room: NA Custom Application Computer Demonstration

Participants

Safwan Halabi, MD, Stanford, CA (*Presenter*) Nothing to Disclose George L. Shih, MD, MS, New York, NY (*Abstract Co-Author*) Consultant, Image Safely, Inc; Stockholder, Image Safely, Inc; Consultant, MD.ai, Inc; Stockholder, MD.ai, Inc; Carol C. Wu, MD, Bellaire, TX (*Abstract Co-Author*) Author, Reed Elsevier Luciano M. Prevedello, MD, MPH, Dublin, OH (*Abstract Co-Author*) Nothing to Disclose Marc D. Kohli, MD, San Francisco, CA (*Abstract Co-Author*) Nothing to Disclose Tessa S. Cook, MD, PhD, Philadelphia, PA (*Abstract Co-Author*) Royalties, Osler Institute Arjun Sharma, MD, Baltimore, MD (*Abstract Co-Author*) Nothing to Disclose Anouk Stein, MD, Paradise Valley, AZ (*Abstract Co-Author*) Consultant, MD.ai, Inc; Stockholder, MD.ai, Inc

For information about this presentation, contact:

safwan.halabi@stanford.edu

TEACHING POINTS

(1) Describe the methodology of curating an image dataset for purposes of a machine learning challenge. (2) Discuss the tools used to crowdsource image annotations. (3) Discuss the statistics of the annotated datasets. (4) Define file standards for the annotated images.

TABLE OF CONTENTS/OUTLINE

Dataset Curation: The NIH ChestX-ray14 dataset contains 112,120 chest X-ray images from 30,805 unique patients with 14 disease labels. For the purposes of the RSNA Machine Learning Challenge, a subset of 30,000 images from the NIH dataset contained: (1) 15,000 radiographs labeled with 'pneumonia', 'consolidation' or 'infiltration'; (2) 7,500 radiographs labeled as 'normal'; and, (3) 7,5000 radiographs labeled as not 'pneumonia' and not 'normal'. All radiographs were converted to DICOM format. Image Annotation Tool: The MD.ai annotation tool (MD.ai, New York, NY) was utilized for the crowdsourcing of image annotation for the following reasons: (1) Ability to assign a block of exams to each annotator and hide overlapping annotations from users; (2) Ability to review all annotations for quality assurance; (3) Ease of use with customized keyboard shortcuts; and, (4) Reporting capabilities with dashboard that show progress from participants. Image Annotation Format: The annotated images were stored in json file format.



AI022-EC-X

The Next Step in Electronic Cleansing for CT Colonography: Unsupervised Machine Learning

All Day Room: NA Custom Application Computer Demonstration

Participants

Rie Tachibana, Boston, MA (*Presenter*) Nothing to Disclose Janne J. Nappi, PhD, Boston, MA (*Abstract Co-Author*) Royalties, Hologic, Inc Royalties, MEDIAN Technologies Hiroyuki Yoshida, PhD, Boston, MA (*Abstract Co-Author*) Patent holder, Hologic, Inc; Patent holder, MEDIAN Technologies;

For information about this presentation, contact:

yoshida.hiro@mgh.harvard.edu

TEACHING POINTS

Electronic cleansing (EC) is used for subtracting tagged fecal materials from CT colonography (CTC) examinations to improve the detection sensitivity of virtual endoscopic fly-through reading. The teaching points of this exhibit are to (1) learn about unsupervised learning as a cutting-edge artificial intelligence (AI) technology for EC in CTC, (2) learn about the advantages and disadvantages of unsupervised and supervised learning, and (3) demonstrate outcomes of unsupervised and supervised learning for EC in CTC examinations.

TABLE OF CONTENTS/OUTLINE

1. Brief history of EC in CTC 2. Advantages and disadvantages of supervised and unsupervised learning in medical imaging 3. How unsupervised machine learning is applied to EC in CTC 4. Example results of unsupervised and supervised EC in clinical CTC cases 5. Characteristic image artifacts and pitfalls in unsupervised and supervised EC methods in CTC



AI030

Crowds Cure Cancer: Help Annotate Data from the Cancer Imaging Archive

All Day Room: AI Community, Learning Center

ABSTRACT

Attendees at this year's RSNA meeting are encouraged to participate in an exciting activity that will provide valuable data to cancer researchers working in deep learning, radiomics and radiogenomics. This booth offers radiologist attendees an opportunity to participate in a 'crowd-sourcing' experiment to accelerate quantitative imaging research. Images are provided by The National Cancer Institute's Cancer Imaging Archive (http://www.cancerimagingarchive.net/), which is a massive public-access resource of cancer radiology images linked to genetic/proteomic, pathology images and clinical data. Many of these cases lack the tumor-location labels needed by computer scientists to jump-start their work on machine learning and quantitative imaging radiomics. Participants will be asked to spend a few minutes anonymously reviewing cases and visually marking their tumor locations. Upon completion, they will receive a ribbon to add to their RSNA badge acknowledging their participation. The data resulting from this process will be openly shared on TCIA with the radiology and computer science communities to accelerate cancer research. Data from last year can be obtained at https://doi.org/10.7937/K9/TCIA.2018.OW73VLO2.



BR112-ED-X

Preparation of Digital Mammograms for the Application of Deep Learning Algorithms

All Day Room: NA Digital Education Exhibit

Participants

Alexandra (Ali) Silver, BSC, Kelowna, BC (*Presenter*) Nothing to Disclose Yuhao Huang, Kelowna, BC (*Abstract Co-Author*) Nothing to Disclose Carson McKay, BSC, Kelowna, BC (*Abstract Co-Author*) Nothing to Disclose Rasika Rajapakshe, PhD, Kelowna, BC (*Abstract Co-Author*) Nothing to Disclose

For information about this presentation, contact:

ali.silver@alumni.ubc.ca

TEACHING POINTS

This educational presentation will illustrate the following: 1. Annotation of Breast abnormalities recorded as DICOM Grayscale Softcopy Presentation State (GSPS) (DICOM PR Modality); 2. De-identification of DICOM files; 3. Description of DICOM PR Graphic Objects including Coordinates, Area, Mean, Standard Deviation and Shape of Object; 4. Utilization of PR Graphic Objects to create a Binary Mask image, referencing to the corresponding mammogram (Image Pair); 5. Generation and display of an Image Pair for each PR file and its referenced mammogram, and; 6. Generation of PNG files from Image Pairs for application in Machine Learning Algorithm.

TABLE OF CONTENTS/OUTLINE

1. Introduction and background on Machine learning. | 2. How Annotation of Breast abnormalities are saved as a DICOM Grayscale Softcopy Presentation State (GSPS) (DICOM PR Modality). | 3. Explanation of PR file format. | 4. Description of the creation of a "PR Viewer" program to create and display the Binary Mask image and its corresponding mammogram. | 5. Utilization of Image Pairs for Machine Learning Algorithm.



CA155-ED-X

Cardiac Image Analysis with Deep Learning Methods

All Day Room: NA Digital Education Exhibit

Participants

Aliasghar Mortazi, MSc, Orlando, FL (*Presenter*) Nothing to Disclose Georgios Z. Papadakis, MD,PhD, Heraklion, Greece (*Abstract Co-Author*) Nothing to Disclose Uygar Teomete, MD, Coral Gables, FL (*Abstract Co-Author*) Nothing to Disclose Ulas Bagci, PhD, MSc, Orlando, FL (*Abstract Co-Author*) Nothing to Disclose

For information about this presentation, contact:

a.mortazi@knights.ucf.edu

TEACHING POINTS

1) They will be familar with novel deep learning approaches 2) They learn about application of deep learning methods in cardiac image analysis 3) Challenges and problems for medical image analysis with using deep learning will be discussed

TABLE OF CONTENTS/OUTLINE

1) Deep-learning methods: -2D/3D CNN - Densely Connected CNN - Unet Densely Connected CNN - Recurrent Neural Network -Generative Adversarial Networks - Reinforcement Learning - CapsuleNet 2) Left Ventricle Analysis: -LV segmentation from myocardial infarct MRI - Automatic Localization of LV in cardiac MRI - Tracking LV endocardium in ultrasound images -LV segmentation from ultrasound - Ejection fraction measurement -ES and ED recognition 3) Myocardium Analysis: -Coronary artery stenosis detection in coronary CT angiography - Measuring wall thickness of myocardium 4) Right Ventricle Analysis: -ARVD detection Measuring -RV volume in cine-MRI 5) Left Atrium & Pulmonary Veins: -Structural analysis of LA and PPVs - Measuring LA wall thickness 6) Coronary Arteries (CA): -CA calcium segmentation -CA segmentation from CT images -Tissue classification of CA 8) Challenges in deep learning for cardiac image analysis Disease diversity, Data scarcity, annotation, motion correctness, data augmentation, optimum architecture 9) Effectiveness of deep learning in future of cardiac image analysis



IN100-ED-X

Robotic Process Automation: Go Beyond Artificial Intelligence in the Radiology Department

All Day Room: NA Digital Education Exhibit

Awards Certificate of Merit

Participants

Norio Nakata, MD, Tokyo, Japan (*Presenter*) Nothing to Disclose Zuojun Wang, MD,PhD, Tokyo, Japan (*Abstract Co-Author*) Nothing to Disclose Takashi Watanabe, Minato, Japan (*Abstract Co-Author*) Nothing to Disclose Tomoyuki Ohta, Tokyo, Japan (*Abstract Co-Author*) Reserch Grant, EA Pharmaceuticals Makiko Nishioka, MD, PhD, Tokyo, Japan (*Abstract Co-Author*) Nothing to Disclose Hiroya Ojiri, MD, Tokyo, Japan (*Abstract Co-Author*) Nothing to Disclose

For information about this presentation, contact:

nakata@jikei.ac.jp

TEACHING POINTS

To learn the operation and benefits of RPA. To learn the feasibility of RPA for radiologists.

TABLE OF CONTENTS/OUTLINE

Robotic process automation (RPA) is an emerging form of clerical process automation technology using software with artificial intelligence (AI) and machine learning capabilities to handle high-volume, repeatable tasks that previously required humans to type, click, and even analyze data in different applications. These tasks can include queries, calculations and maintenance of records and transactions. RPA evolved from screen scraping, workflow automation and AI. RPA has been applied to trading in treasuries, affecting accounting staff involved in the banking area. RPA can be a disruptive force in the healthcare industry. RPA has enabled those in the healthcare field to shift a significant amount of manual, time-intensive and error-prone work from human to machine with incredible results. Hospitals can use RPA for handling patient records, claims, customer support, account management, billing, reporting and analytics. Healthcare providers can leverage AI tools to help their staff analyze routine radiology results more quickly and accurately. RPA can also help radiologists search literature, select imaging protocols, write diagnostic reports, enhance risk management, operate electronic medical records, and arrange their schedules.



IN101-ED-X

Optimization of Imaging Parameters for Use in Medical Imaging Using the Deep Learning Technique

All Day Room: NA Digital Education Exhibit

Participants

Norio Hayashi, PhD, Maebashi, Japan (Presenter) Nothing to Disclose Mika Kogure, Maebashi, Japan (Abstract Co-Author) Nothing to Disclose Natsuki Tsunoda, Maebashi, Japan (Abstract Co-Author) Nothing to Disclose Saki Suzuki, Maebashi, Japan (Abstract Co-Author) Nothing to Disclose Miyu Saito, Maebashi, Japan (Abstract Co-Author) Nothing to Disclose Yusuke Sato, Midori, Japan (Abstract Co-Author) Nothing to Disclose Tomoko Maruyama, Maebashi, Japan (Abstract Co-Author) Nothing to Disclose Hisashi Takeda, Isesaki-City, Japan (Abstract Co-Author) Nothing to Disclose Haruyuki Watanabe, PhD, Maebashi, Japan (Abstract Co-Author) Nothing to Disclose Toshihiro Ogura, PhD, Maebashi, Japan (Abstract Co-Author) Nothing to Disclose Akio Ogura, PhD, Maebashi, Japan (Abstract Co-Author) Nothing to Disclose Yoshito Tsushima, MD, Maebashi, Japan (Abstract Co-Author) Institutional Research Grant, Bayer AG; Institutional Research Grant, DAIICHI SANKYO Group; Institutional Research Grant, Eisai Co, Ltd; Institutional Research Grant, Nihon Medi-Physics Co, Ltd; Institutional Research Grant, FUJIFILM Holdings Corporation ; Institutional Research Grant, Fuji Pharma Co, Ltd; Institutional Research Grant, Siemens AG; Institutional Research Grant, OncoTherapy Science, Inc; Institutional Research Grant, Becton, Dickinson and Company; Speaker, Bayer AG; Speaker, DAIICHI SANKYO Group; Speaker, Eisai Co, Ltd; Speaker, Fuji Pharma Co, Ltd; Speaker, Guerbet SA

TEACHING POINTS

It is necessary to optimize imaging parameters that are used in medical imaging examinations. However, inexperienced medical staff are unable to optimize personalized imaging parameters for individual patients. We developed a system to optimize imaging parameters using the deep learning technique. The teaching points of the exhibit are as follows: 1. To understand the necessity for optimization of imaging parameters for use in medical imaging modalities such as X-ray imaging, computed tomography (CT), and magnetic resonance imaging (MRI) examinations 2. To understand the imaging parameters' optimization system using the deep learning technique 3. To understand how to use the optimization system, as well as to optimize imaging parameters

TABLE OF CONTENTS/OUTLINE

A. Imaging parameters for diagnostic imaging examinations B. Necessity for optimization of imaging parameters C. Concept and outline of an imaging parameters' optimization system using the deep learning technique D. Optimization of imaging parameters and automated image quality check for conventional X-ray examination E. Optimization of imaging parameters and automated image quality check for CT examination F. Optimization of imaging parameters and automated image quality check for MRI examination



IN102-ED-X

Artificial Intelligence Use in Radiology: Development, Current Use, and Present-Day Controversies

All Day Room: NA Digital Education Exhibit

FDA Discussions may include off-label uses.

Participants

Marie Surovitsky, DO, Mineola, NY (*Presenter*) Nothing to Disclose Siavash Behbahani, MD, Mineola, NY (*Abstract Co-Author*) Nothing to Disclose Thomas Harvey, MD, Mineola, NY (*Abstract Co-Author*) Nothing to Disclose Sofya Kalantarova, MD, Mineola, NY (*Abstract Co-Author*) Nothing to Disclose Jonathan Minkin, Mineola, NY (*Abstract Co-Author*) Nothing to Disclose Jason C. Hoffmann, MD, Mineola, NY (*Abstract Co-Author*) Speakers Bureau, Merit Medical Systems, Inc; ; Arielle Sasson, Mineola, NY (*Abstract Co-Author*) Nothing to Disclose Ilana Gitlin, Mineola, NY (*Abstract Co-Author*) Nothing to Disclose

For information about this presentation, contact:

Jason.Hoffmann@nyulangone.org

TEACHING POINTS

1. An understanding of Artificial Intelligence (AI) and its components is essential for radiologists to understand how this will impact their future.2. Patients and radiologists can benefit from systems that rapidly analyze large numbers of images.3. Embracing and incorporating AI is crucial for future success of radiology.

TABLE OF CONTENTS/OUTLINE

General AI review. Differences between machine learning (ML) and deep learning (DL).Define Artificial Neural Networks and explain their role in radiology-specific AI.Why and how AI can help the radiologist and our patients.Highlight studies and current projects to incorporate AI into radiology:-Computer aided detection in mammography and how this differs from contemporary AI-Felix Project (pancreatic cancer detection)-Workflow changes (related to critical findings on Head CT scans)Why radiology must embrace AI.How to integrate AI into radiology practice and training.Current AI limitations, how they can be addressed, future directions, and current controversies:-Who owns the data?-Role of FDA in regulation-How to validate proprietary algorithms-Who is ultimately responsible (radiologist, computer, or developers)?-Will insurance companies reimburse for an AI diagnosis without a radiologist overseeing? Or only in conjunction with a human radiologist evaluating the images?



IN104-ED-X

Automated Construction of the Optimal Structure for 3D CNN by Using the Bayesian Optimization

All Day Room: NA Digital Education Exhibit

Participants

Yasushi Hirano, Ube, Japan (*Presenter*) Nothing to Disclose Takayoshi Ito, BEng, Ube, Japan (*Abstract Co-Author*) Nothing to Disclose Shoji Kido, MD, PhD, Ube, Japan (*Abstract Co-Author*) Nothing to Disclose Shingo Iwano, MD, Nagoya, Japan (*Abstract Co-Author*) Nothing to Disclose

For information about this presentation, contact:

yhirano@yamaguchi-u.ac.jp

TEACHING POINTS

Although weights of convolution layers or fully connected layers in 3D CNNs are automatically optimized in training process, in general the structure of the networks has to be designed manually. Additionally well-built CNNs such as AlexNet or VGG are shared for 2D images, but not for 3D images. Therefore the structure of 3D CNNs has to be manually constructed from scratch. We will show a method for constructing the optimal structure of 3D CNN automatically by using the Bayesian optimization with the Expected Improvement (EI) strategy. For instance, we automatically constructed 3D CNN for classifying lung tumor in 3D chest CT images into benign and malignant ones, and compared the generalization accuracy of the automatically optimized 3D CNN with accuracy of a manually constructed 3D CNN, SVM (RBF kernel and poly kernel) and the random forest. As the result of the classification experiments, generalization accuracy were 81.4%, 70.1%, 69.1%, 70.1% and 65.7%, respectively. It was shown that the Bayesian optimization with the EI strategy had ability to construct 3D CNN with higher performance than the other methods.

TABLE OF CONTENTS/OUTLINE

Introduction The Bayesian optimization Expected Improvement (EI) strategy Comparison of the classification accuracy Conclusion



IN107-ED-X

Data Enhancement of Deep Learning for Medical Image Analysis: How Do We Increase Precisely Labeled Training Images?

All Day Room: NA Digital Education Exhibit

Participants

Shoji Kido, MD, PhD, Ube, Japan (*Presenter*) Nothing to Disclose Shingo Mabu, Ube, Japan (*Abstract Co-Author*) Nothing to Disclose Yasushi Hirano, Ube, Japan (*Abstract Co-Author*) Nothing to Disclose

For information about this presentation, contact:

kido.ai@yamaguchi-u.ac.jp

TEACHING POINTS

The number of medical images is usually not enough for applications using deep learning. So, the data enhancement techniques are important in order to obtain high-performance results by use of deep learning even in the cases of small number of images. The purpose of this exhibit is: 1. To learn data augmentation which increases the size of labeled training images by use of rotations, parallel movement, reflection, and so on. 2. To learn transfer learning which can transfer a network learned with a sufficiently large image dataset such as ImageNet. It offers a way to leverage existing datasets to perform well. 3. To learn Generative Adversarial Networks (GAN) which is the state-of-art technique of image generation. This method can create labeled images similar to original ones and increase training images. 4. To learn unsupervised learning which does not require annotations by radiologists because computers themselves set diagnostic criteria. 5. To learn semi-supervised learning which requires only small number of annotated images. Computers themselves learn using such small number of images and set diagnostic criteria.

TABLE OF CONTENTS/OUTLINE

1. Introduction 2. Data Augmentation 3. Transfer Learning 4. Generative Adversarial Networks (GAN) 5. Unsupervised Learning 6. Semi-supervised Learning 7.Conclusiosn



IN111-ED-X

Machine Learning: Solutions to Shortcomings

All Day Room: NA Digital Education Exhibit

Awards Identified for RadioGraphics

Participants

Curtis L. Simmons, MD, Rochester, MN (*Presenter*) Nothing to Disclose Petro Kostandy, MD, Rochester, MN (*Abstract Co-Author*) Nothing to Disclose Brian J. Bartholmai, MD, Rochester, MN (*Abstract Co-Author*) License agreement, ImBio, LLC; Scientific Advisor, ImBio, LLC; Scientific Advisor, Bristol-Myers Squibb Company

TEACHING POINTS

Overcoming gold standard definition variability, evaluating the robustness of algorithms, outlier impact on algorithms, avoiding overfitting small data sets, impacts of machine learning on current radiology workflows, and current legislative hurdles.

TABLE OF CONTENTS/OUTLINE

1. The gold standard problem: consensus vs a pathological diagnosis 2. Less simplified inputs: A. Inputs forced into definitive yes/no answers. B. Radiologists can convey likelihoods 3. Big data and outliers: A. Computational limits to comparing 3D data over time B. Impacts of pruning the training sets early C. The dilemma of including outliers in training sets 4. Overfitting data sets: A. Limits to extrapolation B. Methods to increase robustness 5. Hurdles of FDA approval A. Limits of consensus gold standards B. Legislative timeline vs technological timeline 6. Radiologist interactions with machine learning: A. Need to check proper data input B. False positive rate leads to ignoring algorithm suggestions C. Overconfidence in algorithms increases error rates



IN113-ED-X

Machine Learning: A Theoretical Stepwise Primer for Radiologists

All Day Room: NA Digital Education Exhibit

Participants

Adarsh Ghosh, MD, NEW DELHI, India (*Presenter*) Nothing to Disclose Devasenathipathy Kandasamy, MD,FRCR, New Delhi, India (*Abstract Co-Author*) Nothing to Disclose

For information about this presentation, contact:

adarsh11g11@gmail.com

TEACHING POINTS

1. Describe a theoretical overview of the steps involved in training a machine learning model- handling data, data preparation, model training and model evaluation.2. Describe feature selection and dimensional reduction as important steps in machine learning.3. Describe the important machine learning models and principle involved in their working.

TABLE OF CONTENTS/OUTLINE

After completing this module you would be able toDescribed the steps involved in Machine LearningStep 1: Preprocessing of raw data1. Missing values and how to handle them2. Outliers and their handling3. Feature Selection: Univariate and multivariate analysis4. Dimensional Reduction: Factor Analysis and Principal Components Analysis. 5. Scaling of variables.Step 2: Training of Algorithm1. Splitting dataset into training, testing and validation datasets: simple/ stratified random sampling.2. Algorithmsa. Supervisedb. Unsupervised c. Reinforcement learning. 3. Logistic regression4. Decision trees5. Support Machine Vectors6. K Nearest Neighbours7. Naïve Bayes8. K means9. Artificial Neural NetworkStep 3: Evaluating and selecting the model1. Accuracy2. Gains chart3. K fold cross validation4. Kolmogorov-Smirnov Chart5. ROC curve.6. Root Mean Square Error



IN116-ED-X

3-Minute Recipe for Deep Learning: Principle, Hardware, and Software

All Day Room: NA Digital Education Exhibit

Participants

Atsushi Teramoto, PhD, Toyoake, Japan (*Presenter*) Nothing to Disclose Hiroshi Fujita, PhD, Gifu City, Japan (*Abstract Co-Author*) Nothing to Disclose

For information about this presentation, contact:

teramoto@fujita-hu.ac.jp

TEACHING POINTS

Artificial Intelligence is changing everything in the world. Particularly, deep learning techniques have the excellent performance; it can help doctors make faster, more accurate diagnoses. There are a lot of publication and software about deep learning. However, principle and computer environment are still difficult to understand for radiologist and radiological technologist. The purpose of this exhibition is to teach the principle of artificial intelligence including machine learning, artificial neural network, and deep learning. Furthermore, hardware and software environment for the deep learning are introduced. The major teaching points of this exhibit are:1. Deep learning is the deep version of artificial neural network, which is one kind of artificial intelligence.2. Convolutional neural network detect the feature from the given image using convolution.3. What kind of hardware and software should we get in order to start the research about deep learning

TABLE OF CONTENTS/OUTLINE

1. Definition of deep learning2. Deep learning basics - Convolutional neural network - Convolution layer - Pooling layer - Fully connected layer3. Hardware and software for deep learning



IN117-ED-X

What Radiologists Should Learn about Machine Learning?

All Day Room: NA Digital Education Exhibit

Participants

Po-Chih Kuo, Taipei, Taiwan (Presenter) Nothing to Disclose Michelle Liou, Taipei, Taiwan (Abstract Co-Author) Nothing to Disclose Yung-Chieh Chen, MD, PhD, Taipei, Taiwan (Abstract Co-Author) Nothing to Disclose Cheng-Yu Chen, MD, Taipei, Taiwan (Abstract Co-Author) Nothing to Disclose

TEACHING POINTS

To introduce the procedure of applying machine learning techniques to medical imaging. To show methods for visualizing and interpreting models obtained by machine learning algorithms. To discuss recent challenges and their potential solutions in machine learning for radiology applications. To conclude what AI skills are necessary for a radiologist.

TABLE OF CONTENTS/OUTLINE

An overview of artificial intelligence, big data, machine learning, and deep learning What's new in machine learning and radiomics? Recent development of models, algorithms, and features Beyond a black box: methods for model visualization and interpretation Challenges and solutions in machine learning for medical applications Would machines replace radiologists? Future directions



IN119-ED-X

The Artificial Intelligence Journal Club: A Multi-Institutional Resident-Driven Web-Based Educational Initiative

All Day Room: NA Digital Education Exhibit

Participants

Patricia Balthazar, MD, Atlanta, GA (*Presenter*) Nothing to Disclose Kevin F. Seals, MD, Los Angeles, CA (*Abstract Co-Author*) Nothing to Disclose Daniel A. Ortiz, MD, Virginia Beach, VA (*Abstract Co-Author*) Nothing to Disclose Lindsey A. Shea, MD, Indianapolis, IN (*Abstract Co-Author*) Nothing to Disclose Shahein H. Tajmir, MD, Boston, MA (*Abstract Co-Author*) Nothing to Disclose Judy W. Gichoya, MBChB,MS, Portland, OR (*Abstract Co-Author*) Nothing to Disclose

Background

Artificial intelligence (AI) and machine learning are rapidly-evolving emerging technologies and undoubtedly the most popular current topic in radiology. One component of the hype can be attributed to job security concerns of machines replacing radiologists. In another common perspective, there is excitement about the disruptive potential of accuracy, productivity and workflow augmentation. The uncertainty is clear, but regardless of how AI will change our future clinical practice, radiology trainees should prepare and take part in this important revolution. Given the lack of formal AI education (or even discussion) during residency, the American College of Radiology Resident and Fellow Section created the AI Journal Club. Lead and organized by 6 residents from multiple institutions across the country, an interactive monthly webinar was created in December 2017. AI-related articles or topics are discussed by invited experts in the field. Email and social media are used to advertise the sessions. Although trainees are the target audience, anyone can register and attend the web-based journal club. The goal of the AI Journal Club is to create an interactive community of trainees and AI experts to discuss key topics in machine learning and learn and grow as a group.

Evaluation

In our 5-month experience, the number of registered participants for each journal club session varied from 94 to 339.

Discussion

Current trainees will be exposed AI and machine learning in their future clinical practices. Beyond imaging interpretation, the promising technology can potentially affect the entire diagnostic imaging chain, including workflow, acquisition, and scheduling. The great interest shown in our resident-driven web-based AI journal club demonstrates that trainees recognize AI to be an important topic to be discussed and understood.

Conclusion

Radiologists of the future, even if not developers and programmers, will need to be able to evaluate AI-related technologies products, and research. There is currently a need for national education of radiology trainees in AI. The AI journal club has successfully started to build a community and represents an important first step in formal AI training for radiologists.

FIGURE

http://abstract.rsna.org/uploads/2018/18011285/18011285_5clw.jpg



IN120-ED-X

Historical Overview of Machine Learning (ML) and Deep Learning in Medical Image Analysis - What are the Sources of the Power of Deep Learning?

All Day Room: NA Digital Education Exhibit

Participants

Kenji Suzuki, PhD, Chicago, IL (*Presenter*) Royalties, General Electric Company; Royalties, Hologic, Inc; Royalties, MEDIAN Technologies; Royalties, Riverain Technologies, LLC; Royalties, Canon Medical Systems Corporation; Royalties, Mitsubishi Corporation; Royalties, AlgoMedica, Inc Amin Zarshenas, MSc, Chicago, IL (*Abstract Co-Author*) Nothing to Disclose

Junchi Liu, MS, Chicago, IL (*Abstract Co-Author*) Nothing to Disclose Yuji Zhao, MSc, Chicago, IL (*Abstract Co-Author*) Nothing to Disclose Yukui Luo, Chicago, IL (*Abstract Co-Author*) Nothing to Disclose

For information about this presentation, contact:

ksuzuki@iit.edu

TEACHING POINTS

1) To survey the history of ML techniques in computer vision and medical image analysis. 2) To overview the ML techniques before and after the introduction of deep learning. 3) To understand the differences between ordinary ML and deep learning. 4) To identify the sources of the power of deep learning.

TABLE OF CONTENTS/OUTLINE

A. Survey of the history of ML in medical image analysis - Class of object/feature-based ML - Class of image/pixel-based ML B. Overview of deep learning - Basic architecture of deep learning models - Various deep learning models - AlexNet, LeNet, ResNet, VGG Net, GAN C. Differences and limitations of ordinary ML and deep learning - Two major reasons for poor performance of object/feature-based ML - End-to-end ML paradigm with deep learning D. Sources of the power of deep learning - Direct training of pixels in images - Depth and width of the architecture E. Interpretation of deep learning models - Deep architecture for higher-level representation of objects - Performance and its dependency on the number of training cases F. Current applications of deep learning in medical imaging - Classification of lesions with deep learning - Segmentation of organs with deep learning - De-noising with deep learning



IN121-ED-X

Seeing Through the Eyes (and Visual Cortex) of a Machine: Convolutional Neural Networks at the Forefront of Machine Intelligence in Medical Imaging

All Day Room: NA Digital Education Exhibit

Participants

Mark F. Conneely, MD, North Chicago, IL (*Presenter*) Nothing to Disclose Kerry L. Conneely, MD, Arlington Hts, IL (*Abstract Co-Author*) Nothing to Disclose Piyush I. Vyas, MD, Lake Forest, IL (*Abstract Co-Author*) Nothing to Disclose Matthew So, North Chicago, IL (*Abstract Co-Author*) Nothing to Disclose David Kasjanski, Chicago, IL (*Abstract Co-Author*) Nothing to Disclose Johnathan Au, North Chicago, IL (*Abstract Co-Author*) Nothing to Disclose Paul Kohanteb, North Chicago, IL (*Abstract Co-Author*) Nothing to Disclose

For information about this presentation, contact:

mark.conneely@rosalindfranklin.edu

TEACHING POINTS

After completing this activity, participants should be able to: 1. Define and describe the basic functional parameters of neural networks and the process of training, testing, and validation in producing predictive models for computer assisted detection and diagnosis. 2. Explain how convolutional neural networks (CNN's) process imaging data. 3. Describe the advantages, challenges, and pitfalls inherent in applying CNN's to medical images for lesion detection and classification. 4. Summarize the history of CNN's, recent developments in their utilization for medical imaging applications, and a few current areas of active research.

TABLE OF CONTENTS/OUTLINE

Introduction Artificial Intelligence, Machine Learning, Neural Networks, and Deep Learning. Machine Learning 101: Training, Testing, and Validation. Artificial Neurons Neural Networks Biology Inspiring Computer Science: The Origins of Convolutional Neural Networks. Feature extraction Convolutions, Kernels, Downsampling, and Max Pooling. Software and Hardware considerations. Eureka! ...Or Perhaps Not. The Problem of Overfitting. CNN Applications in Image Segmentation. Lesion Detection with CNN's. Image and Lesion Classification: Recent Advances. PACS 2.0: When Will Artificial Intelligence Reach the Mainstream Radiologist's Workstation, and What Will It Look Like?



IN122-ED-X

Concepts in Artificial Intelligence: A Primer for Radiologists

All Day Room: NA Digital Education Exhibit

Participants

Harry R. Marshall, MD,PhD, London, ON (*Presenter*) Nothing to Disclose Andrea Para, MSc,MD, Toronto, ON (*Abstract Co-Author*) Nothing to Disclose Aashish Goela, MD,FRCPC, London, ON (*Abstract Co-Author*) Nothing to Disclose

For information about this presentation, contact:

harry.marshall@lhsc.on.ca

TEACHING POINTS

1. The concept of a rational agent is a useful framework for artificial intelligence problems. They have several key components and are modular in nature. We give several examples of different variations of these components that can be 'installed' in the agent, using radiology specific scenarios. 2. Searching through data structures is a necessary task for many agents. We introduce ways to search both without and with domain specific knowledge. 3. Two powerful ways to encode knowledge into an agent are via propositional / first-order logic and probability theory (specifically Bayesian networks). We give a high level overview of these tools with examples. 4. The purpose of machine learning is to improve the agent's components. We summarize some general approaches for learning and put common algorithms and terms in greater context (e.g. 'deep' learning).

TABLE OF CONTENTS/OUTLINE

1. Agents 2. Search 3. Logic 3. Probability 4. Machine learning



IN123-ED-X

Hands-On Machine Learning for Diffusion Tensor Imaging Assessment: From Theory to Practice

All Day Room: NA Digital Education Exhibit

Participants

Felix Paulano-Godino, PhD, Jaen, Spain (*Presenter*) Nothing to Disclose Teodoro M. Noguerol, MD, Jaen, Spain (*Abstract Co-Author*) Nothing to Disclose Rodrigo de Luis-Garcia, Valladolid, Spain (*Abstract Co-Author*) Nothing to Disclose Juan Calabia-del-Campo, Valladolid, Spain (*Abstract Co-Author*) Research funded, SME Giveme5D Antonio Luna, MD,PhD, Jaen, Spain (*Abstract Co-Author*) Consultant, Bracco Group; Speaker, General Electric Company; Speaker, Canon Medical Systems Corporation; Royalties, Springer Nature

For information about this presentation, contact:

f.paulano.j@htime.org

TEACHING POINTS

1. Review the main steps for building an unsupervised machine learning algorithm. 2. Describe how to apply the theoretical concepts into a specific radiological issue such as Diffusion Tensor Imaging (DTI) data assessment. 3. Illustrate the potential radiological and clinical applications for machine learning in the field of DTI for Central Nervous System evaluation.

TABLE OF CONTENTS/OUTLINE

1. Introduction 2. Theoretical basis of machine learning. a. Why use Unsupervised Learning? -Clustering algorithms: k-means, hierarchical clustering, Gaussian mixture models,... b.Data preparation -Principal Component Analysis -Train, validation and test sets c. Issues on the application of a clustering algorithm -Selection of the number of clusters -Initialization and optimization objective - Results analysis: what the results obtained mean? 3. Physical basis of DTI a. Brief description of sequence design and clinical usefulness b. Biological meaning of parameters derived -Mean Diffusivity -Fractional Anisotropy -Radial Diffusivity -Axial Diffusivity 4. How machine learning can help for DTI parameters evaluation? a. Algorithm design: workflow and feasibility b. Clinical practice implementation c. Potential applications 5. Conclusions

Honored Educators

Presenters or authors on this event have been recognized as RSNA Honored Educators for participating in multiple qualifying educational activities. Honored Educators are invested in furthering the profession of radiology by delivering high-quality educational content in their field of study. Learn how you can become an honored educator by visiting the website at: https://www.rsna.org/Honored-Educator-Award/ Antonio Luna, MD - 2018 Honored Educator



IN124-ED-X

Artificial Intelligence Using Neural Network Architecture for Radiology (AINNAR): The Decoding of the Technical Terms in AI

All Day Room: NA Digital Education Exhibit

Participants

Tomoyuki Noguchi, MD, PhD, Shinjuku-Ku, Japan (*Abstract Co-Author*) Nothing to Disclose Yusuke Kawata, MD, Tokyo, Japan (*Abstract Co-Author*) Nothing to Disclose Akihiro Machitori, Chiba, Japan (*Abstract Co-Author*) Nothing to Disclose Yoshitaka Shida, MD, Tokyo, Japan (*Abstract Co-Author*) Nothing to Disclose Takashi Okafuji, MD, Fukuoka, Japan (*Abstract Co-Author*) Nothing to Disclose Masatoshi Hotta, Shinjuku, Japan (*Abstract Co-Author*) Nothing to Disclose Kota Yokoyama, MD, Tokyo, Japan (*Abstract Co-Author*) Nothing to Disclose Ryogo Minamimoto, MD, PhD, Tokyo, Japan (*Abstract Co-Author*) Nothing to Disclose Tsuyoshi Tajima, MD, PhD, Tokyo, Japan (*Abstract Co-Author*) Nothing to Disclose

For information about this presentation, contact:

fuuchiyama@hosp.ncgm.go.jp

TEACHING POINTS

1. To introduce the concept of deep learning and convolutional neural networks (CNNs) 2. To demonstrate the four main operations of CNNs 3. To summarize the outline and details of AINNAR in an easy-to-understand term

TABLE OF CONTENTS/OUTLINE

1. Explain the importance of deep learning in Artificial intelligence (AI) 2. Presentation of features of CNNs 3. Demonstration of four main operations of CNNs A) Convolution B) Non Linearity (ReLU) C) Pooling or Sub Sampling D) Classification (Fully Connected Layer) 4. How to apply CNNs for medical images



IN126-ED-X

Practical Guide to Using PyTorch for Deep Learning Based Image Segmentation in Radiology

All Day Room: NA Digital Education Exhibit

Participants

Yiran Jia, BA, Berkeley, CA (*Presenter*) Nothing to Disclose Thienkhai H. Vu, MD, PhD, San Francisco, CA (*Abstract Co-Author*) Nothing to Disclose Youngho Seo, PhD, San Francisco, CA (*Abstract Co-Author*) Consultant, BioLaurus, Inc Peter Chang, MD, San Francisco, CA (*Abstract Co-Author*) Nothing to Disclose Jae Ho Sohn, MD, San Francisco, CA (*Abstract Co-Author*) Nothing to Disclose

For information about this presentation, contact:

sohn87@gmail.com

TEACHING POINTS

The aim of this abstract is to illustrate practical steps of using deep learning with PyTorch for solving computer vision problems in radiologic imaging research. By walking through how to perform semantic segmentations of breast masses from mammograms, we demonstrate:

- -- how to load and visualize DICOM files in Python
- -- how to pre-process image data and build batch data generator to feed into neural network
- -- how to choose hyperparameters, loss functions, and optimization algorithms in PyTorch
- -- how to train U-Net model in PyTorch
- -- how to analyze errors and validate the result
- -- tips and common pitfalls

TABLE OF CONTENTS/OUTLINE

- Scenario: Given a mammogram, we want to locate the region of breast masses so that we can further analyze and classify them as benign versus malignant.

- Data: DICOM file of mammograms with corresponding segmentation masks
- Technical Requirement: Basic knowledge of Python with numpy and pandas; Linear Algebra; Basic Machine Learning Knowledge
- Load Data and Preprocessing
- Exploratory Data Analysis
- Design U-Net Architecture
- Network Considerations: Hyperparameters, Optimization, Fine-Tuning
- Model Training & Validation
- Visualize Result & Error Analysis



IN127-ED-X

Case Based Approach to Image Classification with PyTorch: A Primer for Novice Machine Learning Practitioners

All Day Room: NA Digital Education Exhibit

Participants

Vaibhavi Shah, Cambridge, MA (*Presenter*) Nothing to Disclose Yiran Jia, BA, Berkeley, CA (*Abstract Co-Author*) Nothing to Disclose Peter Chang, MD, San Francisco, CA (*Abstract Co-Author*) Nothing to Disclose Youngho Seo, PhD, San Francisco, CA (*Abstract Co-Author*) Consultant, BioLaurus, Inc Thienkhai H. Vu, MD, PhD, San Francisco, CA (*Abstract Co-Author*) Nothing to Disclose Jae Ho Sohn, MD, San Francisco, CA (*Abstract Co-Author*) Nothing to Disclose

For information about this presentation, contact:

vbshah@mit.edu

TEACHING POINTS

The objective of this abstract is to demonstrate the use of PyTorch for the application of image classification in radiologic research, specifically as it pertains to predicting breast density from mammogram images. Training a classifier and inference with a classifier will be reviewed as it relates to a breast mammogram dataset, and in the process the following elements will be detailed: Loading and preprocessing raw data (DICOM files) Designing a convolutional neural network and defining its architecture, loss function, hyperparameters, and associated optimizer Training the classifier with preprocessed data Training on a GPU

TABLE OF CONTENTS/OUTLINE

Problem: Mammograms and classifying breast density Imaging: Current status Outlook: Using computer vision as a diagnostic aid Background Minimal medical knowledge about mammograms Basic programming knowledge in Python Basic understanding of machine learning concepts Computer Vision Designing Neural Network Training Model/Inspection Analysis/Visualization Walkthrough Load images Formatting and adjustment Explain Commented Code Implementation of Code Analysis PyTorch details Applications and Tips Applicability to other imaging cases Variability Conclusion



IN129-ED-X

Application of Deep Learning to Pancreatic Imaging - The Radiologists' Perspective

All Day Room: NA Digital Education Exhibit

FDA Discussions may include off-label uses.

Awards Cum Laude

Participants

Linda C. Chu, MD, Baltimore, MD (*Presenter*) Nothing to Disclose Seyoun Park, Baltimore, MD (*Abstract Co-Author*) Nothing to Disclose Satomi Kawamoto, MD, Laurel, MD (*Abstract Co-Author*) Nothing to Disclose Daniel Fadaei Fouladi, MD, Baltimore, MD (*Abstract Co-Author*) Nothing to Disclose Shahab Shayesteh, MD, Baltimore, MD (*Abstract Co-Author*) Nothing to Disclose Karen M. Horton, MD, Baltimore, MD (*Abstract Co-Author*) Nothing to Disclose Alan Yuille, Baltimore, MD (*Abstract Co-Author*) Nothing to Disclose Elliot K. Fishman, MD, Baltimore, MD (*Abstract Co-Author*) Institutional Grant support, Siemens AG; Institutional Grant support, General Electric Company; Co-founder, HipGraphics, Inc

For information about this presentation, contact:

lindachu@jhmi.edu

TEACHING POINTS

1. Deep learning has the potential to revolutionize the practice of radiology through improved disease detection and patient prognostication. 2. Deep learning uses training data and multiple layers of equations to develop the algorithm. 3. Multidisciplinary collaboration between radiologists and computer scientists is essential in building a successful deep learning initiative. 4. Radiologists provide expertise in organ segmentation and pathology annotation. 5. Radiologists can help computer scientists optimize the algorithm through their imaging expertise. 6. Radiologists should help steer future application of deep learning in medical imaging, instead of viewing this new technology as a threat.

TABLE OF CONTENTS/OUTLINE

1. Basic principles of deep learning. 2. Illustrate practical aspects of building a deep learning collaboration, through our experience in applying deep learning to pancreatic imaging: • Multidisciplinary team approach. • Image segmentation and annotation. • Performance in automatic segmentation of normal pancreas. • Performance in automatic detection of pancreatic pathology. • Lessons learned from trouble shooting. 3. Challenges in application of deep learning in current clinical practice. 4. Future directions of deep learning.

Honored Educators

Presenters or authors on this event have been recognized as RSNA Honored Educators for participating in multiple qualifying educational activities. Honored Educators are invested in furthering the profession of radiology by delivering high-quality educational content in their field of study. Learn how you can become an honored educator by visiting the website at: https://www.rsna.org/Honored-Educator-Award/ Elliot K. Fishman, MD - 2012 Honored EducatorElliot K. Fishman, MD - 2014 Honored EducatorElliot K. Fishman, MD - 2016 Honored EducatorElliot K. Fishman, MD - 2018 Honored Educator



IN131-ED-X

Decentralized Deep Learning on a Blockchain

All Day Room: NA Digital Education Exhibit

Participants

John T. Moon, BA, Albany, NY (Presenter) Nothing to Disclose

TEACHING POINTS

Teaching points (3): The purpose of this exhibit is to: 1. To provide a literature review on blockchain and its emerging applications in the healthcare field, and as it specifically relates to imaging in radiology. 2. To educate trainees and clinicians on how blockchain and deep learning in radiology is poised to advance the specialty. 3. To clearly delineate the advantages and potential drawbacks of this ground-breaking technology as it relates to radiological imaging.

TABLE OF CONTENTS/OUTLINE

 Blockchain and deep learning historical overview.
 Modern applications of blockchain and deep learning, respectfully, within and without the healthcare field.
 Current research and guidlines supporting deep learning on a blockchain within radiology. Mechanism and implementation of deep learning on a blockchain for radiological imaging.
 Regulatory and legislative considerations.
 Examination of the impact of blockchain technology on radiology as a field.



IN132-ED-X

Supervised vs. Unsupervised Machine Learning for Radiologists in a Nutshell

All Day Room: NA Digital Education Exhibit

Awards Certificate of Merit

Participants

Sebastian Roehrich, MD, Vienna, Austria (*Presenter*) Nothing to Disclose Helmut Prosch, MD, Vienna, Austria (*Abstract Co-Author*) Nothing to Disclose Johannes Hofmanninger, Vienna, Austria (*Abstract Co-Author*) Siemens AG; Boehringer Ingelheim GmbH Florian Prayer, MD, Vienna, Austria (*Abstract Co-Author*) Nothing to Disclose Jeanny Pan, Vienna, Austria (*Abstract Co-Author*) Nothing to Disclose Georg Langs, Vienna, Austria (*Abstract Co-Author*) Nothing to Disclose

For information about this presentation, contact:

sebastian.roehrich@meduniwien.ac.at

TEACHING POINTS

Supervised and unsupervised machine learning (ML) plays an increasingly important role in radiology. While supervised ML enables the automated detection of known markers, unsupervised ML promises to build models of population-level data, and to identify additional relevant markers. The purpose of this exhibit is: To discern whether a machine learning problem should be tackled with a supervised or unsupervised approach. To understand what information is essential for an efficient collaboration between radiologists and data scientists and how the framework conditions may differ for projects using supervised or unsupervised learning. To review examples of supervised and unsupervised machine learning problem.

TABLE OF CONTENTS/OUTLINE

Supervised and unsupervised machine learning in a nutshell Examples of supervised and unsupervised machine learning problems in radiology Steps for setting up a collaborative project between radiologists and data scientists Framework conditions for projects using a supervised approach Framework conditions for projects using an unsupervised approach Examples of existing applications that utilize supervised and unsupervised learning to improve the clinical workflow in radiology



IN133-ED-X

Artificial Intelligence for the Average Intelligence: A Practical Guide

All Day Room: NA Digital Education Exhibit

Participants

Bryan E. Ashley, MD, Chapel Hill, NC (*Abstract Co-Author*) Nothing to Disclose George R. Wong, MD, Chapel Hill, NC (*Presenter*) Nothing to Disclose

TEACHING POINTS

Understand the basics of artificial intelligence, machine learning, and deep learning. Understand how these systems may be implemented in the future of Radiology. Understand the current capacity and limitations of these automated systems.

TABLE OF CONTENTS/OUTLINE

Background of artificial intelligence: where is began and where is it now. Focus on types of artificial intelligence: machine learning and deep learning to acheive an operable and applicable understanding.Decoding the alphabet soup of AI: CNN, NVIDIA, MNIST Implementation in the future of Radiology with a focus on computer/machine vision: object recognition, identification, and detection. Current capacity and limitations of these automated systems. What can these things do now? Address what we can do to stay informed and ahead of the coming change.



IN137-ED-X

Virtual Radiologists: Current Status of Deep Learning in Radiology and Its Future Trends

All Day Room: NA Digital Education Exhibit

Participants

Sarfaraz Hussein, Orlando, FL (*Presenter*) Nothing to Disclose Aliasghar Mortazi, MSc, Orlando, FL (*Abstract Co-Author*) Nothing to Disclose Harish Raviprakash, Orlando, FL (*Abstract Co-Author*) Nothing to Disclose Naji Khosravan, Orlando, FL (*Abstract Co-Author*) Nothing to Disclose Georgios Z. Papadakis, MD,PhD, Heraklion, Greece (*Abstract Co-Author*) Nothing to Disclose Uygar Teomete, MD, Coral Gables, FL (*Abstract Co-Author*) Nothing to Disclose Ulas Bagci, PhD, MSc, Orlando, FL (*Abstract Co-Author*) Nothing to Disclose

For information about this presentation, contact:

shussein@knights.ucf.edu

TEACHING POINTS

1. Recent advances and applications of deep learning for segmentation, detection and classification tasks in radiology 2. Novel challenges and potential solutions for deep learning methods in radiology

TABLE OF CONTENTS/OUTLINE

1. An overview of latest deep learning techniques: •Dense NET •U-NET •CapsuleNET •Recurrent Networks •Reinforcement Learning •Generative Adversarial Networks 2. Deep learning for Segmentation • Cardiac Imaging o Region Wall thicknesses estimation o Heart segmentation • Prostate Imaging: o Prostate segmentation •Brain Imaging: o Neuroanatomy segmentation •Pulmonary and Abdominal Imaging o Lung and pathology o Pancreas and cysts 3. Deep learning for Detection • Cardiac Imaging o Measuring ejection fraction • Pulmonary and Abdominal Imaging o Lung nodule detection o Renal lesion detection •Breast Imaging: o Lesion Detection •Brain Imaging: o Intracranial hemorrhage 4. Deep learning for Classification •Cardiac Imaging: o Pulmonary artery-vein classification •Brain Imaging o Biomarker for Autism & Alzheimer's •Pulmonary and Abdominal Imaging o Lung nodule diagnosis o IPMN diagnosis •Prostate Imaging: o Lesion diagnosis in US/MRI •Breast Imaging: o Breast Cancer diagnosis 5. Challenges and solutions: optimal architecture, data scarcity, weakly & unsupervised learning, deep visualizations, active and cross modality learning 6. Conclusion and future trends



IN138-ED-X

Strengths, Weakness, Opportunities and Threats: SWOT Analysis of Machine Learning for Radiology Applications

All Day Room: NA Digital Education Exhibit

Participants

Teodoro M. Noguerol, MD, Jaen, Spain (*Presenter*) Nothing to Disclose Felix Paulano-Godino, PhD, Jaen, Spain (*Abstract Co-Author*) Nothing to Disclose Maria Teresa Martin-Valdivia, Jaen, Spain (*Abstract Co-Author*) Nothing to Disclose Mario Martinez-Zarzuela, Valladolid, Spain (*Abstract Co-Author*) Nothing to Disclose Juan Calabia-del-Campo, Valladolid, Spain (*Abstract Co-Author*) Research funded, SME Giveme5D Antonio Luna, MD,PhD, Jaen, Spain (*Abstract Co-Author*) Consultant, Bracco Group; Speaker, General Electric Company; Speaker, Canon Medical Systems Corporation; Royalties, Springer Nature

For information about this presentation, contact:

t.martin.f@htime.org

TEACHING POINTS

1. Review the current situation of machine learning techniques. 2. Describe the main types of machine learning. 3. Review the strengths, weakness, opportunities and threats of machine learning for radiology.

TABLE OF CONTENTS/OUTLINE

1. Introduction 2. Currents concepts a. What is machine learning? b. Artificial intelligence, big data, deep learning and radiomics. c. Update of radiological applications based on machine learning. 3. Main types of machine learning techniques b. Supervised b. Unsupervised c. Semi-supervised d. Specific machine learning techniques in radiology: text-based and image-based. c. Neural networks and deep learning. 4. SWOT analysis of machine learning in radiology a. Strengths. b. Weaknesses. c. Opportunities. d. Threats. 5. Conclusions and take home messages.

Honored Educators

Presenters or authors on this event have been recognized as RSNA Honored Educators for participating in multiple qualifying educational activities. Honored Educators are invested in furthering the profession of radiology by delivering high-quality educational content in their field of study. Learn how you can become an honored educator by visiting the website at: https://www.rsna.org/Honored-Educator-Award/ Antonio Luna, MD - 2018 Honored Educator



PH100-ED-X

Does Deep Learning Help in Diagnosis of Hyperacute Stroke in Noncontrast CT?

All Day Room: NA Digital Education Exhibit

Participants

Noriyuki Takahashi, Akita, Japan (*Presenter*) Nothing to Disclose Toshibumi Kinoshita, MD, PhD, Akita, Japan (*Abstract Co-Author*) Nothing to Disclose Tomomi Omura, Akita, Japan (*Abstract Co-Author*) Nothing to Disclose Keisuke Matsubara, PhD, Akita, Japan (*Abstract Co-Author*) Nothing to Disclose Yongbum Lee, PhD, Niigata, Japan (*Abstract Co-Author*) Nothing to Disclose Mamoru Kato, PhD, Akita, Japan (*Abstract Co-Author*) Nothing to Disclose Hideto Toyoshima, BSc, Akita, Japan (*Abstract Co-Author*) Nothing to Disclose

TEACHING POINTS

To review existing CAD schemes for detecting early ischemic changes of hyperacute stroke in noncontrast CT To present a CAD scheme using deep convolutional neural network (DCNN) To understand the detection performance of the CAD schemes

TABLE OF CONTENTS/OUTLINE

Feature based conventional CAD scheme with anatomical standardization (AS) - Z-score mapping based on a voxel-by-voxel analysis - Classification with handcrafted features based on the z-score mapping CAD scheme with AS using the DCNN - Atlasbased extraction of defined regions according to a quantitative CT scoring method (ASPECTS) - Fine-tuning using a pre-trained model Detection performance of the scheme using the DCNN - Versus that of traditional schemes - Versus that of neuroradiologists Summary: The CAD scheme using the DCNN has higher performance than the existing schemes for detecting early ischemic changes. The AS essential as a pre-processing step for the DCNN for obtaining the higher accuracy in the detection of early ischemic changes. The CAD scheme using the DCNN has the potential comparable to radiologists to detect early ischemic changes of hyperacute stroke in noncontrast CT. Therefore, DCNN-based CAD schemes would be useful in the diagnosis of hyperacute stroke.



PH110-ED-X

Possibility of Deep Learning Technique in Medical Imaging: Can Deep Learning Improve Image Quality?

All Day Room: NA Digital Education Exhibit

Awards Identified for RadioGraphics

Participants

Yuko Nakamura, MD, Hiroshima, Japan (*Presenter*) Nothing to Disclose Toru Higaki, PhD, Hiroshima, Japan (*Abstract Co-Author*) Nothing to Disclose Zhou Yu, Vernon Hills, IL (*Abstract Co-Author*) Employee, Canon Medical Systems Corporation Jian Zhou, PhD, Vernon Hills, IL (*Abstract Co-Author*) Principal Scientist, Canon Medical Systems Corporation; Naruomi Akino, Toyoake, Japan (*Abstract Co-Author*) Nothing to Disclose Kazuo Awai, MD, Hiroshima, Japan (*Abstract Co-Author*) Research Grant, Canon Medical Systems Corporation; Research Grant, Hitachi, Ltd; Research Grant, Fujitsu Limited; Research Grant, Bayer AG; Research Grant, DAIICHI SANKYO Group; Research Grant, Eisai Co, Ltd; Medical Advisory Board, General Electric Company; ; Fuminari Tatsugami, Hiroshima, Japan (*Abstract Co-Author*) Nothing to Disclose Makoto Iida, Hiroshima, Japan (*Abstract Co-Author*) Nothing to Disclose

TEACHING POINTS

a. Deep learning is part of a broader family of machine learning methods based on learning data representations, as opposed to task-specific algorithms. b. Deep learning techniques have been introduced in various areas of medical imaging such as image segmentation and registration, automatic labeling and captioning, and computer-aided detection and diagnosis. c. Deep learning can be applied to reconstruction of images. Deep learning based reconstruction (DLR) can generate CT image with better quality using a deep learning trained by teaching dataset of higher dose CT image reconstructed with model-based iterative reconstruction. d. Unlike other reconstruction technique, DLR can improve CT image quality in various setting.

TABLE OF CONTENTS/OUTLINE

a. What is deep learning? b. Utility of deep learning technique in medical imaging c. Basic principle of deep learning based reconstruction d. Comparison of features between DLR and the current reconstruction techniques e. Case presentations of CT images reconstructed with DLR including cardiac, lung, and abdominal CT



PH117-ED-X

Optimization Method of Hyper-Parameters in Convolutional Neural Network for Medical Image Application

All Day Room: NA Digital Education Exhibit

Awards Certificate of Merit

Participants

Kodai Tanaka, Kusatsu, Japan (*Presenter*) Nothing to Disclose Akiyoshi Hizukuri, Kusatsu, Japan (*Abstract Co-Author*) Nothing to Disclose Ryohei Nakayama, PhD, Kusatsu, Japan (*Abstract Co-Author*) Nothing to Disclose Masaki Ishida, MD, PhD, Tsu, Japan (*Abstract Co-Author*) Nothing to Disclose Kakuya Kitagawa, MD, PhD, Tsu, Japan (*Abstract Co-Author*) Nothing to Disclose Hajime Sakuma, MD, Tsu, Japan (*Abstract Co-Author*) Research Grant, Fuji Pharma Co, Ltd; Research Grant, DAIICHI SANKYO Group; Research Grant, FUJIFILM Holdings Corporation; Research Grant, Siemens AG; Research Grant, Nihon Medi-Physics Co, Ltd; Speakers Bureau, Bayer AG Yasutaka Ichikawa, MD, Tsu, Japan (*Abstract Co-Author*) Nothing to Disclose Hiroki Kobayashi, Kusatsu, Japan (*Abstract Co-Author*) Nothing to Disclose Yuito Takase, Kusatsu, Japan (*Abstract Co-Author*) Nothing to Disclose Yugo Onishi, Kusatsu, Japan (*Abstract Co-Author*) Nothing to Disclose

TEACHING POINTS

Convolutional neural network (CNN) has been applied to various use applications in medical images such as the differentiation of lesions, and the improvement of image quality. Although the CNN has showed high performance in many applications, it is very difficult to appropriately determine a large number of hyper-parameters. The inappropriate hyper-parameters often make significantly decrease of the performance of CNN. This exhibit aims the following points. To understand an architecture and hyper-parameters of the CNN To understand a Bayesian optimization for determining appropriate hyper-parameters of the CNN To demonstrate the application of the CNN with the Bayesian optimization to the differentiation of lesions To demonstrate the application of the CNN with the Bayesian optimization to the improvement of image quality

TABLE OF CONTENTS/OUTLINE

Basic architecture of the CNN Change of performance for the CNN depending on the appropriateness of hyper-parameters Bayesian optimization for determining appropriate hyper-parameters of the CNN Application of the CNN with Bayesian optimization to the differentiation of masses on breast MRI Application of the CNN with Bayesian optimization to the improvement of image quality and spatial resolution on whole heart coronary MRA.



VI109-ED-X

Artificial Intelligence and Interventional Radiology: Current Status, Future Applications, and Related Controversies

All Day Room: NA Digital Education Exhibit

FDA Discussions may include off-label uses.

Participants

Thomas Harvey, MD, Mineola, NY (*Presenter*) Nothing to Disclose Marie Surovitsky, DO, Mineola, NY (*Abstract Co-Author*) Nothing to Disclose Sofya Kalantarova, MD, Mineola, NY (*Abstract Co-Author*) Nothing to Disclose Siavash Behbahani, MD, Mineola, NY (*Abstract Co-Author*) Nothing to Disclose Jonathan Minkin, Mineola, NY (*Abstract Co-Author*) Nothing to Disclose Jason C. Hoffmann, MD, Mineola, NY (*Abstract Co-Author*) Speakers Bureau, Merit Medical Systems, Inc; ; Vanessa Karimi, BS, Mineola, NY (*Abstract Co-Author*) Nothing to Disclose

For information about this presentation, contact:

Jason.Hoffmann@nyulangone.org

TEACHING POINTS

1. Knowledge and appreciation of Artificial Intelligence (AI) in medicine and how it can impact interventional radiology (IR) patients is important for the IR community to pursue and embrace.2. While AI currently does not have a dominant role specifically in IR, many future potential applications exist that may benefit IR patients.

TABLE OF CONTENTS/OUTLINE

AI: Definitions, general review, and currently applications in society and medicineDiscuss potential benefits and drawbacks of AI use in IRReview the present-day uses and studies of AI in medicine, including IR:-Using AI to give patients and clinicians real-time information about IR treatments (The IR "chatbot"/virtual interventional radiologist)-Using AI in conjunction with robots and wireless technology to perform more precise procedural movements and keep the IR physician farther away from the patient/fluoroscope to decrease operator radiation riskEvaluate the controversies that exist with AI in medicine, focusing on those that are most relevant to IR-Can using software such as Syngo or Emboguide transform complex superselective angiography and intervention by computerdriven decision support?-Role of FDA in AI regulation-Validating proprietary AI algorithms-Who is ultimately responsible (IR physician, computer, developers)?-Will insurers reimburse for AI-related procedures?



AI001-SU

RSNA Deep Learning Classroom: Presented by NVIDIA Deep Learning Institute

Sunday, Nov. 25 8:30AM - 4:00PM Room: AI Community, Learning Center

Program Information

Located in the Learning Center (Hall D), this classroom presented by NVIDIA will give meeting attendees a hands-on opportunity to engage with deep learning tools, write algorithms and improve their understanding of deep learning technology. "Attendees must bring a laptop capable of running the most recent version of Chrome."

Sub-Events

AI001-SUA Introduction to Deep Learning

Sunday, Nov. 25 8:30AM - 10:00AM Room: AI Community, Learning Center

Title and Abstract

Introduction to Deep Learning This class will focus on basic concepts of convolutional neural networks (CNNs), and walk the attendee through a working example. A popular training example is the MNIST data set which consists of hand-written digits. This course will use a data set we created, that we call 'MedNIST and consists of 1000 images each from 5 different categories: Chest X-ray, hand X-ray, Head CT, Chest CT, Abdomen CT, and Breast MRI. The task is to identify the image type. This will be used to train attendees on the basic principles and some pitfalls in training a CNN. The attendee will have the best experience if they are familiar with Python programming.

AI001-SUB Data Science: Normalization, Annotation, Validation

Sunday, Nov. 25 10:30AM - 12:00PM Room: AI Community, Learning Center

Title and Abstract

Data Science: Normalization, Annotation, Validation This session will focus on preparation of the image and non-image data in order to obtain the best results from your deep learning system. It will include a discussion of different options for representing the data, how to normalize the data, particularly image data, the various options for image annotation and the benefits of each option. We will also discuss the 'after training' aspects of deep learning including validation and testing to ensure that the results are robust and reliable.

AI001-SUC Introduction to Deep Learning

Sunday, Nov. 25 12:30PM - 2:00PM Room: AI Community, Learning Center

Title and Abstract

Introduction to Deep Learning This class will focus on basic concepts of convolutional neural networks (CNNs), and walk the attendee through a working example. A popular training example is the MNIST data set which consists of hand-written digits. This course will use a data set we created, that we call 'MedNIST and consists of 1000 images each from 5 different categories: Chest X-ray, hand X-ray, Head CT, Chest CT, Abdomen CT, and Breast MRI. The task is to identify the image type. This will be used to train attendees on the basic principles and some pitfalls in training a CNN. The attendee will have the best experience if they are familiar with Python programming.

AI001-SUD 3D Segmentation of Brain MR

Sunday, Nov. 25 2:30PM - 4:00PM Room: AI Community, Learning Center

Title and Abstract

3D Segmentation of Brain MR This session will focus on the use of deep learning methods for segmentation, with particular emphasis on 3D techniques (V-Nets) applied to the challenge of MR brain segmentation. While focused on this particular problem, the concepts should generalize to other organs and image types.



PS10

Opening Session

Sunday, Nov. 25 8:30AM - 10:15AM Room: Arie Crown Theater



AMA PRA Category 1 Credits ™: 1.75 ARRT Category A+ Credit: 1.25

Participants

Vijay M. Rao, MD, Philadelphia, PA (*Presenter*) Nothing to Disclose Bruce R. Thomadsen, PhD, Madison, WI (*Presenter*) Nothing to Disclose Bojan D. Petrovic, MD, Glencoe, IL (*Presenter*) Nothing to Disclose

For information about this presentation, contact:

bpetrovic2@northshore.org

Sub-Events

PS10A Presentation of the Outstanding Educator Award

Participants

David M. Yousem, MD, Baltimore, MD (*Recipient*) Royalties, Reed Elsevier; Speaker, American College of Radiology; Employee, Medicolegal Consultation; ; ;

For information about this presentation, contact:

dyousem1@jhu.edu

PS10B Presentation of the Outstanding Researcher Award

Participants Carolyn C. Meltzer, MD, Atlanta, GA (*Recipient*) Nothing to Disclose

For information about this presentation, contact:

cmeltze@emory.edu

- PS10C Dedication of the 2018 RSNA Meeting Program to the Memory of William G. Bradley Jr, MD, PhD (1948-2017), and Alexander R. Margulis, MD (1921-2018)
- PS10D President's Address: How Emerging Technology Will Empower Tomorrow's Radiologists to Provide Better Patient Care

Participants

Vijay M. Rao, MD, Philadelphia, PA (Presenter) Nothing to Disclose

David C. Levin, MD, Philadelphia, PA (Presenter) Consultant, HealthHelp, LLC; Board Member, Outpatient Imaging Affiliates, LLC

Abstract

With rapid advances in artificial intelligence (AI) and related technologies, radiologists have an opportunity to improve the quality of care they provide to patients, as well as to increase their stature within the medical community and the personal and professional satisfaction they derive from their work. This is true not only in the United States but also around the world. With an aging population and continual growth in imaging procedures globally, a large amount of complex imaging data is available for data mining. AI will enable us to harness the data more effectively. Although AI algorithms for medical imaging are being developed at a fast pace across the globe, many questions remain unanswered regarding computer ethics, regulatory compliance and lack of standards. Digital extraction of quantitative features of lesions that reveal their underlying pathophysiology -- and perhaps even their genetic basis -- are the underpinnings of imaging biomarkers and radiomics. The science of radiology will be greatly enhanced if this potential is actually realized, but it will require a tremendous worldwide effort on the part of all in the field, as well as from organizations like RSNA that are dedicated to advancing the science. Radiologists will also have an opportunity to become integrators or aggregators of diagnostic data. The Interagency Working Group on Medical Imaging of the National Science and Technology Council has proposed the concept of the "diagnostic cockpit." In such a construct, recent findings from other imaging studies, lab results, other test results, key aspects of the patient history and physical exam, and patient demographics and risk factors are all extracted from the EMR, then aggregated to provide the greatest likelihood of not only a correct diagnosis but also a prediction of prognosis and response to personalized therapy. Who is better positioned to lead such an entity than radiologists? The time has come for radiologists to position themselves to provide such leadership in driving this field to the next level. Radiologists will have to increase their knowledge of all aspects of diseases and data science aside from just the imaging aspects. AI applications will provide benefits at every step of the life cycle of an imaging test by increasing the efficiency of the radiology department workflow in many ways, and it will free up some of the time radiologists now spend on image interpretation. That extra time should be spent on greater engagement with patients. This means discussing the imaging tests with them and taking on more responsibility for their total imaging care. Our colleagues in interventional radiology and breast imaging are already doing this, and the rest of the profession must follow suit. If tomorrow's radiologists can accomplish all this, they will become even more essential members of the clinical care team.

PS10E Annual Oration in Diagnostic Radiology: Artificial Intelligence, Analytics, and Informatics: The Future is Here

Participants

Michael P. Recht, MD, New York, NY (*Presenter*) Nothing to Disclose David H. Kim, MD, Middleton, WI (*Introduction*) Shareholder, Cellectar Biosciences, Inc; Shareholder, Elucent Medical;

Abstract

This is an exciting yet challenging time for Radiology. The transformation from a fee for service to a value driven health care system, the increasing sophistication and demands of our patients and referring physicians, the rapid advancements in imaging technology, and the explosive development of artificial intelligence/machine learning all promise significant disruptions to the current practice of Radiology. It is imperative that radiologists face these challenges head on in order to shape our future. To do that, we need to take the lead in utilizing informatics, analytics/business intelligence, and artificial intelligence/machine learning to enhance the value of imaging and radiologists. To demonstrate our value, radiologists must become more integrated into the clinical care team, and more visible and "user-friendly" to both referring physicians and our patients. This, however, is an ever more difficult proposition, due to the increasing demands on our time - for example, the demand for increased productivity, and increasing regulatory requirements - and due to the ongoing geographic dispersion of our practices. The development of several innovations in informatics has helped us meet this challenge. Some examples include virtual rounds and virtual consults, enhanced (multimedia) imaging reports, "collaborative" imaging pathways, radiology-pathology feedback loops, and, most recently, the development of a patient centric radiology mobile app. The use of business analytics and business intelligence is considered essential in most industries. Although the measurement of radiologists' productivity (RVUs) and turnaround times has become commonplace in our field, the use of more advanced metrics and analytics, such as equipment utilization, scheduling efficiency, cost-based accounting, on-time performance, referring physician referral patterns and satisfaction, and service-related costs have been rare in radiology departments. Even when used, the data are typically not real time, and their extraction and display requires the services of dedicated IT or analytics personnel. To truly derive value from data, it is necessary to ensure that the data is accurate, easily accessible, and most importantly, actionable. Examples of how this can be achieved to create value will be presented. The rapid development of artificial intelligence and machine learning is a ubiquitous topic both within the medical literature and at scientific meetings. While many have concentrated on the threat posed by artificial intelligence, others have stressed its potential both to increase the value of imaging and to enhance the radiologist's role in patient care. Examples of how artificial intelligence can be utilized to significantly improve the elements that comprise value in imaging - cost, guality, experience, outcome, appropriateness will be discussed.



SSA09

Gastrointestinal (Machine Learning)

Sunday, Nov. 25 10:45AM - 12:15PM Room: N228



AMA PRA Category 1 Credits ™: 1.50 ARRT Category A+ Credit: 1.75

Participants

Dushyant V. Sahani, MD, Boston, MA (*Moderator*) Research support, General Electric Company Medical Advisory Board, Allena Pharmaceuticals, Inc

Andrew D. Smith, MD, PhD, Birmingham, AL (*Moderator*) President and Owner, Radiostics LLC; President and Owner, eRadioMetrics LLC; President and Owner, Liver Nodularity LLC; President and Owner, Color Enhanced Detection LLC; Patent holder Khaled M. Elsayes, MD, Ann Arbor, MI (*Moderator*) Nothing to Disclose David Fuentes, Houston, TX (*Moderator*) Nothing to Disclose

Sub-Events

SSA09-01 Automated Liver Lesion Segmentation Using Deep Learning

Sunday, Nov. 25 10:45AM - 10:55AM Room: N228

Participants

Sean Sall, San Francisco, CA (Presenter) Researcher, Arterys Inc

Jesse Lieman-Sifry, San Francisco, CA (Abstract Co-Author) Researcher, Arterys Inc

Felix Lau, San Francisco, CA (Abstract Co-Author) Researcher, Arterys Inc

Claude B. Sirlin, MD, San Diego, CA (*Abstract Co-Author*) Research Grant, Gilead Sciences, Inc; Research Grant, General Electric Company; Research Grant, Siemens AG; Research Grant, Bayer AG; Research Grant, ACR Innovation; Research Grant, Koninklijke Philips NV; Research Grant, Celgene Corporation; Consultant, General Electric Company; Consultant, Bayer AG; Consultant, Boehringer Ingelheim GmbH; Consultant, AMRA AB; Consultant, Fulcrum Therapeutics; Consultant, IBM Corporation; Consultant, Exact Sciences Corporation; Advisory Board, AMRA AB; Advisory Board, Guerbet SA; Advisory Board, VirtualScopics, Inc; Speakers Bureau, General Electric Company; Author, Medscape, LLC; Author, Resoundant, Inc; Lab service agreement, Gilead Sciences, Inc; Lab service agreement, ICON plc; Lab service agreement, Intercept Pharmaceuticals, Inc; Lab service agreement, Shire plc; Lab service agreement, Takeda Pharmaceutical Company Limited; Lab service agreement, sanofi-aventis Group; Lab service agreement, Johnson & Johnson; Lab service agreement, NuSirt Biopharma, Inc; Contract, Epigenomics; Contract, Arterys Inc Albert Hsiao, MD,PhD, La Jolla, CA (*Abstract Co-Author*) Founder, Arterys, Inc; Consultant, Arterys, Inc; Consultant, Bayer AG; Research Grant, General Electric Company;

Daniel Golden, PhD, San Francisco, CA (Abstract Co-Author) Employee, Arterys Inc

For information about this presentation, contact:

sean@arterys.com

PURPOSE

To develop an automated deep learning-based method for liver lesion segmentation on MRI scans in order to enable more efficient quantification of lesion size and measurement of growth over time.

METHOD AND MATERIALS

We utilize 1,312 annotated lesions from 607 unique abdominal MRI studies and 393 unique patients. DICOM images and lesion locations were collected as part of standard clinical care. Identified lesions were segmented manually on multiphasic contrastenhanced series by annotators trained in liver lesion segmentation. The median lesion diameter was 15.8 mm, while the median lesion volume was 1.469 mL. We designate an 80%-10%-10% split between the training, validation, and testing sets. We report all metrics on the test set. We use a fully-convolutional neural network that operates on 3D patches, centered on the lesion of interest. The network is a variant of the ENet segmentation architecture.

RESULTS

Our automated contouring method achieved a median volume error of 0.277 mL and a median LLD error of 2.01 mm. The median LLD error is significantly below the LI-RADS 'threshold growth' threshold (5.0mm).

CONCLUSION

Our automated lesion segmentation method yields a low median LLD error, demonstrating that our estimates may be used as part of a semi-automated clinical workflow in which the clinician may review and modify the segmentations. Additionally, we demonstrate that automated volumetric estimates are feasible from MRI and, with further validation, may provide a viable method of tracking tumor volume over time.

CLINICAL RELEVANCE/APPLICATION

An automated liver lesion segmentation system may improve radiologist accuracy and efficiency in quantifying lesion size and measuring growth over time.

SSA09-03 Convolutional Neural Networks Permit Estimation of Whole-Liver Hepatic Proton-Density Fat Fraction from Single or Dual-Echo Chemical-Shift-Encoded MRI

Sunday, Nov. 25 11:05AM - 11:15AM Room: N228

Awards

Student Travel Stipend Award

Participants

Kang Wang, MD, PhD, San Diego, CA (Presenter) Nothing to Disclose Tara A. Retson, MD, PhD, San Diego, CA (Abstract Co-Author) Nothing to Disclose Jonathan C. Hooker, BS, San Diego, CA (Abstract Co-Author) Nothing to Disclose Naeim Bahrami, PhD, MSc, San Diego, CA (Abstract Co-Author) Nothing to Disclose Kevin Blansit, MS, BS, La Jolla, CA (Abstract Co-Author) Nothing to Disclose Evan Masutani, La Jolla, CA (Abstract Co-Author) Nothing to Disclose Claude B. Sirlin, MD, San Diego, CA (Abstract Co-Author) Research Grant, Gilead Sciences, Inc; Research Grant, General Electric Company; Research Grant, Siemens AG; Research Grant, Bayer AG; Research Grant, ACR Innovation; Research Grant, Koninklijke Philips NV; Research Grant, Celgene Corporation; Consultant, General Electric Company; Consultant, Bayer AG; Consultant, Boehringer Ingelheim GmbH; Consultant, AMRA AB; Consultant, Fulcrum Therapeutics; Consultant, IBM Corporation; Consultant, Exact Sciences Corporation; Advisory Board, AMRA AB; Advisory Board, Guerbet SA; Advisory Board, VirtualScopics, Inc; Speakers Bureau, General Electric Company; Author, Medscape, LLC; Author, Resoundant, Inc; Lab service agreement, Gilead Sciences, Inc; Lab service agreement, ICON plc; Lab service agreement, Intercept Pharmaceuticals, Inc; Lab service agreement, Shire plc; Lab service agreement, Enanta; Lab service agreement, Virtualscopics, Inc; Lab service agreement, Alexion Pharmaceuticals, Inc; Lab service agreement, Takeda Pharmaceutical Company Limited; Lab service agreement, sanofi-aventis Group; Lab service agreement, Johnson & Johnson; Lab service agreement, NuSirt Biopharma, Inc; Contract, Epigenomics; Contract, Arterys Inc Albert Hsiao, MD, PhD, La Jolla, CA (Abstract Co-Author) Founder, Arterys, Inc; Consultant, Arterys, Inc; Consultant, Bayer AG; Research Grant, General Electric Company;

For information about this presentation, contact:

kaw016@ucsd.edu

PURPOSE

Confounder-corrected, chemical-shift-encoded (CSE) MRI with 6-echo acquisitions accurately quantifies hepatic proton-density fat fraction (PDFF). However, 6-echo acquisition increases scan time, might result in motion artifact, and limits image resolution of PDFF maps. This study assessed the feasibility of estimating PDFF from the first echo or first 2 echoes of 6-echo CSE MRI using a convolutional neural network (CNN).

METHOD AND MATERIALS

In this IRB-approved and HIPPA-compliant study, we retrospectively identified 355 liver 3T MR exams that included a magnitudebased PDFF sequence comprising 6 gradient-echo images at sequential nominally out- and in-phase echo times. A non-linear fitting algorithm was used to reconstruct the PDFF maps pixel-by-pixel (6-echo PDFF). Using 310 image datasets selected at random, we trained a CNN to estimate 6-echo PDFF maps using only the first echo (1-echo PDFF) or the first two echoes (2-echo PDFF). We tested the CNN in the other 45 PDFF acquisitions. On each axial image containing liver, the liver was segmented and the average PDFF values across all liver pixels was calculated. Per-image mean hepatic 1-echo PDFF and 2-echo PDFF were compared with 6echo PDFF using Pearson correlation and Bland-Altman analyses.

RESULTS

A total of 1065 images were analyzed. Per-image 6-echo PDFF values ranged from 0% to 43%, while R2* ranges from 33 to 195 s-1. Correlations were high for 1-echo vs. 6-echo PDFF (R2=0.99, slope=0.96, intercept=-0.04) and for 2-echo vs. 6-echo PDFF (R2=0.99, slope=0.98, intercept = 0.29). Compared to the the 6-echo method, the 1-echo method showed minimal PDFF overestimation (bias of 0.56%, p<0.01) while the 2-echo method showed minimal PDFF underestimation (bias = -0.12%, p<0.001); 95% limits of agreement were [-1.3%, 2.4%] for 1-echo and [-1.15%, 0.91%] for 2-echo PDFF.

CONCLUSION

A CNN can accurately estimate hepatic PDFF from either the first or first two echoes of a magnitude-based CSE PDFF sequence in livers without substantial iron overload. Further work is required to determine whether these results are generalizable for other pulse sequences, scan parameters or concurrent pathology.

CLINICAL RELEVANCE/APPLICATION

CNN-based whole-liver PDFF estimation from single or two-echo acquisitions might reduce scan time and enable broader clinical use of quantitative fat fraction measurement.

SSA09-04 A New Multi-Model Machine Learning Framework to Improve Hepatic Fibrosis Grading Using Ultrasound Elastography Systems from Different Vendors

Sunday, Nov. 25 11:15AM - 11:25AM Room: N228

Participants

Isabelle Durot, MD, Stanford, CA (*Presenter*) Nothing to Disclose Alireza Akhbardeh, PhD, Stanford, CA (*Abstract Co-Author*) Nothing to Disclose Hersh Sagreiya, MD, Palo Alto, CA (*Abstract Co-Author*) Nothing to Disclose Andreas M. Loening, MD, PhD, Stanford, CA (*Abstract Co-Author*) Research Grant, Koninklijke Philips NV Consultant, ReCor Medical, Inc

Daniel L. Rubin, MD, MS, Stanford, CA (Abstract Co-Author) Nothing to Disclose

For information about this presentation, contact:

durot@stanford.edu

PURPOSE

To show that the diagnostic performance of point shear wave elastography (pSWE) and two-dimensional shear wave elastography (2DSWE) for grading liver fibrosis using shear wave velocity (SWV) combined with a new machine learning (ML) technique, can be as accurate as magnetic resonance elastography (MRE) and can be applied to ultrasound systems from different vendors.

METHOD AND MATERIALS

This IRB-approved retrospective study included two patient groups with chronic liver disease: 1) 123 patients undergoing pSWE (Siemens S2000) and MRE; and 2) 60 patients undergoing 2DSWE (Philips Epiq7) and MRE. For Siemens data, accuracy of median SWV to differentiate clinically non-significant from significant fibrosis was calculated using the published cutoff value of 1.34 m/s, with MRE-based fibrosis grading used as the standard. Next, for both groups, in a technique not using any published US elastography cutoff values, median SWV and true labels from MRE-based grading were input to the Matlab perfcurve function to generate a receiver-operating characteristic (ROC) curve and calculate area-under-the-curve (AUC). Finally, in both groups, four ML algorithms - support vector machines (SVM), logistic regression, naïve Bayes, and quadratic discriminant analysis - using ten SWV measurements as inputs were trained with MRE as the gold standard to obtain MRE-equivalent binary fibrosis grading; scores from the ML algorithms were input into the Matlab perfcurve function to generate ROC AUC, and results were validated using two-fold cross validation.

RESULTS

The performance of median SWV to differentiate clinically non-significant and significant fibrosis (with MRE as the gold standard) was fair for pSWE with the published cutoff value for Siemens (accuracy 55.4%); moderate for Siemens (AUC: 0.73) and Philips (AUC: 0.71) without using a cutoff value; and excellent for an SVM ML algorithm in both groups (Siemens: AUC: 0.96; Philips: AUC: 0.97).

CONCLUSION

The results from Siemens and Philips data suggest that a multi-vendor ML-based algorithm can grade liver fibrosis using ultrasound elastography with excellent diagnostic performance, comparable to MRE. SVMs outperformed the current standard of assessment, median SWV.

CLINICAL RELEVANCE/APPLICATION

The new ML algorithm may be applied to systems from different vendors after validation, providing more comparable and accurate fibrosis grading.

Honored Educators

Presenters or authors on this event have been recognized as RSNA Honored Educators for participating in multiple qualifying educational activities. Honored Educators are invested in furthering the profession of radiology by delivering high-quality educational content in their field of study. Learn how you can become an honored educator by visiting the website at: https://www.rsna.org/Honored-Educator-Award/ Daniel L. Rubin, MD, MS - 2012 Honored EducatorDaniel L. Rubin, MD, MS - 2013 Honored Educator

SSA09-05 A 3D Deep Neural Network for Liver Volumetry in Contrast-Enhanced MRI

Sunday, Nov. 25 11:25AM - 11:35AM Room: N228

Participants

Niklas Verloh, MD, Regensburg, Germany (*Presenter*) Nothing to Disclose Hinrich B. Winther, MD, Hannover, Germany (*Abstract Co-Author*) Nothing to Disclose Christian Hundt, DIPLPHYS,PhD, Mainz, Germany (*Abstract Co-Author*) Nothing to Disclose Kristina I. Ringe, MD, Hannover, Germany (*Abstract Co-Author*) Nothing to Disclose Frank K. Wacker, MD, Hannover, Germany (*Abstract Co-Author*) Nothing to Disclose Bertil Schmidt, Mainz, Germany (*Abstract Co-Author*) Nothing to Disclose Michael Haimerl, Regensburg, Germany (*Abstract Co-Author*) Nothing to Disclose Lukas Beyer, MD, Regensburg, Germany (*Abstract Co-Author*) Nothing to Disclose Christian R. Stroszczynski, MD, Regensburg, Germany (*Abstract Co-Author*) Nothing to Disclose Philipp Wiggermann, Regensburg, Germany (*Abstract Co-Author*) Nothing to Disclose

For information about this presentation, contact:

niklas.verloh@klinik.uni-regensburg.de

PURPOSE

To establish a fully automatic 3D deep learning liver segmentation-system for contrast-enhanced liver MRI.

METHOD AND MATERIALS

Data-sets of Gd-EOB-DTPA-enhanced liver MR images of 100 patients have been selected. The ground truth segmentation of the liver parenchyma in the hepatobiliary phase was performed manually by a resident physician with five years of experience. The dataset was split into a training/validation set (n = 75) and a testing set (n = 25). The artificial neural network (ANN) used in this study is based on 3D-Unet (Cicek et al. 2016, arxiv: 1606.06650). The trained ANN was used to perform a fully automatic image segmentation of the testing set.

RESULTS

The ANN accomplishes a Dice index of 95.1 ± 2.3 % (mean \pm std), an overlap of 90.8 ± 3.9 % and a volume difference of 3.8 ± 6.8 %.

CONCLUSION

This study demonstrates a 3D neural network, which is able to provide a fully automatic segmentation scheme for MRI Images. It is able to segment the liver parenchyma with high precision.

CLINICAL RELEVANCE/APPLICATION

The 3D neural network provides an accurate automatic liver segmentation in MRI; hence it would serve as a useful tool for

radiologists for treatment planning, especially for patients undergoing liver surgery.

SSA09-06 Machine Learning for Rapid Assessment of Outcomes of an Ultrasound Screening and Surveillance Program in Patients at Risk for Hepatocellular Carcinoma

Sunday, Nov. 25 11:35AM - 11:45AM Room: N228

Participants

Hailey Choi, MD, San Francisco, CA (*Presenter*) Nothing to Disclose Imon Banerjee, PhD, Stanford, CA (*Abstract Co-Author*) Nothing to Disclose Hersh Sagreiya, MD, Palo Alto, CA (*Abstract Co-Author*) Nothing to Disclose Aya Kamaya, MD, Stanford, CA (*Abstract Co-Author*) Nothing to Disclose Daniel L. Rubin, MD, MS, Stanford, CA (*Abstract Co-Author*) Nothing to Disclose Terry S. Desser, MD, Stanford, CA (*Abstract Co-Author*) Nothing to Disclose

For information about this presentation, contact:

hailey.choi@ucsf.edu

PURPOSE

To determine large-scale retrospective outcomes of surveillance ultrasound exams in high-risk populations according to the American College of Radiology (ACR) Ultrasound Liver Imaging Reporting and Data System (LI-RADS) classification.

METHOD AND MATERIALS

13,860 ultrasound screening and surveillance exams from 4830 subjects performed between 2007-2017, pre-dating ultrasound LI-RADS recommendations, were assessed. Using more recent reports from May 2017-June 2018, which contained ultrasound LI-RADS specifications (1744 reports), a scalable ensemble machine learning approach was utilized to create a model that can infer ultrasound LI-RADS categories from neural word embedding analysis of the report body text. The model assigned ultrasound LI-RADS categories to the older, free-text reports (12,116 reports). Subjects who underwent serial surveillance exams were identified, and the labeled dataset was assessed for changes in LI-RADS categories over time.

RESULTS

2270 subjects had at least 2 exams. Subjects underwent an average of 5 exams, with mean screening interval of 13 months; mean follow-up duration was 43 months. When applied to the free-text reports, our model scored an average of 0.74 precision, 0.64 recall, and 0.66 F1-score, based on a validation set of 215 reports retrospectively categorized by 2 readers. According to the model's predictions, 1909 (84%) subjects remained in the same LI-RADS category over time: 1875 of these subjects remained in US-1 category, while 26 persisted as US-2; 2 patients had 2 exams each, which were both US-3. 205 (9%) progressed from US-1 to US-2. 95 (4%) alternated between US-1 and US-2. 61 (3%) subjects progressed to US-3 category was US-3.

CONCLUSION

Machine learning enables large-scale retrospective longitudinal evaluation of relatively recent ACR Ultrasound LI-RADS guidelines. Based on our model's predictions, 3% of patients in our cohort developed suspicious lesions to warrant further work-up.

CLINICAL RELEVANCE/APPLICATION

Our experience is the first large-scale assessment of ACR Ultrasound LI-RADS categories with longitudinal outcomes. Although retrospective, our long-term longitudinal data will be helpful in validating and improving current ACR Ultrasound LI-RADS recommendations, as well as in assessing clinical outcomes of HCC surveillance programs.

Honored Educators

Presenters or authors on this event have been recognized as RSNA Honored Educators for participating in multiple qualifying educational activities. Honored Educators are invested in furthering the profession of radiology by delivering high-quality educational content in their field of study. Learn how you can become an honored educator by visiting the website at: https://www.rsna.org/Honored-Educator-Award/ Daniel L. Rubin, MD, MS - 2012 Honored EducatorDaniel L. Rubin, MD, MS - 2013 Honored Educator

SSA09-08 Deep Learning with Convolutional Neural Network for Histopathological Classification of Pancreatic Neuroendocrine Neoplasms: A Preliminary Study

Sunday, Nov. 25 11:55AM - 12:05PM Room: N228

Participants

Yanji Luo, Guangzhou, China (*Presenter*) Nothing to Disclose Huanhui Xiao, Guangzhou, China (*Abstract Co-Author*) Nothing to Disclose Shiting Feng, MD, Guangzhou, China (*Abstract Co-Author*) Nothing to Disclose Ziping Li, MD, PhD, Guangzhou, China (*Abstract Co-Author*) Nothing to Disclose Bingsheng Huang, Shenzhen, China (*Abstract Co-Author*) Nothing to Disclose

For information about this presentation, contact:

luoyanji163@163.com

PURPOSE

To evaluate the efficacy of deep convolutional neural network (DCNN) for the pathological classification of pancreatic neuroendocrine neoplasms (P-NENs) on contrast agent-enhanced computed tomography.

METHOD AND MATERIALS

One hundred and three patients (poor-differentiated [G3], n=19; well-differentiated [G1+G2], n=84) preoperatively investigated by multi spiral computed tomography (MSCT) and subsequently with histopathological proven P-NENs were enrolled. The 103 datasets

were normalized and augmented by multiple preprocessing techniques (rotated, contrast enhanced and noise-added images), and were split into training (81.6%), validation (5.8%), and test set (12.6%) with 8-fold cross validation. The DCNN with the residual learning framework (ResNet), was used to classify the images as having manifestations of poor- or well-differentiated P-NENs. The DCNN was composed of fifty convolutional, one maxpooling, one global average pooling and two fully connected layers. Training and testing were performed eight times. Accuracy, sensitivity, and specificity for categorizing poor- and well-differentiated P-NENs with DCNN model and the area under the receiver operating characteristic curve for poor- versus well-differentiated P-NENs were calculated.

RESULTS

The accuracy, sensitivity, and specificity of classifying poor- and well-differentiated P-NENs were 80.6%, 79.0%, and 81.0%, respectively. The area under the receiver operating characteristic curve for differentiating histopathological grading of P-NENs was 0.79.

CONCLUSION

Deep learning with DCNN showed high diagnostic performance in differentiating histopathological classification of P-NENs at dynamic CT images.

CLINICAL RELEVANCE/APPLICATION

The proposed framework could assist the radiologists in differentiating histopathological grading of P-NENs from contrast agentenhanced CT images and provide prognostic information with regard to patients' outcome.

SSA09-09 Hepatic Steatosis Classification Using Deep Learning with Ultrasonic Radio-Frequency Data

Sunday, Nov. 25 12:05PM - 12:15PM Room: N228

Participants

Aiguo Han, PhD, Urbana, IL (Presenter) Nothing to Disclose

Rohit Loomba, MD, MSc, La Jolla, CA (*Abstract Co-Author*) Grant, Adheron; Grant, Arora; Grant, Bristol-Myers Squibb Company; Grant, DAIICHI SANKYO Group; Grant, Galectin; Grant, Galmed Pharmaceuticals Ltd; Grant, General Electric Company; Grant, GENFIT SA; Grant, Gilead Sciences, Inc; Grant, Immuron Ltd; Grant, Intercept Pharmaceuticals, Inc; Grant, Janseen Inc; Grant, Kinemed; Grant, Madrigal Pharmaceuticals, Inc; Grant, Merck & Co, Inc; Grant, NGM Biopharmaceuticals, Inc; Grant, Promega Corporation Inc; Grant, Siemens AG; Grant, Sirius; Grant, Tobira Therapeutics, Inc

Claude B. Sirlin, MD, San Diego, CA (*Abstract Co-Author*) Research Grant, Gilead Sciences, Inc; Research Grant, General Electric Company; Research Grant, Siemens AG; Research Grant, Bayer AG; Research Grant, ACR Innovation; Research Grant, Koninklijke Philips NV; Research Grant, Celgene Corporation; Consultant, General Electric Company; Consultant, Bayer AG; Consultant, Boehringer Ingelheim GmbH; Consultant, AMRA AB; Consultant, Fulcrum Therapeutics; Consultant, IBM Corporation; Consultant, Exact Sciences Corporation; Advisory Board, AMRA AB; Advisory Board, Guerbet SA; Advisory Board, VirtualScopics, Inc; Speakers Bureau, General Electric Company; Author, Medscape, LLC; Author, Resoundant, Inc; Lab service agreement, Gilead Sciences, Inc; Lab service agreement, ICON plc; Lab service agreement, Intercept Pharmaceuticals, Inc; Lab service agreement, Shire plc; Lab service agreement, Takeda Pharmaceutical Company Limited; Lab service agreement, sanofi-aventis Group; Lab service agreement, Johnson & Johnson; Lab service agreement, NuSirt Biopharma, Inc; Contract, Epigenomics; Contract, Arterys Inc John Erdman, Urbana, IL (*Abstract Co-Author*) Nothing to Disclose

Michael P. Andre, PhD, La Jolla, CA (Abstract Co-Author) Researcher, Siemens AG

William D. O'Brien JR, PhD, Urbana, IL (Abstract Co-Author) Research Grant, Siemens AG

For information about this presentation, contact:

han51@illinois.edu

PURPOSE

To develop a deep learning framework that uses radio-frequency (RF) ultrasound data for settings-independent information extraction, and assess its accuracy for classifying hepatic steatosis in adults with known/suspected nonalcoholic fatty liver disease (NAFLD).

METHOD AND MATERIALS

This was an IRB-approved, HIPPA-compliant prospective study of adults with known/suspected NAFLD. Ultrasound liver images (right lobe) and the underlying raw RF data were acquired intercostally by 2 sonographers using 4C1 and 6C1HD transducers from Siemens S3000. System settings were adjusted for each participant. Twenty liver images for each transducer were acquired for each participant. Gated RF lines from a fixed region of interest were preprocessed and used to train a deep convolutional neural network (CNN) for hepatic steatosis classification, with histology as the reference standard. No effort was made to correct for instrumentation settings. Five-fold cross validation was used for training and test. The model outputs from individual RF lines of all images were aggregated to yield a classification for a patient. As a comparison, B-mode images were graded by 8 radiologists based on their overall impression of hepatic steatosis.

RESULTS

Forty patients (sex: 16M, 24F; age: 55.5±12.3 yo; BMI: 30.2±5.4 kg/m2) were included, of which 22 had no/mild steatosis (grade 0: N=2; grade 1: N=20) and 18 had moderate/severe steatosis (grade 2: N=12; grade 3: N=6). The CNN achieved 80±5% cross-validated accuracy (72±9% sensitivity, 86±4% specificity) for identifying patients with grade 2 or 3 steatosis. By comparison, radiologists' overall impression (grade 2 or 3) for the 6C1HD transducer achieved 68% accuracy (83% sensitivity, 57% specificity) and the overall impression for the 4C1 transducer achieved 72% accuracy (77% sensitivity, 68% specificity) for the same classification.

CONCLUSION

A CNN can automatically classify human patients as having or not having moderate/severe steatosis based on RF lines acquired during liver ultrasounds using variable instrumentation settings. Preliminary findings suggest the CNN may outperform specificity of expert radiologists.

Deep learning using the RF lines acquired during liver ultrasounds could assist radiologists in automatic hepatic steatosis classification.



SSA12

Science Session with Keynote: Informatics (Artificial Intelligence in Radiology: Cutting Edge Deep-Learning)

Sunday, Nov. 25 10:45AM - 12:15PM Room: S406B



AMA PRA Category 1 Credits ™: 1.50 ARRT Category A+ Credit: 1.75

FDA Discussions may include off-label uses.

Participants

George L. Shih, MD, MS, New York, NY (*Moderator*) Consultant, Image Safely, Inc; Stockholder, Image Safely, Inc; Consultant, MD.ai, Inc; Stockholder, MD.ai, Inc;

An Tang, MD, Montreal, QC (*Moderator*) Research Consultant, Imagia Cybernetics Inc; Speaker, Siemens AG; Speaker, Eli Lilly and Company

Synho Do, PhD, Boston, MA (Moderator) Nothing to Disclose

Sub-Events

SSA12-01 Informatics Keynote Speaker: Cutting Edge AI in Radiology

Sunday, Nov. 25 10:45AM - 10:55AM Room: S406B

Participants

An Tang, MD, Montreal, QC (*Presenter*) Research Consultant, Imagia Cybernetics Inc; Speaker, Siemens AG; Speaker, Eli Lilly and Company

For information about this presentation, contact:

an.tang@umontreal.ca

Honored Educators

Presenters or authors on this event have been recognized as RSNA Honored Educators for participating in multiple qualifying educational activities. Honored Educators are invested in furthering the profession of radiology by delivering high-quality educational content in their field of study. Learn how you can become an honored educator by visiting the website at: https://www.rsna.org/Honored-Educator-Award/ An Tang, MD - 2018 Honored Educator

SSA12-02 Predicting Thyroid Nodule Malignancy with Efficient Convolutional Neural Networks

Sunday, Nov. 25 10:55AM - 11:05AM Room: S406B

Awards

Trainee Research Prize - Medical Student

Participants

Ian Pan, MA, Providence, RI (*Presenter*) Nothing to Disclose Matthew T. Stib, MD, Providence, RI (*Abstract Co-Author*) Nothing to Disclose William D. Middleton, MD, Saint Louis, MO (*Abstract Co-Author*) Nothing to Disclose Derek Merck, PhD, Providence, RI (*Abstract Co-Author*) Nothing to Disclose Michael D. Beland, MD, Providence, RI (*Abstract Co-Author*) Research Grant, Canon Medical Systems Corporation; Consultant, General Electric Company

For information about this presentation, contact:

ian_pan@brown.edu

PURPOSE

Various sonographic features of thyroid nodules have been described, and classification systems (i.e., TI-RADS) have been developed to aid radiologists in determining which suspicious nodules require fine needle aspiration (FNA). This study aims to improve our predictive ability by training convolutional neural networks (CNNs) to discriminate between pathology-confirmed benign and malignant thyroid nodules using ultrasound images.

METHOD AND MATERIALS

Our dataset consisted of 151 malignant and 500 benign thyroid nodules from 571 patients, where each nodule contributed 1 longitudinal and 1 transverse ultrasound view. Preprocessing included cropping the nodule of interest and resizing the image to 224 x 224 pixels. The data were divided into 10 training/validation/test folds following a stratified 80%/10%/10% split with no patient overlap. CNNs based on the MobileNet architecture were initialized with pretrained ImageNet weights. A fully-connected layer was first trained for 10 epochs, and the entire network was fine-tuned for 20 epochs. Data were sampled to achieve 50%/50% class balance for each epoch. Data augmentation probability, dropout probability, and learning rate were tuned via randomized search with 60 iterations. Weights with the highest area under the ROC curve (AUC) during validation were used for testing. A malignancy score is determined for each nodule by averaging the predictions for each view across 3 models.

RESULTS

Our model achieved a mean AUC of 0.863 (95% CI: 0.827, 0.898). The median malignancy scores for benign and malignant nodules were 0.162 and 0.618, respectively. With 5 strata, (0-0.2, 0.2-0.4, 0.4-0.6, 0.6-0.8, 0.8-1.0), 5.94%, 18.2%, 29.5%, 65.7%, and 81.4% of nodules in each respective stratum were malignant, compared to an overall malignancy rate of 23.2%. At a threshold of 0.10, the model reduces the number of negative FNAs by 36% while maintaining 95% sensitivity.

CONCLUSION

CNNs fine-tuned on limited data can accurately predict the malignancy potential of sonographically suspicious thyroid nodules. Larger datasets would likely further improve the performance of our classifier. External validation studies are necessary to verify the generalizability of this approach.

CLINICAL RELEVANCE/APPLICATION

CNN malignancy scores calculated from thyroid ultrasound images can be combined with a radiologist's interpretation for improved stratification of nodules to reduce the number of unnecessary FNAs.

SSA12-03 A Deep-learning Method for Fast Detection of Rib Fracture in CT Images: Effect of Computer-Aided Diagnosis to Radiologists

Sunday, Nov. 25 11:05AM - 11:15AM Room: S406B

Participants

Xiaodong LI, Linyi, China (Presenter) Nothing to Disclose

For information about this presentation, contact:

lxd2018rsna@163.com

CONCLUSION

2 reading modes of CAD(CR, SR) can significantly increase the sensitivities of RFD of radiologists. The reading time is shorter by CR than by SR.CR mode can be used as the first option to detect rib fracture by radiologists.

Background

To assess the effect of rib fracture computer-aided diagnosis(CAD) on diagnosis of radiologist.

Evaluation

85 trauma CTs(50 males) with follow-up review CTs were included in the retrospective study.All trauma CTs were subjected to CAD system to generate rib fracture bounding box. The procedure of the CAD system contains ribs segmentation, centerline extraction, rib fracture detection(RFD) based on deep learning algorithm(Faster RCNN), false positive removal and rib fracture localization. 2 senior(NO.1,2) and 2 junior radiologists(NO.3,4) independently evaluated the data using 3 reading modes(without CAD, CR, SR). The fracture line or bone callus growth is the criterion for determining the rib fracture. The follow-up review CTs verified the diagnosis of rib fracture and established the reference standard[1]. All fractures detected by the 4 readers were compared to the reference standard. χ^2 test and rank-sum test were performed to test whether there was significant difference between sensitivities and reading times of 3 reading modes. Abbreviations: without CAD: Radiologists independently evaluated the data as a first reader and then apply the CAD system as a second reader(SR) to review the results.

Discussion

The reference standard identified 281 rib fractures in 85 patients. The sensitivity of RFD with SR 97.2%(273/281;P<0.001) and CR 96.4%(271/281;P<0.001) were significantly higher than that of without CAD 89.7%(252/281). There was no significant sensitivity difference between CR and SR(P>0.3). Senior and junior radiologists used CAD as CR or SR and there was no significant sensitivity difference between 2 modes(P=0.067,P=0.067). Reading time was significantly shorter for CR(98s) compared to that of without CAD(148s;P<0.001) and SR(169s;P<0.001). Reading time of the 3 modes was less in the senior group than in the junior group with significant differences(P<0.001).

SSA12-04 Highly Sensitive Identification and Delineation of Hemorrhagic Stroke Lesion Using Cascaded Deep Learning Model

Sunday, Nov. 25 11:15AM - 11:25AM Room: S406B

Participants

Junghwan Cho, PhD, Lowell, MA (*Presenter*) Nothing to Disclose Manohar Karki, Lowell, MA (*Abstract Co-Author*) Nothing to Disclose Eunmi Lee, Lowell, MA (*Abstract Co-Author*) Nothing to Disclose Jong Kun Kim, MD,PhD, Daegu, Korea, Republic Of (*Abstract Co-Author*) Nothing to Disclose Ki-Su Park, MD,PhD, Daegu, Korea, Republic Of (*Abstract Co-Author*) Nothing to Disclose Dong Eun Lee, MD, Daegu, Korea, Republic Of (*Abstract Co-Author*) Nothing to Disclose Jae Young Choe, MD, Daegu, Korea, Republic Of (*Abstract Co-Author*) Nothing to Disclose Sinyoul Park, MD,PhD, Daegu, Korea, Republic Of (*Abstract Co-Author*) Nothing to Disclose Suk Hee Lee, MD, Daegu, Korea, Republic Of (*Abstract Co-Author*) Nothing to Disclose Suk Hee Lee, MD, Daegu, Korea, Republic Of (*Abstract Co-Author*) Nothing to Disclose Jeoungwoo Sim, MD, Daegu, Korea, Republic Of (*Abstract Co-Author*) Nothing to Disclose Jeoungwoo Son, MD, Gimcheon, Korea, Republic Of (*Abstract Co-Author*) Nothing to Disclose Jeong Ho Lee, MD,PhD, Daegu, Korea, Republic Of (*Abstract Co-Author*) Nothing to Disclose

CONCLUSION

A cascaded deep learning model was developed to identify and delineate hemorrhagic stroke lesion, obtaining overall sensitivity accuracy for classification with 97.91% and segmentation with 83.43%, respectively.

Highly accurate and timely detection of intracranial hemorrhagic stroke is a critical clinical issue for diagnosis decision and treatment in emergency room. Deep learning is a promising approach to solve delayed and missed diagnosis of stroke accident. Accordingly, we developed a cascaded deep learning model trained by a series of different CT window settings as a preprocessing step. It consists of two convolution neural networks (CNNs) for identifying bleeding or not and fully convolutional networks (FCNs) for delineating their lesions.

Evaluation

For this study, we acquired 135,000 CT images from 5,650 patients including 3,000 non-bleeding and 2,650 bleeding. In case of bleeding, five subtypes of intracranial hemorrhage (intraventricular, intraparenchymal, subarachnoid, epidural, and subdural hemorrhage) were well labeled by experts. At first, a cascaded deep learning model was trained to identity whether there is bleeding or not and 5-fold cross validation was conducted. We evaluated sensitivity accuracy by the cascaded model, enabling to review the negative case by the second CNN trained with more narrow window width (40/40 [level/width]) in case that CT image is recognized as negative by the first CNN trained with default brain window setting (50/100). It results in increasing around 1% sensitivity (97.91%) while preserving specificity (98.76%). To delineate lesion of bleeding, the FCNs was trained with 33,300 CT slices using DGX-1 system. We achieved overall precision accuracy ranging from 70% to 90% and recall accuracy ranging from 62% to 88% at different Dice coefficient threshold as true positive decision.

Discussion

In diagnostic accuracy, there is a tradeoff between sensitivity and specificity. But while preserving specificity, the cascaded deep learning model can increase sensitivity in diagnosis of hemorrhagic stroke. It has the capability to help doctors inform any suspected cases.

SSA12-05 Differentiation of Hepatic Masses in Abdominal CT Images Using Texture-Aware Convolutional Neural Networks with Texture Image Patches

Sunday, Nov. 25 11:25AM - 11:35AM Room: S406B

Participants

Hansang Lee, Daejeon, Korea, Republic Of (*Presenter*) Nothing to Disclose Helen Hong, PhD, Seoul, Korea, Republic Of (*Abstract Co-Author*) Nothing to Disclose Heejin Bae, Seoul, Korea, Republic Of (*Abstract Co-Author*) Nothing to Disclose Sungwon Kim, MD, Seoul, Korea, Republic Of (*Abstract Co-Author*) Nothing to Disclose Joonseok Lim, MD, Seoul, Korea, Republic Of (*Abstract Co-Author*) Nothing to Disclose Junmo Kim, Seoul, Korea, Republic Of (*Abstract Co-Author*) Nothing to Disclose

For information about this presentation, contact:

hlhong@swu.ac.kr

hlhong@swu.ac.kr

CONCLUSION

Our method can be applied to the differentiation of various subtypes of hepatic masses including cyst and hemangioma, and early diagnosis of hepatic cancer.

Background

Differentiation of hepatic masses into benign and malignant classes in CT images is an important task for early diagnosis and surgical decision of hepatic cancer. In the cases of small masses, acquisition of intensity and texture features is difficult, making the differentiation challenging. Thus, we propose a deep convolutional neural network (CNN) classification of hepatic masses using texture image patch (TIP) generation to enhance the classification efficiency in small masses.

Evaluation

Our method was evaluated on a dataset consisting of 349 abdominal CT scans including 576 benign and 210 malignant masses. Each mass was manually segmented by the radiologist. In TIP generation, the patches representing only the internal texture of the masses were created by filling the square patch with the segmented mass regions repeatedly. These TIPs have the effect of reflecting the texture information to CNN regardless of the original size of masses. Using these TIPs, the transfer learning (TL) was performed on the ImageNet pre-trained AlexNet to classify the patches into benign or malignant classes. To improve the classification efficiency, we re-trained the random forest (RF) classifier on the deep features extracted from the last feature layer of TL-AlexNet. In experiments, our framework was trained on 390 images(b282, m108), validated on 160 images(b113, m47), and tested on 236 images(b181, m55). The proposed method achieved the accuracy of 87.7% where the comparative methods achieved the accuracies of 83.5%, 80.1%, and 85.2%, without TIP, TL, and RF, respectively.

Discussion

Our TIPs improve the learning efficiency of CNN by augmenting the texture information of small masses and allowing the CNN to focus on the texture information. The TL also plays an important role in learning important imaging features for differentiating the hepatic masses. Instead of obtaining the CNN-classified outputs, re-training the RF classifier on the deep features improves the specificity of the proposed method by enhancing the malignancy detection.

SSA12-06 GrayNet: Medical Generic Image Representations for Deep Learning System of Urinary Stone Detection

Sunday, Nov. 25 11:35AM - 11:45AM Room: S406B

Participants Hyunkwang Lee, Boston, MA (*Presenter*) Nothing to Disclose Anushri Parakh, MBBS, MD, Boston, MA (*Abstract Co-Author*) Nothing to Disclose Sehyo Yune, MD, MPH, Boston, MA (*Abstract Co-Author*) Nothing to Disclose Jeong Hyun Lee, MD, Seoul, Korea, Republic Of (*Abstract Co-Author*) Nothing to Disclose Myeongchan Kim, MD, Boston, MA (*Abstract Co-Author*) Nothing to Disclose Isabelle Hartnett, Boston, MA (*Abstract Co-Author*) Nothing to Disclose Dushyant V. Sahani, MD, Boston, MA (*Abstract Co-Author*) Research support, General Electric Company Medical Advisory Board, Allena Pharmaceuticals, Inc Synho Do, PhD, Boston, MA (*Abstract Co-Author*) Nothing to Disclose

For information about this presentation, contact:

hyunkwanglee@seas.harvard.edu

PURPOSE

The performance of deep-learning based image analysis model developed from an institution is not guaranteed to be achieved when deployed in another if the institutions use different imaging systems with varying scan acquisition and reconstruction settings. We established a pretrained model enriched with medical generic image representations extracted from GrayNet, a dataset for human anatomy recognition with 23 labels and evaluated benefits of GrayNet pretrained models for detecting urinary stones.

METHOD AND MATERIALS

GrayNet contains 322 IV contrast-enhanced whole body CT scans with 120,182 axial slices obtained by CT scanners from two manufacturers (171 from GE and 151 from Siemens). The corresponding virtual unenhanced CT images were generated with a customized transform function. All slices were annotated as 23 radiologist-established anatomical labels. We randomly selected 40 cases for validation and the remainings were used for training of a deep convolutional neural network, Inception-v3. The best model, selected based on validation loss, was reserved as a pretrained model for urinary stone detection. Patients who underwent unenhanced CT scans from two manufacturers (GE and Siemens) for suspected urolithiasis were identified and categorized according to presence (n=128) or absence (n=161) of urinary stones, and then split into train, validation, and test subsets. Inception-v3 models initialized with random, ImageNet, and GrayNet pretrained weights were trained on training datasets from a single manufacturer and both. The optimal models were evaluated on test datasets. Area under the ROC curve (AUC) was measured for evaluation metric.

RESULTS

The performance of the GrayNet model trained on the GE dataset showed higher AUC (0.893) than the ImageNet model (0.833) when tested on the Siemens dataset. Similar trend was observed when models trained on the Siemens dataset and tested on the GE dataset (0.917 from GrayNet, 0.854 from ImageNet). When trained on the combined dataset, the GrayNet model obtained higher AUC than those of ImageNet and random models.

CONCLUSION

The GrayNet pretrained weights enabled better generalization performance, compared to the models initialized with ImageNet pretrained and random weights.

CLINICAL RELEVANCE/APPLICATION

The GrayNet pretrained weights enriched with generic medical image representations can be used as a baseline for deep learning systems for a successful deployment in varying settings.

Honored Educators

Presenters or authors on this event have been recognized as RSNA Honored Educators for participating in multiple qualifying educational activities. Honored Educators are invested in furthering the profession of radiology by delivering high-quality educational content in their field of study. Learn how you can become an honored educator by visiting the website at: https://www.rsna.org/Honored-Educator-Award/ Dushyant V. Sahani, MD - 2012 Honored EducatorDushyant V. Sahani, MD - 2015 Honored EducatorDushyant V. Sahani, MD - 2016 Honored EducatorDushyant V. Sahani, MD - 2017 Honored Educator

SSA12-07 Deep Learning of Clinically Relevant Chest X-Ray Findings on the Combination of Three Large Datasets

Sunday, Nov. 25 11:45AM - 11:55AM Room: S406B

Participants

Satyananda Kashyap, PhD, San Jose, CA (*Abstract Co-Author*) Nothing to Disclose Mehdi Moradi, PhD, San Jose, CA (*Abstract Co-Author*) Employee, IBM Corporation Alexandros Karargyris, San Jose, CA (*Abstract Co-Author*) Employee, IBM Corporation Joy T. Wu, MBChB,MPH, San Jose, CA (*Abstract Co-Author*) Employee, IBM Corporation Murray A. Reicher, MD, Rancho Santa Fe, CA (*Abstract Co-Author*) Chief Medical Officer, Merge Healthcare Incorporated Board Member, Merge Healthcare Incorporated Co-CEO, Health Companion, Inc Former Chairman, DR Systems, Inc Tanveer Syeda-Mahmood, PhD, San Jose, CA (*Presenter*) Employee, IBM Corporation

For information about this presentation, contact:

mmoradi@us.ibm.com

mmoradi@us.ibm.com

CONCLUSION

We have presented a network trained on the largest collection of chest X-ray images with visually observable radiological findings that performs at similar accuracy to networks developed with 14 NIH labels.

Background

Despite deep learning networks now becoming the de facto method of image classification, their relevance to radiologists is limited by the semantics of label used for training such networks. Recent use of image labels such as pneumonia that are not diagnosable from imaging alone have raised concerns on the utility of the networks. We develop a new classifier for chest X-ray images by training it on labels that derived from visually observable radiological findings. We form a new combined data set of 335,688 images from three sources, namely, PLCO Chest X-rays [Gohagan 2000]), Cancer Screening Trial, National Institute of Health (ChestXray14 dataset [Wang 2017]) and the Indiana University dataset [Demner-Fushman 2016]. The 49 original labels assigned to these combined datasets were mapped to the corresponding visually observable findings and regrouped into 20 finding labels. For example, 'consolidation, pneumonia, infiltration, and infiltrate' were all mapped to 'alveolar opacity'. The consolidated dataset with the new labels was used to train a DenseNet121 network architecture [Huang 2016], with 512x512 size input images preprocessed with histogram equalization and intensity normalization.

Evaluation

The dataset was divided to 80% training and 20% validation. The areas under the ROC curve for the 20 findings are: Alveolar opacity: 0.81, Hernia: 0.84, Pneumothorax: 0.86, Atelectasis: 0.87, Aortic atherosclerosis and/or Carotid artery calcification: 0.90, Bone Lesion: 0.77, Enlarged cardiac silhouette: 0.86, Enlarged Hilum: 0.75, Findings consistent with granulomatous disease: 0.76, Hyperaeration: 0.79, Increased reticular markings: 0.71, Mass and/or Nodule: 0.64, Pleural effusion: 0.92, Pleural mass and/or thickening: 0.71, Spinal degenerative changes: 0.89, Tortuous Aorta: 0.89, Vascular redistribution: 0.85, Catheter and/or Tube: 0.89, Missing plus NA: 0.82, Other: 0.69.

Discussion

Label validation particulalry in 'no finding' labels from NIH dataset is under way.

SSA12-08 Automatic Classification and Reporting of Multiple Common Thorax Diseases Using Chest Radiographs

Sunday, Nov. 25 11:55AM - 12:05PM Room: S406B

Participants

Xiaosong Wang, PhD, Bethesda, MD (*Presenter*) Nothing to Disclose Yifan Peng, Bethesda, MD (*Abstract Co-Author*) Nothing to Disclose Le Lu, Bethesda, MD (*Abstract Co-Author*) Employee, NVIDIA Corporation Zhiyong Lu, Bethesda, MD (*Abstract Co-Author*) Nothing to Disclose Ronald M. Summers, MD, PhD, Bethesda, MD (*Abstract Co-Author*) Royalties, iCAD, Inc; Royalties, Koninklijke Philips NV; Royalties, ScanMed, LLC; Research support, Ping An Insurance Company of China, Ltd; Researcher, Carestream Health, Inc; Research support, NVIDIA Corporation; ; ; ;

For information about this presentation, contact:

xiaosong.wang@live.com

PURPOSE

Chest radiographs are one of the most common radiological exams in daily clinical routines. Reporting thorax diseases using chest radiographs is often an entry-level task for radiologist trainees, but it remains a challenging job for learning-oriented machine intelligence. It's due to the shortage of large-scale well-annotated medical image datasets and lack of techniques that can mimic the high-level reasoning of human radiologists. In this work, we show that clinical free-text radiological reports can be utilized as a priori knowledge for tackling these two difficult problems.

METHOD AND MATERIALS

We used a hospital-scale chest radiograph dataset, which consists of 112,120 frontal-view radiographs of 30,805 patients. 14 disease labels observed in images were mined using natural language processing techniques, i.e., atelectasis, cardiomegaly, effusion, infiltrate, mass, nodule, pneumonia, pneumothorax, consolidation, edema, emphysema, fibrosis, pleural thickening, and hernia. We propose a novel text-image embedding neural network (illustrated in the attached figure) for extracting the distinctive image and text representations. Multilevel attention models are integrated into an end-to-end trainable architecture for highlighting the meaningful text words and image regions. We first apply this combined convolutional and recurrent neural network (CNN-RNN) to classify the image by using both image features and text embeddings from associated reports. Furthermore, we transform the framework into a radiograph reporting system by taking only images as input and turning RNN into a generative model.

RESULTS

The proposed framework achieves high accuracy $(0.96\pm0.03 \text{ in AUCs})$ in disease classification using both images and reports on an unseen and hand-labeled dataset (OpenI, 3,643 images). When using only the images as input, the system can also produce significantly improved results $(0.80\pm0.07 \text{ in AUCs})$ compared to the state-of-the-art (0.74 ± 0.08) with a p-value=0.0005. The figure shows sample classification results with generated reports (attended words in red).

CONCLUSION

We illustrate a framework for fully-automated classification and reporting of common thorax diseases in chest radiographs and demonstrate its superior performance compared to the state-of-the-art.

CLINICAL RELEVANCE/APPLICATION

The proposed multi-purpose CADx system can be applied for automatic classification and reporting of common thoracic diseases as a second opinion.

SSA12-09 Deep-learning for Distal Radius Fracture Detection in X-Ray Imaging

Sunday, Nov. 25 12:05PM - 12:15PM Room: S406B

Participants

Maximilian Russe, MD, Freiburg, Germany (*Presenter*) Nothing to Disclose Mathias F. Langer, MD, PhD, Freiburg, Germany (*Abstract Co-Author*) Nothing to Disclose Elmar C. Kotter, MD, MSc, Freiburg, Germany (*Abstract Co-Author*) Editorial Advisory Board, Thieme Medical Publishers, Inc

PURPOSE

Development of a robust algorithm for fracture detection of the distal radius in x-ray imaging for the use in an emergency department.

METHOD AND MATERIALS

Anterior-posterior x-ray images of the wrist from 2013-2017 were classified for fracture or absence of fracture by a consensus reading from a junior and a senior radiologist. Secondary reading was performed by a certified Msk radiologist. 1900 cases were exported for the deep learning study. Data leakage was excluded using only first-time images of the patients. Images where separated into 1351 images for training and 449 for validation. Besides the validation sample for the CNN learning, a separate analysis of the final model was performed using a separate test sample, containing 50 images with and without fractures. For the development of the deep learning model an established Convulsive neuronal network (CNN), GoogLeNet was used. Due network specifications an images distortion using a smashing transformation to 256*256 pixels was needed. The data was augmented using vertical flipping and up to +/- 10° rotation. No manual segmentation or image correction was made. Deep learning was performed by using Torch on Nvidia DIGITS with a standard workplace graphic unit (Nvidia Quadro P4000). Following parameters where used: 1000 training and validation epochs. AdaGrad was used as solver type and the initial learning rate was 0.01.

RESULTS

The training of the CNN took 4.34h of processing time. Final image processing of all 100 test images took 17 seconds. An overall accuracy of the validation sample was achieved with a final value of 94.2%, the overall accuracy of the separate test sample is 90%. The per-class accuracy in the validation sample was for fractures 87.5% and for no fractures 96.4% in the test sample 86% and 94%. These values are comparable and so overfitting of the CNN can be excluded.

CONCLUSION

The created algorithm shows a good detection rate for distal radius fractures. An exclusion of fracture was performed with even a higher accuracy. These results are promising for preliminary classification of x-rays within a clinical setting.

CLINICAL RELEVANCE/APPLICATION

X-ray reading is still a relevant task for fracture detection, fracture detection algorithms can be used to reduce the work load and already could be used for prioritizing work load. Instant preliminary fracture detection can be achieved with this deep learning model and easily implemented in clinical routine.



Machine Learning Theater: Deep Imaging: What Will be the Impact of AI-empowered Image Reconstruction, Diagnosis and Prognosis?: Presented by Quantib

Sunday, Nov. 25 11:00AM - 11:20AM Room: Machine Learning Showcase North Hall

Participants

Wiro Niessen, PhD, Rotterdam, Netherlands (*Presenter*) Co-founder, Quantib BV; Scientific Director, Quantib BV; Shareholder, Quantib BV

Program Information

Machine learning, and especially deep learning is a disruptive technology in the field of medical imaging, impacting medical image acquisition, reconstruction, analysis, and image-based diagnosis and prognosis. In this presentation examples of recent advances of the use of machine learning in these fields will be presented, along with the challenges we face in order to successfully introduce them into clinical practice. I will provide examples showing that the use of AI and big data has large potential to make steps towards precision medicine and precision health, i.e. taking individual variability into account in treatment selection. Specifically, in dementia research, I will show how large scale data analytics in longitudinal population neuroimaging studies, especially when combining imaging with other clinical, biomedical and genetic data, provides a unique angle to study the brain, both in normal ageing and disease, and how this can assist in clinical decision making. I will also discuss the promise and challenges of using state of the art artificial intelligence techniques as deep learning in this domain, to improve diagnostics and prognostics. As a second example I will show how radiomics and deep learning approaches can be used to improve tumor characterization and therapy selection and guidance in oncology, and also here the enormous potential and pitfalls of using artificial intelligence in the interpretation of these data will be discussed. Finally, I will discuss the concept of end-to-end learning, i.e. going directly from the raw data to the end goal, for example disease classification or prognosis. This approach poses the intriguing question whether in medical imaging we always need to reconstruct an image, or whether in certain cases we can directly work from the raw data.



Machine Learning Theater: icobrain - Adding AI to the brAIn: Presented by icometrix

Sunday, Nov. 25 11:30AM - 11:50AM Room: Machine Learning Showcase North Hall

Participants

Dirk Smeets, PhD,DIPLENG, Leuven, Belgium (*Presenter*) Employee, icoMetrix NV Wim Van Hecke, Edegem, Belgium (*Presenter*) Officer, icoMetrix Co-founder, icoMetrix

PROGRAM INFORMATION

Adding AI to the brAIn gives insights on how Machine Learning can enhance productivity, improve diagnostic accuracy and improve patient outcomes for patients with multiple sclerosis, dementia and traumatic brain injury. With the easy-to-integrate software solution icobrain, specialists are provided with an extra set of highly specialized eyes that can uncover abnormalities and discover changes on brain MRI scans. The resulting early assessment of subclinical disease activity accelerates the diagnosis and treatment evaluation of neurological disorders. Moreover, it will be demonstrated that this leads to a faster and more consistent radiological reporting that reduces the radiologist workload and variability.



Machine Learning Theater: Real Time 3D Radiology Portable Platform: Presented by AIExplore

Sunday, Nov. 25 12:00PM - 12:20PM Room: Machine Learning Showcase North Hall

PROGRAM INFORMATION

A real time, portable and interactive web-based 3D radiology system and platform, allowing doctors to analyze 3D radiology datum using their ipads or mobile devices any time any where. A convenient system makes life easier and smarter.



AIS-SUA

Artificial Intelligence Sunday Poster Discussions

Sunday, Nov. 25 12:30PM - 1:00PM Room: AI Community, Learning Center

IN

FDA Discussions may include off-label uses.

Participants

Rikiya Yamashita, MD, PhD, New York, NY (Moderator) Nothing to Disclose

Sub-Events

AI200-SD-SUA1 Effect of Inter-Observer Variability on Deep Learning in Chest X-Rays Station #1

Participants

Harald Ittrich, MD, Hamburg, Germany (*Presenter*) Nothing to Disclose Ivo Matteo Baltruschat, Hamburg, Germany (*Abstract Co-Author*) Nothing to Disclose Leonhard A. Steinmeister, MD, Hamburg, Germany (*Abstract Co-Author*) Nothing to Disclose Michael Grass, PhD, Hamburg, Germany (*Abstract Co-Author*) Employee, Koninklijke Philips NV Axel Saalbach, PHD, Aachen, Germany (*Abstract Co-Author*) Employee, Koninklijke Philips NV Tobias Knopp, DIPLENG, Hamburg, Germany (*Abstract Co-Author*) Nothing to Disclose Gerhard B. Adam, MD, Hamburg, Germany (*Abstract Co-Author*) Nothing to Disclose Hannes Nickisch, Hamburg, Germany (*Abstract Co-Author*) Nothing to Disclose

For information about this presentation, contact:

ittrich@uke.de

PURPOSE

Inter-observer variability is a well-known problem for the development of Deep Learning techniques in chest X-rays, especially for diseases with variable characteristics, where binary annotations vary widely between the individual readers. The aim was to investigate the effect of reader-dependent estimation during the annotation processes for Deep Convolutional Neural Networks (DCNN).

METHOD AND MATERIALS

Two expert radiologists annotated the Indiana dataset, which contains 3125 frontal and lateral conventional chest X-rays, in a multi-label setup with eight representative classes of abnormalities (including pleural effusion, infiltrate, congestion, atelectasis, pneumothorax, cardiomegaly, masses and foreign objects). Inter-observer variability (IOV) for all classes were calculated. We trained a ResNet-50 DCNN (with pre-training on ChestXRay14) using each radiologist's annotation: ExpertNet-1 and ExpertNet-2. In contrast to a binary annotation, the trained DCNNs generate continuous value prediction for each abnormality. For our evaluation, we used a 10 times re-sampling scheme. Within each split, we divided the data into 70% training and 30% testing. To evaluate the similarity of the obtained networks, we computed the Spearman's pairwise rank correlation coefficient between the predictions.

RESULTS

The highest IOV were at congestion and cardiomegaly with $13.6\% \pm 0.57\%$ and $10.61\% \pm 0.67\%$. Despite the differences in the annotation, the network predictions are highly correlated. We estimated rank correlation coefficients of 0.95 ± 0.01 and 0.80 ± 0.03 for cardiomegaly and congestion, respectively. By selecting the best threshold for the classification, we reduced the annotation variability from $13.6\% \pm 0.57\%$ to $3.81\% \pm 0.49\%$ and from $10.61\% \pm 0.67\%$ to $8.36\% \pm 0.78\%$ for congestion and cardiomegaly, respectively.

CONCLUSION

We investigated the effect of inter-observer variability on DCNNs. Even though the assignment of (artificial) binary labels by the two readers led to different datasets, our experiments showed a very high rank correlation between the predictions of ExpertNet-1 and ExpertNet-2.

CLINICAL RELEVANCE/APPLICATION

Generating a consensus ground truth of multiple expert annotation can be time-consuming, but is imperative when developing a CAD-System based on DCNNs.

AI152-ED- Deep Learning-Based Texture Classification for Similar CT Image Retrieval

Station #2

Participants

Hiroaki Takebe, Kawasaki, Japan (*Presenter*) Research collaboration, Fujitsu Limited Yasutaka Moriwaki, Kawasaki, Japan (*Abstract Co-Author*) Research collaboration, Fujitsu Limited Takayuki Baba, Kawasaki, Japan (*Abstract Co-Author*) Research collaboration, Fujitsu Limited Hiroaki Terada, MD, Hiroshima, Japan (*Abstract Co-Author*) Nothing to Disclose Toru Higaki, PhD, Hiroshima, Japan (*Abstract Co-Author*) Nothing to Disclose Kazuo Awai, MD, Hiroshima, Japan (*Abstract Co-Author*) Research Grant, Canon Medical Systems Corporation; Research Grant, Hitachi, Ltd; Research Grant, Fujitsu Limited; Research Grant, Bayer AG; Research Grant, DAIICHI SANKYO Group; Research Grant, Eisai Co, Ltd; Medical Advisory Board, General Electric Company; ; Akio Ozawa, BS, Chiba, Japan (*Abstract Co-Author*) Researcher, Fujitsu Limited Yasuharu Ogino, Tokyo, Japan (*Abstract Co-Author*) Director, Fujitsu Limited Machiko Nakagawa, Tokyo, Japan (*Abstract Co-Author*) Researcher, Fujitsu Limited Kenji Kitayama, Tokyo, Japan (*Abstract Co-Author*) Director, Fujitsu Limited Nobuhiro Miyazaki, Kawasaki, Japan (*Abstract Co-Author*) Research collaboration, Fujitsu Limited;

For information about this presentation, contact:

takebe.hiroaki@jp.fujitsu.com

CONCLUSION

We will be able to retrieve morphologically similar case more accurately by using DCNN for classification of texture and may provide diagnostically helpful information.

FIGURE

http://abstract.rsna.org/uploads/2018/18015959/18015959_5zkd.jpg

Background

When radiologists encounter a difficult case to diagnose, retrieval of morphologically similar cases in which final diagnosis is established may provide clinically useful information. We proposed a novel method which can retrieve morphologically similar cases based on lesion natures and their 3-dimensional (3D) distribution. As an initial trial, we developed a 3D-similar CT image retrieval method for diffuse lung disease (DLD).

Evaluation

In our method, we divided a slice image into blocks and classified texture of each blocks as normal or one of several kinds of lesions, and we represented the quantity of each lesion as histograms along a body based on the 3D model and calculated the similarity between cases by matching these histograms. With this method, the precision of retrieval of similar cases depends heavily upon the precision of texture classification. Then, we evaluated precisions of classification methods that use support vector machine (SVM) and deep convolutional neural network (DCNN) for 4 kinds of lesions, ground glass opacity (GGO), consolidation, honeycomb and emphysema in 63 patients with DLDs. These patients were split into training (55 patients) and test (8 patients). As a result, block images were about 21000 for training and about 3500 for test. Two board-certified radiologists consensually determined nature of DLDs and we regarded the results as the gold standard of lesions' nature. For SVM, image features of local binary pattern (LBP) were extracted from block images. For DCNN, block images were used as inputs of VGG16 network and pre-training was not used. The result showed that VGG16 achieved the precision 94.6%, on the other hand the precision of SVM was 74.2%.

Discussion

The experimental result showed that DCNN proved to be a powerful tool for classifying texture of DLD patients' CT images. We expect that the precision of DCNN will be much better according to increase of data for training.

AI023-EC-SUA Real Time Detection and Labeling of Image Objects: YOLO (You Only Look Once), A Case Study (with Pitfalls) in Training and Running a Deep Network to Detect and Label Objects

Custom Application Computer Demonstration

Participants David W. Piraino, MD, Cleveland, OH (*Presenter*) Medical Advisory Board, Agfa-Gevaert Group; Medical Advisory Board, Siemens AG; Medical Advisory Board, Nuance Communications, Inc Michael J. Ciancibello, Cleveland, OH (*Abstract Co-Author*) Nothing to Disclose James R. Wetzel, BS, Beachwood, OH (*Abstract Co-Author*) Nothing to Disclose Lindsey Marrero, BS, MS, Beachwood, OH (*Abstract Co-Author*) Nothing to Disclose Roseann Spitznagel, Beachwood, OH (*Abstract Co-Author*) Nothing to Disclose

CONCLUSION

Open sources deep neural networks can be used detect, localize, and categories abnormalities on medical images in real time.

FIGURE

http://abstract.rsna.org/uploads/2018/18007883/18007883_jvlz.jpg

Background

Many machine learning models have been developed and trained using the Darknet (https://pjreddie.com/darknet/) deep learning framework to detect, localize, and classify objects in non-medical images from ImageNet (http://image-net.org/). Darknet was developed to provide fast execution of deep learning networks in C. The YOLO (You Only Look Once) object detection system utilizes a convolutional neural network to identify image segments, but unlike other models, is also able to detect and classify images in real time. To apply this technology to radiology, the NIH chest images dataset, available on Kaggle (https://www.kaggle.com/nih-chest-xrays/data), is used in this demonstration for training and test sets.

Evaluation

The NIH dataset, containing around 110,000 chest radiographs, was utilized to train the YOLO convolutional neural network using NVIDIA GeForce GTX Class GPUs. This demonstration will show the steps in developing a machine learning model, which includes data cleansing, data enhancement, training, testing, and attack testing (See Figure using images from NIH dataset). This results in a medical class model which can be used to discover positive findings within medical images, such as atelectasis, cardiomegaly, effusion, infiltration, mass, nodule, pneumonia, and pneumothorax. To create this model, the image bounding boxes from the NIH images are converted to the YOLO format. The model is then retrained with the chest x-ray training set using both the YOLOv2 and YOLOv3 convolutional neural networks and subsequently tested using the test set. A portion of the demonstration will include real time retraining of the model.

Our computer exhibit will show the steps in developing a convolutional neural network for detection, localization, and categorization of objects/abnormalities on chest x-rays from the NIH data set in real time using the Darknet/YOLO object detection system.

AI002-EB A Deep Learning Framework for Radiotherapy Delivery in Thoracic Oncology

All Day Room: AI Community, Learning Center

Participants

Zaid A. Siddiqui, MD, Royal Oak, MI (Presenter) Nothing to Disclose

GENERAL INFORMATION

Meet the Author: The authors of this poster will be available in person to discuss their project during these times: Sunday, November 25 - 12:30-1:30 pm Monday, November 26 - 12:15-1:15 pm

POSTER DESCRIPTION

This presentation provides an overview of deep learning techniques that can assist various aspects of the radiation therapy planning process. The success of deep learning methods for normal tissue segmentation and their potential use in clinical target volumes are reviewed. Techniques to generate synthetic CT scans are also discussed as are their potential uses for MR-based planning or rapid adaptive plans from daily imaging. Finally, we look at the potential applications of deep learning in dose calculation/optimization and in accelerating development of personalized radiotherapy plans.

AI003-EB Ultra Low Dose PET/MRI Imaging of Crohn's Disease Using a Novel Deep Learning Reconstruction Method

All Day Room: AI Community, Learning Center

Participants

Christian Park, DO, Madison, WI (Presenter) Nothing to Disclose

Meet the Author: The authors of this poster will be available in person to discuss their project during these times: Sunday, November 25 - 12:30-1:30 pm

AI008-EB Machine Learning to Predict Risk of Upgrade and Recurrence of Ductal Carcinoma In Situ

All Day Room: AI Community, Learning Center

Participants

Manisha Bahl, MD, MPH, Boston, MA (Presenter) Nothing to Disclose

Regina Barzilay, PhD, Cambridge, MA (Abstract Co-Author) Nothing to Disclose

Constance D. Lehman, MD, PhD, Boston, MA (*Abstract Co-Author*) Research Grant, General Electric Company; Medical Advisory Board, General Electric Company

Meet the Author: The authors of this poster will be available in person to discuss their project during these times: Sunday, November 25 - 12:30-1:00 pm



Machine Learning Theater: QUIBIM Precision 3.0: AI as a Means, Not an End, For Imaging Biomarkers Integration in Clinical Practice: Presented by QUIBIM

Sunday, Nov. 25 12:30PM - 12:50PM Room: Machine Learning Showcase North Hall

Participants

Angel Alberich-Bayarri, PhD, Valencia, Spain (Presenter) Nothing to Disclose

PROGRAM INFORMATION

Tomorrow's radiology is rapidly approaching: imaging biomarkers, radiomics and, of course, AI. However, shouldn't we apply human intelligence to AI? QUIBIM Precision 3.0 provides real value to the radiologist's workflow using AI as a means to an end.



AIS-SUB

Artificial Intelligence Sunday Poster Discussions

Sunday, Nov. 25 1:00PM - 1:30PM Room: AI Community, Learning Center

IN

Participants

Rikiya Yamashita, MD, PhD, New York, NY (Moderator) Nothing to Disclose

Sub-Events

AI201-SD- Automated Foreign Object Detection in Chest X-Ray Images Based on Deep Learning SUB1

Station #1

Participants Chao Huang, PhD, Boston, MA (*Presenter*) Nothing to Disclose Sehyo Yune, MD, MPH, Boston, MA (*Abstract Co-Author*) Nothing to Disclose Myeongchan Kim, MD, Boston, MA (*Abstract Co-Author*) Nothing to Disclose Hyunkwang Lee, Boston, MA (*Abstract Co-Author*) Nothing to Disclose Synho Do, PhD, Boston, MA (*Abstract Co-Author*) Nothing to Disclose

For information about this presentation, contact:

chuang35@mgh.harvard.edu

PURPOSE

Chest X-ray (CXR) is the most commonly utilized imaging modality. In the hospital setting, various foreign objects such as endotracheal tubes or central venous catheters can be seen in CXR. The presence of foreign objects, if not carefully addressed, could impede CXR interpretation but is hard to detect and segment due to the wide variety of size and shape. Here we intend to develop an algorithm that automatically detects and localizes various foreign objects seen in CXR to recognize malposition and rapidly triage CXR.

METHOD AND MATERIALS

We collected 2,400 PA-view CXR images and the associated radiology reports from our institutional database. The images that have foreign objects annotated in the corresponding radiology reports were labelled as positive (1,200 images) and all other images are labelled as negative (1,200 images). A convolutional neural network (CNN) was built, which inputs a CXR image and outputs the probability of foreign object existence along with a heatmap localizing the areas of the image most indicative of foreign objects. We randomly selected 80%, 10%, and 10% of the images for training, validation, and testing, respectively. To avoid overfitting and improve generalization, data augmentation is applied to the images in training dataset with affine transformations (translation, scaling, and rotation).

RESULTS

Althought there were various foreign objects observed in CXR images (catheters, tubes, ECG cables, pacemakers etc.) and we only labeled the images positive and negative, the CNN achieved 99.5% accuracy on separating CXR images without any of these objects from those that has foreign objects. In positive cases, all types of foreign objects were accurately localized using class activation mapping.

CONCLUSION

We developed a CNN-based algorithm that can accurately detect and localize various foreign objects in CXR images without manual annotation and segmentation.

CLINICAL RELEVANCE/APPLICATION

Detecting numerous types of foreign objects without manual segmentation will expedite development of high-performance automated interpretation system for CXR.

AI025-EB- Deep Learning for Discovery of Latent Information in Contrast Free Cardiac CT Images

Hardcopy Backboard

Participants Daniele Della Latta, Massa, Italy (*Presenter*) Nothing to Disclose Gianmarco Santini, Massa, Italy (*Abstract Co-Author*) Nothing to Disclose Nicola Martini, PhD, Massa, Italy (*Abstract Co-Author*) Nothing to Disclose Lorena Maria Zumbo, Massa, Italy (*Abstract Co-Author*) Nothing to Disclose Gabriele Valvano, MSc, Massa, Italy (*Abstract Co-Author*) Nothing to Disclose Andrea Ripoli, PhD, Massa, Italy (*Abstract Co-Author*) Nothing to Disclose Francesco Avogliero, MD, Massa, Italy (*Abstract Co-Author*) Nothing to Disclose Giuli Jamagidze, Massa, Italy (*Abstract Co-Author*) Nothing to Disclose Dante Chiappino, Massa, Italy (*Abstract Co-Author*) Nothing to Disclose

For information about this presentation, contact:

dellalatta@ftgm.it

CONCLUSION

By exploiting the ability of the DCNN to mimic the human visual system and to regenerate the imagery and memory retrieval operations, we propose a novel approach to synthesize contrast enhanced CTimages, starting from contrast free CT thoracic scans. The obtained synthetic CT images allow the quantification of shapes and volumes of the cardiac chambers.

FIGURE

http://abstract.rsna.org/uploads/2018/18015453/18015453_tx5p.jpg

Background

In the European population, the 20% of the CT scans cover the thoracic region. Due to the lack of contrast in the cardiac area, the information about the cardiovascular system remains latent. From the clinical side, it would be important to define the morphology of the cardiac chambers, identifying patients affected by cardiopathies or valvular pathologies. Recently developed Deep Convolutional Neural Networks (DCNN) architectures have achieved breakthrough performance in image processing. Aim of this work is to develop a DCNN able to create contrast enhanced images, starting from contrast free ones.

Evaluation

The study was conducted using both contrast free calcium scoring (CS) and coronary angiography (CTA) CT scans acquired on 200 consecutive patients, during the same cardiac telediastolic phase. By applying rigid registration on CTA and using the CS images as references respiratory motion misalignments were removed. A deconvolutional architecture was chosen for DCNN. Patient's volumes were splitted in 120 cases to train the model, 10 cases for its validation and 70 for the evaluation of its performance. To guarantee a higher generalization power, in the prediction phase data augmentation was used applying random rotation with a max angle of 25 degrees on all the couple of CS and CTA slices provided to the network. The quality of synthesized cardiac image was assessed with Normalized Mutual Information index (NMI) and Peak Signal to Noise Ratio index (PSNR).

Discussion

After 960 training epochs, the model was able to generate synthetic CTA images with a good similarity and contrast dynamics compared to the true CTA images ($NMI=0.95\pm0.04$, $PSNR=53.40\pm1.54$). The high quality of generated images allowed a simple extraction of the left cardiac chambers and the quantification of their volumes.

AI010-EB Utilization of Deep Learning on CT Angiogram to Aid in the Detection of Emergent Large Vessel Occlusion

All Day Room: AI Community, Learning Center

Participants

Anthony D. Yao, Providence, RI (*Presenter*) Nothing to Disclose Matthew T. Stib, MD, Providence, RI (*Abstract Co-Author*) Nothing to Disclose Sumera S. Subzwari, Providence, RI (*Abstract Co-Author*) Nothing to Disclose Amy Wang, Madison, WI (*NON-Presenter*) Luke Zhu, Providence, RI (*Abstract Co-Author*) Nothing to Disclose Jerrold L. Boxerman, MD, PhD, Providence, RI (*Abstract Co-Author*) Nothing to Disclose Grayson L. Baird, PhD, Providence, RI (*Abstract Co-Author*) Nothing to Disclose Ugur Cetintemel, Providence, RI (*Abstract Co-Author*) Nothing to Disclose Ryan A. McTaggart, MD, Barrington, RI (*Abstract Co-Author*) Nothing to Disclose

Meet the Author: The authors of this poster will be available in person to discuss their project during these times: Sunday November 25 1:00-1:30 pm

AI014-EB Deep Learning for Radiological Image Quality Improvement: Impact on the Accuracy of Diagnosis and Organ Segmentation

All Day Room: AI Community, Learning Center

Participants

Leonid Chepelev, MD, PhD, Ottawa, ON (Presenter) Nothing to Disclose

Meet the Author: The authors of this poster will be available in person to discuss their project during these times: Sunday November 25 1:00-1:30pm



Machine Learning Theater: Using AI within Existing Radiology Workflows: Presented by Nuance Communications

Sunday, Nov. 25 1:30PM - 1:50PM Room: Machine Learning Showcase North Hall

Participants

Warren B. Gefter, MD, Philadelphia, PA (Presenter) Nothing to Disclose

Program Information

Artificial Intelligence cannot be deployed in a silo. Integrating the outputs of AI algorithms into the radiologist's clinical workflow presents a number of challenges along with opportunities. Scenarios will be presented to demonstrate how well-designed approaches to workflow integration will enable AI to effectively augment the capabilities of the radiologist while preserving - and enhancing - efficiency and quality.



RC153

Deep Learning in Radiology: How Do We Do It?

Sunday, Nov. 25 2:00PM - 3:30PM Room: E450A



AMA PRA Category 1 Credits ™: 1.50 ARRT Category A+ Credit: 1.75

Participants

Luciano M. Prevedello, MD, MPH, Dublin, OH (Moderator) Nothing to Disclose

LEARNING OBJECTIVES

1) Learn what Deep Learning is and how it may be applied to Radiology. 2) Understand the challenges and benefits of creating a laboratory dedicated to machine learning in Radiology. 3) Be exposed to several applied examples of Deep Learning in Radiology at different institutions.

Sub-Events

RC153A Ohio State University Experience

Participants

Luciano M. Prevedello, MD, MPH, Dublin, OH (Presenter) Nothing to Disclose

LEARNING OBJECTIVES

1) Describe the existing infrastructure to handle pixel and non pixel data at our institution for translational research in machine learning. 2) Learn some applications of Deep Learning in Radiology through examples.

RC153B Stanford University Experience

Participants

Curtis P. Langlotz, MD,PhD, Menlo Park, CA (*Presenter*) Advisory Board, Nuance Communications, Inc; Shareholder, whiterabbit.ai; Advisory Board, whiterabbit.ai; Shareholder, Nines.ai; Consultant, Nines.ai; Shareholder, TowerView Health; Research Grant, Koninklijke Philips NV; Research Grant, Siemens AG; Research Grant, Alphabet Inc;

LEARNING OBJECTIVES

1) Consider the types of clinical problems that are best suited to machine learning solutions. 2) Understand how 'deep' neural networks work, and the technology and people needed for a successful program. 3) Learn about the type of work performed by an artificial intelligence laboratory focused on medical imaging and computer vision. 4) Analyze the key technologies needed to create large annotated training data sets.

RC153C Mayo Clinic Rochester Experience

Participants

Bradley J. Erickson, MD, PhD, Rochester, MN (*Presenter*) Stockholder, OneMedNet Corporation; Stockholder, VoiceIt Technologies, LLC; Stockholder, FlowSigma;

For information about this presentation, contact:

bje@mayo.edu

LEARNING OBJECTIVES

1) Describe Mayo experience with deep learning radiomics technology.



AI001-MO

RSNA Deep Learning Classroom: Presented by NVIDIA Deep Learning Institute

Monday, Nov. 26 8:30AM - 4:00PM Room: AI Community, Learning Center

Program Information

Located in the Learning Center (Hall D), this classroom presented by NVIDIA will give meeting attendees a hands-on opportunity to engage with deep learning tools, write algorithms and improve their understanding of deep learning technology. "Attendees must bring a laptop capable of running the most recent version of Chrome."

Sub-Events

AI001-MOA Introduction to Deep Learning

Monday, Nov. 26 8:30AM - 10:00AM Room: AI Community, Learning Center

Title and Abstract

Introduction to Deep Learning This class will focus on basic concepts of convolutional neural networks (CNNs), and walk the attendee through a working example. A popular training example is the MNIST data set which consists of hand-written digits. This course will use a data set we created, that we call 'MedNIST' and consists of 1000 images each from 5 different categories: Chest X-ray, hand X-ray, Head CT, Chest CT, Abdomen CT, and Breast MRI. The task is to identify the image type. This will be used to train attendees on the basic principles and some pitfalls in training a CNN. The attendee will have the best experience if they are familiar with Python programming.

AI001-MOB Advanced Data Augmentation Using GANs

Monday, Nov. 26 10:30AM - 12:00PM Room: AI Community, Learning Center

Title and Abstract

Advanced Data Augmentation Using GANs Getting 'large enough' data sets is a problem for most deep learning applications, and this is particularly true in medical imaging. Generative Adversarial Networks (GANs) are a deep learning technology in which a computer is trained to create images that look very 'real' even though they are completely synthetic. This may be one way to address the 'data shortage' problem in medicine.

AI001-MOC Multi-modal Classification

Monday, Nov. 26 12:30PM - 2:00PM Room: AI Community, Learning Center

Title and Abstract

Multi-modal Classification This session will focus on multimodal classification. Classification is the recognition of an image or some portion of an image being of one type or another, such as 'tumor' or 'infection'. Multimodal classification means that there are more than 2 classes. While this is logically simple to understand, it presents some unique challenges that will be discussed.

AI001-MOD Introduction to Deep Learning

Monday, Nov. 26 2:30PM - 4:00PM Room: AI Community, Learning Center

Title and Abstract

Introduction to Deep Learning This class will focus on basic concepts of convolutional neural networks (CNNs), and walk the attendee through a working example. A popular training example is the MNIST data set which consists of hand-written digits. This course will use a data set we created, that we call 'MedNIST' and consists of 1000 images each from 5 different categories: Chest X-ray, hand X-ray, Head CT, Chest CT, Abdomen CT, and Breast MRI. The task is to identify the image type. This will be used to train attendees on the basic principles and some pitfalls in training a CNN. The attendee will have the best experience if they are familiar with Python programming.



RC205

Neuroradiology Series: Brain Tumors

Monday, Nov. 26 8:30AM - 12:00PM Room: S406B



FDA Discussions may include off-label uses.

Participants

Soonmee Cha, MD, San Francisco, CA (*Moderator*) Nothing to Disclose Kei Yamada, MD, Kyoto, Japan (*Moderator*) Nothing to Disclose

Sub-Events

RC205-01 Multimodal Molecular Imaging Using Advanced MRI and PET: Applications in Clinical Neuro-Oncology

Monday, Nov. 26 8:30AM - 9:00AM Room: S406B

Participants

Norbert Galldiks, Cologne, Germany (Presenter) Research grant, Wilhelm-Sander Stiftung (Munich, Germany); Advisory board, Abbvie

LEARNING OBJECTIVES

1) To give an overview on the most relevant advanced MRI techniques (i.e., PWI MRI, 2-hydroxyglutatate MRS) and PET tracers (i.e., amino acid PET tracers, radiolabeled somatostatin receptor ligands) to improve diagnostics in the field of clinical Neuro-Oncology.

RC205-02 Robust Pre-Operative Language Mapping in Patients with Brain Tumors: A Feasibility Study

Monday, Nov. 26 9:00AM - 9:10AM Room: S406B

Participants

Mohammad Fakhri, MD, Saint Louis, MO (*Presenter*) Nothing to Disclose Manu S. Goyal, MD, MSc, Saint Louis, MO (*Abstract Co-Author*) Nothing to Disclose Joshua S. Shimony, MD, PhD, Saint Louis, MO (*Abstract Co-Author*) Nothing to Disclose Carl Hacker, Saint Louis, MO (*Abstract Co-Author*) Nothing to Disclose Amrita Hari-Raj, St. Louis, MO (*Abstract Co-Author*) Nothing to Disclose Abraham Z. Snyder, PhD, Saint Louis, MO (*Abstract Co-Author*) Nothing to Disclose

For information about this presentation, contact:

fakhri@wustl.edu

PURPOSE

We evaluate multilevel perceptron (MLP)-based mapping as a tool for identification of language-related resting-state networks in brain tumor patients. Currently available alternative resting state fMRI analysis methods are either biased (e.g., seed-based correlation) or not robust at the single subject level (e.g., Independent Component Analysis), and therefore, not ideal for use in presurgical planning.

METHOD AND MATERIALS

Twenty-one patients with a brain tumor in the vicinity of expressive language areas were included (mean age 42 ±16 years; 71% male). The MLP output was compared to seed-based correlation in two different manually defined language regions of nterst (ROIs). The putative language ROIs were defined using meta-analysis of task-fMRI responses, resting state seed based correlation maps, and direct cortical stimulation language maps. MLP performance in patients was also compared to a cohort of 688 normal subjects.

RESULTS

Upon presentation, 62% of the patients exhibited expressive aphasia prior to the surgical resection. Thirty-two percent of the patients were positive for IDH-1 mutation and 27% had 1p/11q deletion. The MLP was able to reliably map robust language RSN affiliation in putative language areas in all patients (n=21, 100%). Results were similar to those obtained in a cohort of young, healthy subjects. Fisher z-transformed Pearson correlation maps obtained from seed ROIs were strongly spatially correlated with the MLP score in both evaluation ROIs (Spearman rho=0.74 and 0.62, p<0.0001 and p<0.003 respectively).

CONCLUSION

MLP-based language maps are comparable to results obtained using conventional seed-based correlation mapping. MLP-based mapping is reliable in patients with brain tumors. The trained MLP is robust to anatomical shifts owing to mass effects and focal, tumor-related neural dysfunction, hence, is suitable for use in patients with brain tumors.

CLINICAL RELEVANCE/APPLICATION

A trained machine-learning algorithm can reliably identify resting-state language-related networks on an individual basis in patients

with brain tumors in vicinity of the language cortex.

RC205-03 Use of Quantitative Blood Oxygen Level Dependent (qBOLD) in Non-Invasively Determining Glioma Grade, with Correlation through Neuropathology

Monday, Nov. 26 9:10AM - 9:20AM Room: S406B

Participants Pejman Jabehdar Maralani, MD, FRCPC, Toronto, ON (*Presenter*) Nothing to Disclose Julia Keith, MD, Toronto, ON (*Abstract Co-Author*) Nothing to Disclose David Munoz, MD, Toronto, ON (*Abstract Co-Author*) Nothing to Disclose Todd Mainprize, MD, Toronto, ON (*Abstract Co-Author*) Nothing to Disclose Arjun Sahgal, Toronto, ON (*Abstract Co-Author*) Speaker, Medtronic plc; Speaker, Elekta AB; Medical Advisory Board, Varian Medical Systems, Inc; Speaker, Accuray Incorporated; Research Grant, Elekta AB Sean P. Symons, MPH, MD, Toronto, ON (*Abstract Co-Author*) Nothing to Disclose Bradley J. Macintosh, PhD, Toronto, ON (*Abstract Co-Author*) Nothing to Disclose Aimee Chan, Toronto, ON (*Abstract Co-Author*) Nothing to Disclose Sunit Das, MD,PhD, Toronto, ON (*Abstract Co-Author*) Nothing to Disclose David J. Mikulis, MD, Toronto, ON (*Abstract Co-Author*) Stockholder, Thornhill Research Inc; Research Grant, General Electric Company;

For information about this presentation, contact:

pejman.maralani@utoronto.ca

PURPOSE

Quantitative blood oxygen level dependent (qBOLD) magnetic resonance imaging (MRI) has been used as a method to gauge the level of oxygen saturation (SO2) in the tumors of patients with gliomas. We investigated whether there was a difference in the level of oxygenation in different grades of gliomas.

METHOD AND MATERIALS

10 patients were recruited for this prospective, multi-institutional study. Patients underwent a preoperative Ferumoxytol-based qBOLD MRI. Based on visual inspection of SO2 maps from qBOLD imaging, two volumes of interest (VOIs) from the tumor were chosen. Biopsy samples from the VOIs were taken to correlate histopathological measures of hypoxia against qBOLD, and staining was scored by a neuropathologist. Patients with glioblatoma (GBM; WHO Grade IV) was compared with lower-grade astrocytomas. 1 patients' research samples were inconclusive, and therefore excluded from pathological analysis.

RESULTS

Pathology reports indicated that: 1 patient had diffuse astrocytoma (WHO Grade II), 3 patients had anaplastic astrocytoma (WHO Grade III), and 6 patients GBM. When comparing low-SO2 samples, non-GBM patients had on average higher SO2 (26.0% vs 10.6%, p=0.07). Pathology staining of low-SO2 samples showed significantly higher levels of staining in HIF1a (p=0.048), VEGF (p=0.04) and CAIX (p<0.01) in GBM compared to lower-grade gliomas. No significant differences were detectable in the high SO2 (mean, 37.4%) tumors.

CONCLUSION

Levels of oxygenation appear to decrease with increasing glioma grade, and is detectable by qBOLD MRI. Pathological markers of hypoxia support this notion. The threshold for differentiating GBM from lower-grade gliomas appears to be \sim 35% SO2. More subjects are required to confirm these results.

CLINICAL RELEVANCE/APPLICATION

qBOLD MRI can be an alternative method to assess tumor grade when biopsy is not feasible. In light of new hypoxia-targeting therapies, it can also be used to monitor oxygenation state of the tumor during treatment.

RC205-04 Probabilistic Atlases of Pre-Treatment MRI Reveal Hemispheric and Lobe-Specific Spatial Distributions across Molecular Sub-Types of Diffuse Gliomas

Monday, Nov. 26 9:20AM - 9:30AM Room: S406B

Awards

Trainee Research Prize - Medical Student

Participants Niha G. Beig, MS, Cleveland, OH (*Presenter*) Nothing to Disclose Marwa Ismail, PhD, Cleveland, OH (*Abstract Co-Author*) Nothing to Disclose Anant Madabhushi, PhD, Cleveland, OH (*Abstract Co-Author*) Research funded, Koninklijke Philips NV Manmeet Ahluwalia, Cleveland, OH (*Abstract Co-Author*) Nothing to Disclose Pallavi Tiwari, PhD, Cleveland, OH (*Abstract Co-Author*) Nothing to Disclose

For information about this presentation, contact:

niha.beig@case.edu

PURPOSE

Recent WHO classification of diffuse gliomas defined 3 subtypes based on their molecular status: Isocitrate dehydrogenase wild type (IDH-WT), IDH mutant with 1p/19q intact (IDHmut-noncodel), and IDH mutant with 1p/19q co-deletion (IDHmut-codel). Each category represents different prognosis and chemo-sensitivity thus impacting treatment decisions. Previous studies have linked tumor location with patient outcome. In this feasibility study, we developed population atlases of pre-treatment MRI lesions to evaluate whether IDH-WT, IDHmut-codel, IDHmut-noncodel tumors will have spatial proclivity to hemispheric or lobe-specific locations based on their frequency of occurrence.

METHOD AND MATERIALS

150 pre-operative MRI sequences (1.5T/3T T1w, T2w, FLAIR scans, multi-center) of patients diagnosed with diffuse gliomas (65 low grade gliomas and 85 glioblastomas) were considered from TCIA, along with their IDH mutation and 1p/19q co-deletion status. Frequency atlases of tumor occurrence in T2/FLAIR hyper-intensity regions were developed for each sub-type, by averaging voxel intensities across all patients. To compute significant differences (p-value<0.05), voxel-based analysis of differential involvement (ADIFFI) based on two-tailed Fisher's exact test was performed on (a) IDH-WT (n= 91) vs IDH-mut (n=59), and (b) IDHmut-codel (n=13) vs IDHmut-noncodel (n=57) atlases. Prominent clusters were identified and mapped to LONI Probabilistic Brain Atlas (LPBA40) parcellations to provide anatomic localization for each sub-type.

RESULTS

The ADIFFI analysis revealed that IDHmut tumors were predominant in frontal lobe with a frequency of 52.7% occurrence whereas IDH-WT had a multi-centric distribution across parietal and temporal lobes (p<0.005). Prominent cluster of IDHmut-codel was found to be lateralized to the left hemisphere in the cingulate gyrus region, while IDHmut-noncodel had 60% occurrence in the superior frontal gyrus of the right hemisphere (p<0.05).

CONCLUSION

Our analysis suggests spatial proclivity of molecular subtypes to hemispheric and lobe-specific locations in the brain. The spatial localization could serve as an imaging marker for differentiating molecular subtypes of gliomas.

CLINICAL RELEVANCE/APPLICATION

IDHmut-codel have a favorable response to chemoradiation, while IDHmut-noncodel have improved prognosis versus IDH-WT. Identifying radiogenomic markers of sub-types could enable personalized treatments in Gliomas.

RC205-05 High-Tumor Mutation Burden (Hypermutation) in Gliomas Exhibit a Unique Predictive Radiomic Signature

Monday, Nov. 26 9:30AM - 9:40AM Room: S406B

Participants

Islam S. Hassan, MD, Houston, TX (*Abstract Co-Author*) Nothing to Disclose Aikaterini Kotrotsou, PhD, MEng, Houston, TX (*Abstract Co-Author*) Nothing to Disclose Carlos M. Kamiya, Houston, TX (*Abstract Co-Author*) Nothing to Disclose Nabil A. Elshafeey, MD, Houston, TX (*Presenter*) Nothing to Disclose Kristin Alfaro-Munoz, MS, Houston, TX (*Abstract Co-Author*) Nothing to Disclose Pascal O. Zinn, MD, Boston, MA (*Abstract Co-Author*) Nothing to Disclose John F. deGroot, MD, Houston, TX (*Abstract Co-Author*) Nothing to Disclose Rivka R. Colen, MD, Houston, TX (*Abstract Co-Author*) Research Grant, General Electric Company;

For information about this presentation, contact:

rcolen@mdanderson.org

PURPOSE

Increase in tumor mutation burden (TMB) or hypermutation is the excessive accumulation of DNA mutations in cancer cells. Hypermutation was reported in recurrent as well as primary gliomas. Hypermutated gliomas are mostly resistant to alkylating therapies and exhibit a more immunologically reactive microenvironment which makes them a good candidate for immune checkpoint inhibitors. Herein, we sought to use MRI radiomics for prediction of high TMB (hypermutation) in primary and recurrent gliomas.

METHOD AND MATERIALS

In this IRB-approved retrospective study, we analyzed 101 patients with primary gliomas from the University of Texas MD Anderson Cancer Center. Next generation sequencing (NGS) platforms (T200 and Foundation 1) were used to determine the Mutation burden status in post-biopsy (stereotactic/excisional). Patients were dichotomized based on their mutation burden; 77 Non-hypermutated (<30 mutations) and 24 hypermutated (>=30 mutations or <30 with MMR gene or POLE/POLD gene mutations). Radiomic analysis was performed on the conventional MR images (FLAIR and T1 post-contrast) obtained prior to tumor tissue surgical sampling; and rotation-invariant radiomic features were extracted using: (i) the first-order histogram and (ii) grey level co-occurrence matrix. Then, we performed Logistic regression modelling using LASSO regularization method (Least Absolute Shrinkage and Selection Operator) to select best features from the overall features in the dataset. ROC analysis and a 50-50 split for training and testing, were used to assess the performance of logistic regression classifier and AUC, Sensitivity, Specificity, and p-value were obtained.

RESULTS

LASSO regularization (alpha = 1) was performed with all the 4880 features for feature selection and 40 most prominent features were selected for logistic regression modelling. Our 50-50 split ROC analysis showed an accuracy of 94%, sensitivity of 75%, and specificity of 100% and a p-value of 0.0008).

CONCLUSION

An MRI-radiomic phenotype is predictive of the increase in TMB (Hypermutation) in both primary and recurrent gliomas.

CLINICAL RELEVANCE/APPLICATION

Hypermutated gliomas are resistant to alkylating therapies but responsive to immune checkpoint inhibitors. Our proposed radiomic biomarker can be used to guide therapy and patient selection for immunotherapy clinical trials.

RC205-06 Brain Tumor Surveillance Imaging in the Era of Genomics and Personalized Medicine

Monday, Nov. 26 9:40AM - 10:10AM Room: S406B

Participants

Rajan Jain, MD, Hartsdale, NY (Presenter) Consultant, Cancer Panels; Royalties, Thieme Medical Publishers, Inc

For information about this presentation, contact:

rajan.jain@nyumc.org

LEARNING OBJECTIVES

1) To discuss currently used response assessment criteria in brain tumor surveillance, such as Macdonald and RANO criteria and their limitations. 2) Participants will learn how the emergence of genomic markers has brought a paradigm shift in the management and surveillance of gliomas. 3) Participants will learn about the complexities of post-treatment imaging appearance of brain tumors in the new age of targeted immuno-therapies and what functional imaging techniques can add value to conventional surveillance MRI.

RC205-07 Update on Pediatric Brain Tumor Imaging

Monday, Nov. 26 10:20AM - 10:50AM Room: S406B

Participants

Zoltan Patay, MD, PhD, Memphis, TN (Presenter) Nothing to Disclose

For information about this presentation, contact:

zoltan.patay@stjude.org

LEARNING OBJECTIVES

1) Familiarize with new concepts and entities introduced in the 2016 update of the WHO Classification of Tumours of the CNS and pertinent to pediatric brain neoplasms. 2) Review the most recent developments related to the classification of embryonal and ependymal tumors since the publication of the 2016 update. 3) Discuss relevance and implications of the above for the practing radiologist.

RC205-08 Selection of Imaging-based Surrogate Endpoints Depending on a Specific Target of Test Treatment in Phase III Randomized Controlled Trials of Glioblastoma

Monday, Nov. 26 10:50AM - 11:00AM Room: S406B

Participants

Chong Hyun Suh, MD, Seoul, Korea, Republic Of (*Presenter*) Nothing to Disclose Ho Sung Kim, Seoul, Korea, Republic Of (*Abstract Co-Author*) Nothing to Disclose Sang Joon Kim, MD, Seoul, Korea, Republic Of (*Abstract Co-Author*) Nothing to Disclose

PURPOSE

Phase III randomized controlled trials (RCTs) in glioblastoma have used various potential surrogate endpoints with imaging. The surrogacy of imaging-based endpoints remains largely unknown and can be dependent on the type of test treatment. We investigated the surrogacy of imaging-based endpoints as well as their values depending on a specific target of test treatment in patients with glioblastoma.

METHOD AND MATERIALS

A systematic search of phase III RCTs in glioblastoma was performed. Surrogacy between imaging-based endpoints including progression-free survival (PFS), 6 month PFS (6moPFS), 12 month PFS (12moPFS), median PFS, and objective response rate (ORR) with overall survival (OS) were explored using weighted linear regression for the hazard ratio for OS and the hazard ratios or odds ratios for imaging-based endpoints. Subgroup analyses according to disease entity, a specific target of test treatment, and response assessment criteria were performed. The quality of the reporting of efficacy with these IBEs was also evaluated.

RESULTS

Twenty-three RCTs published between 2000 and 2017, covering 8387 patients, met the inclusion criteria. OS showed significant correlations with PFS (standardized ß coefficient [R]=0.719), 6moPFS (R=0.647), and 12moPFS (R=0.638). OS showed nonsignificant correlations with median PFS and ORR. The subgroup analyses consistently showed highly significant correlations between OS and PFS. PFS showed the highest correlations with OS in drugs targeting DNA repair-cell cycle control-epigenetic modifiers (R=0.913) and drugs targeting growth factor receptors-MAPK/PI3K signaling pathways (R=0.962). 12moPFS showed the highest correlations with OS in antiangiogenic therapy, (R=0.821). Trials using RANO criteria showed higher correlation coefficients between OS and PFS, 6moPFS, and 12moPFS than trials using MacDonald criteria. In terms of quality of reporting, there were high proportions of clearly defined primary endpoints (91%) and intent-to-treat analyses (83%). Compared with trials published between 2012 and 2017 were more likely to be supported by industry.

CONCLUSION

Imaging-based endpoints can be surrogates in phase III RCTs of glioblastoma.

CLINICAL RELEVANCE/APPLICATION

The specific target of test treatment and response assessment criteria should be considered in selection of imaging-based endpoints as a surrogate endpoint.

RC205-09 18F-Choline PET/RM in Brain Tumours: Multimodality Imaging in Gliomas Response Assessment

Monday, Nov. 26 11:00AM - 11:10AM Room: S406B

Awards

Student Travel Stipend Award

Participants Valentina Ferrazzoli, MD, Rome, Italy (*Presenter*) Nothing to Disclose Harpreet K. Hyare, MBBS, London, United Kingdom (*Abstract Co-Author*) Nothing to Disclose Ananth Shankar, London, United Kingdom (*Abstract Co-Author*) Nothing to Disclose Christine Tang, MBBS, London, United Kingdom (*Abstract Co-Author*) Nothing to Disclose Ahmed Al-Khayfawee, MRCP,MD, London, United Kingdom (*Abstract Co-Author*) Nothing to Disclose Roberto Floris, MD, Rome, Italy (*Abstract Co-Author*) Nothing to Disclose Francesco Fraioli, MD, London, United Kingdom (*Abstract Co-Author*) Nothing to Disclose

For information about this presentation, contact:

valentinaferrazzoli@hotmail.it

PURPOSE

Evaluation of post-treatment glioma burden remains a significant challenge, particularly in Teenage and Young Adult (TYA) population. Although aminoacid PET has impacted on glioma imaging, 18fluoro-Choline Positron Emission Tomography (ChoPET) is currently more widely available. Purpose was to evaluate ChoPET/MR for post-treatment TYA glioma burden.

METHOD AND MATERIALS

27 TYA (mean age 16 years, 8-22 years) in treatment (radiotherapy e/o chemotherapy) for astrocytic brain tumours (14 WHO III/IV; 13 WHO I/II) were evaluated with ChoPET/MR. 59 follow up scans were retrospectively reviewed; maximum standardized uptake values (SUVmax) and MR features (diameters, enhancement) were recorded. In 13 cases dynamic susceptibility contrast perfusion weighted imaging (DSCpwi) was analyzed; relative cerebral blood volume (rCBV) and SUV in enhancing and non-enhancing tumour volumes (Venh, Vne) and in normal appearing white matter (wm) were calculated (rCBVenh, rCBVne, rCBVwm, SUVenh, SUVne, SUVwm). A blinded nuclear medicine and a radiologist scored the images on tumour probability (1:unlikely-5:definitely). Receiver Operating Characteristic (ROC) analysis was used considering as gold standard for diagnosis the histopathology or follow up. Pearson correlation coefficient was used for SUV and rCBV and independent T-Test for differences in ROIs.

RESULTS

MR sensitivity for residual tumour was 92.7% (85.7% WHO III/IV,81.5% WHO I/II). PET sensitivity was 78.2% (78.6% WHO III/IV, 63.0% WHO I/II). Discrepancy was of 20% (11/12 non enhancing). Significant positive correlation between SUV and rCBV in all ROIs was found (r=0.051, p=0.0016). Tumour component analysis showed significantly higher SUVenh and SUVne than SUVwm (SUVenh:p<0.001, SUVne: p=0.021) and significantly higher rCBVne than rCBVwm (p=0.005). rCBVenh showed only borderline significance (p=0.053).

CONCLUSION

ChoPET is able to detect post-treatment enhancing and non-enhancing tumour but both conventional MR and pwi are superior for evaluating non-enhancing disease. In TYA gliomas follow up a quantitative multimodality evaluation can better identify both enhancing and non-enhancing residual/recurrent disease being promising in the early assessment of tumour response.

CLINICAL RELEVANCE/APPLICATION

In teenage and young-adults gliomas early assessment of tumour response to therapy can be improved by complementary use of PET/MR to evaluate different tumour components.

RC205-10 Prediction of Genomic Profiles and Survival in Glioblastoma Patients: Feasibility of Qualitative and Quantitative Analyses of Arterial Spin-Labeling Perfusion-Weighted Imaging

Monday, Nov. 26 11:10AM - 11:20AM Room: S406B

Participants Roh-Eul Yoo, MD, Seoul, Korea, Republic Of (*Presenter*) Nothing to Disclose Tae Jin Yun, MD, Seoul, Korea, Republic Of (*Abstract Co-Author*) Nothing to Disclose

For information about this presentation, contact:

roheul7@gmail.com

PURPOSE

To explore the feasibility of using arterial spin-labeling perfusion-weighted imaging (ASL-PWI) to predict genomic profiles and survival in glioblastoma (GBM) patients.

METHOD AND MATERIALS

One hundred thirty-two consecutive GBM patients, who had undergone maximal surgical resection or biopsy followed by concurrent chemo- and radiation therapy and adjuvant chemotherapy using temozolomide between January 2011 and November 2015, were included in this retrospective study. CBF at the contrast-enhancing and T2 hyperintense portions on preoperative ASL-PWI were evaluated both qualitatively (hypo- / iso- / hyperperfusion relative to gray matter) and quantitatively (mean and maximal CBFs of tumors normalized with respect to those of contralateral gray matter [nCBFmean and nCBFmax]). The associations between ASL findings and major genomic profiles or survival were evaluated using Mann-Whitney U-test, Fisher's exact test, Spearman rank correlation, and Kaplan-Meier analysis. Receiver operating characteristics analysis was performed to determine the diagnostic performance of the imaging parameters for prediction of genetic biomarkers.

RESULTS

nCBFmean and nCBFmax at contrast-enhancing portions were significantly higher in IDH wild-type group (n = 102) than in IDH mutant (IDH1 or IDH2) group (n = 17) (P = .009 and P = .007, respectively). Sensitivity and specificity for prediction of IDH mutation were 59% and 81% at the optimal cutoff value of 1.13 for nCBFmax. nCBFmax at contrast-enhancing portions tended to be lower in patients with methylated MGMT promoter (n = 65) than in those with unmethylated MGMT promoter (n = 49) (P = .072). No significant associations were found between nCBF and other genetic biomarkers including ATRX, PTEN, p53, and EGFR. Hyperperfusion at contrast-enhancing portions was significantly more common in IDH wild-type group than in IDH mutant group (P = .003). Hyperperfusion was associated with shorter progression-free survival as compared with hypo- or isoperfusion (Median, 6.9 vs. 12.5 vs. 19.3 months; P = .029).

CONCLUSION

ACL DWT may halp popinyaciyaly prodict TDH mytation status and progression free survival in diablastama patients

ASE-PWI Hay help nonlinvasively predict 10 minutation status and progression-free survival in gliobidstoria patients.

CLINICAL RELEVANCE/APPLICATION

ASL-PWI may help noninvasively predict IDH mutation status and progression-free survival in glioblastoma patients and is recommended as part of preoperative tumor evaluation particularly for patients with impaired renal function.

RC205-11 Clinical Data and Vascular Pattern on MRI to Predict Survival in 'De Novo' Glioblastoma

Monday, Nov. 26 11:20AM - 11:30AM Room: S406B

Awards

Student Travel Stipend Award

Participants

Blanca Domenech, MD, Barcelona, Spain (*Presenter*) Nothing to Disclose Alfredo Gimeno Cajal, Barcelona, Spain (*Abstract Co-Author*) Nothing to Disclose Gerard Blasco, RT, Girona, Spain (*Abstract Co-Author*) Nothing to Disclose Pepus Daunis-I-Estadella, Girona, Spain (*Abstract Co-Author*) Nothing to Disclose Carmen Balana, Barcelona, Spain (*Abstract Co-Author*) Nothing to Disclose Jaume Capellades, MD, Barcelona, Spain (*Abstract Co-Author*) Nothing to Disclose Angel Alberich-Bayarri, MD, Valencia, Spain (*Abstract Co-Author*) Nothing to Disclose Kambiz Nael, MD, New York, NY (*Abstract Co-Author*) Medical Advisory Board, Canon Medical Systems Corporation Carlos Leiva-Salinas, MD,PhD, Charlottesville, VA (*Abstract Co-Author*) Nothing to Disclose Rajan Jain, MD, Hartsdale, NY (*Abstract Co-Author*) Consultant, Cancer Panels; Royalties, Thieme Medical Publishers, Inc Marco Essig, MD, Erlangen, Germany (*Abstract Co-Author*) Nothing to Disclose Salvador Pedraza, MD, PhD, Girona, Spain (*Abstract Co-Author*) Nothing to Disclose

For information about this presentation, contact:

bl.domenech@gmail.com

PURPOSE

MRI provides information on the physiologic properties of glioblastomas. In addition to established prognostic markers such as age, performance status, and extent of resection, increased vascularity on contrast-enhanced MRI is associated with shortened survival. We investigated whether glioblastoma vascular pattern (GVP-MRI), combined with clinical variables and other imaging features, could improve the predictive power of survival models.

METHOD AND MATERIALS

From January 2012 through December 2016, 97 consecutive patients (62 men; mean age, 58±15 years) with histologically proven glioblastoma (GLIOCAT substudy) underwent 1.5T-MRI including anatomical, diffusion-weighted, first-pass DSC, and T1-weighted sequences after 0.1 mmol/kg gadobutrol (1 mm isometric voxel). We used Olea Sphere V.3.0 software (Olea Medical, La Ciotat, France) to analyze rCBV, rCBF, mean delay time, and apparent diffusion coefficient in volumes of interest for contrast-enhancing lesion (CEL), non-CEL, and contralateral tissue. Glioblastomas with >5 vessels seen within the lesion on postcontrast T1-weighted images were considered hyper-GVP-MRI. Prognostic factors were evaluated by Kaplan-Meier survival, ROC analyses, and hazard ratios (HR).

RESULTS

Gioblastomas were considered hyper-GVP-MRI in 58 (60.4%) patients. Patients with hyper-GVP-MRI glioblastomas were older, had higher volumeCEL, increased rCBFCEL and poor survival. Combining Stupp protocol (HR: 0.604; 95% CI: 0.459-0.796), age (HR: 0.163; 95% CI: 0.090-0.297), and GVP-MRI (HR: 1.481; 95% CI: 0.909-2.414) best predicted survival at 1 year (AUC 0.901, 83.3% sensitivity, 93.3% specificity, 96.2% PPV, 73.7% NPV).

CONCLUSION

Our preliminary data suggest that combining clinical parameters and vascular pattern on MRI improves survival prediction in 'de novo' glioblastoma. Cross-validation studies in other populations are necessary to test the generalizability of our findings.

CLINICAL RELEVANCE/APPLICATION

Information about baseline risk and prognosis is crucial for assigning patients with glioblastomas to optimized treatment regimens in clinical practice or to subgroups in clinical trials.

RC205-12 Application of Radiomics & Deep-Learning in Brain Tumor Imaging

Monday, Nov. 26 11:30AM - 12:00PM Room: S406B

Participants

Philipp Kickingereder, MD, MBA, Heidelberg, Germany (Presenter) Nothing to Disclose

For information about this presentation, contact:

philipp.kickingereder@med.uni-heidelberg.de

LEARNING OBJECTIVES

1) To understand and critically reflect the impact of radiomics and radiogenomics. 2) To understand the impact of deep-learning for guiding treatment decisions and advancing precision and personalized medicine in neuro-oncology.



RC215

Breast Series: Hot Topics (The In-Person Presentation is Supported by an Unrestricted Educational Grant from Hologic)

Monday, Nov. 26 8:30AM - 12:00PM Room: Arie Crown Theater



AMA PRA Category 1 Credits ™: 3.50 ARRT Category A+ Credits: 4.00

FDA Discussions may include off-label uses.

Participants

Linda Moy, MD, New York, NY (Moderator) Nothing to Disclose

Fiona J. Gilbert, MD, Cambridge, United Kingdom (*Moderator*) Research Grant, Hologic, Inc; Research Grant, General Electric Company; Research Grant, GlaxoSmithKline plc; Research Consultant, Alphabet Inc

Sub-Events

RC215-01 Radiomics

Monday, Nov. 26 8:30AM - 8:50AM Room: Arie Crown Theater

Participants Karen Drukker, PhD, Chicago, IL (*Presenter*) Royalties, Hologic, Inc

For information about this presentation, contact:

kdrukker@uchicago.edu

Active Handout:Karen Drukker

http://abstract.rsna.org/uploads/2018/18000478/RSNA2018_Drukker_Handout RC215-01.pdf

LEARNING OBJECTIVES

1) Identify the scientific premise, motivation, and increasing role of radiomics in medical imaging. 2) Compare 'conventional' radiomics methods and deep learning-based radiomics methods. 3) Assess some of the challenges for radiomics-based decision support systems in becoming powerful players in modern precision medicine.

RC215-02 Quantitative Diffusion-Weighted MRI of Estrogen Receptor-Positive, Lymph Node-Negative Invasive Breast Cancer: Association between Whole-Lesion Apparent Diffusion Coefficient Metrics and Recurrence Risk

Monday, Nov. 26 8:50AM - 9:00AM Room: Arie Crown Theater

Participants

Jin You Kim, MD, Busan, Korea, Republic Of (*Presenter*) Nothing to Disclose Lee Hwangbo, MD, Pusan, Korea, Republic Of (*Abstract Co-Author*) Nothing to Disclose Jin Joo Kim, MD, Busan, Korea, Republic Of (*Abstract Co-Author*) Nothing to Disclose Suk Kim, MD, Pusan, Korea, Republic Of (*Abstract Co-Author*) Nothing to Disclose

For information about this presentation, contact:

youdosa@naver.com

PURPOSE

To investigate possible associations between quantitative apparent diffusion coefficient (ADC) metrics derived from whole-lesion histogram analysis and breast cancer recurrence risk in patients with estrogen receptor (ER)-positive, lymph node-negative invasive breast cancer who underwent the Oncotype DX assay.

METHOD AND MATERIALS

Institutional review board approval was obtained for this retrospective study, which was conducted on 74 women (mean age, 49.3 years) with ER-positive, lymph node-negative invasive breast cancer who underwent the Oncotype DX assay and preoperative diffusion-weighted MRI from July 2015 to January 2018. Histogram analysis of pixel-based ADC data of whole tumors was performed by two radiologists using a software tool and various ADC histogram parameters (mean, minimum, maximum, and 5th, 25th, 50th, 75th, and 95th percentile ADCs) were extracted. The ADC difference value (defined as the difference between minimum and maximum ADC) was calculated to assess intratumoral heterogeneity. Associations between quantitative ADC metrics and Oncotype DX risk groups (low [recurrence score (RS) <18], intermediate (RS 18-30), and high [RS >30]) were evaluated by receiver operating characteristic (ROC) curve and logistic regression analyses.

RESULTS

Whole-lesion histogram analysis showed minimum ADCs, maximum ADCs, and ADC difference values were significantly different between low and non-low (ie, intermediate and high) risk groups (0.604, 1.478, and 0.874×10 -3mm2/s versus 0.374, 1.687, and

 1.321×10 -3mm2/s, respectively; P<0.001, P=0.010, and P<0.001, respectively). The ADC difference value yielded the largest area under the ROC curve (0.771; 95% confidence interval [CI]: 0.650, 0.891; P<0.001) for differentiating the two groups. Multivariate regression analysis showed that the ADC difference value was the only significant factor associated with low Oncotype DX risk group (adjusted odds ratio = 0.998; 95% CI: 0.996, 0.999; P<0.001).

CONCLUSION

The ADC difference value derived from whole-lesion histogram analysis could be helpful for identifying ER-positive, lymph nodenegative invasive breast cancer patients with low risk of recurrence.

CLINICAL RELEVANCE/APPLICATION

In estrogen receptor-positive, lymph node-negative breast cancer, the ADC difference value derived from whole-lesion histogram assessments might serve as quantitative biomarkers of recurrence risk.

RC215-03 Radiomic Phenotypes of Tumor Heterogeneity from Pre-Operative DCE-MRI Predict Breast Cancer Recurrence after 10-Year Follow-Up: Phenotype Discovery and Independent Validation

Monday, Nov. 26 9:00AM - 9:10AM Room: Arie Crown Theater

Participants

Rhea Chitalia, Philadelphia, PA (*Presenter*) Nothing to Disclose Jennifer Rowland, MD, Philadelphia, PA (*Abstract Co-Author*) Nothing to Disclose Elizabeth S. McDonald, MD, Philadelphia, PA (*Abstract Co-Author*) Nothing to Disclose Lauren Pantalone, BS, Philadelphia, PA (*Abstract Co-Author*) Nothing to Disclose Eric A. Cohen, Philadelphia, PA (*Abstract Co-Author*) Nothing to Disclose Aimilia Gastounioti, Philadelphia, PA (*Abstract Co-Author*) Nothing to Disclose Kathleen M. Thomas, BS, Philadelphia, PA (*Abstract Co-Author*) Nothing to Disclose Rebecca Batiste, Philadelphia, PA (*Abstract Co-Author*) Nothing to Disclose Michael D. Feldman, MD, PhD, Philadelphia, PA (*Abstract Co-Author*) Nothing to Disclose NV Advisory Board, XIFIN, Inc Mitchell D. Schnall, MD, PhD, Philadelphia, PA (*Abstract Co-Author*) Nothing to Disclose Emily F. Conant, MD, Philadelphia, PA (*Abstract Co-Author*) Nothing to Disclose Emily F. Conant, MD, Philadelphia, PA (*Abstract Co-Author*) Nothing to Disclose Emily F. Conant, MD, Philadelphia, PA (*Abstract Co-Author*) Nothing to Disclose Emily F. Conant, MD, Philadelphia, PA (*Abstract Co-Author*) Nothing to Disclose Emily F. Conant, MD, Philadelphia, PA (*Abstract Co-Author*) Nothing to Disclose Emily F. Conant, MD, Philadelphia, PA (*Abstract Co-Author*) Nothing to Disclose Emily F. Conant, MD, Philadelphia, PA (*Abstract Co-Author*) Nothing to Disclose Emily F. Conant, MD, Philadelphia, PA (*Abstract Co-Author*) Nothing to Disclose

For information about this presentation, contact:

rhea.chitalia@uphs.upenn.edu

PURPOSE

To validate intrinsic imaging phenotypes of tumor heterogeneity and evaluate their prognostic performance in predicting 10-year recurrence.

METHOD AND MATERIALS

Pre-treatment DCE-MRI scans of 94 women with primary invasive breast cancer and 10-year follow up data available were retrospectively analyzed from a clinical trial cohort at our institution (2002-2006). For each woman, a signal enhancement ratio map was generated for the most representative slice of the primary lesion from which morphologic features were calculated. Radiomic features (histogram, run-length, structural, and co-occurrence matrix features) were extracted and summarized over tumor quadrants. Intrinsic phenotypes of tumor heterogeneity were identified via unsupervised hierarchical clustering applied to the extracted feature vectors, with significant clusters found using Consensus Clustering and the SigClust method. Differences across phenotypes by hormone receptor status, tumor size, post-surgery therapy, TNM staging, and recurrence outcomes were assessed using Chi-square and Kruskal-Wallis tests. An independent dataset of 116 women diagnosed with primary invasive breast cancer (2002-2006), available via The Cancer Imaging Archive, was used to validate phenotype reproducibility. Survival probabilities across phenotypes were evaluated using Kaplan-Meier curves and phenotype cluster assignments were added to a baseline Cox proportional hazards model with established histopathologic prognostic factors to predict RFS.

RESULTS

Three significant phenotypes of low, medium, and high heterogeneity were identified in the discovery cohort and reproduced in the validation cohort (p<0.001). No recurrent cases were found in the low heterogeneity phenotype (p<0.001). Clinical stage, mitotic grade, lymph invasion, and nuclear grade were different across phenotypes (p<=0.02). Kaplan-Meier curves showed significant differences (p<0.001) in RFS probabilities across phenotypes. The augmented model including phenotype assignment had a higher discriminatory capacity (c-statistic= 0.80) compared to a baseline model with only established prognostic factors (c-statistic= 0.65, p<0.01).

CONCLUSION

Intrinsic imaging phenotypes of tumor heterogeneity can predict 10-year recurrence as validated in an independent dataset.

CLINICAL RELEVANCE/APPLICATION

Radiomic phenotypes could provide a non-invasive characterization of tumor heterogeneity to augment personalized prognosis and treatment.

Honored Educators

Presenters or authors on this event have been recognized as RSNA Honored Educators for participating in multiple qualifying educational activities. Honored Educators are invested in furthering the profession of radiology by delivering high-quality educational content in their field of study. Learn how you can become an honored educator by visiting the website at: https://www.rsna.org/Honored-Educator-Award/ Mitchell D. Schnall, MD, PhD - 2013 Honored Educator

RC215-04 Robustness of Computer-aided Diagnosis of Breast Cancer Using Radiomics and Machine Learning Classification of 1,461 Lesions across Populations in China and the United States

Participants

Heather Whitney, PhD, Wheaton, IL (Presenter) Nothing to Disclose

Hui Li, PHD, Chicago, IL (Abstract Co-Author) Nothing to Disclose

Yu Ji, MD, Chicago, IL (Abstract Co-Author) Nothing to Disclose

Alexandra V. Edwards, Chicago, IL (*Abstract Co-Author*) Research Consultant, QView Medical, Inc; Research Consultant, Quantitative Insights, Inc

John Papaioannou, MSc, Chicago, IL (Abstract Co-Author) Research Consultant, QView Medical, Inc.

Peifang Liu, MD, PhD, Tianjin, China (*Abstract Co-Author*) Nothing to Disclose

Maryellen L. Giger, PhD, Chicago, IL (*Abstract Co-Author*) Stockholder, Hologic, Inc; Shareholder, Quantitative Insights, Inc; Shareholder, QView Medical, Inc; Co-founder, Quantitative Insights, Inc; Royalties, Hologic, Inc; Royalties, General Electric Company; Royalties, MEDIAN Technologies; Royalties, Riverain Technologies, LLC; Royalties, Mitsubishi Corporation; Royalties, Canon Medical Systems Corporation

For information about this presentation, contact:

hwhitney@uchicago.edu

PURPOSE

To assess the performance of computer aided diagnosis (CADx) in breast lesions imaged with DCE-MR in two patient cohorts, one in China and one in the United States (US), using extracted radiomic features and machine learning classification.

METHOD AND MATERIALS

Dynamic contrast-enhanced magnetic resonance (DCE-MR) images of 1,461 breast lesions (from China, GE scanners: 300 benign lesions, 302 malignant cancers; from the US, Philips scanners: 268 benign lesions, 591 malignant cancers) were collected under HIPAA and IRB compliance. The lesions were segmented automatically using a fuzzy c-means method. Thirty-eight radiomic features describing size, shape, morphology, kinetics, and texture were extracted using previously reported methods. The performance of CADx for classification between benign lesions and malignant cancers was evaluated with two methodologies: (a) independent training and testing of the datasets, with each set serving as a training set while the other served as a testing set; and (b) tenfold cross validation within each set. Classification was performed using support vector machines with optimization of the hyperparameters. The area under the ROC curve (AUC) served as figure of merit, with its value and standard error determined using the conventional binormal model. The AUCs resulting from (a) and (b) were compared within and between each methodology. Difference in AUC was significantly different when p < 0.05.

RESULTS

When radiomic features extracted from MRIs acquired in China were used to train the machine classifiers and independent testing was conducted on MRIs acquired in the US, AUC = 0.77 (0.02), while the reverse resulted in AUC = 0.79 (0.02). For cross-validation within each set, AUC = 0.82 (0.02) for the US database and AUC = 0.80 (0.02) for the China database. AUCs compared across methodologies failed to show significant difference.

CONCLUSION

Computer aided diagnosis of breast lesions demonstrated potential robustness across independent populations in both independent training/testing and in cross validation.

CLINICAL RELEVANCE/APPLICATION

Radiomic features extracted from DCE-MRI may be robust for classifying breast lesions as benign or malignant across two cohorts (one in China, one in US), enhancing translation to clinical use.

RC215-05 Radiogenomics

Monday, Nov. 26 9:20AM - 9:40AM Room: Arie Crown Theater

Participants

Lars J. Grimm, MD, Durham, NC (Presenter) Editorial Advisory Board, Medscape, LLC; Educational program support, Hologic, Inc

For information about this presentation, contact:

lars.grimm@duke.edu

LEARNING OBJECTIVES

1) Define radiogenomics and describe how it differs from radiomics. 2) Examine the limitations of current radiogenomics research. 3) Assess the utility of radiogenomics in clinical practice. 4) Develop a framework to evaluate future radiogenomics research.

RC215-06 Proteomic Expression Underlying Quantitative MRI Features in Breast Cancer: A Radioproteomics Study

Monday, Nov. 26 9:40AM - 9:50AM Room: Arie Crown Theater

Participants

Ryan M. Hausler, BS, Pittsburgh, PA (*Presenter*) Nothing to Disclose Ruimei Chai, Shenyang, China (*Abstract Co-Author*) Nothing to Disclose Dooman Arefan, PhD, Pittsburgh, PA (*Abstract Co-Author*) Nothing to Disclose Jules H. Sumkin, DO, Pittsburgh, PA (*Abstract Co-Author*) Research Grant, Hologic, Inc; Research Grant, General Electric Company Min Sun, MD,PhD, Pittsburgh, PA (*Abstract Co-Author*) Nothing to Disclose Shandong Wu, PhD, MSc, Philadelphia, PA (*Abstract Co-Author*) Nothing to Disclose

For information about this presentation, contact:

PURPOSE

The complementary analysis of breast cancer via radiology imaging and molecular pathology approaches has spurred radiogenomics and radioproteomics studies. We performed an investigation of the relationships between quantitative radiomic imaging phenotype data and underlying proteomic expression, with the goal of improving precise breast cancer diagnosis and cancer behavior characterization.

METHOD AND MATERIALS

We identified a retrospective cohort of 40 invasive breast cancer patients from a single medical center. Their integrated protein expression data were obtained from The Cancer Genome Atlas study. The proteomic data was acquired via Reverse Phase Protein Array (RPPA) to measure the expression of 217 breast cancer related proteins and phospho-proteins. Dynamic Contrast Enhanced Magnetic Resonance Imaging (DCE-MRI) data of the 40 patients were collected from clinical archive, all acquired with a 1.5T same-vendor scanner. A set of 30 radiomic imaging features were extracted from automatically-segmented tumor volume in all 40 DCE-MRIs to capture tumor morphological and contrast enhancement characteristics. Multivariate linear regression was used to map the associations between each imaging feature with each of the 217 protein expressions, controlling for patient age and cancer stage. A p value was obtained evaluating the significance of the association and was adjusted for multiple comparisons of the selected radiomic feature against every protein. Adjusted p values less than 0.05 were recorded.

RESULTS

The average patient age at scan was 38.7±12 years, 10 (25%) of which were pre- with the rest post-menopausal. We found a variety of expression of cancer related proteins were significantly associated (positively or negatively) with a subset of morphological and contrast enhancement kinetics related imaging features. For example, ERCC5 (a protein responsible for DNA repair following UV-induced damage) is negatively associated with the tumor brightness and contrast agent uptake rates. The full association map is shown in the attached figure.

CONCLUSION

Our study showed that the expression of several cancer related proteins were found to be linearly associated with quantitative DCE-MRI-derived phenotype features in invasive breast tumors.

CLINICAL RELEVANCE/APPLICATION

Radioproteomic studies of cancer can help to decipher how molecular mechanisms may regulate the development of specific tumor phenotypes.

RC215-07 Prediction of 21-gene Recurrence Score in Patients with Estrogen Receptor-positive Early-Stage Breast Cancer Using MRI-based Radiomics Nomogram

Monday, Nov. 26 9:50AM - 10:00AM Room: Arie Crown Theater

Participants

Nam Joo Lee, Seoul, Korea, Republic Of (*Presenter*) Nothing to Disclose Hee Jung Shin, MD, Seoul, Korea, Republic Of (*Abstract Co-Author*) Nothing to Disclose Hwa Jung Kim, Seoul, Korea, Republic Of (*Abstract Co-Author*) Nothing to Disclose Ki Chang Shin, Seoul, Korea, Republic Of (*Abstract Co-Author*) Nothing to Disclose Jong Won Lee, Seoul, Korea, Republic Of (*Abstract Co-Author*) Nothing to Disclose Sae Byul Lee, Seoul, Korea, Republic Of (*Abstract Co-Author*) Nothing to Disclose Eun Young Chae, Seoul, Korea, Republic Of (*Abstract Co-Author*) Nothing to Disclose Woo Jung Choi, MD, Seoul, Korea, Republic Of (*Abstract Co-Author*) Nothing to Disclose Joo Hee Cha, MD, Seoul, Korea, Republic Of (*Abstract Co-Author*) Nothing to Disclose Hak Hee Kim, MD, Seoul, Korea, Republic Of (*Abstract Co-Author*) Nothing to Disclose Ga Young Yoon, MD, Seoul, Korea, Republic Of (*Abstract Co-Author*) Nothing to Disclose

For information about this presentation, contact:

docshin@amc.seoul.kr

PURPOSE

To develop a breast MRI-based radiomics nomogram including pathologic factors which can predict low-risk recurrence score (RS) on 21-gene RS assay in patients with estrogen receptor-positive early-stage breast cancer (EBC).

METHOD AND MATERIALS

From 2011 to 2017, a total of 547 tumors in 539 patients with EBC who underwent preoperative breast MRI were retrospectively included in this study. Among them, low-risk was 320 (58.5%), intermediate-risk was 180 (32.9%), and high-risk was 47 (8.6%). We extracted 744 quantitative MR radiomic features from computerized three-dimensional segmentations of each tumor generated computer-extracted image phenotypes (CEIP) within the intratumoral regions of early post-contrast T1-weighted images, percent enhancement (PE) map, signal enhancement ratio (SER) map, and T2-weighted images. We divided 547 cases into a training set (n=365) and a validation set (n=182). Elastic net was used for feature selection and radiomics score building. Multivariate logistic regression analysis was used to develop a prediction model, we incorporated the radiomics score and independent pathologic risk factors and build a radiomics nomogram. Internal validation for an independent validation set (n=182) was performed.

RESULTS

The radiomics score, which consisted of 24 selected CEIPs, was significantly associated with the prediction of recurrence (C-index, 0.769 for training set and 0.745 for validation set). Independent pathologic predictors contained in the nomogram were progesterone receptor status, nuclear grade, histologic grade, extensive intraductal component, lymphovascular invasion, P53, and Ki67 status, and their C-index was 0.858 for training set and 0.774 for validation set. Addition of radiomics score to the pathologic nomogram showed an incremental value of 0.054 and 0.092, respectively. Radiomics nomogram showed good prediction of low-risk RS, with a C-index of 0.912 for training set and 0.866 for validation set.

CONCLUSION

This study shows that a radiomics nomogram which incorporates the MRI-based radiomics score and pathologic features, can be used to help the preoperative individualized prediction of low-risk RS in patients with EBC.

CLINICAL RELEVANCE/APPLICATION

Prediction nomogram using breast MRI-based radiomics score and pathologic predictors can be used to facilitate the preoperative individualized prediction of low-risk RS on 21-gene RS assay in patients with EBC.

RC215-08 Can Histogram Analysis of Dynamic Contrast-Enhanced MRI and Apparent Diffusion Coefficient Map Predict Molecular Subtypes of Invasive Breast Cancers?

Monday, Nov. 26 10:00AM - 10:10AM Room: Arie Crown Theater

Participants

Joao V. Horvat, MD, Sao Paulo, Brazil (*Presenter*) Nothing to Disclose Doris Leithner, MD, New York, NY (*Abstract Co-Author*) Nothing to Disclose Blanca Bernard-Davila, MPH,MS, New York, NY (*Abstract Co-Author*) Nothing to Disclose Rosa E. Ochoa Albiztegui II, MD, Mexico CIty, Mexico (*Abstract Co-Author*) Nothing to Disclose Danny F. Martinez, BSC,MSc, New York, NY (*Abstract Co-Author*) Nothing to Disclose Olivia Sutton, New York, NY (*Abstract Co-Author*) Nothing to Disclose Elizabeth A. Morris, MD, New York, NY (*Abstract Co-Author*) Nothing to Disclose Sunitha Thakur, PhD, MS, New York, NY (*Abstract Co-Author*) Nothing to Disclose Katja Pinker-Domenig, MD, Vienna, Austria (*Abstract Co-Author*) Nothing to Disclose

For information about this presentation, contact:

joaohorvat@gmail.com

PURPOSE

To evaluate if histogram analysis of dynamic contrast-enhanced (DCE) MRI and apparent diffusion coefficient (ADC) maps with diffusion-weighted imaging (DWI) can predict molecular subtypes of invasive breast cancers.

METHOD AND MATERIALS

In this HIPAA-compliant and IRB-approved study we retrospectively evaluated 91 consecutive patients from January 2011 to January 2013 with invasive ductal carcinoma of the breast who underwent multiparametric MRI with DCE and DWI at our institution. The exclusion criteria were 1) lesion smaller than 1 cm, 2) previous treatment for breast cancer, 3) pathology report unavailable, and 4) poor image quality. One experienced breast radiologist drew a region of interest on DCE MRI and ADC maps on the slice with the largest diameter of the solid portion of the lesion avoiding cystic areas and biopsy markers. The histogram analysis was performed and the mean, variance, kurtosis and skewness were calculated. Molecular breast cancer subtypes were derived by IHC surrogates. Tumors were classified as luminal A if either ER or PR was positive and HER2 was negative, Luminal B if either ER or PR was positive and HER2 positive and triple-negative if ER, PR and HER2 were negative. Nonparametric Mann-Whitney U test and Kruskal-Wallis were used to compare groups of molecular subtypes. P-values <0.05 were accepted to be statistically significant.

RESULTS

The histogram analysis of DCE images and ADC maps of 91 breast cancers demonstrated no significant difference among breast tumor molecular subtypes. Measurements of the mean, variance, kurtosis and skewness were used to compare luminal A/B with HER-2 enriched/triple-negative cancers, without significant results for both DCE (p-value = 0.405, 0.252, 0.667, 0.809) and ADC (0.204, 0.081, 0.941, 0.574), respectively. Histogram measurements were also used to compare luminal A with other subtypes and also demonstrated no significant difference for DCE (0.659, 0.162, 0.516, 0.833) and ADC (0.204, 0.222, 0.495, 0.896).

CONCLUSION

Histogram analysis of DCE MRI and ADC map cannot predict molecular subtypes of invasive breast cancers.

CLINICAL RELEVANCE/APPLICATION

Despite many valuable applications of histogram analysis in diagnostic imaging, it cannot predict molecular subtypes of invasive breast cancers.

RC215-09 CESM Enhancement Pattern and Intensity and Its Correlation to Breast Cancer Immunophenotype: Preliminary Results

Monday, Nov. 26 10:10AM - 10:20AM Room: Arie Crown Theater

Participants

Elzbieta Luczynska, MD, Cracow, Poland (*Presenter*) Nothing to Disclose Sylwia Heinze, PhD, Cracow, Poland (*Abstract Co-Author*) Nothing to Disclose Joanna Niemiec, Cracow, Poland (*Abstract Co-Author*) Nothing to Disclose Agnieszka Adamczyk, Cracow, Poland (*Abstract Co-Author*) Wojciech Rudnicki, MD, Krakow, Poland (*Abstract Co-Author*) Nothing to Disclose

For information about this presentation, contact:

z5luczyn@cyfronet.pl

PURPOSE

The differences in the intensity and pattern of enhancement in CESM between breast carcinomas might result from the differences in the amount of contrast that leaked out from the blood vessels and timely arrested in the interstitium. The aim of this paper is to study the expression of podoplanin in cancer stroma and its relation to breast cancer immunophenotype. Patients with lesions enhancing on CESM were subjected to biopsy - material obtained during biopsies was histopathologically verified. In the present study we retrospectively investigated 97 invasive breast carcinomas diagnosed in 94 patients. This study was performed in compliance with the Declaration of Helsinki and it received the approval of Ethical Committee at the Regional Medical Chamber. For each tumor enhancing on CESM, the intensity and the pattern of enhancement were evaluated. The enhancement of contrast agent uptake was qualitatively assessed as weak/medium or strong ,while the pattern as heterogenous or homogenous. Lymphatic vessels were defined as strongly podoplanin-stained structures with lymphatic vessel characteristics , clearly distinguishable from other tissue structures and cells. We classified tumor stroma as: podoplanin-sparse and podoplanin-rich.

RESULTS

Strong enhancement on CESM was found more frequently in: large tumors (pT>1), node-positive carcinomas, in tumors with podoplanin-sparse stroma vs. tumors with podoplanin-rich stroma . We found no relationship between enhancement on CESM and: tumor grade, histological type of cancer, breast cancer immunophenotype and Ki-67LI. However, in luminal A tumors strong enhancement on CESM was insignificantly more frequent as compared to neoplasms with non-luminal A subtype .

CONCLUSION

In our study prognostic significance of selected CESM features was found for the first time: strong and heterogenous enhancement on CESM was related to poor patients' outcome. In this study, the aforementioned correlation was additionally confirmed by the relationship between strong enhancement on CESM and nodal involvement or large tumor size.

CLINICAL RELEVANCE/APPLICATION

Our results may suggest that intensity and pattern of enhancement on CESM might bring (together with the results of diagnostic imaging methods) not only the confirmation of presence or absence of tumor, but also prognostic information.

RC215-10 Development of MRI-based Radiomics Nomogram for the Prediction of Recurrence in Patients with Luminal-type Breast Cancer: A Nested Case-Control Study

Monday, Nov. 26 10:20AM - 10:30AM Room: Arie Crown Theater

Participants

Bo Yong Chung, Seoul, Korea, Republic Of (*Presenter*) Nothing to Disclose Hee Jung Shin, MD, Seoul, Korea, Republic Of (*Abstract Co-Author*) Nothing to Disclose Hwa Jung Kim, Seoul, Korea, Republic Of (*Abstract Co-Author*) Nothing to Disclose Ki Chang Shin, Seoul, Korea, Republic Of (*Abstract Co-Author*) Nothing to Disclose Eun Young Chae, Seoul, Korea, Republic Of (*Abstract Co-Author*) Nothing to Disclose Woo Jung Choi, MD, Seoul, Korea, Republic Of (*Abstract Co-Author*) Nothing to Disclose Joo Hee Cha, MD, Seoul, Korea, Republic Of (*Abstract Co-Author*) Nothing to Disclose Hak Hee Kim, MD, Seoul, Korea, Republic Of (*Abstract Co-Author*) Nothing to Disclose Ga Young Yoon, MD, Seoul, Korea, Republic Of (*Abstract Co-Author*) Nothing to Disclose

For information about this presentation, contact:

docshin@amnc.seoul.kr

PURPOSE

To determine whether breast MRI-based radiomics nomogram including pathologic factors can predict recurrences or distant metastasis in patients with luminal-type breast cancer (LTBC).

METHOD AND MATERIALS

From 2006 to 2012, a total of 348 patients with LTBC who underwent preoperative breast MRI were retrospectively included in this study. Patients with recurrence were 174. Patients without recurrence were matched in terms of age, stage, and type of chemotherapy, and developed 174 nested case-control pairs. We extracted 804 quantitative MR radiomic features of computerized three-dimensional segmentations of each cancer generated computer-extracted image phenotypes (CEIP) within the intratumoral regions of early post-contrast T1-weighted images, percent enhancement (PE) map, signal enhancement ratio (SER) map, and T2-weighted images. We divided 174 case-control matches into a training set (n=232) and a validation set (n=116). Elastic net was used for feature selection and radiomics score building. Multivariate logistic regression analysis was used to develop the prediction model, we incorporated the radiomics score and independent pathologic risk factors and build a radiomics nomogram. Internal validation for an independent validation set (n=76) was performed.

RESULTS

The radiomics score, which consisted of 14 selected CEIPs, was significantly associated with the prediction of recurrence (C-index, 0.864 for training set and 0.815 for validation set). Independent pathologic predictors contained in the nomogram were progesterone receptor status, P53, lymphovascular invasion, Ki67 status, and lymph node ratio, and their C-index was 0.695 for training set and 0.701 for validation set. Addition of radiomics score to the pathologic nomogram showed an incremental value of 0.211 and 0.177, respectively. Radiomics nomogram showed good prediction of recurrence, with a C-index of 0.906 for training set and 0.878 for validation set.

CONCLUSION

This study shows that a radiomics nomogram which incorporates the MRI-based radiomics score and pathologic features, can be used to help the individualized prediction of local or distant recurrence in patients with LTBC.

CLINICAL RELEVANCE/APPLICATION

Nomogram using breast MRI-based radiomics score and pathologic predictors can be used to facilitate the individualized prediction of recurrence in patients with LTBC.

RC215-11 Horizons with Deep Learning

Monday, Nov. 26 10:40AM - 11:00AM Room: Arie Crown Theater

Participants

Robert M. Nishikawa, PhD, Pittsburgh, PA (*Presenter*) Royalties, Hologic, Inc; Research Grant, Hologic, Inc; Research Consultant, iCAD, Inc; Research Grant, Koios Medical

For information about this presentation, contact:

nishikawarm@upmc.edu

LEARNING OBJECTIVES

1) To understand the importance implementing deep learning tools into a breast imager's workflow. 2) To understand applications of deep learning outside of detection and characterization of breast lesions.

RC215-12 Incorporating Patient Characteristics in Breast Cancer Screening with Deep Convolutional Neural (DCN) Network

Monday, Nov. 26 11:00AM - 11:10AM Room: Arie Crown Theater

Participants

Eric Kim, MD, New York, NY (*Presenter*) Nothing to Disclose Krzysztof J. Geras, New York City, NY (*Abstract Co-Author*) Nothing to Disclose Nan Wu, New York City, NY (*Abstract Co-Author*) Nothing to Disclose Yiqiu Shen, New York City, NY (*Abstract Co-Author*) Nothing to Disclose Jingyi Su, New York City, NY (*Abstract Co-Author*) Nothing to Disclose Sungheon Kim, PhD, New York, NY (*Abstract Co-Author*) Nothing to Disclose Stacey Wolfson, New York, NY (*Abstract Co-Author*) Nothing to Disclose Linda Moy, MD, New York, NY (*Abstract Co-Author*) Nothing to Disclose Kyunghyun Cho, New York City, NY (*Abstract Co-Author*) Nothing to Disclose

For information about this presentation, contact:

kime18@nyumc.org

PURPOSE

To determine if the addition of patient characteristics obtained from the electronic health records may improve the ability of a DCN network to detect and classify lesions on screening mammography.

METHOD AND MATERIALS

This is a retrospective study of a DCN network trained on over 250,000 screening mammograms performed at our institution from 2010-2016. The patients were sorted according to the date of their latest exam and divided into training (first 80%), validation (next 10%), and test (last 10%) sets. In the test phase, only the most recent exam was used for each patient. Patient characteristics including age, family history of breast cancer, and history of prior examinations were extracted from the radiologist reports. The original high-resolution images and extracted side information were utilized as inputs by a multi-column DCN network to classify BI-RADS category. The model was evaluated using area under the receiver operating characteristic curve (AUC) analysis. Analysis was also performed after stratifying patients by age-group and breast density (dense vs non-dense).

RESULTS

The overall performance of the DCN network improved with the addition of patient characteristics in comparison to using images alone (AUC 0.750 vs 0.733). This improvement was especially notable for BI-RADS 0 cases, with an AUC of 0.664 vs 0.618. Performance also generally improved with increasing age, with an average AUC of 0.759 in patients over 70 years of age. Finally, performance of the model is superior in dense breasts vs non-dense breasts (AUC 0.740 vs AUC 0.707).

CONCLUSION

The performance of DCN networks in evaluating screening mammograms increases with the addition of patient characteristics information, especially in the abnormal BI-RADS 0 cases which are the most difficult to evaluate.

CLINICAL RELEVANCE/APPLICATION

End-to-end architectures of DCN networks, like ours, support the incorporation of patient characteristics to increase the accuracy of deep learning algorithms in breast cancer screening.

RC215-13 Detecting Breast Cancer in Mammography: A Deep Learning-Based Computer System versus 101 Radiologists

Monday, Nov. 26 11:10AM - 11:20AM Room: Arie Crown Theater

Participants

Alejandro Rodriguez-Ruiz, Nijmegen, Netherlands (*Abstract Co-Author*) Nothing to Disclose Albert Gubern-Merida, PhD, Nijmegen, Netherlands (*Abstract Co-Author*) Employee, ScreenPoint Medical Kristina Lang, MD,PhD, Malmo, Sweden (*Abstract Co-Author*) Travel support, Siemens AG Speaker, Siemens AG Mireille Broeders, PhD, Nijmegen, Netherlands (*Abstract Co-Author*) Nothing to Disclose Gisella Gennaro, PhD, Padua, Italy (*Abstract Co-Author*) Nothing to Disclose Paola Clauser, MD, Vienna, Austria (*Abstract Co-Author*) Nothing to Disclose Margarita Chevalier, PhD, Madrid, Spain (*Abstract Co-Author*) Nothing to Disclose Thomas H. Helbich, MD, Vienna, Austria (*Abstract Co-Author*) Nothing to Disclose Thomas H. Helbich, MD, Vienna, Austria (*Abstract Co-Author*) Research Grant, Medicor, Inc Research Grant, Siemens AG Research Grant, C. R. Bard, Inc Tao Tan, Nijmegen, Netherlands (*Abstract Co-Author*) Research Grant, QView Medical, Inc Thomas Mertelmeier, PHD, Forchheim, Germany (*Abstract Co-Author*) Employee, Siemens AG; Stockholder, Siemens AG Matthew G. Wallis, MD, Cambridge, United Kingdom (Abstract Co-Author) Nothing to Disclose

Ingvar T. Andersson, MD, PhD, Malmo, Sweden (*Abstract Co-Author*) Nothing to Disclose

Sophia Zackrisson, Malmo, Sweden (*Abstract Co-Author*) Speaker, AstraZeneca PLC ; Speaker, Siemens AG; Travel support, AstraZeneca PLC; Travel support, Siemens AG

Ritse M. Mann, MD, PhD, Nijmegen, Netherlands (*Abstract Co-Author*) Researcher, Siemens AG ; Researcher, Seno Medical Instruments, Inc; Researcher, Identification Solutions, Inc; Researcher, Micrima Limited; Researcher, Medtronic plc; Scientific Advisor, ScreenPoint Medical BV; Scientific Advisor, Transonic Imaging, Inc; Stockholder, Transonic Imaging, Inc Ioannis Sechopoulos, PhD, Atlanta, GA (*Presenter*) Research Grant, Siemens AG; Research Grant, Canon Medical Systems Corporation; Speakers Bureau, Siemens AG; Scientific Advisory Board, Fischer Medical

PURPOSE

To compare the stand-alone performance of a computer-based detection system to that of radiologists in detecting breast cancer on digital mammography (DM).

METHOD AND MATERIALS

Nine multi-reader multi-case (MRMC) study datasets previously used for different performance evaluation purposes in seven countries were collected. Each dataset consisted of DM exams acquired with systems from four different vendors, multiple radiologists' assessments per exam (BI-RADS or probability-of-malignancy scores), and ground truth: yielding a total of 2,458 exams (608 malignant) and interpretations by 101 radiologists (28,373 independent exam interpretations). A deep learning-based computer system (Transpara, ScreenPoint Medical, Nijmegen, The Netherlands) was used to automatically analyze each exam, resulting in a score for suspiciousness of cancer (1-100). Independently for each dataset, the area under the receiver operating characteristic curve (AUC) and the sensitivity at the radiologists' specificity level (case recall) were compared between the computer and radiologists using MRMC analysis of variance.

RESULTS

The performance of the computer system was not significantly different to that of the average of radiologists in eight of nine datasets (AUC differences ranged between -2.6% and +2.5%, P>0.329) and was significantly better in the ninth (+4.6%, P=0.036). At the average specificity of the radiologists, the computer had an equal or higher sensitivity (+0-9%, P>0.083) in all datasets but one (-13%, P=0.066). Comparing individually, the computer had an AUC and sensitivity higher than 53% and 65% of all radiologists, respectively.

CONCLUSION

A computer system based on deep learning has an equivalent performance to radiologists for detecting breast cancer in mammography.

CLINICAL RELEVANCE/APPLICATION

Whether used for decision support (preventing overlook and interpretation errors that are relatively common in the reading of mammography) or as stand-alone readers, computer systems performing at radiologist-like level might herald a breakthrough in the breast cancer detection workflow with mammography. In some situations, where there is a lack of experienced breast radiologists, it might even allow the development or continuation of screening programs.

RC215-14 Improving Accuracy and Efficiency with Concurrent Use of Artificial Intelligence for Digital Breast Tomosynthesis Screening

Monday, Nov. 26 11:20AM - 11:30AM Room: Arie Crown Theater

Participants

Emily F. Conant, MD, Philadelphia, PA (*Presenter*) Grant, Hologic, Inc; Consultant, Hologic, Inc; Grant, iCAD, Inc; Consultant, iCAD, Inc; Speaker, iiCME

Alicia Y. Toledano, DSc, Kensington, MD (Abstract Co-Author) Consultant, iCAD, Inc

Senthil Periaswamy, PhD, Nashua, NH (Abstract Co-Author) Vice President, iCAD, Inc

Sergei V. Fotin, PhD, Nashua, NH (Abstract Co-Author) Principal Scientist, iCAD, Inc; Stockholder, iCAD, Inc

Jonathan Go, Nashua, NH (Abstract Co-Author) Sr. Vice President, iCAD, Inc; ;

Jeffrey W. Hoffmeister, MD, Nashua, NH (Abstract Co-Author) Employee, iCAD, Inc; Stockholder, iCAD, Inc

Justin E. Boatsman, MD, San Antonio, TX (Abstract Co-Author) Consultant, iCad, Inc

For information about this presentation, contact:

Emily.Conant@uphs.upenn.edu

PURPOSE

Screening with Digital Breast Tomosynthesis (DBT) improves accuracy but prolongs reading time when compared to Full-Field Digital Mammography (FFDM) alone. A reader study evaluated concurrent use of Artificial Intelligence (AI) to shorten reading time, while maintaining or improving sensitivity and specificity.

METHOD AND MATERIALS

An AI system based on deep convolutional neural networks was developed to identify suspicious soft tissue and calcific lesions in DBT slices. Findings are outlined in slices, indicating AI's confidence of malignancy with 0-100 scores. A retrospective, fullycrossed, multi-reader, multi-case designed study compared performance of 24 radiologists reading 260 DBT cases both with and without AI. The case set included 65 cancer cases with 66 malignant lesions and 65 cases with biopsy-proven benign lesions. Readings with and without AI occurred in 2 visits separated by a memory washout period of at least 4 weeks. Performance was assessed by measuring Area Under the ROC Curve (AUC) for malignant lesions with AI versus without AI. Reading time, sensitivity, specificity and recall rate were also assessed.

RESULTS

Radiologist performance for detection of malignant lesions, measured by mean AUC, increased 0.057 with use of AI (95% CI: 0.028, 0.087; p < 0.01), from 0.795 without AI to 0.852 with AI. Reading time decreased 52.7% with use of AI (95% CI: 41.8%, 61.5%; p < 0.01), from 64.1 sec without AI to 30.4 sec with AI, using a normalizing transformation to appropriately assess reading times that

were not normally distributed. Sensitivity increased from 77.0% without AI to 85.0% with AI (8.0%; 95% CI: 2.6%, 13.4%; p < 0.01), specificity increased from 62.7% without AI to 69.6% with AI (6.9%; 95% CI: 3.0%, 10.8%; p < 0.01), and recall rate for non-cancers decreased from 38.0% without AI to 30.9% with AI (7.2%; 95% CI: 3.1%, 11.2%; p < 0.01).

CONCLUSION

Concurrent use of AI improves cancer detection with increases of 0.057 in AUC, 8.0% in sensitivity, and 6.9% in specificity; and decreases of 7.2% in recall rate and 52.7% in reading time.

CLINICAL RELEVANCE/APPLICATION

Radiologist's concurrent use of AI for DBT with certainty of finding scores increases detection of breast cancer with significant reduction in reading time while improving sensitivity and specificity.

RC215-15 Breast Cancer Temporal Risk Prediction by Deep Learning and Longitudinal Digital Mammogram Images

Monday, Nov. 26 11:30AM - 11:40AM Room: Arie Crown Theater

Participants

Aly A. Mohamed, PhD, Pittsburgh, PA (*Presenter*) Nothing to Disclose
Wendie A. Berg, MD, PhD, Pittsburgh, PA (*Abstract Co-Author*) Nothing to Disclose
Dooman Arefan, PhD, Pittsburgh, PA (*Abstract Co-Author*) Nothing to Disclose
Jules H. Sumkin, DO, Pittsburgh, PA (*Abstract Co-Author*) Research Grant, Hologic, Inc; Research Grant, General Electric Company
Margarita L. Zuley, MD, Pittsburgh, PA (*Abstract Co-Author*) Investigator, Hologic, Inc
Shandong Wu, PhD, MSc, Philadelphia, PA (*Abstract Co-Author*) Nothing to Disclose

For information about this presentation, contact:

wus3@upmc.edu

PURPOSE

Mammographic breast density is a risk factor and recent studies showed deep learning may identify more predictive imaging risk features than breast density. We performed a study to investigate temporal breast cancer risk prediction by using deep learning models on longitudinal 'normal' screening mammograms acquired prior to diagnosis of breast cancer.

METHOD AND MATERIALS

We conducted a retrospective case-control study on a cohort of 226 patients (1:1 case-control ratio) who underwent standard mammographic screening at our institution during 2006-2013. The unilateral cancer cases (61.3±10.3YO) were all newly diagnosed at 2013 and confirmed by pathology. Asymptomatic cancer-free controls (60.1±10.0 YO) are matched to the cancer cases by age and year of the cancer-diagnosis imaging. All studied women did not have any prior biopsy or recall on mammography. For all cohort, a set of sequential prior 'normal' (negative or benign findings) screening mammogram exams acquired during 2006-2012 were collected (2-8 exams per patient), generating a total of 3263 'normal' images (913 for cancer cases, and 2350 for controls). Those prior images of the cancer-affected breast (for cancer cases) and side-matched breast (for controls) were used to predict the outcome (i.e., case/control status). We compared the prediction in terms of three time periods: (A) all priors from 2006 to 2012, (B) recent priors (1548 images) from 2010 to 2012, and (C) distant priors (1715 images) from 2006 to 2009. The outcome prediction was based on a pre-trained convolutional neural network model (ResNet-50) that was further fine-tuned on our mammograms. 10-fold cross-validation and AUC were used to measure model performance.

RESULTS

81% of cancers and 82% of controls were post- with the rest pre-menopausal, and neither menopausal status nor family history of breast cancer was associated with the outcome. AUC was 0.84 when using all priors, while it was 0.77 or 0.75 when using only the recent or only the distant priors, respectively.

CONCLUSION

Sequential recent or distant prior 'normal' screening mammograms can predict, and their combination is more predictive of, breast cancer development using deep learning models.

CLINICAL RELEVANCE/APPLICATION

Deep learning modeling on longitudinally acquired prior 'normal' screening mammogram images through up to 7 years earlier can enhance temporal prediction of breast cancer development.

RC215-16 Novel Radiomic Descriptor of Tumor Vascular Morphology Identifies Responders to Neo-Adjuvant Chemotherapy on Pre-Treatment Breast MRI

Monday, Nov. 26 11:40AM - 11:50AM Room: Arie Crown Theater

Awards

Trainee Research Prize - Medical Student

Participants Nathaniel Braman, Cleveland, OH (*Presenter*) Nothing to Disclose Prateek Prasanna, Cleveland, OH (*Abstract Co-Author*) Nothing to Disclose Maryam Etesami, MD, New Haven, CT (*Abstract Co-Author*) Nothing to Disclose Donna M. Plecha, MD, Strongsville, OH (*Abstract Co-Author*) Research Grant, Hologic, Inc Anant Madabhushi, PhD, Cleveland, OH (*Abstract Co-Author*) Research funded, Koninklijke Philips NV

For information about this presentation, contact:

nathaniel.braman@case.edu

PURPOSE

Despite significant interest in predicting treatment response prior to breast cancer neo-adjuvant chemotherapy (NAC) from DCE-MRI, prior work has focused on textural patterns of the tumor or parenchyma or deep learning-based approaches that lack direct biological interpretability. In this work, we introduce functional radiomic descriptors of vascular network disorder (VND) and evaluate whether differences in the complexity of tumor-associated vasculature on pre-treatment DCE-MRI can discriminate between patients who do and do not respond to NAC.

METHOD AND MATERIALS

1.5 or 3T DCE-MRI scans of 76 NAC recipients, 24 of whom had surgically confirmed pathological complete response (pCR), were retrospectively analyzed. Average pixel width and slice thickness were .77 mm and 1.22 mm, respectively. Patients were randomly divided into training (n=53, 14 pCR) and testing (n=23, 10 pCR) sets. A semi-interactive scheme was employed to segment the tumor and vascular network. Within a sliding window, vessel orientation was computed for a series of 2-dimensional representations of the vasculature relative to the tumor centroid. Statistics (mean, median, st. dev, skewness, and kurtosis) of the distribution of vessel orientations for each representation were computed, yielding 20 VND features total. Top VND features were selected in the training set using the Wilcoxon rank sum test via three-fold cross validation, then used to train a linear discriminant analysis classifier to predict response in the test set. Performance was compared against (1) intra- and peri-tumoral texture features and (2) a 3 layer LeNet convolutional neural network (CNN).

RESULTS

The top 4 VND features distinguished pCR with an AUC=0.75. pCR was characterized by reduced vascular disorder relative to nonpCR. VND performed comparably or better than other state of the art radiomic approaches, including intra- and peri-tumoral texture (AUC=.75) and deep learning (AUC=.67). Combining predictions from VND, texture features, and CNN yielded the best response prediction accuracy (AUC=0.80).

CONCLUSION

VND features, which capture chaotic vessel network architecture, appear to be associated with NAC response and added predictive value to established radiomic and deep learning approaches.

CLINICAL RELEVANCE/APPLICATION

Quantitative assessment of vessel network architecture as a functional radiomic biomarker could provide interpretable NAC response prediction in breast cancer.

RC215-17 Using Machine Learning to Assess Tumor Metastatic Lymph Nodes and Ki-67 Expression Aggressiveness from Breast MRI Using a Large Clinical Dataset of 300 Cancers from China

Monday, Nov. 26 11:50AM - 12:00PM Room: Arie Crown Theater

Participants

Yu Ji, MD, Chicago, IL (Presenter) Nothing to Disclose

Hui Li, PHD, Chicago, IL (Abstract Co-Author) Nothing to Disclose

Alexandra V. Edwards, Chicago, IL (*Abstract Co-Author*) Research Consultant, QView Medical, Inc; Research Consultant, Quantitative Insights, Inc

John Papaioannou, MSc, Chicago, IL (Abstract Co-Author) Research Consultant, QView Medical, Inc

Peifang Liu, MD, PhD, Tianjin, China (Abstract Co-Author) Nothing to Disclose

Maryellen L. Giger, PhD, Chicago, IL (*Abstract Co-Author*) Stockholder, Hologic, Inc; Shareholder, Quantitative Insights, Inc; Shareholder, QView Medical, Inc; Co-founder, Quantitative Insights, Inc; Royalties, Hologic, Inc; Royalties, General Electric Company; Royalties, MEDIAN Technologies; Royalties, Riverain Technologies, LLC; Royalties, Mitsubishi Corporation; Royalties, Canon Medical Systems Corporation

For information about this presentation, contact:

yuji710@uchicago.edu

PURPOSE

To evaluate quantitative MRI radiomics in the task of identifying metastatic versus nonmetastatic axillary lymph nodes and Ki-67 expression aggressiveness.

METHOD AND MATERIALS

Our research involved a HIPAA-compliant, DCE-MRI database of 300 breast cancer cases. The average age was 47.2 years with a standard deviation of 9.6 years and a range from 25 to 77 years with a median of 47 years. The clinical cohort included 48 low Ki-67 expression (Ki-67 proliferation index < 14%) and 252 cases with high Ki-67 expression (Ki-67 proliferation index >= 14%), indicating a range of tumor aggressiveness. The cohort also included 93 cases with axillary lymph node metastasis and 201 cases without metastasis. The images had been obtained with a gadodiamide-enhanced T1-weighted spoiled gradient-recalled acquisition in the steady state sequence. Primary lesions underwent computerized radiomic analysis in which tumor segmentation and extraction were automatically conducted on an existing CADx workstation. These computer-extracted features included MRI-based phenotypes from six categories: size, shape, morphology, enhancement texture, kinetics, and enhancement-variance kinetics. Radiomic features were input to a Bayesian artificial neural network classifier (BANN) and underwent leave-one-case-out cross validation. Area under the ROC curve (AUC) served as the figure of merit in the classification tasks.

RESULTS

In the task of identifying Ki-67 expression and lymph node status, the analyses of the various radiomic phenotypes yielded AUCs ranging from 0.50 (se = 0.05) to 0.69 (se = 0.04). The Ki-67 MRI-based tumor signature produced an AUC value of 0.71 (se = 0.04). In the task of assessing the status of axillary lymph nodes, the radiomics tumor signature yielded an AUC value of 0.67 (se = 0.03). Both signatures were found to be statistically different from random guessing.

CONCLUSION

Quantitative MRI radiomics conducted on depicted primary breast tumors can contribute to identifying aggressive tumors, including identifying Ki-67 expression and discriminating between metastatic and nonmetastatic lymph nodes, yielding automatic MRI-based prognostic markers for ultimate use in radiogenomics and patient care.

CLINICAL RELEVANCE/APPLICATION

The ability to assess automatically the potential aggressiveness of tumors may elucidate the characteristics of breast cancers for radiogenomics and for use in helping clinician estimate prognosis.



RC253

Preparing your Radiology Practice and IT Department for Big Data

Monday, Nov. 26 8:30AM - 10:00AM Room: S503AB



AMA PRA Category 1 Credits ™: 1.50 ARRT Category A+ Credit: 1.75

Participants

Paul J. Chang, MD, Chicago, IL (*Moderator*) Co-founder, Koninklijke Philips NV; Researcher, Koninklijke Philips NV; Researcher, Bayer AG; Advisory Board, Aidoc Ltd; Advisory Board, EnvoyAI; Advisory Board, Inference Analytics

LEARNING OBJECTIVES

1) The potential of applying "Big Data" approaches to radiology will be discussed. 2) The participant will be introduced to the importance of developing a comprehensive IT architecture and capability beyond the EMR in order to effectively use "Big Data" tools. 3) Strategies for preparing IT for "Big Data" will be discussed.

ABSTRACT

Current and near future requirements and constraints will require radiology practices to continuously improve and demonstrate the value they add to the enterprise. Merely 'managing the practice' will not be sufficient; groups will be required to compete in an environment where the goal will be measurable improvements in efficiency, productivity, quality, and safety. This will require optimally leveraging IT enabled business intelligence, analytics, and data driven workflow. In many ways, this challenge can be described as a "Big Data" problem, requiring the application of newer "Big Data" approaches and tools. Unfortunately, many have discovered that an "EMR centric" IT perspective may severely limit the ability for the enterprise to maximally leverage these newer tools to create differentiable value. This session will provide an introduction to the importance of developing a comprehensive architectural strategy to augment the existing EMR to more effectively consume "Big Data" tools.

Sub-Events

RC253A Getting Your IT Infrastructure Ready for Big Data

Participants

Paul J. Chang, MD, Chicago, IL (*Presenter*) Co-founder, Koninklijke Philips NV; Researcher, Koninklijke Philips NV; Researcher, Bayer AG; Advisory Board, Aidoc Ltd; Advisory Board, EnvoyAI; Advisory Board, Inference Analytics

LEARNING OBJECTIVES

1) The potential of applying "Big Data" and noSQL approaches to radiology will be discussed. 2) The participant will be introduced to the importance of developing a comprehensive IT architecture and capability beyond the EMR in order to effectively use "Big Data" tools. 3) Strategies for preparing IT for business intelligence and analytics will be discussed.

ABSTRACT

Current and near future requirements and constraints will require radiology practices to continuously improve and demonstrate the value they add to the enterprise. Merely 'managing the practice' will not be sufficient; groups will be required to compete in an environment where the goal will be measurable improvements in efficiency, productivity, quality, and safety. This will require optimally leveraging IT enabled business intelligence, analytics, and data driven workflow. In many ways, this challenge can be described as a "Big Data" problem, requiring the application of newer "Big Data" approaches and tools. Unfortunately, many have discovered that an "EMR centric" IT perspective may severely limit the ability for the enterprise to maximally leverage these newer tools to create differentiable value. This session will provide an introduction to the importance of developing a comprehensive architectural strategy to augment the existing EMR to more effectively consume "Big Data" approaches and fully leverage business intelligence and analytics.

RC253B NoSQL Approaches: Beyond the Traditional Relational Database

Participants

Paul J. Chang, MD, Chicago, IL (*Presenter*) Co-founder, Koninklijke Philips NV; Researcher, Koninklijke Philips NV; Researcher, Bayer AG; Advisory Board, Aidoc Ltd; Advisory Board, EnvoyAI; Advisory Board, Inference Analytics

LEARNING OBJECTIVES

1) The distinction between the traditional relational (SQL) database and "NoSQL" approaches will be discussed. 2) The attendees will be given a basic introduction to how "NoSQL" tools, such as Hadoop, MapReduce, MongoDB can be complementary to existing approaches. 3) NoSQL applications and their relevance to radiology will be discussed.

ABSTRACT

Current and near future requirements and constraints will require radiology practices to continuously improve and demonstrate the value they add to the enterprise. Merely 'managing the practice' will not be sufficient; groups will be required to compete in an environment where the goal will be measurable improvements in efficiency, productivity, quality, and safety. This will require optimally leveraging IT enabled business intelligence, analytics, and data driven workflow. These approaches will require the ability to consume and utilize all available enterprise data, including unstructured reports, multimedia objects, etc. Other industries have realized that traditional IT approaches, such as the relational (SQL) database, cannot optimally address these "difficult" data

objects. Many outside of the medical domain have successfully augmented traditional approaches by newer "Big Data" and "NoSQL" methodologies, such as Hadoop, MapReduce, MongoDB, etc. In this session, an introduction to these newer tools will be presented.

RC253C Radiologist Workflow and AI: Challenges and Opportunities

Participants

William W. Boonn, MD, Philadelphia, PA (Presenter) Officer, Nuance Communications, Inc; Shareholder, Nuance Communications, Inc

LEARNING OBJECTIVES

1) A technical overview of machine learning and deep learning will be presented. 2) Applications of machine learning and deep learning in radiology will be illustrated. 3) Challenges in deploying machine learning and deep learning in radiologist workflow and productivity demands will be discussed.

ABSTRACT

Computers in radiology have often promised to deliver faster clinical decisions, more accurate diagnoses, and transformative visualizations. Computer aided diagnostics (CAD) has been deployed to guide radiologists in their detection of abnormalities and identification of disease. Historically, CAD has been based on domain-driven heuristics, and more recently used simple machine learning on structured data. Both of these require extensive manual engineering making them very slow to build, limited in their flexibility, and less accurate than we would like. Deep learning is a new paradigm that offers a transformative solution. Instead of demanding countless human hours of painstaking feature generation and selection, deep learning automatically discovers clinically-relevant features by first architecting a hierarchy of patterns (loosely modelled on the brain's own neural neural networks) and then updating those patterns upon observing examples. As radiology requires complex associative pattern recognition, deep learning is the ideal companion tool. Enlitic is developing a deep neural network of the entire human body that will offer a new way forward in which the radiologist has immediate access to the most relevant clinical information. In this talk, we will present a technical overview of machine learning and deep learning, illustrate its applications in radiology, and detail some of the challenges improving radiological workflow using deep learning poses.

Honored Educators

Presenters or authors on this event have been recognized as RSNA Honored Educators for participating in multiple qualifying educational activities. Honored Educators are invested in furthering the profession of radiology by delivering high-quality educational content in their field of study. Learn how you can become an honored educator by visiting the website at: https://www.rsna.org/Honored-Educator-Award/ William W. Boonn, MD - 2012 Honored Educator



SSC03

Chest (Lung Cancer Screening)

Monday, Nov. 26 10:30AM - 12:00PM Room: E451A



AMA PRA Category 1 Credits ™: 1.50 ARRT Category A+ Credit: 1.75

Participants

Jo-Anne O. Shepard, MD, Boston, MA (*Moderator*) Nothing to Disclose Jane P. Ko, MD, New York, NY (*Moderator*) Research collaboration, Siemens AG

Sub-Events

SSC03-01 Predicting the Likelihood of Various Major Diseases from Lung Cancer Screening Chest CT Using 3D Convolutional Neural Networks

Monday, Nov. 26 10:30AM - 10:40AM Room: E451A

Participants

Aditya U. Sheth, Berkeley, CA (*Presenter*) Nothing to Disclose Youngho Seo, PhD, San Francisco, CA (*Abstract Co-Author*) Consultant, BioLaurus, Inc Peter Chang, MD, San Francisco, CA (*Abstract Co-Author*) Nothing to Disclose Thienkhai H. Vu, MD, PhD, San Francisco, CA (*Abstract Co-Author*) Nothing to Disclose Dmytro Lituiev, San Francisco, CA (*Abstract Co-Author*) Nothing to Disclose Jae Ho Sohn, MD, San Francisco, CA (*Abstract Co-Author*) Nothing to Disclose

For information about this presentation, contact:

sohn87@gmail.com

PURPOSE

A large number of patients undergo annual lung cancer screening with low-dose chest CT. The CT data contains significant information about health of the patient, beyond simple lung cancer status. The National Lung Cancer Screening (NLST) database provides a large dataset with correlated clinical metadata, which can be used to train machine learning algorithms to extract as much useful health information as possible. The aim of the study is to develop and validate a 3D convolutional neural network algorithm on these CT studies to predict the likelihood of various major diseases: diabetes, heart disease, COPD, and stroke.

METHOD AND MATERIALS

We extracted random samples of 16,780 scans from NLST. Data preprocessing consisted of isotropic resolution resizing and standardization to 350 x 350 x 35 pixel size. Data was augmented with random rotations between -15 and 15 degrees. The processed samples were passed through a 3D convolutional neural network (CNN) with architecture loosely inspired by the VGG-Net. Modifications included generalization to 3D dataset, more gradual pooling across the z-axis, and use of batch normalization. Stochastic gradient descent optimizer and sparse categorical crossentropy loss function were utilized. Final results were gathered using a separate testing set extracted from the NLST dataset. Error analysis was conducted.

RESULTS

We performed training and testing for classification of the following diseases: diabetes, heart disease, COPD, and stroke. For each disease respectively, we achieved an ROC AUC of 0.75, 0.70, 0.74, 0.69 on the test sets. ROC curves are displayed in Figure (1). For each of these results, a single radiologist with deep learning expertise manually inspected random samples of correct and incorrect predictions to ensure absence of any systematic errors. None was identified. Testing sets were confirmed to be an accurate representation of the training sets with regards to positive/negative example ratios.

CONCLUSION

Our 3D CNN model successfully predicted the likelihood of various diseases from lung cancer screening chest CT studies.

CLINICAL RELEVANCE/APPLICATION

The algorithm can be used to provide patients with useful health information about major diseases, in addition to the formal lung cancer screening interpretations by radiologists.

SSC03-02 Improving Specificity of Lung Cancer Screening CT Using Deep Learning

Monday, Nov. 26 10:40AM - 10:50AM Room: E451A

Participants

Diego Ardila, Mountain View, CA (*Presenter*) Employee, Alphabet Inc Bokyung Choi, PhD, Mountain View, CA (*Abstract Co-Author*) Employee, Alphabet Inc Atilla P. Kiraly, PhD, Mountain View,, CA (*Abstract Co-Author*) Former Employee, Siemens AG; Employee, Alphabet Inc Sujeeth Bharadwaj, PhD, Mountain View, CA (*Abstract Co-Author*) Employee, Alphabet Inc Joshua J. Reicher, MD, Stanford, CA (*Abstract Co-Author*) Investor, Health Companion, Inc; Consultant, Alphabet Inc Greg Corrado, PhD, Mountain View, CA (*Abstract Co-Author*) Employee, Alphabet Inc Daniel Tse, MD, Mountain View, CA (*Abstract Co-Author*) Employee, Alphabet Inc Lily Peng, MD,PhD, Mountain View, CA (*Abstract Co-Author*) Employee, Alphabet Inc Shravya Shetty, Mountain View, CA (*Abstract Co-Author*) Employee, Alphabet Inc

For information about this presentation, contact:

sshetty@google.com

PURPOSE

Evaluate the utility of deep learning to improve the specificity and sensitivity of lung cancer screening with low-dose helical computed tomography (LDCT), relative to the Lung-RADS guidelines.

METHOD AND MATERIALS

We analyzed 42,943 CT studies from 14,863 patients, 620 of which developed biopsy-confirmed cancer. All cases were from the National Lung Screening Trial (NLST) study. We randomly split patients into a training (70%), tuning (15%) and test (15%) sets. A study was marked "true" if the patient was diagnosed with biopsy confirmed lung cancer in the same screening year as the study. A deep learning model was trained over 3D CT volumes (400x512x512) as input. We used the 95% specificity operating point based on the tuning set, and evaluated our approach on the test set. To estimate radiologist performance, we retrospectively applied Lung-RADS criteria to each study in the test set. Lung-RADS categories 1 to 2 constitute negative screening results, and categories 3 to 4 constitute positive results. Neither the model nor the Lung-RADS results took into account prior studies, but all screening years were utilized in evaluation.

RESULTS

The area under the receiver operator curve of the deep learning model was 94.2% (95% CI 91.0, 96.9). Compared to Lung-RADS on the test set, the trained model achieved a statistically significant absolute 9.2% (95% CI 8.4, 10.1) higher specificity and trended a 3.4% (95% CI -5.2, 12.6) higher sensitivity (not statistically significant).Radiologists qualitatively reviewed disagreements between the model and Lung-RADS. Preliminary analysis suggests that the model may be superior in distinguishing scarring from early malignancy.

CONCLUSION

A deep learning based model improved the specificity of lung cancer screening over Lung-RADS on the NLST dataset and could potentially help reduce unnecessary procedures. This research could supplement future versions of Lung-RADS; or support assisted read or second read workflows.

CLINICAL RELEVANCE/APPLICATION

While Lung-RADS criteria is recommended for lung cancer screening with LDCT, there is still an opportunity to reduce false-positive rates which lead to unnecessary invasive procedures.

SSC03-03 New Algorithm Incorporating Machine Learning Improves Lung Cancer Risk Calculation on Screening CT Scans

Monday, Nov. 26 10:50AM - 11:00AM Room: E451A

Participants

Cheng Ting Lin, MD, Baltimore, MD (*Presenter*) Nothing to Disclose Yuliang Li, Baltimore, MD (*Abstract Co-Author*) Nothing to Disclose Matthew Garner, Baltimore, MD (*Abstract Co-Author*) Nothing to Disclose Nadege Fackche, Baltimore, MD (*Abstract Co-Author*) Nothing to Disclose Samata Kakkad, Baltimore, MD (*Abstract Co-Author*) Nothing to Disclose Zaver M. Bhujwalla, PhD, Baltimore, MD (*Abstract Co-Author*) Nothing to Disclose Susumu Mori, PhD, Baltimore, MD (*Abstract Co-Author*) Nothing to Disclose Susumu Mori, PhD, Baltimore, MD (*Abstract Co-Author*) Nothing to Disclose Calum MacAulay, Vancouver, BC (*Abstract Co-Author*) Nothing to Disclose David Ettinger, Baltimore, MD (*Abstract Co-Author*) Nothing to Disclose Malcolm Brock, Baltimore, MD (*Abstract Co-Author*) Nothing to Disclose Stephen Lam, MD, Vancouver, BC (*Abstract Co-Author*) Nothing to Disclose Peng Huang, Baltimore, MD (*Abstract Co-Author*) Nothing to Disclose

For information about this presentation, contact:

clin97@jhmi.edu

PURPOSE

Lung-RADS is widely used to classify nodules detected on lung cancer screening CT. Using data from the National Lung Cancer Screening Trial (NLST), we examined whether integration of patient demographics, clinical history, and CT texture features could improve our ability to predict long-term lung cancer development. Since most screening CTs detect early stage lung cancers, we further examined if our algorithm could predict cancer progression and overall survival in patients with resected stage I lung cancers.

METHOD AND MATERIALS

Demographics, clinical history, and baseline CT images from 24,386 NLST participants were analyzed using survival machine learning (SML). Nodule volume was calculated by V=3.14LR2 where L=longest diameter, R=longest perpendicular diameter/2. Subjects were partitioned into 4 risk groups to test hazards ratios (HR). The SML partition was compared to that from Lung-RADS. For the stage I lung cancer subgroup, the time from lung cancer diagnosis to death was used as the SML endpoint.

RESULTS

At the time of baseline CTs, the 4 risk groups were classified by: high (largest nodule L>10mm, V>6358mm3; n=85), mid-high (largest nodule L>10mm, V<=6358mm3; n=1219), mid-low (largest nodule L= $5\sim10$ mm, smoking>40 years; n=1736), and low (all

others; n=21346). Compared to our low risk group, HRs for time to lung cancer onset were 91.5, 11.1, 4.0 for high, mid-high, and mid-low risk groups respectively (all p<0.0001). In contrast, the HRs from Lung-RADS categories 4, 3, and 2 were 5.68, 1.27, and 0.75 respectively as compared to category 1 (p values: <0.0001, 0.056, 0.058). For stage 1 lung cancers, demographics, nodule margins, lymph node enlargement, and blood vessel involvement jointly affected the rate of cancer progression and overall patient survival.

CONCLUSION

Using the NLST data, our new classification outperforms Lung-RADS in stratifying risk and predicting long-term lung cancer development. Furthermore, in pathologically defined stage 1 patients who received surgery, our new classification can identify those with poor survival suggesting that it can do so independently of cancer stage.

CLINICAL RELEVANCE/APPLICATION

Our new classification outperforms Lung-RADS in stratifying risk and predicting long-term lung cancer development and can identify stage 1 patients with poor survival suggesting that it can do so independently of cancer stage.

SSC03-04 Effect of Semiautomated Segmentation and Computer-Aided Detection of Lung Nodules on Lung Cancer Screening with Low Dose CT: Experience from a Nationwide Lung Cancer Screening Project

Monday, Nov. 26 11:00AM - 11:10AM Room: E451A

Participants

Eui Jin Hwang, Seoul, Korea, Republic Of (*Presenter*) Nothing to Disclose Jin Mo Goo, MD, PhD, Seoul, Korea, Republic Of (*Abstract Co-Author*) Research Grant, Samsung Electronics Co, Ltd; Research Grant, Lunit Inc Hyae Young Kim, MD, PhD, Goyang-si, Korea, Republic Of (*Abstract Co-Author*) Nothing to Disclose Jaeyoun Yi, Seoul, Korea, Republic Of (*Abstract Co-Author*) Officer, Coreline Soft, Co Ltd Yeol Kim I, Goyang-Si, Korea, Republic Of (*Abstract Co-Author*) Nothing to Disclose

For information about this presentation, contact:

ken921004@hotmail.com

PURPOSE

To evaluate the effect of semiautomated segmentation and computer-aided detection (CAD) system for lung nodule on lung cancer screening based on the Lung-RADS.

METHOD AND MATERIALS

We utilized the data from an ongoing nationwide multi-center lung cancer screening project with low dose chest CT. This project started with a visual assessment and manual measurement system (a manual system) and changed into a cloud-based software system which equipped with a semiautomated nodule segmentation and CAD system (a software system). In a software system, an average diameter of a nodule for the Lung-RADS was calculated on a plane showing the maximal cross sectional area of a nodule. For this study, an average diameter on axial planes was also calculated. We compared the number of detected lung nodules and distribution of Lung-RADS categories between two systems. When the results of before and after CAD were available (the number of cases, 2374), the effect of CAD was evaluated.

RESULTS

The number of cases and the number of nodules for both systems are as follows: a manual system, 1821 cases, 1630 nodules; a software system, 4665 cases, 6116 nodules. Significantly greater number of nodules (0.90 vs. 1.31 nodule/case) were detected at a software system. The size of nodule was significantly larger (5.5 vs. 4.6 mm) at a software system, but there was no significant difference in the size of nodules between two systems when axial planes were used in calculating an average diameter in a software system. Both the per-case (9.8% vs. 17.4%) and per-nodule (12.9% vs. 17.9%) proportion of positive test (category 3/4) were significantly higher at a software system. By applying the CAD results, not only the number of the detected nodules (0.77 vs. 1.23 nodule/case) but also the per-case proportion of positive test (11.6% vs. 17.1%) were significantly increased.

CONCLUSION

By applying a semi-automated segmentation and CAD system, the number of detected nodules and the proportion of positive test were significantly increased.

CLINICAL RELEVANCE/APPLICATION

Semiautomated segmentation and CAD have important effects on the Lung-RADS positive rate. Therefore, detailed guidelines should be provided for the use of software in lung cancer screening.

SSC03-05 Randomized Clinical Trial of CAD versus No CAD as First Reader of Lung Cancer Screening CT: Preliminary Report

Monday, Nov. 26 11:10AM - 11:20AM Room: E451A

Participants

Ren Yuan, MD,PhD, Vancouver, BC (*Presenter*) Nothing to Disclose John R. Mayo, MD, Vancouver, BC (*Abstract Co-Author*) Speaker, Siemens AG Renelle Myers, MD, Vancouver, BC (*Abstract Co-Author*) Nothing to Disclose Sukhinder Atkar-Khattra, BSC, Vancouver, BC (*Abstract Co-Author*) Nothing to Disclose Isaac Streit, Vancouver, BC (*Abstract Co-Author*) Nothing to Disclose John Yee, MD, Vancouver, BC (*Abstract Co-Author*) Nothing to Disclose Kyle Grant, MD, Vancouver, BC (*Abstract Co-Author*) Nothing to Disclose Alexander Lee, MD, Vancouver, BC (*Abstract Co-Author*) Nothing to Disclose Anna L. Mcguire, MD, Vancouver, BC (*Abstract Co-Author*) Nothing to Disclose Colin Jacobs, PhD, Nijmegen, Netherlands (*Abstract Co-Author*) Stockholder, Thirona BV; Co-founder, Thirona BV; Research Grant, Varian Medical Systems, Inc; Research Grant, Canon Medical Systems Corporation Martin Tammemagi, St. Catharines, ON (*Abstract Co-Author*) Nothing to Disclose Stephen Lam, MD, Vancouver, BC (*Abstract Co-Author*) Nothing to Disclose

For information about this presentation, contact:

ren.yuan@bccancer.bc.ca

PURPOSE

The accuracy of radiologists reading lung cancer screening CT in a previous study shows a false-negative rate (FN) of 3.5% to 8.1%. The purpose of this study was to assesses if CAD can reduce the FN and CT reading time.

METHOD AND MATERIALS

We conducted a randomized trial in 148 smokers participating in our ongoing Lung Cancer Screening Project (75M:73F, 66±7yrs, 59 ex- vs. 89 current-smoker). Chest CTs were randomized into two arms. In the CAD and Technician first arm (CAD+Tech-1st), CAD findings were displayed first, a technician accepted or rejected CAD findings and added probable nodule(s), then a chest radiologist accepted or rejected the CAD +Tech findings additional nodule(s). In the RAD-first arm (RAD-1st) the same radiologist read the CT first with CAD marks hidden, then turned on CAD to accept true nodules including those only found by CAD and delete the non-nodule CAD findings. The number of true nodules and reading time were recorded.

RESULTS

The reading times were 6.2 ± 3.4 min (range: 2-18) vs. 8.3 ± 5.4 min (range: 3-30) for CAD+Tech-1st vs. RAD-1st arms (p=0.012) for CTs with >=1 nodule; and 4.4 ± 1.5 min (range: 2-10) vs. 8.7 ± 9.5 min (range: 3-30) for those without nodules (p=0.07). By the three detection methods, 212 true nodules were found in 97 CTs in the CAD+Tech-1st arm. CAD detected 82 and technician added 93 true nodules, giving a combined sensitivity of 83%. There were 37/212 nodules found only by the radiologist; 12/37 were the most important nodule, and 1/37 was the only nodule that drove follow-up. In the RAD-1st arm 71 true nodules were found in 51 CTs; 36/71 (51%) were found by both CAD and radiologist. The radiologist missed 2 true nodules in 2 participants (2/51, 4%) which were detected by CAD and altered their follow-up protocol. The radiologist's detection sensitivity slightly increased with CAD (97% to 100%). CAD missed 33/71(46%) true nodules found by the radiologist, 16/33 (48%) were key nodules and 11/16 were the only nodule, changing follow-up.

CONCLUSION

CAD+Tech speed up the radiologist's nodule detection on screening chest CT. CAD detected nodules in 4% subjects where no nodule was identified by the radiologist, changing imaging follow-up protocol.

CLINICAL RELEVANCE/APPLICATION

While CAD+Tech as first reader cannot replace the radiologist, CAD could play an important role in lung cancer screening by saving radiologists' time, and importantly reduce their FN rate by 4%.

SSC03-06 Understanding Gaps Between Mental Health and Radiology Care: Population-based Cross-Sectional Survey Analysis of Lung Cancer Screening Eligibility and Smoking Prevalence Among Patients with Mental Illness

Monday, Nov. 26 11:20AM - 11:30AM Room: E451A

Participants

Efren J. Flores, MD, Boston, MA (*Presenter*) Nothing to Disclose Diego Lopez, Boston, MA (*Abstract Co-Author*) Nothing to Disclose Gary X. Wang, MD, PhD, Boston, MA (*Abstract Co-Author*) Nothing to Disclose McKinley Glover IV, MD, Boston, MA (*Abstract Co-Author*) Nothing to Disclose Kelly E. Irwin, MD, MPH, Boston, MA (*Abstract Co-Author*) Nothing to Disclose Elyse Park, PhD, MPH, Boston, MA (*Abstract Co-Author*) Nothing to Disclose Constance D. Lehman, MD, PhD, Boston, MA (*Abstract Co-Author*) Nothing to Disclose Soard, General Electric Company Jo-Anne O. Shepard, MD, Boston, MA (*Abstract Co-Author*) Nothing to Disclose Anand K. Narayan, MD, PhD, Boston, MA (*Abstract Co-Author*) Nothing to Disclose

For information about this presentation, contact:

ejflores@mgh.harvard.edu

PURPOSE

Prior studies have found that patients with mental illness are more likely to smoke compared with patients without mental illness. Lung Cancer Screening (LCS) with LDCT decreases lung cancer mortality in eligible current or former smokers. There is limited population-based information about LCS eligibility in patients with mental illness. Our purpose was to determine if patients with selfreported mental illness are more likely to be eligible for LCS and smoking cessation interventions compared to patients without mental illness using nationally representative federal cross-sectional survey data.

METHOD AND MATERIALS

Retrospective analysis of 2015 National Health Interview Survey (NHIS), a nationally representative, federal cross sectional survey was conducted. Individuals 55-77 yrs without lung cancer were included. The proportion of survey participants eligible for LCS was calculated and compared in patients with and without self-reported mental illness. Multiple variable logistic regression analyses were conducted comparing LCS eligibility in patients with and without self-reported mental illness, adjusted for potential confounders (age, race, and insurance status). Adjusted odds ratios were calculated with 95% confidence intervals. Analyses were performed accounting for complex survey design elements.

RESULTS

11,325 individuals between ages 55-77 were included (mean age 64.1, 52.8% female, 74.9% white) of whom 2.8% reported at least

one mental illness. Of individuals with self reported mental illness, 18.7% met eligibility criteria for LCS and 25.8% were current smokers. Of individuals without self reported mental illness, 10.6% met eligibility criteria for LCS and 12.9% were current smokers. Patients self-reporting mental illness were more likely to be eligible for LCS (Adjusted OR 1.89, 95% CI 1.30 to 2.75, p = 0.001) and more likely to be current smokers (Adjusted OR 2.20, 95% CI 1.59 to 3.07, p < 0.001) than patients without mental illness.

CONCLUSION

Patients with self-reported mental illness have a higher smoking prevalence and are nearly twice as likely to be eligible for LCS compared with patients without mental illness.

CLINICAL RELEVANCE/APPLICATION

Radiologists have an opportunity to collaborate with psychiatry and primary care in developing targeted LCS outreach efforts for patients with mental illness who are at increased risk of developing lung cancer due to their higher smoking prevalence.

SSC03-07 Lung Cancer Screening in a Socioeconomically Disadvantaged Population: Baseline and 1st Annual Rescreening Results

Monday, Nov. 26 11:30AM - 11:40AM Room: E451A

Awards

Trainee Research Prize - Resident

Participants

Charles H. Li, MD, Los Angeles, CA (*Presenter*) Nothing to Disclose Phillip Guichet, MD, New York, NY (*Abstract Co-Author*) Nothing to Disclose Steven Cen, PhD, Los Angeles, CA (*Abstract Co-Author*) Nothing to Disclose Beringia Liu, MPH, Los Angeles, CA (*Abstract Co-Author*) Nothing to Disclose Bhushan Desai, MBBS, MS, Los Angeles, CA (*Abstract Co-Author*) Nothing to Disclose Cameron Hassani, MD, Los Angeles, CA (*Abstract Co-Author*) Nothing to Disclose Leah M. Lin, MD, Los Angeles, CA (*Abstract Co-Author*) Nothing to Disclose Farhood Saremi, MD, Los Angeles, CA (*Abstract Co-Author*) Nothing to Disclose Bonnie Garon, MD, Los Angeles, CA (*Abstract Co-Author*) Nothing to Disclose Ana Maliglig, MD, MPH, Los Angeles, CA (*Abstract Co-Author*) Nothing to Disclose Alison Wilcox, MD, Los Angeles, CA (*Abstract Co-Author*) Nothing to Disclose Alison Wilcox, MD, Los Angeles, CA (*Abstract Co-Author*) Nothing to Disclose

For information about this presentation, contact:

chrisleemd@gmail.com

PURPOSE

To describe the results of the first two rounds of screening of our clinical low-dose CT lung cancer screening program targeting a minority, socioeconomically disadvantaged, high-risk population different from that studied in the National Lung Screening Trial.

METHOD AND MATERIALS

All participants met USPSTF and/or NCCN eligibility criteria for lung cancer screening. A coordinator enrolled eligible individuals, scheduled their screening exams, and organized their transportation.

RESULTS

1029 individuals were referred from 7/21/2015 through 3/20/2018. 119 individuals declined screening, and 230 were unable to be contacted. Of 717 participants who agreed to participate, 411 met eligibility criteria for lung cancer screening. 370 patients underwent their baseline LDCT during this time period. 203 males (55%) and 167 females received baseline LDCT, with a mean age of 60 years. The median pack-years was 42 (range 20-132), and 81% of participants were current smokers. The ethnic makeup of the population was 77% black, 9% white, 8% Hispanic/Latino, and 5% Asian. 57% of participants had no more than a high school education. 33% of participants reported occupational exposure to one or more lung carcinogens. 84% (312) of patients received a Lung-RADS score of 1 (92) or 2 (220), 8% (29) received a score of 3, 5% (19) a score of 4A, and 3% a score of 4B (8) or 4X (2). 3 patients have been diagnosed with lung cancer to date: 1 stage IIB, 1 stage IIIB, and 1 stage IV. 28% (105) of patients had potentially significant incidental findings including interstitial lung disease (16), severe emphysema (14), aortic aneurysm (7), moderate-severe coronary calcifications (45), extrapulmonary masses (32), and pulmonary hypertension (4). 54% (147/271) of participants who were due for annual rescreening returned for their first annual LDCT. 93% (136) of these patients received a Lung-RADS score of 1 (21) or 2 (115), 3% (4) received a score of 3, 1% (2) a score of 4A, and 3% a score of 4B (5) or 4X (0).

CONCLUSION

Lung cancer screening with LDCT in a minority, socioeconomically disadvantaged, high-risk population is feasible but may yield a different lung cancer profile than screening in more privileged communities. Adherence to annual rescreening and follow-up recommendations is challenging in this population.

CLINICAL RELEVANCE/APPLICATION

Minority, socioeconomically disadvantaged populations may experience different benefits from LDCT lung cancer screening.

Honored Educators

Presenters or authors on this event have been recognized as RSNA Honored Educators for participating in multiple qualifying educational activities. Honored Educators are invested in furthering the profession of radiology by delivering high-quality educational content in their field of study. Learn how you can become an honored educator by visiting the website at: https://www.rsna.org/Honored-Educator-Award/ Cameron Hassani, MD - 2018 Honored EducatorFarhood Saremi, MD - 2015 Honored Educator

SSC03-08 Performance of the Vancouver Risk Calculator Compared to ACR Lung-RADS in an Urban, Diverse Clinical Lung Cancer Screening Cohort

Participants Abraham Kessler, BA, Bronx, NY (*Abstract Co-Author*) Nothing to Disclose Robert Peng, MD, Bronx, NY (*Presenter*) Nothing to Disclose Edward Mardakhaev, MD, Bronx, NY (*Abstract Co-Author*) Nothing to Disclose Charles S. White, MD, Baltimore, MD (*Abstract Co-Author*) Consultant, Koninklijke Philips NV Linda B. Haramati, MD, MS, Bronx, NY (*Abstract Co-Author*) Spouse, Board Member, Kryon Systems Ltd

For information about this presentation, contact:

kessler.abraham@gmail.com

PURPOSE

To compare the performance of the Vancouver Risk Calculator (VRC) with ACR Lung-RADS for a lung cancer screening cohort in an urban, diverse clinical setting.

METHOD AND MATERIALS

IRB approval was obtained. All lung cancer screening patients who had their initial screening CT from December 2012-June 2016 demonstrating a nodule comprised the study population. Each exam was assigned a Lung-RADS score, with 4A and 4B considered positive. The VRC calculates the risk of cancer at different thresholds using 9 patient and imaging variables, with a 5% threshold considered positive. Analysis was performed on a per-patient level based on the largest nodule. Follow-up information was obtained via EMR, cancer registry and NDI. Patients with initial studies suspicious for malignancy but without histologic confirmation were adjudicated on a case-by-case basis. Performance characteristics to predict lung cancer were compared for Lung-RADS and VRC.

RESULTS

486 patients, 261(53.7%) women, mean age 63 ± 5.2 , comprised the study population. Mean follow-up time was 36.9 ± 11.1 months, and 61(12.6%) patients were lost to follow-up. Lung cancer was diagnosed in 35(7.2%). Lung-RADS had 10 FP and 14 FN while VRC 5% had 30 FP and 8 FN. Overall sensitivity, specificity and accuracy for Lung-RADS was 61.1%, 97.8%, and 94.9% and for VRC 5% was 77.8%, 93.3%, and 92.2%, respectively.

CONCLUSION

In comparison with Lung-RADS, the VRC demonstrated higher sensitivity but lower specificity and accuracy in predicting malignancy among patients in a diverse clinical lung cancer screening program.

CLINICAL RELEVANCE/APPLICATION

LungRADS and VRC achieved complementary results in a diverse urban clinical lung cancer screening program. Use of the two, in concert, may improve lung cancer prediction.

SSC03-09 Lung MRI as a Cost-Effective Alternative to Low-Dose CT Lung Cancer Screening: A Markov Cohort Analysis

Monday, Nov. 26 11:50AM - 12:00PM Room: E451A

Awards

Student Travel Stipend Award

Participants

Bradley D. Allen, MD, Chicago, IL (Presenter) Nothing to Disclose

Mark L. Schiebler, MD, Madison, WI (Abstract Co-Author) Stockholder, Stemina Biomarker Discovery, Inc; Stockholder, HealthMyne, Inc;

Gregor Sommer, Basel, Switzerland (Abstract Co-Author) Nothing to Disclose

Hans-Ulrich Kauczor, MD, Heidelberg, Germany (*Abstract Co-Author*) Research Grant, Siemens AG Research Grant, Bayer AG Speakers Bureau, Boehringer Ingelheim GmbH Speakers Bureau, Siemens AG Speakers Bureau, Koninklijke Philips NV Speakers Bureau, Bracco Group Speakers Bureau, AstraZeneca PLC

Juergen Biederer, MD, Heidelberg, Germany (Abstract Co-Author) Nothing to Disclose

Timothy J. Kruser, MD, Chicago, IL (Abstract Co-Author) Nothing to Disclose

James C. Carr, MD, Chicago, IL (*Abstract Co-Author*) Research Grant, Astellas Group; Research support, Siemens AG; Speaker, Siemens AG; Advisory Board, Guerbet SA

Gordon Hazen, PhD, Evanston, IL (Abstract Co-Author) Nothing to Disclose

For information about this presentation, contact:

bdallen@northwestern.edu

PURPOSE

The purpose of this study was to evaluate the potential performance of lung MRI (MRI) vs. low dose CT (LDCT) using a Markov model of lung cancer screening. We hypothesized that MRI would be a cost-effective alternative to LDCT.

METHOD AND MATERIALS

We converted the MISCAN Lung microsimulation of lung cancer progression into a Markov cohort model with transition probabilities based on histology/stage. Our model uses published data to specify lung cancer incidence and background non-lung cancer mortality based on gender, age and smoking burden, and survival after diagnosis by gender, histology and stage. Published LDCT screening sensitivity (Sn) and specificity (Sp) by stage/histology was used to populate the LDCT model parameters. For MRI, the Sn and Sp were based on published data of solid nodules using size and T2 contrast-to-noise ratio. Our model follows a large cohort of age-60 males with 2 packs/day smoking history for 20 years. The time-0 composition of the cohort was a mixture of well and undiagnosed cancer patients from the model when run from age 42. At each annual screening, portions of the surviving cohort experience true/false, positive/negative outcomes with true positives moving to treatment. Costs for screening LDCT (\$256), work-

up, and treatment were extracted from CMS procedure cost data and the literature. Sensitivity analysis was performed on Sn/Sp of MRI and costs of MRI. Results of interest include life-years/patient (LYs), net monetary benefit (NMB), and cost-effectiveness (C/E) of MRI relative to LDCT.

RESULTS

LYs for MRI screening were 13.28 vs. 13.29 for LDCT. Using an acceptable cost/LY of \$100,000, MRI resulted in a net-monetary benefit (NMB) of \$3,744 over LDCT. MRI saves \$2656/patient over LDCT, while losing only 3.97 life days, for a favorable C/E ratio of \$244,189/LY. Cost ranging from \$256 to \$375 result in a favorable C/E ratio for MRI.

CONCLUSION

Based on this simulation, MRI provides an equivalent LY benefit with cost-savings over LDCT lung cancer screening at reasonable MRI costs. This finding is driven by improved specificity of MRI for solid nodule characterization.

CLINICAL RELEVANCE/APPLICATION

Markov simulation of a high-risk screening cohort shows that Lung MRI has the potential to be a cost-effective alternative to lowdose CT screening.



SSC07

Science Session with Keynote: Genitourinary (New Techniques for Renal Imaging)

Monday, Nov. 26 10:30AM - 12:00PM Room: S503AB



AMA PRA Category 1 Credits ™: 1.50 ARRT Category A+ Credit: 1.75

Participants

John R. Leyendecker, MD, Dallas, TX (*Moderator*) Nothing to Disclose David D. Childs, MD, Clemmons, NC (*Moderator*) Nothing to Disclose

Sub-Events

SSC07-01 Genitourinary Keynote Speaker: Renal Mass Characterization: Quantitation, Radiomics, and Machine Learning

Monday, Nov. 26 10:30AM - 10:40AM Room: S503AB

Participants

Ivan Pedrosa, MD, Dallas, TX (Presenter) Nothing to Disclose

SSC07-02 Utility of Google TensorFlow™ Inception Machine Learning to Discriminate Clear Cell Renal Cell Carcinoma from Oncocytoma on Multiphasic CT

Monday, Nov. 26 10:40AM - 10:50AM Room: S503AB

Participants

Heidi Coy, Los Angeles, CA (*Presenter*) Nothing to Disclose Kevin Hseih, Los Angeles, CA (*Abstract Co-Author*) Nothing to Disclose Willie Wu, Los Angeles, CA (*Abstract Co-Author*) Nothing to Disclose Fabien Scalzo, PhD, Los Angeles, CA (*Abstract Co-Author*) Nothing to Disclose Mahesh B. Nagarajan, PhD, Los Angeles, CA (*Abstract Co-Author*) Nothing to Disclose Jonathan R. Young, MD, Sacramento, CA (*Abstract Co-Author*) Nothing to Disclose Michael L. Douek, MD, MBA, Los Angeles, CA (*Abstract Co-Author*) Nothing to Disclose Steven S. Raman, MD, Santa Monica, CA (*Abstract Co-Author*) Nothing to Disclose

For information about this presentation, contact:

hcoy@mednet.ucla.edu

PURPOSE

Although a renal mass can have imaging features of a typical clear cell renal cell carcinoma (ccRCC) on CT, up to 30% of these are found to be benign after surgery, most commonly oncocytoma (ONC). The purpose of our study was to develop a machine learningbased renal lesion classifier using open source Google TensorFlow[™] Inception (TCI) Machine Learning to discriminate ccRCC from ONC on four-phase CT.

METHOD AND MATERIALS

With IRB approval and HIPAA compliance, we derived a cohort of 176 patients with 195 lesions (131 patients with 125 ccRCCs; 61 patients with 49 ONC) with preoperative four phase (unenhanced (UN), corticomedullary (CM), nephrographic (NP), excretory (EX)) CT imaging. Regions of interest were drawn around the tumor on every slice in each phase to create a 3D tumor volume. To preprocess the DICOM data into a format currently supported by TCI, 3D tumor data was extracted in the x, y and z plane and converted into a red, green and blue (RGB) jpeg image using the three color channels to encode each slice. 70% of the data was used in the training set and 30% in the testing set. We investigated several approaches to convert the data into a set of 2D JPEG images that adequately represented each tumor and were used to train the final layer of the neural network model.

RESULTS

When we analyzed 3 mid-slices of the tumor in the x, y and z plane in each post contrast phase, the EX phase had the highest accuracy in classifying both ccRCC (79.6%) and Onc (59.5%) compared to the accuracy in the CM (ccRCC=78.3%, Onc=46%) and NP (ccRCC=77.2%, Onc=46.5%) phases. The highest accuracy in classifying ccRCC was obtained by submitted all x,y and z planes in all phases as one image to TCI with an accuracy of 82.5%, however this lowered the correct classification of Onc to 52.2%.

CONCLUSION

In this pilot study, TCI enabled independent classification of clear cell RCC from oncocytoma on a four phase MDCT with an accuracy of 82.5%.

CLINICAL RELEVANCE/APPLICATION

A TCI based method if developed and validated prospectively may be an adjunct to radiologists for discrimination between clear cell RCC and Oncocytoma on multiphasic CT minimizing diagnostic uncertainty and enabling more accurate patient triage.

ssc07-03 Differentiation of Renal Cell Carcinoma and Oncocytoma Using Machine Learning-Based MR Radiomics

Monday, Nov. 26 10:50AM - 11:00AM Room: S503AB

Participants Yijun Zhao, Changsha, China (Presenter) Nothing to Disclose Harrison X. Bai, MD, Philadelphia, PA (Abstract Co-Author) Nothing to Disclose Dhanya Mahesh, Philadelphia, PA (Abstract Co-Author) Nothing to Disclose Chang Su, New Haven, CT (Abstract Co-Author) Nothing to Disclose Ken Chang, Boston, MA (Abstract Co-Author) Nothing to Disclose Paul Zhang, MD, PhD, Philadelphia, PA (Abstract Co-Author) Nothing to Disclose Hui Liu, Changsha, China (Abstract Co-Author) Nothing to Disclose Dehong Peng, Changsha, China (Abstract Co-Author) Nothing to Disclose Mandeep S. Dagli, MD, Philadelphia, PA (Abstract Co-Author) Nothing to Disclose Terrance Gade, Philadelphia, PA (Abstract Co-Author) Nothing to Disclose Michael C. Soulen, MD, Philadelphia, PA (Abstract Co-Author) Royalties, Cambridge University Press; Consultant, Guerbet SA; Research support, Guerbet SA; Research support, BTG International Ltd; Consultant, Merit Medical Systems, Inc; Proctor, Sirtex Medical Ltd; Consultant, Terumo Corporation; Consultant, Bayer AG Zishu Zhang, MD, PhD, Ypsilanti, MI (Abstract Co-Author) Nothing to Disclose William.s Stavropoulos, Philadelphia, PA (Abstract Co-Author) Nothing to Disclose

For information about this presentation, contact:

zhaoyj25@126.com

PURPOSE

To build a random forest predictive model for distinguishing between renal cell carcinoma (RCC) and oncocytoma that integrates clinical, preoperative, and multimodal automated features.

METHOD AND MATERIALS

Forty-one patients with histologically confirmed renal tumors (23 RCCs; 18 oncocytomas) were identified from a single institution. Two experts (HL and DP), with 23 and 10 years of experience of reading body MR respectively, blinded to the histologic diagnoses, made image diagnosis based on the preoperative MR images (T2-weighted and T1-contrast enhanced sequences). Histogram, geometric and texture features were extracted from preoperative MR images. Using a random forest algorithm, automated features were integrated with clinical data to generate a multivariate predictive model. Receiving operating characteristic curves (ROCs) and areas under the curve (AUCs) were used to assess model performance by using the Delong method for statistical comparison of ROCs.

RESULTS

Patients with oncocytoma had higher mean age than patients with RCC (65.8 ± 7.7 vs. 58.7 ± 11.4 years, p=0.022). Tumor size did not differ significantly between RCC and oncocytoma (average of 2.3 ± 0.9 vs. 2.5 ± 1.0 cm; p = 0.620). For each patient, 5 clinical features and 10566 automated features were included in the model. After feature reduction, 32 features remained. This included 30 T1-contrast enhanced features and 2 T2-weighted features. The tested model achieved accuracy of 80.5% (AUC = 0.80) with sensitivity of 82.6% and specificity of 77.8%. Shape Volume-Compactness (T1C), NGTDM-Busyness (T1C), GLSZM-ZSV (T1C), and Shape Volume-Volume (T2WI) were the features contributing most to the model. Compared to our model, expert 1 achieved accuracy of 63.4% (AUC = 0.59; p = 0.019) with 95.7% sensitivity and 22.2% specificity, and expert 2 achieved accuracy of 57.5% (AUC = 0.55; p = 0.005) with 65.2% sensitivity and 44.4% specificity.

CONCLUSION

Preliminary results using machine learning algorithms demonstrated improved accuracy in differentiation of RCC and oncocytoma when compared with expert interpretation. Further validation is needed in a larger cohort.

CLINICAL RELEVANCE/APPLICATION

Oncocytoma, a benign tumor, that cannot typically be distinguished from RCC based on routine clinical imaging. A machine learning based approach with high accuracy would potentially spare patients unnecessary surgery, ablation, and biopsy.

SSC07-04 The Utility of Radiomic Features in Differentiation of Clear Cell Renal Cell Carcinoma from Non-Clear Cell Renal Cell Carcinoma: A Preliminary Study

Monday, Nov. 26 11:00AM - 11:10AM Room: S503AB

Participants Jian Wen Li, Nanjing, China (*Presenter*) Nothing to Disclose Chang Sheng Zhou, BS, Nanjing, China (*Abstract Co-Author*) Nothing to Disclose Xiuli Li, Beijing, China (*Abstract Co-Author*) Nothing to Disclose Ping Gong, Beijing, China (*Abstract Co-Author*) Nothing to Disclose Long Jiang Zhang, MD, PhD, Nanjing, China (*Abstract Co-Author*) Nothing to Disclose GM Lu, Nanjing, China (*Abstract Co-Author*) Nothing to Disclose

For information about this presentation, contact:

kimonlee@163.com

PURPOSE

To investigate the ability of radiomic features derived from the corticomedullary phase images to differentiate clear cell renal cell carcinoma (RCC) from non-clear cell RCC.

METHOD AND MATERIALS

This study involved 450 patients with 463 tumors histopathologically diagnosed as clear cell RCC (n=362), papillary RCC (n=54) or

chromophobe RCC (n=47), whose corticomedullary phase images were available. To conduct the study, 80% (n=371) and 20% (n=92) tumors were randomly selected as development and validation cohorts keeping the ratio of clear cell RCC to non-clear cell RCC consistent. Using the development cohort, a discriminative subset from 1023 radiomic features was selected by SVM with LASSO regularization. Receiver operating characteristic analysis was conducted to assess the predictive ability of the selected CT radiomic features in differentiation of clear cell RCC from non-clear cell RCC in the validation cohort. For contrast, a radiologist, with 6 years of experience in genitourinary imaging, was instructed to predict the subtypes (clear cell or non-clear cell RCC) of the validation cohort. The chi-square test was conducted to compare the accuracies between the SVM model and the radiologist.

RESULTS

Our research demonstrated that the SVM model combining 15 features was strongly discriminative in differentiation of clear cell RCC from non-clear cell RCC in the validation cohort. The sensitivity, specificity, overall accuracy, and area under the curves for the SVM model in the validation cohort were 84.7% (61/72), 85% (17/20), 84.8% (78/92), and 0.905, while the sensitivity, specificity, and overall accuracy for the radiologist were 94.4% (68/72), 60% (12/20), and 86.9% (80/92). According to the chi-square test, there was no statistically significant difference between the accuracies of the SVM model and the radiologist (p=0.672).

CONCLUSION

This study demonstrated that CT radiomic features derived from the corticomedullary phase images can aid in the differentiation of renal cell carcinoma subtypes, which is comparable to experienced radiologists.

CLINICAL RELEVANCE/APPLICATION

The effective SVM model combining 15 radiomic features could help the clinical management of patients with renal cell carcinoma, especially patients with non-clear cell renal cell carcinoma.

SSC07-05 Differentiation of Renal Lipid-Poor Angiomyolipoma from Renal Cell Carcinoma by Machine Learning Based on Whole-Tumor Texture Features of Three-Phase CT Images

Monday, Nov. 26 11:10AM - 11:20AM Room: S503AB

Participants

Enming Cui, MD, Jiangmen, China (*Presenter*) Nothing to Disclose Wansheng Long, MD, Guangdong, China (*Abstract Co-Author*) Nothing to Disclose Fan Lin, MD, Shenzhen, China (*Abstract Co-Author*) Nothing to Disclose Xiangmeng Chen, MD, Jiangmen, China (*Abstract Co-Author*) Nothing to Disclose Zhuangsheng Liu, Jiangmen, China (*Abstract Co-Author*) Nothing to Disclose

For information about this presentation, contact:

cem2008@163.com

PURPOSE

To determine the diagnostic performance of machine learning in the differentiation of lipid-poor angiomyolipoma (Ip-AML) from renal cell carcinoma (RCC) based on whole-tumor quantitative texture features of three-phase CT images.

METHOD AND MATERIALS

A total of 40 patients with 41 pathologically proven Ip-AML and 95 patients with 97 pathologically proven RCCs were included by this retrospective study. All patients underwent three-phase CT study which consisted of precontrast phase (PCP), corticomedullary phase (CMP) and nephrographic phase (NP). Texture features were extracted from whole-tumor images at three-phase, single PCP, CMP and NP, respectively. Then support vector machine with recursive feature elimination method based on five-fold cross-validation (SVM-RFECV) were utilized to establish the discriminative classifiers. The performance of classifiers based on three-phase, single PCP, CMP and NP were determined and compared with each other. The performance of machine learning classifier in the differentiation of Ip-AML from RCC was compared with morphological interpretation by radiologists using Receiver operating character (ROC) analysis.

RESULTS

43, 34, 24, 20 features subset were extracted as candidate features in three-phase, PCP, CMP and NP by Boruta package for python respectively. Among of these, 13, 24, 9 12 optimal feature subset further screened by SVM-RFECV entered to establish machine learning classifier in the differentiation of Ip-AML and RCC. The classifier base on three-phase whole tumor images achieved the best performance in discriminating Ip-AML from RCC, with the highest accuracy, area under curve (AUC), sensitivity, and specificity of 92.78%, 0.96, 92.78% and 92.78%, respectively. The performance of morphological interpretation by radiologist was inferior to machine learning classifier in differentiating Ip-AML and RCC, with lower accuracy, AUC, sensitivity and specificity of 69.57%, 0.66, 36.59% and 89.69%.

CONCLUSION

Machine learning classifier based on whole-tumor texture features from three-phase images could reach more accurate discrimination between Ip-AML and RCC than conventional morphological interpretation.

CLINICAL RELEVANCE/APPLICATION

Machine learning classifier is more powerful than morphological interpretation by radiologists and is recommended as part of a MR study prior to renal tumor removal.

SSC07-06 Is Dual-Energy CT (DECT) Of Renal Masses Ready For Prime Time? Diagnostic Accuracy of Conventional Attenuation Change and Iodine Concentration Thresholds at Rapid-kVp-Switch DECT for Detection of Enhancement in Renal Masses

Monday, Nov. 26 11:20AM - 11:30AM Room: S503AB

Participants Nima Sadoughi, MD, Ottawa, ON (*Presenter*) Nothing to Disclose Satheesh Krishna, MD, Ottawa, ON (*Abstract Co-Author*) Nothing to Disclose Matthew D. McInnes, MD, PhD, Ottawa, ON (*Abstract Co-Author*) Nothing to Disclose Blair MacDonald, Ottawa, ON (*Abstract Co-Author*) Nothing to Disclose Nicola Schieda, MD, Ottawa, ON (*Abstract Co-Author*) Nothing to Disclose

For information about this presentation, contact:

nschieda@toh.on.ca

PURPOSE

Iodine concentration (i[]), measured on DECT, is an alternative to attenuation difference (Δ HU) for diagnosis of enhancement in renal masses. Reported i[] thresholds vary and may be too high to detect enhancement in hypoenhancing papillary renal cell carcinoma (pRCC). This study re-evaluates rapid-kVp-switch DECT i[] thresholds for diagnosis of enhancement in SRMs.

METHOD AND MATERIALS

With IRB approval, we evaluated 34 renal masses (including 9 pRCC) diagnosed histologically and 30 benign cysts with renal mass protocol rapid-kVp-switch DECT between 2015-2017. A blinded Radiologist measured i[] (mg/mL) and Δ HU. Enhancement was defined as: 1) i[]>2 mg/mL (Marin et al., Kaza et al.) 2) i[]>1.6 mg/mL (Zarzour et al.) and 3) Δ HU>20 HU. Diagnostic accuracy was tabulated and compared by ROC analysis.

RESULTS

There were no differences in age, gender or size of lesions between groups (p>0.05). Using i[]>2.0 mg/mL achieved sensitivity/specificity/Area under ROC curve (AUC) of 73.3%/100%/0.87. 23.5% (8/34) pRCCs were misclassified as non-enhancing with i[] ranging from 0.7-1.6 mg/mL. Using i[]>1.2 mg/mL, sensitivity/specificity/AUC of 86.7%/100%/0.93 was achieved. 11.8% (4/34) pRCCs were misclassified as non-enhancing with i[] range from 0.7-0.9 mg/mL. Using Δ HU>20 HU achieved sensitivity/specificity/AUC of 93.3%/94.1%/0.94. 5.9% (2/34) pRCCs were misclassified as non-enhancing and 6.7% (2/30) cysts were misdiagnosed as enhancing due to pseudoenhancement. There was no difference in AUC comparing the three methods for detecting enhancement (p>0.05), with higher false negatives encountered with i[] and false positives encounterd with Δ HU.

CONCLUSION

Published iodine concentration thresholds for enhancement in renal masses measured at DECT result in substantial false negative results among hypoenhancing papillary RCC, with the 1.2 mg/mL threshold outperforming 2.0 mg/mL. Δ HU is more sensitive for detection of enhancement compared to iodine concentration but with higher false positive results due to pseudoenhancement.

CLINICAL RELEVANCE/APPLICATION

 Δ HU remains a robust method to diagnose enhancement in renal masses and is more sensitive for detection of low level enhancement in papillary tumors compared to published iodine concentration values; however, DECT remains valuable for diagnosis of pseudoenhancement.

SSC07-07 The Reality of Dual-Energy CT Iodine Quantification in High-Attenuating Renal Lesion: A Comparison to Standard Hounsfield Units Attenuation

Monday, Nov. 26 11:30AM - 11:40AM Room: S503AB

Participants

Mathias Meyer, Durham, NC (*Presenter*) Researcher, Siemens AG; Researcher, Bracco Group Federica Vernuccio, MD, Palermo, Italy (*Abstract Co-Author*) Research support, Siemens AG Christoph Schabel, MD, Durham, NC (*Abstract Co-Author*) Nothing to Disclose Fernando Gonzalez, Santiago, Chile (*Abstract Co-Author*) Nothing to Disclose Bhavik N. Patel, MD,MBA, Stanford, CA (*Abstract Co-Author*) Nothing to Disclose Rendon C. Nelson, MD, Durham, NC (*Abstract Co-Author*) Research Consultant, General Electric Company; Research Consultant, Nemoto Kyorindo Co, Ltd; Consultant, VoxelMetrix, LLC; Co-owner, VoxelMetrix, LLC; Advisory Board, Bracco Group; Advisory Board, Guerbet SA; Research Grant, Nemoto Kyorindo Co, Ltd; Speakers Bureau, Bracco Group; Royalties, Wolters Kluwer nv Daniele Marin, MD, Durham, NC (*Abstract Co-Author*) Research support, Siemens AG

PURPOSE

To determine if dual-energy CT (DECT) derived iodine quantification allows accurate characterization of indeterminate highattenuating renal lesions, and to identify technique- and patient-related variables that may influence lesion characterization.

METHOD AND MATERIALS

220 patients with 265 high-attenuating renal lesions (mean attenuation 54 33HU; 83 malignant lesions) were included in this retrospective IRB-approved, HIPAA-compliant study. Each patient underwent a single-energy unenhanced CT followed by nephrographic phase DECT using four different state-of-the-art DECT platforms (two rapid-kV-switching DECT [rsDECT] systems and two dual-source DECT systems [dsDECT]). Quantitative iodine concentration values and conventional enhancement (Δ HU) were calculated for each lesion. Receiver operating characteristics area under the curve (AUC) for renal lesion characterization were determined. To calculate diagnostic accuracy, surgical resection with histological workup, biopsy, and imaging follow-up for >24 months were used to determine the final category. Receiver operation characteristics, with dedicated area under the curves (AUC) were calculated to differentiate malignant from benign renal lesions. Nominal logistic regression analysis was performed to identify technique- and patient-related variables that may influence lesion characterization.

RESULTS

Diagnostic accuracy for lesion characterization was significantly higher using Δ HU (AUC: 0.93 with an optimal cut-off of 20HU), compared to iodine concentration values (AUC: 0.83; p<0.0001). Optimal iodine concentration thresholds were significantly different for the rsDECT system (2.0mg/ml with AUC of 0.84) compared to the dsDECT system (1.0mg/ml with an AUC of 0.87) (p<0.0001). Using the dedicated iodine thresholds resulted in 32 false positive findings and 20 false negative findings. Lesion location relative to the dual-energy field of view, patient size and DECT platform did not demonstrate any effect on lesion characterization.

CONCLUSION

Conventional measurements of enhancement yield statistically significant higher accuracy compared to iodine concentration measurements for the characterization of indeterminate high-attenuating renal lesions.

CLINICAL RELEVANCE/APPLICATION

Conventional measurements of enhancement is statistically significantly superior to iodine concentration measurements in the characterization of indeterminate high-attenuating renal lesions.

SSC07-08 Clinical Evaluation of Virtual Unenhanced Images from Second-Generation Dual-Energy CT Gemstone Spectral Imaging

Monday, Nov. 26 11:40AM - 11:50AM Room: S503AB

Awards

Student Travel Stipend Award

Participants

Jennifer Xiao, MD, Seattle, WA (*Presenter*) Nothing to Disclose Janet M. Busey, MS, Seattle, WA (*Abstract Co-Author*) Nothing to Disclose David A. Zamora, MS, Seattle, WA (*Abstract Co-Author*) Nothing to Disclose Achille Mileto, MD, Seattle, WA (*Abstract Co-Author*) Nothing to Disclose

For information about this presentation, contact:

jmxiao@uw.edu

PURPOSE

To assess virtual unenhanced (VUE) images from a second-generation dual-energy CT gemstone spectral imaging (GSI) technology and to evaluate how measured attenuation compares to that from true unenhanced (TUE) images.

METHOD AND MATERIALS

Our single-center, retrospective study was IRB-approved and HIPAA-compliant. Fifty-seven subjects (32 men, 25 women; mean age, 65 years) underwent a contrast-enhanced CT of the abdomen on a second-generation dual-energy CT GSI technology with fast kV switching (80/140 kV) between September 2017 and March 2018 for hematuria work-up (n=42) and renal mass evaluation (n=15). TUE images were acquired in all cases in single-energy mode at 120 kV. TUE and VUE images were reconstructed at a slice thickness of 2.5 mm. Attenuation values of liver, pancreas, kidneys, adrenal glands, psoas muscle, subcutaneous fat, aorta, IVC, and main portal vein were measured on TUE and VUE images. In addition, attenuation values were obtained from 24 patients with renal mass (cystic, n=5; solid, n=19). Number of renal stones detected on TUE and VUE were also recorded. Data were analyzed using a Student paired t-test.

RESULTS

There was no significant difference in measured attenuation between TUE and VUE images throughout the abdomen (P>.05, for all comparisons). Mean attenuation values from solid and cystic renal lesions were not significantly different (TUE: 18.4 HU and 9.8 HU vs. VUE: 18.6 HU and 8 HU; P=.76 and P=.38, respectively). We observed a significant difference in number of detected renal stones between TUE (n= 21) and VUE (n= 12) images (P=.01).

CONCLUSION

VUE images obtained from contrast-enhanced data acquired on a second-generation dual-energy CT with GSI technology represent a good approximation of TUE images for noncontrast evaluation of abdominal organs and focal renal lesions. Nevertheless, our preliminary data indicate that a considerable number of small renal stones may not be detected.

CLINICAL RELEVANCE/APPLICATION

Prospective implementation of VUE images may render opportunities for decreased radiation exposure in multi-phase abdominal CT protocols for evaluation of genitourinary pathology.

SSC07-09 Clinical Decision Algorithm for the Evaluation of Renal Cystic Lesions Using Single-Phase Split-Filter Dual-Energy CT

Monday, Nov. 26 11:50AM - 12:00PM Room: S503AB

Participants

Aurelio Cosentino, MD, Torino, Italy (*Abstract Co-Author*) Nothing to Disclose Verena Hofmann, Basel, Switzerland (*Abstract Co-Author*) Nothing to Disclose Daniel Boll, Basel, Switzerland (*Abstract Co-Author*) Nothing to Disclose Benjamin M. Yeh, MD, San Francisco, CA (*Abstract Co-Author*) Research Grant, General Electric Company; Consultant, General Electric Company; Author with royalties, Oxford University Press; Shareholder, Nextrast, Inc; Research Grant, Koninklijike Philips NV; Research Grant, Guerbet SA; ; Matthias Benz, MD, Basel, Switzerland (*Abstract Co-Author*) Nothing to Disclose Markus M. Obmann, MD, San Francisco, CA (*Presenter*) Nothing to Disclose

For information about this presentation, contact:

Markus.Obmann@usb.ch

PURPOSE

To evaluate the diagnostic performance of single source split-filter dual energy CT (tbDECT) to exclude enhancement in renal cystic lesions at venous phase abdominal CT.

METHOD AND MATERIALS

A total of n=230 simple or minimally complicated renal cysts were identified in n=51 consecutive patients who underwent both abdominal tbDECT and magnetic resonance (MR) examination; the latter was used as the 'gold standard' to classify the cysts as Bosniak I or Bosniak II. Material decomposition images were processed off of venous phase series and regions of interest (ROI) were placed within each cystic lesion, blindly to MR. For each ROI, four parameters were assessed simultaneously (Virtual Unenhanced attenuation values [HU], contrast enhancement attenuation values [HU], iodine density [mg/dl] and ROI size [cm2]) to test different approaches for lesion characterization. Renal cysts were considered as not enhancing if contrast enhancement (CM) <= 10 HU and iodine density (IOD) <= 0.5 mg/dl. The ROI was considered small if size <= 0.2 cm2.

RESULTS

Using MR n=207 Bosniak I and n=23 Bosniak II cysts were identified. At virtual unenhanced images, 48% of the cysts were not hypodense (> 10 HU). Both CM and IOD alone gave high percentages of pseudoenhancement (false positive 47% and 33% respectively). The combination of criteria (IOD first then CM) improved specificity to 79%. Exclusion of small ROIs reduced false positives to 3%. An algorithm for the exclusion of enhancement, combining all the criteria, was created.

CONCLUSION

The combined evaluation of multiple criteria provided by tbDECT correctly characterizes Bosniak I and II renal cysts as not enhancing, reduces false positive findings and potentially avoids unnecessary work-ups. We propose an algorithm that can be easily implemented in clinical practice.

CLINICAL RELEVANCE/APPLICATION

Excluding enhancement in renal cystic lesions with 97% of specificity, applying an easy to use algorithm on single-phase dualenergy images from single source, split-filter twin-beam dual-energy CT.



SSC09

Science Session with Keynote: Informatics (Artificial Intelligence in Radiology: Bleeding Edge)

Monday, Nov. 26 10:30AM - 12:00PM Room: E450A



AMA PRA Category 1 Credits ™: 1.50 ARRT Category A+ Credit: 1.75

FDA Discussions may include off-label uses.

Participants

George L. Shih, MD, MS, New York, NY (*Moderator*) Consultant, Image Safely, Inc; Stockholder, Image Safely, Inc; Consultant, MD.ai, Inc; Stockholder, MD.ai, Inc;

Ronald M. Summers, MD, PhD, Bethesda, MD (*Moderator*) Royalties, iCAD, Inc; Royalties, Koninklijke Philips NV; Royalties, ScanMed, LLC; Research support, Ping An Insurance Company of China, Ltd; Researcher, Carestream Health, Inc; Research support, NVIDIA Corporation; ; ; ;

Safwan Halabi, MD, Stanford, CA (Moderator) Nothing to Disclose

Sub-Events

SSC09-01 Informatics Keynote Speaker: Bleeding Edge Medical AI

Monday, Nov. 26 10:30AM - 10:40AM Room: E450A

Participants

Ronald M. Summers, MD, PhD, Bethesda, MD (*Presenter*) Royalties, iCAD, Inc; Royalties, Koninklijke Philips NV; Royalties, ScanMed, LLC; Research support, Ping An Insurance Company of China, Ltd; Researcher, Carestream Health, Inc; Research support, NVIDIA Corporation; ;; ;

SSC09-02 Relationship Learning and Organization of Significant Radiology Image Findings for Lesion Retrieval and Matching

Monday, Nov. 26 10:40AM - 10:50AM Room: E450A

Awards

Trainee Research Prize - Fellow

Participants Ke Yan, Bethesda, MD (*Presenter*) Nothing to Disclose Xiaosong Wang, PhD, Bethesda, MD (*Abstract Co-Author*) Nothing to Disclose Le Lu, Bethesda, MD (*Abstract Co-Author*) Employee, NVIDIA Corporation Ling Zhang, Bethesda, MD (*Abstract Co-Author*) Nothing to Disclose Adam P. Harrison, PhD, Bethesda, MD (*Abstract Co-Author*) Nothing to Disclose Mohammad Hadi Bagheri, MD, Bethesda, MD (*Abstract Co-Author*) Nothing to Disclose Ronald M. Summers, MD,PhD, Bethesda, MD (*Abstract Co-Author*) Nothing to Disclose Ronald M. Summers, MD,PhD, Bethesda, MD (*Abstract Co-Author*) Royalties, iCAD, Inc; Royalties, Koninklijke Philips NV; Royalties, ScanMed, LLC; Research support, Ping An Insurance Company of China, Ltd; Researcher, Carestream Health, Inc; Research support, NVIDIA Corporation; ; ; ;

For information about this presentation, contact:

yankethu@foxmail.com

PURPOSE

Radiologists mark and measure significant image findings in their daily work to assess patients' conditions and therapy responses. These large-scale and diverse clinical annotations can be great data sources to train data-hungry algorithms (e.g. deep learning) for medical image analysis. However, they are basically unsorted and lack semantic annotations like the lesion type and location. We aim to organize and explore them by learning a deep feature embedding for each lesion. It can help us to 1) know their types and locations; 2) find similar lesions in different patients, i.e. content-based lesion retrieval; and 3) find similar lesions in the same patient, i.e. lesion matching across scans for disease tracking.

METHOD AND MATERIALS

We built a large-scale and comprehensive dataset, DeepLesion, by mining the PACS. It contains 32,735 lesions from 10,594 CT studies of 4,427 patients. The lesions are quite diverse, and include e.g. lung nodules, liver lesions, adenopathy, and bone lesions. The train/val/test sets have 70%, 15%, 15% of the data split in patient level. We learn a feature embedding for each lesion that keeps the similarity relationship of the type, location, and size, i.e. lesions with similar attributes should have similar embeddings. We get the lesion types and locations by label propagation and self-supervised body-part regression. Size is directly obtained from the radiological marking. A triplet network with a sequential sampling strategy is utilized to learn the embedding. The network is a multiscale multi-crop convolutional neural network that can exploit both context and detail of the lesion images. The learned embeddings can be applied in lesion retrieval and matching by nearest neighbor searching.

RESULTS

In the test set of DeepLesion, we achieve 91.5±0.1%, 92.8±0.0%, and 94.9±0.0% accuracy in lesion retrieval w.r.t. the lesions'

type, location, and size, respectively. The area-under-curve value for lesion matching is 95.9% in a manually labeled test set of 1313 lesions from 103 patients.

CONCLUSION

We proposed an algorithm to learn feature embeddings for a variety of lesions to encode their type, location, and size. Experiments showed its effectiveness in lesion retrieval and matching.

CLINICAL RELEVANCE/APPLICATION

The proposed algorithm can be used in content-based lesion retrieval and intra-patient lesion matching, which can help radiologists find similar lesions and track lesions in follow-up studies.

SSC09-03 Multi-Stage Deep Disassembling Networks for Generating Bone-Only and Tissue-Only Images from Chest Radiographs

Monday, Nov. 26 10:50AM - 11:00AM Room: E450A

Participants

Jaehong Aum, Seoul, Korea, Republic Of (*Presenter*) Employee, Lunit Inc Sunggyun Park, Seoul, Korea, Republic Of (*Abstract Co-Author*) Employee, Lunit Inc Donggeun Yoo, Seoul, Korea, Republic Of (*Abstract Co-Author*) Employee, Lunit Inc Chang Min Park, MD, PhD, Seoul, Korea, Republic Of (*Abstract Co-Author*) Nothing to Disclose Eui Jin Hwang, Seoul, Korea, Republic Of (*Abstract Co-Author*) Nothing to Disclose

For information about this presentation, contact:

sgpark@lunit.io

CONCLUSION

Deep neural network based automatic disassembling network for CRs is demonstrated and its performance is validated by SSIM proving its potential to improve interpretability of CRs and aid pysicians for accurate diagnosis.

Background

Dual-energy subtraction technique produces bone-only and tissue-only images to improve interpretability of chest radiographs (CRs). However, the use of this technique was limited because it requires a specialized hardware device for capturing the CRs. In order to overcome this limitation, we developed a deep disassembling networks for CRs (DDCN) which generates bone-only and tissue-only images from a normal CR.

Evaluation

To develop DDCN, we collected a total of 617 CRs with both bone-only and tissue-only images, which were produced by dual energy subtraction technique. To clean the dataset, we excluded 100 cases with suboptimal image quality. Furthermore, we refined the remaining 517 cases using guided filter and non-local means filter to remove image noises. Subsequently, we randomly divided the 517 datasets into the training dataset (n=467) and validation dataset (n=50). We designed a novel two-stage deep convolutional network where the first-stage is designed for observing context of a CR and the second-stage is for producing bone-only and tissue-only images given the first-stage output. The network is constructed with residual architecture, 40 convolutions for the first-stage and 14 convolutions for the second-stage. We quantitatively measured the performance of our network using SSIM which measures the structure difference between a given ground truth image and our network-producing image. In validation dataset, the measured SSIM comparing ground truth tissue-only images and our network-producing results was 0.9678. When we limit the region of interest (ROI) as lung area, the SSIM was measured as 0.9835. In the case of bone-only image, it was 0.9877 and 0.9870 when we limit ROIs as whole image and lung area, respectively.

Discussion

DDCN produces bone-only and tissue-only images from CRs taken by conventional X-ray device. We believe it is the first introduction of deep neural network for disassembling bone and tissue from a CR.

SSC09-04 Non-invasive Tracking of Cancer Evolution using Deep Learning-Based Longitudinal Image Analysis

Monday, Nov. 26 11:00AM - 11:10AM Room: E450A

Participants

Yiwen Xu, PhD, Boston, MA (*Presenter*) Nothing to Disclose Ahmed Hosny, MSc, Cambridge, MA (*Abstract Co-Author*) Nothing to Disclose Thibaud Coroller, MS, Boston, MA (*Abstract Co-Author*) Nothing to Disclose Roman Zeleznik, Boston, MA (*Abstract Co-Author*) Nothing to Disclose Raymond H. Mak, MD, Boston, MA (*Abstract Co-Author*) Nothing to Disclose Hugo Aerts, PhD, Boston, MA (*Abstract Co-Author*) Stockholder, Sphera Inc

PURPOSE

Tumors are continuously evolving biological systems, and medical imaging is uniquely poised to monitor those changes in patients, before, during, and after treatment. While it is trivial to track tumor lesions over space and time, it is much harder to develop models encompassing all the time points. Here we investigated the use of recurrent deep learning network capable of analysing time series CT images of locally advanced non-small cell lung cancer (NSCLC) patients.

METHOD AND MATERIALS

Dataset A consists of 179 stage III NSCLC patients treated with definitive radiation therapy (581 scans, mean 3.2 scans per patient). This dataset was separated into independent training/tuning (n=107), and test (n=72) cohorts. Transfer learning through convolutional neural networks (CNN) merged with a recurrent neural network was trained on serial scans. Survival was analyzed for a separate test set with AUC and Kaplan Meier curves. Further pathologic response validation of the CNN model was performed on Dataset B (n=79 patients, 158 scans, 2 per patient) treated with chemoradiation followed by surgery. This cohort was used to

validate pathological tumor response and compared to performance with volume change.

RESULTS

Enhanced performance on the test set was observed with the addition of each follow-up scan into the CNN model for 2-year survival (AUC=0.64, 0.69, 0.74, p<0.05), comporable results were demonstrated for one-year survival. The models with 3 follow-up scans showed strong stratification power for high and low risk groups of the predictions using Kaplan-Meier analysis (Log-rank, p<0.05). The hazard ratios for the one-year and 2-year survival models were 6.16 and 2.38, respectively (p<0.05). The CNN model significantly stratified pathological responders and cases of gross residual disease in Dataset B (AUC=0.65, p<0.05), with predictive results comparable to tumour volume change.

CONCLUSION

This study demonstrates promising results using deep learning to combine patient scans at multiple time points to improve clinical survival and response predictions. Pathologic validation of this biomarker was shown on an independent validation cohort.

CLINICAL RELEVANCE/APPLICATION

Tracking of cancer evolution using deep learning applied to medical imaging showed promising predictions of patient outcome and pathologic response, without the need for manual tumor contours.

SSC09-05 Interpretation of Computed Tomography Without Reconstruction: Reading Sinograms to Detect Intracranial Hemorrhage

Monday, Nov. 26 11:10AM - 11:20AM Room: E450A

Participants

Chao Huang, PhD, Boston, MA (*Presenter*) Nothing to Disclose Hyunkwang Lee, Boston, MA (*Abstract Co-Author*) Nothing to Disclose Sehyo Yune, MD, MPH, Boston, MA (*Abstract Co-Author*) Nothing to Disclose Myeongchan Kim, MD, Boston, MA (*Abstract Co-Author*) Nothing to Disclose Synho Do, PhD, Boston, MA (*Abstract Co-Author*) Nothing to Disclose

For information about this presentation, contact:

chuang35@mgh.harvard.edu

PURPOSE

In the current medical practice, diseases or conditions, such as intracranial hemorrhage (ICH), are usually diagnosed using reconstructed images that are generated from sophisticated reconstruction algorithms. In this study, we explore the feasibility to directly detect ICH from non-contrast head computed tomography (CT) in data domain instead of image domain by applying deep learning techniques on CT sinograms.

METHOD AND MATERIALS

A total of 889 head CT examinations were retrieved from our institutional database, and each axial slice was annotated by 5 boardcertified neuroradiologists. The pixel values of CT images were then converted into linear attenuation coefficients, upon which the 2D parallel-beam Radon transforms were applied to generate simulated sinograms. To investigate the effects of number of projection views and detector size on ICH detection, 3 sets of sinograms were produced: '360 x 729', '120 x 240' and '40 x 80', where 'm x n' means the sinogram obtained from m projection views and n detectors. The sinograms were then randomly splitted into training (635 cases), validation (127 cases) and testing (127 cases) sets, which were used to train, validate, and evaluate a convolutional neural network (CNN) that inputs a sinogram and outputs the probability of ICH. To improve generalization, data augmentation was used for training by applying affine transformations (translation, scaling, rotation and reflection) on CT image slices followed by Radon transforms. For comparison, another CNN was built and trained with reconstructed CT images.

RESULTS

The CNN model using CT images as inputs achieved 91.5% test accuracy on ICH detection, and the models using " 360×729 ", " 120×240 " and " 40×80 " sinograms as inputs detected ICH with 80.2%, 78.1%, and 76.7% accuracy, respectively.

CONCLUSION

This study shows the potential of direct detection of ICH using CT raw data without image reconstruction. The results also suggest the possibility of using sparse projection views and large-size detectors without sacrificing the ICH detection accuracy, which could lower the radiation dose and equipment costs.

CLINICAL RELEVANCE/APPLICATION

Direct detection of critical conditions like ICH using sinograms without image reconstruction will save the processing time that is critical in situations like emergency rooms. The potential of radiation dose and equipment cost reduction is also of interest to radiologists.

SSC09-06 Image Annotation by Eye Tracking: Accuracy and Precision of Centerlines of Obstructed Small Bowel Segments Placed Using Eye Trackers

Monday, Nov. 26 11:20AM - 11:30AM Room: E450A

Participants

Alfredo Lucas, BSC, La Jolla, CA (Abstract Co-Author) Nothing to Disclose

Kang Wang, MD, PhD, San Diego, CA (Abstract Co-Author) Nothing to Disclose

Cynthia S. Santillan, MD, San Diego, CA (Abstract Co-Author) Consultant, Robarts Clinical Trials, Inc

Albert Hsiao, MD, PhD, La Jolla, CA (*Abstract Co-Author*) Founder, Arterys, Inc; Consultant, Arterys, Inc; Consultant, Bayer AG; Research Grant, General Electric Company;

Claude B. Sirlin, MD, San Diego, CA (*Abstract Co-Author*) Research Grant, Gilead Sciences, Inc; Research Grant, General Electric Company; Research Grant, Siemens AG; Research Grant, Bayer AG; Research Grant, ACR Innovation; Research Grant, Koninklijke

Philips NV; Research Grant, Celgene Corporation; Consultant, General Electric Company; Consultant, Bayer AG; Consultant, Boehringer Ingelheim GmbH; Consultant, AMRA AB; Consultant, Fulcrum Therapeutics; Consultant, IBM Corporation; Consultant, Exact Sciences Corporation; Advisory Board, AMRA AB; Advisory Board, Guerbet SA; Advisory Board, VirtualScopics, Inc; Speakers Bureau, General Electric Company; Author, Medscape, LLC; Author, Resoundant, Inc; Lab service agreement, Gilead Sciences, Inc; Lab service agreement, ICON plc; Lab service agreement, Intercept Pharmaceuticals, Inc; Lab service agreement, Shire plc; Lab service agreement, Enanta; Lab service agreement, Virtualscopics, Inc; Lab service agreement, Alexion Pharmaceuticals, Inc; Lab service agreement, Takeda Pharmaceutical Company Limited; Lab service agreement, sanofi-aventis Group; Lab service agreement, Johnson & Johnson; Lab service agreement, NuSirt Biopharma, Inc; Contract, Epigenomics; Contract, Arterys Inc Paul M. Murphy II, MD, PhD, San Diego, CA (*Presenter*) Nothing to Disclose

For information about this presentation, contact:

pmmurphy@ucsd.edu

PURPOSE

To determine the accuracy and precision of centerlines of obstructed small bowel segments placed using eye trackers.

METHOD AND MATERIALS

This HIPAA-compliant IRB-approved retrospective pilot study included seven subjects diagnosed with small bowel obstruction (SBO) by CT. For each subject, an obstructed segment of bowel was chosen. Three observers then annotated the centerline of the segment with three methods: manual fiducial placement or visual fiducial placement using either a Tobii x3-120 or 4c eye tracker, which report the location on the screen at which an observer is looking. This location was mapped to 3D coordinates within the CT volume using a custom 3D Slicer module. Each annotation was repeated three times. The distance between centerlines was calculated after alignment using dynamic time warping (DTW) to account for the variable number of fiducials placed. Intra-observer DTW distance between manual and visual centerlines was calculated as measure of accuracy. Intra- and inter-observer DTW distances between centerlines placed with each method were calculated as measures of precision. One-sample t-tests were performed to assess whether mean DTW distances were less than 1.5 or 3 cm for each measure of accuracy or precision respectively.

RESULTS

DTW distances between manual and visual centerlines ranged from 1.1 ± 0.2 to 1.8 ± 0.2 cm, and were significantly less than 1.5 cm for two of three observers using both visual methods (P<0.01). Intra- and inter-observer DTW distances for manual centerlines were 0.6 ± 0.1 and 0.8 ± 0.2 cm, and for visual centerlines ranged from 1.0 ± 0.4 to 1.9 ± 0.6 cm, but were less than 3.0 cm in all cases (P<0.01).

CONCLUSION

Eye trackers may be used for visual annotation of the centerlines of obstructed small bowel segments with accuracy and precision that compare favorably to the threshold diameter of 3 cm for diagnosis of SBO on CT. Accuracy varied among observers, but precision was consistently favorable.

CLINICAL RELEVANCE/APPLICATION

SBO is a common and important disease, for which machine learning tools have yet to be developed. Image annotation is a critical first step in machine learning, but manual annotation of small bowel is prohibitively time-consuming. Image annotation by eye tracking is sufficiently accurate and precise relative to the diameter of obstructed small bowel to serve as a potential first step in the development of machine learning tools that facilitate diagnosis of SBO on CT.

SSC09-07 Big Data Interpretability: Automatically Identify Mislabeled Data in Medical Imaging Deep Learning

Monday, Nov. 26 11:30AM - 11:40AM Room: E450A

Participants Degan Hao, MS, Pittsburgh, PA (*Presenter*) Nothing to Disclose Lei Zhang, PhD, Pittsburgh, PA (*Abstract Co-Author*) Nothing to Disclose Bingjie Zheng, MD, Zhengzhou, China (*Abstract Co-Author*) Nothing to Disclose Margarita L. Zuley, MD, Pittsburgh, PA (*Abstract Co-Author*) Investigator, Hologic, Inc Ruimei Chai, Shenyang, China (*Abstract Co-Author*) Nothing to Disclose Shandong Wu, PhD, MSc, Philadelphia, PA (*Abstract Co-Author*) Nothing to Disclose

For information about this presentation, contact:

deh95@pitt.edu

PURPOSE

In big data applications, data quality and variations can significantly influence performance of deep learning models. Manual labeling or natural language processing-based labeling inevitably generates some mislabeled data. We developed a dedicated method for deep learning to automatically identify potentially mislabeled data.

METHOD AND MATERIALS

We proposed a novel algorithm framework using entropy loss and influence functions to measure data's relevance and correlation strengths with respect to classification performance in convolutional neural network (CNN) models. We identified a clinically-acquired digital mammographic imaging data and their BI-RADS breast density categories (a/b/c/d). Category a (fatty) and d (extremely dense) each has 350 images, while Category b (scattered fibroglandular density) and c (heterogeneously dense) each has 2,000 images. We implemented a CNN-based binary classification model on distinguishing Category a vs d and another similar model for Category b vs c. We did two experiments: 1) Before training models, we purposely flipped the labels for 10% randomly selected data in each category and used our method to identify those flipped data; and 2) We ran our method on the original unflipped data to identify those potentially mislabeled images by radiologists and evaluate the effect by using a published scheme that assesses the "correctness" of clinically-assigned BI-RADS breast density categories.

The AUC is 0.99 and 0.96 for the Category a vs d model and for the Category b vs c model, respectively. For experiment 1), our method can identify 98% of the purposely flipped data in Category a and d, and 92% in Category b and c, by automatically examining as small as only 30% of the full dataset. For experiment 2), there is 78% (or 96%) overlap in the potentially mislabeled data between those identified by our method and those specified by the "correctness" assessment method, by examining 50% (or 90%) of the full dataset.

CONCLUSION

We developed an automated method for deep learning and demonstrated it can identify vast majority of mislabeled data in the BIRADS-based clinical breast density assessment in digital mammograms.

CLINICAL RELEVANCE/APPLICATION

Fully-automated identification of mislabeled data for deep learning can significantly improve data quality, model's performance and reliability, as well as stratified data interpretability.

SSC09-08 Approaching Chest-CT-Level Performance on Chest X-Rays with Deep-Learning

Monday, Nov. 26 11:40AM - 11:50AM Room: E450A

Participants

Tarun Raj, Mumbai, India (*Presenter*) Employee, Qure.ai Pooja Rao, MBBS,PhD, Mumbai, India (*Abstract Co-Author*) Employee, Qure.ai Prashant Warier, PhD, Mumbai, India (*Abstract Co-Author*) Employee, Qure.ai Manoj D. Tadepalli, BEng, Mumbai, India (*Abstract Co-Author*) Employee, Qure.ai Bhargava Reddy, Mumbai, India (*Abstract Co-Author*) Employee, Qure.ai Preetham Putha, BEng, Mumbai, India (*Abstract Co-Author*) Employee, Qure.ai Justy Antony Chiramal, MBBS,MD, Mumbai, India (*Abstract Co-Author*) Research Consultant, Qure.ai

For information about this presentation, contact:

tarun.raj@qure.ai

PURPOSE

To determine whether deep learning algorithms can detect abnormalities on chest X-rays (CXR) before they are visible to radiologists.

METHOD AND MATERIALS

We trained deep learning models to identify abnormal X-rays and CXR opacities using a set of 1,150,084 chest X-Rays. We used a retrospectively obtained independent set of de-identified chest X-rays from patients who had undergone a chest CT scan within 1 day (TS-1, n=187), 3 days (TS-3, n=197) and 10 days (TS-10, n=230) of the X-ray to evaluate the algorithms' ability to detect abnormalities that were not visible to the radiologist at the time of reporting on the X-ray. Natural language processing algorithms were used to establish ground truth from radiologist reports of the CT scans, on 2 parameters - 'any abnormality' and 'hyperdense abnormality (HA)' - defined as any abnormal focal or diffuse hyperdense abnormality in the lung fields including but not limited to nodule, mass, fibrosis and calcification. The CT scans were used as ground truth to evaluate the accuracy of the original CXR report and the deep learning algorithms.

RESULTS

Of 187 CT scans in TS-1, 153 contained an HA. 52 of these (34%) had been picked up on the original CXR by the reporting radiologist, and 63 of these (41%) were picked up by the deep learning algorithm. Of 180 abnormal scans in TS-1, 106 (59%) had been picked up as abnormal on the original CXR by the reporting radiologist, and 120 of these (67%) were picked up by the deep learning algorithm. To detect HA, this amounts to an accuracy of 0.49, sensitivity of 0.41 and specificity of 0.85 for the algorithm, versus an accuracy of 0.44, sensitivity of 0.34 and specificity of 0.91 for the original radiologist read of the chest X-ray. To detect any abnormality, the accuracy, sensitivity, and specificity are 0.67,0.67 and 0.71 respectively for the algorithm, and 0.59,0.59 and 0.71 respectively for the reporting radiologist. Similar results were observed on TS-3 and TS-10, as shown in the figure below

CONCLUSION

Deep learning algorithms can pick up abnormalities that have been missed on chest X-rays but identified on a subsequent chest CT.

CLINICAL RELEVANCE/APPLICATION

Using deep learning algorithms to screen chest X-rays could result in higher sensitivity at identifying abnormal scans than currently possible, with only a small corresponding increase in the number of false positives.

ssc09-09 A Portable Automated X-Ray Imaging System and Reading Solution for Screening Lung Diseases

Monday, Nov. 26 11:50AM - 12:00PM Room: E450A

Participants Girish Srinivasan, Palatine, IL (*Presenter*) Nothing to Disclose Woo Jung Shim, Seoul, Korea, Republic Of (*Abstract Co-Author*) Nothing to Disclose Zafar Fawad, Santa Monica, CA (*Abstract Co-Author*) Nothing to Disclose Sung-Hong Park, Daejeon, Korea, Republic Of (*Abstract Co-Author*) Nothing to Disclose Huan M. Luu, BSC, Daejeon, Korea, Republic Of (*Abstract Co-Author*) Nothing to Disclose

For information about this presentation, contact:

srinivasan.girish@gmail.com

CONCLUSION

The AXIR system allows clinicians to save time and money while providing patients with good service at any location. The AI-based

automation facilitates its use as a screening and diagnosis tool, allowing doctors to make real-time decisions with high precision and reliability. The system, in the future, may cover other anatomical regions while the AI-engine can be enhanced to diagnose broader disease indications.

Background

A chest x-ray is a commonly used examination for screening and diagnosis of lung diseases. Artificial intelligence (AI) solutions, for automated image analysis, have been implemented as cloud-based solutions centered on hospitals with well-equipped infrastructures. However, two-thirds of the planet does not have access to radiology services due to lack of infrastructure and expertise. We have developed a portable automated X-ray imaging system and reading solution (AXIR) with embedded AI technology to solve this problem.

Evaluation

The AXIR system comprises of a low power portable generator (3kW), a wireless detector (resolution > 4lp/mm), an image preprocessing tool, an AI-based analysis engine, and a mobile viewer. The AI engine screens images for abnormalities and displays the location. Abnormalities can further be classified as pleural effusion, cardiomegaly, opacity, infiltrate, consolidation, fibrosis, hilar enlargement, and calcification. The AI models were trained using public datasets and with images acquired using the AXIR system. The system is being validated at a poor infrastructure site handling about 1000 chest X-rays / month. The performance of the system is evaluated by measuring the accuracy, sensitivity, and specificity of diagnosis.

Discussion

Access to diagnostic imaging services has a great impact on public health and can potentially increase, for example, early detection. AXIR's portable X-ray system with embedded AI-based analytics is a novel highly accessible medical device. In our initial test, we achieved a diagnostic accuracy of 92% with a sensitivity of 94% and specificity of 90%. At our pilot site, the system reduced the diagnosis time from an average of 3 days to less than 10 minutes and brought the patient re-visit rate down to 1% from 20%.



SSC12

Physics (MR: New Techniques, Systems, Evaluation)

Monday, Nov. 26 10:30AM - 12:00PM Room: N226



AMA PRA Category 1 Credits ™: 1.50 ARRT Category A+ Credit: 1.75

FDA Discussions may include off-label uses.

Participants

Robert E. Lenkinski, PhD, Dallas, TX (*Moderator*) Research Grant, Koninklijke Philips NV Research Consultant, Aspect Imaging Peter A. Hardy, PhD, Lexington, KY (*Moderator*) Nothing to Disclose Yi Wang, PhD, New York, NY (*Moderator*) Nothing to Disclose

Sub-Events

SSC12-01 Impact of Respiratory Training in Improving Image Quality: A Study Based on Free Breathing T1 Star VIBE MRI

Monday, Nov. 26 10:30AM - 10:40AM Room: N226

Participants

Ma Guangming, MMed, Xianyang City, China (*Presenter*) Nothing to Disclose Dang Shan, Xianyang, China (*Abstract Co-Author*) Nothing to Disclose Tian Qian, MMed, Xianyang City, China (*Abstract Co-Author*) Nothing to Disclose Nan Yu, MD, Xian Yang, China (*Abstract Co-Author*) Nothing to Disclose Lei Yuxin, MMed, Xianyang City, China (*Abstract Co-Author*) Nothing to Disclose Shaoyu Wang, Shanghai, China (*Abstract Co-Author*) Nothing to Disclose Chenwang Jin, Xi'an, China (*Abstract Co-Author*) Nothing to Disclose

For information about this presentation, contact:

416725386

PURPOSE

Our objective was to estimate the impact of respiratory training in improving image quality of images obtained from T1 Star VIBE magnetic resonance imaging (MRI).

METHOD AND MATERIALS

This prospective study was approved by the local ethics committee. Totally of 6 volunteers were in the study. The volunteers underwent 3 Tesla MR scanner (Siemens-Skyra) using T1 Star VIBE for two times within 24-48h. The MRI protocol (MAGNETOM 3.0T SKYRA MR scanner, Siemens healthcare, Erlangen, Germany) included a Prototyped T1-weighted 3D Star VIBE sequence(TE/TR:1.39/2.79,slice thickness 1.2mm)and T2 blade. The volunteers accepted MRI examination directly at the first scan, while they receive respiratory training before the MRI examination to make them keeping calm and breathing evenly. The observation of lung markings were used to evaluate image quality of each examination. The display of lung markings were observed in three zone (upper, middle and bottom according to the T4 and T8 vertebra level) by two experienced radiologists independently. And a 3-point system were used (3-point: no artifacts, noise, or with a little artifacts, less noise, the image quality is better; 2-point: more artifacts, more noise, image quality is acceptable; 1-point: obvious artifacts, large noise, image quality is poor.) The image quality of T1 Star VIBE MRI in two scans were compared.

RESULTS

All the volunteers finished MRI examination. The image quality scores of three zones(upper, middle and bottom) in first scans were 2.5 ± 0.55 , 2.17 ± 0.75 , 1.5 ± 0.55 , and those were 2.83 ± 0.41 , 2.67 ± 0.52 , 2.33 ± 0.82 in the second scans. The image quality scores of the lower part of the lungs had significant difference among the two groups(t=2.71, p=0.042).

CONCLUSION

Respiratory training could improve the image quality, especially at the bottom of the lung and increase the lesion detection rate and accuracy of diagnosis.

CLINICAL RELEVANCE/APPLICATION

Respiratory training may be used to improve the image quality of images obtained from T1 Star VIBE magnetic resonance imaging.

ssc12-02 MRI Safety: Digital Measurement of Magnetically Induced Torque Based on ASTM F2213

Monday, Nov. 26 10:40AM - 10:50AM Room: N226

Mushtaq Musadik, Jena, Germany (*Abstract Co-Author*) Nothing to Disclose Rene Aschenbach, MD, Jena, Germany (*Abstract Co-Author*) Nothing to Disclose Florian Burckenmeyer, Jena, Germany (*Presenter*) Nothing to Disclose Ioannis Diamantis, Jena, Germany (*Abstract Co-Author*) Nothing to Disclose Niklas P. Eckardt JR, MD, Neuengonna, Germany (*Abstract Co-Author*) Nothing to Disclose Ulf K. Teichgraeber, MD, Jena, Germany (*Abstract Co-Author*) Research Consultant, W. L. Gore & Associates, Inc Research Consultant, Siemens AG Research Consultant, CeloNova BioSciences, Inc Research Consultant, General Electric Company

CONCLUSION

Ferromagnetic stainless steel screws may exhibit large magnetically induced torque within the homogeneous magnetic field during MRI examination. For analysing of these magnetically induced torque a digital measuring device could be developed, which allows to simplify and accelerated the standard test method ASTM F2213.

Background

Performing MRI examinations in patients who use implantable medical devices involve safety risks both for the patient and the implant. The aim was a digital measuring device for measuring magnetically induced torque on medical implants in magnetic field center of 1.5T and 3T MR scanner.

Evaluation

An MR-safe measuring platform was developed according to the standard ASTM F2213 and combined with a precision balance (PCB 1600-2, Kern & Shon GmbH, Germany). The evaluation was performed with stainless steel screws (length 24, 47 and 71 mm) and a neurostimulator (LibraXP, St. Jude Medical, USA) in the magnetic field center of a 1.5T and 3T MRI (Magnetom Avanto and Magnetom Prisma, Siemens, Germany). The torque was measured at 10-degree increments as the implant was rotated relative to the static magnetic field for all possible orientations of the object.

Discussion

The measured force depends on the object orientation within the static magnetic field. The neurostimulator had a torque of 1 + 1 N*mm (maximum 3 N*mm) for a rotation about the vertical axis, 39 + 20 Nmm (maximum 64 N*mm) for rotation about the longitudinal axis and 40 + 20 N * mm (maximum 64 N*mm)) for a rotation about the transverse axis. This corresponds to a maximum acting force of 1.28 N (mass 0.131 kg). The magnetostatic torque is proportional to the length of the test object. For the stainless steel screws, the torque is 66 + 37 N*mm (maximum 108 N*mm) for a length of 24 mm, 139 + 86 Nmm (maximum 247 N*mm) for a length of 47 mm and 252 + 145 Nmm (maximum 434 N*mm) for a length of 71 mm.

SSC12-03 Numerical Simulation of Thermal Risk Assessment for a Compact MR Scanner

Monday, Nov. 26 10:50AM - 11:00AM Room: N226

Participants

Matthew Tarasek, PhD, Niskayuna, NY (*Abstract Co-Author*) Employee, General Electric Company Yunhong Shu, PhD, Rochester, MN (*Abstract Co-Author*) Nothing to Disclose Desmond Yeo, Niskayuna, NY (*Abstract Co-Author*) Employee, General Electric Company Ek T. Tan, MENG, Rochester, MN (*Abstract Co-Author*) Employee, General Electric Company John Huston III, MD, Rochester, MN (*Abstract Co-Author*) Stockholder, Resoundant, Inc Royalties, Resoundant, Inc Matthew A. Bernstein, PhD, Rochester, MN (*Presenter*) Former Employee, General Electric Company Thomas K. Foo, PhD, Niskayuna, NY (*Abstract Co-Author*) Employee, General Electric Company

For information about this presentation, contact:

tarasek@ge.com

PURPOSE

Brain imaging on conventional MRI scanners commonly relies on a whole-body (WB) radiofrequency (RF) transmit coil to provide a uniform excitation (B1+) field. As such, patient RF power deposition may be an issue during high RF duty-cycle scanning. A recently developed compact 3T (C3T) MRI scanner with high performance gradients [1,2] has a dedicated RF transmit coil that exposes only the head region. For neuroimaging, the C3T scanner may provide lower RF power deposition compared to conventional WB scanners, thus enabling the development of advanced neuroimaging techniques.

METHOD AND MATERIALS

A 16-rung high-pass birdcage head coil (127.74 MHz, 37-cm ID, driven in quadrature) was modelled using full-wave electromagnetic FDTD simulation software, Sim4Life (ZMT, Zurich, Switzerland). Simulations were performed to predict specific absorption rate (SAR) distributions using the Duke human body model as a test phantom at a landmark location of the glabella. A large-diameter standard 3T 16-rung WB birdcage coil was also modeled for comparison. Input power on the larger coil was scaled to reach the same average B1+ for the glabella slice as in the C3T, and scaled SAR maps were used as inputs to a time-dependent Penne's bioheat equation [3] thermal solver. All thermal simulations were run using 200W continuous input power for 60 minutes, with the proper scaling for the WB coil according to B1+. All material properties were set to nominal literature values [4].

RESULTS

The following were observed as a result of the simulations of the C3T compared to whole-body MRI: (i) ~20% reduced average SAR in the head and neck region, (ii) lower (5.5° C vs 6.5° C) peak temperature rise in the brain regions, and (iii) minimal (~0°C) temperature rise in the neck region was observed in the C3T scanner compared to the ~7°C rise in the WB MRI, due to reduced body mass exposure in the dedicated scanner.

CONCLUSION

The C3T provides a reduction of ~20% in thermal risk over a conventional whole-body MRI due to the much smaller exposed body mass to achieve the same B1+ excitation field in the brain. This allows for improved performance from the SAR demanding applications. 1.FooT,MRM,2018 2.WeaversP,MPhys,2016 3.Pennes.JAPhys1948 4.GabrielS,PMB1996

CLINICAL RELEVANCE/APPLICATION

Advanced neuroimaging techniques require faster imaging thus creating potential for increased patient heating. Here we investigate the thermal risk of a recently developed head-only MRI scanner.

SSC12-04 Improving Resolution, Distortion, and SNR of Clinical Diffusion Weighted Images Using Deep Learning

Monday, Nov. 26 11:00AM - 11:10AM Room: N226

Participants

Junshen Xu, Beijing, China (*Presenter*) Nothing to Disclose Nan Liu, Shanghai, China (*Abstract Co-Author*) Employee, Shanghai United Imaging Healthcare Co, Ltd Xiaodong Ma, Beijing, China (*Abstract Co-Author*) Nothing to Disclose Jun Xie, Shanghai, China (*Abstract Co-Author*) Employee, Shanghai United Imaging Healthcare Co, Ltd Guobin Li, Shanghai, China (*Abstract Co-Author*) Employee, Shanghai United Imaging Healthcare Co, Ltd Zhenkui Wang, Shanghai, China (*Abstract Co-Author*) Employee, Shanghai United Imaging Healthcare Co, Ltd Nan-Jie Gong, Houston, TX (*Abstract Co-Author*) Employee, UIH America, Inc Kui Ying, PhD, Beijing, China (*Abstract Co-Author*) Nothing to Disclose

PURPOSE

Diffusion weighted images (DWI) are commonly acquired with single-shot Echo-planar imaging (EPI) sequence, which is suffered from image distortion due to eddy current and B0 field inhomogeneity as well as low resolution especially in clinical settings. Multi-shot DWI has been demonstrated to outperform single-shot DWI in these aspects with optimized SNR. However, multi-shot DWI has not been widely adopted clinically due to long scan time.

METHOD AND MATERIALS

We proposed a method of generating high-quality DWI from its low-quality counterpart using fully convolutional neural network. Brain DWI data were acquired with a 3T MR system (uMR 780) using both single-shot (128*128) and four-shots (160*160) EPI sequences. The multi-shot EPI DWI, which has higher resolution and less distortion, served as ground truth in training process. Our dataset contains 38 pairs of single-shot and multi-shot DWI. Each pair of images were resized to 320x320 and then cropped randomly to generate 50 patches (128x128). To make full use of available data and reduce the bias, we adopted a 10-fold cross validation in experiments.

RESULTS

For quantitative evaluation, we calculated peak signal-to-noise ratio (PSNR) and structural similarity index (SSIM). Results showed that the proposed method gain 4.2dB in PSNR and 0.22 in SSIM compared with single-shot DWI. Additionally, perceptual results showed that our neural network can recover details and reduce distortion in single-shot DWI.

CONCLUSION

Results imply that we can improve resolution, SNR and reduce distortion of single-shot EPI-DWI using deep neural network, which potentially enables acquiring high quality DWI without lengthening scan time.

CLINICAL RELEVANCE/APPLICATION

This method could improve resolution, SNR and reduce distortion of clinical DW images without lengthening scan time.

ssc12-05 Fast Field-Cycling MRI Technology: Prototype Human Scanner and First Clinical Results

Monday, Nov. 26 11:10AM - 11:20AM Room: N226

Participants

David Lurie, Aberdeen, United Kingdom (*Presenter*) Research Grant, General Electric Company Lionel M. Broche, PhD, Aberdeen, United Kingdom (*Abstract Co-Author*) Nothing to Disclose Gareth R. Davies, MSc, DPhil, Aberdeen, United Kingdom (*Abstract Co-Author*) Nothing to Disclose German Guzman Gutierrez, MD,MPH, Aberdeen, United Kingdom (*Abstract Co-Author*) Nothing to Disclose Mary J. Macleod, MBChB,PhD, Aberdeen, United Kingdom (*Abstract Co-Author*) Nothing to Disclose Peter J. Ross, PhD, Aberdeen, United Kingdom (*Abstract Co-Author*) Nothing to Disclose

For information about this presentation, contact:

d.lurie@abdn.ac.uk

PURPOSE

A prototype human-scale Fast Field-Cycling (FFC) MRI scanner has been built, allowing good quality images at ultra-low field (0.2 mT) with enhanced T1-contrast. It has been used to image the brain in patients with acute ischemic stroke.

METHOD AND MATERIALS

FFC-MRI is a new method, designed to image at ultra-low field while preserving signal-to-noise ratio (SNR) and image quality. The main field (B0) is switched between values during the pulse sequence, with polarization at the scanner's highest field, evolution (relaxation) at low field, followed by gradients, RF pulses and signal detection at high field. Our in-house-built prototype scanner has a water-cooled resistive magnet (Tesla Engineering, UK; bore 0.5 m, length 2 m) providing a maximum field of 0.2 T, with the evolution field controllable between 0.2 mT and 0.2 T; switching time between fields is 20 ms. A home-built head birdcage coil (8.5 MHz) was used. Scanner control is via a commercial console (MR Solutions, UK), running pulse sequences which include control of B0. Magnet current (up to 1950 A) is from a low-noise power supply amplifier (International Electric Company, Finland). Following research ethics committee approval, patients (N=10) with acute ischemic stroke were recruited and gave informed consent. They were scanned by FFC-MRI within 24-96 h after presentation. Duration of the FFC-MRI examination was typically 45 minutes, including setup, scout and FFC images at five evolution fields (0.2 mT to 200 mT). Patients were scanned by CT prior to FFC-MRI and some had 3 T MRI (N=2) including DWI.

RESULTS

The usable range of B0 during the evolution period was validated in phantoms. In scans of patients with acute ischemic stroke, T1-

weighted FFC-MRI images exhibited hyper-intense regions, with contrast increasing markedly as the evolution magnetic strength field decreased, with maximum lesion intensity at the lowest field used (0.2 mT). The infarct region seen by FFC-MRI correlated well with the appearance in CT and DWI (where appropriate) images.

CONCLUSION

A whole-body FFC-MRI scanner was built and has been used to image the brain in patients with ischemic stroke, in the first-ever clinical demonstration of this technology.

CLINICAL RELEVANCE/APPLICATION

FFC-MRI is a new modality which can generate diagnostic-quality images at ultra-low magnetic fields (e.g. 0.2 mT), with significantly-enhanced endogenous T1-contrast compared to conventional MRI.

SSC12-06 Joint Cardiovascular Magnetic Resonance Image Reconstruction and Segmentation Using Deep Learning Image-to-Image Translation

Monday, Nov. 26 11:20AM - 11:30AM Room: N226

Participants

James W. Goldfarb, PhD, Roslyn, NY (*Presenter*) Nothing to Disclose Jie J. Cao, MD, Roslyn, NY (*Abstract Co-Author*) Nothing to Disclose

PURPOSE

To develop and test a joint image reconstruction and semantic segmentation method for functional right and left ventricular cardiovascular MR imaging.

METHOD AND MATERIALS

Image-to-image translation using a generative adversarial network (GAN) was implemented using PyTorch v 0.3.0, translating source radial CMR sinograms (r-theta space) to semantic segmentation of the left and right ventricles. 1700 short axis cardiac MR images were used for training (n=1400), simulation and validation(n=300). Each had expert manual segmentation of the LV and RV bloodpools. Deep learning via a U-net convolutional neural network was used for image-to-image translation (so-called 'pix2pix'), providing semantic segmentation masks of the RV and LV directly from raw CMR k-space data. The U-net Generator was trained with an adversarial loss for 100 epochs. Reconstruction/segmentation of the RV and LV was studied with undersampling factors of up to 8. The Sørensen-Dice similarity index was used to compare RV and LV masks to manual segmentation in validation data, undersampled simulations, and prospectively collected CMR radial exams (n=15).

RESULTS

The GAN trained quickly, providing excellent segmentation of both the LV and RV with LV Dice index= 0.989 ± 0.003 (range: 0.975-0.996) and RV Dice Index = 0.986 ± 0.005 (range: 0.938-0.995). Deep learning provided segmentation consistent with clinical standards, where trabeculae and papillary muscles are included inside of ventricular bloodpool segmentations. With an acceleration factor of 8, quality segmentations were maintained with slightly reduced Dice Indices: LV Dice index= 0.961 ± 0.016 (range: 0.872 - 0.993); RV Dice index= 0.937 ± 0.023 (range: 0.734-0.981). In-vivo prospective reconstructions using complex radial CMR data yielded similar Dice Indices.

CONCLUSION

Image-to-image translation is a viable method for radial MR image reconstruction and provides a framework for image reconstruction, acceleration and segmentation. In this proof-of-concept study, simulations confirmed the feasibility of quantitative LV and RV imaging with image-to-image translation and prospective in vivo radial imaging yielded encouraging results with acceleration factors of up to 8.

CLINICAL RELEVANCE/APPLICATION

A deep learning approach is presented which 'translates' CMR data directly to quantitative LV and RV segmentation and eliminates the need for conventional backprojection and gridding along with manual segmentation.

ssc12-07 Optimization of Pulse Sequence Ordering for Automated Fat and Iron Quantification

Monday, Nov. 26 11:30AM - 11:40AM Room: N226

Participants Daniel J. Margolis, MD, Los Angeles, CA (*Presenter*) Consultant, Blue Earth Diagnostics Ltd Alexander Gavlin, MD, Bronx, NY (*Abstract Co-Author*) Nothing to Disclose Andrea S. Kierans, MD, New York, NY (*Abstract Co-Author*) Nothing to Disclose

For information about this presentation, contact:

djm9016@med.cornell.edu

PURPOSE

Commercially available pulse sequences with dedicated post-processing software can automate the creation of maps for fat and iron quantification and make them readily available on picture archiving and communication systems (PACS) workstations, obviating the need for dedicated post-processing to be performed by the radiologist. These most commonly use a gradient multi-echo Dixon technique for derivation of fat percent (or per mille, "per thousand") and R2*, from which iron deposition can be extrapolated. However, as patients at risk for fat or iron accumulation generally also have diffuse liver disease, these scans are often combined with contrast-enhanced imaging using a hepatobiliary agent (e.g., gadoxetate disodium) with a 20-minute delayed scan in the hepatobiliary phase for improved lesion detection. This results in "down time" between the equilibration phase, generally before 5 minutes after contrast administration, and the hepatobiliary phase. It is attractive to perform as many pulse sequences as possible during this "down time," but only if they are not adversely affected by the accumulation of the contrast administration, the degree to which contrast accumulation affects signal for these acquisitions is unknown.

RESULTS

Twelve subjects were identified. Two were excluded as outliers (one for severe steatosis, one for iron overload). Adequate measurement of FP and R2* was performed before and after contrast for the remaining 10 patients. The student's t-test showed no significant difference for FP (p=0.21) but a significant increase in measured R2* after contrast (p=0.02). The control chart shows increased variability for those R2* values acquired after contrast.

CONCLUSION

Time is the ultimate non-renewable resource. Therefore, time optimization of magnetic resonance imaging is an important consideration for optimal utilization of resources. However, this should not sacrifice diagnostic accuracy, and thereby decrease value. This investigation of fat and iron quantification shows that fat quantification appears relatively unaffected by accumulation of a T1- and T2*-shortening contrast agent, whereas R2* is unreliably increased in this setting. Fat/water quantification to measure the degree of steatosis might therefore be possible in the delayed post-contrast phase, whereas quantification of iron accumulation must be done prior to contrast administration. The control chart in this case shows the opposite of the expected effect for R2*, with an increase in variability after the intervention (contrast administration).

METHODS

The gradient multi-echo Dixon sequences were acquired before and approximately 15 minutes after administration of gadoxetate disodium (Eovist, Bayer) at 0.025 mmol/kg and 2.0 mL/sec (LiverLab q-Dixon, Siemens Healthineers, TR/TE 15.6/2.4, 4 degree flip angle, 3.5 mm slice thickness) with automated deconvolution of R2* and fat per mille (FP) maps on the scanner and sent to PACS. All sequential patients during one month were de-identified and a region of interest at least 3 cm in diameter was drawn on a motion-free image of the right lobe, with the average value recorded. The values before and after administration of gadoxetate disodium were evaluated using paired student's t-test. A "control chart" is created showing values before and after administration of contrast.

PDF UPLOAD

http://abstract.rsna.org/uploads/2018/18016666/18016666_hnxa.pdf

SSC12-08 Management of Image Artifacts on a Clinical 7T MRI Scanner

Monday, Nov. 26 11:40AM - 11:50AM Room: N226

Participants Andrew Fagan, Rochester, MN (*Presenter*) Nothing to Disclose

Kirk M. Welker, MD, Rochester, MN (*Abstract Co-Author*) Nothing to Disclose Joel P. Felmlee, PhD, Rochester, MN (*Abstract Co-Author*) Nothing to Disclose Matthew A. Frick, MD, Rochester, MN (*Abstract Co-Author*) Nothing to Disclose Kimberly K. Amrami, MD, Rochester, MN (*Abstract Co-Author*) Nothing to Disclose

For information about this presentation, contact:

Fagan.Andrew@mayo.edu

PURPOSE

In 2017, 7T MRI entered the clinical arena with a first scanner obtaining 510(k) FDA clearance for clinical brain and knee imaging. As with previous generations of 7T (research) scanners, significant image artifacts were prevalent in the images from this system, arising from the underlying physics of the interaction of the 297 MHz radiofrequency (RF) energy with the dielectric properties of tissue and also from RF coil issues. In this paper, we present the development of techniques to mitigate these artifacts.

METHOD AND MATERIALS

Image non-uniformities arising from B1+ transmit (due to complex interference of RF waves) and B1- receive (due to RF coil receiver sensitivity problems) inhomogeneities were mitigated through the use of custom-made high permittivity dielectric pads made from a combination of CaTiO3, BaTiO3, hydroxyethyl-cellulose and D2O. Pads of differing dimensions were developed for different anatomical sites. Inter-voxel dephasing with signal drop-out due to significant magnetic susceptibility effects (e.g. at the base of the brain) was minimized through the use of localized B0 shimming techniques. Distortions arising from long echo trains were mitigated through the use of high image acquisition acceleration factors facilitated by the SNR increase at 7T. Control of receiver and transmitter bandwidths were used to minimize the in- and through-plane chemical shift artifacts.

RESULTS

Tailored dielectric pads increased the SNR in areas of signal deficit by up to 27% and improved overall image uniformity. Clinical protocols were established for routine scanning in the brain (e.g. for seizure, tramautic brain injury, neurovascular diseases, fMRI-based surgical planning) and knee (e.g. meniscal tear, nerve visualization, cartilage repair); example images will be presented.

CONCLUSION

7T MRI offers significant advantages over lower-field systems, arising primarily from increased SNR and image contrast possibilities. However, the successful management of image artifacts and the development of consistent diagnostic image quality across all patient cohorts is key to its integration into a routine clinical workflow.

CLINICAL RELEVANCE/APPLICATION

This paper presents clinical protocols developed on a new generation of 7T MRI scanner, which successfully managed image artifacts and resulted in diagnostic image quality.

SSC12-09 Evaluation of Deep-Learning-Based Technology for Reducing Gadolinium Dosage in Contrast-Enhanced MRI Exams

Monday, Nov. 26 11:50AM - 12:00PM Room: N226

Participants Enhao Gong, PhD, Stanford, CA (*Presenter*) Stockholder, Subtle Medical Jonathan Tamir, BSC, Berkeley, CA (*Abstract Co-Author*) Research support, General Electric Company; Stockholder, Subtle Medical, Inc John Pauly, Stanford, CA (*Abstract Co-Author*) Research support, General Electric Company Max Wintermark, MD, Lausanne, Switzerland (*Abstract Co-Author*) Advisory Board, General Electric Company; Consultant, More Health; Consultant, Magnetic Insight; Consultant, Icometrix; Consultant, Nines;

Greg Zaharchuk, MD, PhD, Stanford, CA (*Abstract Co-Author*) Research Grant, General Electric Company; Stockholder, Subtle Medical;

For information about this presentation, contact:

enhaog@stanford.edu

PURPOSE

Gadolinium Deposition is one of the most urgent issues facing radiology community. In this work, we further validated a Deep Learning based contrast-boost method, on 200 patients with mixed indications, and demonstrated the generalization and robustness of the deep learning based solution to reducing gadolinium dosage while maintaining diagnostic quality.

METHOD AND MATERIALS

Dataset: A cohort of 200 patients were included in this study, with mixed indications and recieving clinically routine contrastenhanced MRI (CE-MRI) exams. Sequences: Pre-contrast (zero-dose), post-contrast after 10% dosage administration (low-dose) and post-contrast after 100% dosage administration (full-dose) was collected with 3D T1 IR-FSPGR sequences for each patient. Method: Different series from the same patient wer corregistered and normalized. A deep convolutional neural network (3D U-Net) was trained to learn the approximation of the full-dose CE-MRI using low-dose and zero-dose images. 5-fold cross-validation was used to generate results for evaluation. Evaluation: Quantitatve metrics (PSNR, RMSE, SSIM) were used to evaluate the improvement of the enhanced contrast using deep learning. Qualitative metrics (image quality, contrast enhancement quality) were used to evaluate the result of the DL based enhancement. A non-infereiority test was conducted to demonstrate the performance of the method and validate the capability of reducing dosage without image quality loss.

RESULTS

Quantitative metrics demonstrated consistent (~4dB in PSNR and 10% in SSIM) and significant (p<0.001) quality improvement of the deep learning based solution, compared with low-dose CE-MRI. Qualitative ratings showed non-significant differences between the proposed method and acquired full-dose CE-MRI images, which was also verified with the non-inferiority testing. Initial results also demonstrated the possibility of synthesizing full-dose CE-MRI images with zero-dose MR images only.

CONCLUSION

With a large dataset, we demonstrated the DL solution can generalize well, achieving robust and significant quality improvement over the low-dose CE-MRI, using 10% or even less gadolinum dosage. It enables significantly (at least 10x) gadolinium dosage reduction without sacrificing diagnositic quality.

CLINICAL RELEVANCE/APPLICATION

Deep Learning solution is valuable in clinical radiology for fighting against gadolinium deposition.

Honored Educators

Presenters or authors on this event have been recognized as RSNA Honored Educators for participating in multiple qualifying educational activities. Honored Educators are invested in furthering the profession of radiology by delivering high-quality educational content in their field of study. Learn how you can become an honored educator by visiting the website at: https://www.rsna.org/Honored-Educator-Award/ Max Wintermark, MD - 2018 Honored Educator



ML21

Machine Learning Theater: Artificial Intelligence: Implications for Advanced Imaging and Precision Medicine: Presented by Siemens Healthineers

Monday, Nov. 26 11:00AM - 11:20AM Room: Machine Learning Showcase North Hall

Participants

Puneet Sharma, Princeton, NJ (Presenter) Research Director, Siemens AG

Participants

Tommaso Mansi, PhD, Princeton, NJ

Program Information

Artificial intelligence (AI) is transforming care delivery and expanding precision medicine. Siemens Healthineers has served as a pioneer in AI development for more than 20 years, and new deep learning technology now enables us to automate complex diagnostics and support optimal treatment. Our AI-powered solutions address major challenges that the healthcare field faces. Right now, the demand for diagnostic services outstrips the supply of experts in the workforce. Developing solutions for managing this ever-increasing workload is a crucial task for the healthcare sector. And, while the workload is growing, diagnostics and treatment are also becoming more complex. Diagnostic experts and physicians need a new set of tools that can handle large volumes of medical data quickly and accurately. This would allow for more objective treatment decisions based on quantitative data and tailored to the needs of every patient. To provide this new toolset, we need to draw on the power of AI.



ML22

Machine Learning Theater: Adaptive Intelligence and Radiologist Efficiency: Presented by Philips

Monday, Nov. 26 11:30AM - 11:50AM Room: Machine Learning Showcase North Hall

Participants

Homer H. Pien, PhD, Boston, MA (Presenter) Officer, Koninklijke Philips NV; Sr. Vice President, Koninklijke Philips NV

Program Information

As healthcare delivery continues its evolution towards value-based care, so must radiology. Adaptive Intelligence helps radiologists be more efficient, and fosters more direct contribution to screening, diagnosis and treatment of patients. This talk will provide examples of where we have found success, and where challenges still lie ahead.



ML23

Machine Learning Theater: AI Improves Imaging Workflow for MR and PET Exams: Faster, Safer, and Smarter: Presented by Subtle Medical

Monday, Nov. 26 12:00PM - 12:20PM Room: Machine Learning Showcase North Hall

Participants

Greg Zaharchuk, MD, PhD, Stanford, CA (*Presenter*) Research Grant, General Electric Company; Stockholder, Subtle Medical; Enhao Gong, PhD, Stanford, CA (*Presenter*) Stockholder, Subtle Medical

Program Information

Subtle Medical provides AI and Deep Learning solutions to significantly enhance image quality for medical imaging such as PET and MRI. Studies demonstrate the AI technologies can further enhance images acquired with 4x faster protocols and 75%-90% lowdose protocols. Subtle Medical is partnering with industry leaders to deliver its AI solutions into clinical environment, enabling faster, safer and smarter imaging workflow.



AIS-MOA

Artificial Intelligence Monday Poster Discussions

Monday, Nov. 26 12:15PM - 12:45PM Room: AI Community, Learning Center



Participants

Ryan Chamberlain, PhD, Minneapolis, MN (Moderator) Employee, ImBio, LLC

Sub-Events

AI202-SD- Automatic Contrast Enhancement Detection on Head CT

Station #1

Participants Bernardo Henz, MSc, Porto Alegre, Brazil (*Abstract Co-Author*) Nothing to Disclose Jose E. Venson, MSc, Porto Alegre, Brazil (*Presenter*) Nothing to Disclose Alesson Scapinello, Porto Alegre, Brazil (*Abstract Co-Author*) Nothing to Disclose Daniel Souza, Porto Alegre, Brazil (*Abstract Co-Author*) Nothing to Disclose Cesar C. Cavion, MD, Porto Alegre, Brazil (*Abstract Co-Author*) Nothing to Disclose Felipe C. Kitamura, MD, MSC, Sao Paulo, Brazil (*Abstract Co-Author*) Developer, DASA

CONCLUSION

Our results showed high accuracy in the detection of contrast on head CT scans. As future work, we are planning validation experiments in a clinical environment

Background

Intravenous administration of iodinated contrast media has undeniable importance in the evaluation of computed tomography (CT) scans for several clinical indications. The information about contrast administration is usually in the DICOM metadata. However, in teleradiology services, this parameter is frequently not available in a standardized way, being difficult to be automatically populated in the report. Consequently, incorrect contrast information represents 8.73% of report errors in our teleradiology, causing financial and even potentially legal disruptions to diagnostic services. In order to reduce this error rate, we propose a solution to automatically detect contrast enhancement by using convolutional neural networks.

Evaluation

We selected 500 head CT scans randomly and anonymously, ensuring a balanced distribution between the classes: non-contrastenhanced and contrast-enhanced. Preparing the data: Given that the number of slices of each exam differs, we decided to train a CNN to classify a single image into one of the two classes. Instead of using all slices of an exam, we only take the ones in the range [0.40,0.60] in the z-axis, also cropping the xy-axes to get the sinus rectus. This totalizes more than 10k 192x192 images for training. Strategies used for data augmentation were random rotations, translations, brightness and contrast adjustments, and addition of noise. Our architecture: Our model consists of 6 convolutional and 2 fully-connected layers. After training, our network was able to predict the class of a single image with 93% of accuracy. Exam classification: When classifying an exam, we used a voting scheme to account for the probability of each prediction being correct. In other words, the higher the chance of a prediction being correct, the higher its weight in the voting. By using this scheme, the accuracy of predicting the class of the exam is 98%.

Discussion

Automatic contrast detection is important to avoid errors in reports and optimize the diagnostic flow.

AI026-EB- An Artificial Intelligence-Based System for Triaging of Digital Mammography Exams

Hardcopy Backboard

Participants

David Richmond, Newton, MA (*Presenter*) Senior Data Scientist, IBM Watson Health Maggie Kusano, Mississauga, ON (*Abstract Co-Author*) Employee, IBM Corporation Guy Amit, PhD, Haifa, Israel (*Abstract Co-Author*) Employee, IBM Corporation Ayelet Akselrod-Ballin, San Jose, CA (*Abstract Co-Author*) Employee, IBM Corporation Efrat Hexter, San Jose, CA (*Abstract Co-Author*) Employee, IBM Corporation Simona Rabinovici-Cohen, Haifa, Israel (*Abstract Co-Author*) Employee, IBM Corporation Yoel Shoshan, Haifa, Israel (*Abstract Co-Author*) Employee, IBM Corporation David Wilson, Cambridge, MA (*Abstract Co-Author*) Employee, IBM Corporation Grant Covell, Cambridge, MA (*Abstract Co-Author*) Employee, IBM Corporation Andjela Azabagic, Brooklyn, NY (*Abstract Co-Author*) Former Employee, IBM Corporation Bill Stoval, Cambridge, MA (*Abstract Co-Author*) Employee, IBM Corporation Marwan Sati, PhD, Mississauga, ON (*Abstract Co-Author*) Employee, IBM Corporation

For information about this presentation, contact:

david.richmond@ibm.com

CONCLUSION

A framework for automated processing of medical images within clinical environments has been developed and shown in this early pilot to automatically triage MG studies based on an AI- algorithm.

FIGURE

http://abstract.rsna.org/uploads/2018/18020191/18020191_3w6t.jpg

Background

Breast screening programs have been established worldwide to facilitate early detection and treatment of breast cancer. However, healthcare quality and affordability initiatives, an aging population, increased data from emerging modalities, and a shortage of radiologists have led to unmanageable throughput, resulting in delayed diagnosis and physician burnout. In this paper we present an AI-based framework for triaging digital screening mammography (MG) exams based on likelihood of cancer.

Evaluation

A deep learning model was trained to infer a patient's likelihood of abnormality based on her 4-view screening MG exam. The model was integrated in a new platform for automated processing of images within hospital IT and cloud environments. Digital MG studies were de-identified from partner sites and secondary usage rights secured. Normal MGs were defined as screening studies assessed as BI-RADS 1 or 2, confirmed by 4+ years of follow up normal exams. Abnormal MGs were defined as screening studies that were recalled, and led to positive or negative biopsy within 1 year. The system was initially trained on 1192 screening MGs and then tested on a held-out set of 323 screening MGs from a new hospital site, enriched with suspicious cases (165 normal, 158 abnormal). The system achieved a sensitivity of 95% and specificity of 20%. In other words, the system correctly triaged 20% of the BI-RADS 1 and 2 exams as normal. For a cancer prevalence of 0.5%, this corresponds to an NPV of 99.87%. In cross-validation on a set of 1578 MG studies (~700 normal, ~900 abnormal), the system achieved a specificity of 40% at 95% sensitivity, with an ROC AUC of 0.84.

Discussion

The system identified a significant portion of normal exams from the worklist, effectively highlighting more complex and challenging cases. We are continuing training with 10,000 screening MGs, and expect that the system will learn to identify more normal studies, further refining the remaining complex cases.

AI143-ED- Deep Learning Techniques for Automated Segmentation of Diffuse Lung Disease Opacities on CT MOA2 Images

Station #2

Participants Shoji Kido, MD, PhD, Ube, Japan (*Presenter*) Nothing to Disclose Kanako Murakami, Ube, Japan (*Abstract Co-Author*) Nothing to Disclose Noriaki Hashimoto, Ube, Japan (*Abstract Co-Author*) Nothing to Disclose Yasushi Hirano, Ube, Japan (*Abstract Co-Author*) Nothing to Disclose Shingo Mabu, Ube, Japan (*Abstract Co-Author*) Nothing to Disclose Kenji Suzuki, PhD, Chicago, IL (*Abstract Co-Author*) Royalties, General Electric Company; Royalties, Hologic, Inc; Royalties, MEDIAN Technologies; Royalties, Riverain Technologies, LLC; Royalties, Canon Medical Systems Corporation; Royalties, Mitsubishi Corporation; Royalties, AlgoMedica, Inc

For information about this presentation, contact:

kido.ai@yamaguchi-u.ac.jp

TEACHING POINTS

To segment diffuse lung disease opacities on CT images accurately is important for quantitative pathological evaluation such as radiomics. However, it is difficult to segment pathological lungs correctly by use of conventional algorithms because contours of lungs are blurring by pathological opacities such as consolidation. The state-of-art deep learning techniques can segment lungs with diffuse lung opacities correctly compared with conventional methods. The purpose of this exhibit is: 1. To learn segmentation by use of convolutional neural network (CNN) with a sliding window on a pixel-by-pixel. 2. To learn segmentation by use of fully convolutional neural network (FCN) where the last fully-connected layer of CNN is substituted by another convolution layer with a large 'receptive field'. 3. To learn segmentation by use of U-Net which has ladder networks. U-Net is the state-of-art semantic segmentation algorithm of biological images, and it requires small number of image data. 4. To learn neural network convolution (NNC) which is one of other types of simple structure neural networks. It requires a small number of images and calculation time.

TABLE OF CONTENTS/OUTLINE

1. Introduction, 2. Segmentation by use of CNN with a sliding window. 3. Segmentation by use of FCN. 4. Segmentation by use of U-Net. 5. Segmentation by use of NNC. 5. Conclusion.

AI027-EB- Abdominal Segmentation for Body Composition Using Deep-Learning U-Net MOA

Hardcopy Backboard

Participants Alexander Weston, Rochester, MN (*Presenter*) Nothing to Disclose Panagiotis Korfiatis, PhD, Rochester, MN (*Abstract Co-Author*) Nothing to Disclose Kenneth Philbrick, Rochester, MN (*Abstract Co-Author*) Nothing to Disclose Timothy L. Kline, PhD, Rochester, MN (*Abstract Co-Author*) Nothing to Disclose Naoki Takahashi, MD, Rochester, MN (*Abstract Co-Author*) Nothing to Disclose Bradley J. Erickson, MD, PhD, Rochester, MN (*Abstract Co-Author*) Stockholder, OneMedNet Corporation; Stockholder, VoiceIt Technologies, LLC; Stockholder, FlowSigma;

For information about this presentation, contact:

CONCLUSION

U-Net is an accurate method of 3D abdominal segmentation based on 2D imaging data. This is important for accurately assessing body composition.

FIGURE

http://abstract.rsna.org/uploads/2018/18020348/18020348_7m3i.jpg

Background

Body composition (defined as the amount and distribution of fat and muscle present in the body) is a well-known indicator of overall physical health. There are several methods to assess body composition but the most accurate is abdominal CT (or MRI) imaging, which is often already included in the clinical workflow. A limitation to this approach is the need for abdominal segmentation which is time consuming. For this reason, single-slice analysis of body composition is common.

Evaluation

We trained a deep convolutional neural network (U-Net) on 2430 transverse CT scans at the level of the L3 vertebra. We segmented the abdomen into subcutaneous, muscle, visceral adipose, visceral organ, and bone compartments. Gold-standard segmentation was performed with a semiautomated method with manual correction. On the test set, U-Net had a Dice score of 0.98 on the subcutaneous, 0.96 on muscle, and 0.94 on visceral adipose compartments (compared to the gold-standard). Additionally, the accuracry of our algorithm met or exceeded that of manual segmentation by 2 experts (subcutaneous: 0.98 vs 0.95, muscle: 0.95 vs 0.93, viscera: 0.99 vs 0.99). We evaluated performance of our algorithm on transverse CT scans taken at the level of the L4 vertebra (a different level from our training data) which was not significantly different than accuracy at the L3 level. Finally, we evaluated the performance of our trained U-Net on a secondary dataset of 2369 transverse CT scans taken from subjects with a different underlying condition.

Discussion

Our algorithm is an accurate method of assessing body composition. It is generalizable to a different population of subjects. It accurately segments multiple levels of the abdomen despite the fact that it is trained on the L3 level alone. It is therefore capable of 3D segmentation with limited 2D training data. We demonstrate that 3D segmentation to assess body composition is more accurate than the current gold-standard of single-slice segmentation due to the variability in subject anatomy, including shifting GI contents.

Honored Educators

Presenters or authors on this event have been recognized as RSNA Honored Educators for participating in multiple qualifying educational activities. Honored Educators are invested in furthering the profession of radiology by delivering high-quality educational content in their field of study. Learn how you can become an honored educator by visiting the website at: https://www.rsna.org/Honored-Educator-Award/ Naoki Takahashi, MD - 2012 Honored Educator

AI204-SD- Semi-Automatic RECIST Labeling on CT Scans with Cascaded Convolutional Neural Networks

Station #3

Participants

Youbao Tang, PhD, Bethesda, MD (*Presenter*) Nothing to Disclose Adam P. Harrison, PhD, Bethesda, MD (*Abstract Co-Author*) Nothing to Disclose Mohammad Hadi Bagheri, MD, Bethesda, MD (*Abstract Co-Author*) Nothing to Disclose Jing Xiao, Shenzhen, China (*Abstract Co-Author*) Nothing to Disclose Ronald M. Summers, MD,PhD, Bethesda, MD (*Abstract Co-Author*) Royalties, iCAD, Inc; Royalties, Koninklijke Philips NV; Royalties, ScanMed, LLC; Research support, Ping An Insurance Company of China, Ltd; Researcher, Carestream Health, Inc; Research support, NVIDIA Corporation; ; ; ;

For information about this presentation, contact:

youbao.tang@nih.gov

PURPOSE

Response evaluation criteria in solid tumors (RECIST) is the standard measurement for tumor extent to evaluate treatment responses in cancer patients. Using RECIST annotation faces two main challenges: 1) measuring tumor diameters requires a lot of professional knowledge and is time-consuming. Consequently, it is difficult and expensive to manually annotate large-scale datasets, e.g., those used in large clinical trials or retrospective analyses. 2) RECIST marks are often subjective and prone to inconsistency among different observers. However, consistency is critical in assessing actual lesion growth rates, which directly impacts patient treatment options. To overcome these problems, we propose a cascaded convolutional neural network based method to semi-automatically label RECIST annotations.

METHOD AND MATERIALS

The stacked hourglass networks (SHN) is employed for RECIST estimation, where a relationship constraint loss is introduced to improve the estimation accuracy. Regardless of class, the lesion regions may have large variability in sizes, locations and orientations in different images. To make our method robust to these variations, the lesion region first needs to be normalized before feeding into SHN. The spatial transformer network is used for lesion region normalization, where a localization network is designed for lesion region and transformation parameter prediction. Thus, given a region of interest by a radiologist, our method directly outputs its RECIST annotation. We train our system on a large scale lesion dataset where 32,735 RECIST annotations from 4,459 patients are performed by multiple radiologists over a multi-year period.

RESULTS

500 lesions from 200 patients have three manual RECIST annotations and are used for test. The mean and standard deviation of inter-reader variation of long diameter are 3.40 ± 5.24 mm, while those for the variation between our system and the manual annotations are 2.67 ± 3.95 mm. The results demonstrate that our system performs more stably and with less variability.

CONCLUSION

Our approach only requires a rough bounding box drawn by a radiologist and produces stable RECIST annotations, suggesting that RECIST can be reliably obtained with reduced labor and time.

CLINICAL RELEVANCE/APPLICATION

If coupled with a reliable lesion localization framework, our approach can be made fully automatic. As such, the proposed system can potentially provide a highly positive impact to clinical workflows.

AI203-SD-MOA4 Prostate Cancer Lesion Segmentation and Gleason Score Prediction Using Multi-parametric MRI via Deep Residual Neural Network

Station #4

Participants Ruiming Cao, Los Angeles, CA (*Presenter*) Nothing to Disclose Sepideh Shakeri, Los Angeles, CA (*Abstract Co-Author*) Nothing to Disclose Xinran Zhong, Los Angeles, CA (*Abstract Co-Author*) Research support, Siemens AG Amirhossein Mohammadian Bajgiran, MD, Los Angeles, CA (*Abstract Co-Author*) Nothing to Disclose Sohrab Afshari Mirak, MD, Los Angeles, CA (*Abstract Co-Author*) Nothing to Disclose David S. Lu, MD, Los Angeles, CA (*Abstract Co-Author*) Nothing to Disclose David S. Lu, MD, Los Angeles, CA (*Abstract Co-Author*) Consultant, Medtronic plc; Speaker, Medtronic plc; Consultant, Johnson & Johnson; Research Grant, Johnson & Johnson; Consultant, Bayer AG; Research Grant, Bayer AG; Speaker, Bayer AG Dieter R. Enzmann, MD, Los Angeles, CA (*Abstract Co-Author*) Nothing to Disclose Steven S. Raman, MD, Santa Monica, CA (*Abstract Co-Author*) Nothing to Disclose Kyunghyun Sung, PhD, Los Angeles, CA (*Abstract Co-Author*) Research support, Siemens AG

For information about this presentation, contact:

rcao@mednet.ucla.edu

PURPOSE

To automatically contour prostate cancer (PCa) lesion and to predict Gleason score (GS) by training a deep residual neural network (ResNet) from multi-parametric MRI (mp-MRI).

METHOD AND MATERIALS

In collaboration with Department of Pathology, we utilized GS-labeled whole-mount histopathology after radical prostatectomy to identify and segment PCa lesion on mp-MRI as ground-truth. A total number of 98 pre-operative mp-MRI cases were acquired on 3T MRI systems (Skyra and Prisma, Siemens), and normalized T2-weighted (T2w) imaging, apparent diffusion coefficient (ADC) and transfer constant (Ktrans) were used for training and testing the ResNet. We input each slice of mp-MRI to a fully-supervised ResNet to predict PCa lesion contour and GS. Specifically, we have built a 101-layer ResNet with atrous convolutional filters which help to compensate the misalignment between different imaging sequences. The model was trained using a weighted pixel-wise cross-entropy loss, which optimizes the prediction of both PCa lesion contour and GS. We randomly selected 74 cases consisting a total of 1056 mp-MRI slices as training set and tested the trained ResNet with the remaining 24 cases. For testing, the ResNet had to determine the presence and quantity of lesions on a given slice before segmentation.

RESULTS

Two experienced abdominal radiologists, with 33 years and 25 years of clinical experience respectively, were asked to independently score the quality of predicted lesion contours from 1 (completely missed) to 5 (sufficiently similar to the ground-truth) based on the ground-truth segmentation for each lesion in testing cases. 77.4% lesion contour predictions received 3 (minimal overlap) or above with 100% inter-rater agreement. Out of those predictions, on average 68.8% received 4 (significant overlap) or above with 79.2% agreement. Of those predictions scored 3 or above, clinically significant lesions (GS3+4 or above) were classified with 81.8% precision and 100% recall.

CONCLUSION

This study used state-of-the-art ResNet for PCa lesion segmentation and GS prediction. In 24 testing cases, the ResNet had achieved 77.4% success rate in lesion segmentation and 81.8% precision in predicting clinically significant lesion.

CLINICAL RELEVANCE/APPLICATION

This study aims to improve diagnosis of prostate cancer and to further assist clinical decision making for proper treatment.

AI004-EB Development and Visual Assessment of a Deep Learning System for Automated Tuberculosis Screening Using Chest Radiographs

All Day Room: AI Community, Learning Center

Participants

Tae Kyung Kim, Baltimore, MD (Presenter) Nothing to Disclose

Meet the Author: The authors of this poster will be available in person to discuss their project during these times Monday, November 26 - 12:15-12:45 pm



ML24

Machine Learning Theater: Actionable Intelligence and the Future of Precision Health: Presented by CorTechs Labs

Monday, Nov. 26 12:30PM - 12:50PM Room: Machine Learning Showcase North Hall

Participants

Nathan White, PhD, San Diego, CA (Presenter) Nothing to Disclose

Program Information

Precision health has the ability to transform healthcare from a reactive treatment-focused mindset to a proactive prevention and wellness-focused discipline. Learn about how actionable intelligence can utilize the power of quantitative imaging with the integration of genetic and clinical data to empower patient and physician decision-making.



RCA23

Introduction to Machine Learning and Texture Analysis for Lesion Characterization (Hands-on)

Monday, Nov. 26 12:30PM - 2:00PM Room: S401AB



AMA PRA Category 1 Credits ™: 1.50 ARRT Category A+ Credit: 1.75

FDA Discussions may include off-label uses.

Participants

Kevin Mader, DPhil,MSc, Basel, Switzerland (*Moderator*) Employee, 4Quant Ltd; Shareholder, 4Quant Ltd Kevin Mader, DPhil,MSc, Basel, Switzerland (*Presenter*) Employee, 4Quant Ltd; Shareholder, 4Quant Ltd Barbaros S. Erdal, PhD, Columbus, OH (*Presenter*) Nothing to Disclose Joshy Cyriac, Basel, Switzerland (*Presenter*) Nothing to Disclose

For information about this presentation, contact:

mader@biomed.ee.ethz.ch

joshy.cyriac@usb.ch

LEARNING OBJECTIVES

1) Review the basic principles of machine learning. 2) Learn what texture analysis is and how to apply it to medical imaging. 3) Understand how to combine texture analysis and machine learning for lesion classification tasks. 4) Learn the how to visualize and analyze results. 5) Understand how to avoid common mistakes like overfitting and incorrect model selection.

ABSTRACT

During this course, an introduction to machine learning and image texture analysis will be provided through hands on examples. Participants will use with open source as well as freely available commercial platforms in order to achieve tasks such as image feature extraction, statistical analysis, building models, and validating them. Imaging samples will include both 2D and 3D datasets from a variety of modalities (CT, PET, MR). The course will begin with a brief overview of important concepts and links to more detailed references. The concepts will then be directly applied in visual, easily understood workflows where the participants will see how the images are processed, features and textures are extracted and how publication ready statistics and models can be built and tested.



AIS-MOB

Artificial Intelligence Monday Poster Discussions

Monday, Nov. 26 12:45PM - 1:15PM Room: AI Community, Learning Center



Participants

Ryan Chamberlain, PhD, Minneapolis, MN (Moderator) Employee, ImBio, LLC

Sub-Events

AI205-SD- Solid Renal Tumor Detection Using Convolutional Neural Networks

Station #1

Participants Osvaldo Landi Junior, MD, Sao Paulo, Brazil (*Presenter*) Nothing to Disclose Hanna R. Dalla Pria, MD, Sao Paulo, Brazil (*Abstract Co-Author*) Nothing to Disclose Juliana C. Yoshitani, MD, Sao Paulo, Brazil (*Abstract Co-Author*) Nothing to Disclose Lucas Pereira, Goiania, Brazil (*Abstract Co-Author*) Nothing to Disclose Felipe C. Kitamura, MD, MSC, Sao Paulo, Brazil (*Abstract Co-Author*) Developer, DASA Daisy T. Kase, Sao Paulo, Brazil (*Abstract Co-Author*) Nothing to Disclose Marcelo Arcuri, MD, Sao Paulo, Brazil (*Abstract Co-Author*) Nothing to Disclose Anderson Soares, Goiania, Brazil (*Abstract Co-Author*) Nothing to Disclose Marcio Ricardo T. Garcia, MD, Sao Paulo-SP, Brazil (*Abstract Co-Author*) Nothing to Disclose Nitamar Abdala, MD, PhD, Mogi Das Cruzes, Brazil (*Abstract Co-Author*) Nothing to Disclose

For information about this presentation, contact:

osv.landi@gmail.com

CONCLUSION

The present model proved to be able to differentiate solid renal tumors from normal kidneys with a high accuracy rate. It's refinement and implementation could help to guide patients through healthcare system workflows, aiding in early tumor detection and thus allowing prompt intervention for better clinical outcomes.

Background

The wide application of diagnostic imaging methods in recent years has lead to an increasing number of incidental tumors, including kidney tumors. These lesions are often presented as early-stage localized renal malignancies, which has possibly contributed to the reduced mortality and morbidity of renal cancer as a whole due to its early detection. In addition, while the standard care for these patients is excision, nephron sparing surgery has emerged as an oncologically equivalent alternative to radical nephrectomy in most cases of localized renal cell carcinoma, reducing the negative sequelae of traditional surgical interventions, such as chronic kidney disease. In this study, we propose a convolutional neural network (CNN) model to detect solid renal tumors in abdominal computed tomography, with potential to collaborate in early detection and consequent improvement to patient prognosis.

Evaluation

This retrospective study was approved by our institutional review board, and written informed consent was waived. A total of 73 anonymized abdominal computed tomography studies were selected based on the hospital records. Kidney images were cropped from these studies in axial, coronal and sagittal axis, yielding 951 normal kidney images and 888 solid renal tumor images. This dataset was randomized in the patient level into training (65%), validation (15%) and test (20%) subsets. After preprocessing, an in-house CNN with ice modules was trained from scratch with online data augmentation. Optimization was done with random grid search and regularization.

Discussion

In the present study, our model achieved up to 79% accuracy for differentiating normal kidneys from solid renal tumors, with a precision of 91.81%, recall of 59%, f-score of 71.88% and area under the ROC curve of 0.89.

AI206-SD- Improving Radiology Appointment Wait Time Prediction with Machine Learning MOB2

Station #2

Participants Steven P. Guitron, MS,BS, Boston, MA (*Presenter*) Nothing to Disclose Darren P. Parke, BA,MA, Boston, MA (*Abstract Co-Author*) Nothing to Disclose Oleg S. Pianykh, Newton Highlands, MA (*Abstract Co-Author*) Nothing to Disclose

CONCLUSION

We implemented a real-time model that can generate accurate wait time predictions using only common RIS data. Using machine learning with large predictor sets significantly improved the prediction quality. Our approach can be easily replicated at other facilities to provide patients with the most accurate wait time information.

Radiology patients can be frustrated by the seemingly opaque experience of waiting for their exams as daily wait time patterns can change significantly. Previously, to address this problem at Massachusetts General Hospital, a simple 3-predictor linear regression model was made to display estimated patient wait times. By studying the nonlinearity of historical waits, our goal was to develop a more accurate model that could better capture wait time fluctuations using the power of machine learning (ML).

Evaluation

Raw data was pulled from the hospital's Radiology Information System (RIS). 52 predictors were automatically generated, including line size, previous wait times, and appointment lengths. A custom ML library was developed, and several models were implemented: least squares regression, elastic net, lasso, generalized linear model, and random forest. After training each, the model with the least error is chosen to predict wait times. To display real time predictions, models are stored in the database with expiration dates. The expired models are retrained, enabling capture of any changes in patient workflow. Performance was optimized to compute predictions in less than 2 sec. Thus, the algorithm was optimized to automatically choose which model to use and when to retrain, completely unsupervised. Additionally, our algorithm provides an interactive display of recent prediction history, where less accurate predictions can be investigated.

Discussion

Using our ML-based model, we explained up to 60.4% of out-of-sample variance (improved from 0% with the 3-predictor model). Using a popular CT resource, we improved average prediction error from 30.72 min to 19.83 min. Our best models can predict better than the historical average 74% of the time.

AI208-SD-MOB3 3D Context Enhanced Region-based Convolutional Neural Network for Universal Lesion Detection in a Large Database of 32,735 Manually Measured Lesions on Body CT

Station #3

Participants

Ke Yan, Bethesda, MD (Presenter) Nothing to Disclose

Mohammad Hadi Bagheri, MD, Bethesda, MD (*Abstract Co-Author*) Nothing to Disclose Ronald M. Summers, MD, PhD, Bethesda, MD (*Abstract Co-Author*) Royalties, iCAD, Inc; Royalties, Koninklijke Philips NV; Royalties, ScanMed, LLC; Research support, Ping An Insurance Company of China, Ltd; Researcher, Carestream Health, Inc; Research support, NVIDIA Corporation; ; ; ;

For information about this presentation, contact:

yankethu@foxmail.com

PURPOSE

Detecting lesions from CT scans is an important yet challenging problem because non-lesions and lesions can have similar appearance. 3D context is very helpful in such differentiation tasks. However, most existing detection frameworks of convolutional neural networks (CNNs) are designed for 2D images. Methods which use 3D information are either not efficient or memory-consuming. In this paper, we propose 3D context enhanced region-based CNN (3DCE) to incorporate 3D context information efficiently by aggregating feature maps of 2D images. Besides, current lesion detectors can typically find only one kind of lesion. We develop a universal lesion detector that covers all kinds of lesions in one framework.

METHOD AND MATERIALS

The universal lesion detector relies on the DeepLesion dataset, which was collected by us and contains 32,735 lesions manually annotated on CT scans. It includes a variety of lesions such as lung nodules, liver tumors, adenopathy, bone lesions, etc. The proposed 3DCE is designed based on a 2D region-based fully convolutional network. To incorporate 3D information, we input 3M slices to the network. The central slice contains the ground-truth bounding-box and the other slices provide the 3D context. They are grouped to M 3-channel images. M feature maps are then extracted and concatenated to aggregate 3D information. We combine this fused feature map and the lesion proposals generated by a region proposal network to obtain the final detection results. 3DCE is memory-friendly, easy to train, less prone to overfitting, with the training and inference process both end-to-end (requiring only one run).

RESULTS

The train/val/test sets of the challenging DeepLesion dataset contain 70%, 15%, 15% of the data split in patient level. On the test set, the sensitivity of 3DCE at 4 false positives per image is 84.37%, compared to 80.32% of the baseline faster RCNN algorithm. Smaller lesions and bone lesions benefit more from 3D information (5% and 8% improvement).

CONCLUSION

We proposed an algorithm to leverage the 3D context when detecting lesions in volumetric data. It consistently improved the detection accuracy on the DeepLesion dataset.

CLINICAL RELEVANCE/APPLICATION

The proposed algorithm can be applied in all automated lesion detection problems where 3D context is helpful. The universal lesion detector can help radiologists find all types of lesions, which is more useful than single-purpose detectors in practice.

AI209-SD-MOB4 Recognition of Pediatric Long-Bone Fractures in the Setting of Variable Open Growth Plates by Convolutional Neural Networks

Station #4

Participants

Zbigniew Starosolski, PhD, Houston, TX (*Presenter*) Stockholder, Alzeca Biosciences, LLC J. H. Kan, MD, Houston, TX (*Abstract Co-Author*) Nothing to Disclose Ananth Annapragada, PhD, Houston, TX (*Abstract Co-Author*) Stockholder, Alzeca Biosciences, LLC Stockholder, Sensulin, LLC Stockholder, Abbott Laboratories Stockholder, Johnson & Johnson

For information about this presentation, contact:

PURPOSE

Convolutional neural networks (CNNs) show promise for radiologic imaging interpretation. Fracture morphology heterogeneity in the setting of skeletal immaturity with variable appearances of physes and apophyses are a challenge for automatic classification. The purpose of this study was to evaluate the effect of CNN architecture on the computer-aided diagnosis (CAD) of long-bone fractures in pediatric patients of age 3 months to 18 years.

METHOD AND MATERIALS

An IRB approved dataset obtained at a children's hospital from 2015-18 that included 1444 pediatric fractures and 1147 normal radiographs of the appendicular skeleton was used. Fracture locations were recorded in image coordinates for further dataset generation. Radiographs were patched into 512x512 imagesets from the raw DICOM images. Patches were automatically generated in a random fashion along the calculated centerline of the long bone. Training set including 256000 patches with fractures and the same number showing normal bone. The validation set and test set each had 32000 images for each class. Four different CNN architectures were tested: VGG19, U-net and with the utilization of transfer learning Xception and DenseNet.

RESULTS

The accuracies of classification for relatively shallow VGG19, U-net (10 and 26 layers respectively) were 50.0% and 52.9% respectively. Transfer learning networks Xception and DenseNet (126 and 201 layers respectively) resulted in 71.3% and 65.8% respectively. The latest CNNs achieved specificity 81.7% and 86.3%, sensitivity 60.9% and 45.3% respectively. The majority of the false negative exams included indistinct fracture lines or were one of the fracture types not well represented in the training set. The false positive exams were all not well represented in the training set and constituted fractures near a joint line of the lower extremity.

CONCLUSION

The most accurate binomial fracture classification was recorded by well parameterized CNNs using transfer learning. The automated patch approach eliminated image scaling, and allowed localization of the classified fracture within a relatively narrow spatial domain.

CLINICAL RELEVANCE/APPLICATION

Binomial fracture identification is possible by CNN architecture on CAD of pediatric long bone fractures in the setting of open growth plates and apophyses and is able to distinguish fractures from physius. We expect that with the larger representation of each fracture type accuracy will improve.

AI009-EB Machine Learning-based Virtual Metastasis Biopsy as an Early Predictor of Tumor Progression and Resistance Mutation Acquisition in Colon Cancer Patients

All Day Room: AI Community, Learning Center

Participants

Dania Daye, MD, PhD, Philadelphia, PA (Presenter) Nothing to Disclose

Azadeh Tabari, Boston, MA (Abstract Co-Author) Nothing to Disclose

Katherine P. Andriole, PhD, Dedham, MA (*Abstract Co-Author*) Research Grant, NVIDIA Corporation; Research Grant, General Electric Company; Research Grant, Nuance Communications, Inc; Advisory Board, McKinsey & Company, Inc Michael S. Gee, MD, PhD, Boston, MA (*Abstract Co-Author*) Nothing to Disclose

Meet the Author: The authors of this poster will be available in person to discuss their project during these times: Monday, November 26 - 12:45-1:15 pm

AI016-EB Detection of Obstructive and Restrictive Lung Disease on Chest Radiography Using Machine Learning and Integrated Pulmonary Function Data

All Day Room: AI Community, Learning Center

Participants

Jessica Chan, MD, Salt Lake City, UT (*Presenter*) Nothing to Disclose Ricardo Bigolin Lanfredi, MS,BS, Salt Lake City, UT (*Abstract Co-Author*) Nothing to Disclose Tolga Tasdizen, PhD, Salt Lake City, UT (*Abstract Co-Author*) Nothing to Disclose Tao Li, MS, Salt Lake City, UT (*Abstract Co-Author*) Intern, Koninklijke Philips NV Vivek Srikumar, PhD, Salt Lake City, UT (*Abstract Co-Author*) Nothing to Disclose Clement Vachet, MBA,MS, Salt Lake City, UT (*Abstract Co-Author*) Nothing to Disclose Joyce D. Schroeder, MD, Boulder, CO (*Abstract Co-Author*) Nothing to Disclose

Meet the Author: The authors of this poster will be available in person to discuss their project during these times: Monday November 26 12:45-1:15pm



ML25

Machine Learning Theater: AI: Fad or Forever: Presented by MaxQ AI

Monday, Nov. 26 1:00PM - 1:20PM Room: Machine Learning Showcase North Hall

Participants

Gene Saragnese, Andover, MA (Presenter)

Program Information

Instead of more data and analysis, radiologists need solutions and tools that provide answers while seamlessly integrating into the current workflow, PACS systems, medical imaging hardware, and healthcare clouds. This discussion is a preview of the Symposium presentation Tuesday (CS35) where we will explore the promise of AI - and how by embracing it - radiologists will usher in a new era of healthcare. These support tools provide deep clinical insights into challenging cases - such as a brain hemorrhage - to help guide the clinical team through a series of critical decisions with improved speed and accuracy to enhance access and treatment for the patient.



ML26

Machine Learning Theater: Medical Imaging: Challenges and Opportunities: Presented by Google Cloud

Monday, Nov. 26 1:30PM - 1:50PM Room: Machine Learning Showcase North Hall

PROGRAM INFORMATION

Two thirds of the world's population lacks access to medical imaging. Specialist capacity, equipment availability, and adequate training often can limit the availability of imaging services, particularly in remote areas.

Google Cloud has been working with organizations around the world to use Cloud technology to help eliminate some of the barriers. For example, Google Cloud has been investing heavily in Machine Learning capabilities designed specifically for the healthcare industry. Arie Meir, PhD & Product Manager for Google Cloud will explain more about the new tools Google has built for developing Machine Learning applications in healthcare.

Andre Targino, Lead AI Researcher at Portal Telemedicina (a Google Cloud partner) with be joining onstage to present some of his team's work on iterative model development to support AI assisted telediagnostics.

Join Arie Meir & Andre Targiono on 11/26 from 1:30 PM - 1:50 PM CT at the ML Theatre to learn more about how Cloud and Machine Learning can transform access, reduce costs and enhance quality of radiology services across the globe. Also, be sure stop by Google Cloud's booth #7161 to see more examples of how Google Cloud is helping to increase access to healthcare around the world.



MSMI23

Molecular Imaging Symposium: Neurologic MI Applications

Monday, Nov. 26 1:30PM - 3:00PM Room: S405AB



AMA PRA Category 1 Credits ™: 1.50 ARRT Category A+ Credit: 1.75

FDA Discussions may include off-label uses.

Participants

Alexander Drzezga, MD, Cologne, Germany (*Moderator*) Consultant, Siemens AG; Consultant, Bayer AG; Consultant, General Electric Company; Consultant, Eli Lilly and Company; Consultant, The Piramal Group; Speakers Bureau, Siemens AG; Speakers Bureau, Bayer AG; Speakers Bureau, General Electric Company; Speakers Bureau, Eli Lilly and Company; Speakers Bureau, The Piramal Group Satoshi Minoshima, MD, PhD, Salt Lake City, UT (*Moderator*) Consultant, Hamamatsu Photonics KK; Research Grant, Hitachi, Ltd; Research Grant, Nihon Medi-Physics Co, Ltd;

Sub-Events

MSMI23A Brain MI in Dementia

Participants

Alexander Drzezga, MD, Cologne, Germany (*Presenter*) Consultant, Siemens AG; Consultant, Bayer AG; Consultant, General Electric Company; Consultant, Eli Lilly and Company; Consultant, The Piramal Group; Speakers Bureau, Siemens AG; Speakers Bureau, Bayer AG; Speakers Bureau, General Electric Company; Speakers Bureau, Eli Lilly and Company; Speakers Bureau, The Piramal Group

LEARNING OBJECTIVES

1) Gain overview on types of molecular neuropathology involved in the development of different forms of dementia and understand currently discussed disease concepts. 2) Learn about the currently available methods for imaging molecular pathology such as amyloid-deposition and tau-aggregation in dementia and their current status of validation. 3) Gain insights on the clinical value of the individual available methods and their combination with regard to earlier detection, more reliable diagnosis and therapy monitoring of disease.

MSMI23B Dopaminergic Imaging in Parkinsonian Syndrome

Participants

Kirk A. Frey, MD, PhD, Ann Arbor, MI (*Presenter*) Consultant, MIM Software Inc; Stockholder, General Electric Company; Stockholder, Johnson & Johnson; Stockholder, Novo Nordisk AS; Stockholder, Bristol-Myers Squibb Company; Stockholder, Merck & Co, Inc;

LEARNING OBJECTIVES

1) Understand the molecular targets available for imaging of presynaptic dopaminergic synapses. 2) Appreciate the diagnostic characteristics of dopamine transporter imaging in movement disorder syndromes. 3) Master the appropriate use settings for clinical application of dopamine transporter imaging. 4) Appreciate alternative molecular imaging approaches that may offer value in distinction between movement disorders in the future.

MSMI23C Clinical Trials and Approval Process for New Brain MI

Participants Peter Herscovitch, MD, Bethesda, MD (*Presenter*) Nothing to Disclose

For information about this presentation, contact:

herscovitch@nih.gov

LEARNING OBJECTIVES

Describe the U.S. Food and Drug Administration (FDA) approval process for new radiopharmaceuticals for molecular brain imaging.
 Describe the U.S. Medicare approval process for new radiopharmaceuticals for molecular brain imaging.
 Explain the features and current results of the IDEAS Study: Imaging Dementia-Evidence for Amyloid Scanning Study.
 List the evolving requirements for demonstrating the value of diagnostic imaging, with emphasis on radiopharmaceuticals for molecular brain imaging.

ABSTRACT

The final steps in clinical translation of molecular imaging radiopharmaceuticals for brain studies are approval by the U.S. Food and Drug Administration (FDA) for marketing and by insurance carriers for reimbursement. Given the age of patients most likely to require brain imaging studies for neurodegenerative disorders, coverage approval by the U.S. Centers for Medicare and Medicaid (CMD, 'Medicare') is crucial. This talk will discuss the FDA requirements for approval of a radiopharmaceutical, with a focus on amyloid brain imaging. It should be noted that FDA approval does not necessarily lead to Medicare approval, especially for PET agents. The CMS approval process will be outlined, including the increasing need to demonstrate the ability of PET imaging to provide improved health outcomes. CMS coverage with evidence development (CED) of PET amyloid imaging agents will be described, with a focus on the design, implementation, and current results of the Imaging Dementia-Evidence for Amyloid Scanning (IDEAS) Study. MSMI23D Machine Learning in Brain MI

Participants

Satoshi Minoshima, MD, PhD, Salt Lake City, UT (*Presenter*) Consultant, Hamamatsu Photonics KK; Research Grant, Hitachi, Ltd; Research Grant, Nihon Medi-Physics Co, Ltd;

LEARNING OBJECTIVES

1) Gain insights on available methods of molecular imaging in dementia and their significance. 2) Gain insights in principles and value of dopaminergic imaging in Parkinsonian syndromes. 3) Gain understanding in approval processes for new brain molecular imaging tracers and ongoing clinical trials.



MSRO23

BOOST: Head and Neck-Science Session

Monday, Nov. 26 1:30PM - 2:30PM Room: E450A



AMA PRA Category 1 Credit ™: 1.00 ARRT Category A+ Credit: 1.00

FDA Discussions may include off-label uses.

Participants

Carryn Anderson, MD, Iowa City, IA (Moderator) Nothing to Disclose

John C. Grecula, MD, Columbus, OH (Moderator) Research Grant, Teva Pharmaceutical Industries Ltd; Research Grant, Soligenix, Inc;

Sub-Events

MSR023-01 Low-Lying Lymph Node (LLLN) Involvement in Human Papillomavirus (HPV)-Associated Oropharyngeal Carcinoma (OPC)

Monday, Nov. 26 1:30PM - 1:40PM Room: E450A

Awards

Student Travel Stipend Award

Participants

Timothy Lin, BA, Bellaire, TX (Presenter) Nothing to Disclose Hesham Elhalawani, MD, MSc, Houston, TX (Abstract Co-Author) Nothing to Disclose Baher Elgohari, MBBCh, Houston, TX (Abstract Co-Author) Nothing to Disclose James M. Debnam, MD, Houston, TX (Abstract Co-Author) Nothing to Disclose Amit Jethanandani, MPH, Houston, TX (Abstract Co-Author) Nothing to Disclose Abdallah S. Mohamed, MD, MSc, Houston, TX (Abstract Co-Author) Nothing to Disclose S. J. Frank, MD, Houston, TX (Abstract Co-Author) Board Member, C4 Imaging LLC Stockholder, C4 Imaging LLC Advisory Board, Elekta AB Erich M. Sturgis, MD, Houston, TX (Abstract Co-Author) Nothing to Disclose Jack Phan, MD, PhD, Houston, TX (Abstract Co-Author) Nothing to Disclose Jay Reddy, MD, PhD, Houston, TX (Abstract Co-Author) Nothing to Disclose Clifton D. Fuller, MD, PhD, Houston, TX (Abstract Co-Author) Research Consultant, Elekta AB; Research Grant, Elekta AB; Speaker, Elekta AB William H. Morrison, MD, Houston, TX (Abstract Co-Author) Nothing to Disclose Heath Skinner, MD, PhD, Houston, TX (Abstract Co-Author) Nothing to Disclose David I. Rosenthal, Houston, TX (Abstract Co-Author) Advisory Board, Bristol-Myers Squibb Company Advisory Board, Merck KGaA Research support, Merck KGaA Adam S. Garden, MD, Houston, TX (Abstract Co-Author) Nothing to Disclose Brandon Gunn, MD, Galveston, TX (Abstract Co-Author) Nothing to Disclose

For information about this presentation, contact:

tlin4@mdanderson.org

PURPOSE

To characterize the incidence/pattern of LLLN involvement in HPV-associated OPC and correlation with outcomes after radiation therapy (RT).

METHOD AND MATERIALS

We reviewed diagnostic/planning images and clinical data of an IRB-approved cohort of HPV-associated OPC patients (pts) treated with definitive RT at our institution from 2004-13. Demographics and outcomes were retrieved from the medical records. LLLN+ were defined as any radiographically involved level IV or Vb nodes. AJCC 8th edition staging was used. Actuarial outcomes were calculated using Kaplan-Meier and compared by log-rank test. One-way analysis of variance was used to compare proportions.

RESULTS

In 796 pts, the incidence of LLLN+ was 12%, 13% in base of tongue and 10% in tonsil primaries, 10% in N1, 17% in N2, and 48% in N3. Median follow-up was 58 months (IQR: 42-77). Induction chemotherapy (IC) was used in 80% vs. 37% and concurrent in 78% vs. 65% for those with vs. without LLLN involvement, respectively. The proportion of LLLN+ patients receiving IC was 70%, 93%, and 100% for those with N1, N2, and N3 disease, respectively (p=.0034). Overall, LLLN+ was associated with worse 5-year rates for all disease control endpoints tested except freedom from distant metastasis (FDM) with a trend for OS. In patients with N1 disease, LLLN-involvement was associated with worse rates of FDM (87% vs. 94%, p=.0214); no significant differences were observed in N2 or N3 subgroups for any endpoint. In patients who received IC, LLLN+ was associated with worse 5-year local control (LC), regional control (RC), and relapse-free survival (RFS), differences ranging from 6-11% (p-value<0.004 for each). When stratified by IC and N-category, LLLN+ was associated with lower FDM rates in N1 (86% vs. 94%, p=.014) but not N2 or N3 disease.

CONCLUSION

Reflective of the patterns of care of those treated during this study time frame, most pts with LLLN+ received IC, which could have potentially offset any adverse correlation with subsequent distant failure. However, LLLN+ correlated with other disease control endpoints (LC, RC, and RFS), and thus could be considered a marker of regionally advanced disease in HPV-associated OPC, even for those with lower stage.

CLINICAL RELEVANCE/APPLICATION

LLLLN involvement was associated with poorer disease control outcomes, and a potential influence of IC on subsequent distant failure is hypothesized.

MSR023-02 Automatic Gross Tumor Volume (GTV) Delineation for Nasopharyngeal Carcinoma (NPC) Radiotherapy on Multi-modal MRI: A Deep Learning Model Trained from 1000 Patient Dataset

Monday, Nov. 26 1:40PM - 1:50PM Room: E450A

Participants

Fu Li, Guangzhou, China (*Presenter*) Nothing to Disclose Yao Lu, Guangzhou, China (*Abstract Co-Author*) Nothing to Disclose Ying Sun, Guangzhou, China (*Abstract Co-Author*) Nothing to Disclose Li Lin, Guangzhou, China (*Abstract Co-Author*) Nothing to Disclose

For information about this presentation, contact:

lifu5@mail.sysu.edu.cn

PURPOSE

GTV delineation of NPC is a critical and time-consuming process during intensity modulated radiotherapy. We are developing an automatic deep learning GTV delineation approach for NPC radiotherapy on multi-model MRI.

METHOD AND MATERIALS

With IRB approval, we retrospectively collected 1012 patients who underwent intensity modulated radiotherapy for NPC from Sept. 2016 to Aug. 2017. Multi-model MRIs (T1, T1C, T1W, T2) were acquired for GTV delineation of each patient with Philips MR imaging system and covered large variations in scanning parameters. Three experienced radiotherapists manually marked the GTV contours on MRI series (1 to 2 hours per case). In this study, a modified 3D U-net deep learning network was trained to perform volume-to-volume delineation of GTV. Multi-modal MRIs were regard as different channel input of the 3D U-net and feature maps from various layers were concatenated with deep supervision to generate the output as the corresponding GTV likelihood map. Binary cross-entropy was applied as loss function for network training. To increase receptive fields and capture contextual information, two-stride convolution was used to downsample feature maps instead of maxpooling operator. Besides, clinical anatomy characteristics were explored as post-processing to protect normal tissues and further improve the model performance. We randomly split the entire data set into training (850 cases) and independent testing (162 cases). Dice coefficient (DC), average percent volume error (AVE) and average absolute volume error (AAVE) were used to compare the computed GTV results with the experts' manual results.

RESULTS

The average DC, AVE and AAVE on test data are 0.79 ± 0.05 , -0.09 ± 0.21 , and 0.19 ± 0.13 , respectively. Comparing to 1-2 hours by the readers, our deep learning delineation takes less than 15 seconds per case.

CONCLUSION

Our results demonstrated the feasibility of deep learning approach for automatic GTV delineation of NPC during intensity modulated radiotherapy. Our automatic tool achieves good delineation quality on NPC GTV and greatly reduces the delineation time by hundred times compared to clinical doctors.

CLINICAL RELEVANCE/APPLICATION

Radiotherapy is one of the efficient routine treatment for NPC and accurate delineation of GTV is a key step in radiotherapy. Our automatic tool has potential to reduce the variability between human readers as well as improve the efficiency of the whole procedure.

MSR023-03 Using Artificial Intelligence to Predict Oropharyngeal Cancer Recurrence After Radiation Therapy

Monday, Nov. 26 1:50PM - 2:00PM Room: E450A

Participants William Su, New York, NY (*Presenter*) Nothing to Disclose Martin Kang, New York, NY (*Abstract Co-Author*) Nothing to Disclose Yading Yuan, New York, NY (*Abstract Co-Author*) Nothing to Disclose Richard L. Bakst, MD, New York, NY (*Abstract Co-Author*) Nothing to Disclose

For information about this presentation, contact:

richard.bakst@mountsinai.org

PURPOSE

HPV derived oropharyngeal cancers are less aggressive and more radiosensitive compared to non-HPV derived oropharyngeal cancers. In the HPV era, treatment de-escalation is one of the main areas of focus for clinical trials. However, recurrences still occur in HPV derived disease and can follow unique patterns, so it is important to identify patients at high risk of recurrence and ensure that they do not receive de-intensified treatment. Artificial intelligence can be used to analyze radiomic signatures and potentially predict recurrence. This would allow for personalized treatment planning based on radiographic risk profiles. Our purpose was to demonstrate that deep learning models have the potential to assess radiographic risk factors for oropharyngeal cancer recurrence.

METHOD AND MATERIALS

Radiotherapy planning CT scans of 108 patients with histologically proven oropharyngeal cancer were acquired from the TCIA Head-Neck-PET-CT collection. In this collection, all patients with recurrent cancer or metastases at presentation were excluded. Of 108 cases, 44 had loco-regional or distant recurrence of cancer after definitive radiation treatment. For each patient, a volume of interest (VOI) that embraces the Gross Tumor Volume was extracted from the entire CT scan. After being preprocessed for dimension standardization and intensity normalization, the VOI was input into a VGG16 based neural network to obtain a discriminative score, which indicates an estimate of the probability of recurrence of that tumor. Receiver Operating Characteristic (ROC) analysis was used to evaluate the classification performance of the VGG-based model.

RESULTS

By using 4-fold cross validation, the VGG-based classification model achieved an average accuracy of 0.59 and AUC of 0.60.

CONCLUSION

Our study shows that deep learning models have potential in predicting oropharyngeal cancer recurrence. This can eventually pave the way towards individualized radiation dosage planning based on radiomic signatures. A larger, multi-institutional dataset is required to further validate the model for clinical application.

CLINICAL RELEVANCE/APPLICATION

Artificial intelligence can be used to analyze radiographic features on CT simulation scans to predict recurrence risk and tailor radiation dosages in the HPV era of oropharyngeal cancers.

MSR023-04 A Phase II, Proof-of-Concept Clinical Study of an Oral Mouth Rinse Containing Sandalwood Oil (SAO) for the Prevention of Oral and Oropharyngeal Mucositis Associated with (Chemo-) Radiation Therapy in Head and Neck Cancer Patients

Monday, Nov. 26 2:00PM - 2:10PM Room: E450A

Participants

Chul S. Ha, MD, San Antonio, TX (*Presenter*) Investigator, Santalis Pharmaceuticals, Inc Ying Li, MD, San Antonio, TX (*Abstract Co-Author*) Investigator, Santalis Pharmaceuticals, Inc Carol Jenkins, RN,MS, San Antonio, TX (*Abstract Co-Author*) Nothing to Disclose Corey Levenson, PhD, San Antonio, TX (*Abstract Co-Author*) Officer, Santalis Pharmaceuticals

PURPOSE

Mucositis is one of the most debilitating side effects in patients treated with (chemo-) radiation therapy for head and neck cancer. This study was intended to evaluate the efficacy in alleviating mucositis, safety and tolerability of SAO (0.25% aqueous solution of an anti-inflammatory and anti-microbial essential oil from Santalum album trees).

METHOD AND MATERIALS

Patients to be treated with (chemo-) radiation therapy (>= 60 Gy) for cancers of oral cavity/oropharynx were asked to swish and gargle for 30 seconds, and spit, with 15 ml of the SAO three times a day throughout the radiation therapy. Pain in the oral cavity/oropharynx was measured using the numerical rating pain scale (NRPS) and mucositis was graded using the RTOG scale every week. Our data were compared with historical data in table 2 (incidence of mucositis), figure 1 (mean mucositis grade) and figure 2 (mean oral pain grade) from MD Anderson Cancer Center (MDACC) (doi:10.1016/j.ijrobp.2007.01.053) and table 4 (incidence of mucositis) from Memorial Sloan Kettering Cancer Center (MSKCC) (doi:10.1016/j.ijrobp.2010.10.041).

RESULTS

Fourteen subjects were enrolled but 6 withdrew (4 of them due to taste/smell of the rinse, 1 due to fatigue, 1 due to perceived ineffectiveness of the rinse). Among the 8 who completed the course of SAO treatment, 6 were treated with chemo-radiation and 2 with radiation only. IMRT was used for everyone. The median dose was 6,996 cGy in 33 fractions. There were no serious adverse events from SAO. The mean RTOG mucositis grades from weeks 3,6 and 9 were 1.125, 2.125 and 1.875. Two of 8 patients experienced mucositis >= 3. The corresponding mean NRPS were 3.700, 4.988 and 3.875.

CONCLUSION

The incidence of mucositis >= 3 were 70% from MDACC and 22% from MSKCC. Distribution of our mean NRPS and RTOG mucositis data compared favorably against figures 1 and 2 from MDACC. Though SAO was difficult to use due to poor taste/smell, it was otherwise well tolerated and appears to have enough signal to warrant further development as a potential alleviator of mucositis.

CLINICAL RELEVANCE/APPLICATION

This is a proof-of-concept clinical trial for an oral mouth rinse containing Sandalwood Oil for the prevention of mucositis associated with (chemo-) radiation therapy in head and neck cancer patients. We believe our results have generated enough signal to pursue further development of this preparation.

MSR023-05 Locoregional Patterns of Failure (POF) following Therapeutic Dose Neck Radiation Therapy (RT) for Un-Resected Anaplastic Thyroid Cancer (ATC)

Monday, Nov. 26 2:10PM - 2:20PM Room: E450A

Awards

Student Travel Stipend Award

Participants

Amit Jethanandani, MPH, Houston, TX (*Presenter*) Nothing to Disclose Mona K. Jomaa, MD,PhD, Cairo, Egypt (*Abstract Co-Author*) Nothing to Disclose Maria E. Cabanillas, Houston, TX (*Abstract Co-Author*) Research funded, Exelixis, Inc Abdallah S. Mohamed, MD, MSc, Houston, TX (*Abstract Co-Author*) Nothing to Disclose Renata Ferrarotto, MD, Houston, TX (*Abstract Co-Author*) Nothing to Disclose Mark Zafereo, MD, Houston, TX (*Abstract Co-Author*) Nothing to Disclose Adam S. Garden, MD, Houston, TX (*Abstract Co-Author*) Nothing to Disclose William H. Morrison, MD, Houston, TX (*Abstract Co-Author*) Nothing to Disclose Heath Skinner, MD, PhD, Houston, TX (*Abstract Co-Author*) Nothing to Disclose S. J. Frank, MD, Houston, TX (*Abstract Co-Author*) Board Member, C4 Imaging LLC Stockholder, C4 Imaging LLC Advisory Board, Elekta AB

Jack Phan, MD, PhD, Houston, TX (Abstract Co-Author) Nothing to Disclose

Jay Reddy, MD, PhD, Houston, TX (Abstract Co-Author) Nothing to Disclose

David I. Rosenthal, Houston, TX (Abstract Co-Author) Advisory Board, Bristol-Myers Squibb Company Advisory Board, Merck KGaA Research support, Merck KGaA

Clifton D. Fuller, MD,PhD, Houston, TX (Abstract Co-Author) Research Consultant, Elekta AB; Research Grant, Elekta AB; Speaker, Elekta AB

Brandon Gunn, MD, Galveston, TX (Abstract Co-Author) Nothing to Disclose

PURPOSE

Despite aggressive therapy, patients (pts) with ATC often develop locoregional progression (LRP). We aimed to identify the pattern of LRP in pts with un-resected ATC who received therapeutic doses of neck RT (>45 Gy).

METHOD AND MATERIALS

An institutional ATC database was retrospectively reviewed for pts who received neck RT from 01/00-08/17. ATC pts with unresected disease were eligible if they received RT > 45 Gy at our institution and had follow-up CTs to assess for LRP. Progressive gross tumor volumes (rGTVs) were segmented on diagnostic CTs that demonstrated LRP (rCTs) and were reviewed by a head and neck radiation oncologist. rCTs were co-registered with treatment planning CTs (pCTs) using deformable image registration (VelocityAI 3.0.1). rGTVs were compared to original RT plans using a centroid-based approach. Failures were classified into 5 types based on pre-defined spatial/dosimetric criteria; A (central high dose), B (central elective dose), C (peripheral high dose), D (peripheral elective dose), and E (extraneous dose).

RESULTS

129 ATC pts received neck RT; of these, 103 had available plans and only 73 had plans and follow-up CTs. Of the 73, pts were excluded for prior resection (n=37) or if RT dose was \leq 45 Gy (n=17). Thus, 19 formed the cohort. Most (79%) were Caucasian; median age was 63.5 years; 58% were stage IVC; 95% received IMRT; and all received systemic therapy. Median RT dose was 66 Gy (IQR: 59-66); median dose per fraction was 2 Gy (IQR: 1.7-2.2). Median follow-up was 7.9 mos. Six pts (31.5%) developed LRP and 16 rGTVs were identified (6 in 1 pt, 4 in 1, 3 in 1, and 1 in 3 each). Median time to LRP was 2.3 mos (range: 0-43). Of rGTVs, 7 were local (thyroid bed) and 9 were regional (1 in the paratracheal region; 1 in base of tongue [BOT]; 3 in node levels IIa; 1 in III; 2 in IV; and 1 in paraspinal musculature [PSM]). Type A was the most common rGTV POF (56%), followed by Types E (31%; 3 nodal, 1 BOT, and 1 PSM), B and C (8% each). Actuarial locoregional control (LRC) was 73% at 6 and 12 mos. Four living patients without LRP had a median follow-up of 27.5 mos (range: 9.3-65).

CONCLUSION

The identified POF was largely Type A and rapid (<6 mos), suggestive of a radiation resistance profile.

CLINICAL RELEVANCE/APPLICATION

Rapid neck progression was avoided in most ATC pts and some exhibited durable neck control, which could allow pts to receive subsequent systemic or targeted therapies.

MSR023-06 A Population-Based Study of the Effects of Therapy, Primary Tumor Characteristics, and Metastatic Disease Sites on Survival in Patients with Metastatic Head and Neck Cancer

Monday, Nov. 26 2:20PM - 2:30PM Room: E450A

Awards

Student Travel Stipend Award

Participants Justin Budnik, MD, Rochester, NY (*Presenter*) Nothing to Disclose Nicholas J. Denunzio, MD, PhD, Boston, MA (*Abstract Co-Author*) Nothing to Disclose Michael T. Milano, MD, PhD, Chicago, IL (*Abstract Co-Author*) Nothing to Disclose Deepinder Singh, MD, Rochester, NY (*Abstract Co-Author*) Nothing to Disclose

PURPOSE

Data is emerging that multimodality therapy (MMT) may improve overall survival (OS) in patients with metastatic head and neck cancer (M1-HNC). We aim to investigate the effects of MMT, tumor characteristics, and sites of metastatic disease on OS in M1-HNC patients using the Surveillance, Epidemiology, and End Results (SEER) database.

METHOD AND MATERIALS

2,827 patients from the SEER 18 registry diagnosed with M1-HNC from 2010-2014 were analyzed. Patients coded as having metastatic disease in bone, brain, liver, and lung were identified. Kaplan-Meier analyses and Cox proportional hazards models were used to assess the impact of MMT, primary tumor characteristics, and metastatic disease sites on OS.

RESULTS

Most patients were male (n=2,169, 76.7%), and had squamous carcinoma histology (n=2,009, 71.1%). Median age was 60 years and median OS was 10 months. Oropharynx (n=900, 31.8%) was the most common primary site. Patients coded as having metastases in lung and not in bone, brain, or liver (n=958, 33.9%) were the most common metastatic disease category. 518 patients (18.3%) received cancer-directed surgery (CDS), 1,458 patients (51.6%) received radiation (RT), and 1,690 patients (59.8%) received chemotherapy (CT). 579 patients (20.5%) received neither CDS, nor RT, nor CT (no therapy-group). With Cox regression accounting for age, sex, race, primary site, histology, grade, T stage, N stage, and metastatic sites, those who received CDS, RT, and CT (n=172, 6.1%) had the largest OS benefit (HR=0.22, 95% CI 0.17-0.28, p<0.001) compared to the no therapygroup. Patients receiving RT and CT were the most common MMT combination (n=879, 31.1%), and had improved OS (HR=0.35, 95% CI 0.30-0.40, p<0.001) compared to the no therapy-group. Primary and metastatic disease site-specific analyses showed that MMT combinations provided and OS benefit at all primary sites in the head and neck region and across metastatic sites with the exception of those coded as having metastases in bone and lung, and not in brain and liver.

CONCLUSION

In this hypothesis-generating study MMT is associated with improved OS in patients with M1-HNC. The OS benefit persists across primary and metastatic disease sites. Prospective study of MMT in M1-HNC patients is warranted.

CLINICAL RELEVANCE/APPLICATION

In this population-based, hypothesis-generating study multimodality therapy is associated with improved overall survival in patients with metastatic head and neck cancer.



CS23

Innovations in High Resolution Imaging: Presented by the Institute for Advanced Medical Education (IAME), educational grant provided by Canon Medical Systems

Monday, Nov. 26 2:00PM - 3:30PM Room: S101AB

Participants

Vincent Dousset, MD, PhD, Bordeaux, France (Presenter) Nothing to Disclose

Mathias Prokop, PhD, Nijmegen, Netherlands (*Presenter*) Speakers Bureau, Bracco Group; Speakers Bureau, Bayer AG; Research Grant, Canon Medical Systems Corporation; Speakers Bureau, Canon Medical Systems Corporation; Research Grant, Siemens AG; Speakers Bureau, Siemens AG; Departmental spinoff, Thirona; Departmental licence agreement, Varian Medical Systems, Inc; ;

СМЕ

CME Credit is available through a third-party provider: www.appliedradiology.org/cc3

RSVP Link

https://www.appliedradiology.org/RSNA18/default.aspx



RCC24

Clinical Decision Support: From Theory to Clinical Practice

Monday, Nov. 26 2:30PM - 4:00PM Room: S501ABC



AMA PRA Category 1 Credits ™: 1.50 ARRT Category A+ Credit: 1.75

Participants

Emanuele Neri, MD, Pisa, Italy (Moderator) Nothing to Disclose

LEARNING OBJECTIVES

1) To explore the strategy of implementation of CDS in US and Europe. 2) To report the clinical implementation and impact of CDS in a real setting. 3) To preview the future implementation of artificial intelligence in CDS.

Sub-Events

RCC24A How Can Radiologists Implement Decision Support Systems in Clinical Routine: ACR View

Participants Bibb Allen JR, MD, Birmingham, AL (*Presenter*) Nothing to Disclose

LEARNING OBJECTIVES

1) Apply lessons learned from the Medicare Demonstration project to implement effective Cllinical Decision Support (CDS) programs. 2) Formuate strategies for compliance with current regulations requiring CDS.

RCC24B How Can Radiologists Implement Decision Support Systems in Clinical Routine: ESR View

Participants

Boris Brkljacic, MD, PhD, Zagreb, Croatia (Presenter) Nothing to Disclose

For information about this presentation, contact:

boris@brkljacic.com

LEARNING OBJECTIVES

1) To learn about the use of imaging referral guidelines in Europe. 2) To understand the challenges of implementing a CDS for heterogeneous European countries. 3) To describe the varying experiences of implementing CDS and imaging referral guidelines in different countries.

RCC24C Results and Lessons from Brigham and Women's Hospital

Participants

Ramin Khorasani, MD, Boston, MA (Presenter) Nothing to Disclose

LEARNING OBJECTIVES

1) Briefly review existing federal regulations pertinent to imaging clinical decision support. 2) Discuss design, implementation and results of large scale imaging CDS intervention at Brigham and Women's Hospital. 3) Contrast results and discuss implications from CDS interventions that have and have not impacted ordering physician behavior. 4) Recommend strategies to optimize imaging CDS implementation to improve quality and enable and promote evidence-based practice.

RCC24D Application of Machine Learning in Clinical Decision Support Systems

Participants

Tarik K. Alkasab, MD, PhD, Boston, MA (Presenter) Nothing to Disclose



SSE04

Cardiac (MRI: General Topics)

Monday, Nov. 26 3:00PM - 4:00PM Room: N226



AMA PRA Category 1 Credit ™: 1.00 ARRT Category A+ Credit: 1.00

FDA Discussions may include off-label uses.

Participants

Pamela K. Woodard, MD, Saint Louis, MO (*Moderator*) Research agreement, Siemens AG; Research, Eli Lilly and Company; Research, F. Hoffmann-La Roche Ltd; ; ; ; ; ;

Harold I. Litt, MD, PhD, Philadelphia, PA (Moderator) Research Grant, Siemens AG ; ; ;

Sub-Events

SSE04-01 Convolutional Neural Network Based Guidance System for Multiplanar Cardiac MRI

Monday, Nov. 26 3:00PM - 3:10PM Room: N226

Awards Student Travel Stipend Award

Participants Kevin Blansit, MS,BS, La Jolla, CA (*Presenter*) Nothing to Disclose Tara A. Retson, MD, PhD, San Diego, CA (*Abstract Co-Author*) Nothing to Disclose Evan Masutani, La Jolla, CA (*Abstract Co-Author*) Nothing to Disclose Naeim Bahrami, PhD, MSc, San Diego, CA (*Abstract Co-Author*) Nothing to Disclose Kang Wang, MD,PhD, San Diego, CA (*Abstract Co-Author*) Nothing to Disclose Albert Hsiao, MD,PhD, La Jolla, CA (*Abstract Co-Author*) Founder, Arterys, Inc; Consultant, Arterys, Inc; Consultant, Bayer AG; Research Grant, General Electric Company;

For information about this presentation, contact:

kblansit@eng.ucsd.edu

PURPOSE

Cardiac MRI (cMRI) is the gold standard for quantitative cardiac evaluation. However, it requires specialized training and expertise to perform. To advance the accessibility and quality of cMRI, we developed a convolutional neural network (CNN) to localize key cardiac landmarks to guide plane prescription. We hypothesize that CNN-based landmark localization may generate similar imaging planes to those acquired by a dedicated cardiac technologist.

METHOD AND MATERIALS

With HIPAA-compliance and IRB waiver of informed consent, we retrospectively collected clinical cMRIs performed at our institution from February 2012 to June 2017, including 472 short axis (SAX) and 892 long axis (LAX) cine series. Anatomic landmarks were annotated by expert radiologists. U-Net CNNs were implemented to predict the location of these structures using heatmap localization. Data was split into 80% of cases for training and 20% for testing. SAX, 4, 3, and 2 chamber planes were computed from predicted anatomic localizations. We analyzed performance of localization by calculating distances between predictions and ground truth annotation, and report mean error and standard deviations. We assessed plane prescription by calculating the angle difference between CNN-predicted planes and those acquired by the technologist. Angle bias, mean error, and standard deviations are reported for each plane orientation.

RESULTS

From LAX images, the mean distance between annotation and predicted location was 7.70±5.90 mm for apex and 5.70±4.02 mm for the mitral valve. For SAX images, the mean distance was 11.99±7.80 mm for aortic valve, 10.20±5.65 mm for mitral valve, 12.56±5.10 mm for pulmonic valve, and 11.99±6.43 mm for tricuspid valve. For SAX stack prescription, average angle bias, mean error, and standard deviations were -7.80°, 7.80°±5.44°. For LAX prescriptions, average angle bias, mean error, and standard deviations were 5.64°, 6.65°±5.22° for 4-chamber, 10.86°, 11.95°±8.02° for 3-chamber, and 4.21°, 7.46°±7.36° for 2-chamber.

CONCLUSION

CNN-based anatomic localization is a feasible strategy for planning cMRI imaging planes. In this study, we show that this approach can produce imaging planes similar to those chosen by dedicated cardiac technologists.

CLINICAL RELEVANCE/APPLICATION

CNNs have the potential to improve the quality and accessibility of MRI, and may even benefit complex examinations like cardiac MRI, which require multiple double oblique image planes.

SSE04-02 Deep Learning for Accelerated CMR Image Reconstruction

Participants

Jo Schlemper, London, United Kingdom (*Presenter*) Nothing to Disclose Chen Qin, London, United Kingdom (*Abstract Co-Author*) Nothing to Disclose Jose Caballero, London, United Kingdom (*Abstract Co-Author*) Nothing to Disclose Ozan Oktay, PhD, London, United Kingdom (*Abstract Co-Author*) Nothing to Disclose Wenjia Bai, DPhil, London, United Kingdom (*Abstract Co-Author*) Nothing to Disclose Giacomo Tarroni, London, United Kingdom (*Abstract Co-Author*) Nothing to Disclose Anthony Price, London, United Kingdom (*Abstract Co-Author*) Nothing to Disclose Jo Hajnal, London, United Kingdom (*Abstract Co-Author*) Nothing to Disclose Daniel Rueckert, PhD, London, United Kingdom (*Abstract Co-Author*) Nothing to Disclose

For information about this presentation, contact:

jo.schlemper11@imperial.ac.uk

PURPOSE

CMR acquisition is inherently time consuming and requires multiple breath-holds, which is not only challenging for many patients, but it also makes the modality susceptible to motion artefacts. The aim of this study is to accelerate the CMR data acquisition by reducing the amount of k-space data needed for reconstructing images from undersampled data.

METHOD AND MATERIALS

Fully sampled, short-axis cardiac cine MR scans from 10 volunteers were acquired. Each scan contains a single slice SSFP acquisition with 30 temporal frames, resolution of 256x256 pixels, FOV of 320x320 mm with slice thickness 10mm. The recombined single-coil images were retrospectively undersampled respecting a linear frequency/phase encode structure, while the central 8 lines in k-space were always included. Deep learning-based iterative denoising algorithms are proposed: 3D-convolutional neural network (CNN) and 2D-convolutional recurrent neural network (CRNN). The networks were trained to directly output clean image from the aliased image. The proposed methods were compared to state-of-the-art compressed sensing approaches: kt-FOCUSS and kt-SLR. The methods were evaluated using peak signal-to-noise ratio (PSNR) and reconstruction speed. We considered acceleration factors 6 and 9 and performed 3-fold cross validation.

RESULTS

The networks were trained within three days on GPU GeForce GTX 1080. Even from small number of training subjects one could train a network that works well on test data. For acceleration factor 6, PSNR was 32.5, 34.6, 37.2 and 37.37 dB for kt-FOCUSS, kt-SLR, CRNN and CNN respectively. For acceleration factor 9, the numbers were 29.7, 31.4, 33.3 and 34.95 dB respectively. The reconstruction speeds were 15, 450, 6 and 10 seconds respectively.

CONCLUSION

We have proposed deep learning-based approaches for CMR image reconstruction, which both outperform current state-of-the-art both in terms of speed and reconstruction quality for single-coil, retrospective undersampling study.

CLINICAL RELEVANCE/APPLICATION

The method will be able to accelerate the CMR acquisition, which reduces burden on patients and improves image quality. In future, parallel imaging extension and implementation on scanner is expected.

SSE04-03 Multiparametric Cardiovascular Magnetic Resonance Imaging Assessment in End Stage Renal Disease Patients with Preserved Left Ventricular Ejection Fraction

Monday, Nov. 26 3:20PM - 3:30PM Room: N226

Participants

Xuhui Zhou, MD, PhD, Shenzhen, China (*Abstract Co-Author*) Nothing to Disclose Ling Lin, MD, Leiden, Netherlands (*Presenter*) Nothing to Disclose Qiuxia Xie, Guangzhou, China (*Abstract Co-Author*) Nothing to Disclose Yang Peng, Guangzhou, China (*Abstract Co-Author*) Nothing to Disclose Hildo J. Lamb, MD, PhD, Leiden, Netherlands (*Abstract Co-Author*) Nothing to Disclose

For information about this presentation, contact:

l.lin@lumc.nl

PURPOSE

Early detection of cardiac dysfunction in end stage renal disease (ESRD) patients is beneficial but challenging. Our study aimed to evaluate myocardial strain and tissue characteristic changes by cardiovascular magnetic resonance (CMR) imaging in ESRD patients with preserved left ventricular ejection fraction (LVEF), especially focused on those with no echocardiographic evidence of diastolic dysfunction.

METHOD AND MATERIALS

29 ESRD patients (17 males; mean age 44±11 years) with LVEF >50% in ultrasonagraphy and 43 healthy volunteers (24 males; mean age 43±10 years) underwent CMR imaging including cine, native T1 and T2 mapping. LV function, global LV strains as well as LV myocardial native T1 and T2 of the mid-cavity slice were measured and compared between the two groups. Correlations between LVMASS and CMR parameters were analyzed. According to ASE/EACVI recommendations for the evaluation of LV diastolic function by echocardiography, ESRD group were divided into normal diastolic function subgroup (n=11) and diastolic dysfunction subgroup (n=18). CMR parameters were compared among the two subgroups and the healthy group.

RESULTS

Native T1 and T2 were statistically higher in ESRD group ($1296.2\pm38.4ms$, $44.0\pm2.8ms$) than healthy group ($1260.1\pm51.9ms$, $41.0\pm1.7ms$; p=0.002, p<0.001). LV Global longitudinal strain (GLS) and global circumferential strain (GCS) were statistically

impaired in ESRD group (-14.5 \pm 2.9%, -16.4 \pm 3.0%) compared with the healthy group (-16.5 \pm 2.2%, -18.2 \pm 2.5%; p=0.002, 0.008). Increased LVMASS was strongly associated with impaired LV GLS and GCS (r= 0.72, 0.73; p<0.001) in ESRD group. In subgroup with normal diastolic function, T2 (43.2 \pm 1.5ms) and LV GLS (-14.3 \pm 3.0%) were statistically different from those in the healthy group (p=0.002, 0.008), while native T1 and LV GCS were similar with those in the healthy group.

CONCLUSION

ESRD patients with preserved LVEF demonstrated higher myocardial native T1, T2, and impaired LV GLS and GCS compared with healthy people. Myocardial edema and decreased myocardial compliance might exist in ESRD patients with preserved LVEF and normal diastolic function, as indicated by higher T2 and impaired LV GLS.

CLINICAL RELEVANCE/APPLICATION

Early stage of myocardial fibrosis, edema and decreased myocardial compliance might exist in ESRD patients with preserved LVEF, even when their diastolic function is normal on echocardiography.

SSE04-04 Subharmonic Aided Pressure Estimation (SHAPE) for Obtaining Intra-Cardiac Pressures Noninvasively in Real-Time: Preliminary Results

Monday, Nov. 26 3:30PM - 3:40PM Room: N226

Participants

Cara Esposito, Philadelphia, PA (Abstract Co-Author) Nothing to Disclose Jaydev K. Dave, PHD, Philadelphia, PA (Presenter) Research Grant, Koninklijke Philips NV; Equipment support, Lantheus Medical Imaging, Inc; Equipment support, General Electric Company Flemming Forsberg, PhD, Philadelphia, PA (Abstract Co-Author) Research Grant, Canon Medical Systems Corporation; Research Grant, General Electric Company; Research Grant, Siemens AG; Research Grant, Lantheus Medical Imaging, Inc Maureen McDonald, MBA, Philadelphia, PA (Abstract Co-Author) Nothing to Disclose Priscilla Machado, MD, Philadelphia, PA (Abstract Co-Author) Nothing to Disclose Kris Dickie, Burnaby, BC (Abstract Co-Author) Employee, Clarius Mobile Health Corp Ira S. Cohen, Philadelphia, PA (Abstract Co-Author) Nothing to Disclose Praveen Mehrotra, MD, Philadelphia, PA (Abstract Co-Author) Nothing to Disclose Michael Savage, MD, Philadelphia, PA (Abstract Co-Author) Nothing to Disclose David Fischman, Philadelphia, PA (Abstract Co-Author) Nothing to Disclose Nicholas J. Ruggiero II, MD, Philadelphia, PA (Abstract Co-Author) Nothing to Disclose Paul Walinsky, MD, Philadelphia, PA (Abstract Co-Author) Nothing to Disclose Andrew Boyle, Philadelphia, PA (Abstract Co-Author) Nothing to Disclose Eron Sturm, Philadelphia, PA (Abstract Co-Author) Nothing to Disclose Marguerite Davis, Philadelphia, PA (Abstract Co-Author) Nothing to Disclose

For information about this presentation, contact:

jaydev.dave@jefferson.edu

PURPOSE

Subharmonic aided pressure estimation (SHAPE) utilizes subharmonic signals from ultrasound contrast agents for pressure estimation. The purpose of this work was to evaluate the efficacy of intra-cardiac SHAPE using Definity (Lantheus Medical Imaging) and Sonazoid (GE Healthcare) microbubbles in patients scheduled for cardiac catheterization procedures.

METHOD AND MATERIALS

Patients scheduled for left and/or right heart catheterization procedures were recruited into this IRB-approved study. During the catheterization procedure, 15 patients received an infusion of Definity (2 activated vials mixed in 50 mL saline; 4-10 mL per minute) and 3 patients received a co-infusion of Sonazoid (infusion rate (mL/hour) = 0.18 x body weight in kg) and saline (120 mL/hour). During contrast infusion, the patients were scanned using a customized interface developed on a SonixTablet scanner (BK Ultrasound; interface developed using C/C++ and cross-platform Qt libraries (The Qt Company)) to determine optimum incident acoustic output (IAO; from a set of 16 pre-configured acoustic outputs coded from 0 or minimum to 15 or maximum) eliciting ambient pressure sensitive growth phase subharmonics for SHAPE, on a per-patient basis. Previously determined optimal parameters for Definity (ftransmit: 3.0 MHz; a chirp down pulse) and Sonazoid (ftransmit: 2.5 MHz; square wave pulse) were used for data acquisition. Correlation coefficient between the SHAPE and pressure catheter data was computed using MATLAB (2016A, The MathWorks, Inc.).

RESULTS

The IAO's at which the best correlation coefficient obtained between the SHAPE and pressure catheter data varied on a perpatient basis from coded values of 3 to 15 (patient BMI range: 22.7-64.6). Data with Definity infusion showed that the correlation coefficient between SHAPE and pressure catheter for the left ventricle (LV) was -0.8 ± 0.03 (mean \pm standard deviation; n = 10) and for the right ventricle (RV) was -0.8 ± 0.08 (n = 12). Data with Sonazoid infusion showed the correlation coefficient between SHAPE and pressure catheter for the LV was -0.8 ± 0.04 (n = 2) and the RV was -0.8 (n = 1).

CONCLUSION

Preliminary results indicate a good correlation (correlation coefficient range: -0.7 to -0.9) between SHAPE and pressure-catheter based intra-cardiac pressures.

CLINICAL RELEVANCE/APPLICATION

Intra-cardiac SHAPE may become an effective noninvasive alternative to cardiac catheterization procedures.

SSE04-05 Transient Ischemic Dilation and Coronary Artery Disease Burden in Cardiac MRI

Monday, Nov. 26 3:40PM - 3:50PM Room: N226

For information about this presentation, contact:

jmyan@mcw.edu

PURPOSE

Transient Ischemic Dilation (TID) is a well-established finding in nuclear myocardial perfusion imaging (MPI) and is a marker for coronary artery disease (CAD) severity. Stress perfusion cardiac MRI (CMR) offers significantly improved spatial and temporal resolution relative to MPI and allow for direct measurement of the LV wall cavity dimensions. Despite these advantages, CMR-derived TID ratios are not well established and thus not utilized in the clinical setting for CAD severity. The aim of this study was to confirm whether TID occurs during stress perfusion CMR and define a TID ratio that predict the presence and severity of CAD.

METHOD AND MATERIALS

Patients who underwent a complete stress CMR from 2012-2016 were included in the study. Imaging studies were analyzed and stress and rest left ventricular (LV) area at three myocardial cross-sections, basal, mid, and apex, was recorded. Coronary angiographic data for all patients with this information available was reviewed. TID ratio was calculated as the LV cavity area minus papillary muscles at stress versus rest. Global TID ratio was calculated by taking the mean of the segments (basal, mid, and apex) for each patient. Patients were classified into High Risk group if angiography results show >= 70% stenosis in the proximal LAD, >= 70% stenosis in the Left Main, >=90% lesion in more than 2 major vessels, or prior CABG with >=70% graft lesion. Unpaired t-test was used to compare mean values of High Risk and Low Risk groups and a ROC analysis was performed to determine the global TID ratio that differentiated patients with High Risk CAD versus Low Risk CAD.

RESULTS

One hundred forty three patients underwent stress CMR. Fourteen patients met criteria for High Risk CAD on coronary angiography, while the remainder had either negative stress or positive stress with low risk CAD. Mean Global TID ratio for high risk group was 1.18 vs 0.98 in the low risk group (p = 0.004). AUC in the ROC analysis was 0.734 (p=0.004). Associated criterion maximizing specificity revealed global TID ratio > 1.16 with a sensitivity of 57% and specificity of 85%.

CONCLUSION

Significant dilation in the LV area at stress occurs when severe CAD is present compared to rest.

CLINICAL RELEVANCE/APPLICATION

A global stress to rest ratio of 1.16 in cardiac stress MRI may provide an additional marker for identifying high-risk multi-vessel CAD.

SSE04-06 Is Cardiac MR Indispensable for Assessing the Cardiac Mass?: Based on the Review of 10-Years of Hospital Records

Monday, Nov. 26 3:50PM - 4:00PM Room: N226

Participants

Ji Eun Park, Seongnam, Korea, Republic Of (*Presenter*) Nothing to Disclose Eun Ju Chun, MD, PhD, Seongnam-Si, Korea, Republic Of (*Abstract Co-Author*) Nothing to Disclose Jeong A Kim, MD, Goyangsi, Korea, Republic Of (*Abstract Co-Author*) Nothing to Disclose Jin Young Yoo, MD, Cheongju, Korea, Republic Of (*Abstract Co-Author*) Nothing to Disclose Yeonyee E Yoon, Sengnam, Korea, Republic Of (*Abstract Co-Author*) Nothing to Disclose

PURPOSE

Although cardiac magnetic resonance (MR) is useful for assessing cardiac mass, it has limited to use as the first modality because of high cost and long scan times. Therefore, we aimed to evaluate how MR is effective in assessing the cardiac mass based on the review of 10-years of hospital records.

METHOD AND MATERIALS

We hypothesized that cardiac mass is firstly detected with echocardiography, and further evaluated with CT and MR. On the basis of echocardiography from 2008 to 2017 in single tertiary hospital, we searched patients with cardiac mass using ICD code and keywords. Cardiac mass was classified by the location (intracardiac, valve and extracardiac) and evaluated the transferred ratio to next modality (CT or MR) from echocardiography according to mass location. Finally, we evaluated why the clinician performed MR and how successful that goal was achieved.

RESULTS

In a total of 718 adults (390 males, 62.6 ± 18.7 years) with cardiac mass (282 intracardiac mass, 262 valve mass, 174 extracardiac mass) which detected on echocardiography, 406 patients (56.5%) were performed CT. Among them, CT performed ratio is highest for extracardiac mass (92.0%) followed by intracardiac mass (66.0%) and valve mass (22.9%), sequentially. MR was performed in 64 patients (8.9%); 16 patients with directly performed MR, 48 patients were performed MR after CT. Role of MR in assessing the cardiac mass was as follows; tissue characterization (n=36), differentiation of thrombus from tumor (n=15) and detection of invasiveness (n=25). After MR, the successful rate which met the goals of MR was highest for detection of invasiveness (92.0%), followed by differentiation of thrombus (80.0%) and tissue characterization (61.1%).

CONCLUSION

Valve mass may be sufficient with echocardiography, and extracardiac mass requires CT to assess the extent. CMR is useful for determine invasiveness and differentiate thrombus from tumor than tissue characteristics

CLINICAL RELEVANCE/APPLICATION

From this review of our data, the efficacy of CMR for assessing cardiac mass might be higher to determine the invasiveness and differentiate the thrombus from tumor than to detect tissue characteristics.



SSE11

Genitourinary (Imaging of Renal Stones)

Monday, Nov. 26 3:00PM - 4:00PM Room: S102CD



AMA PRA Category 1 Credit ™: 1.00 ARRT Category A+ Credit: 1.00

FDA Discussions may include off-label uses.

Participants

Mitchell E. Tublin, MD, Pittsburgh, PA (Moderator) Nothing to Disclose

Sub-Events

SSE11-01 Three Dimensional Texture Analysis with Machine Learning Provides Incremental Predictive Information for Successful Shock Wave Lithotripsy in Patients with Kidney Stones

Monday, Nov. 26 3:00PM - 3:10PM Room: S102CD

Participants

Manoj Mannil, Zurich, Switzerland (*Presenter*) Nothing to Disclose Jochen von Spiczak, MD,MSc, Zurich, Switzerland (*Abstract Co-Author*) Nothing to Disclose Christian Fankhauser, Zurich, Switzerland (*Abstract Co-Author*) Nothing to Disclose Thomas Hermanns, Zurich, Switzerland (*Abstract Co-Author*) Nothing to Disclose Hatem Alkadhi, MD, Zurich, Switzerland (*Abstract Co-Author*) Nothing to Disclose

PURPOSE

To determine the predictive value of three-dimensional texture analysis (3D-TA) in computed tomography (CT) images for successful shock wave lithotripsy (SWL) in patients with kidney stones.

METHOD AND MATERIALS

Patients with pre and postoperative CT scans, previously untreated kidney stones and a stone diameter of 5-20 mm were included. A total of 224 3D-TA features of each kidney stone, including the attenuation measured in Hounsfield Units (HU), and the clinical variables body mass index (BMI), initial stone size, and skin-to-stone distance (SSD) were analyzed using five commonly used machine learning models. The data set was split in a ratio of 2/3 for model derivation and 1/3 for validation. Machine learning-based predictions for SWL success in the validation cohort were evaluated calculating sensitivity, specificity, and the area-under-the-curve (AUC).

RESULTS

For SWL success the three clinical variables BMI, initial stone size and SSD showed AUCs of 0.68, 0.58 and 0.63 respectively and no predictive information for HU could be noted. By use of a RandomForest classifier using three 3D-TA features an AUC of 0.79 could be observed. By combining 3D-TA features and clinical variables, the discriminatory accuracy improved further with an AUC of 0.85 for 3D-TA features and SSD, an AUC of 0.8 for 3D-TA features and BMI and an AUC of 0.81 for 3D-TA and stone size.

CONCLUSION

Our in-vivo study indicates the potential of 3DTA of urinary stone CT enabling the prediction of successful stone disintegration with SWL with high accuracy.

CLINICAL RELEVANCE/APPLICATION

Selected 3D-TA features provide incremental predictive value for successful SWL, which allows stratifying patients with symptomatic kidney stones to either primary SWL or Ureterorenoscopy.

SSE11-02 Usefulness of Computer Aided Detection of Urinary Stones in Computed Tomography Kidney Ureter Bladder using Convolutional Neural Networks: Preliminary Study

Monday, Nov. 26 3:10PM - 3:20PM Room: S102CD

Participants

Sung Bin Park, MD, Seoul, Korea, Republic Of (*Presenter*) Nothing to Disclose Hyun Jeong Park, Seoul, Korea, Republic Of (*Abstract Co-Author*) Nothing to Disclose Eun Sun Lee, MD, PhD, Seoul, Korea, Republic Of (*Abstract Co-Author*) Nothing to Disclose Jong Beum Lee, Seoul, Korea, Republic Of (*Abstract Co-Author*) Nothing to Disclose Byung Ihn Choi, MD, PhD, Seoul, Korea, Republic Of (*Abstract Co-Author*) Nothing to Disclose

For information about this presentation, contact:

pksungbin@paran.com

Computed tomography kidney ureter bladder (CTKUB) is the method of choice for diagnosing urinary stones. The purpose of this study is to develop a computer aided detection (CAD) algorithm for identifying a urinary stone in thin slice CTKUB.

METHOD AND MATERIALS

Thin slices (3 mm) CTKUB (120 kVp and 150 mAs) in patients with suspicious of stone disease were included in the study. The labeling of urinary stones or not in CTKUB as reference standard was performed by an expert radiologist. 5,268 urinary stones and 4,980 non-urinary stones on CTKUB images were evaluated for training dataset. 551 urinary stones and 528 non-urinary stones on CTKUB images were evaluated for validation dataset. The convolutional neural network was consisted of 8 convolution layers, 9 fully connected layers and softmax classifier. The diagnostic performance of CAD algorithm for identifying a urinary stone from combination of three different image planes (axial, coronal and sagittal) in thin slice CTKUB using convolutional neural network was analyzed.

RESULTS

In training dataset, the performance was almost perfect. In validation dataset, the CAD algorithm was classified all 551 urinary stones as stones. It was also classified 528 non-urinary stones as 527 non-urinary stones and 1 urinary stone. The sensitivity, specificity, accuracy, positive predictive value and negative predictive value of CAD algorithm were 100%, 99.8%, 99.9%, 99.8% and 100%, respectively.

CONCLUSION

CAD algorithm in thin slice CTKUB using convolutional neural network can have high diagnostic performance for urinary stone detection. Prospective further studies involving more participants and focusing on the factors affecting clinical practice such as stone size, location (ureter, kidney) are needed.

CLINICAL RELEVANCE/APPLICATION

In view of its high accuracy, we believe CAD algorithm in thin slice CTKUB using convolutional neural network can be used as an initial examination in patients with suspicious of stone disease.

SSE11-03 Efficacy of Single-Source Rapid kV-Switching Dual-Energy CT for Characterization of Non-Uric Acid Renal Stones: A Prospective Ex-Vivo Study Using Anthropomorphic Phantom

Monday, Nov. 26 3:20PM - 3:30PM Room: S102CD

Awards

Student Travel Stipend Award

Participants Roberto Cannella, MD, Pittsburgh, PA (*Presenter*) Nothing to Disclose Mohammed Shahait, Pittsburgh, PA (*Abstract Co-Author*) Nothing to Disclose Alessandro Furlan, MD, Pittsburgh, PA (*Abstract Co-Author*) Book contract, Reed Elsevier; Research Grant, General Electric Company; Consultant, General Electric Company Joel D. Bigley, Pittsburgh, PA (*Abstract Co-Author*) Nothing to Disclose Timothy Averch, Pittsburgh, PA (*Abstract Co-Author*) Nothing to Disclose Amir Borhani, MD, Pittsburgh, PA (*Abstract Co-Author*) Consultant, Guerbet SA; Author, Reed Elsevier

For information about this presentation, contact:

rob.cannella89@gmail.com

PURPOSE

To investigate the accuracy of rapid kV-switching single-source dual-energy computer tomography for prediction of classes of nonuric acid stones.

METHOD AND MATERIALS

Non-uric-acid renal stones retrieved via percutaneous nephrolithotomy were prospectively collected between January 2017 and February 2018 in a single institution. Only stones >5mm and with pure composition (i.e. >80% composed of one element) were studied. Stone composition was determined using Fourier Transform Infrared Spectroscopy. The stones were scanned in 32 cm-wide anthropomorphic whole body phantom in a location mimicking the kidneys. Image acquisition was performed using a single-source rapid-kVp switching CT scanner. The effective atomic number (Zeff) and the attenuation (HU) at 40 kev, 70 kev, and 140 kev virtual monochromatic sets of images were extracted by placing a ROI at the largest cross-sectional areas. Ratios between the attenuations at different energy levels were calculated. Mean values of different stone classes were compared using ANOVA and student t-test. Difference between the actual class of stone and the predicted class of stone based on vendor-recommended Zeff thresholds were assessed. A p-value <0.05 was considered statistically significant. Receiver operating curves (ROC) and area under curve (AUC) with 95% confidence intervals were calculated to assess the efficacy of each parameter.

RESULTS

The final study sample included 31 stones from 31 patients consisting of 2 (6%) struvite, 4 (13%) cysteine and 25 (81%) calciumbased pure stones. The mean size of the stones was 9.9 ± 2.4 mm. The mean Zeff of the stones was 12.0 ± 0.41 for calcium-based, 10.1 ± 0.14 for struvite, and 9.9 ± 0.57 for cysteine stones which were statistically different (p<0.001). In 16 cases (51.6%), there was discrepancy between the actual stone class and the predicted class based on vendor-recommended thresholds. Zeff had the best efficacy for differentiation of different stone classes. The calculated AUC was for 0.947 for Zeff; 0.833 for HU40; 0.880 for HU70 and 0.893 for HU140.

CONCLUSION

Zeff has superior performance to HU and attenuation ratios for differentiation of different classes of non-uric-acid stones.

CLINICAL RELEVANCE/APPLICATION

Non-invasive determination of composition of urinary stone has important clinical implication in guiding the decision making algorithm

for stone treatment.

SSE11-04 Dual-Energy Spectral CT Characterization of Urinary Calculi In Vivo

Monday, Nov. 26 3:30PM - 3:40PM Room: S102CD

Participants Xiaohu Li, MD, Hefei, China (*Presenter*) Nothing to Disclose Yongqiang Yu, MD, Hefei, China (*Abstract Co-Author*) Nothing to Disclose Jianying Li, Beijing, China (*Abstract Co-Author*) Employee, General Electric Company

PURPOSE

To explore the feasibility of using dual-energy energy spectral CT to determine the components of urinary calculi in vivo

METHOD AND MATERIALS

Fifty-seven cases of patients with urinary calculi were included in the present eighty-nine stones, with GSI (gemstone spectral imaging) scan using AW4.6 workstation for image analysis indexes:GSI scan mode (Effective atomic number), the material (Materia Density) calcium water ratio (calcium water ratio, CWR),50keV and 70keV single energy CT value. The differences of 4 indexes were compared. According the infrared spectrum analysis results as the reference standard. Compared with spectrum diagnosis ,we can conclude that sensitivity, specificity and positive predictive value, negative predictive value of pure uric acid stones, pure non-uric acid stones, stones mixed . Retrospective study of involving 24 cases of single component calculi (11 pieces of uric acid stones, 9 pieces of calcium oxalate, 3 pieces of calcium phosphate stones) and 53 cases of mixed stones.Stones were respectively measuring the effective atomic number, CWR, 50ke V, 70keV single energy CT value and we can compare the indexes of different groups with the one way anova.

RESULTS

The infrared spectrum analysis results as the reference standard, the sensitivity for analysis pure uric acid calculi, pure non-uric acid stones and mixed stones were 100%, 91.7%, 97.0%, respectively; with specificity of 100%, 97.4%, 95.7%, respectively; with the positive predictive value of 100%, 84.6% 98.5% respectively and the negative predictive value were 100%, 98.7%, 91.7%, respectively.

CLINICAL RELEVANCE/APPLICATION

It is useful to reduce the occurrence of complications if we can make a definite diagnosis of stone composition before surgery.

SSE11-05 Role of Single Source Dual Energy CT in Evaluation of Chemical Composition of Urinary Tract Calculi

Monday, Nov. 26 3:40PM - 3:50PM Room: S102CD

Participants

CHANDRESH O. KARNAVAT, Mumbai, India (*Abstract Co-Author*) Nothing to Disclose Niravkumar K. Kadavani, MBBS, Mumbai, India (*Presenter*) Nothing to Disclose Ritu M. Kakkar, MBBS, DMRD, Mumbai, India (*Abstract Co-Author*) Nothing to Disclose Shrinivas B. Desai, MD, Mumbai, India (*Abstract Co-Author*) Nothing to Disclose

For information about this presentation, contact:

chand.k.13@gmail.com

PURPOSE

To evaluate the diagnostic accuracy of Single Source Dual Energy CT in characterisation of renal stones with biochemical analysis as reference

METHOD AND MATERIALS

This was a prospective study carried out at a tertiary care centre for a period of 3 years using Gemstone Spectral Imaging in single source dual energy CT scanner- GE Discovery CT750 HD. A total of 70 patients with renal calculi who underwent single source dual energy CT and subsequent surgery were included in the study. Both high and low energy data sets are acquired simultaneously for axial and helical acquisitions at the full 50 cm field of view. Dual-energy data were processed by the GSI general protocol on the CT workstation (Advantage Windows, version 4.2; GE Healthcare). A region of interest (ROI) was applied over the renal stone viewed on the bone window settings occupying approximately 50% of the stone area on axial images. Using GSI software effective atomic number of the ROI area Z (Zeff) was calculated and stones were characterised. Post surgery biochemical analyses of these stones were sent to a common laboratory. All results of dual energy CT were compared to the biochemical analysis by applying kappa statistics

RESULTS

Out of 70 patients, 43 were male and rest were female. The age group of patients ranged from 25 to 70 years (mean 47 years). Out of 48 calcium oxalate stones on dual energy CT, 47 were calcium oxalate and one was mixed. Out of 12 struvite stones on dual energy CT, 10 were struvite and 2 were mixed. Single cysteine stone detected on dual energy CT was found to be mixed stone on biochemistry. All 7 ammonium urate stones on dual energy were found to be same on biochemistry. Single mixed stone detected on dual energy CT showed similar result on biochemistry. Weighted kappa was found to be 0.835 which indicates very good agreement between two different diagnostic tests

CONCLUSION

Single Source Dual energy CT scan has a role in accurately assessing the chemical composition of the urinary tract calculi

CLINICAL RELEVANCE/APPLICATION

Chemical composition of the urinary tract calculi using Single Source Dual Energy CT has significant impact on medical management of patient with stone disease

SSE11-06 Comparison of CT-Index and Effective Z Analysis for Characterization of Urinary Stones with Dual-Energy CT: A Phantom Study

Monday, Nov. 26 3:50PM - 4:00PM Room: S102CD

Participants

Felice A. Burn, MD, Aarau, Switzerland (*Presenter*) Nothing to Disclose Daniel Mueller, Zurich, Switzerland (*Abstract Co-Author*) Nothing to Disclose Sebastian T. Schindera, MD, Aarau, Switzerland (*Abstract Co-Author*) Nothing to Disclose

For information about this presentation, contact:

felice.burn@ksa.ch

PURPOSE

To assess the accuracy of CT-index and effective Z value (atomic number) derived from dual-energy CT for differentiation of uric acid from non-uric acid stones and to further characterize the subgroup of non-uric acid stones.

METHOD AND MATERIALS

Total of 64 urinary stones from humans (32 uric acid and 32 non-uric acid stones with subgroups of oxalate, struvite, brushite and apatite) were included in the study. The stones were placed in an anthropomorphic CT-phantom (diameter, 30 cm). All stones underwent an x-ray diffraction analysis representing the gold standard and they had a high purity and homogeneity of at least 90% in their compositions. The phantom was scanned on a 360-slice MDCT scanner (Aquilion ONE Vision, Canon Medical) with a dual-energy mode using tube voltages of 135 and 80 kVp. The acquired datasets were automatically segmented and postprocessed with commercially available software. The CT-index and the effective Z, which was derived from raw data-based dual-energy analysis, was assessed. A statistical receiver operating characteristics (ROC) analysis and multivarable discrimination analysis was performed.

RESULTS

The differentiation of uric acid stones from non-uric acid stones were significant, using the CT-index (p < 0.001) and the effective Z value (p < 0.01). The use of the effective Z and CT-index allow further separation in subcategories as uric acid, oxalat, apatit, brushit and struvit stones (Figure 1), whereas this separation is less accurate than for the differentiation of uric acid from non-uric acid stones. If the CT-index and the effective Z values were taken both in consideration a subgroup analysis shows. If the CT-index and the effective Z values were taken both in consideration a subgroup analysis shows more powerful options in differentiation.

CONCLUSION

CT-index and effective Z values, derived from dual-energy CT, allow very accurate differentiation of uric acid from non-uric acid stones. The differentiation of non-uric acid subgroups is not very reliable for both parameters separately. However, the combinations of both parameters in the evaluation of subgroups can improve the separation of non-uric acid stones.

CLINICAL RELEVANCE/APPLICATION

Improved characterization of renal stone compositions with dual-energy CT using CT index and effective Z value in combination has a direct impact on the clinical management and therefor may improve patient outcome and may reduce treatment costs.



SSE14

Informatics (Artificial Intelligence in Radiology: More Cutting-Edge Deep Learning)

Monday, Nov. 26 3:00PM - 4:00PM Room: E353C



AMA PRA Category 1 Credit ™: 1.00 ARRT Category A+ Credit: 1.00

FDA Discussions may include off-label uses.

Participants

Norio Nakata, MD, Tokyo, Japan (*Moderator*) Nothing to Disclose Nabile M. Safdar, MD, Milton, GA (*Moderator*) Nothing to Disclose Safwan Halabi, MD, Stanford, CA (*Moderator*) Nothing to Disclose Alexandre Cadrin-Chenevert, MD, St Charles Borromee, QC (*Moderator*) Nothing to Disclose

Sub-Events

SSE14-01 Machine Learning Fully Automatic Analysis of Vertebrae Trabecular Bone Mineral Density in 10,000 CTs: Groundwork for Opportunistic Osteoporosis Screening

Monday, Nov. 26 3:00PM - 3:10PM Room: E353C

Participants

Thomas J. Re, MD, Princeton, NJ (*Presenter*) Consultant, Siemens AG Bogdan Georgescu, PhD, Princeton, NJ (*Abstract Co-Author*) Employee, Siemens AG Guillaume J. Chabin, MS, Princeton, NJ (*Abstract Co-Author*) Employee, Siemens AG Sasa Grbic, Princeton, NJ (*Abstract Co-Author*) Employee, Siemens AG Dorin Comaniciu, PhD, Princeton, NJ (*Abstract Co-Author*) Employee, Siemens AG

For information about this presentation, contact:

sasa.grbic@siemens-healthineers.com

CONCLUSION

ML technology can be exploited to perform large-scale investigations of CT-tBMD on this and other large cohorts as groundwork for developing CT-based osteoporosis screening.

Background

Opportunistically CT measured vertebral trabecular bone mineral density (CT-tBMD) has been proposed as a possible alternative to DEXA measurements for assessing osteoporosis in cases where a body CT is performed for other motives (trauma, surgery, oncology, COPD, etc). Such an application will require better understanding of CT-tBMD ranges in health and pathology. Previous works, using traditional semi-automatic quantization methods, have been of limited cohort size. Recent developments in machine learning (ML) applied to analyze medical imaging data have increased robustness and accuracy enabling accurate automated segmentation of anatomic structures. We applied a ML pipeline to a large public cohort containing CT and correlated clinical data (COPDgene.org) to demonstrate the viability of using such technology for large-scale tBMD studies.

Evaluation

Deep Reinforcement Learning and Adversarial Deep Image-to-Image ML networks were trained with 4560 manually segmented vertebrae from 380 CTs. A pipeline incorporating this network and 5% erosion algorithm, for trabecular bone isolation, was developed. It showed a 4.5% prediction error when tested on another 834 manually segmented vertebrae. The pipeline was applied to 9554 chest CTs from the COPDGene cohort and correlated to available corresponding clinical data. Results demonstrate a downward trend of BMD with age with slightly more rapid decline in later years for women than men. The data demonstrated significantly lower BMD in subjects diagnosed with osteoporosis, with history of compression or hip fracture (p-values<0.01). Processing time was 5.9 sec per series on a 3 GPU workstation.

Discussion

These findings agree with previous ones obtained by traditional semi-automatic techniques on smaller cohorts. Novelty in this work is the use of an ML based and fully automatic pipeline which provides precision and scalability and permits rapid application to the current and other large cohorts.

SSE14-02 Towards Hierarchical Optimization of Pretrained Deep Learning Models for Tuberculosis Screening in Chest Radiograph

Monday, Nov. 26 3:10PM - 3:20PM Room: E353C

Participants

Jeonghwan Gwak, Seoul, Korea, Republic Of (*Abstract Co-Author*) Nothing to Disclose Chang Min Park, MD, PhD, Seoul, Korea, Republic Of (*Abstract Co-Author*) Nothing to Disclose Jae Won Choi, MD, Seoul, Korea, Republic Of (*Presenter*) Nothing to Disclose Hyungjin Kim, MD, Seoul, Korea, Republic Of (*Abstract Co-Author*) Nothing to Disclose Eui Jin Hwang, Seoul, Korea, Republic Of (*Abstract Co-Author*) Nothing to Disclose Jin Mo Goo, MD, PhD, Seoul, Korea, Republic Of (*Abstract Co-Author*) Research Grant, Samsung Electronics Co, Ltd; Research Grant, Lunit Inc

For information about this presentation, contact:

james.han.gwak@gmail.com

CONCLUSION

We verified that hierarchical optimization process could assist to optimize the pretrained deep learning models by developing and incorporating hierarchical and structured feature information.

Background

Tuberculosis (TB) is a chronic infectious disease and thus early screening is critical in alleviating its transmission and reducing reproductive rate. While there are a few researches for the given task in chest radiograph through developing new deep learning models and simply using fixed pretrained models, there are very rare researches on further optimizing pretrained models to improve the performance.

Evaluation

We focused on optimizing pretrained models using hierarchical optimization process using iterative adaptive fixation and release operations and parallel model building. Based on the implications of high-level abstractions, lower layers in pretrained models will have more general feature information (e.g., edges) and upper layers keep domain-specific feature information (e.g., object parts or objects). The optimization is done by making a parallel pool consisting of 10 instances of a pretrained deep learning model and by bypassing through fixation/release of convolution layers with slightly perturbed feature information and then fine-tuning is repeatedly done until the gradient changes become negligible. Finally, the winner will be selected as the best model. We used 7,000 normal patients' chest radiograph images, and 7,000 TB patients' images for training using the hierarchical optimization. As the pretrained models, we used GoogLeNet, ResNet-152 and Inception-ResNet-V2. For validation and test, we used two independent datasets each consisting of 300 normal patients' images and 150 TB patients' images. Results showed that the area under the receiver operating characteristics curves (AUCs) of GoogLeNet, ResNet-152 and Inception-ResNet-V2 were 0.97, 0.99 and 0.99, respectively. For comparison, the AUCs of the models without such optimization process obtained 0.89, 0.93, 0.92, respectively.

Discussion

We proposed a method of optimizing pretrained deep learning models in a hierachical manner. Further study is required to deal with class-imbalanced dataset issues.

SSE14-03 Understanding Deep Learning: Insights from a Classifier Trained to Predict Contrast Enhanced Phase from Abdominal CT Imaging

Monday, Nov. 26 3:20PM - 3:30PM Room: E353C

Participants

Kenneth Philbrick, Rochester, MN (*Presenter*) Nothing to Disclose Zeynettin Akkus, PhD, Rochester, MN (*Abstract Co-Author*) Nothing to Disclose Timothy L. Kline, PhD, Rochester, MN (*Abstract Co-Author*) Nothing to Disclose Panagiotis Korfiatis, PhD, Rochester, MN (*Abstract Co-Author*) Nothing to Disclose Naoki Takahashi, MD, Rochester, MN (*Abstract Co-Author*) Nothing to Disclose Bradley J. Erickson, MD, PhD, Rochester, MN (*Abstract Co-Author*) Stockholder, OneMedNet Corporation; Stockholder, VoiceIt Technologies, LLC; Stockholder, FlowSigma;

For information about this presentation, contact:

Philbrick.Kenneth@mayo.edu

CONCLUSION

The data that we report here demonstrates that voxel level visualizations provide powerful insight into the precise anatomical regions of imaging which activate a network. Investigating the anatomical structures identified in these maps may provide key insight for systems (e.g., tumor) where well performing deep learning models exist but defining radiological signatures are unknown.

Background

The imaging features identified by deep learning classifiers are difficult to describe directly. Deep learning classifiers learn to identify images by optimizing a series of non-linear functions to activate on texture and shapes. The effect of this, is that for a given multilayer network, multiple visually different inputs can act to strongly activate a network's output. Multiple techniques (attention maps, grad-cam maps, saliency maps, guided backpropagation maps, and saliency-attention maps) have been purported to provide insight as to the specific imaging features identified by a deep learning model. We directly investigated the utility of these methods in a radiology context.

Evaluation

Typical organ enhancement patterns that follow vascular contrast agent administration are well understood. We leveraged this and developed a deep learning classifier to identify contrast enhanced renal scan phase from whole slice CT data. The classifier exceeded 90% accuracy on the test set. We utilized this classifier to explore the utility of attention maps, grad-cam maps, saliency maps, guided backpropagation maps, and saliency-attention maps to identify the imaging features our model utilized to predict scan phase.

Discussion

Saliency maps and guided back propagation maps identify voxels in input imaging which promote model prediction. For most scans these visualizations identified similar anatomical regions which directly reflect renal scan phase (renal: cortex, medulla, artery, vein, aorta, and vene cava). Attention maps, grad-cam maps, and saliency-attention maps illustrate layer activations and indirectly identified the anatomy responsible for these activations. As a whole, these maps indicated that the kidneys were responsible classification but could not clearly localize the features.

Honored Educators

Presenters or authors on this event have been recognized as RSNA Honored Educators for participating in multiple qualifying educational activities. Honored Educators are invested in furthering the profession of radiology by delivering high-quality educational content in their field of study. Learn how you can become an honored educator by visiting the website at: https://www.rsna.org/Honored-Educator-Award/ Naoki Takahashi, MD - 2012 Honored Educator

SSE14-04 Multi-Class Deep Learning for Classification of Thoracic Radiographs to Enable Accurate and Efficient Workflow

Monday, Nov. 26 3:30PM - 3:40PM Room: E353C

Participants

Jennie S. Crosby, BS, Chicago, IL (Presenter) Nothing to Disclose

Thomas J. Rhines, Chicago, IL (Abstract Co-Author) Nothing to Disclose

Feng Li, MD, PhD, Chicago, IL (Abstract Co-Author) Nothing to Disclose

Heber MacMahon, MD, Chicago, IL (*Abstract Co-Author*) Consultant, Riverain Technologies, LLC Stockholder, Hologic, Inc Royalties, UCTech Research support, Koninklijke Philips NV Consultant, General Electric Company

Maryellen L. Giger, PhD, Chicago, IL (*Abstract Co-Author*) Stockholder, Hologic, Inc; Shareholder, Quantitative Insights, Inc; Shareholder, QView Medical, Inc; Co-founder, Quantitative Insights, Inc; Royalties, Hologic, Inc; Royalties, General Electric Company; Royalties, MEDIAN Technologies; Royalties, Riverain Technologies, LLC; Royalties, Mitsubishi Corporation; Royalties, Canon Medical Systems Corporation

For information about this presentation, contact:

jenniea@uchicago.edu

PURPOSE

DICOM header information is frequently used to classify image types within the clinical radiological workflow, however, if a header contains incorrect or missing fields, it cannot be reliably used for classification. To expedite image transfer and interpretation, we trained a convolutional neural network in the task of classifying chest radiographs into 4 categories: AP/PA images, lateral images, soft tissue images and bone images (for dual energy studies).

METHOD AND MATERIALS

Our research included 5669 clinical thoracic radiographs. One set of 1911 radiographs, acquired Feb. 2006 to Feb. 2017, was manually sorted into the four categories. The manually sorted set consisted of 818 AP/PA images, 419 lateral images, 389 soft tissue images, and 285 bone images. Classifying the images using DICOM header information alone left 38% unclassified. Using TensorFlow (Google, 2015), an AlexNet architecture network was trained from scratch, in which 1242 images (65%) were used for training, 382 images (20%) for validation, and 287 images (15%) for testing. Next, the trained network was applied to an independent set of 3758 additional images yielding 68 (1.8%) images misclassified, 65% of which were soft tissue and AP/PA images.

RESULTS

The network classified Images with a high accuracy (98.19%). An important task for clinical workflow is the distinction between an AP/PA and its associated lateral view to ensure correct organization of the imaging sequence as well as appropriate image processing and CAD application. The AUC for distinguishing between AP/PA and lateral was 0.9998 ± 0.0002 . Other results included AUC= 0.9979 ± 0.0005 in distinguishing between soft tissue and AP/PA images and AUC=1 in distinguishing between soft tissue and bone images. In addition to high performance, the rapid classification of images could be applied in a hospital setting without disruption of clinical workflow. The model was trained in 5 min and classified 3758 images in 3 min. By comparison, an experienced human sorter took about 11.6 hours to classify the test set.

CONCLUSION

A trained convolutional neural network can classify different radiographic projections from the same study, most notably AP/PA vs. lateral, with high speed and accuracy.

CLINICAL RELEVANCE/APPLICATION

A trained neural network can be used in a clinical setting to quickly and accurately classify radiographs by image type to ensure correct organization of the study sequence.

SSE14-05 Deep-Learning Renal Segmentation for Fully Automated Radiation Dose Estimation in Radionuclide Therapy

Monday, Nov. 26 3:40PM - 3:50PM Room: E353C

Participants

Price Jackson, PhD, Melbourne, Australia (*Presenter*) Nothing to Disclose Nicholas Hardcastle, PHD, St Leonards, Australia (*Abstract Co-Author*) Nothing to Disclose Noel Dawe, Parkville, Australia (*Abstract Co-Author*) Nothing to Disclose Michael S. Hofman, MBBS, East Melbourne, Australia (*Abstract Co-Author*) Nothing to Disclose Tomas Kron, PHD, East Melbourne, Australia (*Abstract Co-Author*) Nothing to Disclose Rodney Hicks, MBBS, East Melbourne, Australia (*Abstract Co-Author*) Nothing to Disclose

For information about this presentation, contact:

Price.Jackson@petermac.org

PURPOSE

Convolutional neural networks have been shown to be powerful tools to assist with object detection and, like a human observer, may be trained based on a relatively small cohort of reference subjects. Rapid, accurate organ recognition in medical imaging permits a variety of new quantitative diagnostic techniques. In the case of therapy with targeted radionuclides, it may permit comprehensive radiation dose analysis in a manner that would often be prohibitively time-consuming using conventional methods.

METHOD AND MATERIALS

An automated image segmentation tool was developed based on 3-dimensional convolutional neural networks to detect right and left kidney contours on low-dose, non-contrast CT images. The model training set involved 89 manually-contoured cases and was then tested on a cohort of 24 patients receiving therapy with 177Lu-PSMA-617 for metastatic prostate cancer. Automatically generated contours were compared with those drawn by expert and assessed for similarity based on dice score, mean distance-to-agreement and total segmented volume. Further, the contours were applied to voxel dose maps computed from post-treatment quantitative SPECT imaging and renal dose estimates using automated and manual means were evaluated for statistical bias.

RESULTS

Neural network segmentation was able to identify right and left kidneys in all patients with a high degree of accuracy. Mean dice score was 0.91 ± 0.05 and 0.86 ± 0.18 for right and left kidneys, respectively, with associated mean distances-to-agreement of 2.0 ± 1.0 and 4.0 ± 7.5 millimetres. The system was integrated into the hospital image database, returning contours for a selected study in approximately 90 seconds. Poor performance was observed in 3 patients with cystic kidneys of which only few were included in the training data. Mean radiation absorbed dose based on automated contours was within 4.0% of that computed with manual segmentation.

CONCLUSION

Automated contouring using convolutional neural networks shows promise in providing quantitative assessment of functional SPECT and PET images; in this case demonstrating comparable accuracy for radiation dose interpretation in radionuclide therapy relative to a human observer.

CLINICAL RELEVANCE/APPLICATION

The primary application of this research is quantitative diagnosis and improved nuclear medicine treatment personalisation.

SSE14-06 Using Active Learning and Domain Adaptation to Train a 3D-Unet for Liver Segmentation at a High Volume Liver Transplant Center

Monday, Nov. 26 3:50PM - 4:00PM Room: E353C

Participants

Brett Marinelli, MD,MS, New York, NY (*Abstract Co-Author*) Nothing to Disclose Michael Martini, BA, New York, NY (*Abstract Co-Author*) Nothing to Disclose Martin Kang, New York, NY (*Abstract Co-Author*) Nothing to Disclose Anthony Costa, PhD, New York, NY (*Abstract Co-Author*) Nothing to Disclose Eric K. Oermann, MD, New York, NY (*Abstract Co-Author*) Nothing to Disclose Ivan Jambor, MD,PhD, Turku, Finland (*Presenter*) Speakers Bureau, Koninklijke Phillips NV

For information about this presentation, contact:

brett.marinelli@gmail.com

PURPOSE

To demonstrate the ability of a deep learning model to automatically assess liver volume utilizing publicly available data and active learning that successfully transfers to an external cohort at a high volume transplant center.

METHOD AND MATERIALS

131 CTs and liver segmentations were used from the MICCAI Grand Challenge LiTS dataset. 257 clinically acquired CTs (CACs) were collected from an institution's PACs where liver volumetry was recorded. CACs are from between 1/2014 - 12/2016 and include145 pre-transplant evaluations (56%), 159 cirrhotics (62%), 92 hepatocellular carcinoma cases (36%), and 18 prospective living liver transplant donors (7.0%). A preprocessing pipeline standardized all images to 128x128x128 voxels. As a benchmark, a 3D-UNet convolutional neural network (CNN) was trained on an 80/20 train/validation split of the LiTS dataset. Then, a 3D-UNet was fit to a training set composed of the LiTS dataset augmented by six copies of five CACs in an active learning framework. A semi-automatic GrowCut method was used for segmentation of active learning cases with Slicer3D. The CAC dataset excluding active learning scans was used as the comparative test set. Dice similarity validation scores were recorded. Successful volume measurement was defined as a difference within 200cc. Median and 1st-3rd interquartile range (IQR) were reported for both tested models. A paired student's t-test compared performance before and after implementation of active learning.

RESULTS

The benchmark model demonstrated a 0.90 Dice on the LiTS validation set, successful volume measurements in 139/257 livers and median absolute difference of 180 mL (IQR 80-311 mL) in the test set. The active learning approach demonstrated a 0.84 Dice on the LiTS validation cohort, successful volume measurements in 150/252 livers and a median absolute difference of 160 mL (IQR 67-313mL). The active learning approach yielded superior results (P=0.04).

CONCLUSION

Combining active learning and domain adaptation for liver segmentation can significantly improve model performance at capturing liver volumes utilizing publicly available datasets while deploying the model at a high volume liver transplant center.

CLINICAL RELEVANCE/APPLICATION

We describe methods that use a deep learning model for automatically assessing liver volume with publicly available data and active learning that successfully transfers to an external cohort at a high volume transplant center.



SSE18

Neuroradiology/Head and Neck (Thyroid and Parathyroid Imaging)

Monday, Nov. 26 3:00PM - 4:00PM Room: E351



AMA PRA Category 1 Credit ™: 1.00 ARRT Category A+ Credit: 1.00

Participants

Christine M. Glastonbury, MBBS, San Francisco, CA (*Moderator*) Author with royalties, Reed Elsevier Paul M. Bunch, MD, Winston-Salem, NC (*Moderator*) Nothing to Disclose

Sub-Events

SSE18-01 Thyroid Nodules on Ultrasound: Effect of Computer-Aided Diagnosis (CAD) on Radiologists' Performance with a Large Clinical Diagnostic Population

Monday, Nov. 26 3:00PM - 3:10PM Room: E351

Participants Feng Han MD PhD

Feng Han, MD,PhD, Guangzhou, China (*Presenter*) Nothing to Disclose Xiao Luo, Guangzhou, China (*Abstract Co-Author*) Nothing to Disclose Min Xu, Guangzhou, China (*Abstract Co-Author*) Nothing to Disclose An-Hua Li, MD, Guangzhou, China (*Abstract Co-Author*) Nothing to Disclose

For information about this presentation, contact:

hanfeng@sysucc.org.cn

PURPOSE

To evaluate the effect of computer-aided diagnosis (CAD) on different level radiologists' performance for discriminating malignant from benign thyroid nodules on US images.

METHOD AND MATERIALS

From January 2013 to December 2017, thyroid nodules with decisive diagnosis on the basis of pathologic results were consecutively enrolled. The observer study was conducted with four experienced radiologists and four radiology fellows, all of whom analyzed the thyroid nodules using 2017 ACR TIRADS first without and subsequently with CAD software. The performance of each observer without and with the CAD was assessed by measuring the area under the receiver operating characteristics curve (Az), sensitivity, specificity, PPV and NPV. To quantify the changes in clinical management decisions with the CAD aid, we computed for each radiologist the number of malignant and benign nodules for which the clinical management decision was changed. Concordance between observers in classing the thyroid nodules was measured in without and with CAD conditions.

RESULTS

In total, 1065 thyroid nodules from 1035 patients were included; 382 (35.87%) were benign and 683 (64.13%) were malignant. Use of the CAD resulted in an improvement of the average performance of the 8 observers, as measured by means of a statistically significant increase in Az value (0.840-0.853; p < .000), sensitivity (86.44%-87.52%; p < .000) and inter-observer agreements(0.744-0.769; p < .05) A statistically significant difference was not found in the specificity without and with the computer aid (38.74%-38.55%; p = .20). On the basis of TI-RADS assessments, it was estimated that with CAD, each observer, on average, correctly recommended 1.02% (7/683) of additional biopsies and also increased 0.37% (1.4/382) of unnecessary biopsies.

CONCLUSION

Computer-aided diagnosis can help radiologists improve their sensitivity in detection of thyroid malignancies and also increased the rate of unnecessary biopsies.

CLINICAL RELEVANCE/APPLICATION

To aid diagnosis for inexperienced radiologists and decrease workload

SSE18-02 Comparision of Morphology and Enhancement Characteristics of Ectopic and Eutopic Parathyroid Adenomas.

Monday, Nov. 26 3:10PM - 3:20PM Room: E351

Participants

Harika Tirumani, MBBS, MD, Little Rock, AR (*Presenter*) Nothing to Disclose Rohan Samant, MD, Little Rock, AR (*Abstract Co-Author*) Nothing to Disclose Raghu H. Ramakrishnaiah, MBBS, FRCR, Little Rock, AR (*Abstract Co-Author*) Nothing to Disclose Jennifer L. McCarty, MD, Houston, TX (*Abstract Co-Author*) Nothing to Disclose Stephen J. Geppert, MD, Little Rock, AR (*Abstract Co-Author*) Nothing to Disclose Rudy L. Van Hemert JR, MD, Little Rock, AR (*Abstract Co-Author*) Nothing to Disclose Edgardo J. Angtuaco, MD, Little Rock, AR (*Abstract Co-Author*) Nothing to Disclose

For information about this presentation, contact:

htirumani@uams.edu

PURPOSE

4D-CT is a novel technique for pre-surgical localization of parathyroid adenomas (PA). PA can be eutopic or ectopic. Detection of ectopic PA is crucial for surgical success especially if patient has multigland disease with both eutopic and ectopic PA. Purpose of our study is to determine the differences in morphology and enhancement characteristics between eutopic and ectopicPA which will help in increasing the confidence of radiologist for suggesting high probability.

METHOD AND MATERIALS

This is an IRB approved retrospective study of 232 patients with surgically proven PA who underwent 4D CT imaging for pre surgical localization of PA between 2014 and 2017. All 4D CT scans were performed with initial noncontrast followed by 30 sec and 90 sec postcontrast images on 64 slice MDCT scanner. Contrast washout ratios (CWR) were calculated by measuring Hounsfield units (HU) of PA on the noncontrast, 30 second post contrast early arterial exam (30A) and on the 90 second post contrast delayed exam (90D). CWR = $[100 \times (HU \text{ on } 30A - HU \text{ on } 90D)/HU \text{ on } 30A]$.

RESULTS

Out of 232 patients, 186 patients - 1 gland, 37 patients - 2 gland, 6 patients - 3 gland and 3 patients - 4 gland adenomas constituting a total of 290 radiologically diagnosed lesions. Out of these, 25 (6M, 17F) PA were in ectopic and 265 (37M, 228F) PA were eutopic. Out of 290 radiologically reported lesions, 242 lesions (21 Ectopic and 221 Eutopic) matched to the adenomas found on surgery and pathology constituting to 242 radiological-surgical-pathology matched lesions. 48 lesions were false positive, which did not correlate with the location on surgical pathology. Morphological characteristics like shape, size, heterogeneity were studied and compared between eutopic and ectopic adenomas. Enhancement characteristics of eutopic and ectopic adenomas were compared and were categorized at 10% washout intervals, for example: 1-10%, 11-20% and so on.

CONCLUSION

1. 217 out of 265 eutopic adenomas and 20 out of 25 ectopic adenomas demonstrated contrast washout ratios between 31%-80% and did not demonstrate significant difference in washout characteristics. 2. Size and shape of ectopic PA did not show significant influence on washout characteristics. 3. Measurement of contrast enhancement and washout dynamics is limited in lesions with large cystic areas.

CLINICAL RELEVANCE/APPLICATION

Detection of ectopic PA is crucial for surgical success especially in the setting of multigland disease.

SSE18-03 The Assessment of Cervical Lymph Node Metastasis from Thyroid Cancers: A Quantitative Analysis on Multiphasic CT

Monday, Nov. 26 3:20PM - 3:30PM Room: E351

Participants

Aysegul Gursoy Coruh, MD, ANKARA, Turkey (*Presenter*) Nothing to Disclose Caglar Uzun, Ankara, Turkey (*Abstract Co-Author*) Nothing to Disclose Melahat Kul, Ankara, Turkey (*Abstract Co-Author*) Nothing to Disclose Zehra Akkaya, Ankara, Turkey (*Abstract Co-Author*) Nothing to Disclose Kursat Gokcan, Ankara, Turkey (*Abstract Co-Author*) Nothing to Disclose Atilla Elhan, Ankara, Turkey (*Abstract Co-Author*) Nothing to Disclose

For information about this presentation, contact:

draysegulgursoy@gmail.com

PURPOSE

Purpose: The purpose of this study was to evaluate the diagnostic performance of multiphasic CT in the discrimination of metastatic lymph nodes of papillary (PTC) and medullary (MTC) thyroid cancers from non-metastatic ones with the use of quantitative parameters.

METHOD AND MATERIALS

Materials-methods: This study enrolled 62 pathologically proven metastatic and 62 benign lymph nodes from 23 thyroid cancer patients (19 PTC and 4 MTC). Multiphasic CT was utilized by using non-enhanced, arterial (25-second delay) and venous (80second delay) phases. Two readers independently measured mean tissue attenuation values (MAV) of metastatic and benign lymph nodes. The relative wash in and wash out percentages were calculated and were defined as: arterial MAV-nonenhanced MAV/nonenhanced MAV, venous MAV- arterial MAV/arterial MAVx100; respectively.

RESULTS

Results: The difference in MAV between metastatic and benign lymph nodes for the PTC were maximum in the arterial phase (p<0.001). The arterial phase showed the highest diagnostic performance compared with other phases for the PTC (AUC±SE:0.98±0.01; %95 CI: 0.96-1). A cutoff value of 97.5 HU for the arterial phase had a sensitivity of 96.3% (%95 CI: 87.5-99%) and specificity of 94.4% (%95 CI: 84.8-98.1%), positive predictive value (PPV) of 97.2% and negative predictive value (NPV) of 92.6% in the discrimination of metastatic lymph nodes from PTC (p<0.001). Metastatic lymph nodes from MTC showed progressive enhancement compared to benign lymph nodes and the venous phase showed the highest diagnostic performance in discrimination between metastatic and benign lymph nodes (p<0.05). A MAV cutoff of 112.5 HU in the venous phase predicted metastatic lymph nodes from MTC with a sensitivity of 87.5%, specificity of 75%, (p=0.015).

CONCLUSION

The detection of metastatic lymph nodes from thyroid cancers can be achievable with the use of quantitative parameters in

multiphasic CT. Metastatic lymph nodes from PTC show strong uptake of contrast in the arterial phase and wash out of contrast in the venous phase. Whereas, metastatic lymph nodes from MTC show progressive enhancement in the venous phase.

CLINICAL RELEVANCE/APPLICATION

Determination of metastatic lymph nodes is an important problem in thyroid cancers. Complete resection of the primary disease and metastases is the one of the important factor in the survival.

SSE18-04 Retrospective Analysis of Thyroid Ultrasound Recommendations Using Thyroid Imaging Reporting and Data System (TI-RADS) Scoring

Monday, Nov. 26 3:30PM - 3:40PM Room: E351

Awards

Student Travel Stipend Award

Participants

Charles E. Runyan III, MD, Phoenix, AZ (*Presenter*) Nothing to Disclose Alexia Tatem, BS, Cave Creek, AZ (*Abstract Co-Author*) Nothing to Disclose Samantha Matz, DO, Phoenix, AZ (*Abstract Co-Author*) Nothing to Disclose Albert Roh, MD, Phoenix, AZ (*Abstract Co-Author*) Nothing to Disclose Mary J. Connell, MD, Phoenix, AZ (*Abstract Co-Author*) Nothing to Disclose

PURPOSE

Breast Imaging, Reporting, and Data System (BI-RADS) has been used to standardize mammogram reports and recommendations; Thyroid Imaging, Reporting, and Data System (TI-RADS) seeks to do the same. We compared our institution's prior biopsy recommendations on ultrasound reports to what the recommendations would have been using TI-RADS.

METHOD AND MATERIALS

Our study was a retrospective review of 449 thyroid nodules which were assessed by ultrasound and subsequently biopsied. We collected the description of the lesion and the original recommendations from the radiology report. Pathology results were collected. Three radiologists then performed blinded and independent evaluations of each exam; a TI-RADS score was assigned to each thyroid nodule. Recommendations based on TI-RADS were compared with prior recommendations and biopsy results.

RESULTS

449 thyroid nodules were identified by review of biopsies. Had we implemented TI-RADS, we would have recommended 102 fewer biopsies (23%). No nodules for which a biopsy was initially recommended but not recommended by TI-RADS criteria demonstrated a clinically significant malignancy at biopsy. Incidental foci of papillary carcinoma found within benign follicular nodules less than 0.5cm were considered not clinically relevant, as studies have shown that 5-30% of autopsies have found occult papillary carcinoma in patients who died of unrelated causes. Our positive predictive value before implementing TI-RADS was 8.2%. Utilizing TI-RADS, our positive predictive value is 10.5%, a ~25% difference.

CONCLUSION

There was a decrease in the number of thyroid biopsies that would have been recommended when using TI-RADS. We demonstrated a 23% decrease in the number of recommended biopsies without decreasing our ability to identify clinically significant malignancies. Findings suggest that implementing TI-RADS will decrease the number of negative biopsies performed, which will decrease patient risk and worry as well as save the health system from the cost of these additional procedures. Our study is limited by only selecting patients who underwent biopsy. Due to our inclusion criteria, we did not assess for any missed malignancies in nodules presumed to be benign on prior ultrasound reports.

CLINICAL RELEVANCE/APPLICATION

Use of TI-RADS for thyroid nodule biopsy recommendations can greatly reduce the number of biopsies recommended without missing a clinically significant malignancy.

SSE18-05 Machine Learning Optimization of 4D-CT and 99m-Technetium Sestamibi for Preoperative Localization in Patients with Primary Hyperparathyroidism

Monday, Nov. 26 3:40PM - 3:50PM Room: E351

Participants

Laurent Dercle, MD, New York, NY (*Presenter*) Nothing to Disclose Yu-Kwang Donovan Tay, MD, New York, NY (*Abstract Co-Author*) Nothing to Disclose Gaia Tabacco, MD, New York, NY (*Abstract Co-Author*) Nothing to Disclose Prachi Dubey, MD, NY, NY (*Abstract Co-Author*) Nothing to Disclose Gul Moonis, MD, New York, NY (*Abstract Co-Author*) Nothing to Disclose Randy Yeh, MD, New York, NY (*Abstract Co-Author*) Nothing to Disclose

For information about this presentation, contact:

ry2210@cumc.columbia.edu

PURPOSE

The purpose of this study is to apply machine learning to 4D-CT and 99mTechnetium sestamibi (MIBI) for preoperative localization of hyperfunctioning parathyroid glands in patients with primary hyperparathyroidism (PHPT). Our aim is to develop a model and decision tree algorithm to maximize diagnostic accuracy.

METHOD AND MATERIALS

A retrospective study of 400 patients who underwent combined imaging protocol of 4D-CT and MIBI SPECT/CT and subsequent parathyroidectomy was performed. Four parathyroid glands were assumed for each patient (n=1600). Reference standard was surgical pathology. Both 4D-CT and MIBI were interpreted by two nuclear radiologists. Using machine learning, a random-forest tree

algorithm using 3-fold cross validation was trained and validated to predict the probability of a parathyroid gland as positive hyperfunctioning gland on pathology (adenoma or hyperplasia). A total of 17 variables were used, including 4 clinical, 10 biological, and 3 imaging variables. Imaging variables included 4D-CT, MIBI, and combined 4D-CT+MIBI.

RESULTS

Of 1600 parathyroid glands, 521 were abnormal on surgical pathology. The model output was probability of a gland as positive on pathology. The final model selected variables of combined 4D-CT+MIBI and preoperative serum PTH and Calcium crossproduct (PTH*Ca). The AUC of the model was 0.99 (95 CI: .984-.996) and outperformed AUC of radiologist interpretation of 4D-CT and MIBI, alone and in combination. When both 4D-CT and MIBI are positive, the probability of a true positive is 97% (n=305) and when either test is positive, the probability is 75% (n=164). When both tests are negative, the gland is a true negative in 96% of cases if PTH*Ca is > 1232 (n=333), 92% of cases if PTH*Ca>675 and <1232 (n=563) and 81% of cases if PTH*Ca<675 (n=297).

CONCLUSION

Diagnostic accuracy of preoperative 4D-CT and MIBI is improved with machine learning compared with radiologist interpretation. A decision tree algorithm simplified into three variables selected by machine learning can provide probability of correct classification of each parathyroid gland as normal or abnormal and guide the surgeon to pursue minimally invasive parathyroidectomy or 4-gland exploration.

CLINICAL RELEVANCE/APPLICATION

Machine learning-derived model and decision tree algorithm can improve diagnostic accuracy of preoperative localization of 4D-CT and 99mTechnetium Sestamibi for patients with primary hyperparathyroidism.

SSE18-06 Utility of Ultrasound Elastography (Acoustic Radiation Force Impulse Imaging) in the Diagnosis of Parathyroid Adenoma in Correlation with Sestamibi Scan

Monday, Nov. 26 3:50PM - 4:00PM Room: E351

Participants

Sooraj Prasannakumar, MBBS, Chennai, India (*Presenter*) Nothing to Disclose Sudhakar H. K., DMRD, MD, Chennai, India (*Abstract Co-Author*) Nothing to Disclose Meera K., DMRD, MD, Chennai, India (*Abstract Co-Author*) Nothing to Disclose Jayasudha Sambedu, MBBS,DMRD, Chennai, India (*Abstract Co-Author*) Nothing to Disclose Sandhya Gh JR, MBBS, Chennai, India (*Abstract Co-Author*) Nothing to Disclose Ajai R. Kattoju, MBBS, Chennai, India (*Abstract Co-Author*) Nothing to Disclose

For information about this presentation, contact:

spsoorajp@gmail.com

PURPOSE

In this study we consider applying the technique of ARFI with Virtual Touch Quantification (a type of quantitative elastography) in diagnosis of parathyroid adenomas(most common cause of primary hyperparathyroidism), to prospectively assess whether this technique can increase the diagnostic value of ultrasound approaching nearer to or more than the sensitivity and specificity of sestamibi scan.

METHOD AND MATERIALS

This was a prospective observational study conducted in the department of radiodiagnosis of our institution from October 2016 to December 2017. The study population consisted of 36 patients(n=36) with clinical suspicion of primary hyperparathyroidism with positive Sestamibi scan for parathyroid adenoma irrespective of ultrasound results(done prior to the Sestamibi scan). The parathyroid adenoma was first identified by grey scale imaging features and then a region of interest for elastography was placed within the lesion and the stiffness of the lesion using ARFI-VTQ values were obtained. Five successful measurements were taken for ARFI -VTQ(measured in meters per second) and the median value was calculated.

RESULTS

Ultrasound elastography was performed on all the 36 cases of adenomas and the median ARFI-VTQ values were calculated. The mean ARFI values of the corresponding adjacent thyroid tissue were also calculated. The mean ARFI-VTQ values of adenomas was $(1.72\pm0.45m/s)$. The mean ARFI-VTQ values of normal thyroid tissue was $(2.66\pm0.38m/s)$. There was a statistically significant difference between the two variables with [p <0.0001]. The study shows a consistently low elastography values for adenomas than adjacent thyroid tissue and other lesions which mimic adenomas like lymph nodes. Thus ultrasound along with ARFI-VTQ values has high accuracy in diagnosing adenomas.

CONCLUSION

Ultrasound elastography(withARFI-VTQ) is an excellent tool which enhances the diagnostic value of ultrasound in parathyroid adenomas when used along with B-mode ultrasound and doppler.

CLINICAL RELEVANCE/APPLICATION

In clinically diagnosed patients of hyperparathyroidism ultrasound ARFI-VTQ can be applied as a solitary imaging modality(in place of sestamibi), since it is an excellent diagnostic imaging tool in the diagnosis of normally located parathyroid adenomas with high accuracy.



SSE23

Physics (Breast X-Ray Imaging)

Monday, Nov. 26 3:00PM - 4:00PM Room: S502AB



AMA PRA Category 1 Credit ™: 1.00 ARRT Category A+ Credit: 1.00

FDA Discussions may include off-label uses.

Participants

Srinivasan Vedantham, PhD, Tucson, AZ (*Moderator*) Research collaboration, Koning Corporation Hilde Bosmans, PhD, Leuven, Belgium (*Moderator*) Co-founder, Qaelum NV Research Grant, Siemens AG

Sub-Events

SSE23-01 Radiation Dose Reduction in Digital Breast Tomosynthesis (DBT) by Means of Neural Network Convolution (NNC) Deep Learning

Monday, Nov. 26 3:00PM - 3:10PM Room: S502AB

Participants

Junchi Liu, MS, Chicago, IL (Abstract Submitter) Nothing to Disclose

Amin Zarshenas, MSc, Chicago, IL (Abstract Co-Author) Nothing to Disclose

Syed Ammar Qadir, Chicago, IL (Abstract Co-Author) Nothing to Disclose

Limin Yang, MD, PhD, Iowa City, IA (Abstract Co-Author) Nothing to Disclose

Laurie L. Fajardo, MD, MBA, Park City, UT (*Abstract Co-Author*) Consultant, Hologic, Inc; Consultant, Siemens AG; Consultant, FUJIFILM Holdings Corporation;

Kenji Suzuki, PhD, Chicago, IL (*Presenter*) Royalties, General Electric Company; Royalties, Hologic, Inc; Royalties, MEDIAN Technologies; Royalties, Riverain Technologies, LLC; Royalties, Canon Medical Systems Corporation; Royalties, Mitsubishi Corporation; Royalties, AlgoMedica, Inc

For information about this presentation, contact:

jliu118@hawk.iit.edu

PURPOSE

To reduce cumulative radiation exposure and lifetime risks for radiation-induced cancer from breast cancer screening, we developed novel NNC deep learning for radiation dose reduction in DBT.

METHOD AND MATERIALS

Our original NNC deep learning employed patched-based neural network regression in a convolutional manner to convert lower-dose (LD) to higher-dose (HD) tomosynthesis images. We trained NNC with quarter-dose (25% of the standard dose: 12mAs at 32kVp) raw-projection images and corresponding "teaching" higher-dose (HD) images (200% of the standard dose: 99mAs at 32kVp) of a breast cadaver phantom acquired with a DBT system (Selenia Dimensions, Hologic). Once trained, NNC no longer requires HD images. It converts new LD images to images that look like HD images; thus the term "virtual" HD (VHD) images. We reconstructed tomosynthesis slices on a research DBT system. To determine a dose reduction rate, we acquired 4 studies of another test phantom at 4 different doses (1.35, 2.7, 4.04, and 5.39mGy entrance dose). Structural SIMilarity(SSIM) index was used to evaluate the image quality. For further testing, we collected half-dose (50% of the standard dose: 32±14 mAs at 33±5 kVp) and full-dose (100% of the standard dose: 68±23mAs at 33±5kvp) images of 51 clinical cases with the DBT system at Univ. of Iowa Hospitals & Clinics. We evaluated resulting images in a blinded observer study with 35 breast radiologists to rate and distinguish blinded VHD and real full-dose DBT images.

RESULTS

NNC converted quarter-dose images (1.35mGy; SSIM: 0.88) of the testing cadaver phantom to VHD images with image quality (SSIM:0.97) equivalent to 119% dose images (6.41mGy), achieving 79% dose reduction. In our blinded observer study, 21(60%) of 35 breast radiologists either preferred VHD images over real full-dose images or could not distinguish between the two. The difference in image quality between the two was not statistically significant (P=0.37). The time required to process each study was 0.48 sec. on a GPU (GTX Titan Z, Nvidia).

CONCLUSION

Blinded observer study with 35 radiologists demonstrated that VHD images converted by our deep-learning technology were equivalent to full-dose DBT images. Our cadaver phantom experiment demonstrated 79% dose reduction.

CLINICAL RELEVANCE/APPLICATION

Substantial radiation dose reduction would benefit patients by reducing the lifetime risk of radiation-induced cancer from DBT screening.

Participants

Martin J. Yaffe, PhD, Toronto, ON (*Presenter*) Research collaboration, General Electric Company; Shareholder, Volpara Health Technologies Limited; Co-founder, Mammographic Physics Inc; Research Consultant, BHR Pharma LLC

Etta D. Pisano, MD, Charleston, SC (*Abstract Co-Author*) Researcher, Freenome Holdings Inc; Researcher, Real Imaging Ltd; Researcher, Therapixel; Researcher, DeepHealth, Inc; Researcher, ToDos

Aili K. Maki, BEng, Toronto, ON (Abstract Co-Author) Research collaboration, General Electric Company; Contractor, Mammographic Physics, Inc

James G. Mainprize, PhD, Toronto, ON (*Abstract Co-Author*) Institutional research agreement, General Electric Company Gordon Mawdsley, BS, Toronto, ON (*Abstract Co-Author*) Director, Medical Physics Incorporated Research collaboration, General Electric Company

Sam Shen, Toronto, ON (Abstract Co-Author) Employee, Mammographic Physics Inc; Research collaboration, General Electric Company

Ruth C. Carlos, MD, MS, Ann Arbor, MI (Abstract Co-Author) Nothing to Disclose

Kathy D. Miller, MD, Indianapolis, IN (Abstract Co-Author) Nothing to Disclose

Christopher E. Comstock, MD, New York, NY (Abstract Co-Author) Nothing to Disclose

For information about this presentation, contact:

martin.yaffe@sri.utoronto.ca

PURPOSE

To describe and provide preliminary results from a remote-monitoring QC program developed to provide assessment of quality and rapid feedback in a screening trial. The program is being used in the randomized TMIST trial of screening with breast tomosynthesis versus digital mammography. TMIST is expected to include 125 sites in the US and Canada and will recruit 164,986 women who will be imaged up to 5 times over 4 years.

METHOD AND MATERIALS

The QC program is based on imaging of phantoms by the technologist at each site and digital transmission to a central analysis server. Phantoms assess signal and noise properties, artifacts, spatial resolution and geometric fidelity of the imaging system. The analysis is performed automatically with results made available to technologists on a password protected web site. Technical information from the DICOM header, stripped of personal identifiers, from every clinical image is available for analysis of doses, exposure factors and compression parameters..

RESULTS

As of April 2018, initial QC data from 87 units at the first 29 TMIST sites were available, including de-identified screening mammogram header data from 60 units at the first 25 sites. The most frequent technical problems were due to electronic interference, dustlike artifacts and the compression force being reported in the header as '0. Problems were also noted due to duplication of image submission from the same individual as separate cases and noncompliance with the QC protocol. In addition, it was noted that digital detectors were occasionally replaced without technical documentation. This was accompanied by changes in signal-to-noise performance. Based on 881 examinations, the mean dose (CC + MLO) was 4.2 mGy for 2D digital mammograms and 8.2 mGy for tomosynthesis. The presentation will report on results up to November, 2018.

CONCLUSION

Use of a centralized remote data collection QC system reduces technologist labor at the site and reduces subjectivity in testing. This approach enables consistent analysis and rapid reporting of QC results.

CLINICAL RELEVANCE/APPLICATION

Sensitivity and specificity of breast cancer detection depend critically on the technical image quality. The credibility of the results from the TMIST trial requires that the image quality of both modalities is verified. In addition, experience from this trial will provide data to help define the essential elements of the standard QC program for tomosynthesis.

Honored Educators

Presenters or authors on this event have been recognized as RSNA Honored Educators for participating in multiple qualifying educational activities. Honored Educators are invested in furthering the profession of radiology by delivering high-quality educational content in their field of study. Learn how you can become an honored educator by visiting the website at: https://www.rsna.org/Honored-Educator-Award/ Ruth C. Carlos, MD, MS - 2015 Honored EducatorRuth C. Carlos, MD, MS - 2018 Honored Educator

SSE23-03 Visual Grading Characteristics Analysis of Propagation-Based X-Ray Phase Contrast Mammography

Monday, Nov. 26 3:20PM - 3:30PM Room: S502AB

Participants

Seyedamir Tavakoli Taba, Sydney, Australia (*Abstract Co-Author*) Nothing to Disclose Sarah J. Lewis, PhD,MEd, Sydney, Australia (*Abstract Co-Author*) Nothing to Disclose Patrycja Baran, Parkville, Australia (*Abstract Co-Author*) Nothing to Disclose Matthew Dimmock, Clayton, Australia (*Abstract Co-Author*) Nothing to Disclose Mikkaela McCormack, Heidelberg, Australia (*Abstract Co-Author*) Nothing to Disclose Sheridan Mayo, Clayton, Australia (*Abstract Co-Author*) Nothing to Disclose Sheridan Mayo, Clayton, Australia (*Abstract Co-Author*) Nothing to Disclose Yakov Nesterets, Clayton, Australia (*Abstract Co-Author*) Nothing to Disclose Christopher Hall, Clayton, Australia (*Abstract Co-Author*) Nothing to Disclose Jane Fox, Clayton, Australia (*Abstract Co-Author*) Nothing to Disclose Zdenka Prodanovic, Clayton, Australia (*Abstract Co-Author*) Nothing to Disclose Darren Lockie, FRANZCR, Southbank, Australia (*Abstract Co-Author*) Nothing to Disclose Daniel Hausermann, Clayton, Australia (*Abstract Co-Author*) Nothing to Disclose Giuliana Tromba, PhD, Trieste, Italy (*Abstract Co-Author*) Nothing to Disclose

For information about this presentation, contact:

amir.tavakoli@sydney.edu.au

PURPOSE

While all current x-ray based breast imaging modalities rely on minimal differences in soft tissue x-ray attenuation (absorption contrast), phase-contrast imaging has the capacity to also visualise variations in x-ray refraction (phase contrast). For x-ray energies typically used in breast imaging, the phase contrast can be substantially larger than the absorption contrast, presenting an opportunity to improve soft tissue visualisation especially in mammographically dense breasts. The goal of this study was to evaluate the radiological quality of images produced by the x-ray propagation-based phase-contrast computed tomography (PB-CT) technique at two different x-ray energies in comparison to absorption-based CT images collected at the same radiation dose (4 mGy).

METHOD AND MATERIALS

Twenty-seven synchrotron-based CT images of a full-size breast mastectomy specimen were reconstructed. Nine images were absorption-based CT at 32 KeV, nine images were PB-CT at 32 KeV and nine were PB-CT at 38 KeV. A group of breast specialist radiologists and medical imaging experts compared the radiological quality of the three sets of images based on various image quality criteria. Visual grading characteristics (VGC) analysis was conducted and VGC curves were obtained. The area under the VGC curve (0<=AUCVGC<=1) was calculated as the measure of the difference in image quality between two compared sets of images.

RESULTS

The results show that the radiological quality ratings of PB-CT 32 KeV images were significantly higher than absorption-based CT images (AUCVGC=0.879, p<=.001) and PB-CT 38 KeV images (AUCVGC=0.795, p<=.001). The image quality ratings were not significantly different between PB-CT 38 KeV images and absorption-based CT images (AUCVGC=0.567, p=.076).

CONCLUSION

Phase-contrast PB-CT mammography can be used to produce images with substantially higher radiological quality compared to conventional absorption-based images, but this advantage appears to be dependent on beam energy. The results from this study should provide a strong basis for future experimental and clinical protocols for further optimisation of this novel and promising approach to breast imaging.

CLINICAL RELEVANCE/APPLICATION

PB-CT of the breast is expected to deliver improved image quality compared to current x-ray modalities and become a viable method for early diagnosis of breast cancer in the future.

SSE23-04 Evaluation of American College of Radiology (ACR) Mammography Accreditation Phantom Image Quality of a Grid-Less and Software-Based Scatter Correction Technology

Monday, Nov. 26 3:30PM - 3:40PM Room: S502AB

Participants

Anzi Zhao, MS, Cleveland, OH (*Presenter*) Nothing to Disclose Katie Hulme, MS, Cleveland, OH (*Abstract Co-Author*) Nothing to Disclose

PURPOSE

To evaluate the quality of ACR mammography accreditation phantom images acquired with a grid-less and software-based scatter correction technology - Progressive Reconstruction Intelligently Minimizing Exposure (PRIME).

METHOD AND MATERIALS

3 Siemens Mammomat Inspiration units with PRIME were utilized in this study. The same ACR phantom was imaged on all units. 20 2D phantom images were acquired on each unit using a phototimed technique (W/Rh, 28kVp, AEC segmentation off, dose level 'normal', exam tag 'QC RAW'), of which 10 were acquired with grid in position and 10 were acquired with PRIME. Mode of acquisition was varied in a random order. 10 additional PRIME images were acquired on one unit with a resolution test pattern to assess spatial resolution. Contrast-to-noise ratio (CNR), signal-to-noise ratio (SNR), and standard deviation (SD) of phantom images were evaluated using the method in Siemens quality control manual. Incident air kerma and average glandular dose (AGD) were measured and calculated for each exposure. A total of 60 phantom images were scored by 4 qualified medical physicists and 2 experienced mammography technologists on a diagnostic workstation in clinical viewing conditions, and using ACR phantom evaluation guidelines with demographics hidden.

RESULTS

With PRIME, all images failed CNR criteria (>=2) with significantly lower CNR and higher SD than grid-based images by as much as 43% and 23%, respectively; SNR was reduced by 2-4%; spatial resolution was unaffected at 7 mm/lp; AGD was reduced by up to 16%. Visual scoring by 6 viewers resulted in no significant difference between the two types of images. Minor degradation on average score of masses on PRIME images compared to grid-based images (4.1 vs 4.2) was noted on one unit. All viewers agreed on the notable difference in image appearance and noise texture when PRIME was employed.

CONCLUSION

PRIME didn't penalize ACR phantom scoring, although there was a significant degradation of CNR on PRIME images because of the increased noise. The clinical implications of differences in noise texture warrant further investigation. Although PRIME offers moderate dose savings, clinicians should still be aware of potential effects on image appearance.

CLINICAL RELEVANCE/APPLICATION

DDIME technology corrects coattor radiation and anables and loss full field digital mammagraphy at lower nations average alandular

PRIME LECTIONOGY COTTECTS SCALLET TAUALION and enables grid-less full new digital manifoldiaphy at lower patient average glandular dose, with comparable image quality.

SSE23-05 Mammographic Compression Variability Increased after Removing Real-Time Pressure Indicator

Monday, Nov. 26 3:40PM - 3:50PM Room: S502AB

Participants

Monique G. van Lier, MSc, Amsterdam, Netherlands (*Presenter*) Employee, SigmaScreening BV Jerry E. De Groot, PhD, Amsterdam, Netherlands (*Abstract Co-Author*) Employee, SigmaScreening BV Woutjan Branderhorst, PhD, Amsterdam, Netherlands (*Abstract Co-Author*) Employee, SigmaScreening BV Laura J. Schijf, MD, Amsterdam, Netherlands (*Abstract Co-Author*) Nothing to Disclose Cornelis A. Grimbergen, PhD, Amsterdam, Netherlands (*Abstract Co-Author*) Founder, SigmaScreening BV Employee, SigmaScreening BV Board Member, SigmaScreening BV Patent holder, SigmaScreening BV Gerard J. den Heeten, MD,PhD, Nijmegen, Netherlands (*Abstract Co-Author*) Founder, SigmaScreening BV; Scientific Advisor, SigmaScreening BV; Patent Holder, SigmaScreening BV; Stock options, Volpara Health Technologies Limited; Medical Advisory Board, Volpara Health Technologies Limited

For information about this presentation, contact:

m.g.vanlier@amc.nl

CONCLUSION

When replacing a paddle with a pressure indicator, in a group of technicians familiar with the indicator, by a conventional paddle, the variability increased significantly leading to more unfavorable over- and under-compression.

Background

A certain level of breast flattening in mammography is needed to obtain a high quality image. Generally accepted and quantifiable standards do not exists. Recent studies show that the level of compression pressure at exposure influences screening performance. Attempts are made to standardize the compression procedure by introducing pressure-based compression using a paddle equipped with a real-time pressure indicator. We aimed to study the impact on compression practice when replacing the pressure-based paddle with a conventional paddle without pressure indication in group experienced technicians.

Evaluation

Mammographic compression pressure was retrospectively obtained from mammographic images (VolparaAnalytics) and evaluated in two datasets from the same radiology department with the same technician team. The first dataset (4 years, n=11.561 compressions) was collected when using a compression paddle equipped with a real-time pressure indicator aiming for a 10kPa (75mmHg) compression pressure. The second dataset (3 months, n=1331 compressions) was collected 4 months after the mammography system with pressure indicator was replaced by a system without pressure indicator. The average compression pressure and variance significantly (P<0.001) increased from 11.23 \pm 0.04 kPa to 11.60 \pm 0.14 kPa (mean \pm SEM) after removal of the pressure indicator. The proportion of compressions in the pressure range 5-15 kPa decreased from 87.4% to 77.9%. The proportion of high pressures (>15kPa) almost doubled (11.0% to 18.8%) and low pressures (<5kPa) more than doubled (1.6% to 3.3%).

Discussion

When removing the pressure indicator, the initially low variability is increasing rapidly, indicating that an indicator is needed to remain high compression reproducibility. An increase in over- and under-compression can ultimately lead to decreased mammographic performance.

SSE23-06 Development of Low Dose Digital Mammography Platform by Image Reconstruction Using Deep Learning Algorithm: A Preliminary Study

Monday, Nov. 26 3:50PM - 4:00PM Room: S502AB

Participants

Su Min Ha, MD, Seoul, Korea, Republic Of (*Presenter*) Nothing to Disclose Eunhee Kang, Daejon, Korea, Republic Of (*Abstract Co-Author*) Nothing to Disclose Jong Chul Ye, PhD, Daejon, Korea, Republic Of (*Abstract Co-Author*) Nothing to Disclose Hak Hee Kim, MD, Seoul, Korea, Republic Of (*Abstract Co-Author*) Nothing to Disclose

PURPOSE

To investigate whether low dose mammography can be reconstructed to standard dose mammography using the new deep learning algorithm.

METHOD AND MATERIALS

14 specimens from 14 patients who underwent total mastectomy for primary breast cancer were included. Specimen mammograms were obtained with standard routine dose and reduced sequential doses; 80% of routine dose, 60%, 40%, 20% and 10%. The proposed de-noising method is designed based on semi-supervised learning with cycle consistency loss. Most of the mammography has Automatic Exposure Control (AEC) system which chooses an appropriate current X-ray source. The routine dose and 20% dose level images were selected as training dataset. Since the noise levels between two images are different and unavoidable slight mismatch due to potential deformation between multiple acquisitions, we developed the semi-supervised learning using cyclic consistency. We trained two generators (network G and F) and two discriminators (network Dx and Dy). Since we had 14 datasets, we performed cross-validation. Last, image quality of reconstructed low dose image was compared with the standard full dose image and was qualitatively rates as follows; 1= poor, 2= fair, 3= equal, 4=better.

RESULTS

As more radiation dose was decreased, noise was increased and contrast resolution was decreased accordingly. However, in the reconstructed images, noise was decreased and contrast resolution was rather improved. Overall, when we evaluated the lesions according to Breast imaging-reporting and data system lexicon, and with consideration of underlying breast parenchyma density,

the reduced dose of 20% cut-off of standard full dose showed no significant difference in image quality compared with standard dose mammography.

CONCLUSION

The image quality of reconstructed low dose mammography using the new deep learning algorithm is comparable with standard dose mammography until dose reduction cut-off 20% of standard full dose. Therefore, the radiation dose of mammography could be considerably reduced using this deep learning algorithm.

CLINICAL RELEVANCE/APPLICATION

Image reconstruction using the new deep learning algorithm is effective in dose reduction of mammography, especially in young women with high risk who are routinely examined with mammography for screening.



SPSI24

Special Interest Session: Demystifying Machine Learning and Artificial Intelligence for the Radiologist

Monday, Nov. 26 4:30PM - 6:00PM Room: E451A



AMA PRA Category 1 Credits ™: 1.50 ARRT Category A+ Credit: 1.75

Participants

Safwan Halabi, MD, Stanford, CA (*Moderator*) Nothing to Disclose Ruth C. Carlos, MD, MS, Ann Arbor, MI (*Moderator*) Nothing to Disclose

LEARNING OBJECTIVES

1) Practical introduction to machine learning and artificial intelligence including allaying fears of joblessness among radiologists while providing potential scenarios of what being a radiologist in the era of artificial intelligence might entail. 2) Describe cutting-edge examples of research and clinical applications of AI and machine learning in imaging, using the High Impact Clinical Trials (HICT) format of research presentation followed by a topic discussant. 3) Discuss the future applications of machine learning and artificial intelligence.

ABSTRACT

The application of machine learning and artificial intelligence in medicine, and especially radiology, has caught the attention of physicians, researchers and the global tech industry. While some radiologists worry their jobs will be taken over by software, others are optimistic that this technology will make image interpretation faster, more accurate and pertinent. Coupling the increasing amounts of data radiologists have to interpret with decreasing reimbursement, artificial intelligence software has the potential to reinvent the entire radiology practice from exam ordering to diagnosis. What distinguishes this special interest session is the combination that addresses the current concerns of radiologists, presents leading edge research and provides insight into the impact of current technology on future practice.

Sub-Events

SPSI24A The Lowdown: Introduction to Machine Learning and Artificial Intelligence (Or Machines Will Not Take Our Jobs)

Participants

Bradley J. Erickson, MD, PhD, Rochester, MN (*Presenter*) Stockholder, OneMedNet Corporation; Stockholder, VoiceIt Technologies, LLC; Stockholder, FlowSigma;

LEARNING OBJECTIVES

View learning objectives under main course title.

SPSI24B The Reality: Current Application of Machine Learning and Artificial Intelligence in Clinical Radiology and Research

Participants

Jayashree Kalpathy-Cramer, MS, PhD, Charlestown, MA (*Presenter*) Consultant, Infotech Software Solution Kristen W. Yeom, MD, Palo Alto, CA (*Presenter*) Nothing to Disclose Bhavik N. Patel, MD, MBA, Stanford, CA (*Presenter*) Nothing to Disclose

For information about this presentation, contact:

kalpathy@nmr.mgh.harvard.edu

LEARNING OBJECTIVES

View learning objectives under main course title.

SPSI24C The Fantasy: Future Applications of Machine Learning and Artificial Intelligence in Radiology and Radiogenomics

Participants

Bradley J. Erickson, MD, PhD, Rochester, MN (*Presenter*) Stockholder, OneMedNet Corporation; Stockholder, VoiceIt Technologies, LLC; Stockholder, FlowSigma;

For information about this presentation, contact:

bje@mayo.edu

LEARNING OBJECTIVES

View learning objectives under main course title.

SPSI24D Q&A



AI001-TU

RSNA Deep Learning Classroom: Presented by NVIDIA Deep Learning Institute

Tuesday, Nov. 27 8:30AM - 4:00PM Room: AI Community, Learning Center

Program Information

Located in the Learning Center (Hall D), this classroom presented by NVIDIA will give meeting attendees a hands-on opportunity to engage with deep learning tools, write algorithms and improve their understanding of deep learning technology. "Attendees must bring a laptop capable of running the most recent version of Chrome."

Sub-Events

AI001-TUA 3D Segmentation of Brain MR

Tuesday, Nov. 27 8:30AM - 10:00AM Room: AI Community, Learning Center

Title and Abstract

3D Segmentation of Brain MR This session will focus on the use of deep learning methods for segmentation, with particular emphasis on 3D techniques (V-Nets) applied to the challenge of MR brain segmentation. While focused on this particular problem, the concepts should generalize to other organs and image types.

AI001-TUB Introduction to Deep Learning

Tuesday, Nov. 27 10:30AM - 12:00PM Room: AI Community, Learning Center

Title and Abstract

Introduction to Deep Learning This class will focus on basic concepts of convolutional neural networks (CNNs), and walk the attendee through a working example. A popular training example is the MNIST data set which consists of hand-written digits. This course will use a data set we created, that we call 'MedNIST' and consists of 1000 images each from 5 different categories: Chest X-ray, hand X-ray, Head CT, Chest CT, Abdomen CT, and Breast MRI. The task is to identify the image type. This will be used to train attendees on the basic principles and some pitfalls in training a CNN. The attendee will have the best experience if they are familiar with Python programming.

AI001-TUC Data Science: Normalization, Annotation, Validation

Tuesday, Nov. 27 12:30PM - 2:00PM Room: AI Community, Learning Center

Title and Abstract

Data Science: Normalization, Annotation, Validation This session will focus on preparation of the image and non-image data in order to obtain the best results from your deep learning system. It will include a discussion of different options for representing the data, how to normalize the data, particularly image data, the various options for image annotation and the benefits of each option. We will also discuss the 'after training' aspects of deep learning including validation and testing to ensure that the results are robust and reliable.

AI001-TUD Multi-modal Classification

Tuesday, Nov. 27 2:30PM - 4:00PM Room: AI Community, Learning Center

Title and Abstract

Multi-modal Classification This session will focus on multimodal classification. Classification is the recognition of an image or some portion of an image being of one type or another, such as 'tumor' or 'infection'. Multimodal classification means that there are more than 2 classes. While this is logically simple to understand, it presents some unique challenges that will be discussed.



MSQI31

Quality Improvement Symposium: Value in Imaging 1: Value in Radiology

Tuesday, Nov. 27 8:30AM - 10:00AM Room: S402AB



AMA PRA Category 1 Credits ™: 1.50 ARRT Category A+ Credit: 1.75

Participants

Jonathan B. Kruskal, MD, PhD, Boston, MA (Moderator) Author, Wolters Kluwer nv

LEARNING OBJECTIVES

To define the concept and definition of value relative to clinical radiology practice.
 To describe how value can be measured.
 To define strategies for improving delivery of value.

Additional Information

RSNA will award Quality Essentials Certificates of Completion to RSNA 2018 attendees who successfully participate. Participants who achieve a score of 80% or higher on the SAM test questions will be eligible to receive the certificates.

Sub-Events

MSQI31A What is Value in Radiology?

Participants Jonathan B. Kruskal, MD, PhD, Boston, MA (*Presenter*) Author, Wolters Kluwer nv

For information about this presentation, contact:

jkruskal@bidmc.harvard.edu

LEARNING OBJECTIVES

To define the concept and definition of value relative to clinical radiology practice.
 To describe how value can be measured.
 To define strategies for improving delivery of value.

Honored Educators

Presenters or authors on this event have been recognized as RSNA Honored Educators for participating in multiple qualifying educational activities. Honored Educators are invested in furthering the profession of radiology by delivering high-quality educational content in their field of study. Learn how you can become an honored educator by visiting the website at: https://www.rsna.org/Honored-Educator-Award/ Jonathan B. Kruskal, MD, PhD - 2012 Honored EducatorJonathan B. Kruskal, MD, PhD - 2016 Honored Educator

MSQI31B The Patient Perspective on Radiology Value

Participants

Tessa S. Cook, MD, PhD, Philadelphia, PA (Presenter) Royalties, Osler Institute

For information about this presentation, contact:

tessa.cook@uphs.upenn.edu

LEARNING OBJECTIVES

1) Discuss what patients value most in their encounters with a radiology practice. 2) Describe challenges patients face in navigating their care in radiology. 3) Understand innovations in care design that could address challenges patients face in radiology.

MSQI31C How Machine Learning will Optimize our Value

Participants

Curtis P. Langlotz, MD,PhD, Menlo Park, CA (*Presenter*) Advisory Board, Nuance Communications, Inc; Shareholder, whiterabbit.ai; Advisory Board, whiterabbit.ai; Shareholder, Nines.ai; Consultant, Nines.ai; Shareholder, TowerView Health; Research Grant, Koninklijke Philips NV; Research Grant, Siemens AG; Research Grant, Alphabet Inc;

LEARNING OBJECTIVES

1) Review the clinical constraints and needs that radiologists face. 2) Critique the role of computer aided detection in radiology. 3) Understand the role of artificial intelligence across the image life cycle, including detection. 4) Discuss how artificial intelligence will change the practice of radiology.



RC305

Neuroradiology Series: Artificial Intelligence in Neuroradiology

Tuesday, Nov. 27 8:30AM - 12:00PM Room: S406B



AMA PRA Category 1 Credits ™: 3.50 ARRT Category A+ Credits: 4.00

Participants

Greg Zaharchuk, MD, PhD, Stanford, CA (*Moderator*) Research Grant, General Electric Company; Stockholder, Subtle Medical; Christopher P. Hess, MD, PhD, Mill Valley, CA (*Moderator*) Nothing to Disclose

Sub-Events

RC305-01 AI: An Introduction for Neuroradiologists

Tuesday, Nov. 27 8:30AM - 9:00AM Room: S406B

Participants

Yvonne W. Lui, MD, New York, NY (Presenter) Research collaboration, Siemens AG; Advisor, Bold Brain Ventures

LEARNING OBJECTIVES

1) Introduce basic concepts, ideas, and terminology of machine learning. 2) Review array of machine learning applications in neuroimaging.

RC305-02 Residual Extraction Approach in the Deep Learning With 3D Convolutional Ladder Network for Differential Diagnosis of Idiopathic Normal Pressure Hydrocephalus and Alzheimer's Disease

Tuesday, Nov. 27 9:00AM - 9:10AM Room: S406B

Participants

Ryusuke Irie, MD, Tokyo, Japan (*Presenter*) Nothing to Disclose Yujiro Otsuka, Tokyo, Japan (*Abstract Co-Author*) Nothing to Disclose Koji Kamagata, Tyuuouku, Japan (*Abstract Co-Author*) Nothing to Disclose Michimasa Suzuki, MD, Minato-Ku, Japan (*Abstract Co-Author*) Nothing to Disclose Akihiko Wada, MD, Izumo, Japan (*Abstract Co-Author*) Nothing to Disclose Masaaki Hori, MD, Tokyo, Japan (*Abstract Co-Author*) Nothing to Disclose Tomoko Maekawa, MD, Tokyo, Japan (*Abstract Co-Author*) Nothing to Disclose Shohei Fujita, MD, Tokyo, Japan (*Abstract Co-Author*) Nothing to Disclose Christina Andica, Tokyo, Japan (*Abstract Co-Author*) Nothing to Disclose Madoka Nakajima, Tokyo, Japan (*Abstract Co-Author*) Nothing to Disclose Masakazu Miyajima, Hongo, Japan (*Abstract Co-Author*) Nothing to Disclose Yumiko Motoi, Tokyo, Japan (*Abstract Co-Author*) Nothing to Disclose Shigeki Aoki, MD, PhD, Tokyo, Japan (*Abstract Co-Author*) Nothing to Disclose

PURPOSE

Idiopathic normal pressure hydrocephalus (iNPH) and Alzheimer's disease (AD) are geriatric diseases and common as causes of dementia. As a treatment approach is quite different, it is important to diagnose iNPH and AD correctly. The purpose of this study was to differentiate iNPH and AD by deep learning method.

METHOD AND MATERIALS

Twenty-three patients with iNPH (11 male and 12 female: mean age 74.6 years) and 23 patients with AD (11 male and 12 female: mean age 75.0 years) were included in this study. Diagnosis of iNPH was made according to the criteria of probable iNPH proposed by the Japanese Clinical Guidelines for Idiopathic Normal Pressure Hydrocephalus, and that of AD was made according to the criteria of probable AD by the National Institute of Neurologic and Communicative Disorders and Stroke/Alzheimer's Disease and Related Disorders Association. All patients underwent brain MRI with 3 T unit and we used only whole-brain three dimensional (3D) T1-weighted images in this study. We designed fully-automated, end-to-end 3D deep learning model to differentiate iNPH and AD. The model consists of residual extraction part followed by neural network classifier. In the residual extraction part, we build 3D convolutional ladder network to reconstruct 3D volume to be extracted from original 3D volume. The residual volume is then fed again into the encoder to obtain residual feature map. The feature map is used as an input of subsequent neural network classifier. We evaluated an accuracy of our model in differentiation of iNPH and AD by leave-one-out cross-validation. We also evaluated validity of the result by visualizing important area in the original input image with Gradient-weighted Class Activation Mapping.

RESULTS

Twenty out of 23 cases in iNPH and 20 out of 23 cases in AD were correctly diagnosed (predictive value was 87.0%). The area under the receiver operating characteristic curve was 0.91. The time taken for diagnosis was about 1 to 2 seconds per case.

CONCLUSION

Residual extraction approach in the deep learning method was useful for the differential diagnosis of iNPH and AD.

CLINICAL RELEVANCE/APPLICATION

Deep learning with residual extraction approach can help radiologists in the diagnosis of dementia which is difficult to be differentiated clinically.

RC305-03 Automated Classification of Alzheimer's Disease by Interregional Correlation Matrix in Structural MR Images

Tuesday, Nov. 27 9:10AM - 9:20AM Room: S406B

Participants

Xiangzhu Zeng, MD, Beijing, China (*Presenter*) Nothing to Disclose Huishu Yuan, Beijing, China (*Abstract Co-Author*) Nothing to Disclose Yan Liu, Beijing, China (*Abstract Co-Author*) Nothing to Disclose Ling Wang, Chengdu, China (*Abstract Co-Author*) Nothing to Disclose Zheng Wang, MS, Beijing, China (*Abstract Co-Author*) Nothing to Disclose

For information about this presentation, contact:

xiangzhuzeng@126.com

PURPOSE

Based on compartmental sparse feature selection method, interregional correlation matrix of structural magnetic resonance data was built for identification of Alzheimer's disease (AD) from the healthy and compared with voxel-based volume of gray matter (GM) method.

METHOD AND MATERIALS

198 AD (AD group) cases and 148 healthy control (HC group) cases were investigated (table 1). For all cases, High-resolution 3D T1WI images were acquired on a SIEMENS Trio 3T scanner or a GE 750 3T scanner. 148 AD and 100 HC cases were in training set and 50 AD and 50 HC for testing. Sparse principal component analysis (SPCA) method was used to extract sparse principal components (SPCs) for 32 ROIs of the cerebrum according to AAL template and feature parameter value Yi of SPCs was obtained for each ROI. Then interregional correlation matrix of Yi of 32 ROIs is built and 16 distinct ROIs are selected according to analyzing the interregional correlation coefficients between Hippocampus and other ROIs. Yi of SPCs and the volume of GM of 17 distinct ROIs as variables in support vector machine (SVM) classifier (Figure 1).

RESULTS

1. Interregional correlation matrix of Yi of 32 ROIs is built and 16 distinct ROIs (Amygdala, parahippocampal gyrus, caudate, anterior cingulum, middle cingulum, posterior cingulum, superior orbital frontal lobe, inferior orbital frontal lobe, middle orbital frontal lobe, medial orbital frontal lobe, fusiform gyrus, insula, putamen, thalamus, middle temporal pole and superior temporal pole) with high correlation with Hippocampus were selected (r>0.3, p<0.05) (Figure 2). 2. Yi and the volume of GM of 17 ROIs (above 16 ROIs and Hippocampus) used as feature variable of SVM, The classification accuracy for Yi and the volume of GM is 0.84 and 0.82 respectively. 3. There is a strong correlation between Yi of hippocampus and volume of it (r=0.963, p<0.001). Yi has much higher correlation with MMSE score (r=0.586, p<0.001) than volume (r=0.393, p<0.001) (Table 2).

CONCLUSION

Our results revealed high classification accuracy for AD diagnosis by using SPCA method combined with interregional correlation matrix of structural MR data. The feature parameter value Yi of our method is more accurate than volume of GM to quantify cerebral atrophy of AD.

CLINICAL RELEVANCE/APPLICATION

The method of SPCA combined with interregional correlation matrix is an effective computer-aided diagnosis method to help clinician to identify AD.

RC305-04 Comparison of Machine Learning Models for Prediction of Alzheimer's Disease (AD)

Tuesday, Nov. 27 9:20AM - 9:30AM Room: S406B

Participants

Qingchen Diao, Shenzhen, China (*Abstract Co-Author*) Nothing to Disclose Silun Wang, MD, PhD, Shenzhen, China (*Presenter*) Nothing to Disclose Sang Na, MS, Shenzhen, China (*Abstract Co-Author*) Nothing to Disclose Wanshun Wei, Shenzhen, China (*Abstract Co-Author*) Nothing to Disclose

For information about this presentation, contact:

wangsilun@gmail.com

PURPOSE

Alzheimer's disease (AD) is a type of neurodegenerative disease that is the most common form of dementia. The purpose of this study is to compare investigate the diagnostic accuracy of machine learning methods for predicting AD via structural information of brain.

METHOD AND MATERIALS

T1-weighted 3D MPRAGE images were collected from the Alzheimer's Disease Neuroimaging Initiative (ADNI). We recruited 88 AD patients and 142 normal controls (mean age 71.7 \pm 5.9 vs 71.4 \pm 4.8, p>0.05). The raw data was firstly processed by FreeSurfer to generate the subcortical segmentation, cortical parcellation and segmentation of hippocampus. We then trained three types of machine learning algorithms, namely support vector machine (SVM), random forest (RF) and naive bayes, on the 80% of dataset and evaluated accuracy, sensitivity, positive predictive value (PPV), specificity and negative predictive value (NPV) on the rest of dataset. Grid search associated with cross validation is used to get the best hyper-parameter (including kernels of SVM) of each algorithm.

RESULTS

For each patient, 163 brain structural data were generated including 70 cortex thickness, 68 brain volume, 10 volume of ventricle, 15 subsegment of hippocampus for each raw MRI images. In terms of classify AD patients, RF has best diagnostic accuracy of 95.7%, sensitivity of 83.3%, PPV of 100%, specificity of 100% and NPV of 94.4%. However, SVM (accuracy 84.8%, sensitivity 58.3%, precision 77.8%, PPV 94.1%, NPV 86.5%) and naive bayes (accuracy 82.6%, sensitivity 58.3%, PPV 70.0%, specificity 91.2%, NPV 86.1%) show worse performances. We further found that entorhinal cortical thickness, hippocampal tail volume and molecular layer of hippocamus, especially in left brain, are top-3 important features, which have largest Gini importance and mean decrease impurity (0.1038, 0.0514, 0.0457 respectively).

CONCLUSION

Random forestRF has better diagnostic performance compared to SVM and naive bayes. RF shows highly precision and specificity and thus is appropriate for screening testing use in population study. In addition, machine learning identifies that thinner of entorhinal cortical thickness and smaller of hippocampal tail play a key role in AD patients.

CLINICAL RELEVANCE/APPLICATION

Machine learning based on FreeSurfer-processed MRI images may accuraty predict AD,

RC305-05 Radiomics Based on Multi-Contrasts MRI Allows Precisely Differentiate Glioma Subtypes and Predict Tumor Proliferative Behaviors

Tuesday, Nov. 27 9:30AM - 9:40AM Room: S406B

Participants

Changliang Su, Wuhan, China (*Presenter*) Nothing to Disclose Wenzhen Zhu, MD, PhD, Wuhan, China (*Abstract Co-Author*) Nothing to Disclose Ju Zhang, Wuhan, China (*Abstract Co-Author*) Nothing to Disclose Chengxia Liu, Wuhan, China (*Abstract Co-Author*) Nothing to Disclose Nanxi Shen I, MD, Wuhan, China (*Abstract Co-Author*) Nothing to Disclose Xiaowei Chen, Wuhan, China (*Abstract Co-Author*) Nothing to Disclose

For information about this presentation, contact:

suchangliang2008@163.com

PURPOSE

To explore the feasibility of radiomics based on anatomical, diffusion- and perfusion-weighted MRI in differentiating gliomas subtypes and predicting tumor proliferation.

METHOD AND MATERIALS

220 pathology confirmed gliomas and ten contrasts were included in the retrospective analysis. After registed to T2FLAIR images and resampled to 1 mm3 isotropically, 431 radiomics features were extracted from each included contrast maps in semi-automatic defined tumor volume. For single contrast and the combination of all contrast maps, partial correlation analysis revealed correlations between radiomics features and pathological biomarkers, and multivariate models were built to identify the best predictive models with adjusted 0.632+ bootstrap AUC.

RESULTS

In univariate analysis, both non-wavelet and wavelet radiomics features correlated significant with tumor grades and Ki-67. The max R was 0.557 (p=2.04E-14) in T1C for tumor grades, and 0.395 (p=2.33E-07) in ADC for Ki-67. In multi-variate analysis, the combination of all contrast radiomics features had the highest AUCs in both differentiating glioma subtypes and predicting proliferation, when compared with single contrast images. For low/high-grade gliomas, the best AUC was 0.911. In differentiating subtypes gliomas, the best AUC was 0.896 in grade II-III, 0.997 for grade II-IV, and 0.881 in grading III-IV. In reflecting levels of proliferation, multi-contrasts features leaded to an AUC of 0.936.

CONCLUSION

Multi-contrasts Radiomics supplys complementary information on both geometric characters and molecular biological traits, which correlated significantly with tumor grades and proliferation. Combined all contrasts radiomics models might precisely predict glioma biological behaviors, which may attribute to pre-surgical personal diagnosis.

CLINICAL RELEVANCE/APPLICATION

The precisely predicting tumor subtypes and proliferation levels based multi-contrasts MRI radiomics allows accurate evlation of pre-surgical gliomas, which may facillate the development of precise medicine, even in those patients from poor areas, who suffer from expensive cost on genetic detections.

RC305-06 Accelerating and Standardizing Stroke Patient Triaging with Deep Learning

Tuesday, Nov. 27 9:40AM - 10:10AM Room: S406B

Participants

Kim Mouridsen, Aarhus, Denmark (Presenter) Shareholder and Officer, Cercare Medical

LEARNING OBJECTIVES

1) Describe how deep learning may be applied to predict most likely tissue outcome in acute ischemic stroke. 2) Compare different approaches to prediction of outcome with machine learning. 3) Explain basic considerations in constructing and training deep learning models.

RC305-07 Data Preparation, Segmentation, and Deployment for Neuroradiology AI Applications

For information about this presentation, contact:

mmuelly@stanford.edu

LEARNING OBJECTIVES

1) Recognize the impact of data and label quality on machine learning models. 2) Understand the components involved in end to end development of machine learning models for clinical applications.

RC305-08 Whole-Tumor Texture and Morphology Analyses of Conventional and Diffusion Tensor Imaging For Determination of Grades and Histological Subtypes in Meningiomas Using Machine Learning

Tuesday, Nov. 27 10:50AM - 11:00AM Room: S406B

Participants

Yaewon Park, MD, Seoul, Korea, Republic Of (*Presenter*) Nothing to Disclose Jongmin Oh, Seoul, Korea, Republic Of (*Abstract Co-Author*) Nothing to Disclose Seng Chan You, Suwon, Korea, Republic Of (*Abstract Co-Author*) Nothing to Disclose Kyunghwa Han, PhD, Seoul, Korea, Republic Of (*Abstract Co-Author*) Nothing to Disclose Sung Soo Ahn, MD, Seoul, Korea, Republic Of (*Abstract Co-Author*) Nothing to Disclose Yoon Seong Choi, MD, Seoul, Korea, Republic Of (*Abstract Co-Author*) Nothing to Disclose Yoon Seong Choi, MD, Seoul, Korea, Republic Of (*Abstract Co-Author*) Spouse, Stockholder, Medi Whale Jong Hee Chang, Seoul, Korea, Republic Of (*Abstract Co-Author*) Nothing to Disclose Se-Hoon Kim, Seoul, Korea, Republic Of (*Abstract Co-Author*) Nothing to Disclose Seung-Koo Lee, MD, PhD, Seoul, Korea, Republic Of (*Abstract Co-Author*) Nothing to Disclose

For information about this presentation, contact:

yaewonpark@yuhs.ac

PURPOSE

To evaluate the role of texture and morphology analyses of postcontrast T1-weighted images, apparent diffusion coefficient (ADC) and fractional anisotropy (FA) maps bases on the entire tumor volume, in differentiation of grades and histological subtypes of meningiomas.

METHOD AND MATERIALS

Eighty-five patients with pathologically diagnosed meningiomas (low grade [benign], 61; high-grade [atypical and anaplastic], 24), who underwent postcontrast T1-weighted and diffusion tensor imaging, were included in the discovery set. The postcontrast-T1 weighted image, ADC and the fractional anisotropy maps were analyzed to derive volume-based data of the entire tumor. Texture and morphology analyses were correlated with the meningioma grades and histological subtypes. Support vector machines were trained to build classification models for the determination of meningioma grade. We tested the model in a temporal external validation set (37 patients; low-grade, 27; high-grade, 10).

RESULTS

Various texture and morphology parameters differed significantly according to meningioma grades. The best classification system for the prediction of meningioma grades had a maximum area under the curve of 0.905 and 0.878 in the discovery and validation sets, respectively. Various texture parameters differed significantly between fibroblastic and non-fibroblastic subtypes.

CONCLUSION

Whole-tumor texture and morphology features of postcontrast T1-weighted images, ADC and fractional anisotropy maps are useful for differentiating meningioma grades.

CLINICAL RELEVANCE/APPLICATION

Texture and morphology features of postcontrast T1-weighted images, ADC and fractional anisotropy maps may aid in preoperative grading of meningiomas, which influences treatment planning.

RC305-09 The Added Prognostic Value of Radiological Phenotypes to Clinical Features in IDH-Wild Type Lower Grade Gliomas Using Machine Learning

Tuesday, Nov. 27 11:00AM - 11:10AM Room: S406B

Awards

Student Travel Stipend Award

Participants

Chae Jung Park, MD, Seoul, Korea, Republic Of (*Presenter*) Nothing to Disclose Kyunghwa Han, PhD, Seoul, Korea, Republic Of (*Abstract Co-Author*) Nothing to Disclose Sung Soo Ahn, MD, Seoul, Korea, Republic Of (*Abstract Co-Author*) Nothing to Disclose Yoon Seong Choi, MD, Seoul, Korea, Republic Of (*Abstract Co-Author*) Spouse, Stockholder, Medi Whale Sohi Bae, MD, Seoul, Korea, Republic Of (*Abstract Co-Author*) Nothing to Disclose Seung-Koo Lee, MD, PhD, Seoul, Korea, Republic Of (*Abstract Co-Author*) Nothing to Disclose

PURPOSE

To investigate the additional prognostic value of MR imaging phenotypes to clinical features using machine learning in patients with IDH-wild type lower grade gliomas

METHOD AND MATERIALS

Dragnarative MDTe of 112 nationte with histonathologically confirmed TDU wild type grade TT or TTT gliamae were retrognactively

analyzed according to the Visually Accessible Rembrandt Images (VASARI) features set. A radiologic risk score (RRS) for overall survival (OS) and progression free survival (PFS) was produced by selected features and their regression coefficients from Elastic net regression model with 100 times of repeated cross validation. Multivariable Cox analysis was performed including age, Karnofsky Performance score (KPS), grade, extent of resection and RRS. The added predictive value of RRS was calculated by comparing Cindices between multivariable Cox models with and without RRS. The difference of C-indices was validated by bootstrap with 1,000 times of resampling.

RESULTS

Elastic net Cox regression model revealed 15 different MR imaging phenotypes that were significantly associated with OS and PFS, respectively. According to multivariable Cox analysis, RRS obtained from these imaging phenotypes was an independent predictor for both OS (HR 3.322, p < 0.001) and PFS (HR 2.605, p < 0.001). The model with RRS showed better performance in predicting survival than that without RRS (C-index for OS: 0.722 vs. 0.806, C-index for PFS: 0.706 vs. 0.773). The differences of C-indices in two models were statistically significant after bootstrap testing.

CONCLUSION

RRS derived from MRI features was independent predictors for survival in patients with IDH-wild type lower grade gliomas. Addition of RRS to prognosis prediction model significantly improved performance.

CLINICAL RELEVANCE/APPLICATION

IDH-wild type lower grade gliomas are known to be similar to glioblastoma in terms of genetic alterations and prognostically heterogeneous. Radiological phenotypes may have added prognostic value in patients with IDH-wild type lower grade gliomas.

RC305-10 Magnetic Resonance Textural Analysis on Contrast Enhanced 3D-SPACE Images in Assessment of Consistency of Pituitary Macroadenoma

Tuesday, Nov. 27 11:10AM - 11:20AM Room: S406B

Participants

Wenting Rui, Shanghai, China (*Presenter*) Nothing to Disclose Yue Wu, Shanghai, China (*Abstract Co-Author*) Nothing to Disclose Zengyi Ma, Shanghai, China (*Abstract Co-Author*) Nothing to Disclose Xiao Xu, Shanghai, China (*Abstract Co-Author*) Nothing to Disclose Junhai Zhang, Shanghai, China (*Abstract Co-Author*) Nothing to Disclose Zhenwei Yao, Shanghai, China (*Abstract Co-Author*) Nothing to Disclose

For information about this presentation, contact:

wennyrui@126.com

PURPOSE

To explore the value of magnetic resonance textural analysis (MRTA) in assessing consistency of pituitary macroadenoma (PMA) based on contrast enhanced 3D-SPACE images.

METHOD AND MATERIALS

Fifty-three patients with PMA that underwent contrast enhanced 3D-SPACE scanning by 3.0T MRI and endoscopic trans-sphenoidal surgery were included in the present study. Consistency levels of PMA were evaluated intraoperatively by two neurosurgeons. Each resection specimen was stained with H&E and anti-collagen IV. MRTA was conducted and texture features were calculated by Omni Kinetics software. An unpaired t-test was used to analyze the differences of texture features between relative soft and hard PMAs. Receiver operating characteristic curves by individual and combined features were used to calculate the diagnostic accuracy of MRTA in predicting consistency.

RESULTS

First-order energy and second-order correlation negatively correlated with hard PMAs, while first-order entropy and second-order variance, sum variance, and sum entropy positively correlated with tumor stiffness. All showed significant differences between soft and medium consistency PMAs (P<0.05). Diagnostic accuracy of combined negative features could achieve an area under the curve (AUC) of 0.819, sensitivity of 88.9%, specificity of 61.5%, positive predictive value (PPV) of 70.6%, negative predictive value (NPV) of 84.2% and positive features could achieve an AUC of 0.836, sensitivity of 85.2%, specificity of 69.2%, PPV of 74.2%, NPV of 81.8% (P<0.001).

CONCLUSION

MRTA using contrast enhanced 3D-SPACE images is helpful for assessing PMA consistency preoperatively and noninvasively.

CLINICAL RELEVANCE/APPLICATION

Consistency level of PMA determines surgery approach and resection rates. MRTA based on contrast enhanced 3D-SPACE images may help assess consistency of PMAs preoperatively and noninvasively, which can guide the appropriate surgery approach to increase resection rates and reduce long-term recurrence.

RC305-11 Real-World Performance of Deep-Learning-based Automated Detection System for Intracranial Hemorrhage

Tuesday, Nov. 27 11:20AM - 11:30AM Room: S406B

Participants Hyunkwang Lee, Boston, MA (*Presenter*) Nothing to Disclose Sehyo Yune, MD,MPH, Boston, MA (*Abstract Co-Author*) Nothing to Disclose Stuart R. Pomerantz, MD, Boston, MA (*Abstract Co-Author*) Research Grant, General Electric Company Mohammad Mansouri, MD, MPH, Framingham, MA (*Abstract Co-Author*) Nothing to Disclose Ramon G. Gonzalez, MD, PhD, Boston, MA (*Abstract Co-Author*) Nothing to Disclose Michael H. Lev, MD, Boston, MA (*Abstract Co-Author*) Consultant, General Electric Company; Institutional research support, General Electric Company; Stockholder, General Electric Company; Consultant, MedyMatch Technology, Ltd; Consultant, Takeda Pharmaceutical Company Limited; Consultant, D-Pharm Ltd Synho Do, PhD, Boston, MA (*Abstract Co-Author*) Nothing to Disclose

For information about this presentation, contact:

hyunkwanglee@seas.harvard.edu

PURPOSE

Most of currently published deep learning studies in medical image analysis report their performance using carefully selected data. To use such tools in the clinical practice, however, it is critical to know how they work with the real-world data. Here, we evaluated the applicability of our ICH detection system in the clinical setting by comparing the model performance on the real-world cases to the performance on the selected dataset.

METHOD AND MATERIALS

We previously trained and validated the deep learning system for ICH detection using a total of 904 cases of 5mm, non-contrast head CT scans - 625 cases with ICH and 279 cases without ICH. Six board-certified neuroradiologists annotated all 2D axial slices according to the presence of ICH based on consensus. For evaluating the model, we retrieved an additional, non-overlapping set of 200 cases - 100 with ICH and 100 without ICH - with exclusion of cases with any history of brain surgery, intracranial tumor, intracranial device placement, skull fracture, or cerebral infarct. For performance evaluation in the real-world setting, all non-contrast head CT scans acquired at a single emergency department for three months from September to November 2017 were obtained. Collected were 2,606 consecutive cases including 163 cases with ICH.

RESULTS

Area under the receiver operating curve (AUC) was 0.993 for detecting the presence of ICH on the 200 selected cases with sensitivity of 98.0%, specificity of 95.0%, and negative predictive value of 97.9%. The same model achieved AUC of 0.834 on the real-world cases with sensitivity of 87.1%, specificity of 58.3%, and negative predictive value of 98.5% at the high sensitivity operating point.

CONCLUSION

The deep-learning-based ICH detection model achieved lower sensitivity and specificity when tested on real-world data compared to when tested on the selected data that excluded potentially confusing cases. However, the negative predictive values were similar in the two test datasets.

CLINICAL RELEVANCE/APPLICATION

The performance of deep-learning based systems should be evaluated on the real-world data before being used in the clinical practice to assist clinicians in interpreting the automated output.

RC305-12 The Present and Future of Deep Learning in Neuroradiology: What Can We Do Now and What We Will Be Able to Accomplish

Tuesday, Nov. 27 11:30AM - 12:00PM Room: S406B

Participants Peter Chang, MD, San Francisco, CA (*Presenter*) Nothing to Disclose

For information about this presentation, contact:

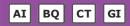
changp6@uci.edu



RC309

Gastrointestinal Series: Advances in Abdominal CT (The In-Person Presentation is Supported by an Unrestricted Educational Grant from GE Healthcare, Life Sciences)

Tuesday, Nov. 27 8:30AM - 12:00PM Room: E451A



AMA PRA Category 1 Credits ™: 3.50 ARRT Category A+ Credits: 4.00

FDA Discussions may include off-label uses.

Participants

Benjamin M. Yeh, MD, San Francisco, CA (*Moderator*) Research Grant, General Electric Company; Consultant, General Electric Company; Author with royalties, Oxford University Press; Shareholder, Nextrast, Inc; Research Grant, Koninklijike Philips NV; Research Grant, Guerbet SA; ;

Avinash R. Kambadakone, MD, Boston, MA (Moderator) Nothing to Disclose

Meghan G. Lubner, MD, Madison, WI (Moderator) Grant, Koninklijke Philips NV; Grant, Johnson & Johnson;

George L. Shih, MD, MS, New York, NY (*Moderator*) Consultant, Image Safely, Inc; Stockholder, Image Safely, Inc; Consultant, MD.ai, Inc; Stockholder, MD.ai, Inc;

Arun Krishnaraj, MD, MPH, Charlottesville, VA (Moderator) Nothing to Disclose

For information about this presentation, contact:

arunk@virginia.edu

akambadakone@mgh.harvard.edu

mlubner@uwhealth.org

LEARNING OBJECTIVES

1. Review topics around Machine Learning 2. Discuss applications of multi-energy CT 3. Review usage of oral contrast media and associated controversies 4. Discuss CT imaging biomarkers for oncologic and non oncologic applications 5. Review innovations in Health IT.

Sub-Events

RC309-01 Machine Learning

Tuesday, Nov. 27 8:30AM - 8:55AM Room: E451A

Participants

George L. Shih, MD, MS, New York, NY (*Presenter*) Consultant, Image Safely, Inc; Stockholder, Image Safely, Inc; Consultant, MD.ai, Inc; Stockholder, MD.ai, Inc;

For information about this presentation, contact:

george@cornellradiology.org

LEARNING OBJECTIVES

1) Basic concepts of machine learning and deep learning. 2) Exciting areas of abdominal machine learning research. 3) Future of abdominal AI.

RC309-02 Machine Learning-based Radiomics Improve Prediction of Metastatic Disease Progression in Patients with Colon Cancer

Tuesday, Nov. 27 8:55AM - 9:05AM Room: E451A

Participants Dania Daye, MD, PhD, Philadelphia, PA (*Presenter*) Nothing to Disclose Azadeh Tabari, Boston, MA (*Abstract Co-Author*) Nothing to Disclose Michael S. Gee, MD, PhD, Boston, MA (*Abstract Co-Author*) Nothing to Disclose

For information about this presentation, contact:

dania.daye@gmail.com

PURPOSE

Intra-tumor heterogeneity is independently associated with worse patient prognosis in several cancer subtypes. This study investigates the role of quantitative tumor heterogeneity MRI features in predicting metastatic disease progression in patients with colon cancer.

METHOD AND MATERIALS

In this IDR-annrovad ratrospactive study, we identified 51 patients with stage 4 colon cancer who underwant MDI for liver

metastasis evaluation. Standard clinical prognostic variables were collected. The largest hepatic lesion was identified on the portal venous phase T1-weighted post-contrast images and segmented. MR radiomic feature vectors were extracted from each lesion using 50 morphological and texture features. Six-month metastatic disease progression was assessed, with progression defined as appearance of new hematogeneous metastatic lesions. Univariate logistic regression analysis was used to assess the contribution of the features to disease progression prediction. A linear support vector machine (SVM) machine learning technique was applied to the imaging phenotype vector and to the clinical prognostic variables to predict disease progression. The classifiers were trained and tested using 10-fold cross validation. ROC analysis, area under the curve (AUC) and Delong's test were used to assess classification performance.

RESULTS

13 of 51 patients (26%) exhibited metastatic disease progression. Mean time to disease progression was 109 \pm 5.9 days. Tumor entropy, dissimilarity and GLCM standard deviation exhibited significant differences in mean values between patients exhibiting progression and those who did not (p=0.02, p=0.03 and p=0.03, respectively). Univariate regression revealed three features independently associated with metastatic disease progression: tumor promenance (p=0.03), homogeneity (p=0.03), and variance (p=0.02). An SVM model that incorporates imaging-based heterogeneity features resulted in improved model performance for disease progression prediction (AUC of 0.86), compared to the model that only included standard prognostic clinical variables (AUC=0.54) (p<0.001).

CONCLUSION

Quantitative tumor heterogeneity MRI features improve prediction of metastatic disease progression in patients with colon cancer.

CLINICAL RELEVANCE/APPLICATION

Machine learning-based tumor radiomics may improve disease progression prediction and may inform decisions regarding locoregional vs systemic therapy in patients with oligometastatic disease.

RC309-03 A Multiphase Convolutional Dense Network For Classification of Focal Liver Lesions on Dynamic Contrast-Enhanced CT

Tuesday, Nov. 27 9:05AM - 9:15AM Room: E451A

Participants

Cao Sue, MD, Guangzhou, China (*Presenter*) Author Hui Liu, Shanghai, China (*Abstract Co-Author*) Nothing to Disclose Meng Ye, Shanghai, China (*Abstract Co-Author*) Nothing to Disclose Wenqi Shi, Guangzhou, China (*Abstract Co-Author*) Author Simin Chen, Guangzhou, China (*Abstract Co-Author*) Author Dashan Gao, San Diego, CA (*Abstract Co-Author*) Author Yunqiang Chen, San Diego, CA (*Abstract Co-Author*) Author Sichi Kuang, Guangzhou, China (*Abstract Co-Author*) Author

Hanxi Zhang, Guangzhou, China (Abstract Co-Author) Author

Claude B. Sirlin, MD, San Diego, CA (*Abstract Co-Author*) Research Grant, Gilead Sciences, Inc; Research Grant, General Electric Company; Research Grant, Siemens AG; Research Grant, Bayer AG; Research Grant, ACR Innovation; Research Grant, Koninklijke Philips NV; Research Grant, Celgene Corporation; Consultant, General Electric Company; Consultant, Bayer AG; Consultant, Boehringer Ingelheim GmbH; Consultant, AMRA AB; Consultant, Fulcrum Therapeutics; Consultant, IBM Corporation; Consultant, Exact Sciences Corporation; Advisory Board, AMRA AB; Advisory Board, Guerbet SA; Advisory Board, VirtualScopics, Inc; Speakers Bureau, General Electric Company; Author, Medscape, LLC; Author, Resoundant, Inc; Lab service agreement, Gilead Sciences, Inc; Lab service agreement, ICON plc; Lab service agreement, Intercept Pharmaceuticals, Inc; Lab service agreement, Shire plc; Lab service agreement, Takeda Pharmaceutical Company Limited; Lab service agreement, sanofi-aventis Group; Lab service agreement, Johnson & Johnson; Lab service agreement, NuSirt Biopharma, Inc; Contract, Epigenomics; Contract, Arterys Inc Jin Wang, MD, Guangzhou, China (*Abstract Co-Author*) Nothing to Disclose

For information about this presentation, contact:

wangjin3@mail.sysu.edu.cn

PURPOSE

To develop and assess an automated multiphase convolutional dense network (MP-CDN) to classify focal liver lesions (FLLs) of different pathological types on multiphase computed tomography (CT).

METHOD AND MATERIALS

Following ethics committee approval with waived informed consent requirement, 359 patients with a total of 517 FLLs scanned on a 320-row CT scanner using a multiphase (pre-contrast, arterial, portal venous, and delayed phases) protocol between 2012-2017 were retrospectively enrolled. FLLs were classified by contemporaneous histology as hepatocellular carcinoma (HCC, n=111), metastases (mets, n=112), benign FLL (i.e., hemangioma, focal nodular hyperplasia, adenoma; n=162), and hepatic abscess (n=132). A MP-CDN classifier with a sequential input of 4 CT contrast-enhanced phases was developed to automatically classify each FLL. 410 FLLs (88 HCCs, 89 mets, 128 benign FLLs, 105 abscesses) were used for training; 107 FLLs (23 HCCs, 23 mets, 34 benign FLLs, 27 abscesses) were used for testing. The performance of MP-CDN classification was assessed in the testing dataset: accuracy was calculated from the confusion matrix; the area under the receiver operating characteristic curve (AUC) was calculated from the softmax probability outputted from the last layer of the MP-CDN.

RESULTS

The mean classification accuracy in the testing dataset was 81.3% (87/107). The AUC for differentiating each lesion type from the other 3 lesion types was 0.92, 0.99, 0.88 and 0.96 for HCC, mets, benign FLLs, and hepatic abscess, respectively.

CONCLUSION

A MP-CDN accurately classified FLLs detected on multiphase CT over a 6-year period as HCC, mets, benign FLLs and hepatic abscess. If independently validated in a large, diverse cohort imaged with a variety of CT scanners and protocols, MP-CDN may be

a potential method to assist radiologists for differential diagnosis of malignant and benign FLLs.

CLINICAL RELEVANCE/APPLICATION

MP-CDN may be a potential method to assist radiologists for differential diagnosis of malignant and benign FLLs and to facilitate management decisions in clinical practice.

RC309-04 Development and Validation of a Deep Learning System for Staging Liver Fibrosis Using Contrast-Enhanced CT Images of the Liver

Tuesday, Nov. 27 9:15AM - 9:25AM Room: E451A

Participants

Jong Keon Jang, MD, Seoul, Korea, Republic Of (*Presenter*) Nothing to Disclose Gyu Jin Choi, Seoul, Korea, Republic Of (*Abstract Co-Author*) Nothing to Disclose Seung Soo Lee, MD, Seoul, Korea, Republic Of (*Abstract Co-Author*) Nothing to Disclose Yu Sub Sung, Seoul, Korea, Republic Of (*Abstract Co-Author*) Nothing to Disclose Woo Hyun Shim, Seoul, Korea, Republic Of (*Abstract Co-Author*) Nothing to Disclose Ho Sung Kim, Seoul, Korea, Republic Of (*Abstract Co-Author*) Nothing to Disclose Jin-Young Choi, Seoul, Korea, Republic Of (*Abstract Co-Author*) Nothing to Disclose Yedaun Lee, MD, Busan, Korea, Republic Of (*Abstract Co-Author*) Nothing to Disclose Bo-Kyeong Kang, MD, Seoul, Korea, Republic Of (*Abstract Co-Author*) Nothing to Disclose Jin Hee Kim, MD, Seoul, Korea, Republic Of (*Abstract Co-Author*) Nothing to Disclose So Yeon Kim, MD, Seoul, Korea, Republic Of (*Abstract Co-Author*) Nothing to Disclose So Yeon Kim, MD, Seoul, Korea, Republic Of (*Abstract Co-Author*) Nothing to Disclose Eunsil Yu, MD, Seoul, Korea, Republic Of (*Abstract Co-Author*) Nothing to Disclose

PURPOSE

To develop and validate a deep learning system (DLS) based on convolutional neural network for staging liver fibrosis using computed tomography (CT) images of the liver.

METHOD AND MATERIALS

A DLS for CT-based staging of liver fibrosis was created using a development dataset that included portal venous phase CT images for 7461 patients with pathologically confirmed liver fibrosis. The diagnostic performance of the DLS was evaluated in test datasets for 891 patients. The influence of patient characteristics and CT techniques on the accuracy of the DLS was evaluated by logistic regression analysis. In a subset of 421 patients, the diagnostic performance of the DLS was compared with that of the radiologist's assessment, aminotransferase-to-platelet ratio index (APRI), and fibrosis-4 index using the area under the receiver-operating characteristic curve (AUROC) and Obuchowski index.

RESULTS

DLS had a staging accuracy of 79.4% (707/891) and an AUROC of 0.96 (95% CI 0.95-0.97), 0.97 (CI 0.96-0.98), and 0.95 (CI 0.94-0.96) for diagnosing significant fibrosis (F2-4), advanced fibrosis (F3-4), and cirrhosis, respectively. In multivariate analysis, only pathologic fibrosis stage significantly affected the staging accuracy of the DLS (P = .016 and P = .013 for F1 and F2, respectively, compared with F4), while etiology and CT technique did not. The DLS (Obuchowski index 0.94) outperformed the radiologist's interpretation, APRI, and fibrosis-4 index (range of Obuchowski indices, 0.71-0.81, P < .001) for staging liver fibrosis.

CONCLUSION

The DLS allows accurate staging of liver fibrosis using CT images and appears to be a promising assessment tool.

CLINICAL RELEVANCE/APPLICATION

Considering its high diagnostic performance and robustness to CT imaging techniques, the CT-based deep learning system would be a useful clinical tool for assessing liver fibrosis using routine portal venous phase CT images of the liver.

RC309-05 New Applications of Multi-energy CT

Tuesday, Nov. 27 9:25AM - 9:50AM Room: E451A

Participants

Benjamin M. Yeh, MD, San Francisco, CA (*Presenter*) Research Grant, General Electric Company; Consultant, General Electric Company; Author with royalties, Oxford University Press; Shareholder, Nextrast, Inc; Research Grant, Koninklijike Philips NV; Research Grant, Guerbet SA; ;

For information about this presentation, contact:

ben.yeh@ucsf.edu

LEARNING OBJECTIVES

1) Review scenarios in which single-energy CT and other diagnostic imaging tests may be problematic. 2) Describe capabilities of multi-energy CT, including recent advances. 3) Discuss case scenarios where multi-energy CT improves diagnoses or clinical decision making. 4) Review potential pitfalls of multi-energy CT. 5) Describe future advances and applications of multi-energy CT.

RC309-06 Measuring Fat Fraction with Dual-Layer Spectral CT Material Attenuation Decomposition Plots: An Iodine-Independent Method for Imaging Hepatic Steatosis

Tuesday, Nov. 27 9:50AM - 10:00AM Room: E451A

Participants Todd C. Soesbe, PhD, Dallas, TX (*Presenter*) Nothing to Disclose Matthew A. Lewis, PhD, Dallas, TX (*Abstract Co-Author*) Research collaboration, CMR Naviscan Corporation; Research collaboration, QT Ultrasound, LLC Lakshmi Ananthakrishnan, MD, Irving, TX (*Abstract Co-Author*) Nothing to Disclose John R. Leyendecker, MD, Dallas, TX (*Abstract Co-Author*) Nothing to Disclose Yin Xi, PhD, Dallas, TX (*Abstract Co-Author*) Nothing to Disclose Takeshi Yokoo, MD, PhD, Dallas, TX (*Abstract Co-Author*) Nothing to Disclose Robert E. Lenkinski, PhD, Dallas, TX (*Abstract Co-Author*) Research Grant, Koninklijke Philips NV Research Consultant, Aspect Imaging

PURPOSE

To determine the accuracy and iodine-independence of fat fraction measurements obtained from dual-layer spectral CT material attenuation decomposition (MAD) plots. Accuracy was evaluated using an MRI verified phantom, while iodine-independence was evaluated in patients with contrast-enhanced multiphase CT.

METHOD AND MATERIALS

Spectral CT derived photoelectric effect and Compton scatter images were used to create a 2D histogram (MAD plot) that allowed for differentiation and segmentation of fat, liver, and iodine. MAD plot fat fraction accuracy was determined using an anthropomorphic phantom and four 50 mL vials containing different ratios of homogenized bovine liver and lard (0, 25, 50, and 100% fat by volume). The phantom was scanned on both a Philips Ingenia 3.0 T MRI and a Philips IQon dual-layer spectral CT (120 kVp and 140 kVp) with the MRI fat fraction measurements (mDIXON Quant) used as the reference standard. ROI data from the MRI and spectral CT fat fraction maps were compared to the known fat fraction. For proof of concept in vivo, MAD plot fat fraction accuracy between pre- and post-contrast spectral CT was determined in four patients with varying degrees steatosis. Non-contrast and contrast-enhanced MAD plot fat fraction maps were compared using three ROIs per image, placed in similar liver locations.

RESULTS

For the phantom data, Bland-Altman analysis showed the mean difference (mean+/-sigma) between the known and measured fat fraction percent was MRI = 1.61+/-1.23, 120kVp = 0.52+/-1.77, and 140kVp = 0.80+/-1.94. MAD plot fat fraction maps at 120 kVp and 140 kVp were comparable in accuracy to the MRI mDIXON quant fat fraction map. Bland-Altman analysis for the in vivo liver data showed that the mean difference between the pre- and post-contrast measured fat fraction percent was Venous = 0.21+/-1.57 and Delayed = -0.61+/-1.78. Therefore, the MAD plot fat fraction map was independent of iodine.

CONCLUSION

MAD plots are an accurate method for measuring fat fraction with dual-layer spectral CT ex vivo, with potential for in vivo contrast-enhanced CT. The MAD plot method is translatable to other types of dual-energy spectral CT systems and could potentially measure volumetric fat fraction.

CLINICAL RELEVANCE/APPLICATION

With this method any patient receiving an abdominal CT (with or without iodine) can have their liver fat fraction measured, which would help to detect early stage and asymptomatic fatty liver disease.

RC309-07 Can Quantitative Iodine Parameters on DECT Replace Perfusion CT Parameters in Colorectal Cancers?

Tuesday, Nov. 27 10:00AM - 10:10AM Room: E451A

Participants

Hyo-Jin Kang, MD, Seoul, Korea, Republic Of (*Presenter*) Nothing to Disclose Se Hyung Kim, MD, Seoul, Korea, Republic Of (*Abstract Co-Author*) Nothing to Disclose Jae Seok Bae, MD, Seoul, Korea, Republic Of (*Abstract Co-Author*) Nothing to Disclose Sun Kyung Jeon, MD, Seoul, Korea, Republic Of (*Abstract Co-Author*) Nothing to Disclose Joon Koo Han, MD, Seoul, Korea, Republic Of (*Abstract Co-Author*) Nothing to Disclose

PURPOSE

To determine the correlation between iodine concentrations derived from dual-energy CT (DECT) and perfusion CT (PCT) parameters in patients with pathologically-proven colorectal cancers (CRC), and to evaluate their reproducibility and respective radiation exposures.

METHOD AND MATERIALS

Institutional review board approval and written informed consents were obtained for this study. Forty-one patients with CRCs who underwent same day DECT and PCT were prospectively enrolled. Three radiologists independently analyzed iodine concentration of the tumors and iodine ratios (ratio of lesion to aorta (IRa) or to infrarenal IVC (IRv)) from DECT as well as blood flow (BF), blood volume (BV), permeability (PMB), and mean transit time (MTT) from PCT. Pearson R and linear correlation, paired t-test and intraclass correlation coefficients (ICCs) were used.

RESULTS

Significant correlations were found between iodine parameters from DECT and PCT parameters: iodine concentration of tumors and BF (r=0.29, P=0.06), BV (r=0.32, P=0.04), PMB (r=0.34, P=0.03), and MTT (r=-0.38, P=0.02); iodine ratio (IRa) and MTT (r=-0.32, P=0.04); and iodine ratio (IRv) and BF (r=0.32, P=0.04) and PMB (r=0.44, P=<0.01). DECT showed better intra- and interobserver agreements (ICC=0.98, 0.90 in iodine concentration; 0.98, 0.91 in IRa; and 0.91, 0.93 in IRv, respectively) than PCT (ICC=0.90, 0.78 in BF; 0.82, 0.76 in BV; 0.75, 0.75 in PMB; 0.64, 0.79 in MTT, respectively). As for radiation dosage, CTDIvol and DLP in DECT (10.48±1.84mGy and 519.7±116.7mGy·cm) were significantly lower than those of PCT (75.76mGy and 911mGy·cm) (P<0.01).

CONCLUSION

Iodine parameters from DECT are significantly correlated with PCT parameters, but have higher intra- and inter-observer agreements and lower radiation exposure.

CLINICAL RELEVANCE/APPLICATION

As iodine parameters derived from DECT are significantly correlated with perfusion parameters while allowing better intra- and interobserver agreements and lower radiation exposure, DECT may be a good alternative to PCT in the assessment of the tumor hemodynamics in patients with CRC.

RC309-08 Oral Contrast Media Controversies

Tuesday, Nov. 27 10:15AM - 10:40AM Room: E451A

Participants Avinash R. Kambadakone, MD, Boston, MA (*Presenter*) Nothing to Disclose

For information about this presentation, contact:

akambadakone@mgh.harvard.edu

LEARNING OBJECTIVES

1) Explain the indications and benefits of oral contrast media in abdomen/pelvis CT. 2) Understand the controversies in the role of oral contrast media in various clinical settings including ER, oncology and routine abdominal scans. 3) Optimize the use of oral contrast media to improve diagnosis.

RC309-09 Spectral Photon-Counting CT Multi-Phase Liver Imaging with Dual Contrast Agent

Tuesday, Nov. 27 10:40AM - 10:50AM Room: E451A

Participants Salim Si-Mohamed, Lyon, France (*Presenter*) Nothing to Disclose Valerie Tatard-Leitman, PhD, Lyon, France (*Abstract Co-Author*) Nothing to Disclose Daniela Pfeiffer, MD, Munich, Germany (*Abstract Co-Author*) Nothing to Disclose Monica Sigovan, PhD, Lyon, France (*Abstract Co-Author*) Nothing to Disclose Daniel Bar-Ness, Bron, France (*Abstract Co-Author*) Nothing to Disclose Loic Boussel, MD, Lyon, France (*Abstract Co-Author*) Nothing to Disclose Philippe C. Douek, MD, PhD, Lyon, France (*Abstract Co-Author*) Nothing to Disclose Peter B. Noel, PhD, Munich, Germany (*Abstract Co-Author*) Nothing to Disclose

For information about this presentation, contact:

salim.si-mohamed@chu-lyon.fr

PURPOSE

To demonstrate the feasibility of dual-contrast multiphase imaging of the liver using Spectral Photon-Counting CT via K-edge imaging.

METHOD AND MATERIALS

The experiments were performed on 3 rabbits following approval by the local ethics committee. We used a 5 energy bins prototype spectral photon-counting CT (Philips Healthcare, Haifa, Israel), tube voltage of 120 kVp, tube current of 100 mA. The iodine contrast agent (Iomeron, 400 mg/mL, 1.5 mL/kg, Bracco) was injected first, followed by the gadolinium contrast agent (gadoteridol, 0.5 M, 5 mL/kg, Bracco) 21 seconds later, and acquisitions were done 10 seconds after the second injection. This protocol allowed performing two different phases imaging of the liver, i.e. arterial (gadolinium) and portal (iodine). Conventional HU and quantitative material decomposition iodine and specific K-edge gadolinium images were obtained.

RESULTS

The gadolinium K-edge and iodine material decomposition images allowed the discrimination between the two contrast agents, which was not possible using the conventional CT images. Moreover, we observed a dual-phase imaging matching the expected pharmacokinetics of the two contrast media. The iodine injected enhanced the liver parenchyma while the gadolinium injected enhanced the arteries. These results were confirmed by measuring the attenuation values (HU) and the concentrations (mg/mL) of contrast agents in the aorta (conventional CT: 1130 ± 17.6 HU; gadolinium: 20.9 ± 1.2 ; iodine: 6.8 ± 0.4), hepatic arteries (conventional CT: 474.6 ± 44.3 ; gadolinium: 7.7 ± 0.8 ; iodine: 0.7 ± 0.4), portal vein (conventional CT: 233.6 ± 15.1 ; gadolinium: -0.1 ± 0.6 ; iodine: 2.5 ± 0.4) and liver parenchyma (conventional CT: 143.9 ± 11.2 ; gadolinium: -0.6 ± 0.7 ; iodine: 3.6 ± 0.4).

CONCLUSION

Spectral Photon-Counting CT allows in vivo dual contrast qualitative and quantitative liver multi-phase imaging in a single acquisition. This finding pinpoints major clinical applications in multiphase imaging with no registration issues and with the additional value of reducing radiation dose to patients by decreasing the number of acquisitions.

CLINICAL RELEVANCE/APPLICATION

Spectral Photon-Counting CT allows the qualitative discrimination between two contrast agents injected sequentially in the liver, enabling to reduce radiation dose to patients by combining liver arterial and portal phases into a single acquisition.

RC309-10 Machine Learning Based Quality Assurance for CT Arterial Phase Timing to Ensure Robust Measurement of Tumor Density in Hepatocellular Carcinoma Patients

Tuesday, Nov. 27 10:50AM - 11:00AM Room: E451A

Awards

Trainee Research Prize - Fellow

Participants Laurent Dercle, MD, New York, NY (*Presenter*) Nothing to Disclose Jingchen Ma, NYC, NY (*Abstract Co-Author*) Nothing to Disclose Fatima-Zohra Mokrane, MD, Toulouse, France (*Abstract Co-Author*) Nothing to Disclose Ai-ping Chen, Nanjing, China (*Abstract Co-Author*) Nothing to Disclose Deling Wang, Guangzhou, China (*Abstract Co-Author*) Nothing to Disclose Lin Lu, New York, NY (Abstract Co-Author) Nothing to Disclose

Lawrence H. Schwartz, MD, New York, NY (Abstract Co-Author) Committee member, Celgene Corporation Committee member,

Novartis AG Committee member, ICON plc Committee member, BioClinica, Inc

Chuanmiao Xie I, MD, PhD, Guangzhou, China (Abstract Co-Author) Nothing to Disclose

Binsheng Zhao, DSc, New York, NY (*Abstract Co-Author*) License agreement, Varian Medical Systems, Inc; Royalties, Varian Medical Systems, Inc; License agreement, Keosys SAS; License agreement, Hinacom Software and Technology, Ltd;

For information about this presentation, contact:

ld2752@cumc.columbia.edu

PURPOSE

Several treatment response criteria shifted towards categorizing response as a decrease in tumor size and/or density. We aimed to increase the reproducibility of the measurement of tumor density at the arterial phase in Hepatocellular carcinoma (HCC) by developing and validating a semi-Automatic arterial-timing Classification Algorithm based on the analysis of the pharmacokinetiC distribution of the Iodinated contrast Agent a Single timepoint (ACACIAS).

METHOD AND MATERIALS

Using dynamic CT-images of 69 HCC pts, we trained (48 pts, 1930 timepoints) and validated (21 pts, 837 timepoints) ACACIAS to categorize arterial-timing into five phases according to the time to arterial peak: early (E0) < -15s < pre-peak (Pre1) < -5s < peak (P2) < +5s < post-peak (Post3) < +15s < late (L4). The random forest algorithm built the model based on the average density in predefined ROIs. Using an independent testing set, we delineated and calculated the average density of biopsy-proven HCC in 90 pts with cirrhotic liver at three phases: non-contrast enhanced 'NCP', arterial 'AP' and portal 'PVP'.

RESULTS

In the validation set, ACACIAS predicted correctly phases E0, Pre1, P2, Post3, and L4 in respectively 92%, 58%, 86%, 30%, and 99% of pts. Inter-patient variability in the duration of the arterial peak (5-95th percentiles of Full Width at Half Maximum: 10.6-27.5s) explained lower accuracies of ACACIAS in Pre1 and Post3 phases. In the testing set, 96% of NCP and 97% of PVP were correctly classified. The predicted arterial timing of AP was E0, Pre1, P2, Post3, and L4 in respectively 1, 34, 13, 25, and 17 pts and was associated with a significant difference in mean tumor density: 68, 55, 60, 71, and 60HU. The arterial HCC enhancement peaked at phase Post3 (+17%), (P<0.02, ANOVA).

CONCLUSION

ACACIAS predicted arterial timing accurately based on iodine biodistribution on medical images. A peak of HCC tumor density (+17%) was observed at the arterial phase 'Post3'. ACACIAS could improve extraction of tumor quantitative imaging biomarkers and monitoring of anti-cancer therapy efficacy by ensuring reproducible arterial phase acquisitions.

CLINICAL RELEVANCE/APPLICATION

ACACIAS ensures a reproducible tumor density measurement at arterial phase for treatment response assessment, as well as wideranging applications since tumor density is a surrogate of vascularity.

RC309-11 CT Imaging Biomarkers

Tuesday, Nov. 27 11:00AM - 11:25AM Room: E451A

Participants

Meghan G. Lubner, MD, Madison, WI (Presenter) Grant, Koninklijke Philips NV; Grant, Johnson & Johnson;

For information about this presentation, contact:

mlubner@uwhealth.org

LEARNING OBJECTIVES

1. Discuss known and emerging CT imaging biomarkers in non-oncologic applications using liver disease as an example. 2. Review oncologic applications of CT texture analysis using colorectal neoplasms and renal cell carcinoma as examples.

LEARNING OBJECTIVES

1) Discuss a variety of quantitative features (size/volume, morphology, texture) that can be obtained retrospectively from CT data for both oncologic and non-oncologic applications.

Honored Educators

Presenters or authors on this event have been recognized as RSNA Honored Educators for participating in multiple qualifying educational activities. Honored Educators are invested in furthering the profession of radiology by delivering high-quality educational content in their field of study. Learn how you can become an honored educator by visiting the website at: https://www.rsna.org/Honored-Educator-Award/ Meghan G. Lubner, MD - 2014 Honored EducatorMeghan G. Lubner, MD - 2015 Honored EducatorMeghan G. Lubner, MD - 2018 Honored Educator

RC309-12 Quantitative Imaging in Spectral Detector CT: Suitability of Iodine Maps for Oncologic Imaging: An Initial Evaluation in Phantoms and 75 Patients

Tuesday, Nov. 27 11:25AM - 11:35AM Room: E451A

Participants

Nils Grosse Hokamp, MD, Cleveland, OH (*Presenter*) Nothing to Disclose Nuran Abdullayev, MD, Cologne, Germany (*Abstract Co-Author*) Nothing to Disclose Max Schlaak, Cologne, Germany (*Abstract Co-Author*) Nothing to Disclose Christian Wybranski, MD, Magdeburg, Germany (*Abstract Co-Author*) Nothing to Disclose Thorsten Persigehl, MD, New York, NY (*Abstract Co-Author*) Nothing to Disclose Thomas Streichert, Cologne, Germany (*Abstract Co-Author*) Nothing to Disclose Jasmin A. Holz, PhD, Cologne, Germany (*Abstract Co-Author*) Nothing to Disclose Hatem Alkadhi, MD, Zurich, Switzerland (*Abstract Co-Author*) Nothing to Disclose David C. Maintz, MD, Koln, Germany (*Abstract Co-Author*) Nothing to Disclose Stefan Haneder, MD, Cologne, Germany (*Abstract Co-Author*) Nothing to Disclose

For information about this presentation, contact:

nils.grosse-hokamp@uk-koeln.de

PURPOSE

Iodine maps are available from spectral detector computed tomograph (SDCT). They visualize the distribution of iodinated contrast media and allow for its quantification. Hence, they are a promising technique in oncologic imaging with respect to both, initial diagnosis (benign vs malignant) and follow-up examinations (therapy monitoring). In order to exploit a potential benefit in this respect, it is necessary to understand the intra- and inter-individual consistency of these.

METHOD AND MATERIALS

To evaluate accuracy of the reconstruction algorithm, an anthropomorphic liver phantom was repetitively examined at different time points; further images were reconstructed repetitively. Regions of interest (ROI) were placed automatically at identical positions using an in-house developed software. In addition, we included 75 patients, that underwent double (n=50) or triple (n=25) SDCT examination in this retrospective, IRB-approved study. Patients with significant change in liver function as indicated by laboratory results were excluded. Three ROI were drawn in each the liver parenchyma and the portal vein (PV) in portal-venous phase. Iodine uptake (IU) was normalized to the PV (IU_norm). Empirical standard deviation of the mean (ESD) was used and used to determine inter-scan and intra-individual consistency of IU_norm in phantoms and patients, respectively.

RESULTS

In phantoms, ESD between different acquisitions and timepoints was as low as 1.3%. InMean iodine uptake of the liver parenchyma was 2.2 ± 0.8 mg/ml (ranging from 0.5 - 4.8 mg/ml), IU_norm was 0.40 ± 0.07 . Intra-individual consistency was rather high as indicated by an ESD of 7.7% showing a wide range from -44% - +36%.

CONCLUSION

Iodine quantification using Iodine maps from SDCT is technically feasible; however, in in-vivo measurements at different timepoints, intra-individual iodine quantification of the liver differs. Among other reasons, this is likely due to offsets in timing of image acquisition and not necessarily attributed to the specific reconstruction algorithm.

CLINICAL RELEVANCE/APPLICATION

Measurements of iodine uptake should be interpreted carefully when considering them for clinical decision making.

RC309-13 Innovations in Health IT

Tuesday, Nov. 27 11:35AM - 12:00PM Room: E451A

Participants

Arun Krishnaraj, MD, MPH, Charlottesville, VA (Presenter) Nothing to Disclose

For information about this presentation, contact:

arunk@virginia.edu

LEARNING OBJECTIVES

Identify policies impacting the spread of innovation in health IT. 2) Assess the role of greater transparency of health care data.
 Describe how mobile and wearables are impacting the collection of health data.



RC353

Deep Learning & Machine Intelligence in Radiology

Tuesday, Nov. 27 8:30AM - 10:00AM Room: S406A



AMA PRA Category 1 Credits ™: 1.50 ARRT Category A+ Credit: 1.75

Participants

Paul J. Chang, MD, Chicago, IL (*Moderator*) Co-founder, Koninklijke Philips NV; Researcher, Koninklijke Philips NV; Researcher, Bayer AG; Advisory Board, Aidoc Ltd; Advisory Board, EnvoyAI; Advisory Board, Inference Analytics

Sub-Events

RC353A Introduction to Deep Learning

Participants

Luciano M. Prevedello, MD, MPH, Dublin, OH (Presenter) Nothing to Disclose

LEARNING OBJECTIVES

1) Understand the principles of knowledge extraction from data (Machine Learning). 2) Understand main intuitions behind deep machine learning models (Deep Learning). 3) Understand how Deep Learning can be applied to medical image analysis and the main challenges associated to the application of Deep Learning in this domain.

RC353B Deep Learning and Machine Intelligence in Radiology: A Reality Check

Participants

Paul J. Chang, MD, Chicago, IL (*Presenter*) Co-founder, Koninklijke Philips NV; Researcher, Koninklijke Philips NV; Researcher, Bayer AG; Advisory Board, Aidoc Ltd; Advisory Board, EnvoyAI; Advisory Board, Inference Analytics

LEARNING OBJECTIVES

1) A "realistic" perspective on how deep learning and machine intelligence can add value to radiology will be discussed. 2) The significant challenges with respect to practical implementation of deep learning/machine intelligence offerings by existing radiology workflow and existing IT infrastructure will be reviewed. 3) Strategies for preparing the radiology department and IT for deep learning/machine intelligence will be discussed.

ABSTRACT

Current and near future requirements and constraints will require radiology practices to continuously improve and demonstrate the value they add to the healthcare enterprise. Merely 'managing the practice' will not be sufficient; groups will be required to compete in an environment where the goal will be measurable improvements in efficiency, productivity, quality, and safety. There has been great interest (as well as fear and hype) regarding the application of deep learning and other machine intelligence approaches to help improve the radiology value proposition. This session will attempt to provide a "reality check" on how these potentially promising technologies might be used by radiology and the significant challenges involved. Topics that will be covered include: • How can we best apply deep learning/machine intelligence to add "true value?" • How do we confidently validate the performance of these technologies? • How can our existing IT systems "feed and consume" these technologies efficiently and at scale? • How can we best harmonize the human radiologist with these machine agents?

RC353C Deep Learning: How to Get Started

Participants

Abdul Hamid Halabi, Santa Clara, CA (Presenter) Developer, NVIDIA Corporation; Spouse, Employee, Covenant Pathology



CS31

Artificial Intelligence: Impact and Implications to Radiology: Presented by Philips Healthcare

Tuesday, Nov. 27 9:00AM - 10:30AM Room: S101AB

Participants

Julius Chapiro, MD, New Haven, CT (*Presenter*) Research Grant, Koninklijke Philips NV; Research Grant, Guerbet SA; Consultant, Guerbet SA; Consultant, Eisai Co, Ltd

Lawrence N. Tanenbaum, MD, New York, NY (*Presenter*) Speaker, General Electric Company; Speaker, Siemens AG; Speaker, Guerbet SA; Speaker, Koninklijke Philips NV; Consultant, Enlitic, Inc; Consultant, icoMetrix NV; Consultant, CorTechs Labs, Inc; Consultant, Arterys Inc

Michael P. Recht, MD, New York, NY (Presenter) Nothing to Disclose

Kevin W. McEnery, MD, Houston, TX (*Presenter*) Advisor, Koninklijke Philips NV Research Agreement, Koninklijke Philips NV John J. Smith, MD, JD, Washington, DC (*Presenter*) Partner, Hogan Lovells US LLP

PROGRAM INFORMATION

This panel will be an open discussion format among the expert panelists to provide insights on some of the most pressing issues the introduction of AI into Radiology faces. Data, regulatory, workflow, adoption, applications and potential displacement will all be touched upon, guided by questions from the audience.

СМЕ

This course does not offer CME credit.



CS32

Expanding Precision Medicine along Clinical Pathways with AI Powered Decision Support: Presented by Siemens Healthineers

Tuesday, Nov. 27 9:00AM - 10:00AM Room: S102AB

Participants

Mitchell D. Schnall, MD, PhD, Philadelphia, PA (*Presenter*) Nothing to Disclose Mohamed Abazeed, MD, PhD, Cleveland, OH (*Presenter*) Nothing to Disclose Razvan Ionasec, PhD, Princeton, NJ (*Presenter*) Employee, Siemens AG

PROGRAM INFORMATION

Balancing the challenge of standardization while personalizing patient-centric options is at the forefront of integrated decisionmaking for healthcare provider. Combining in-vitro, in-vivo and genomics data and extracting insights with the help of AI and thereby driving more precise diagnosis and treatment decisions along clinical pathways is the focus of this symposium.



CS33

Medical Imaging: The Path Forward: Presented by Google Cloud

Tuesday, Nov. 27 9:00AM - 10:30AM Room: S105D

Participants

Gregory J. Moore, MD, PhD, Mountain View, CA (*Presenter*) Nothing to Disclose Michael Muelly, MD, Mountain View, CA (*Presenter*) Employee, Google LLC; Partner, ClariPACS LLC

PROGRAM INFORMATION

Electronic health records, medical imaging, and genomics are examples of healthcare data types which can drive clinical and operational decisions on individuals and populations. However, in a world where data is growing at unprecedented rates, a new strategy and a new set of tools is required to capture the promises of Big Data in the healthcare space. Cloud computing is rapidly changing the way that healthcare data is handled. By creating novel opportunities to use scaled data aggregation to train machine learning models, Cloud computing can enable improvements in operational efficiency and clinical decision support. Google Cloud is at the forefront of the application of Cloud computing to healthcare. In this symposium, the Google Cloud team will present a perspective on data management, analytics and machine learning with specific focus on medical imaging applications. In conjunction with our customers and our partners, we will share what we have learned, the challenges we have encountered, , and the opportunities for innovation moving forward.

СМЕ

This course does not offer CME credit.



SSG02

Cardiac (Coronary Atherosclerosis)

Tuesday, Nov. 27 10:30AM - 12:00PM Room: S104B



AMA PRA Category 1 Credits ™: 1.50 ARRT Category A+ Credit: 1.75

Participants

James C. Carr, MD, Chicago, IL (*Moderator*) Research Grant, Astellas Group; Research support, Siemens AG; Speaker, Siemens AG; Advisory Board, Guerbet SA

Konstantin Nikolaou, MD, Tuebingen, Germany (Moderator) Advisory Panel, Siemens AG; Speakers Bureau, Siemens AG; Speaker Bureau, Bayer AG

Arthur E. Stillman, MD, PhD, Atlanta, GA (Moderator) Nothing to Disclose

Sub-Events

SSG02-01 Incremental Prognostic Value of Coronary Artery Disease-Reporting and Data System (CAD-RADS) Scores Over Coronary Artery Calcium Scores (CACS) for Major Adverse Cardiovascular Event in Stroke Patients Without Chest Pain

Tuesday, Nov. 27 10:30AM - 10:40AM Room: S104B

Participants

Kyungsun Nam, MD, Seoul, Korea, Republic Of (*Presenter*) Nothing to Disclose Jin Hur, MD, Seoul, Korea, Republic Of (*Abstract Co-Author*) Nothing to Disclose Dong Jin Im, Seoul, Korea, Republic Of (*Abstract Co-Author*) Nothing to Disclose Young Joo Suh, MD, Seoul, Korea, Republic Of (*Abstract Co-Author*) Nothing to Disclose Yoo Jin Hong, MD, Seoul, Korea, Republic Of (*Abstract Co-Author*) Nothing to Disclose Hye-Jeong Lee, MD, Seoul, Korea, Republic Of (*Abstract Co-Author*) Nothing to Disclose Young Jin Kim, MD, Seoul, Korea, Republic Of (*Abstract Co-Author*) Nothing to Disclose Byoung Wook Choi, MD, Seoul, Korea, Republic Of (*Abstract Co-Author*) Nothing to Disclose

For information about this presentation, contact:

namks0216@yuhs.ac

PURPOSE

The aim of this study was to investigate the prognostic value of coronary artery disease-reporting and data system (CAD-RADS) scores and determine the additional risk stratification benefit of CAD-RADS scores compared to coronary artery calcium score (CACS) and coronary artery disease (CAD) extent classifications in ischemic stroke patients without cardiac symptoms.

METHOD AND MATERIALS

From January 2013 to August 2014, 615 ischemic stroke patients who had at least one risk factor for CAD without chest pain underwent coronary computed tomography angiography (CCTA) and were included for final analysis. CT images were evaluated for CACS, extent of CAD and CAD-RADS scores. The primary endpoint was major adverse cardiovascular events (MACEs) defined as cardiovascular death, nonfatal myocardial infarction, unstable angina (UA) requiring hospitalization, revascularization and recurrent ischemic stroke event. Cox regression analyses were used to identify associations between CAD-RADS results and MACEs. Cstatistics were calculated to compare discriminatory values of each model.

RESULTS

During the median follow-up period of 3.11 years, there were a total of 78 MACEs. Of 615 patients, 24.7% were classified as CAD-RADS 0, 19.3% as CAD-RADS 1, 17.6% as CAD-RADS 2, 18.5% as CAD-RADS 3, 15.6% as CAD-RADS 4A, 2.1% as CAD-RADS 4B, and 2.1% as CAD-RADS 5. CACS, CAD extent classification and CAD-RADS scores independently stratified risk of future MACEs (all p < 0.05). C-statistics revealed that both CAD extent classification and CAD-RADS scores improved risk stratification beyond CACS (C-index: 0.753 vs 0.698, p < 0.001 and 0.726 vs 0.698, p = 0.041, respectively).

CONCLUSION

In ischemic stroke patients without chest pain, CAD-RADS score had prognostic value for future MACE. In addition, CAD-RADS score provide additional risk-discrimination over CACS.

CLINICAL RELEVANCE/APPLICATION

CAD-RADS score provides additional risk-discrimination over CACS for the future major adverse cardiovascular events and can be recommended in the assessment of cardiovascular risk of stroke patient without chest pain.

SSG02-02 Machine Learning Outperforms CAD-RADS in Finding Optimal Prognostic Plaque Characteristics on Coronary CT Angiograms

Tuesday, Nov. 27 10:40AM - 10:50AM Room: S104B

Participants

Kevin M. Johnson, MD, New Haven, CT (*Presenter*) Nothing to Disclose Hilary E. Johnson, Madison, CT (*Abstract Co-Author*) Nothing to Disclose Yang Zhao, New Haven, CT (*Abstract Co-Author*) Nothing to Disclose David A. Dowe, MD, Absecon, NJ (*Abstract Co-Author*) Nothing to Disclose Lawrence H. Staib, PhD, New Haven, CT (*Abstract Co-Author*) Nothing to Disclose

For information about this presentation, contact:

kevin.johnson@yale.edu

PURPOSE

To use machine learning to find an optimal combination of coronary artery imaging features on CT angiography for the prediction of all cause mortality and coronary deaths, myocardial infarction and revascularization

METHOD AND MATERIALS

CT angiography was performed and risk factor data collected. Arteries were scored using CAD-RADS and 4 other published methods and compared to a score derived using machine learning. Causes of death were determined using the National Death Index. Myocardial infarction and revascularizations were discovered by follow-up letters. Prognostic results were compared using the area under the receiver operating characteristic curves.

RESULTS

7117 patients were imaged and followed for a mean of 9.0 years. There were 414 deaths from all causes, 79 attributed to coronary artery disease as the underlying or contributing cause, 51 myocardial infarctions (MI) and 231 revascularizations. The two best machine learning models were linear discriminant with diagonal covariance matrix and a classification neural network. Respective areas under the ROC curve were 0.76 and 0.77 for all cause mortality, 0.82 and 0.82 for coronary deaths or MI, and 0.87 and 0.88 for CHD or MI or revascularization. The corresponding CAD-RADS results were 0.71, 0.79 and 0.86.

CONCLUSION

Machine learning outperformed CAD-RADS for prediction of death and coronary events.

CLINICAL RELEVANCE/APPLICATION

Machine learning can be used to provide a prognostic score on coronary CT angiography that is comparable to or better than CAD-RADS.

SSG02-03 Development of a Deep Learning Algorithm for Predicting the Coronary Artery Calcium Score Using Retinal Images

Tuesday, Nov. 27 10:50AM - 11:00AM Room: S104B

Participants

Tyler Hyungtaek Rim, Seoul, Korea, Republic Of (*Abstract Co-Author*) Stockholder, Medi-whale Inc Taegeun Choi, Seoul, Korea, Republic Of (*Abstract Co-Author*) Stockholder, Mediwhale Seongjung Kim, Seoul, Korea, Republic Of (*Abstract Co-Author*) Stockholder, Mediwhale Yoon Seong Choi, MD, Seoul, Korea, Republic Of (*Presenter*) Spouse, Stockholder, Medi Whale

For information about this presentation, contact:

awaitingyourfeedback@gmail.com

PURPOSE

To determine if deep learning networks could be trained to estimate coronary artery calcium score (CACS) in heart CT scan from retinal images.

METHOD AND MATERIALS

All patients who obtained both ophthalmic examination and heart CT angiography at the tertiary center. Automated extraction of an OCT and retinal images was performed and linked to clinical end points from the electronic medical records. A deep neural network was trained to categorize images as either CACS<=10 (normal) or CACS>=100 (abnormal). We used the Modified VGG 11 model. We inserted one global average pooling layer instead of 2 fully-connected layers. To avoid overfitting, we had the data augmentation. At the SoftMax layer, the image that passed over the network was shown normal or abnormal binary probability value. Accuracy and Area under the receiver operating characteristic was estimated.

RESULTS

A total of 23,177 retinal images based on 15,056 examinations from 2,419 patients, who have received heart CT angiography including CACS, were extracted. At the examination level, we achieved an area under the ROC curve of 78.43% with an accuracy of 70%. At a patient level, we achieved an area under the ROC curve of 85.53% with an accuracy of 77.9%.

CONCLUSION

Using the non-invasive retinal examination including fundus photographs and OCT, deep learning networks show an impressive ability to predict the CACS, which is one of most important marker of heart disease.

CLINICAL RELEVANCE/APPLICATION

Deep-learning based screening of fundus photographs and OCT may have potential for a surrogate marker without radiation

exposure for high-risk patients with high coronary artery calcium score.

SSG02-04 Coronary Calcium Content Extracted by Machine Learning Methods from Incidental CT Scans Improves Coronary Heart Disease Prediction Accuracy

Tuesday, Nov. 27 11:00AM - 11:10AM Room: S104B

Participants

Noam Barda, Tel Aviv, Israel (*Presenter*) Nothing to Disclose Eldad Elnekave, MD, Shefayim, Israel (*Abstract Co-Author*) Employee, Zebra Medical Vision Ltd Noa Dagan, MD, MPH, Tel Aviv, Israel (*Abstract Co-Author*) Nothing to Disclose Orna Bregman-Amitai, BSC, Shefayim, Israel (*Abstract Co-Author*) Employee, Zebra Medical Vision Ltd Ran Balicer, MD,PhD, Tel Aviv, Israel (*Abstract Co-Author*) Nothing to Disclose

For information about this presentation, contact:

noamba@clalit.org.il

PURPOSE

Despite significant reductions in the last few decades, coronary heart disease (CHD) remains a significant cause of mortality. Many risk factors for CHD can be mitigated by lifestyle changes and pharmacological interventions, making risk calculation for individuals an important part of prevention. Accordingly, quantification of risk is integrated into prevailing management guidelines. Determination of coronary calcium content has been shown to allow improvement in risk calculation, but requires specialized tests that are not often performed. We present a novel algorithmic method that allows for the extraction of coronary calcium scores from incidental chest CTs performed for other indications, and demonstrate its utility in improving prediction accuracy over the American Heart Association (AHA) 2013 pooled risk model in a retrospective cohort study.

METHOD AND MATERIALS

There were 14,866 patients aged 30-74 with no prior CHD diagnosis included. CT scans and different covariates for the model were extracted in the two years prior to the index date (1 June 2012). Patients were followed-up for five years. Prediction performance results were compared between the AHA 2013 model (base model) and the same model with the novel coronary calcium score inserted as an additional predictor (augmented model). Both were logistic regression models and were trained on the sample population to allow comparison. For measures requiring a threshold, 3.5% risk over 5 years was chosen.

RESULTS

Based on the likelihood ratio test, the augmented model was superior to the base model (p-value <0.001). Similarly, the augmented model achieved superior performance for all performance measures: sensitivity increased 0.85%, specificity increased 4.9%, area under the ROC curve increased by 2.2% and there was a 4.5% categorical net reclassification improvement.

CONCLUSION

In this study, use of a novel biomarker extracted using a machine learning algorithm from incidental CT scans improves predictive accuracy compared to the commonly used model. This improvement occurs both in theoretical and practical measurements of model utility; in actual use it would translate into better clinical decisions.

CLINICAL RELEVANCE/APPLICATION

Coronary calcium content extracted via novel machine learning methods from incidental CTs significantly improves coronary heart disease prediction.

SSG02-05 Radiomics of Coronary Artery Calcium in the Framingham Heart Study

Tuesday, Nov. 27 11:10AM - 11:20AM Room: S104B

Awards

Student Travel Stipend Award

Participants

Parastou Eslami, PhD, Boston, MA (Presenter) Nothing to Disclose Chintan Parmar, Boston, MA (Abstract Co-Author) Nothing to Disclose Borek Foldyna, MD, Boston, MA (Abstract Co-Author) Nothing to Disclose Jan-Erik Scholtz, MD, Boston, MA (Abstract Co-Author) Nothing to Disclose Alexander Ivanov, BS, Boston, MA (Abstract Co-Author) Nothing to Disclose Roman Zeleznik, Boston, MA (Abstract Co-Author) Nothing to Disclose Michael T. Lu, MD, Boston, MA (Abstract Co-Author) Nothing to Disclose Maros Ferencik, MD, Boston, MA (Abstract Co-Author) Nothing to Disclose Vasan Ramachandran, Boston, MA (Abstract Co-Author) Nothing to Disclose Kristin Baltrusaitis, Boston, MA (Abstract Co-Author) Nothing to Disclose Joseph M. Massaro, PhD, Boston, MA (Abstract Co-Author) Nothing to Disclose Ralph D'Agnostino, PhD, Boston, MA (Abstract Co-Author) Nothing to Disclose Christopher J. O'Donnell, MD, MPH, West Roxbury, MA (Abstract Co-Author) Nothing to Disclose Hugo Aerts, PhD, Boston, MA (Abstract Co-Author) Stockholder, Sphera Inc Udo Hoffmann, MD, Boston, MA (Abstract Co-Author) Institutional Research Grant, Kowa Company, Ltd; Institutional Research Grant, Abbott Laboratories; Institutional Research Grant, HeartFlow, Inc; Institutional Research Grant, AstraZeneca PLC

For information about this presentation, contact:

peslami1@mgh.harvard.edu

PURPOSE

To assess whether detailed coronary artery calcium (CAC) characterization based on radiomic feature extraction followed by machine learning improves prediction of cardiovascular (CV) events.

METHOD AND MATERIALS

Participants from the Offspring and third Generation cohorts of the community-based Framingham Heart Study who underwent chest CT between 2002 and 2005 were followed over a median of 9.1 years for cardiovascular events (CV) events (myocardial infarction, stroke, or death). Of those, 624 participants who had excellent image quality and CAC (Agatston score (AS)> 0) were randomly divided into discovery (n=318) and validation cohorts (n=306). CAC was segmented manually using 3DSlicer, and about 2000 radiomic features (based on intensity, shape, and texture of CAC) were extracted using pyRadiomics software. In the derivation cohort, we used an internal minimum redundancy maximum relevancy algorithm (without knowledge of events) to identify the 20 highest ranked features. Finally, a random forest classifier was used to optimize decision trees for prediction for CV events. The weighted predictive probability of events for each of the 20 features was summarized into a radiomic score. The performance of this score was tested independent in the validation cohort.

RESULTS

The discovery (66.1% men, 58.1 ± 11.1 age) and validation cohorts (61.4% men, 59.3 ± 11.2 age) had similar CV risk profile, median AS, and CV event rates (30/318 = 9.7% and 29/306=9.5%, respectively). In adjusted multivariate analysis (for Framingham risk factors and AS), participants in the validation cohort, who had radiomic scores in the mid and upper tertiles had significantly higher risk for events as compared to the lower tertile (mid: HR= 9.3, p=0.03, upper: HR=16.5, p=0.007). The area under the curve (AUC) was higher for AS, radiomic score (RS), and combined AS/RS were 0.73, 0.76 and 0.79; respectively in the overall population. Performance was best in the subgroup with AS <300 (n=250, Figure)

CONCLUSION

This proof-of-concept study demonstrates that detailed CAC characterization based on radiomic feature extraction predicts CV events independent of traditional risk factors and AS. Further validation is necessary to determine clinical impact.

CLINICAL RELEVANCE/APPLICATION

Artificial intelligence may identify a prognostically important radiomic signature of CAC.

Honored Educators

Presenters or authors on this event have been recognized as RSNA Honored Educators for participating in multiple qualifying educational activities. Honored Educators are invested in furthering the profession of radiology by delivering high-quality educational content in their field of study. Learn how you can become an honored educator by visiting the website at: https://www.rsna.org/Honored-Educator-Award/ Udo Hoffmann, MD - 2015 Honored Educator

SSG02-06 Identification of Invasive and Radionuclide Imaging Markers of Plaque Vulnerability Using Computed Tomography Radiomics

Tuesday, Nov. 27 11:20AM - 11:30AM Room: S104B

Participants

Marton Kolossvary, MD, Budapest, Hungary (*Presenter*) Creator and Developer - Radiomics Image Analysis Jonghanne Park, MD, Seoul, Korea, Republic Of (*Abstract Co-Author*) Nothing to Disclose Ji-In Bang, Seoul, Korea, Republic Of (*Abstract Co-Author*) Nothing to Disclose Jinlong Zhang, MD, Seoul, Korea, Republic Of (*Abstract Co-Author*) Nothing to Disclose Joo Myung Lee, MD,PhD, Seoul, Korea, Republic Of (*Abstract Co-Author*) Nothing to Disclose Jin Chul Paeng, Seoul, Korea, Republic Of (*Abstract Co-Author*) Nothing to Disclose Bela Merkely, MD,PhD, Budapest, Hungary (*Abstract Co-Author*) Nothing to Disclose Baga Narula, MD, PhD, Orange, CA (*Abstract Co-Author*) Nothing to Disclose Takashi Kubo, MD,PhD, Wakayama, Japan (*Abstract Co-Author*) Nothing to Disclose Bashi Akasaka, MD,PhD, Wakayama, Japan (*Abstract Co-Author*) Nothing to Disclose Ban-Kwon Koo, Seoul, Korea, Republic Of (*Abstract Co-Author*) Nothing to Disclose Ban-Kwon Koo, Seoul, Korea, Republic Of (*Abstract Co-Author*) Nothing to Disclose Ban-Kwon Koo, Seoul, Korea, Republic Of (*Abstract Co-Author*) Nothing to Disclose Ban-Kwon Koo, Seoul, Korea, Republic Of (*Abstract Co-Author*) Nothing to Disclose Pal Maurovich-Horvat, MD, PhD, Pecs, Hungary (*Abstract Co-Author*) Nothing to Disclose

For information about this presentation, contact:

marton.kolossvary@gmail.com

PURPOSE

Several invasive and radionuclide imaging markers of coronary plaque vulnerability have been described. Identification of these imaging biomarkers by a single, widely available non-invasive technique may provide an opportunity to identify vulnerable plaques and vulnerable patients in daily clinical practice. Therefore, our aim was to assess the diagnostic accuracy of coronary computed tomography angiography (CTA) derived radiomic features to identify attenuated plaque using intravascular ultrasound (IVUS), thincap fibroatheroma per optical coherence tomography and radionucleide uptake using sodium fluoride positron emission tomography morphologic (NaF18-PET) as compared to conventional qualitative and quantitative CT metrics.

METHOD AND MATERIALS

We analyzed 44 plaques in 25 patients using IVUS, OCT, NaF18-PET and coronary CTA. We assessed 7 conventional qualitative and quantitative plaque characteristics and calculated 935 radiomic parameters. We calculated receiver operating characteristics area under the curve (AUC) values using a 5-fold cross validation with 1000 repeats to assess diagnostic accuracy. We used the Kolmogorov-Smirnov test to compare the distribution of AUC values resulting from the cross-validations.

RESULTS

Radiomics outperformed conventional metrics to identify attenuated plaque per intravascular ultrasound, thin-cap fibroatheroma by optical coherence tomography and metabolically active plaques per sodium fluoride positron emission tomography in CT images (AUC: 0.72 vs 0.59; 0.80vs 0.66; 0.87 vs 0.65; p<0.001 all; respectively).

CONCLUSION

Computed tomography radiomics may allow the non-invasive identification of invasive and radionuclide imaging biomarkers.

Radiomics is able to identify morphologic and metabolic high-risk plaque features currently olny identifiable using invasive and radionucleide imaging, which are both important components of plaque instability.

SSG02-07 Epicardial Fat is Increased in the HIV Population and Associated to Coronary Artery Plaque Burden

Tuesday, Nov. 27 11:30AM - 11:40AM Room: S104B

Participants Manel Sadouni, MD, Montreal, QC (*Presenter*) Nothing to Disclose Madeleine Durand, MD,MSc, Montreal, QC (*Abstract Co-Author*) Nothing to Disclose Irina Boldeanu, Montreal, QC (*Abstract Co-Author*) Nothing to Disclose Samer Mansour, Montreal, QC (*Abstract Co-Author*) Researc Grant, Abbott Laboratories Cecile Tremblay, MD, Montreal, QC (*Abstract Co-Author*) Nothing to Disclose Carl Chartrand-Lefebvre, MD,MSc, Montreal, QC (*Abstract Co-Author*) Nothing to Disclose Sayer AG; Research Grant, Bracco Group; Research collaboration, TeraRecon, Inc; Research collaboration, Siemens AG

For information about this presentation, contact:

sadounim89@gmail.com

PURPOSE

HIV patients are exposed to a higher risk of coronary artery disease (CAD) compared to non-infected patients. The exact mechanism responsible for this increased risk is not well understood. HIV individuals are also exposed to changes in body fat distribution characterized by greater ectopic fat. These changes may play a role in promoting atherosclerosis. Epicardial fat, which is the ectopic fat related to the heart, may play a unique role because of its location near to the coronary arteries. We hypothesize that epicardial fat volume is increased in the HIV patients and correlates with total coronary plaque volume, and with low attenuation plaque volume, which is a marker of plaque vulnerability.

METHOD AND MATERIALS

This is a cross sectional study, nested in the Canadian HIV and Aging Cohort Study (CHACS), a large prospective cohort following more than 800 HIV+ and HIV- patients. Consecutive CHACS participants with low to intermediate cardiovascular risk without symptoms or past CAD were invited to undergo cardiac computed tomography (CT) and coronary plaque imaging with CT angiography. Volume measurement of epicardial fat, total atherosclerotic plaque and low-attenuation plaque were performed. Association between epicardial fat volume, coronary plaque volume and low attenuation plaque volume was assessed using multivariate linear regression.

RESULTS

A total of 246 participants underwent cardiac CT scans. 173 were HIV+ and 73 were HIV-. HIV+ patients had greater epicardial fat volume indexed to body mass index (BMI) than HIV- patients (p = 0.03). In the HIV infected group, epicardial fat volume was associated with duration of antiretroviral therapy use ($\beta = 1.45$, p = 0.004). After adjustment for traditional cardiovascular risk factors, BMI and waist circumference, epicardial fat volume was significantly associated with total plaque volume ($\beta = 1.99$, p = 0.04) and low attenuation plaque volume ($\beta = 0.86$, p = 0.01).

CONCLUSION

Epicardial fat volume is increased in the HIV participants . The association of epicardial fat volume with antiretroviral therapy duration and subclinical coronary artery plaque may suggest a potential mechanism that could explain the increased risk for CAD in the HIV population.

CLINICAL RELEVANCE/APPLICATION

Epicardial fat is increased in HIV patients and correlates with total coronary plaque volume and low attenuation plaque volume, a CT marker of plaque vulnerability.

SSG02-08 Subclinical Coronary Atherosclerosis among Individuals with HIV on Antiretroviral Therapy

Tuesday, Nov. 27 11:40AM - 11:50AM Room: S104B

Participants

Irina Boldeanu, Montreal, QC (*Presenter*) Nothing to Disclose Manel Sadouni, MD, Montreal, QC (*Abstract Co-Author*) Nothing to Disclose Samer Mansour, Montreal, QC (*Abstract Co-Author*) Researc Grant, Abbott Laboratories Cecile Tremblay, MD, Montreal, QC (*Abstract Co-Author*) Nothing to Disclose Madeleine Durand, MD,MSc, Montreal, QC (*Abstract Co-Author*) Nothing to Disclose Carl Chartrand-Lefebvre, MD,MSc, Montreal, QC (*Abstract Co-Author*) Equipment support, Koninklijke Philips NV; Equipment support, Bayer AG; Research Grant, Bracco Group; Research collaboration, TeraRecon, Inc; Research collaboration, Siemens AG

For information about this presentation, contact:

chartrandlef@videotron.ca

PURPOSE

To compare coronary plaque burden and characteristics between HIV-infected and non-HIV-infected participants

METHOD AND MATERIALS

This cross-sectional study nested in a large prospective cohort was approved by the local Institutional Review Board. All subjects provided written consent. Consecutive HIV+ and HIV- participants were prospectively recruited for cardiac computed tomography (CT). Eligibility criteria were males/females, no known coronary artery disease, low/intermediate 10-yr Framingham risk score (FRS, 5-20%), no CT contraindication. Coronary calcium scoring was done with non-contrast CT, and contrast-enhanced CT for plaque (calcified vs noncalcified, volume) and lumen assessment. Imaging assessors were blinded to HIV status. Analyses used multivariate multiple linear and logistic regression models.

RESULTS

A total of 246 participants (173 HIV+ (93% males), 73 HIV- (81 % males)) were included, with similar age (mean 55 yo, p=0.69) and FRS (median 11 %, p=0.53). Diabetes (10% vs 1.4 %, p=0.01) and smoking (28% vs 14 %, p=0.02) were more frequent in HIV+ than HIV- participants, and elevated LDL cholesterol less frequent in HIV+ participants (20% vs 32%, p=0.07). Median duration of HIV infection in HIV+ participants was 18 yrs. All were on antiretroviral therapy (median 15 yrs). After adjusting for diabetes, smoking and LDL cholesterol, prevalence and plaque extent was similar between HIV+ and HIV- participants (72 % vs 69 %, p= 0.37; 2.9 \pm 3.0 vs 2.7 \pm 3.8 plaques/participant, p= 0.53). HIV+ participants showed more frequent noncalcified and less frequent calcified plaques than HIV- participants (0.3 \pm 0.7 vs 0.1 \pm 0.5, p=0.01; 1.4 \pm 2.4 vs 2.0 \pm 2.0 plaques/participants, p=0.006). Number of mixed plaques (1.0 \pm 1.4 vs 0.6 \pm 1.4 plaques/participant, p= 0.27), mean calcium score (148 vs 141, p=0.81), plaque volume (273 vs 218 mm3, p=0.91) and prevalence of >= 70% stenosis (10% vs 6%, p=0.40) were similar between HIV+ and HIV- participants.

CONCLUSION

Noncalcified plaques are more frequent in asymptomatic HIV+ individuals under antiretroviral therapy, while calcified plaques are less frequent, in comparison to HIV- individuals, after adjustment of cardiovascular risk factors.

CLINICAL RELEVANCE/APPLICATION

Noncalcified plaques are usually considered more vulnerable plaques. Our findings suggest one anatomic substrate that could explain the increased risk of myocardial infarction in the HIV population.

SSG02-09 Atherosclerosis of Coronary Arteries in HIV Patients on Routine Non-Gated CT Chest: Incidence, Characteristics, and Risk Factors

Tuesday, Nov. 27 11:50AM - 12:00PM Room: S104B

Participants

Mayil S. Krishnam, MBBS, MRCP, Orange, CA (*Presenter*) Nothing to Disclose Edgar Karanjah, MBChB, Orange, CA (*Abstract Co-Author*) Nothing to Disclose Eduardo Hernandez-Rangel, MD, Monterrey, Mexico (*Abstract Co-Author*) Nothing to Disclose Eun Jin Chae, MD, PhD, Seoul, Korea, Republic Of (*Abstract Co-Author*) Nothing to Disclose

PURPOSE

To evaluate the incidence and risk factors of subclinical coronary artery calcification (CAC) in patients with Human Immunodeficiency Virus (HIV) infection.

METHOD AND MATERIALS

We retrospectively reviewed 143 HIV patients (M:F = 119:24; mean age, 46.4) who underwent routine non-gated CT of thorax, from May 2010 to November 2015. Each of the four main coronary arteries was identified-left main stem (LMS), left anterior descending (LAD), left circumflex (LCX), and right coronary artery (RCA)- on CT images. Calcification in each artery was categorized as absent, mild, moderate, or severe by a radiologist. A multivariate logistic regression was performed to find independent risk factors for positive CAC. Clinical and laboratory parameters reflecting the status of HIV infection, including CD4 count, viral load, duration since HIV diagnosis, and status of antiretroviral treatment.

RESULTS

Forty-one patients (28.7%) showed calcifications in one or more coronary arteries. LAD (n=38, 92.7%) was most commonly affected, followed by LCX (n=18, 43.9%) and RCA (n=13, 31.7%). CAC deposited at the proximal portion in LAD and LCX (76.3%, 77.7%, respectively) while at the mid to distal portion in RCA (61.5%). Age of CAC+ group (53.9 years) was significantly higher than that (43.4 years) of CAC- group (p < 0.001). Minimum age of HIV patient with positive CAC was 24yrs. Duration of HIV infection in CAC+ group (12.3 years) was significantly higher than that (8.6 years) in CAC- group (p<0.0344). The mean viral load was significantly lower value in CAC+ group compared to that in CAC- group (76K versus 414K, p=0.02). CAC+ group showed significantly higher CD4 cell counts than CAC- group (mean=355.9 versus 175.3, p=0.0053). There was no significant difference in HAART status between the two groups (current HAART receivers 84.4% versus 85.7%, p=0.539). On multivariate logistic regression, age, HIV duration, and CD4 were significantly associated with CAC+ (p-values<.05)

CONCLUSION

Patients with HIV showed early onset and increased incidence of CAC and associated with higher CD4 cell counts. Duration of HIV is an independent risk factor for coronary artery calcification, in addition to age of patients.

CLINICAL RELEVANCE/APPLICATION

Awareness of increased risk of atherosclerosis development in young-age HIV-infected patients is crucial for primary prevention of future cardiovascular events.



SSG03

Chest (Lung Nodule)

Tuesday, Nov. 27 10:30AM - 12:00PM Room: S504AB



AMA PRA Category 1 Credits ™: 1.50 ARRT Category A+ Credit: 1.75

FDA Discussions may include off-label uses.

Participants

Sudhakar N. Pipavath, MD, Mercer Island, WA (*Moderator*) Adjudicator, Gilead Sciences, Inc Mark L. Schiebler, MD, Madison, WI (*Moderator*) Stockholder, Stemina Biomarker Discovery, Inc; Stockholder, HealthMyne, Inc;

Sub-Events

SSG03-01 Deep Learning-Based Computer-Aided Detection System for Multiclass Multiple Lesions on Chest Radiographs: Observers' Performance Study

Tuesday, Nov. 27 10:30AM - 10:40AM Room: S504AB

Awards Student Travel Stipend Award

Participants

Jooae Choe, MD, Seoul, Korea, Republic Of (*Presenter*) Nothing to Disclose Sang Min Lee, MD, Seoul, Korea, Republic Of (*Abstract Co-Author*) Nothing to Disclose Kyunghee Lee, MD, PhD, Seongnam, Korea, Republic Of (*Abstract Co-Author*) Nothing to Disclose Kyu-Hwan Jung, PhD, Seoul, Korea, Republic Of (*Abstract Co-Author*) Stockholder, VUNO Inc Jaeyoun Yi, Seoul, Korea, Republic Of (*Abstract Co-Author*) Officer, Coreline Soft, Co Ltd Sang Min Lee, MD, Seoul, Korea, Republic Of (*Abstract Co-Author*) Nothing to Disclose Joon Beom Seo, MD, PhD, Seoul, Korea, Republic Of (*Abstract Co-Author*) Nothing to Disclose

For information about this presentation, contact:

sangmin.lee.md@gmail.com

PURPOSE

To evaluate the added value of a deep-learning based computer-aided detection (CAD) system for multiclass multiple lesions on radiographs when radiologists read chest radiographs.

METHOD AND MATERIALS

We developed new CAD system using deep learning for detecting multiple lesions with 4 different patterns (nodule/mass, interstitial opacity, pleural effusion, and pneumothorax) on chest radiograph. To train the deep learning network, 17917 images were collected in two tertiary hospitals. Numbers of normal and abnormal patients are 11000 and 6917, respectively. We labeled disease type and delineate region of interests (ROI) drawn as ground truths by two thoracic radiologists with consensus. To validate the effect of the developed CAD on observer's performance, 9 observers including 7 board-certified radiologists and two radiology residents reviewed 200 chest radiographs twice with two weeks interval. 200 chest radiographs consists of 100 normal and 100 abnormal (nodule/mass: 60, interstitial opacity: 10, pleural effusion: 10, pneumothorax: 10) chest radiographs. The diagnostic performance of the developed CAD, observers with and without CAD were evaluated and compared using jackknife free-response receiver operating characteristic (JAFROC) figure of merits (FOMs) on a per-lesion basis. The reading time for review was recorded.

RESULTS

The developed CAD showed FOMs of 0.931 for nodule/mass, 0.900 for interstitial opacity, 1 for pleural effusion, and 1 for pneumothorax. The mean FOMs of 9 observers without CAD were 0.916 for nodule/mass, 0.922 for interstitial opacity, 0.944 for pleural effusion, and 0.978 for pneumothorax. After applying the CAD, the mean FOMs of 9 observers were 0.942 for nodule/mass, 0.900 for interstitial opacity, 0.967 for pleural effusion, and 1 for pneumothorax. Except for interstitial opacity, the accuracy of three patterns with CAD increased. The mean reading time was 91.5 minutes \pm 53.2 without CAD and 79.1 minutes \pm 28.2 with CAD.

CONCLUSION

The deep-learning based CAD may help improve observer performance for reading chest radiograph as well as reducing reading time.

CLINICAL RELEVANCE/APPLICATION

The deep-learning based CAD has the potential to improve observer efficiency in terms of accuracy and reading and may provide preliminary interpretation for chest radiographs.

SSG03-02 A Retrospective, Multi-Center Clinical Study for Validating Increased Lesion Detection Accuracy of Radiologists When Using Computer-Aided Detection System in Reading Digital Chest X-Ray Images

Awards Student Travel Stipend Award

Participants

Yongsik Sim, MD, Seoul, Korea, Republic Of (*Presenter*) Nothing to Disclose Myung Jin Chung, MD, Seoul, Korea, Republic Of (*Abstract Co-Author*) Research Grant, General Electronic Company; Research Grant, Samsung Electronics Co, Ltd; Research Grant, Lunit Inc Elmar C. Kotter, MD, MSc, Freiburg, Germany (*Abstract Co-Author*) Editorial Advisory Board, Thieme Medical Publishers, Inc Synho Do, PhD, Boston, MA (*Abstract Co-Author*) Nothing to Disclose Kyunghwa Han, PhD, Seoul, Korea, Republic Of (*Abstract Co-Author*) Nothing to Disclose Hanmyoung Kim, MS, Suwon, Korea, Republic Of (*Abstract Co-Author*) Employee, Samsung Electronics Co, Ltd Seungwook Yang, PhD, Suwon, Korea, Republic Of (*Abstract Co-Author*) Employee, Samsung Electronics Co, Ltd Dong-Jae Lee, Suwon, Korea, Republic Of (*Abstract Co-Author*) Employee, Samsung Electronics Co, Ltd Byoung Wook Choi, MD, Seoul, Korea, Republic Of (*Abstract Co-Author*) Nothing to Disclose

For information about this presentation, contact:

ysim1@yuhs.ac

PURPOSE

To evaluate performance of radiologists detecting pulmonary malignant nodules assisted by deep-learning based computer-aided detection (CAD) software, compared with performance of radiologist or CAD alone.

METHOD AND MATERIALS

Each of four participating centers in three countries retrospectively collected 150 lung cancer radiographs and 50 normal radiographs. Normal x-ray images are from healthy adults, confirmed by a CT scan taken within 14 days. Each cancer x-ray image has 1 to 3 pathologically confirmed nodule(s), whose sizes are between 1 and 3 centimeters. The estimated location of each nodule was marked on x-ray image referring to the CT scan. 12 radiologists from 4 institutions with various experiences independently analyzed a set of x-ray images and marked region of interests (ROIs) on each radiograph in suspicion of a nodule. Deep learning-based computer-aided detection (CAD) software was applied to find suspicious nodules on chest radiographs. Finally, 12 radiologists reviewed whole set of images with assistance of CAD, accepting or dismissing ROIs suggested by CAD. Sensitivity and false negative per image (FPPI) of radiologist alone, CAD alone and radiologist with CAD were statistically analyzed.

RESULTS

The overall sensitivity and FPPI of the CAD system were 63.75% and 0.20, which was not statistically distinct from those of radiologists. The average sensitivity of radiologists appeared to increase significantly from 65.1% to 70.3%, after aided by the CAD software (p<0.0001). The average FPPI was 0.2 and 0.18, without and with CAD, respectively. The decline of FPPI was significant (p=0.0006). On subgroup analysis, incremental effects of CAD on nodule detection sensitivity were not affected by radiologists' experience, size, location, type (primary or metastatic) of nodules and modality of acquisition.

CONCLUSION

The average sensitivity and FPPI of our CAD system were not statically different from those of radiologists. When radiologists were assisted by the CAD, overall sensitivity increased significantly while FPPI seemed to decrease. Incremental effect of the CAD system was not affected by radiologist's experience, characteristics of a nodule or modality, which can support the potential general use of this software.

CLINICAL RELEVANCE/APPLICATION

Radiologists' performance in lung cancer nodule detection can be improved with a deep learning-based CAD system regarding both sensitivity and false positive rate.

SSG03-03 Nodule Size Measurement: Automatic or Human-Which is Better for Predicting Lung Cancer in a Brock Model?

Tuesday, Nov. 27 10:50AM - 11:00AM Room: S504AB

Participants

Sarim Ather, MBChB, PhD, Oxford, United Kingdom (*Presenter*) Nothing to Disclose Carlos Arteta, Oxford, United Kingdom (*Abstract Co-Author*) Employee, Optellum Ltd Nicholas Dowson, Oxford, United Kingdom (*Abstract Co-Author*) Employee, Optellum Ltd Lyndsey C. Pickup, MEng, DPhil, Oxford, United Kingdom (*Abstract Co-Author*) Employee, Optellum Ltd Petr Novotny, Oxford, United Kingdom (*Abstract Co-Author*) Employee, Optellum Ltd Catarina Santos, Oxford, United Kingdom (*Abstract Co-Author*) Employee, Optellum Ltd Heiko Peschl, Oxford, United Kingdom (*Abstract Co-Author*) Employee, Optellum Ltd Heiko Peschl, Oxford, United Kingdom (*Abstract Co-Author*) Nothing to Disclose Maria Tsakok, Oxford, United Kingdom (*Abstract Co-Author*) Nothing to Disclose William Hickes, MSc, Oxford, United Kingdom (*Abstract Co-Author*) Nothing to Disclose Samia Hussain, Oxford, United Kingdom (*Abstract Co-Author*) Nothing to Disclose Jerome M. Declerck, PhD, Oxford, United Kingdom (*Abstract Co-Author*) Employee, Optellum Ltd; Co-founder, Optellum Ltd Vaclav Potesil, Oxford, United Kingdom (*Abstract Co-Author*) Employee, Optellum Ltd; Co-founder, Optellum Ltd Vaclav Potesil, Oxford, United Kingdom (*Abstract Co-Author*) Employee, Optellum Ltd; Co-founder, Optellum Ltd Vaclav Potesil, Oxford, United Kingdom (*Abstract Co-Author*) Employee, Optellum Ltd Founder, Optellum Ltd Employee, Hocoma AG Timor Kadir, Oxford, United Kingdom (*Abstract Co-Author*) Employee, Optellum Ltd; Fergus V. Gleeson, MBBS, Oxford, United Kingdom (*Abstract Co-Author*) Consultant, Alliance Medical Limited; Consultant, Blue Earth Diagnostics Ltd; Consultant, Polarean, Inc

For information about this presentation, contact:

sarim.ather@ouh.nhs.uk

PURPOSE

To assess the impact of automated segmentation of pulmonary nodules by measuring the accuracy of the prediction of malignancy

using the Brock University Cancer Prediction Model.

METHOD AND MATERIALS

Retrospective analysis was carried out of 7927 nodules (of which 314 were malignant) from 5394 patients who were scanned as part of the US NLST (mean age 62±5 years; of which 3192 were male). Following BTS guidelines, nodules <5mm in size were excluded, but all other nodules were included regardless of type, attenuation, and margin. Automatic 3D nodule segmentations were generated via a deep learned model and initiated with a single click point inside the nodule. We used the following methods for measuring nodule size: the NSLT radiologist measurements, D2D, the long axis from the automatic segmentations, D3D, and in order to characterize the nodule volumes more accurately, the volumes of the automatic segmentations, V, were converted to an equivalent linear size using the equation for a sphere. Each was tested as the size term in the standard Brock model to generate a malignancy risk and Area-Under-the-Receiver-Operating-Characteristics (AUC-ROC) curve calculated.

RESULTS

The AUC-ROC was 85.96% (95% confidence interval (CI): 84.33, 87.76) for D2D, 86.64 (95% CI: 85.04, 88.19) for D3D, and 88.17 (95% CI: 86.71, 89.82) for Dsph. The expected increase in AUC Dsph offers over D2D is 2.21 (95% CI: 1.28, 3.12).

CONCLUSION

The automatic nodule size measurements outperformed the manual radiologist measurements in predicting lung cancer as an input to the Brock model. The non-axial Dsph, which is derived from the volumetric segmentation outperforms both long axis-based methods. Assessing nodule segmentation by measuring prediction efficacy is a viable alternative to overlap measures such as DICE.

CLINICAL RELEVANCE/APPLICATION

Automatic segmentation removes the need for manual extraction of axial diameters of lung nodules. It is not subject to intra- and inter-radiologist variation thereby improving consistency.

SSG03-04 Effect of Artificial Intelligence Based Vessel Suppression and Automatic Detection of Part-Solid and Ground-Glass Nodules on Low-Dose Chest CT

Tuesday, Nov. 27 11:00AM - 11:10AM Room: S504AB

Awards Student Travel Stipend Award

Participants

Ramandeep Singh, MBBS, Boston, MA (*Presenter*) Nothing to Disclose Chayanin Nitiwarangkul, MD, Boston, MA (*Abstract Co-Author*) Nothing to Disclose

Jo-Anne O. Shepard, MD, Boston, MA (*Abstract Co-Author*) Nothing to Disclose

Fatemeh Homayounieh, MD, Chelsea, MA (Abstract Co-Author) Nothing to Disclose

Atul Padole, MD, Boston, MA (Abstract Co-Author) Nothing to Disclose

Shaunagh McDermott, FFR(RCSI), Boston, MA (Abstract Co-Author) Nothing to Disclose

Mannudeep K. Kalra, MD, Boston, MA (Abstract Co-Author) Research Grant, Siemens AG; Research Grant, Canon Medical Systems Corporation

Subba R. Digumarthy, MD, Boston, MA (Abstract Co-Author) Nothing to Disclose

Brent Little, MD, Boston, MA (Abstract Co-Author) Author, Reed Elsevier; Editor, Reed Elsevier

PURPOSE

Most studies with CAD and artificial intelligence (AI) software have focused on solid lung nodules. We assessed the effect of AIbased vessel suppression (AI-VS) and automatic detection (AI-AD) on ground glass (GGN) and part-solid lung nodules (PSN) in lowdose CT (LDCT).

METHOD AND MATERIALS

Our study included 100 LDCT examinations with mixed attenuation pulmonary nodules (average diameter>5mm) identified from the National Lung Cancer Screening Trial (NLST). These exams were not used in training or validation of the AI software (ClearRead CT, Riverain Inc.). All 100 LDCT were processed to generate three image series per case - unprocessed, AI-VS, and AI-AD series with annotated lung nodules. Two thoracic radiologists (R1: 3-year experience, R2: 27-year experience) independently assessed the unprocessed images alone, then together with AI-VS series, and finally with AI-AD. For each assessment, number of all > 5mm with location & size of dominant GGN and PSN were recorded. Descriptive statistics and student t tests were performed for data analysis.

RESULTS

On unprocessed images, R1 and R2 detected 278 nodules (123 PSN, 155 GGN) and 269 (117 PSN, 152 GGN), respectively (p>0.05). With addition of AI-VS images, R1 and R2 detected 290 nodules (126 PSN, 164 SSN) and 293 (132 PSN, 161 GGN), respectively, which were significantly greater than those detected without the AI-VS (p=0.004). AI-VS aided in detection of solid component in 22 PSN which were deemed SSN by both readers. Conversely, AI-AD annotated only 75 PSN and 54 GGN (total 129 nodules). In 21 patients, AI-AD did not detect the dominant PSN or SSN; it detected 14 false positive nodules (vessels, atelectasis, anterior junctional line). Average respective sizes of 69-matched and detected PSN on unprocessed and AI-AD series were 15 ±7 mm and 13 ± 6 mm (p=0.07).

CONCLUSION

AI-VS improves detection and characterization of GGN and PSN on LDCT of the chest. Specifically, improved and easier detection of the solid component in non-solid nodules with AI-VS can avoid false down-grading of Lung-RADS category, and thus help in appropriate patient management.

CLINICAL RELEVANCE/APPLICATION

AI software can aid in improved detection and confident detection of ground-glass and part-solid lung nodules on low dose chest CT.

Honored Educators

Presenters or authors on this event have been recognized as RSNA Honored Educators for participating in multiple qualifying educational activities. Honored Educators are invested in furthering the profession of radiology by delivering high-quality educational content in their field of study. Learn how you can become an honored educator by visiting the website at: https://www.rsna.org/Honored-Educator-Award/ Subba R. Digumarthy, MD - 2013 Honored EducatorBrent Little, MD - 2018 Honored Educator

SSG03-05 Evaluation of Lung Nodules with FDG PET-CT: The Value of MIP Reconstructions in Conventional Thoracic CT Images During Shallow Breathing versus Images in Deep Inspiration

Tuesday, Nov. 27 11:10AM - 11:20AM Room: S504AB

Participants Montserrat Alemany, Uppsala, Sweden (*Presenter*) Nothing to Disclose Tomas Hansen, MD, PhD, Uppsala, Sweden (*Abstract Co-Author*) Nothing to Disclose Carlos Trampal, Uppsala, Sweden (*Abstract Co-Author*) Nothing to Disclose Jens Sorensen, Uppsala, Sweden (*Abstract Co-Author*) Nothing to Disclose

For information about this presentation, contact:

montserrat.alemany.ripoll@akademiska.se

PURPOSE

Detection of small lung nodules is important for apropiate staging of cancer. There is controversy in literature about the value of adding a separate CT of the lungs in deep inspiration. Radiation dose is no longer an issue with the use of modern equipment because only aproximately 3 mSv are added to the usual dose. The purpose of this study was to assess the value of additional thoracic CT in deep inspiration and the use of maximum intensity projection (MIP) reconstructions in PET-CT of oncologic patients.

METHOD AND MATERIALS

186 consecutive patients (99 male and 89 female; mean age,72 years; range: 26-93 y) underwent FDG PET-CT for one of the following indications: characterization of a new detected lung nodule/mass (n=101), staging of cancer (n=31), therapy respons monitoring (n=33), suspicion of tumor relapse (n=19) and cancer of unknown origin (n=2). After PET-CT acquisition with shallow breathing, a thoracic CT in deep inspiration was performed to all patients (slide thickness: 1.25 mm). MIP of the two sets of lung images were performed. Two experienced radiologist analyzed the 4 sets of CT studies. The number of lung nodules was recorded. Lung nodule was defined as a rounded opacity smaller than 10 mm completely surrounded by lung parenchyma. The clinical relevance of the eventual discrepancies between CT studies was analized (i.e. upstaging).

RESULTS

120/186 patients presented with nodules. PET-CT with shallow breathing detected 393 nodules, and 578 when MIP images were analized. Thoracic CT with deep inspiration found 534 nodules and 905 when MIP was used. The number of detected nodules increased from free breathing to breathe hold CT in 42 patients. The detected number of nodules with breath hold technique compared with free breathing increased increased in 51 patients when MIP was used. The extradetected nodules were considered clinical relevant in 7/120 (6%) of patients because they influence patient management for example by increasing TNM staging.

CONCLUSION

According to our results the addition of deep inspiration thoracic CT with MIP reconstructions can be recommended in clinical practice because this approach yields better performance in TNM staging in oncologic patients.

CLINICAL RELEVANCE/APPLICATION

Addition of deep inspiration CT with MIP reconstructions to conventional FDG PET-CT in oncologic patients yields better performance in TNM staging.

SSG03-06 Deep Learning for Rule-Out of Unnecessary Follow-Up in Patients with Incidentally Detected, Indeterminate Pulmonary Nodules: Results on an Independent Dataset

Tuesday, Nov. 27 11:20AM - 11:30AM Room: S504AB

Participants

Heiko Peschl, Oxford, United Kingdom (*Abstract Co-Author*) Nothing to Disclose Carlos Arteta, Oxford, United Kingdom (*Abstract Co-Author*) Employee, Optellum Ltd Lyndsey C. Pickup, MEng, DPhil, Oxford, United Kingdom (*Abstract Co-Author*) Employee, Optellum Ltd; Co-founder, Optellum Ltd Maria Tsakok, Oxford, United Kingdom (*Abstract Co-Author*) Nothing to Disclose Sarim Ather, MBChB, PhD, Oxford, United Kingdom (*Pesenter*) Nothing to Disclose Samia Hussain, Oxford, United Kingdom (*Abstract Co-Author*) Nothing to Disclose William Hickes, MSc, Oxford, United Kingdom (*Abstract Co-Author*) Nothing to Disclose William Hickes, MSc, Oxford, United Kingdom (*Abstract Co-Author*) Research Grant, Mirada Medical Ltd Petr Novotny, Oxford, United Kingdom (*Abstract Co-Author*) Employee, Optellum Ltd Catarina Santos, Oxford, United Kingdom (*Abstract Co-Author*) Employee, Optellum Ltd Emily Fay, Oxford, United Kingdom (*Abstract Co-Author*) Employee, Optellum Ltd Jerome M. Declerck, PhD, Oxford, United Kingdom (*Abstract Co-Author*) Employee, Optellum Ltd Vaclav Potesil, Oxford, United Kingdom (*Abstract Co-Author*) Employee, Optellum Ltd Founder, Optellum Ltd Finitor Kadir, Oxford, United Kingdom (*Abstract Co-Author*) Employee, Optellum Ltd Founder, Optellum Ltd Vaclav Potesil, Oxford, United Kingdom (*Abstract Co-Author*) Employee, Optellum Ltd Founder, Optellum Ltd Fergus V. Gleeson, MBBS, Oxford, United Kingdom (*Abstract Co-Author*) Consultant, Alliance Medical Limited; Consultant, Blue Earth Diagnostics Ltd; Consultant, Polarean, Inc

For information about this presentation, contact:

Heiko.Peschl@ouh.nhs.uk

PURPOSE

To assess the follow-up rule-out accuracy of a convolutional neural network (CNN) in patients with incidentally detected, indeterminate pulmonary nodules in a multi-site, heterogeneous population.

METHOD AND MATERIALS

The US National Lung Screening Trial (NLST) dataset was manually curated and used to create a training set: each reported nodule and cancer was located, contoured and diagnostically characterised (9310 benign nodule patients; 1058 cancer patients). All patients with solid and semi-solid nodules of 6mm and above, where benign nodules and cancers could be confidently identified by clinicians (5972 patients, of which 575 were cancer patients), were selected. A CNN was trained using Deep Learning and three thresholds for benign rule-out were calculated at three levels of sensitivity: 100%, 99.5% and 99%. An independent dataset of patients with incidentally detected indeterminate pulmonary nodules was retrospectively collected from a tertiary referral centre and surrounding hospitals in the UK with a heterogeneous mix of scan parameters, manufacturers and clinical indications (610 patients, 698 nodules, 5-15mm). Diagnosis was established according to British Thoracic Society guidelines (2015). The dataset contained 50 cancers from 47 patients (7% of all nodules). Performance was evaluated by measuring the specificity at the three benign rule-out thresholds; i.e. to measure the proportion of benign nodules correctly stratified while missing no or few cancers. Overall Area-Under-the-ROC-Curve analysis (AUC) was also calculated.

RESULTS

The specificity (sensitivity) was 24% (100%), 24% (100%) and 48.6% (100%) at the three thresholds respectively. AUC was 0.93 (95%CI = 0.90-0.96).

CONCLUSION

On this independent dataset, the CNN was able to correctly classify just under half of the benign nodules whilst not misclassifying any cancers.

CLINICAL RELEVANCE/APPLICATION

Our work shows the potential of CNNs in ruling out benign pulmonary nodules and therefore reducing the need for follow up scans in a large number of patients.

SSG03-07 A Decision Analysis of Follow-Up and Treatment Algorithms for Subsolid Pulmonary Nodules

Tuesday, Nov. 27 11:30AM - 11:40AM Room: S504AB

Participants

Mark M. Hammer, MD, Saint Louis, MO (*Presenter*) Nothing to Disclose Lauren Palazzo, Boston, MA (*Abstract Co-Author*) Nothing to Disclose Andrew Eckel, Boston, MA (*Abstract Co-Author*) Nothing to Disclose Eduardo J. Mortani Barbosa JR, MD, Philadelphia, PA (*Abstract Co-Author*) Nothing to Disclose Chung Yin Kong, PhD, Boston, MA (*Abstract Co-Author*) Nothing to Disclose

For information about this presentation, contact:

markmhammer@gmail.com

PURPOSE

To use simulation modeling based on evidence from the literature to evaluate several management strategies and treatment options for patients with ground glass nodules (GGNs).

METHOD AND MATERIALS

We developed a Monte Carlo model for patients with GGNs as they underwent follow-up per Lung-RADS for up to ten years. Nodules could grow and develop solid components over time. Rates of clinically-significant malignancy were calibrated to data from the National Lung Cancer Screening Trial. We investigated modifications to the follow-up schedule and tested different treatment strategies, specifically lobectomy, radiation therapy, and no therapy.

RESULTS

Overall, 2.3% of nodules represented clinically significant malignancies, and 6.3% of nodules were treated. Only 29.8% of Lung-RADS 4B/4X nodules were clinically-significant malignancies. We compared outcomes of patients with Lung-RADS 2 nodules followed at 1-, 2-, and 3-year intervals; overall survival at 10 years of follow-up was similar, ranging from 74.7% (annual) to 73.5% (triennial). We also evaluated 10-year outcomes from Lung-RADS 4B/4X non-solid nodules treated with different modalities; at 10 years, overall survival was highest in the radiation therapy arm, at 83.9%, and lowest in the no treatment arm, at 78.1%.

CONCLUSION

Our results suggest a conservative approach to the follow-up and treatment of GGNs. The follow-up interval for GGNs can be increased to 3 years with minimal change in outcomes. Our results also favor the use of radiation therapy when a nodule has met criteria for treatment. Prospective randomized trials are needed to evaluate thresholds for management and different treatment modalities for GGNs.

CLINICAL RELEVANCE/APPLICATION

Conservative management strategies for non-solid nodules, such as triennial follow-up for Lung-RADS 2 nodules and radiation therapy instead of lobectomy for Lung-RADS 4B/4X nodules, are preferable to more aggressive treatment.

SSG03-08 A Robust Model for Prediction of Pulmonary Nodule Malignancy with CT Scans

Tuesday, Nov. 27 11:40AM - 11:50AM Room: S504AB

Participants

Jianlin Wu, MD, Dalian, China (*Abstract Co-Author*) Nothing to Disclose Wen Tang, Beijing, China (*Abstract Co-Author*) Employee, Infervision Inc Rongguo Zhang, Beijing, China (*Abstract Co-Author*) Employee, Infervision Inc Tianci Song, Beijing, China (*Abstract Co-Author*) Employee, Infervision Inc Chen Xia, Beijing, China (*Abstract Co-Author*) Nothing to Disclose Yufeng Deng, PhD, Durham, NC (*Presenter*) Employee, Infervision Inc Kai Liu, Shanghai, China (*Abstract Co-Author*) Nothing to Disclose Yi Xiao, Shanghai, China (*Abstract Co-Author*) Nothing to Disclose Shiyuan Liu, PhD, Shanghai, China (*Abstract Co-Author*) Nothing to Disclose

PURPOSE

Pulmonary nodules could be early manifestations of lung cancer, but the morphological complexity makes it difficult to differentiate benign and malignant nodules. This paper proposes two deep learning models aiming to accurately determine the malignancy of pulmonary nodules from CT images.

METHOD AND MATERIALS

Model-1 was adapted from the winning model in Data Science Bowl 2017.. We chose ResNet as its backbone and integrated U-Net and Capsule Network architectures to enable the model to comprehensively capture multiscale features of pulmonary nodules. Model-2 took extracted features from Model-1 as input to a random forest classifier to further predict nodule malignancy, as inspired from the NoduleX model. Two datasets were adopted to validate the performance of the proposed two models. Dataset 1 contains 1061 samples (benign/malignant: 703/353) from Lung Image Database Consortium and Image Database Resource Initiative (LIDC-IDRI), and Dataset 2 consists of 1117 samples (benign/malignant: 354/763) provided by collaborating hospitals. Nodules in both datasets were biopsy or surgery proven, and pathology diagnoses were used as gold standard. We randomly selected 20% from each dataset as the testing set and used the rest 80% as the training set. We trained and tested our two models on the above two datasets respectively.

RESULTS

On Dataset 1 (LIDC-IDRI), Model-1 achieved an AUC of 0.91 in the prediction of pulmonary nodule malignancy while Model-2 achieved an AUC of 0.96. On Dataset 2, Model-1 again reached a high AUC of 0.90, which significantly outperformed the Model-2 with AUC=0.80.

CONCLUSION

Model-1 showed consistently high accuracy in pulmonary nodule malignancy prediction on both the LIDC dataset and CT scans collected from collaborating hospitals. Our two models achieved comparable results with NoduleX model which had got the state-of-the-art performance in LIDC dataset. The experimental results demonstrated that Model-1 showed more stable performance across datasets and had better model robustness. The strength of Model-1 may lie in its Capsule Network structure that could extract more universally informative features and the end-to-end deep learning architecture.

CLINICAL RELEVANCE/APPLICATION

Our proposed model can serve as a useful tool for early diagnosis of lung cancer and has the potential to be applied in clinical treatment planning.

SSG03-09 External Validation of the McWilliams Model to Predict Probability of Cancer in Pulmonary Nodules using NLST Data

Tuesday, Nov. 27 11:50AM - 12:00PM Room: S504AB

Participants Audrey Winter, PhD, Los Angeles, CA (*Presenter*) Nothing to Disclose William Hsu, PhD, Los Angeles, CA (*Abstract Co-Author*) Research Grant, Siemens AG

For information about this presentation, contact:

AWinter@mednet.ucla.edu

PURPOSE

Lung cancer screening results in the discovery of an estimated 1.57 million screen- and incidentally-detected pulmonary nodules. Prediction models, which estimates the probability of lung cancer in pulmonary nodules detected on computed tomography (CT) can potentially aid in manage patients and minimize overdiagnosis. Thus, we performed an external validation of an existing model developed by McWilliams et al (doi:10.1056/NEJMoa1214726).

METHOD AND MATERIALS

Based on the inclusion/exclusion criteria stated by McWilliams, we identified 7,879 non-calcified nodules greater than 4 mm discovered at the baseline CT screening with at least 2 years of follow-up using data from the CT arm of the National Lung Screening Trial (NLST). We assessed model discrimination (the ability to distinguish between cancer/not cancer) and calibration (the agreement between predicted and observed probabilities). We identified differences between PanCan, the derivation dataset, and NLST. The regression coefficient and the intercept coefficient were estimated by fitting a logistic regression on NLST. We also attempted to update and recalibrate the model. Finally, we evaluated whether the addition of new covariates such as body mass index, smoking status, pack-years and asbestos improved performance.

RESULTS

While the AUC of the model was good 0.905 [0.882-0.928]), the histogram plot showed that whether a nodule was cancer/not cancer could not be well-separate (see Figure, left). The calibration plot showed that the model tended to overestimate the probability of cancer. Following methods in Steyerberg et al (doi: 10.1002/sim.1844), the updated model achieved an AUC of 0.914 [0.892-0.936] and a better calibration (see Figure, right). Emphysema (p=0.03) and nodule spiculation (p<0.01) had a significantly different effect in the NLST cohort compared to the PanCan. Among the new covariates, only the pack-year history was found to be significant (p<0.01).

CONCLUSION

While the model achieved high AUC, discrimination and calibration remain suboptimal, motivating our efforts to improve additional clinical, imaging, and the evolution of covariates over time that could influence performance.

CLINICAL RELEVANCE/APPLICATION

External validation is necessary to access constalizability of a prediction model to new patients. We show how discrimination and

external valuation is necessary to assess generalizability of a prediction model to new patients, we show now discrimination and calibration can be examined to assess how models can likely enter in clinical practice.



SSG06

Informatics (Artificial Intelligence in Radiology: No Pixels or Fake Pixels)

Tuesday, Nov. 27 10:30AM - 12:00PM Room: N230B



AMA PRA Category 1 Credits ™: 1.50 ARRT Category A+ Credit: 1.00

FDA Discussions may include off-label uses.

Participants

Luciano M. Prevedello, MD, MPH, Dublin, OH (*Moderator*) Nothing to Disclose Norio Nakata, MD, Tokyo, Japan (*Moderator*) Nothing to Disclose John Mongan, MD,PhD, San Francisco, CA (*Moderator*) Research funded, General Electric Company; Research funded, Enlitic, Inc; Consultant, Siemens AG; Spouse, Employee, AbbVie Inc George L. Shih, MD, MS, New York, NY (*Moderator*) Consultant, Image Safely, Inc; Stockholder, Image Safely, Inc; Consultant, MD.ai, Inc; Stockholder, MD.ai, Inc;

Sub-Events

SSG06-01 Deep Learning for the Automatic Detection of Urgent Radiology Findings from Free-Text Radiology Reports

Tuesday, Nov. 27 10:30AM - 10:40AM Room: N230B

Participants

Yuhao Zhang, Stanford, CA (*Presenter*) Nothing to Disclose Ian Pan, MA, Providence, RI (*Abstract Co-Author*) Nothing to Disclose Derek Merck, PhD, Providence, RI (*Abstract Co-Author*) Nothing to Disclose Jonathan S. Movson, MBChB, Providence, RI (*Abstract Co-Author*) Nothing to Disclose Matthew T. Stib, MD, Providence, RI (*Abstract Co-Author*) Nothing to Disclose Christopher Manning, Stanford, CA (*Abstract Co-Author*) Nothing to Disclose Curtis P. Langlotz, MD,PhD, Menlo Park, CA (*Abstract Co-Author*) Advisory Board, Nuance Communications, Inc; Shareholder, whiterabbit.ai; Advisory Board, whiterabbit.ai; Shareholder, Nines.ai; Consultant, Nines.ai; Shareholder, TowerView Health; Research Grant, Koninklijke Philips NV; Research Grant, Siemens AG; Research Grant, Alphabet Inc;

For information about this presentation, contact:

zyh@stanford.edu

PURPOSE

Reliably identifying and communicating urgent radiology findings are crucial to the diagnosis and treatment of diseases. We describe a deep learning algorithm to automatically detect urgent radiology findings from free-text reports and evaluate its performance on a multi-institutional corpus.

METHOD AND MATERIALS

Radiology reports of 156,992 studies from Nov. 2017 to Feb. 2018 were collected from 3 hospitals. These reports were categorized by experts using 4 levels of acuity (1=normal, 2=routine, 3=priority and 4=critical). Reports also received a binary label as requiring follow-up or not. We randomly stratified the reports into a 70% training, a 10% validation, and a 20% test set. For classification we developed a 2-layer long short-term memory (LSTM) network followed by a term weighting layer. We then use the weighted sum of the LSTM states as a vector representation of the report to get the probabilistic estimate of the urgency level. To enable knowledge transfer from a larger corpus, we trained word vectors with the GloVe algorithm on 4.5 million reports and use them to initialize the word vectors used in our network. Additionally, the term weighting layer provided interpretable information about which words were weighted most heavily towards the decision.

RESULTS

We evaluate our algorithm on 3 tasks: (1) binary classification of the reports into urgent (categories 3-4) vs. non-urgent (categories 1-2) findings; (2) binary classification into follow-up vs. non-follow-up recommended; and (3) 4-way classification for acuity categories 1-4. Results for task 1, 2, and 3 are AUC=0.951, AUC=0.961, and micro-averaged F1=0.846, respectively. In comparison, a baseline naive Bayes classifier with hand-tuned lexical features achieves 0.911, 0.915, and 0.773 for the 3 tasks. Task 3 F1 drops to 0.833 when we initialize the word vectors randomly, suggesting that some knowledge was transferred from the larger corpus. Term weighting results showed the network placed a high weight on 'no abnormalities' for normal studies or 'large effusion' for priority studies.

CONCLUSION

Deep learning algorithms can reliably detect urgent radiology findings from free-text radiology reports and provide highly interpretable results.

CLINICAL RELEVANCE/APPLICATION

Automatic detection of urgent radiology findings with natural language processing and deep learning is a useful technique for

SSG06-02 Automated Determination of Radiology Reports Requiring Urgent Communication Using Intelligent Word Embeddings

Tuesday, Nov. 27 10:40AM - 10:50AM Room: N230B

Awards

Trainee Research Prize - Medical Student

Participants

Scott B. Werwath, Berkeley, CA (*Presenter*) Nothing to Disclose Hari Trivedi, MD, San Francisco, CA (*Abstract Co-Author*) Nothing to Disclose Jason F. Talbott, MD, PhD, San Francisco, CA (*Abstract Co-Author*) Nothing to Disclose Thienkhai H. Vu, MD, PhD, San Francisco, CA (*Abstract Co-Author*) Nothing to Disclose Youngho Seo, PhD, San Francisco, CA (*Abstract Co-Author*) Nothing to Disclose Jae Ho Sohn, MD, San Francisco, CA (*Abstract Co-Author*) Nothing to Disclose

For information about this presentation, contact:

sohn87@gmail.com

CONCLUSION

The model performed extremely well at the task of detecting urgent findings in radiology reports. This model can be further tested in real clinical workflow to further assess its value as a detection tool.

Background

Radiology exams can reveal findings that require the immediate attention of clinicians. Radiologists are responsible for ensuring communication of urgent findings because it may affect patient safety and management. Leveraging Natural Language Processing (NLP) and machine learning (ML) techniques, we developed a model that can predict the likelihood that a radiology report contains findings that require urgent communication.

Evaluation

80,649 radiology reports from a variety of modalities and body parts were extracted from a single institution. Reports were labeled as containing urgent findings if the impression included phrases like 'results communicated to'; these phrases were then removed from the reports to blind the model to ground-truth. Feature selection followed the 'Intelligent Word Embeddings' model: applying standard tokenization, performing negation and phrase identification, using RadLex for synonym detection, and training fastText document embeddings on the processed reports. A variety of different classifiers (convolutional neural network, support vector machine, random forests, and multi-layer perceptions (MLP)) were trained on the document embedding vectors. The accuracies of the classifiers were compared on an internal test set of 8,779 reports and an external test set from a different hospital of 20,208 reports.

Discussion

The linear bag-of-words MLP was the best performing model, achieving an ROC-AUC of 0.94 on validation data, which corresponded to 84% accuracy at 90% sensitivity and an F1 score of 0.87. The model also achieved ROC-AUCs of 0.90 and 0.87 on the internal and external test data, respectively. A web version of the model is also provided for real-time and crowdsourced review: bit.ly/2Ikhce1

SSG06-03 Rule-Based Natural Language Processing Algorithm for Automated Parsing of Clinical Radiology Reports

Tuesday, Nov. 27 10:50AM - 11:00AM Room: N230B

Participants

Sasank Chilamkurthy, BEng, Mumbai, India (*Abstract Co-Author*) Employee, Qure.ai Swetha Tanamala, BEng, MENG, Mumbai, India (*Presenter*) Employee, Qure.ai Rohit Ghosh, BEng, MENG, Mumbai, India (*Abstract Co-Author*) Employee, Qure.ai Pooja Rao, MBBS, PhD, Mumbai, India (*Abstract Co-Author*) Employee, Qure.ai Mustafa Biviji, MBBS, DMRD, Nagpur, India (*Abstract Co-Author*) Nothing to Disclose

For information about this presentation, contact:

sasank.chilamkurthy@qure.ai

PURPOSE

Clinical radiology reports are usually written in free-form text rather in a structured format. In this work, we develop and validate rule based natural language processing (NLP) algorithm to parse these reports into structured data consumable by other information systems.

METHOD AND MATERIALS

Anonymized clinical radiology reports of 290,155 (development dataset) and 1,779 (Q2k dataset) head CT scans were used to develop and validate the algorithms. Target findings were intracranial hemorrhage and its subtypes, intraparenchymal, intraventricular, subdural, extradural and subarachnoid hemorrhages, skull fracture, midline shift and mass effect. Rules based on keywords and regular expressions were constructed to account for the variations in reporting of the these findings in development dataset. Additionally, grammar rules were created to identify the negations in a sentence. To validate the results of this rule based algorithm, we established gold standards of Q2k dataset by manually going through them. We measure sensitivity and specificity of the algorithm for each finding against this gold standard.

RESULTS

Average sensitivity and specificity of the algorithm across the target findings on Q2k dataset are 0.9841 and 0.9956 respectively.

Least performing finding was subdural hemorrhage with sensitivity of 0.9318 (95% CI 0.8134-0.9857) and specificity of 0.9965 (95% CI 0.9925-0.9987) while skull fracture was inferred perfectly with sensitivity of 1 (95% CI 0.9745-1.000) and specificity of 1 (95% CI 0.9977-1.000). A previous similar study on head CT reports, but with machine learning based NLP algorithms, reported average sensitivity and specificity of 0.9025 and 0.9172 across findings.

CONCLUSION

In this work, we showed that rule based NLP algorithms can identify the findings from free text clinical radiology reports with very high accuracies. Their performance is superior to that of machine learning based NLP algorithms which require annotation of reports instead of rule creation.

CLINICAL RELEVANCE/APPLICATION

This algorithm can be used to retrieve studies with desired findings from a PACS for research or educational purposes, or to train AI algorithms.

SSG06-05 Restoration of Motion-corrupted MR Images Using Deep Adversarial Networks

Tuesday, Nov. 27 11:10AM - 11:20AM Room: N230B

Participants

Karim Armanious, MSc, Stuttgart, Germany (*Presenter*) Nothing to Disclose Thomas Kuestner, DIPLENG, Stuttgart, Germany (*Abstract Co-Author*) Nothing to Disclose Sergios Gatidis, MD, Tubingen, Germany (*Abstract Co-Author*) Nothing to Disclose Bin Yang, PhD,DIPLENG, Stuttgart, Germany (*Abstract Co-Author*) Nothing to Disclose

PURPOSE

Motion artifacts are a frequent source of image quality deterioration in MRI. Existing motion correction strategies mostly focus on prospective compensation of motion artifacts during acquisition. Currently, strategies for retrospective correction of acquired MR images are very limited. The purpose of this work is to implement and evaluate a framework for retrospective restoration of motion-corrupted MR images using deep adversarial networks.

METHOD AND MATERIALS

Our proposed framework consists of two main components trained simultaneously. The first component is a multi-scale deep architecture consisting of 70 convolutional layers for high-resolution image restoration of MR images. The second component is a convolutional neural network (CNN), which classifies the output of the first multi-scale network as realistic or not. The training of the network is done in the adversarial fashion of generative-adversarial networks, where competition between the two components drives the multi-scale network to improve its performance until a detailed motion-free MR image is acquired. The framework was trained on a dataset of 1500 T1 weighted MR images of the head and pelvis regions from 11 volunteers. Image data were paired such that a motion-free and a motion-corrupted image were acquired. Evaluation of the trained model was carried out on a separate dataset of 600 MR images from 4 patients. The quality of the motion corrected images was attested quantitatively in comparison to MR images without motion correction using the SSIM metric. Additionally, qualitative performance was rated by 2 radiologists using a 4-point score (4: best).

RESULTS

The developed framework achieved state-of-the-art results on MR motion correction for rigid motion artifacts. Motion-corrected images achieved an average score of 2.9 by radiologists in comparison to 1.2 for images without motion correction and to 3.7 for motion-free MR images. In addition, SSIM score of motion corrected images has improved by 27.3 % indicating a remarkable reduction of artifacts.

CONCLUSION

Motion artifacts can be retrospectively corrected using a deep adversarial framework, enabling a high-resolution restoration of MR images.

CLINICAL RELEVANCE/APPLICATION

This project enables the extraction of valuable information from motion-corrupted MR images. This can be used to enhance the accuracy of post-processing tasks, such as segmentation and organ volume estimation.

SSG06-06 Predicting Exam Cancellations Using Machine Learning: Towards Optimized Radiology Scheduling

Tuesday, Nov. 27 11:20AM - 11:30AM Room: N230B

Participants

William Hsu, PhD, Los Angeles, CA (*Presenter*) Research Grant, Siemens AG Jay Won, Los Angeles, CA (*Abstract Co-Author*) Nothing to Disclose Sarah E. Luery, Los Angeles, CA (*Abstract Co-Author*) Nothing to Disclose Cleo K. Maehara, MD, Brookline, MA (*Abstract Co-Author*) Nothing to Disclose

For information about this presentation, contact:

whsu@mednet.ucla.edu

PURPOSE

The capacity of a radiology department is constrained by the number of imaging slots, which is related to the availability of imaging equipment. However, while slots may be filled in advance, last minute cancellations and no-shows may result in underutilization that could have otherwise accommodated additional patients. We evaluated the use of a machine learning approach called gradient boosting trees that were trained on scheduling and medical record data to predict whether an exam would be canceled.

METHOD AND MATERIALS

Using data from 150,000 past scheduled exams during a 2 year time period, we examined whether each exam was completed or

canceled. Metadata about an exam such as its description, modality, anatomical region, duration, site/location, patient demographics (age, gender, associated diagnostic codes), and timestamps (date of scheduling, exam completion) were used as inputs to the model. For each cancellation, we recorded the date and reason. A gradient boosting is a machine learning method that generates a set of decision trees from training data by minimizing the average value of a loss function and incrementally expanding the model. A final prediction is generated based on the collective sum of each tree's prediction. A five-fold cross-validation was used to train and test the model. A random sample of 6,000 exams was set aside from each training set to tune the model hyperparameters.

RESULTS

A total of 44,928 exams (30%) were canceled, many of which are provider-initiated (e.g., erroneous order). Of the canceled exams, 13,962 (31%) were canceled by the patient (in advance or no-show). The average area under the curve across all of the folds was 0.742 + -0.004. The most predictive features included patient age, day/time of the scheduled exam, location, and whether the exam was an x-ray or ultrasound.

CONCLUSION

We demonstrate a prediction model with a limited set of clinical and exam variables is still capable of yielding meaningful predictions. We are exploring other factors such as the distance of the patient to the imaging site, weather and traffic, prior history of cancellations, and payor as ways to improve the model's accuracy.

CLINICAL RELEVANCE/APPLICATION

A model to predict exam cancellations may assist departments with identifying and avoiding such occurrences through outreach (e.g., proactive reminders) and mitigation of underlying issues (e.g., difficulty coming to the site, denial by payors).

SSG06-07 Generative Adversarial Neural Networks in the Creation of Synthetic Chest Radiographs: Can We Fool the Experts?

Tuesday, Nov. 27 11:30AM - 11:40AM Room: N230B

Participants

Ishan Deshpande, Chamaign, IL (*Presenter*) Nothing to Disclose Alex G. Schwing, PhD, Urbana, IL (*Abstract Co-Author*) Nothing to Disclose Sanmi Koyejo, PhD, Urbana, IL (*Abstract Co-Author*) Nothing to Disclose Nasir A. Siddiqui, MD, Oak Brook, IL (*Abstract Co-Author*) Nothing to Disclose Ayis T. Pyrros, MD, Hinsdale, IL (*Abstract Co-Author*) Research Consultant, Document Storage Systems, Inc David A. Forsyth, PhD, Urbana, IL (*Abstract Co-Author*) Nothing to Disclose

For information about this presentation, contact:

ayis.pyrros@dupagemd.com

PURPOSE

Generative Adversarial Neural Networks (GANs), are a form of unsupervised machine learning, utilizing competitive neural networks, which can synthesize realistic images unique from training data. GANs can theoretically allow a near limitless supply of unique and HIPAA compliant cases, which could be used for both computer and human training. The purpose of this study was to determine if chest radiographs synthesized from a GAN could fool radiologists.

METHOD AND MATERIALS

A GAN was trained using a sliced Wasserstein distance criterion, with modifications to suppress variance in the estimate of the sliced Wasserstein distance. Training data is the NIH Chest X-ray8 dataset, using 60,000 images. All frontal radiographic views were used regardless of findings. Synthetic radiographs, 512x512 pixels, were created in PNG format. De novo real/acquired chest radiograph images and synthetic images were randomly assorted into testing sets consisting of pairs of one real and one synthetic image, with the same resolution. These images were then presented to 12 ABR-certified radiologists, with a median experience of 10-15 years. The radiologists were then asked to distinguish between synthetic and real images using a two-alternative forced choice, with random timers between 2-10 seconds. Subjects were presented with as many pairs as they were willing to judge.

RESULTS

GAN training took approximately 70 hours on an NVIDIA P100. The generation of a synthetic image takes on average 2ms on an NVIDIA Titan-X. Overall, expert readers were able to detect the synthetic image in 61% of over 1300 pairs viewed (chance is 50%; this corresponds to a sensitivity of 61% and a specificity of 39%). There is significant variation between subjects, with some subjects reliably able to identify real images quite accurately (3 % of GAN images identified as real) and others reliably detecting GAN images as real (85%).

CONCLUSION

Current GAN methods can generate unique realistic chest radiographs in arbitrary quantities. These radiographs can pass as real images, when presented to radiologists.

CLINICAL RELEVANCE/APPLICATION

Current applications include anonymizing datasets and training images for humans and machines. Improvements could allow generating images guaranteed to contain a particular disease, to show a rare disease state, enhance image quality, create unique views, or to show possible future disease states implied by a current radiograph.

SSG06-08 Realistic CT Images Generation Using Condition Generative Adversarial Network (cGAN) for Accurate Segmentation of Hemorrhagic Stroke

Tuesday, Nov. 27 11:40AM - 11:50AM Room: N230B

Participants Manohar Karki, Lowell, MA (*Presenter*) Nothing to Disclose For information about this presentation, contact:

mkarki@caidesystems.com

PURPOSE

Investigate the quality of synthetic brain CT images generated using a cGAN, and their use as augmentation data for accurate detection and dilineation of hemorrhagic stroke.

METHOD AND MATERIALS

Well labeled intracranial hemorrhage on 33391 CT images from 2647 patients consisting of 5 subtypes: intraparenchymal, intraventricular, subarachnoid, epidural and subdural hemorrhages were obtained. Existing GAN implementation on tensorflow framework and images of 256 x 256 were used. Images from 80% of patients were used for training and 20% set aside for testing. Segmented ground truth images were used as the condition to steer the generation process. 2.5%, 10% and 50% of original training data were trained for 10, 50, 100 and 200 epochs each. Because evaluating generated images using a single traditional metric did not reflect the quality of images well, we used a combination of metrics. FCN Scores, Clarity (based on average blurriness) and a classifier that distinguishes between generated images and original images at various thresholds were used. FCN scores were obtained by evaluating the dice similarity coefficients (DSC) of generated images on an existing segmentation algorithm specifically trained only on the original dataset. The best GAN model chosen was then used to generate additional images as training to improve a fully convolutional neural network (FCN) for segmentation.

RESULTS

Using 2.5% of original data, generated images helped to increase sensitivity by 16.7% and DSC by 38%. The increase using 10% of original data was 56.5% and 28.8% for sensitivity and DSC respectively. Whereas using 50% of original data, the increase was 26.7% and 22.6% for sensitivity and DSC respectively.

CONCLUSION

Conditional GANs were effective in generating realistic images that increased detection and delineation performance compared to model trained with just original data. Both dice coefficients and sensitivity increased with the usage of synthetic CT images as augmentation.

CLINICAL RELEVANCE/APPLICATION

Realistic synthetic images generated from accurate labels could help studies and medical tools that rely on access to labeled medical images for training and validation.

SSG06-09 Self PET Attenuation Correction Using Conditional Generative Adversarial Networks

Tuesday, Nov. 27 11:50AM - 12:00PM Room: N230B

Participants

Karim Armanious, MSc, Stuttgart, Germany (*Presenter*) Nothing to Disclose Marc Fischer, MSc, Stuttgart, Germany (*Abstract Co-Author*) Nothing to Disclose Bin Yang, PhD,DIPLENG, Stuttgart, Germany (*Abstract Co-Author*) Nothing to Disclose Sergios Gatidis, MD, Tubingen, Germany (*Abstract Co-Author*) Nothing to Disclose

PURPOSE

Current methods for PET attenuation correction rely on the existence of an attenuation map generated by a second imaging modality which is mostly CT. In certain situations, CT is not available and attenuation correction is performed by estimating an attenuation map using MRI or by importing externally acquired CT images. In this work, we present and evaluate a framework for self attenuation correction of PET data using conditional Generative Adversarial Networks (cGAN) which does not require an accompanying modality.

METHOD AND MATERIALS

The principle idea of the proposed method is to generate an artificial CT image only based on non-corrected PET data. This CT image can then be used for subsequent PET attenuation correction. Our method is based on a cGAN trained on a dataset of corresponding PET/CT brain images from 38 patients. The cGAN consists of three separate convolutional neural networks (CNNs). The first network translates an uncorrected PET image into a synthetic corresponding CT image. The two remaining networks compare the low and high-frequency components respectively between the synthetically generated CT images and the ground-truth CT images. As a result, the generator network is able to match the global structure as well as the texture and style of the desired output. The proposed method was evaluated on a dataset of PET/CT images of the head region from 8 patients. Quantitative comparison between synthetic and ground truth CT images was carried out using the Structural SIMilarity (SSIM) index. In addition, qualitative performance to judge the clinical fidelity of the synthetic CT images was rated by 2 radiologists using a 4-point score (4: best).

RESULTS

The developed method succeeded in translating uncorrected input PET images into highly realistic synthetic CT images. The image quality of synthetic CT images received an average score of 3.1 by radiologists in comparison to 3.7 for real images. Quantitative correlation between our synthetic CT images and corresponding ground truth CT images is indicated by an SSIM score of 0.914.

CONCLUSION

Attenuation correction of PET images without further image modalities is feasible and could be achieved by utilizing cGANs.

CLINICAL RELEVANCE/APPLICATION

The proposed method can be used for fast and reliable attenuation correction of PET data in situations where no CT can be

acquired for this purpose. An extension to whole body imaging is conceivable.



SSG08

Musculoskeletal (Machine Learning and Artificial Intelligence)

Tuesday, Nov. 27 10:30AM - 12:00PM Room: S102CD



AMA PRA Category 1 Credits ™: 1.50 ARRT Category A+ Credit: 1.75

FDA Discussions may include off-label uses.

Participants

Martin Torriani, MD, Lincoln, MA (*Moderator*) Nothing to Disclose Bao H. Do, MD, Stanford, CA (*Moderator*) Nothing to Disclose

Sub-Events

SSG08-01 SpineNet: Automated Vertebra and Disc Gradings Using Deep Learning

Tuesday, Nov. 27 10:30AM - 10:40AM Room: S102CD

Participants

Timor Kadir, Oxford, United Kingdom (*Presenter*) Employee, Optellum Ltd; Andrew Zisserman, PhD, MA, Oxford, United Kingdom (*Abstract Co-Author*) Nothing to Disclose Jeremy Fairbank, Oxford, United Kingdom (*Abstract Co-Author*) Nothing to Disclose Amir Jamaludin, Oxford, United Kingdom (*Abstract Co-Author*) Nothing to Disclose Jill Urban, Oxford, United Kingdom (*Abstract Co-Author*) Nothing to Disclose

PURPOSE

To assess the performance of an fully automated deep learning method in producing radiological gradings of spinal MRI in the context of management of chronic back pain

METHOD AND MATERIALS

A dataset comprising images of 12,018 individual discs from 2009 patients were retrospetively collected from 6 different referrral centers in the UK, Hungary, Slovenia and Italy in a previous EU project (Genodisc). The primary selection for recruitment to Genodisc was "patients who seek secondary care for their back pain or spinal problem" and were sourced from routine clinical management. The MRI machines and protocols varied between the sites but included at least one standard T2 sagittal MRI acquisition which, for consistency, was used for all of the results reported here, though the system is capable of using the T1 and axial images also. The scans were annotated with the following radiological scores by a single experienced spinal radiologist: Pfirmann grade, disc narrowing, endplate defects, marrow changes, spondylolisthesis and central canal stenosis. To test the radiologist's intra-rater variability, they repeated their grading on a subset of 200 patients randomly interdispersed throughout the entire dataset. For training, the dataset was split into a 80:10:10 train:validation:test sets on a per patient basis (not per disc). This resulted in 1806 patients (10,836 discs) for training and 203 patients (1,224 discs) for testing. A multi-class Convolutional Neural Network (CNN) was trained using Deep Learning to predict all of the gradings. Accuracy was measured by comparing the output of the system to the radiologist annotations using class-balanced accuracy. Multi-way cross-validation was used to test the efficacy and repeatability of the system.

RESULTS

The average class balanced accuracy for the SpineNet system was 86.3% (+/- 0.3). This compares favourably to the radiologists intra-rater repeatability of 82.5%.

CONCLUSION

The SpineNet system can produce accurate and repeatable gradings for a range of spinal MRI radiological gradings used in chronic back-pain clinical management and research. Such gradings may be used to augment the radiologist report, improve consistency and communication with the referring physician.

CLINICAL RELEVANCE/APPLICATION

Quantitative gradings of spinal degeneration may be a useful adjunct to routine qualitative report of spinal MRI and improve communication with the referring phylcian.

SSG08-02 Can a Machine Diagnose an Anterior Cruciate Ligament Tear? Fully-Automated Detection System Using Deep Learning

Tuesday, Nov. 27 10:40AM - 10:50AM Room: S102CD

Participants Bochen Guan, Madison, WI (*Abstract Co-Author*) Nothing to Disclose Fang Liu, PhD, Madison, WI (*Abstract Co-Author*) Nothing to Disclose Humberto G. Rosas, MD, Madison, WI (*Abstract Co-Author*) Nothing to Disclose Kevin Lian, Verona, WI (*Abstract Co-Author*) Nothing to Disclose Ali Guermazi, MD, PhD, Boston, MA (*Abstract Co-Author*) Shareholder, Boston Imaging Core Lab, LLC ; Research Consultant, Merck KGaA; Research Consultant, sanofi-aventis Group; Research Consultant, TissueGene, Inc; Research Consultant, OrthoTrophix, Inc; Research Consultant, AstraZeneca PLC; Research Consultant, General Electric Company; Research Consultant, Pfizer Inc Richard Kijowski, MD, Madison, WI (*Presenter*) Research support, General Electric Company; Consultant, Boston Imaging Core Lab, LLC

For information about this presentation, contact:

N/A

PURPOSE

To investigate the use of a deep learning (DL) approach to create a fully-automated prediction model for detecting anterior cruciate ligament (ACL) tears of the knee joint.

METHOD AND MATERIALS

The propsed deep learning approach consisted of two neural networks connected in a cascaded fashion to create a fullyautomated processing pipeline. The first network performed rapid segmentation of the intercondylar notch on two to three consecutive image slices, while the second classification network evaluated structural abnormalities within the segmented anatomic region. Sagittal proton density-weighted fast spin-echo (PD-FSE) and fat-suppressed T2-weighted fast spin-echo (T2-FSE) sequences were acquired using the same 3T scanner on the knees of 200 subjects (100 subjects with a torn ACL and 100 subjects with an intact ACL at subsequently performed knee arthroscopy). The DL method was trained to detect ACL tears using both the PD-FSE and T2-FSE images on 100 randomly chosen subjects and evaluated on the remaining 100 subjects. Diagnostic performance of the DL method was assessed with receiver operation characteristic (ROC) and area under curve (AUC) analysis using arthroscopy as the reference standard. The diagnostic performance of a musculoskeletal radiology fellow and an experienced fellowship-trained musculoskeletal radiologist for detecting ACL tears in the same subject poulation was also calculated.

RESULTS

For the fellow and radiologist, the sensitivity (95%CI) for detecting ACL tears was 94% (81%-99%) and 97% (86%-100%) respectively, while the specificity (95%CI) was 98% (92%-100%) and 98% (92%-100%) respectively. In comparison, the sensitivity (95%CI) and specificity (95%CI) for the DL method for detecting ACL tears at the optimal threshold by the Youden index was 89% (74%-97%) and 98% (92%-100%) respectively. The AUC (95%CI) for the DL method was 0.942 (0.876-0.979, p<0.001), indicating high overall diagnostic performance.

CONCLUSION

A fully-automated DL approach showed high diagnostic performance for detecting surgically confirmed ACL tears, but its sensitivity was slightly lower than human readers indicating the need for larger training datasets to maximize diagnostic performance.

CLINICAL RELEVANCE/APPLICATION

A fully-automated DL approach trained on a small image dataset shows promise for detecting ACL tears but requires further optimization to achieve diagnostic performance comparable to human readers.

Honored Educators

Presenters or authors on this event have been recognized as RSNA Honored Educators for participating in multiple qualifying educational activities. Honored Educators are invested in furthering the profession of radiology by delivering high-quality educational content in their field of study. Learn how you can become an honored educator by visiting the website at: https://www.rsna.org/Honored-Educator-Award/ Ali Guermazi, MD, PhD - 2012 Honored Educator

SSG08-03 Deep Learning For CT Spine Fracture Detection

Tuesday, Nov. 27 10:50AM - 11:00AM Room: S102CD

Awards

Student Travel Stipend Award

Participants Karen Cheng, MD, Orange, CA (*Presenter*) Nothing to Disclose Charles Lin, Irvine, CA (*Abstract Co-Author*) Nothing to Disclose Daniel S. Chow, MD, Orange, CA (*Abstract Co-Author*) Nothing to Disclose Peter Chang, MD, San Francisco, CA (*Abstract Co-Author*) Nothing to Disclose

For information about this presentation, contact:

pchang077@gmail.com

PURPOSE

To evaluate a multi-step deep learning tool, based on convolutional neural networks (CNN), for fully-automated localization of vertebral bodies and detection of fracture on CT.

METHOD AND MATERIALS

After IRB approval, an institutional database was queried to identify patients with cervical, thoracic or lumbar CT obtained between January 2016 and 2017. For each patient, sagittal bone reconstructions were used to manually generate bounding cubes for each vertebral body. Additionally, all levels with a vertebral body fracture were identified. Final annotations were confirmed through visual inspection by a board-certified radiologist. A 3D mask R-CNN architecture based on a feature pyramid backbone was used to regress bounding cube locations for each vertebrae (Figure 1A). Subsequently, each vertebrae was cropped, resampled and used as input into a second 3D residual CNN for detection of fracture (Figure 1B). The 34-layer residual CNN architecture was implemented with bottleneck layers and all-convolutional design (no pooling). Performance was assessed on per vertebrae and per patient levels.

RESULTS

A total of 440 patients were included in this study. 88 of which had at least one vertebral body fracture. Overall. 174 of 3.206

individual levels contained a fracture. Accuracy, AUC, sensitivity, specificity, PPV and NPV were 0.961, 0.956, 0.845, 0.967, 0.590, 0.991 (per-vertebrae) and 0.859, 0.836, 0.875, 0.823, 0.558, 0.963 (per-patient). Combined, serial inference for the 3D mask R-CNN followed by the 3D residual CNN required 2.19 seconds per patient on a single GPU workstation.

CONCLUSION

A custom deep learning based tool is accurate for detection of vertebral body fracture. Given the potential subtle appearance of fractures and high resolution of CT spine imaging, a two-part serial architecture was required to integrate complimentary large field-of-view (vertebral body localization) and small field-of-view (fracture detection) information needed for this task.

CLINICAL RELEVANCE/APPLICATION

A high-performing deep learning tool for CT spine fracture detection can be used for rapid triage in the acute trauma setting, optimizing radiology workflow and expediting patient care.

SSG08-04 Automatic Detection of Distal Radius Fractures in X-Ray Images using Deep Learning

Tuesday, Nov. 27 11:00AM - 11:10AM Room: S102CD

Participants

Christian A. Bluethgen, MD,MSc, Zurich, Switzerland (*Presenter*) Nothing to Disclose Ilaria Vittoria de Martini, Zurich, Switzerland (*Abstract Co-Author*) Nothing to Disclose Anton S. Becker, MD, Zurich, Switzerland (*Abstract Co-Author*) Nothing to Disclose Thomas Frauenfelder, MD, Zurich, Switzerland (*Abstract Co-Author*) Nothing to Disclose

For information about this presentation, contact:

christian.bluethgen@usz.ch

PURPOSE

The aim of this study was to evaluate the diagnostic performance of a multi-purpose, deep-learning based image analysis software for the detection of wrist fractures.

METHOD AND MATERIALS

In this retrospective study, patients with suspected wrist fractures on X-ray imaging studies ordered by the ER department between 2016 and 2017 were included. After applying exclusion criteria (e.g. presence of osteosynthesis material), the remaining X-ray images were labeled for the presence of radius fractures. In uncertain cases, CT studies were consulted, excluding cases missing CT confirmation. The cases were randomly split into training and test set (85% and 15%, respectively). A multi-purpose image analysis software was trained for the decision whether a distal radius fracture was present on the X-ray image. Training data was augmented (e.g. by horizontal flipping, shifting, rotating, scaling). The test set was subsequently processed by the trained system. Performance was measured as area under the ROC curve (AUC) from the score the software assigned to each image. Sensitivity and specificity were calculated at the optimal threshold as indicated by Youden's index. Finally, the test set was evaluated by an attending radiologist and a radiology resident with 16 and 2 years of experience, respectively.

RESULTS

The included images featured 171 cases with fractures and 562 controls, amounting to 733 X-ray images of 277 different patients. The training and evaluation set consisted of 573 and 160 X-ray images, respectively. The diagnostic performance of the trained software on the test set of 160 X-ray images was excellent with an AUC of 0.91 (95%-CI 0.85-0.95). It therefore performed comparable to a radiology resident (AUC 0.87, p=0.25) but worse than the attending radiologist (AUC 0.98, p<0.01). Sensitivity and specificity of the software at the optimal threshold were calculated to be 88.5% and 89.9%, respectively. Heatmaps drawn as an image overlay by the software indicated areas suspicious for defects as useful visual feedback. The interreader agreement of the human readers was substantial with a Cohen's kappa of 0.71 (95%-CI 0.60-0.82).

CONCLUSION

The software was able to detect wrist fractures with high sensitivity and specificity, using only a small dataset for training. It performed on a par with the radiology resident reader.

CLINICAL RELEVANCE/APPLICATION

Deep-learing based software is useful for the detection of wrist fractures.

SSG08-05 Multi-Tissue Segmentation for Body Composition Using a Deep Convolutional Neural Network

Tuesday, Nov. 27 11:10AM - 11:20AM Room: S102CD

Awards

Student Travel Stipend Award

Participants

Benjamin Wang, MD, Boston, MA (*Presenter*) Nothing to Disclose Andrew Tsao, Boston, MA (*Abstract Co-Author*) Nothing to Disclose Martin Torriani, MD, Lincoln, MA (*Abstract Co-Author*) Nothing to Disclose

For information about this presentation, contact:

mtorriani@mgh.harvard.edu

PURPOSE

To develop and test a deep convolutional neural network (CNN) to automatically segment abdominal CT images for body composition measures. We hypothesized that a deep CNN would achieve high accuracy using a limited training dataset and data augmentation.

METHOD AND MATERIALS

We manually segmented single-slice CT images obtained at the level of L4 (80kV, 70mAs, 10mm slice thickness, 50cm field of view) in 160 subjects for determination of body composition. Manual segmentation was performed on 512x512 pixel images to label 6 classes: background, muscle, bone, bowel/solid organs, visceral and subcutaneous fat. Twenty cases were segregated for a test dataset. The remaining 140 underwent a processing pipeline of histogram equalization followed by data augmentation (N=2,000), which included random deformations, horizontal mirroring, Poisson noise, cropping and magnification. We trained our model from scratch on Keras/Tensorflow using an 80/20 training/validation split and a U-Net architecture (8 batch size, 50 epochs, dropout 0.3, initial learning rate 0.0001, softmax). Testing was performed to obtain the Dice (F1) score as a parameter to compare the similarity between manual vs. CNN-based multi-class segmentation.

RESULTS

The overall mean Dice score was 96% (median 97%, range, 94-98). Mean Dice scores for each class were: background 98% (median 98%, range, 96-99), bone 87% (86%, 83-92), subcutaneous fat 94% (96%, 87-98), muscle 91% (91%, 84-97), bowel/solid organs 89% (90%, 83-94), and visceral fat 81% (88%, 45-93). Visceral fat demonstrated the broadest accuracy range, which may derive from its more variable quantity and morphology, representing an important focus to improve algorithm performance.

CONCLUSION

Our results show overall accurate automated abdominal CT segmentation for body composition using a deep CNN algorithm, trained on a limited dataset with data augmentation. While segmentation accuracy was generally high for most classes (>81%), improvement of algorithm performance will focus on strategies to increase visceral fat segmentation accuracy. This workflow may serve as a basis for future models aimed at automated segmentation of entire abdominal CT studies for body composition.

CLINICAL RELEVANCE/APPLICATION

Deep CNN algorithms for tissue segmentation are promising methods to obtain body composition measurements, and may allow efficient and automatic data extraction in opportunistic and population studies.

SSG08-06 End to End Solution for Complete Thigh Muscle Semantic Segmentation from Musculoskeletal CT using Deep Learning

Tuesday, Nov. 27 11:20AM - 11:30AM Room: S102CD

Participants

Hasnine A. Haque, DSc, PhD, Hino, Japan (*Presenter*) Employee, General Electric Company; Researcher, Keio University School of Medicine Science

Masahiro Hashimoto, Shinjuku-Ku, Japan (Abstract Co-Author) Nothing to Disclose

Nozomu Uetake, Hino, Japan (Abstract Co-Author) Nothing to Disclose

Masahiro Jinzaki, MD, Tokyo, Japan (Abstract Co-Author) Support, Canon Medical Systems Corporation; ;

For information about this presentation, contact:

N/A

PURPOSE

The goal is to develop and validate a 2.5D deep learning neural network (DLNN) to automatically classify thigh muscle into 10 classes and evaluate its classification accuracy over 2D DLNN.

METHOD AND MATERIALS

The clinical dataset consists of 48 thigh volume(TV) cropped from 24 anonymized non-contrast CT DICOM of lower extremities. Cropped volumes were aligned with femur axis and resample in 2mm voxel spacing. To reduce the annotation workload, final expert ground truth annotation was created by editing the predicted labels of muscle by a newly developed stacked U-Net DLNN. Stacked U-Net produces relatively higher segmentation accuracy on smaller muscles even when it is trained with small number annotated datasets. Proposed 2.5D DLNN consists of three 2D U-Net(optimizer: Adam, Ir=1e-4,decay=1e-3) trained with axial, coronal and sagittal muscle slices respectively. A voting algorithm was used to combine the output of 2D U-Nets to create final segmentation. 2.5D U-Net was trained on PC(Intel Xeon 2.20GHz 128GB, NVIDIA Tesla P100-SXM2-16GB) with 38 TV(Epoch:100, Batch:32) and the remaining 10 TV were used to evaluate segmentation accuracy of 10 classes within Thigh. The result segmentation of both left and right thigh were de-cropped to original CT volume space. Finally, segmentation accuracies were compared between proposed DLNN and 2D U-Net(axia).

RESULTS

Average segmentation DSC score accuracy of all classes with 2.5D U-Net as 91.18% and Housdorff distance(HD) as 17mm. We found DSC score for 2D U-Net was 2.9% lower and HD was more than four times higher than the that of 2.5D U-Net.

CONCLUSION

Successfully implemented end-to-end solution for complete automatic classification with reasonable accuracy of thigh muscle into 10 classes . The same could be easily extend to muscle segmentation of any other body parts (lower limb, arm, shoulder etc.). To date, there is no other study of deep machine learning algorithm used except our study for CT based semantic muscle segmentation.

CLINICAL RELEVANCE/APPLICATION

Muscle segmentation functionality on PACS may improve visibility and can enable automatic quantitative evaluation of muscle atrophy with the disease progression. Change in volume or shapes of muscles will enable therapeutic interventions to be targeted to the affected regions only.

SSG08-07 A Deep-Learning System for Fully-Automated Muscle Assessment on Abdominal CT for Opportunistic Detection of Sarcopenia

Participants Joseph E. Burns, MD, PhD, Orange, CA (*Presenter*) Nothing to Disclose Jianhua Yao, PhD, Bethesda, MD (*Abstract Co-Author*) Royalties, iCAD, Inc Joseph J. Chen, BS, Orange, CA (*Abstract Co-Author*) Nothing to Disclose Ronald M. Summers, MD,PhD, Bethesda, MD (*Abstract Co-Author*) Royalties, iCAD, Inc; Royalties, Koninklijke Philips NV; Royalties, ScanMed, LLC; Research support, Ping An Insurance Company of China, Ltd; Researcher, Carestream Health, Inc; Research support, NVIDIA Corporation; ; ; ;

For information about this presentation, contact:

jburns@uci.edu

PURPOSE

Central sarcopenia is a risk factor for mortality in multiple cancers, liver transplantation, cirrhosis, and trauma, and represents a topic of interest in multiple medical and surgical specialties to help guide patient management. We have created a fully-automated deep-learning system to opportunistically analyze truncal musculature for sarcopenia detection on CT scans obtained as part of the patient's routine clinical care

METHOD AND MATERIALS

First, individual lumbar vertebral bodies are segmented to separate bone from soft tissue, and create reference anatomic levels for muscle analysis, via thresholding, morphologic operations, and aggregated intensity profiles. Next, muscle groups at reference vertebral levels are segmented on axial images by a holistically nested neural network through image-to-image training and classification. There are varying reference level and muscle group standards for sarcopenia determination in different medical and surgical specialties. To accommodate this, the system performs analysis for multiple muscle groups and vertebral levels. Segmentation accuracy was assessed via Dice Similarity Coefficient, a measure of overlap between manual and automated segmentations. The system was trained on contrast enhanced portal venous phase CTs of 51 patients and tested on 51 cases (average age 67 (range 59-81), 53 F, 49 M). For demonstration here, the system was designed to calculate sarcopenia via the standard cutoff value for L3 SMI (skeletal muscle index: L3 axial muscle area cm2/patient ht m2) of < 3.62cm2/m2 for women and <4.93 cm2/m2 for men, as proposed by international consensus of cancer cachexia

RESULTS

The Dice coefficients for the psoas, paraspinous, and total abdominal muscle groups in the training and testing sets were 0.953 + -0.015 and 0.938 + -0.028, respectively at the level of the third lumbar vertebra. The mean normalized L3MI was 5.02 + -1.45 cm2/m2 for women and 6.18 + -1.83 cm2/m2 for men. Sarcopenia was present in 15.4% (8/52) of women and 13.3% (6/45) of men

CONCLUSION

This fully-automated system can robustly detect, accurately segment, and generate quantitative statistics for multiple abdominal wall muscle groups at multiple lumbar vertebral levels on CT scans

CLINICAL RELEVANCE/APPLICATION

Automated quantification of sarcopenia may guide patient management in pre-treatment risk assessment and surgical planning, and act as a platform to facilitate large scale clinical trials

SSG08-08 Machine-Learning-Based Discovery of Sexual Dimorphism of Hand and Wrist Radiographs

Tuesday, Nov. 27 11:40AM - 11:50AM Room: S102CD

Participants

Sehyo Yune, MD, MPH, Boston, MA (*Presenter*) Nothing to Disclose Hyunkwang Lee, Boston, MA (*Abstract Co-Author*) Nothing to Disclose Shahein H. Tajmir, MD, Boston, MA (*Abstract Co-Author*) Nothing to Disclose Michael S. Gee, MD, PhD, Boston, MA (*Abstract Co-Author*) Nothing to Disclose Synho Do, PhD, Boston, MA (*Abstract Co-Author*) Nothing to Disclose

For information about this presentation, contact:

sehyo.yune@mgh.harvard.edu

PURPOSE

Skeletal sexual dimorphism develops mostly in the pelvis during puberty. Although prior work has shown higher second-to-fourth digit ratio and smaller carpal bones in women compared to men, the distributions of these measures substantially overlap for women and men. We aim to create a machine-learning algorithm to distinguish sex from hand and wrist radiographs and evaluate its performance by comparing it to radiologists'.

METHOD AND MATERIALS

We compiled a dataset of 10,607 (5,148 male and 5,459 female) radiographs of hand and wrist from a cohort of patients, ranging from 5 years to 80 years of age. A total of 7,461 radiographs were used for training, and 1,573 images separate from the training data were randomly selected for validation. Images from the remaining 1,573 cases were reserved for testing. The images were labeled solely with the sex of the subject. We fine-tuned an ImageNet-pretrained VGG16 convolutional neural network (CNN) on our training dataset. The best CNN, selected based on the validation loss, then provided automated prediction of sex, which was compared to the sex in the medical record. To compare the performance with human radiologists, we randomly selected 50 cases for which the CNN correctly predicted sex. Two radiologists independently read the hand and wrist radiographs and predicted sex for these 50 cases. The radiologists were blinded to clinical information of the patients but were allowed to use reference such as the Greulich and Pyle atlas while reading the radiographs.

RESULTS

Of the 1,573 radiographs tested, the algorithm predicted sex correctly with 95.4% accuracy (95.2% in female and 95.7% in male).

The two radiologists showed 58% (45.8% in female and 69.2% in male) and 46% (50% in female and 57.7% in male) accuracy. The class activation maps (CAM) showed that the CNN mostly focused on 2nd and 3rd metacarpal base or 4th and 5th metacarpal head in women, and radioulnar/radiocarpal joint or 2nd, 3rd, and 4th metacarpophalangeal joints in men.

CONCLUSION

We developed an algorithm that accurately distinguishes men and women from hand and wrist radiographs in children as well as in adults.

CLINICAL RELEVANCE/APPLICATION

The current study shows the discovery of previously unrecognized radiologic features using machine learning. It could be used in screening of disorders affecting sexual development.

SSG08-09 Automated Radiograph Based Preoperative Measurements in FAI Patients Utilizing Deep Learning

Tuesday, Nov. 27 11:50AM - 12:00PM Room: S102CD

Participants

Simukayi Mutasa, MD, New York, NY (*Presenter*) Nothing to Disclose Zenas Igbinoba, New York, NY (*Abstract Co-Author*) Nothing to Disclose Michael J. Rasiej, MD, New York, NY (*Abstract Co-Author*) Nothing to Disclose Tony T. Wong, MD, New York, NY (*Abstract Co-Author*) Nothing to Disclose

For information about this presentation, contact:

s.mutasa@columbia.edu

PURPOSE

Utilize deep learning to obtain preoperative measurements from radiographs in patients with femoroacetabular impingement.

METHOD AND MATERIALS

A retrospective study of patients with femoroacetabular impingement was performed. 181 unique patients who underwent CT scan of the hip for preoperative measurement of alpha angle (AA), acetabular version (AV), femoral version (FV) and lateral center edge (LCE) were identified. The training set consisted of 1084 radiographs. This was made up of available preoperative false profile, Dunn, frog leg and AP radiographs (n=419) and augmented with digitally reconstructed radiographs (DRRs) generated from the CT scans at different views (n=665). A novel convolutional neural network (CNN) based on a DenseNet architecture with 54 hidden layers and a regression head was trained on 256x256 input images to predict LCE measurement. For testing AA, AV, and FV measurements, both a regression output and a binary classifier for normal and abnormal ranges were tested. Parameters were tuned based on a 20% validation group generated from the training set. The sequestered testing set consisted of 95 preoperative radiographs at various views and corresponding measurements from accompanying CT scans.

RESULTS

Overall mean absolute error (MAE) and standard deviation of the error for LCE measurement was $3.2^{\circ} \pm 2.3^{\circ}$. Performance of the network was best on false profile views of the hip ($3.0^{\circ} \pm 2.2^{\circ}$) but this difference was not statistically significant. AA, AV and FV prediction performance was evaluated, however the performance of the network was not predictive in the current implementation.

CONCLUSION

Deep learning techniques applied to radiographs can be used for quantitative measurement of LCE. With further modification and additional examples, quantitative measurement of AA, AV and FV may be possible.

CLINICAL RELEVANCE/APPLICATION

An accurate, automated system designed to obtain FAI measurements from radiographs can obviate the need for CT and has the potential to decrease healthcare costs, decrease patient exposure to radiation and increase radiologist efficiency.



SSG13

Physics (CAD/Machine Learning)

Tuesday, Nov. 27 10:30AM - 12:00PM Room: S404AB



AMA PRA Category 1 Credits ™: 1.50 ARRT Category A+ Credit: 1.75

Participants

Heang-Ping Chan, PhD, Ann Arbor, MI (*Moderator*) Institutional research collaboration, General Electric Company Kenneth R. Hoffmann, PhD, Buffalo, NY (*Moderator*) Stockholder, Imagination Software Corporation; Officer, Imagination Software Corporation ;

Sub-Events

SSG13-01 Deep Learning-Based Automatic Chest PA Screening System for Various Devices and Hospitals

Tuesday, Nov. 27 10:30AM - 10:40AM Room: S404AB

Participants

Woong Bae, Seoul, Korea, Republic Of (*Abstract Co-Author*) Nothing to Disclose Sejin Park, MS, Seoul, Korea, Republic Of (*Abstract Co-Author*) Employee, VUNO Inc Kyu-Hwan Jung, PhD, Seoul, Korea, Republic Of (*Presenter*) Stockholder, VUNO Inc Joon Beom Seo, MD, PhD, Seoul, Korea, Republic Of (*Abstract Co-Author*) Nothing to Disclose Namkug Kim, PhD, Seoul, Korea, Republic Of (*Abstract Co-Author*) Stockholder, Coreline Soft, Co Ltd

For information about this presentation, contact:

iorism@vuno.co

PURPOSE

To ensure generalization performance in various hospitals, we developed a deep learning based automatic Chest PA screening System which can detect 5 class findings and performs well on various devices. Its performance was evaluated by using FROC and FOM in various devices.

METHOD AND MATERIALS

Our system can detect 5 class findings which are nodule, consolidation, pleural effusion, interstitial opacity, pneumothorax. We used chest radiographs(PA view) collected from 2013 to 2015 at two hospitals. There were 18,869 labeled CRs comprised of 11,181 normal and 1,943 nodule, 1,293 consolidation, 1,867 pleural effusion, 1,406 interstitial opacity, 1,179 pneumothorax CRs. All abnormal CRs were clinically confirmed by CT scans. Thus, we could collected elaborate segmentation label data. Furthermore, our data were acquired in various devices, the first hospital has x-ray detectors from 3 manufacturers(GE, FUJI, Canon), and the other has devices from 2 manufacturers(Philips, LISTEM). We used only data from the first hospital for training and then used all data of other hospital as test data.

RESULTS

In the test dataset, our screening performance showed AUC of 0.99, with an sensitivity, specificity of 97.6%, 97.9%, respectively. For each class findings, Our system achieved FROC and FP per scan of 81.2% / 0.72, 84.4% / 1.41, 83.1% / 0.35, 85.7% / 1.45, 91.6% / 0.78 for nodule, consolidation, pleural effusion, interstitial opacity, pneumothorax, respectively. In FOM performance, sensitivity is 84.7%, 91.5%, 93.7%, 97.9%, 97.2%.

CONCLUSION

Our screening system demonstrated reliable performance in various devices and multi hospitals. It also showed competitive results in detecting location and classification of 5 class findings.

CLINICAL RELEVANCE/APPLICATION

Our system demonstrates reliable performance on various devices on multiple findings using CAD.

SSG13-02 Curriculum Learning from Patch to Image for Pulmonary Abnormal Pattern Screening in Chest-PA X-Ray: Intra- and Extra-Validation on Multi-Center Datasets

Tuesday, Nov. 27 10:40AM - 10:50AM Room: S404AB

Participants

Beomhee Park, Seoul, Korea, Republic Of (*Presenter*) Nothing to Disclose Namkug Kim, PhD, Seoul, Korea, Republic Of (*Abstract Co-Author*) Stockholder, Coreline Soft, Co Ltd Joon Beom Seo, MD, PhD, Seoul, Korea, Republic Of (*Abstract Co-Author*) Nothing to Disclose Sang Min Lee, MD, Seoul, Korea, Republic Of (*Abstract Co-Author*) Nothing to Disclose Kyunghee Lee, MD, PhD, Seongnam, Korea, Republic Of (*Abstract Co-Author*) Nothing to Disclose Yongwon Cho, Seoul, Korea, Republic Of (*Abstract Co-Author*) Nothing to Disclose Eunsol Lee, MD, Seoul, Korea, Republic Of (*Abstract Co-Author*) Nothing to Disclose

Younghoon Cho, MD, Seoul, Korea, Republic Of (Abstract Co-Author) Nothing to Disclose

For information about this presentation, contact:

beomheep@gmail.com

PURPOSE

To propose and validate a computer aided detection (CAD) for detecting 5 kinds of pulmonary abnormalities in chest-PA X-ray using multicenter data with a curriculum learning strategy to train entire images after training lesion-specified image patches to guide the CAD toward better local minima.

METHOD AND MATERIALS

Chest-PA X-rays collected from two hospitals, which consisted of 10137 healthy subjects and 3244 patients including 944, 550, 280, 1364, and 331 patients with nodule (ND), consolidation (CS), interstitial opacity (IO), pleural effusion (PE) and pneumothorax (PT) from XXX (X1), and 1035 healthy subjects and 4404 patients including 1189, 853, 1009, 998 and 944 patients with ND, CS, IO, PE and PT from YYY (Y1), respectively. 60% and 20% of X1 dataset were used for training and validation. 20% of X1 and Y1 datasets were used for test. Every abnormality lesion was manually drawn by expert thoracic radiologists. Using these regions, image patches were used to specifically train the regional patterns of abnormalities. Entire images were used to fine-tune the network subsequently. Modified resnet-50 architecture for multi-label problem was used to train weak supervisions. To assess the effectiveness of our approach, we compared it with or without this strategy using six-measures including area under the curve (AUC), accuracy, sensitivity, specificity, positive predictive value (PPV), and negative predictive value.

RESULTS

Both models converged well and weights were extracted at the minimum loss on validation set. With curriculum learning, the AUC in X1 test set was 93.2, 88.6, 97.7, 99.5, 96.6% for ND, CS, IO, PE, and PT, respectively. Compared to the model without this strategy, performance improvement was achieved in all metrics, and PPV showed the largest improvement of 11.3% and 4.6% for X1 and Y1.

CONCLUSION

The proposed curriculum learning strategy successfully showed the outperforming results compared with baseline through multicenter validation, which could be used in case of the smaller dataset with complex task.

CLINICAL RELEVANCE/APPLICATION

This curriculum learning strategy could be useful in case of computer-aided detection (CAD) on the smaller dataset with complex task such as CAD on abnormalities of chest-PA X-ray.

SSG13-03 Data Augmentation via Synthetic Mammograms for Improved Training of a Deep Learning Breast Mass Detection Algorithm

Tuesday, Nov. 27 10:50AM - 11:00AM Room: S404AB

Participants

Kenny H. Cha, PhD, Silver Spring, MD (*Presenter*) Nothing to Disclose Nicholas Petrick, PhD, Silver Spring, MD (*Abstract Co-Author*) Nothing to Disclose Aria Pezeshk, PhD, Silver Spring, MD (*Abstract Co-Author*) Nothing to Disclose Christian G. Graff, PhD, Silver Spring, MD (*Abstract Co-Author*) Nothing to Disclose Diksha Sharma, Silver Spring, MD (*Abstract Co-Author*) Nothing to Disclose Andreu Badal, PhD, Silver Spring, MD (*Abstract Co-Author*) Nothing to Disclose Berkman Sahiner, PhD, Silver Spring, MD (*Abstract Co-Author*) Nothing to Disclose

For information about this presentation, contact:

kenny.cha@fda.hhs.gov

PURPOSE

To evaluate whether training data augmentation using synthetic mammograms may improve the performance of a deep learning system for mass detection.

METHOD AND MATERIALS

Synthetic mammograms were generated from procedurally generated compressed breast phantoms containing masses. The anthropomorphic phantoms were modeled for four different breast density categories, and the masses were modeled with different sizes, shapes and margins. MC-GPU, a Monte Carlo-based x-ray transport simulation code that generates clinically-realistic radiographic projection images, was used to project the 3D phantoms into synthetic mammograms. A total of 530 mammograms with 677 masses were generated. We used Faster R-CNN for our deep learning network with pre-training from ImageNet using ResNet-101 architecture. From the Curated Breast Imaging Subset of Digital Database for Screening Mammography (CBIS-DDSM) data set, we used 573 mammograms (607 masses) for training, and 170 mammograms (177 masses) for testing, all of which contained masses. We compared the detection performance of the Faster R-CNN when the network was trained using only the CBIS-DDSM training images, and when the network was augmented with the 530 synthetic mammograms. FROC analysis was performed to compare performances with and without the synthetic mammograms.

RESULTS

When trained on the CBIS-DDSM data set alone, the Faster R-CNN detected 68.4% (121/177) of the masses on the test set. With the augmented training set, the test set detection prescreening sensitivity was 83.6% (148/177). The difference between the two FROC curves was statistically significant using JAFROC (p = 0.005). At 1 false positive per image (FP/image), the test set detection sensitivity was 60.5% (107/177) when trained on CBIS-DDSM alone, and was 68.9% (122/177) when trained with the augmented data set. The difference was statistically significant using McNemar's test (p = 0.001).

CONCLUSION

Our study domonstrator that it is possible to concrete high quality synthetic mammagrams using procedurally concreted breast

our study demonstrates that it is possible to generate high quality synthetic mannograms using procedurally generated breast phantoms and Monte Carlo simulation, that can be used to enlarge the training data set and improve the performance of deep learning systems for mass detection on mammograms.

CLINICAL RELEVANCE/APPLICATION

Training data set can be a limiting factor for deep learning applied to medical imaging tasks. This study shows our synthetic mammograms are useful for data augmentation in computer-aided detection.

SSG13-04 Comparison of Transfer Learning and Deep Feature Extraction Strategies for Breast Cancer Classification in Mammography Using Deep Neural Networks

Tuesday, Nov. 27 11:00AM - 11:10AM Room: S404AB

Participants

Ravi K. Samala, PhD, Ann Arbor, MI (*Presenter*) Nothing to Disclose Heang-Ping Chan, PhD, Ann Arbor, MI (*Abstract Co-Author*) Institutional research collaboration, General Electric Company Lubomir M. Hadjiiski, PhD, Ann Arbor, MI (*Abstract Co-Author*) Nothing to Disclose Mark A. Helvie, MD, Ann Arbor, MI (*Abstract Co-Author*) Institutional Grant, General Electric Company Nicholas Szerman, Ann Arbor, MI (*Abstract Co-Author*) Nothing to Disclose

PURPOSE

To study the differences between using a pre-trained deep convolutional neural network (DCNN) as feature extractor and a finetuned DCNN using transfer learning for classification of malignant and benign masses in mammography.

METHOD AND MATERIALS

3,578 mass lesions from 3,411 mammograms were collected with IRB approval. Three DCNN structures: AlexNet, InceptionV1 (GoogLeNet) and VGG16 that had success in ImageNet classification were used in this study. All the DCNNs were pretrained on ImageNet data for a 1000-class object classification task and then applied to mammographic mass classification. When used as a feature extractor, the features from the first fully connected layers (*FF*) were extracted and a random forest classifier (RF-*FF*) is trained. Under the transfer learning paradigm, two transfer strategies: freezing up to the first convolutional layer (*CF*) and freezing up to the last convolutional layer (*CL*) were studied, which led to four mammography-trained classifiers: mDCNN-*CF* and mDCNN-*CL* with DCNN classifier (consisting of fully connected layers and softmax) and random forest classifier using *FF* features. All the strategies were validated in a 4-fold cross-validation approach while keeping all the views from the same patient together in the same fold. The experiments were repeated ten times with different random stochastic initializations.

RESULTS

ImageNet-trained feature extractor RF-*FF* obtained mean AUCs of 0.77, 0.58 and 0.74 for AlexNet, InceptionV1 and VGG16, respectively. Mammography fine-tuned mDCNN-*CF* and mDCNN-*CL* reached mean AUCs of 0.83 and 0.79, respectively, as the best among the three structures. mDCNN-*CF*-RF-*FF* and mDCNN-*CL*-RF-*FF* also reached similar AUCs of 0.83 and 0.79, respectively. The fine-tuned mDCNNs achieved higher accuracy than without transfer learning.

CONCLUSION

Although DCNN trained with images from a different domain may be used as a deep feature extractor for medical imaging, transfer learning in the target domain has significant advantages where some of the deeper layers can be fine-tuned for the target task. In transfer learning, replacing the DCNN classifier with an external classifier like the random forest classifier does not improve the classifier performance.

CLINICAL RELEVANCE/APPLICATION

With the prolific usage of deep learning in medical imaging, it is important to understand the effectiveness of the features extracted by different DCNN structures with and without transfer learning.

SSG13-05 Detecting Mal-Positioned Endotracheal (ET) Tubes in Portable Chest X-Ray (CXR) Images: Comparing Deep Learning Models with Hand-Engineered Approach on Carina Detection

Tuesday, Nov. 27 11:10AM - 11:20AM Room: S404AB

Participants Zhimin Huo, PhD, Pittsford, NY (*Presenter*) Employee, Carestream Health, Inc Hui Zhao, Rochester, NY (*Abstract Co-Author*) Nothing to Disclose Jane Zhang, Rochester, NY (*Abstract Co-Author*) Nothing to Disclose

For information about this presentation, contact:

zhiminhuo@yahoo.com

PURPOSE

Comparing performances in detecting carina location from deep learning and hand-engineered approaches

METHOD AND MATERIALS

ET tubes are the most commonly used tubes for ICU patents. Mal-positioned ET tubes may lead to collapsed lungs. The ET tube tip placement relative to carina location in a CXR image is used to determine if an ET tube is properly positioned. However, the carina, a ridge of cartilage in the trachea that occurs between the division of the two main bronchi, can be hard to detect on CXR images. Our previously developed hand-engineered approach includes the detection of lungs, spine and aortic arch to identify an initial ROI. Carina location is detected using template matching and feature analysis within the ROI. In this study, we investigate convolutional neural networks (CNN) based models, i.e., the faster R-CNN and U-Net, to detect carina locations. The R-CNN was trained with initial weights from a pre-trained model. U-Net was trained from scratch. Both models were trained on 994 portable CXR images, validated on 136 images, and tested on 212 images. The carina location (x,y) on each image was identified by an experienced radiologist for the 212 testing images and by a trained scientist for the rest of images. The carina detection accuracy was measured by the distance between the human-identified and computer detected locations in terms of <=5mm, 10 mm and beyond. Each image has only one detection from each approach; detections beyond 10 mm from the truth are regarded as a miss or FP detection.

RESULTS

R-CNN yielded sensitivities of 92% (98%) and 60% (88%) and 58% (87%) for <=5 (10) mm on the training, validation and testing data, respectively . U-Net yielded sensitivities of 94% (94%), 64% (85%) and 67% (89%) for <=5 (10) mm on the training, validation and testing data, respectively. Our hand-engineered approach yielded a sensitivity of 52% (74%) for <=5 (10) mm on the same 212 testing images. The CNN based models yielded a similar performance in detecting carina location measured within 10 mm of truth with more than 10% improvement on average than that of the hand-engineered approach.

CONCLUSION

Use of CNN based models substantially improved carina detection accuracy and performance robustness.

CLINICAL RELEVANCE/APPLICATION

Accurate detection of carina locations in CXR images can help timely detection of mal-positioned ET tubes, thus improving the care and treatment management for critically ill patients in ICU.

SSG13-06 Classification of Glioblastoma Using Machine Learning and Delta-Radiomic Signature Derived from Dynamic Susceptibility Enhanced MRI

Tuesday, Nov. 27 11:20AM - 11:30AM Room: S404AB

Participants

Xiaofeng Yang, PhD, Atlanta, GA (*Presenter*) Nothing to Disclose Jiwoong J. Jeong, BS, Atlanta, GA (*Abstract Co-Author*) Nothing to Disclose Bing Ji, Atlanta, GA (*Abstract Co-Author*) Nothing to Disclose Liya Wang, MD, Shenzhen, China (*Abstract Co-Author*) Nothing to Disclose Yang Lei, Atlanta, GA (*Abstract Co-Author*) Nothing to Disclose Tian Liu, PhD, Atlanta, GA (*Abstract Co-Author*) Nothing to Disclose Arif N. Ali, MD, MS, Chicago, IL (*Abstract Co-Author*) Nothing to Disclose Walter J. Curran JR, MD, Atlanta, GA (*Abstract Co-Author*) Nothing to Disclose Hui Mao, PhD, Atlanta, GA (*Abstract Co-Author*) Nothing to Disclose

For information about this presentation, contact:

xyang43@emory.edu

PURPOSE

Glioblastoma (GBM) is the most aggressive cancer with poor prognosis due to its heterogeneity. The purpose of this study is to improve the tissue characterization of these highly heterogeneous tumors using delta-radiomic signature of dynamic susceptibility contrast enhanced (DSC) MR images, which are commonly used to derive blood perfusion parameters to the tumor, with machine learning approaches.

METHOD AND MATERIALS

Multiparametric magnetic resonance (MR) images of 25 patients with histo-pathologically confirmed 13 high and 12 low grade GBM were taken using a standard brain tumor imaging protocol. All DSC images were registered to FLAIR images. The tumor contours from FLAIR images and its contralateral regions of the normal tissue were used to extract delta-radiomic features from each DSC image over the entire volume of DSC time course images before applying feature selection methods. The most informative and non-redundant features (signature) were selected to train a random forest to differentiate high-grade (HG) and low-grade (LG) tumors while feature correlation limits were applied to remove redundancies. Then a leave-one-out cross-validation random forest was applied to the dataset to classify GBMs. To evaluate the performance of our proposed classification method, overall prediction accuracy, confidence, sensitivity and specificity were calculated.

RESULTS

Analysis of the predictions showed that our method consistently predicted the tumor grade of 24 out of 25 patients correctly (0.96). Based on the leave-one-out cross-validation, the mean prediction accuracy was 0.95 ± 0.10 for HG and 0.85 ± 0.25 for LG. The area under the receiver operating characteristic curve (AUC) was 0.94.

CONCLUSION

Our method performed well in classifying high and low grade GBMs based on the DSC MRI data. This study shows that deltaradiomic features of DSC MRI are correlated with GBM grades and may be use to improve imaging characterizing of gliomas. The performance of our method in interrogating DSC MRI data will be explored further using combined spatial and temporal deltaradiomic features.

CLINICAL RELEVANCE/APPLICATION

This study explores the new computational approach of delta-radiomic signature and machine learning to extract additional information from clinically applied DSC MR images to better classify GBMs.

SSG13-07 U-Net-Based Deep-Learning Bladder Segmentation in CT Urography

Tuesday, Nov. 27 11:30AM - 11:40AM Room: S404AB

Participants

Xiangyuan Ma, Ann Arbor, MI (*Abstract Co-Author*) Nothing to Disclose Lubomir M. Hadjiiski, PhD, Ann Arbor, MI (*Presenter*) Nothing to Disclose Jun Wei, PhD, Ann Arbor, MI (*Abstract Co-Author*) Nothing to Disclose Heang-Ping Chan, PhD, Ann Arbor, MI (*Abstract Co-Author*) Institutional research collaboration, General Electric Company Kenny H. Cha, PhD, Silver Spring, MD (*Abstract Co-Author*) Nothing to Disclose Richard H. Cohan, MD, Ann Arbor, MI (*Abstract Co-Author*) Co-author, Wolters Kluwer nv Elaine M. Caoili, MD, MS, Ann Arbor, MI (*Abstract Co-Author*) Nothing to Disclose Ravi K. Samala, PhD, Ann Arbor, MI (*Abstract Co-Author*) Nothing to Disclose Chuan Zhou, PhD, Ann Arbor, MI (*Abstract Co-Author*) Nothing to Disclose Yao Lu, Guangzhou, China (*Abstract Co-Author*) Nothing to Disclose

For information about this presentation, contact:

maxyuan@mail2.sysu.edu.cn

PURPOSE

To develop a U-Net based deep learning approach (U-DL) for bladder segmentation in CT urography (CTU) as a critical component for computer-aided diagnosis (CAD) of bladder cancer and treatment planning.

METHOD AND MATERIALS

Bladder segmentation in CTU remains a challenge because the bladder often contains regions filled with intravenous contrast and without contrast. We previously developed a bladder segmentation method using deep-learning convolution neural network (DL-CNN) and level sets within an user-input bounding box. However, some cases with poor image quality or with advanced bladder cancer spreading into the neighboring organs caused inaccurate segmentation. We have newly developed an automated U-DL method to identify the bladder boundary in CTU cases. The entire CTU slice containing bladder is used as input to the U-DL without the need for a bounding box. The output of U-DL is the corresponding bladder likelihood mask of the slice. No level set is used as a post-processing step. We trained the U-DL with a mini-batched stochastic gradient descent algorithm by minimizing a binary cross-entropy cost function using 7629 bladder slices from 81 CTU cases. The segmentation performance was evaluated using 92 independent test cases. 3D hand-segmented contours were obtained as reference standard for all cases. The segmentation accuracy was evaluated relative to the reference standard in terms of the average volume intersection ratio (AVI), average percent volume error (AVE), average absolute volume error (AAVE), average minimum distance (AMD), and the Jaccard index (JI).

RESULTS

For the independent test set, the AVI, AVE, AAVE, AMD, and JI for segmentation with U-DL were $93.0\pm9.8\%$, $-3.0\pm13.9\%$, $8.9\%\pm11.1\%$, 2.7 ± 2.0 mm, $85.1\%\pm10.9\%$, respectively. With DL-CNN and level sets, the corresponding values were $81.9\%\pm12.1\%$, $10.2\%\pm16.2\%$, $14.0\%\pm13.0\%$, 3.6 ± 2.0 mm, and $76.2\%\pm11.8\%$, respectively. The improvement for all measures were statistically significant (p<0.001).

CONCLUSION

Compared to the previous method using DL-CNN and level sets, the U-DL is more accurate and does not depend on an user-input bounding box. Further work is underway to improve the U-DL as a fully automated method for segmentation of the bladder.

CLINICAL RELEVANCE/APPLICATION

Bladder segmentation is a crucial step for detection of bladder cancer and wall thickening in CAD and for treatment planning. This study developed a highly accurate method for bladder segmentation.

SSG13-08 Automated Detection of Hemorrhage and Fracture Regions in Head and Neck CT of the Trauma Patient in Emergency Rooms Using 3D Convolutional Neural Networks with Strong and Weak Labels

Tuesday, Nov. 27 11:40AM - 11:50AM Room: S404AB

Participants

Areum Lee, Seoul, Korea, Republic Of (*Presenter*) Nothing to Disclose Beomhee Park, Seoul, Korea, Republic Of (*Abstract Co-Author*) Nothing to Disclose Namkug Kim, PhD, Seoul, Korea, Republic Of (*Abstract Co-Author*) Stockholder, Coreline Soft, Co Ltd Hyun-Jin Bae, PhD, Seoul, Korea, Republic Of (*Abstract Co-Author*) Nothing to Disclose Younghwa Byeon, Seoul, Korea, Republic Of (*Abstract Co-Author*) Nothing to Disclose Inhwan Kim I, Seoul, Korea, Republic Of (*Abstract Co-Author*) Nothing to Disclose Gil-Sun Hong, MD, Seoul, Korea, Republic Of (*Abstract Co-Author*) Nothing to Disclose Jeong Hyun Lee, MD, PhD, Seoul, Korea, Republic Of (*Abstract Co-Author*) Nothing to Disclose

For information about this presentation, contact:

namkugkim@gmail.com

PURPOSE

To purpose and validate detection of hemorrhage and fracture using 3D convolutional neural network (CNN) with weak supervision in head and neck CT of brain trauma patient in emergency rooms.

METHOD AND MATERIALS

Brain CT images were acquired from 1785 healthy subjects and 2661 patients including 2451 and 1122 patients with hemorrhage including EDH, ICH and SDH and fracture, respectively. Weakly labeled data could lead to training failure due to high complexity and dimensionality problems. To solve of this problem, we used additional 169 patient's data with information of areas of fracture and hemorrhage were labeled. Using this hard labeled data, 3D patch images were extracted and trained before training weak supervision. After that, the network was fine-tuned using weak supervision with a relatively large amount of data. 3D CNN architecture was designed based on VGGNet-16 and global average pooling was performed before the prediction layer to extract the class activation map. Two independent networks were used to train and detect hemorrhages and fractures individually and evaluated in terms of accuracy, sensitivity, specificity, positive predictive value (PPV), and negative predictive value (NPV).

RESULTS

Our proposed method performance for hemorrhage detection showed 87.7%, 87.7%, and 87.6% and fracture detection showed 80.5%, 69.5%, and 87.8% for accuracy, sensitivity, and specificity. In addition, PPV and NPV of hemorrhage detection and fracture detection were 91.5%, 82.5% and 79.0%, 81.3%, respectively.

CONCLUSION

We proposed fully automated detection system using deep learning networks for brain injury patients in emergency rooms. The system helps to radiologists and physicians in emergency rooms reducing the diagnosis time and human errors. The automated detection system could be applied in various kinds of other abnormal detection with strong and week labels.

CLINICAL RELEVANCE/APPLICATION

This study could be used for CAD on hemorrhage and fracture in head and neck CT of brain trauma patient in emergency rooms.

SSG13-09 Quantitative MRI Radiomics in the Task of Distinguishing Between Malignant and Benign Breast Lesions in a Large Clinical Dataset from China

Tuesday, Nov. 27 11:50AM - 12:00PM Room: S404AB

Participants

Yu Ji, MD, Chicago, IL (Presenter) Nothing to Disclose

Hui Li, PHD, Chicago, IL (Abstract Co-Author) Nothing to Disclose

Alexandra V. Edwards, Chicago, IL (Abstract Co-Author) Research Consultant, QView Medical, Inc; Research Consultant, Quantitative Insights, Inc

John Papaioannou, MSc, Chicago, IL (Abstract Co-Author) Research Consultant, QView Medical, Inc

Peifang Liu, MD, PhD, Tianjin, China (Abstract Co-Author) Nothing to Disclose

Maryellen L. Giger, PhD, Chicago, IL (*Abstract Co-Author*) Stockholder, Hologic, Inc; Shareholder, Quantitative Insights, Inc; Shareholder, QView Medical, Inc; Co-founder, Quantitative Insights, Inc; Royalties, Hologic, Inc; Royalties, General Electric Company; Royalties, MEDIAN Technologies; Royalties, Riverain Technologies, LLC; Royalties, Mitsubishi Corporation; Royalties, Canon Medical Systems Corporation

For information about this presentation, contact:

yuji710@uchicago.edu

PURPOSE

To evaluate the potential of quantitative MRI radiomics in the task of distinguishing between malignant and benign breast lesions in a large clinical dataset from China.

METHOD AND MATERIALS

Our research involved a clinical DCE-MRI database of 600 breast cases retrospectively acquired under a HIPAA-compliant with a waiver of consent IRB protocol. The average ages of the 300 benign and 300 malignant patients were 41.8 and 47.2 years with a standard deviation of 9.5 and 9.6 years, respectively. Characteristics of the breast cancers included clinical and histopathologic findings on axillary lymph nodes and tumors. Once each lesion was indicated to our radiomics workstation, the machine learning algorithm automatically segmented and extracted radiomic features on the primary lesion, including those from six categories: size, shape, morphology, enhancement texture, kinetics, and enhancement-variance kinetics. The selected feature subset was input to a Bayesian artificial neural network (BANN) classifier and underwent leave-one-case-out cross validation. Area under the receiver operating characteristic (ROC) curve (AUC) served as the figure of merit in the task of distinguishing between malignant and benign breast lesions.

RESULTS

In the task of distinguishing between malignant and benign breast lesions, the analyses of each radiomic feature demonstrated AUC values ranging from 0.53 (se = 0.02) to 0.78 (se = 0.02). A subset of features that characterize lesion irregularity, margin sharpness, textural and kinetics were selected. The resulting radiomic lesion signature from the BANN classifier yielded an AUC value of 0.88 (se = 0.01).

CONCLUSION

Quantitative MRI radiomics demonstrated promising classification performance in distinguishing between malignant and benign breast lesions in a large clinical dataset from China.

CLINICAL RELEVANCE/APPLICATION

Our computerized radiomic analysis method has potential to aid clinicians in improving breast cancer diagnosis and patient management.



ML32

Machine Learning Theater: The Potential of a Web Platform to Transform Medical Imaging with AI and Cloud Computation: Presented by ARTERYS, Inc.

Tuesday, Nov. 27 11:30AM - 11:50AM Room: Machine Learning Showcase North Hall

Participants

Fabien Beckers, San Francisco, CA (*Presenter*) Founder and CEO, Arterys Inc Michael Poon, MD, New York, NY (*Presenter*)



ML33

Machine Learning Theater: Finding a Similar Case to Understand Yours-The Impact of Search on Clinical Radiology: Presented by contextflow

Tuesday, Nov. 27 12:00PM - 12:20PM Room: Machine Learning Showcase North Hall

Participants

Georg Langs, Vienna, Austria (Presenter) Nothing to Disclose

Program Information

The heterogeneity of clinical cases, and corresponding medical imaging data often makes in-depth assessment necessary for diagnosis. Search for similar cases is a paradigm that enables clinicians to view cases or cohorts sharing characteristics with a present case, together with the underlying evidence. Since the information needed for similarity evaluation is highly complex, and holds substantial natural variability not associated with disease, it poses a challenging machine learning problem. In the talk we will present techniques and results demonstrating how machine learning algorithms can identify markers and metrics to find comparable cases and cohorts that are informative during diagnosis.



AIS-TUA

Artificial Intelligence Tuesday Poster Discussions

Tuesday, Nov. 27 12:15PM - 12:45PM Room: AI Community, Learning Center

IN

Participants

Ryan Chamberlain, PhD, Minneapolis, MN (Moderator) Employee, ImBio, LLC

Sub-Events

Station #1

Awards Student Travel Stipend Award

Participants

Tafadzwa Chaunzwa, BEng, MS, Boston, MA (*Presenter*) Nothing to Disclose Yiwen Xu, PhD, Boston, MA (*Abstract Co-Author*) Nothing to Disclose Raymond H. Mak, MD, Boston, MA (*Abstract Co-Author*) Nothing to Disclose David Christiani, MD, Boston, MA (*Abstract Co-Author*) Nothing to Disclose Michael Lanuti, MD, Boston, MA (*Abstract Co-Author*) Nothing to Disclose Andrea Shafer, MPH, Boston, MA (*Abstract Co-Author*) Nothing to Disclose Nancy Diao, DSc, Boston, MA (*Abstract Co-Author*) Nothing to Disclose Hugo Aerts, PhD, Boston, MA (*Abstract Co-Author*) Stockholder, Sphera Inc

For information about this presentation, contact:

tafadzwa.chaunzwa@yale.edu

CONCLUSION

Transfer-learning is a viable approach to building powerful deep-learning based tools for image analysis and performing prognostic calculations in early-stage NSCLC. This model can aid clinical decision making in the treatment of lung cancer.

Background

In this study we present a deep-learning model that can act as a non-invasive biomarker in early stage Non-Small Cell Lung Cancer (NSCLC). Our model would be able to assign patients to short term or long term survival groups, based on computed tomography (CT) characteristics.

Evaluation

Pre-treatment CT studies were retrieved for 186 NSCLC surgical Stage-I patients at Massachusetts General Hospital between 2004 and 2010. Median follow-up from time of diagnosis was 1074 days, with 90.3% 2-year survival. To mitigate bias against a low probability event (mortality), data augmentation was performed on the training and validation images (n = 178). A VGG-16 deep neural network pretrained on ImageNet was used, with fine-tuning of the last two convolutional layers, dense layers, and softmax for stratification. Inputs of this model were 50 x 50 mm2 patches. Training was performed on 144 labeled CT scans, matched to one of two groups based on 2 year survival. 34 samples were used for initial cross-validation.

Discussion

Our model stratified patients with long term and short term survival in an independent test set of 46 patients (accuracy of 87%, AUC=0.92, p<0.0023). Given the relatively small datasets encountered in this and other clinical studies, optimal results would not have been attained by training a deep-learning model from scratch (AUC=0.89, p<0.0041). By tailoring a powerful solution for other computer vision tasks, we were able to build a robust prognostic model. A multivariate linear model of conventional clinical prognostic factors (age, gender, tumor stage IA/1B, histology, and smoking status) had a significant but lower predictive performance (AUC=0.665).

AI213-SD-TUA2 Synthetic PET Generator: A Novel Method to Improve Lung Nodule Detection by Combining Outputs from a Pix2pix Conditional Adversarial Network and a Convolutional Neural Network Based Malignancy Probability Estimator

Station #2

Participants

Vasanthakumar Venugopal, MD, New Delhi, India (*Abstract Co-Author*) Nothing to Disclose Abhijith Chunduru, MENG, Bengaluru, India (*Presenter*) Stockholder, Predible Health Suthirth Vaidya, BEng, MENG, Bengaluru, India (*Abstract Co-Author*) Employee, Predible Health Vidur Mahajan, MBBS, New Delhi, India (*Abstract Co-Author*) Nothing to Disclose Harsh Mahajan, MD, MBBS, New Delhi, India (*Abstract Co-Author*) Nothing to Disclose

For information about this presentation, contact:

CONCLUSION

Synthetic PET images can potentially increase the sensitivity of malignant nodule detection from Lung CT images. Such a modality can be easier for radiologists to understand than naive probability heatmaps. Further research is required to investigate the effect of potential biases and investigate appropriate clinical application.

Background

Assessment of malignancy of lung nodules on CT scans is a subjective and arduous task for radiologists with low reported accuracy rates, especially for small nodules. We propose a novel method to generate a synthetic PET image of the lung from CT images using Conditional Generative Adversarial Networks (cGAN) that can improve the sensitivity of the radiologist in the detection of malignant lung nodules.

Evaluation

We used a combination of a PET Generator combined with a Malignancy Probability Estimator to generate a synthetic PET image from Lung CT scan. The PET Generator is a conditional adversarial network (pix2pix) trained on slices containing the Lung from 100 PET-CT scans which were acquired on patients suspected or diagnosed with Lung Cancer. The model performed at a mean squared error of 0.08 when compared in SUV units. The malignancy probability estimator is a 20-layer deep residual convolutional neural network trained on a dataset of 1595 scans from the NLST trial. The model performed produced a ROC of 0.89 when tested on 822 patients. The outputs of the PET Generator provides a background for overlaying outputs of the Malignancy Probability Estimator which together produce the synthetic PET image.

Discussion

When tested on a dataset of 30 images, the synthetic PET model performed at a mean squared error of 0.08 when compared in SUV units. The malignancy model was independently tested on 350 scans and produced an AUC of 0.89. A dataset of 22 malignant scans is used to benchmark performance of malignancy detection. Using the CT scan alone, three radiologists had sensitivities of 86%, 81% and 72% in detecting malignant studies. Using the synthetic PET as an additional modality, an increased sensitivity of 95% can be obtained. However, it is important to note that the SUV values detected on the nodules were not correlated with the actual SUV values.

AI006-EB Radiomic Modeling to Predict Risk of Vertebral Compression Fracture After Stereotactic Body Radiation Therapy for Spinal Metastases

All Day Room: AI Community, Learning Center

Participants

Chengcheng Gui, Baltimore, MD (Presenter) Nothing to Disclose

Meet the Author: The authors of this poster will be available in person to discuss their project during these times Tuesday, November 27 12:15-12:45 pm



LL23

Lunch and Learn: Real-World Deployment of Deep Learning for Breast Cancer Screening: Presented by Kheiron Medical Technologies (invite-only)

Tuesday, Nov. 27 12:30PM - 1:30PM Room: S403B

Participants

Peter D. Kecskemethy, PhD, London, United Kingdom (*Presenter*) Stockholder, Kheiron Medical Technologies Ltd Hugh Harvey, MBBS, London, United Kingdom (*Presenter*) Employee, Kheiron Medical Christopher C. Austin, MBBCh, MSc, Seattle, WA (*Presenter*)

Program Information

Kheiron is at the cutting edge of deep learning technology for breast cancer screening, and leading the way for healthcare and industry collaborations in real-world deployment of deep learning technologies. Please join us for this lunchtime session where we will use our experiences of partnerships and real-world deployment to explore and discuss this exciting new space, including: - the organizational benefits and challenges posed by the next generation of supportive technology - how radiologists can take a leading role in the development and adoption of deep learning in radiology - discussion on the challenges faced by the industry, including structural changes and operations of professional bodies, individual providers, and nationwide programs.

RSVP Link

https://www.kheironmed.com/rsna



ML34

Machine Learning Theater: The Hype, the Reality, and the Global Landscape of Medical AI: Presented by Infervision

Tuesday, Nov. 27 12:30PM - 12:50PM Room: Machine Learning Showcase North Hall

Participants

Kuan Chen, Beijing, China (Presenter) Employee, Infervision Inc

Program Information

Infervision is a pioneer and industry leader in medical AI headquartered in Beijing, China. Founded in January 2015, Infervision is committed to employ AI and deep learning technologies to analyze medical images to aid radiologists. We adhere to the principle of 'From the clinic, to the clinic', have developed highly effective tools to help radiologists make faster and more accurate diagnoses not only in China, but across the globe.



AIS-TUB

Artificial Intelligence Tuesday Poster Discussions

Tuesday, Nov. 27 12:45PM - 1:15PM Room: AI Community, Learning Center

IN

FDA Discussions may include off-label uses.

Participants Ryan Chamb

Ryan Chamberlain, PhD, Minneapolis, MN (Moderator) Employee, ImBio, LLC

Sub-Events

AI215-SD- Impact of Deep Learning-based CT Denoising on Normal Anatomical Structures in Low Dose Chest TUB1 CT: FBP vs IRT vs Deep Learning

Station #1 Participants

Semin Chong, MD, Seoul, Korea, Republic Of (*Presenter*) Research Consultant, Samsung Electronics Co, Ltd Jong H. Kim, PhD, Seoul, Korea, Republic Of (*Abstract Co-Author*) Nothing to Disclose Kyungmin Lee, Seoul, Korea, Republic Of (*Abstract Co-Author*) Nothing to Disclose

CONCLUSION

DL image denoising is expected to provide the same or better quality than the IRT in the mediastinum and airway. However, IRT also seems to have some limitations now, and it is thought that more software improvement or machine training is needed to apply DL technology to pulmonary parenchyma.

Background

The dramatic development of CT image denosing technology enabled to achieve ultra low-dose CT scans. Deep learning (DL) based techniques are applied in image processing algorithms to solve many difficulties in image reconstruction and lead to changes in paradigm. In this study, we propose the possibility of DL method to reduce image noise and compare it with FBP and IRT.

Evaluation

We evaluated a new CT denoising solution (ClariCT+, ClariPI, Seoul, South Korea) based on a fully convolutional deep learning (DL) model, which was trained by using 11,500 slices of normal patients with two-tissue mode where soft tissue and lung tissue were segmented and were used for training of two separate denoising models. All images (n = 30) were acquired by applying FBP, IRT (i4 and i6, iDose, Philips Healthcare, The Netherlands) and DL (DLmd and DLstr, moderate and strong denosing levels). Mean (HU), SD (HU), and area(mm2) of ROI were measured for mediastinum (aortic arch), right lung, left lung, and airway (trachea) using a fixed size ROI in each image.

Discussion

Mean of mediastinum and left lung did not differ statistically between FBP, IRT, and DL. Mean of right lung was significantly different between FBP and DLstr. Mean and SD of airway were not significantly different between DLmd and DLstr. The SD of the mediastinm decreased statistically significantly from FBP to DLstr, but there was no statistically significant difference between i4 and i6, DLmd and DLstr, and DLmd and DLstr for right lung, left lung and airway, respectively. In this study, reducing the image noise applied to the mediastinum was the most ideal and showed anatomical characteristics suitable for the hypothesis. However, some lungs showed instability of the mean HU when DL was applied, and DL as well as IRT were not consistent in SD reduction. One interesting point was that the mean and SD of the trachea were consistent when applying DL.

AI216-SD-TUB2 Machine Learning for Identifying the Value of Digital Breast Tomosynthesis using Data from a Multicentre Retrospective Study

Station #2

Participants

Ahmed M. Alaa, Los Angeles, CA (*Abstract Co-Author*) Nothing to Disclose Fiona J. Gilbert, MD, Cambridge, United Kingdom (*Presenter*) Research Grant, Hologic, Inc; Research Grant, General Electric Company; Research Grant, GlaxoSmithKline plc; Research Consultant, Alphabet Inc Yuan Huang, Cambridge, United Kingdom (*Abstract Co-Author*) Nothing to Disclose Mihaela van der Schaar, Oxford, United Kingdom (*Abstract Co-Author*) Nothing to Disclose

CONCLUSION

Machine learning helps to identify subpopulations of women who benefit most from DBT, and can be used to design individualized screening.

Background

We sought to identify subgroups of women for whom digital breast tomosynthesis (DBT) showed improved diagnostic accuracy for different types of malignant lesions than 2D mammography. The study used multicenter retrospective data from 6,040 women (934 biopsy-confirmed cancers) who underwent both DBT and 2D mammography. An ensemble of 20 state-of-the-art machine learning models was created to predict biopsy outcomes based on radiological classification of 2D and DBT images, Volpara breast

composition measures and age. We used this ensemble to assess the diagnostic accuracy of DBT- and 2D-based predictors, to identify subgroups of women for whom DBT is more informative, and to quantify the value of the individual predictors with respect to different types of malignant lesions.

Evaluation

Accuracy and precision of DBT-based and 2D-based predictive models were evaluated using the area under receiver operating characteristic curve (AUC-ROC) and the area under precision-recall curve (AUC-PR), respectively. At the population level, DBT-based models significantly outperformed 2D-based models in terms of both AUC-ROC ($0.943 \pm 0.009 \text{ vs } 0.915 \pm 0.018$) and AUC-PR ($0.812 \pm 0.042 \text{ vs } 0.776 \pm 0.051$). The gains achieved by DBT-based models were superior in patient groups with fibroglandular volume ranging from 40 cm³ - 80 cm³, and in invasive lobular cancers compared to ductal tumours. The gain from DBT became insignificant for patients >60 years old or with fibroglandular volume exceeding 80 cm³.

Discussion

Using state-of-the-art machine learning techniques, we established that DBT mammography is significantly more informative than 2D mammography, especially for patients with moderate fibroglandular breast volume but was not advantageous in those women > 60 years or in those with dense breast volume >80cm3. For both DBT and 2D imaging, our machine learning models lead to higher detection rates and fewer false alarms.

AI218-SD- Patient Data Adapted Deep Learning for Multi-Label Chest X-Ray Classification TUB3

Station #3

Participants

Ivo Matteo Baltruschat, Hamburg, Germany (*Presenter*) Nothing to Disclose Hannes Nickisch, Hamburg, Germany (*Abstract Co-Author*) Koninklijke Philips NV Michael Grass, PhD, Hamburg, Germany (*Abstract Co-Author*) Employee, Koninklijke Philips NV Tobias Knopp, DIPLENG, Hamburg, Germany (*Abstract Co-Author*) Nothing to Disclose Axel Saalbach, PHD, Aachen, Germany (*Abstract Co-Author*) Employee, Koninklijke Philips NV

For information about this presentation, contact:

i.baltruschat@uke.de

PURPOSE

Neural network based chest X-ray image classification can serve multiple purposes in diagnostic radiology. These include the reordering of task lists for the radiologist, the exclusion of pathology up to diagnosis prediction. Most neural networks train pure image data against the multi-label chest X-ray classification. Here, we include additional patient data e.g. patient age and gender as well as the view position in the training. Together with the images, we evaluate the improvement in classification accuracy.

METHOD AND MATERIALS

We used the ChestXray14 dataset with about 112120 images for training of our neural networks and investigated the ResNet-50 architecture in the experiments. Following up on early work in this domain, we considered transfer learning with and without finetuning as well as the training of a dedicated X-ray network. Furthermore, we included a network integrating non-image data (patient age, gender, and acquisition type) in the classification pipeline. In a systematic evaluation using a 5 times re-sampling scheme and a multi-label loss function, we evaluated the performance of the different approaches for pathology classification by ROC statistics. In this context, we observed the best performance for the X-ray specific ResNet-50 integrating non-image data.

RESULTS

For our empirical assessment, we evaluated two different setups with varying network schemes and architectures with and without patient data inclusion. For all pathologies, we performed an ROC analysis and computed the area under curve (AUC). The mean AUC increases across all pathologies from 73.0 ± 1.1 to 74.8 ± 1.1 (±1.8) / 81.7 ± 1.0 to 82.0 ± 0.9 (±0.3) for off-the-shelf / fine-tuned networks.

CONCLUSION

Neural network based chest X-ray image classification profits from patient data inclusion in contrast to pure image data based multi-label classification. Increased mean AUC results can be achieved for the majority of target pathologies.

CLINICAL RELEVANCE/APPLICATION

Automatic multi-label chest X-ray classification based on neural networks can improve various processes in diagnostic radiology. By combining image and patient data the diagnosis prediction can be improved.

AI007-EB Artificial Intelligence-Assisted Automated Detection and Outcome Prediction of Subarachnoid Hemorrhage: Techniques and Educational Approaches

All Day Room: AI Community, Learning Center

Participants

Weimeng Ding, Montreal, QC (*Presenter*) Nothing to Disclose Jack W. Luo, Montreal, QC (*Abstract Co-Author*) Nothing to Disclose Josep L. Dolz, MD, Terrassa, Spain (*NON-Presenter*) Nothing to Disclose Ismail Ben Ayed, London, ON (*NON-Presenter*) Research, General Electric Company Jaron Chong, MD, Montreal, QC (*Abstract Co-Author*) Nothing to Disclose

Meet the Author: The authors of this poster will be available in person to discuss their project during these times: Tuesday November 27 12:45-1:15pm



ML35

Machine Learning Theater: Human + Machine: The Future of AI Augmented Radiology: Presented by Enlitic

Tuesday, Nov. 27 1:00PM - 1:20PM Room: Machine Learning Showcase North Hall

Participants

Kevin Lyman, CEO, Enlitic - San Francisco, CA

Program Information

With the healthcare industry expected to cope with 116 billion medical images by 2021 radiologists are being pushed far beyond their alloted 3-second analysis per image. Deep learning technology promises much-needed relief to radiologists, improving their ability to identify and characterize abnormalities while surfacing key patient insights. Join Enlitic CEO Kevin Lyman in the Machine Learning Theatre as he demonstrates the latest innovations and augmented radiology solutions from Enlitic, providing a first-look at how this technology is being integrated into existing workflows and deployed in clinical settings to make radiologists faster, and more accurate.



ML36

Machine Learning Theater: How AI Can Improve Diagnostic Performance and Reduce Reading Time in Breast Tomosynthesis: Presented by iCAD

Tuesday, Nov. 27 1:30PM - 1:50PM Room: Machine Learning Showcase North Hall

Participants

Senthil Periaswamy, PhD, Nashua, NH (Presenter) Vice President, iCAD, Inc

Program Information

iCAD will share how its innovative breast health AI solution, built on the latest deep learning technology, improves breast cancer detection, reduces recalls and improves reading efficiency for digital breast tomosynthesis.



CS35

AI: Fad or Forever: Presented by MaxQ AI

Tuesday, Nov. 27 2:00PM - 3:30PM Room: S102AE

Participants

Gene Saragnese, Andover, MA (*Presenter*) Ajay Choudhri, MD, Trenton, NJ (*Presenter*) Norman J. Beauchamp JR, MD, Grand Rapids, MI (*Presenter*) Research Grant, Koninklijke Philips NV

PARTICIPANTS

Brian Casey, Editor-in-Chief, AuntMinnie.com San Francisco, CA (Moderator)

PROGRAM INFORMATION

Despite holding much promise, many new innovations in personalized medicine, genomics and now AI have dramatically increased the amount of imaging data to interpret, which has put extreme pressure on radiologists to balance reading more cases in less time while maintaining a high level of accuracy and confidence. Instead of more data and analysis, radiologists need solutions and tools that provide answers while seamlessly integrating into the current workflow, PACS systems, medical imaging hardware, and healthcare clouds. This session will explore the promise of AI - and how by embracing it - radiologists will usher in a new era of healthcare. In particular, the potential to improve triage, annotation, and diagnostic rule-out of intracranial hemorrhage in acute care settings. In the hands of highly skilled radiologists, these AI support tools provide deep clinical insights into challenging cases - such as ICH - to help guide the clinical team through a series of critical decisions with improved speed and accuracy to enhance access and treatment for the patient. AI-enabled solutions hold great promise as 'imaging plus' support tools that will greatly benefit the care of acute patients as well as collaborating clinicians in emergency rooms across the globe. Hear directly from a panel of experts on the potential of new AI-enabled solutions for radiologists working within the acute care space.

СМЕ

This course does not offer CME credit.

RSVP

https://maxq.ai/rsna-2018



RCA34

Leveraging Machine Learning Techniques and Predictive Analytics for Knowledge Discovery in Radiology (Hands-on)

Tuesday, Nov. 27 2:30PM - 4:00PM Room: S401AB



AMA PRA Category 1 Credits ™: 1.50 ARRT Category A+ Credit: 1.75

Participants

Kevin Mader, DPhil,MSc, Basel, Switzerland (*Moderator*) Employee, 4Quant Ltd; Shareholder, 4Quant Ltd Kevin Mader, DPhil,MSc, Basel, Switzerland (*Presenter*) Employee, 4Quant Ltd; Shareholder, 4Quant Ltd Barbaros S. Erdal, PhD, Columbus, OH (*Presenter*) Nothing to Disclose Joshy Cyriac, Basel, Switzerland (*Presenter*) Nothing to Disclose

LEARNING OBJECTIVES

1) Review the basic principles of predictive analytics. 2) Be exposed to some of the existing validation methodologies to test predictive models. 3) Understand how to incorporate radiology data sources (PACS, RIS, etc) into predictive modeling. 4) Learn how to interpret results and make visualizations.

ABSTRACT

During this course, an introduction to machine learning and predictive analytics will be provided through hands on examples on imaging metadata (scan settings, configuration, timestamps, etc). Participants will use open source as well as freely available commercial platforms in order to achieve tasks such as image metadata and feature extraction, statistical analysis, building models, and validating them. Imaging samples will include datasets from a variety of modalities (CT, PET, MR) and scanners. The course will begin with a brief overview of important concepts and links to more detailed references. The concepts will then be directly applied in visual, easily understood workflows where the participants will see how the data are processed, features are selected, and models are built.



SSJ18

Neuroradiology (Artificial Intelligence in Neuroimaging)

Tuesday, Nov. 27 3:00PM - 4:00PM Room: E451B



AMA PRA Category 1 Credit ™: 1.00 ARRT Category A+ Credit: 1.00

FDA Discussions may include off-label uses.

Participants

Max Wintermark, MD, Lausanne, Switzerland (*Moderator*) Advisory Board, General Electric Company; Consultant, More Health; Consultant, Magnetic Insight; Consultant, Icometrix; Consultant, Nines;

Mark D. Herbst, MD, PhD, Saint Petersburg, FL (Moderator) Nothing to Disclose

Sub-Events

SSJ18-01 Automated Detection of Abnormality in Multi-Parametric Brain MRI Using an Artificial Intelligence 3D Pipeline

Tuesday, Nov. 27 3:00PM - 3:10PM Room: E451B

Participants

Kambiz Nael, MD, New York, NY (*Presenter*) Medical Advisory Board, Canon Medical Systems Corporation
Benjamin L. Odry, PhD, Princeton, NJ (*Abstract Co-Author*) Employee, Siemens AG
Chen Yang, PhD, New York, NY (*Abstract Co-Author*) Nothing to Disclose
Mariappan Nadar, Princeton, NJ (*Abstract Co-Author*) Nothing to Disclose
Bin Lou, Princeton, NJ (*Abstract Co-Author*) Employee, Siemens AG
Thomas Re, Princeton, NJ (*Abstract Co-Author*) Nothing to Disclose
Bogdan Georgescu, PhD, Princeton, NJ (*Abstract Co-Author*) Nothing to Disclose
Bogdan Georgescu, PhD, Princeton, NJ (*Abstract Co-Author*) Employee, Siemens AG
Bernd Stoeckel, PhD, Princeton, NJ (*Abstract Co-Author*) Employee, Siemens AG
Dorin Comaniciu, PhD, Princeton, NJ (*Abstract Co-Author*) Employee, Siemens AG
David S. Mendelson, MD, Larchmont, NY (*Abstract Co-Author*) Spouse, Employee, Novartis AG; Advisory Board, Nuance
Communications, Inc; Advisory Board, General Electric Company; Advisory Board, Canon Medical Systems Corporation; Advisory Board, Bayer AG; Advisory Board, Nines
Zahi A. Fayad, PhD, New York, NY (*Abstract Co-Author*) Nothing to Disclose

For information about this presentation, contact:

kambiznael@gmail.com

PURPOSE

With rapid growth and increasing use of brain MRI, there has been a significant interest in automated image processing and classification of brain MRI scans to supplant human interpretation and improve workflow. In this study we aim to assess the diagnostic accuracy of an AI 3D pipeline in classifying multi-parametric brain MRI to normal vs. abnormal.

METHOD AND MATERIALS

A total of 1,516 consecutive clinical brain MRI studies including sagittal T1W and axial FLAIR, ADC and B1000 sequences were selected from our institution HIPAA compliant imaging registry. Brain MR studies were obtained using standardized protocol across 1.5T MR scanners from two manufacturers (GE and Siemens). Each sequence was reformatted to common resolution to accommodate for differences between vendors. A board certified neuroradiologist assigned each case to normal vs. abnormal based on the review of clinical report of each case. Consequently, 88% of the MRI scans were marked as abnormal. A 3D AI pipeline was developed: first, a deep reinforcement learning based landmark detection was used to estimate positioning and brain coverage. Brain was extracted using an adversarial dense image-to-image based technique then sequence-independent dense convolutional networks were trained in a supervised way, with data augmentation (random rotation, translation and added noise at each iteration), and merged to flag abnormal cases. Training was performed on 1,566 cases (200,448 images - 85% abnormal) with class weights to address class imbalance, testing included 175 cases (22,400 images - 84% abnormal).

RESULTS

Receiver operating characteristic (ROC) analysis showed that an area-under-the-curve (AUC) of 0.90 with accuracy of 86%, sensitivity of 85%, and specificity of 89% for our detection pipeline.

CONCLUSION

Our proposed intelligent pipeline accurately identifies abnormal brain MRIs from the individual patients. If its potential is realized, it can be used as a clinical tool to flag abnormal MRIs, allowing for improved triage and timely interpretation of abnormal scans in a busy and large clinical practice.

CLINICAL RELEVANCE/APPLICATION

Our proposed automated and intelligent 3D pipeline can flag abnormal brain MRI scans, catering available human expertise in interpreting abnormal cases in a timely manner.

SSJ18-02 Multi-Metric Characterization of Resting-State Functional Connectivity for Machine Learning Classification in Major Brain Networks

Tuesday, Nov. 27 3:10PM - 3:20PM Room: E451B

Participants

Rosaleena Mohanty, MS, Madison, WI (*Presenter*) Nothing to Disclose Veena A. Nair, PhD, Madison, WI (*Abstract Co-Author*) Nothing to Disclose Vivek Prabhakaran, MD, PhD, Fitchburg, WI (*Abstract Co-Author*) Nothing to Disclose

PURPOSE

Population differences have been identified based on resting-state functional connectivity (FC) derived from blood-oxygen-leveldependent (BOLD) response using machine learning classification. While Pearson's correlation is the conventional metric used to quantify FC, it may not capture the true dynamic and non-linear relationship between BOLD responses from distinct brain regions. This motivates the need for a more complete notion of FC for better classification performance.

METHOD AND MATERIALS

Ten-minute eyes closed functional MRI were acquired on 3T GE MR750 scanner from 50 right-handed healthy participants consisting of 25 older (age=57.5±7.1 years; 13 females; education=16.68 years) and 25 younger (age=23.9±5.9 years; 13 females; education=16.76 years) participants. Data were preprocessed using standard steps on SPM12 to extract the BOLD time courses in 6 major brain networks. Network-wise FC was computed based on 8 distinct metrics: cross-correlation, coherence, mutual information, dynamic time warping (DTW) distance, Euclidean distance, cityblock distance, wavelet coherence and the conventional Pearson's correlation. Individual and combined discriminatory power of the metrics was assessed using a linear support vector machine classifier to differentiate between the older and younger groups for each network. Neighborhood component analysis and leave-one-out cross-validation were used for feature selection and evaluation of classification performance respectively.

RESULTS

Groups were significantly different in age (p-value<0.001) but not in gender distribution or education. Comparative results showed that Pearson's correlation may not always be the optimal choice for FC. The combined metric performed comparable/better than individual metrics for each network. This could imply that a more meaningful definition of FC encompassing linear, non-linear, dynamic, time-, frequency- and wavelet-domain information could be created for classification by drawing contributions from multiple metrics.

CONCLUSION

Combining the inter-dependencies in BOLD signals in time, frequency and wavelet domains could provide a more comprehensive notion of FC for population-based classification using machine learning.

CLINICAL RELEVANCE/APPLICATION

Multi-metric characterization offers a more complete definition of FC and could be useful in delineating group differences between patient and healthy population using machine learning classification.

SSJ18-03 Use of a Deep Convolutional Neural Network for Automated Detection of Intracranial Hemorrhage

Tuesday, Nov. 27 3:20PM - 3:30PM Room: E451B

Awards

Student Travel Stipend Award

Participants Chad W. Farris, MD,PhD, Boston, MA (*Presenter*) Nothing to Disclose Arjun Majumdar, Lexington, MA (*Abstract Co-Author*) Nothing to Disclose Brian Telfer, Lexington, MA (*Abstract Co-Author*) Nothing to Disclose Jonathan E. Scalera, MD, Boston, MA (*Abstract Co-Author*) Nothing to Disclose

For information about this presentation, contact:

Chad.Farris@bmc.org

PURPOSE

The purpose of this study is to investigate the possibility of automated detection of all varieties of intracranial hemorrhage (ICH), including epidural (EDH), subdural (SDH), subarachnoid (SAH), intraparenchymal (IPH), and intraventricular (IVH) on unenhanced head CT examinations (HCT) using a deep residual convolutional neural network (DRCNN) in all possible clinical scenarios, including initial HCT for diagnosis of ICH, follow-up HCT for known ICH, and post-operative HCT after surgical intervention.

METHOD AND MATERIALS

IRB approved retrospective HIPAA compliant study with requirement for informed consent waived. Included cases were identified through a keyword search of our RIS for HCT with ICH and normal HCT (NHCT) between 7/1/2014-7/1/2016. A total of 95 ICH cases and 46 NHCT cases were included in this study. The hemorrhages in the ICH cases were segmented by hand using an inhouse MATLAB annotation tool. The DRCNN was trained using 60 annotated ICH cases and validated with 5 ICH cases. The trained DRCNN was then tested on 30 ICH cases (with many of the cases including different types of hemorrhage for a total of 56 hemorrhages) and 46 NHCT cases using two different DRCNN thresholds for hemorrhage detection and minimal post-processing of the DRCNN output. The percentage of hemorrhages detected, and the false positive rate (FPR) were evaluated at each of the DRCNN thresholds. For the lower DRCNN threshold, a minimum number of DRCNN identified pixels containing hemorrhage was employed to consider the case positive for hemorrhage to limit the FPR.

RESULTS

The DRCNN with a high threshold (HT) for ICH detection correctly detected 70% (39/56) ICH including, 0% (0/1) EDH, 60% (6/10) SDH, 50% (6/12) SAH, 81% (17/21) IPH, and 83% (10/12) IVH. The DRCNN with a low threshold (LT) for ICH detection correctly

detected 89% (50/56) ICH including, 100% (1/1) EDH, 80% (8/10) SDH, 83% (10/12) SAH, 90% (19/21) IPH, and 100% (12/12) IVH. The DRCNN with a HT for ICH detection had a FPR of 2% (1/46 NHCTs evaluated). The DRCNN with a LT for ICH detection had a FPR of 28% (13/46 NHCTs evaluated).

CONCLUSION

DRCNNs can be trained to successfully detect all types of ICH on HCT examinations in all possible clinical scenarios.

CLINICAL RELEVANCE/APPLICATION

Automated detection of intracranial hemorrhages could potentially be used clinically to help triage completed unread examinations and assist with detection of subtle hemorrhages.

SSJ18-04 Substantially Shortened Brain and Lumbar Spine MR Scan Times with a Machine Learning-Based Iterative Image Reconstruction Algorithm

Tuesday, Nov. 27 3:30PM - 3:40PM Room: E451B

Participants

Lawrence N. Tanenbaum, MD, New York, NY (*Presenter*) Speaker, General Electric Company; Speaker, Siemens AG; Speaker, Guerbet SA; Speaker, Koninklijke Philips NV; Consultant, Enlitic, Inc; Consultant, icoMetrix NV; Consultant, CorTechs Labs, Inc; Consultant, Arterys Inc

Wende N. Gibbs, MD, MA, Pasadena, CA (Abstract Co-Author) Nothing to Disclose

Blake A. Johnson, MD, Saint Louis Park, MN (*Abstract Co-Author*) Consultant, Medic Vision Imaging Solutions, Ltd; Consultant, MR Instruments, Inc; Consultant, icoMetrix NV; Consultant, Minnetronix

Inna Varaganov, MD, Haifa, Israel (Abstract Co-Author) Consultant, Medic Vision Imaging Solutions, LTD

John M. Gomori, MD, Jerusalem, Israel (Abstract Co-Author) Consultant, Medic Vision Imaging Solutions, Ltd; Advisory Board, NVision

Adi Pais, PhD, Tirat Carmel, Israel (*Abstract Co-Author*) Employee, Medic Vision Imaging Solutions, Ltd Tal Aharoni, MSc, Haifa, Israel (*Abstract Co-Author*) Employee, Medic Vision Imaging Solutions, Ltd Roni Shreter, MD, Haifa, Israel (*Abstract Co-Author*) Nothing to Disclose

For information about this presentation, contact:

nuromri@gmail.com

PURPOSE

To evaluate the scan time shortening potential of a novel 3D image enhancement algorithm for brain and lumbar spine MRI exams.

METHOD AND MATERIALS

Fifty-six subjects (mean age 48+/-16 years) were scanned on four 1.5T scanners (Philips-Ingenia: 18 brain, 6 spine; Siemens-Aera: 9 brain, 2 spine; General Electric Signa-HDxt: 10 brain, Optima MR450w 11 spine), at three different sites using the site's routine clinical protocols as well as an average of ~30% shorter scan time-reduced variants. The time-reduced variant protocols were set by altering routine acquisition parameters, trading scan time reductions, mainly, for decreased signal to noise ratio. The faster, SNR challenged scans were processed with a novel 3D image enhancement algorithm (iQMR by Medic Vision Ltd.) and compared with the corresponding sites' routine scans (153 brain scans and 43 lumbar spine scans). Independent, blinded, side-by-side comparisons of diagnostic quality, visual image quality, presence of artifacts and brain gray-white matter differentiation were performed by six neuroradiologists for brain data and three neuroradiologists for spine data, using a 5-point Likert-scale (3= equal, >3 processed image is superior).

RESULTS

The processed-reduced scan time images (614 brain reads, 129 lumbar spine reads) were rated higher or equal to the conventional routine scans with respect to diagnostic quality (brain: median=3, mode=3, mean=2.94+/-0.39; spine: median=3, mode=3, mean=3.05+/-0.39), visual image quality (brain: median=3, mode=3, mean=2.83+/-0.69; spine: median=3, mode=3, mean=3.14+/-0.77), the presence of artifacts (brain: median=3, mode=3, mean=2.91+/-0.54; spine: median=3, mode=3, mean=3.11+/-0.66) and for brains, gray-white matter differentiation (median=3, mode=3, mean=2.91+/-0.46).

CONCLUSION

iQMR processed, reduced scan time images were similar in overall image quality to standard protocols with a reduction of MRI exam scan time of about 30%.

CLINICAL RELEVANCE/APPLICATION

iQMR can produce clinically acceptable MR images at significantly shorter scan times, facilitating patient comfort and clinical practice workflow. Faster scans could potentially decrease motion artifacts and reduce the need for repeat scans.

ssj18-05 Radiomics-Based Prediction of Malignant Potential in Patients with Parotid Gland Cancer

Tuesday, Nov. 27 3:40PM - 3:50PM Room: E451B

Participants

Hidemi Kamezawa, Omuta, Japan (*Presenter*) Nothing to Disclose Hidetaka Arimura, PhD, Fukuoka, Japan (*Abstract Co-Author*) Nothing to Disclose Ryuji Yasumatsu, Fukuoka, Japan (*Abstract Co-Author*) Nothing to Disclose Mazen Soufi, Nara, Japan (*Abstract Co-Author*) Nothing to Disclose Shu Haseai, Fukuoka, Japan (*Abstract Co-Author*) Nothing to Disclose Kenta Ninomiya, Fukuoka, Japan (*Abstract Co-Author*) Nothing to Disclose

PURPOSE

Prediction of malignant potential (low+intermediate and high grades) in patients with parotid gland cancer (PGC) is crucial in determination of treatment approaches. Although the fine needle aspiration cytology (FNAC) is performed for prediction of malignant

potential for PGC, various researchers have reported the prediction accuracy of malignant potential in PGC by the FNAC, which depends on the operator experience, was from 69 to 92%. Therefore, we developed the radiomics-based prediction of malignant potential in patients with parotid gland cancer.

METHOD AND MATERIALS

A total of 972 radiomic features (statistic, texture, wavelet-based features) were extracted from tumor regions in preoperative T1and T2-weighted images of 42 PGC patients. Radiomic signatures for prediction of malignant potential in PGC patients were generated by using least absolute shrinkage and selection operator (LASSO), which is one of sparse coding approaches that performs both feature selection and regularization to avoid the curse of dimensionality. Malignant potential for PGC was predicted by using Gaussian support vector machine (G-SVM), which is a machine learning classifier. The accuracy and the mean area under the receiver operating characteristic curve (AUC) of G-SVM model by a leave-one-out cross validation test were evaluated.

RESULTS

The 5 features, which included T1_LLH_Skewness, T1_HLH_Min, T2_gray-level non-uniformity (GLN), T2_LLH_Long Run Emphasis (LRE), and T2_LLH_Small Zone High Gray-Level Emphasis (SZHGE), were selected by LASSO as the radiomic signatures for the malignant potential for PGC. The prediction accuracy of the malignant potential for PGC by using the G-SVM based on the selected 5 features was 90.5%, and the AUC was 0.96 with a sensitivity of 0.90 and a specificity of 0.90.

CONCLUSION

The proposed approach demonstrated high accuracy in classification of the malignant potential for PGC. Our results suggested that the proposed approach based on radiomics using preoperative MR images could be feasible to predict the malignant potential for PGC.

CLINICAL RELEVANCE/APPLICATION

The proposed approach contributes to the higher accuracy and lower intra- and inter-observer variabilities for prediction of malignant potential in parotid gland cancer.

SSJ18-06 Brain Tumor Segmentation on Fluid-Attenuated Inversion Recovery MRI Using Transfer Learning on U-Net

Tuesday, Nov. 27 3:50PM - 4:00PM Room: E451B

Participants

Naeim Bahrami, PhD, MSc, San Diego, CA (*Presenter*) Nothing to Disclose Ashwin Srikant, San Diego, CA (*Abstract Co-Author*) Nothing to Disclose Albert Hsiao, MD,PhD, La Jolla, CA (*Abstract Co-Author*) Founder, Arterys, Inc; Consultant, Arterys, Inc; Consultant, Bayer AG; Research Grant, General Electric Company; Nikdokht Farid, MD, San Diego, CA (*Abstract Co-Author*) Nothing to Disclose Carrie R. McDonald, PhD, La Jolla, CA (*Abstract Co-Author*) Nothing to Disclose

For information about this presentation, contact:

nabahrami@ucsd.edu

PURPOSE

Lesion assessment of glioma hyperintense volumes on fluid-attenuated inversion recovery (FLAIR) MRI is important for surgery, treatment planning, and genomic analysis. Manual delineation of the hyperintense region is time-consuming and subject to interand intra-operator variability. The purpose of this study is to assess the feasibility of FLAIR hyperintense region segmentation using a fully automated convolutional neural network (CNN) technique.

METHOD AND MATERIALS

We retrospectively collected 151 patients (363 time points) with low and high-grade gliomas. Each of the patients had a 3D T2weighted FLAIR sequence with TE/TR = 126/6000 ms, TI = 863, and FOV = 24 cm. Prior to analysis, raw data were corrected for bias field and distortion, image registration, and skull stripping. FLAIR hyperintense volumes were segmented semi-automatically (Amira software package, Visage Imaging) on the co-registered images by two trained image analysts and approved by a boardcertified neuro-radiologist with expertise in neuro-oncology. We developed a 2D U-net algorithm for segmentation and serially trained the model with images containing large lesions, small lesions, and no lesions. Three hundred of the cases were used for training and sixty-three were used for validation. We evaluated our model using Dice coefficients between the manually segmented and CNN-derived FLAIR volumes on the validation set.

RESULTS

Our proposed model segmented the hyperintense regions with the average Dice coefficient of 0.85. In 79% of patients, the dice coefficient was more than 0.8. Prediction of FLAIR volume from our cascaded U-net model closely matched with expert annotation (p=0.91).

CONCLUSION

In this study, we demonstrate the utility of a fully-automated CNN technique for segmenting the hyperintense region on FLAIR. We increased the performance of our model with transfer learning from images with large hyperintense regions to the images with no lesion. Implementation of this CNN into the clinical workflow may help improve the ROI drawing performance and reduce the discrepancies among image analysts.

CLINICAL RELEVANCE/APPLICATION

We present a fully automated technique for tumor segmentation of the FLAIR MRI of the patients with gliomas. Our model will increase accuracy of clinical interpretations by standardizing and quantifying the determination of the FLAIR hyperintense volume as a crucial part of Response Assessment in Neuro-Oncology (RANO).



SSJ22

Physics (Image Reconstruction)

Tuesday, Nov. 27 3:00PM - 4:00PM Room: N227B



AMA PRA Category 1 Credit ™: 1.00 ARRT Category A+ Credit: 1.00

FDA Discussions may include off-label uses.

Participants

Xiaochuan Pan, PhD, Chicago, IL (*Moderator*) Research Grant, Bondent Imaging; Research Grant, Canon Medical Systems Corporation; Stockholder, Clarix Imaging

Xiangyang Tang, PhD, Atlanta, GA (Moderator) Research Grant, SINOVISION Technology Co, Ltd

Sub-Events

SSJ22-01 Modified Model Based Iterative Reconstruction Method to Improve CT Number Accuracy in Low-Dose CT

Tuesday, Nov. 27 3:00PM - 3:10PM Room: N227B

Participants

John W. Hayes, MS, Madison, WI (*Presenter*) Nothing to Disclose Ran Zhang, PhD, Madison, WI (*Abstract Co-Author*) Nothing to Disclose Daniel Gomez-Cardona, PhD, Rochester, MN (*Abstract Co-Author*) Nothing to Disclose Juan Pablo Cruz Bastida, Madison, WI (*Abstract Co-Author*) Nothing to Disclose Guang-Hong Chen, PhD, Madison, WI (*Abstract Co-Author*) Research funded, General Electric Company Research funded, Siemens AG

For information about this presentation, contact:

jwhayes@wisc.edu

PURPOSE

Recent theoretical and experimental studies about CT number accuracy in low dose CT have shown that filtered backprojection (FBP) and conventional model based iterative reconstruction (MBIR) methods are biased by an amount that is dose and contrast dependent. This work validates that the data weighting scheme in the MBIR framework is the culprit for both these biases and that a more optimal weighting scheme has been found to eliminate bias across all dose and contrast levels.

METHOD AND MATERIALS

Raw CT data was acquired for two phantoms on a benchtop CT system using a photon counting detector (XC-HYDRA FX50, XCounter AB, Sweden). The Catphan phantom (Catphan 600, Phantom Laboratory, Salem, New York) was scanned at several dose levels in the range 69-367 mAs, with 50 repeated scans for each dose level. A customized head phantom was also scanned in the range 40-400 mAs, with 30 repeated scans for each dose level. Reference images for each phantom were obtained by averaging the pre-log projections for the highest dose level across all repetitions, and then performing FBP reconstruction. These references served as the experimental ground truth. For each dose level and reconstruction method (FBP, MBIR, proposed MBIR), bias images were calculated by subtracting the reference image from the mean of the reconstructions of each repeated scan. Bias was measured in 4 small inserts of varying contrast in the Catphan phantom. Bias images of the Catphan and head phantoms were also assessed across the image field of view (FOV).

RESULTS

There are three main results: 1) The theoretical relationship bias= $\pm a/mAs*(1+\beta\Delta HU)$ was validated experimentally for both FBP (positive polarity) and conventional MBIR (negative polarity). 2) The proposed MBIR method, which uses a modified weighting scheme, eliminates bias for each contrast and dose level in the Catphan phantom. 3) The proposed MBIR method demonstrates promising preliminary results for reducing bias across the FOV in a more complex anthropomorphic head phantom.

CONCLUSION

The proposed MBIR method maintains CT number accuracy of varying contrast across dose levels by using a theoretically based modified data weighting scheme.

CLINICAL RELEVANCE/APPLICATION

Certain tasks, e.g. detection of acute cerebral venous sinus thrombosis (CVST), rely on CT number estimation. It is critical the CT reconstruction method maintains accurate HU values.

ssj22-02 Joint Reconstruction of Low-Count PET and Undersampled MR in PET/MR Using Deep Learning

Tuesday, Nov. 27 3:10PM - 3:20PM Room: N227B

Junshen Xu, Beijing, China (*Presenter*) Nothing to Disclose Tuoyu Cao, PhD, Houston, TX (*Abstract Co-Author*) Employee, Medical Device Manufactor Zheng Zhang, MD, Shanghai, China (*Abstract Co-Author*) Employee, Healthcare Device Manufactor Lingzhi Hu, PhD, Houston, TX (*Abstract Co-Author*) Employee, UIH America, Inc Nan-Jie Gong, Houston, TX (*Abstract Co-Author*) Employee, UIH America, Inc Hongcheng Shi, Shanghai, China (*Abstract Co-Author*) Nothing to Disclose Kui Ying, PhD, Beijing, China (*Abstract Co-Author*) Nothing to Disclose

PURPOSE

Acquiring low-count PET and undersampled MR can shorten PET/MR scan time, which, however, may also lead to noisy PET images and MR images with artifacts. The goal of this report is to evaluate whether deep learning method can reconstruct high-quality PET/MR images from its low-quality counterpart, potentially enabling shorter scan time in PET/MR. We also compared the proposed model with single modality models to investigate whether the resulting image quality can benefit from sharing features of the two modalities in the network.

METHOD AND MATERIALS

We developed a fully convolutional encoder-decoder network to predict high quality PET and MR images from low-count PET and undersampled MR. Concatenate skip connections and strategy of residual learning is adopted to restore high resolution details. Brain PET/MR data are acquired with a simultaneous PET/MR system (uPMR790, United Imaging Healthcare) from 50 patients who received 0.12 mCi/kg FDG. To generate low-count PET, the PET list-mode data was randomly undersampled for 10% events. Both standard-count and low-count PET images were reconstructed with OSEM (4 iterations, 20 subsets). Undersampled T1 weight MR is generated using radial sampling in k-space with sampling rate equal to 10%. Standard-count PET and fully sampled MR were taken as ground-truth in network training.

RESULTS

Models were trained on 40 patients and evaluated on the other 10 patients. The proposed joint model gains 4.5/7.9dB in peak signal-to-noise ratio (PSNR) and 0.036/0.42 in structural similarity index (SSIM) compared with low-count PET/undersampled MR. When compared with the single modality model of PET/MR, results shows that our joint model has an improvement of 0.97/0.15dB in PSNR and 0.006/0.0012 in SSIM.

CONCLUSION

Using a deep learning algorithm, we can estimate high-quality PET and MR images from low-count PET and undersampled MR images. Results also showed that joint reconstruction of PET and MR by sharing features in network can improve image quality of two modalities compared with single modality model.

CLINICAL RELEVANCE/APPLICATION

This method was demonstrated promising in greatly reducing the scan time in PET/MR imaging by up to 90%.

SSJ22-03 Implementation of a CT Reference Library Containing Manufacturer-Neutral Projection Data, Images, and Clinical Metadata

Tuesday, Nov. 27 3:20PM - 3:30PM Room: N227B

Participants

Taylor Moen, Rochester, MN (*Presenter*) Nothing to Disclose Jayse Weaver, Rochester, MN (*Abstract Co-Author*) Nothing to Disclose Cynthia H. McCollough, PhD, Rochester, MN (*Abstract Co-Author*) Research Grant, Siemens AG Phillip Edwards, Rochester, MN (*Abstract Co-Author*) Nothing to Disclose David R. Holmes Iii, PhD, Rochester, MN (*Abstract Co-Author*) Nothing to Disclose Lifeng Yu, PhD, Chicago, IL (*Abstract Co-Author*) Nothing to Disclose Baiyu Chen, PhD, New York, NY (*Abstract Co-Author*) Nothing to Disclose Joel G. Fletcher, MD, Rochester, MN (*Abstract Co-Author*) Grant, Siemens AG; Consultant, Medtronic plc; ;

For information about this presentation, contact:

mccollough.cynthia@mayo.edu

PURPOSE

A manufacturer-neutral CT projection data (PD) format (DICOM-CT-PD) has been previously developed and used to allow access to CT PD and the scanner information required for image reconstruction. Access to such data was not previously possible, limiting the ability of reconstruction scientists to work with patient data. In this work, we aim to construct a reference DICOM-CT-PD library containing patient PD with corresponding images and clinically relevant metadata, and to publish this library for public access.

METHOD AND MATERIALS

CT images and PD were acquired from three different manufacturers for three clinical scanners at routine dose levels for head, chest and abdomen exams. The PD were converted to the DICOM-CT-PD format and a lower dose exam was simulated for each PD set using a validated noise-insertion method. Radiologists reviewed each case and marked lesion locations and diagnosis. Reference truth was obtained from the patient medical record, either from histology or subsequent imaging. Metadata such as lesion location, diagnosis, and source of truth were acquired for each case and formatted into a reference report. Each case was anonymized to remove protected health information for transfer to an NCI-hosted public data archive, The Cancer Imaging Archive (TCIA).

RESULTS

450 total cases from Siemens (n=150), GE (n=150), and Philips (n=150) scanners were obtained, including both negative and positive patient cases. PD are available for two dose levels, routine full dose and simulated low dose (25% of routine dose for head and abdomen cases and 10% of routine dose for chest cases). Routine dose image series are available for all of the cases, and reduced dose images are additionally available for exams acquired on a Siemens scanner. Clinical metadata are organized in an easy to use spreadsheet. The assembled projection, image and clinical data provide a rich data library with which CT image reconstruction scientists can validate their algorithms.

CONCLUSION

A large patient library containing manufacturer-neutral PD, the corresponding full dose images, and clinical reference information has been developed and is being made available through the TCIA.

CLINICAL RELEVANCE/APPLICATION

The successful implementation of this library will provide open source CT PD with correlated images and clinical information to investigators for reconstruction research and development.

ssj22-04 Motion Compensation in Liver SPECT using Simultaneous X-Ray and Nuclear Imaging

Tuesday, Nov. 27 3:30PM - 3:40PM Room: N227B

Participants

Martijn Dietze, Utrecht, Netherlands (*Presenter*) Nothing to Disclose Remco Bastiaannet, Utrecht, Netherlands (*Abstract Co-Author*) Nothing to Disclose Britt Kunnen, Utrecht, Netherlands (*Abstract Co-Author*) Nothing to Disclose Sandra v. Velden, Utrecht, Netherlands (*Abstract Co-Author*) Nothing to Disclose Marnix G. Lam, MD, Utrecht, Netherlands (*Abstract Co-Author*) Nothing to Disclose Max A. Viergever, Utrecht, Netherlands (*Abstract Co-Author*) Nothing to Disclose Hugo W. de Jong, PhD, Utrecht, Netherlands (*Abstract Co-Author*) Nothing to Disclose

PURPOSE

Quantitative accuracy of liver SPECT/CT is crucial for e.g. dosimetry in radioembolization, but due to respiratory motion limited in precision. Motion can be compensated for in the reconstruction, but in clinical practice this requires an external device for the tracking of the motion signal and a prior motion vector field estimate to link the motion signal to organ movements, complicating the acquisition. A device under development, which simultaneously measures x-ray and nuclear projections, could be used to retrieve both measures intrinsically. Such a data-driven approach eliminates the need for external devices and provides a real-time vector field. The purpose of this work is to evaluate the performance of the proposed motion compensation technique using simulations.

METHOD AND MATERIALS

Nuclear and x-ray projections of a realistic digital phantom with respiratory motion were generated using Monte Carlo simulations for several breathing patterns. X-ray projections were sampled at 1 to 5 Hz; nuclear projections were acquired continuously. Total x-ray imaging dose was varied from 1 to 1000 μ Gy. The motion signal was extracted from x-ray projections by calculation of the center of mass and then used to bin the projections into gates. The x-ray gates were individually reconstructed and registered onto each other, resulting in the vector field to be included in the nuclear reconstruction.

RESULTS

The respiratory motion signal was accurately extracted from the x-ray projections, provided the x-ray sampling rate was greater than 2 Hz and the motion was stable in amplitude. The total minimally required dose for x-ray sampling was 10 μ Gy for a 5 minute scan. The inclusion of motion correction into the SPECT reconstruction improved contrast-to-noise ratio, in comparison with no motion correction, from 11.9 \pm 0.5 to 19.1 \pm 0.7.

CONCLUSION

The proposed motion compensation technique has the potential to improve quantitative SPECT reconstructions. Additionally, the need for external devices and a prior vector field estimate are eliminated. Only a limited amount of dose is required to obtain significantly improved results, paving the way for clinical use.

CLINICAL RELEVANCE/APPLICATION

Liver radioembolization requires quantitative SPECT to study the activity distribution. In order to improve accuracy and personalize dosimetry, motion should be accounted for in reconstructions.

SSJ22-05 Motion Compensated Reconstruction of the Aortic Valve for Non-Gated Helical CT Scans

```
Tuesday, Nov. 27 3:40PM - 3:50PM Room: N227B
```

Participants

Clemens Spink, Hamburg, Germany (*Presenter*) Nothing to Disclose Tanja Elss, Hamburg, Germany (*Abstract Co-Author*) Doctorate student, Koninklijke Philips NV Rolf Bippus, Hamburg, Germany (*Abstract Co-Author*) Employee, Koninklijke Philips NV Michael Morlock, PhD, Hamburg, Germany (*Abstract Co-Author*) Nothing to Disclose Gerhard B. Adam, MD, Hamburg, Germany (*Abstract Co-Author*) Nothing to Disclose Gunnar K. Lund, MD, Hamburg, Germany (*Abstract Co-Author*) Nothing to Disclose Michael Grass, PhD, Hamburg, Germany (*Abstract Co-Author*) Nothing to Disclose

PURPOSE

Precise CT imaging is prerequisite for reliable planning of transcatheter aortic valve implantation (TAVI). Especially in non-gated CT scans, cardiac motion leads to severe artifacts in the reconstructed CT images. Blurring of the valve and the neighboring vascular anatomy potentially result in incorrect device sizing. A second pass motion correction method for non-gated helical CT scans with a pitch <1 is introduced here.

METHOD AND MATERIALS

The new post-processing method was applied to five non-gated clinical datasets acquired with a 256-slice CT scanner (Brilliance iCT, Philips Healthcare). Redundancy in the helical projection data was used to generate three image volumes at identical spatial positions, but different time points. During each reconstruction a subset of detector rows was selected which may be either overlapping or fully separated depending on the pitch size. The 3D edge-filtering scheme included Gaussian smoothing for noise reduction, gradient calculation for edge enhancement, non-maximum-suppression and hysteresis thresholding for reduction of incoherent edges. The sparse filter results were taken as input for an elastic registration to estimate the displacement of each

voxel between the given time points. Reconstructed datasets were evaluated with a TAVI planning software (IntelliSpace Portal, Philips Healthcare) by two blinded readers.

RESULTS

The method achieved significant motion artifact reduction in CT aortic valve reconstructions. A removal of doubled structures at the aortic boundaries could be observed, as well as reduced blurring compared to the uncompensated reconstructions.

CONCLUSION

Motion compensated reconstruction is feasible for non-gated helical CT scans using edge filtering and image based registration for motion estimation. Reconstructed CT image datasets may improve planning and device selection for TAVI procedures.

CLINICAL RELEVANCE/APPLICATION

Motion compensated reconstruction yields reduced artifact levels at the aortic valve in non-gated helical CT scans with a pitch <1.

SSJ22-06 Multi-Channel GAN: A Machine Learning Approach to Parallel MRI Reconstruction

Tuesday, Nov. 27 3:50PM - 4:00PM Room: N227B

Participants Pengyue Zhang, Stony Brook, NY (*Presenter*) Nothing to Disclose Fusheng Wang, Stony Brook, NY (*Abstract Co-Author*) Nothing to Disclose Yulee Li, Greenvale, NY (*Abstract Co-Author*) Nothing to Disclose

For information about this presentation, contact:

pengyue.zhang@stonybrook.edu

PURPOSE

Magnetic resonance imaging (MRI) has a low imaging speed. MRI acceleration relies on undersampling that may introduce aliasing artifacts in image reconstruction. Here we propose a machine learning approach that can automatically learn parallel MRI mechanisms underlying multi-channel k-space data and reconstruct high-quality MR images from undersampled data.

METHOD AND MATERIALS

Parallel MRI is a standard approach to imaging acceleration on clinical MRI scanners. This approach can effectively suppress aliasing artifacts associated with undersampling, but requires an additional calibration procedure that limits the overall imaging speed. Here a deep learning based neural network model, multi-channel generative adversarial network (multi-channel GAN), is developed to process multi-channel raw MRI data. This model can learn parallel MRI reconstruction mechanisms underlying a large amount of multi-channel k-space data. The trained model can be used to reconstruct images from undersampled data without calibration, thereby providing a higher imaging speed than conventional parallel MRI. In our approach, the basic unit of multi-channel GAN has two sub-networks: a generator network which learns the relationship between undersampled and fully-sampled data and a discriminator network which justifies if the generated data are real. The whole model consists of the same number of basic unit networks as that of radiofrequency channels on the MRI scanner for parallel MRI reconstruction. The training process uses a stochastic gradient descent and back-propagation algorithm. The trained multi-channel generator network is used to perform image reconstruction.

RESULTS

We evaluate the proposed method with a total of 170 sets of 2D multi-channel brain MRI images. Figure 1 shows an example of reconstruction results with an undersampling factor of 5. It is found that the machine learning method outperforms other state-of-the-art parallel MRI reconstruction methods.

CONCLUSION

We demonstrate a machine learning approach to parallel MRI reconstruction. This approach can generate high-quality images from undersampled data without calibration, providing a higher imaging speed than conventional parallel MRI.

CLINICAL RELEVANCE/APPLICATION

The machine learning approach to parallel MRI reconstruction can enhance diagnostic MRI quality, shorten clinical MRI procedures and improve clinical MRI throughput.



RC425

Mini-course: Image Interpretation Science - Computational Perception

Tuesday, Nov. 27 4:30PM - 6:00PM Room: S103AB



AMA PRA Category 1 Credits ™: 1.50 ARRT Category A+ Credit: 1.75

Participants

Elizabeth A. Krupinski, PhD, Atlanta, GA (*Coordinator*) Nothing to Disclose Ehsan Samei, PhD, Durham, NC (*Coordinator*) Research Grant, General Electric Company; Research Grant, Siemens AG; Advisory Board, medInt Holdings, LLC; License agreement, 12 Sigma Technologies; License agreement, Gammex, Inc

For information about this presentation, contact:

ekrupin@emory.edu

LEARNING OBJECTIVES

1) Provide an overview of the types and applications of CAD being developed and used today. 2) Summarize the evidence and controversies regarding clinical impact of CAD. 3) Describe future trends in CAD research.

ABSTRACT

Medical images constitute a core portion of the information physicians utilize to render diagnostic and treatment decisions. At a fundamental level, the diagnostic process involves two aspects - visually inspecting the image (perception) and rendering an interpretation (cognition). Key indications of expert interpretation of medical images are consistent, accurate and efficient diagnostic performance, but how do we know when someone has attained the level of training required to be considered an expert? How do we know the best way to present images to the clinician in order to optimize accuracy and efficiency? The advent of digital imaging in many clinical specialties, including radiology, pathology and dermatology, has dramatically changed the way that clinicians view images, how residents are trained, and thus potentially the way they interpret image information, emphasizing our need to understand how clinicians interact with the information in an image during the interpretation process. With improved understanding we can develop ways to further improve decision-making and thus improve patient care.

Sub-Events

RC425A AI in Clinical Radiology

Participants

Maryellen L. Giger, PhD, Chicago, IL (*Presenter*) Stockholder, Hologic, Inc; Shareholder, Quantitative Insights, Inc; Shareholder, QView Medical, Inc; Co-founder, Quantitative Insights, Inc; Royalties, Hologic, Inc; Royalties, General Electric Company; Royalties, MEDIAN Technologies; Royalties, Riverain Technologies, LLC; Royalties, Mitsubishi Corporation; Royalties, Canon Medical Systems Corporation

For information about this presentation, contact:

m-giger@uchicago.edu

LEARNING OBJECTIVES

1) Become familiar with AI, including machine learning and deep learning methods, for use in radiology. 2) Become aware of the potential challenges involved when developing and applying AI to radiological interpretations. 3) Become familiar with some of the future potentials and plans for AI In radiology.

RC425B Intersection of Imaging Informatics and Perception

Participants

Katherine P. Andriole, PhD, Dedham, MA (*Presenter*) Research Grant, NVIDIA Corporation; Research Grant, General Electric Company; Research Grant, Nuance Communications, Inc; Advisory Board, McKinsey & Company, Inc

For information about this presentation, contact:

kandriole@bwh.harvard.edu

LEARNING OBJECTIVES

1) Provide a basic overview of Medical Imaging Informatics. 2) Describe ways in which an understanding of visual perception informs the development and use of Imaging Informatics data visualization tools. 3) Assess ways Imaging Informatics can impact image interpretation.

RC425C Radiologist Interpretation in the Era of AI

Participants

Curtis P. Langlotz, MD,PhD, Menlo Park, CA (*Presenter*) Advisory Board, Nuance Communications, Inc; Shareholder, whiterabbit.ai; Advisory Board, whiterabbit.ai; Shareholder, Nines.ai; Consultant, Nines.ai; Shareholder, TowerView Health; Research Grant, Koninklijke Philips NV; Research Grant, Siemens AG; Research Grant, Alphabet Inc;

LEARNING OBJECTIVES

1) Review the history of radiology reporting. 2) Describe the common pitfalls and mistakes in today's radiology reports. 3) Learn to improve the quality of radiology reports. 4) Assess how the radiology report will evolve in the era of artificial intelligence.



RC453

Deep Learning-An Imaging Roadmap

Tuesday, Nov. 27 4:30PM - 6:00PM Room: E451B



AMA PRA Category 1 Credits ™: 1.50 ARRT Category A+ Credit: 1.75

FDA Discussions may include off-label uses.

Participants

Paula M. Jacobs, PhD, Bethesda, MD (Moderator) Nothing to Disclose

For information about this presentation, contact:

Paula.Jacobs@nih.gov

LEARNING OBJECTIVES

1) Understand the framework of 'Deep Learning', Machine Learning, and Neural Net computer algorithms. 2) Comprehend what aspects of radiology practice are most amenable to machine learning deployment. 3) Understand the academic, commercial and clinical perspectives on how the field will likely develop and how NCI's Cancer Imaging Archive (TCIA) can accelerate development of this new technology.

ABSTRACT

Deep Learning, an independent self-learning computational environment that uses multilayered computational neural nets, has generated considerable excitement (as well as concerns and misperceptions) in medical imaging. Deep learning computational techniques, such as convolutional neural networks (CNNs) generate multiple layer feature classifiers that extract disease relevant features from entire regions of medical images without the need for localization or pre-segmentation of lesions. Although CNNs require training on very large image datasets that encompass particular disease expressions, they can be diagnostically effective since no human input of segmentation features such as size, shape, margin sharpness, texture, and kinetics are required. But their immediate and future applicability as tools for unsupervised medical decision-making are, as yet, not well understood by most clinical radiologists. This overview session of Deep Learning will provide a clearer picture by presenters who are active in that field and who can clarify how the unique characteristics of Deep Learning could impact clinical radiology. It will address how radiologists can contribute to, and benefit from, this new technology. Topics of this multi-speaker session will cover: 1) the general principles of deep learning computational schemas and their mechanisms of handling image inputs and outputs. 2) new technology including hardware shifts in microprocessors from CPU's to GPU devices that offer significant computational advantages 3) how to ensure that Deep Learning results are consistently clinically relevant and meaningful including nodal element tuning and provability so as to assure medical care consistency and reproducibility. 4) how to develop and leverage datasets for deep learning on archives such as the NIH The Cancer Imaging Archive (TCIA) including requirements for input image dataset magnitude and completeness of disease spectrum representation. 5) how to embed essential non-imaging data needed as inputs, (e.g. EHR, outcome, cross-disciplinary metadata, and the data pre-processing required to make DICOM ready for Deep Learning. The presentations will be at a level understandable and relevant to the RSNA radiologist audience.

Sub-Events

RC453A Computer Science Deep Learning Research by the Academic Community

Participants

Fred W. Prior, PhD, Little Rock, AR (Presenter) Nothing to Disclose

LEARNING OBJECTIVES

1) Understand the basic concepts of Machine Learning and Deep Learning and how they differ. 2) Gain insights into how these techniques are being used in quantitative imaging (Radiomic) research.

RC453B Commercial Development and Deployment of Deep Learning Technology

Participants

Abdul Hamid Halabi, Santa Clara, CA (Presenter) Developer, NVIDIA Corporation; Spouse, Employee, Covenant Pathology

RC453C Radiology Clinician Perspectives

Participants

Andrea G. Rockall, FRCR, MRCP, London, United Kingdom (Presenter) Speaker, Guerbet SA

LEARNING OBJECTIVES

1) Understand the differences between an algorithm that works in the lab and one that works in clinical practice. 2) Identify common weaknesses in study design that can lead to better apparent performance than might be realized in practice. 3) Recognize challenges in practical workflow that might impede clinical adoption of some tools.

Honored Educators

Presenters or authors on this event have been recognized as RSNA Honored Educators for participating in multiple qualifying

educational activities. Honored Educators are invested in furthering the profession of radiology by delivering high-quality educational content in their field of study. Learn how you can become an honored educator by visiting the website at: https://www.rsna.org/Honored-Educator-Award/ Andrea G. Rockall, FRCR,MRCP - 2017 Honored Educator



SPSH40

Hot Topic Session: Fast MSK MR Imaging

Wednesday, Nov. 28 7:15AM - 8:15AM Room: E450A



AMA PRA Category 1 Credit ™: 1.00 ARRT Category A+ Credit: 1.00

FDA Discussions may include off-label uses.

Participants

Soterios Gyftopoulos, MD, Scarsdale, NY (Moderator) Nothing to Disclose

For information about this presentation, contact:

Soterios.Gyftopoulos@nyumc.org

LEARNING OBJECTIVES

1) Describe the evolution of MRI and the reasons for and against the implementation of fast MR imaging. 2) Describe the advantages and disadvantages of current and emerging techniques for fast MR imaging. 3) Describe how machine learning can be used to accelerate MR imaging.

Sub-Events

SPSH40A Fast MR Imaging: What, How, and Why

Participants Soterios Gyftopoulos, MD, Scarsdale, NY (*Presenter*) Nothing to Disclose

For information about this presentation, contact:

Soterios.Gyftopoulos@nyumc.org

LEARNING OBJECTIVES

1) Review the evolution of MR imaging from its inception to its current state. 2) Discuss the reasons for and against fast MR imaging.

SPSH40B Current Techniques for Fast MR Imaging

Participants

Naveen Subhas, MD, Shaker Heights, OH (Presenter) Research support, Siemens AG

LEARNING OBJECTIVES

1) Review current techniques that are available to obtain faster MRI scans including abbreviated MRI, single sequence 3D MRI and parallel imaging. 2) Discuss advantages and limitations of these techniques.

SPSH40C Emerging Techniques for Fast MR Imaging

Participants

Jan Fritz, MD, Baltimore, MD (*Presenter*) Research Grant, Siemens AG; Scientific Advisor, Siemens AG; Scientific Advisor, Alexion Pharmaceuticals, Inc; Speaker, Siemens AG

For information about this presentation, contact:

jfritz9@jhmi.edu

LEARNING OBJECTIVES

1) To review new and emerging acceleration techniques for 2D and 3D MRI. 2) To identify advantages and limitations of the different acceleration techniques. 3) To apply the most appropriate acceleration techniques for various clinical scenarios of musculoskeletal MRI.

SPSH40D Machine Learning for Fast MR Imaging

Participants Michael P. Recht, MD, New York, NY (*Presenter*) Nothing to Disclose

For information about this presentation, contact:

michael.recht@nyumc.org

LEARNING OBJECTIVES

1) Explain the basic concepts behind using machine learning for MR image reconstruction. 2) Understand the advantages provided

by machine learning image reconstruction.



AI001-WE

RSNA Deep Learning Classroom: Presented by NVIDIA Deep Learning Institute

Wednesday, Nov. 28 8:30AM - 4:00PM Room: AI Community, Learning Center

Program Information

Located in the Learning Center (Hall D), this classroom presented by NVIDIA will give meeting attendees a hands-on opportunity to engage with deep learning tools, write algorithms and improve their understanding of deep learning technology. "Attendees must bring a laptop capable of running the most recent version of Chrome."

Sub-Events

AI001-WEA Data Science: Normalization, Annotation, Validation

Wednesday, Nov. 28 8:30AM - 10:00AM Room: AI Community, Learning Center

Title and Abstract

Data Science: Normalization, Annotation, Validation This session will focus on preparation of the image and non-image data in order to obtain the best results from your deep learning system. It will include a discussion of different options for representing the data, how to normalize the data, particularly image data, the various options for image annotation and the benefits of each option. We will also discuss the 'after training' aspects of deep learning including validation and testing to ensure that the results are robust and reliable.

AI001-WEB Introduction to Deep Learning

Wednesday, Nov. 28 10:30AM - 12:00PM Room: AI Community, Learning Center

Title and Abstract

Introduction to Deep Learning This class will focus on basic concepts of convolutional neural networks (CNNs), and walk the attendee through a working example. A popular training example is the MNIST data set which consists of hand-written digits. This course will use a data set we created, that we call 'MedNIST and consists of 1000 images each from 5 different categories: Chest X-ray, hand X-ray, Head CT, Chest CT, Abdomen CT, and Breast MRI. The task is to identify the image type. This will be used to train attendees on the basic principles and some pitfalls in training a CNN. The attendee will have the best experience if they are familiar with Python programming.

AI001-WEC Advanced Data Augmentation Using GANs

Wednesday, Nov. 28 12:30PM - 2:00PM Room: AI Community, Learning Center

Title and Abstract

Advanced Data Augmentation Using GANs Getting 'large enough' data sets is a problem for most deep learning applications, and this is particularly true in medical imaging. Generative Adversarial Networks (GANs) are a deep learning technology in which a computer is trained to create images that look very 'real' even though they are completely synthetic. This may be one way to address the 'data shortage' problem in medicine.

AI001-WED 3D Segmentation of Brain MR

Wednesday, Nov. 28 2:30PM - 4:00PM Room: AI Community, Learning Center

Title and Abstract

3D Segmentation of Brain MR This session will focus on the use of deep learning methods for segmentation, with particular emphasis on 3D techniques (V-Nets) applied to the challenge of MR brain segmentation. While focused on this particular problem, the concepts should generalize to other organs and image types.



RC553

Deep Learning: Applying Machine Learning to Multi-disciplinary Precision Medicine Data Sets

Wednesday, Nov. 28 8:30AM - 10:00AM Room: E451B



AMA PRA Category 1 Credits ™: 1.50 ARRT Category A+ Credit: 1.75

FDA Discussions may include off-label uses.

Participants

Paula M. Jacobs, PhD, Bethesda, MD (Moderator) Nothing to Disclose

Maryellen L. Giger, PhD, Chicago, IL (*Presenter*) Stockholder, Hologic, Inc; Shareholder, Quantitative Insights, Inc; Shareholder, QView Medical, Inc; Co-founder, Quantitative Insights, Inc; Royalties, Hologic, Inc; Royalties, General Electric Company; Royalties, MEDIAN Technologies; Royalties, Riverain Technologies, LLC; Royalties, Mitsubishi Corporation; Royalties, Canon Medical Systems Corporation

John B. Freymann, BS, Rockville, MD (*Presenter*) Nothing to Disclose Joel Saltz, MD, PhD, Stony Brook, NY (*Presenter*) Nothing to Disclose Hugo Aerts, PhD, Boston, MA (*Presenter*) Stockholder, Sphera Inc

For information about this presentation, contact:

Paula.Jacobs@nih.gov

john.freymann@nih.gov

m-giger@uchicago.edu

LEARNING OBJECTIVES

1) Understand the strategy NIH National Cancer Institute is making to link clinical imaging with other existing patient-case 'metadata' archives. 2) Learn to navigate the patient-specific database silos (genetics, proteomics, clinical demographics) so as to strengthen Machine Learning research. 3) By specific use-case examples attendees will comprehend the advantage such imaging and disparate-type metadata links offer to clinically relevant cancer research.

ABSTRACT

Abstract: This didactic session will provide clinician researchers with examples of ongoing machine learning research in imaging combined with clinical and 'omics data sets, along with examples of where to find and how to link existing cancer image archive cases to other public-access stored databases that contain same-patient demographics, genetics, proteomic, and pathology images. Many of these disparate data types may be presently unfamiliar to imagers - such as mass spectroscopy data that arises from cellular proteomic analysis that propel the need for urgently forming new cross-disciplinary research teams. These datasets, often stored separately by different professional specialty teams, constitute critical complementary elements ultimately needed for reliable Machine Learning. This session pivots out from the clinical images available in the NCI Cancer Imaging Archive (TCIA) collections that acts as the point of origin for linking same-patient demographics, pathology, proteomics, and genetic data so that machine learning efforts can be more scientifically robust.



CS41

Medical Imaging Analytics & AI: Technologies and Solutions for Better Healthcare Today and in the Future: Presented by Intel®

Wednesday, Nov. 28 9:00AM - 10:30AM Room: S101AB

PARTICIPANTS

Dave Ryan, Intel Corp.; Prashant Shah, Intel Corp.; Parsa Mirhaji, MD, Ph.D., Einstein and Montefiore; Gene Saragnese, MaxQ AI; Eliot Siegel, MD, Veterans Affairs Maryland Healthcare System; Lei Xing, MD, Ph.D., Stanford University; Greg Zaharchuk, MD, Ph.D, Stanford University; Eric King, Intel Corp.

PROGRAM INFORMATION

Artificial Intelligence is disrupting the medical imaging market with technologies and solutions to improve clinician workflow and enable clinicians to address unmet needs of patients. This session will look at the adoption of AI in Medical Imaging from multiple perspectives. Section 1: Introduction to AI technologies that are most relevant for medical imaging today including deep learning and computer vision that drive enhanced performance and increase clinician productivity. Section 2: Real examples of AI at work today. AI is already helping to augment radiologists' work, reducing mundane tasks and helping identify the most complex cases for them to target their expertise involving Deep Learning and Computer Vision. Section 3: There is an exploding startup ecosystem at the intersection of AI and Medical Imaging. We'll look at the disruptors poised to change medical imaging in the next 3 to 5 years.

RSVP

http://www.cvent.com/d/jbqw4l



RCA42

From Texture Analysis to Deep Learning for Lesion Characterization (Hands-on)

Wednesday, Nov. 28 10:30AM - 12:00PM Room: S401AB



AMA PRA Category 1 Credits ™: 1.50 ARRT Category A+ Credit: 1.75

Participants

Kevin Mader, DPhil,MSc, Basel, Switzerland (*Moderator*) Employee, 4Quant Ltd; Shareholder, 4Quant Ltd Kevin Mader, DPhil,MSc, Basel, Switzerland (*Presenter*) Employee, 4Quant Ltd; Shareholder, 4Quant Ltd Barbaros S. Erdal, PhD, Columbus, OH (*Presenter*) Nothing to Disclose Joshy Cyriac, Basel, Switzerland (*Presenter*) Nothing to Disclose

LEARNING OBJECTIVES

1) Review the basic principles of machine learning. 2) Learn what texture analysis is and how to apply it to medical imaging. 3) Understand how to combine texture analysis and machine learning for lesion classification tasks.

ABSTRACT

During this course, an introduction to machine learning and image texture analysis will be provided through hands on examples. Participants will use open source as well as freely available commercial platforms in order to achieve tasks such as image feature extraction, statistical analysis, building models, and validating them. Imaging samples will include both 2D and 3D datasets from a variety of modalities (CT, PET, MR). The course will begin with a brief overview of important concepts and links to more detailed references. The concepts will then be directly applied in visual, easily understood workflows where the participants will see how the images are processed, features and textures are extracted and how publication ready statistics and models can be built and tested.



SSK02

Breast Imaging (Artificial Intelligence)

Wednesday, Nov. 28 10:30AM - 12:00PM Room: E451B



AMA PRA Category 1 Credits ™: 1.50 ARRT Category A+ Credit: 1.75

FDA Discussions may include off-label uses.

Participants

Despina Kontos, PhD, Philadelphia, PA (*Moderator*) Nothing to Disclose

Maryellen L. Giger, PhD, Chicago, IL (*Moderator*) Stockholder, Hologic, Inc; Shareholder, Quantitative Insights, Inc; Shareholder, QView Medical, Inc; Co-founder, Quantitative Insights, Inc; Royalties, Hologic, Inc; Royalties, General Electric Company; Royalties, MEDIAN Technologies; Royalties, Riverain Technologies, LLC; Royalties, Mitsubishi Corporation; Royalties, Canon Medical Systems Corporation

Sub-Events

SSK02-01 Using Deep Convolutional Neural Networks to Predict Readers' Estimates of Mammographic Density from Raw and Processed Mammographic Images

Participants

Georgia Ionescu, Manchester, United Kingdom (*Abstract Co-Author*) Nothing to Disclose Martin Fergie, Manchester, United Kingdom (*Abstract Co-Author*) Nothing to Disclose Michael Berks, Manchester, United Kingdom (*Abstract Co-Author*) Nothing to Disclose Elaine Harkness, PhD, Manchester, United Kingdom (*Abstract Co-Author*) Nothing to Disclose Johan Hulleman, Manchester, United Kingdom (*Abstract Co-Author*) Nothing to Disclose Adam Brentnall, London, United Kingdom (*Abstract Co-Author*) Nothing to Disclose Jack Cuzick, London, United Kingdom (*Abstract Co-Author*) Nothing to Disclose Gareth Evans, Manchester, United Kingdom (*Abstract Co-Author*) Nothing to Disclose Susan M. Astley, PhD, Manchester, United Kingdom (*Presenter*) Nothing to Disclose

PURPOSE

Mean percentage density assessed visually by two independent readers using Visual Analogue Scales (VAS) has a strong association with breast cancer risk, but is resource-intensive and impractical for stratified screening. We describe a fully-automated method for predicting this mammographic percent density measure from raw (for processing) or processed (for presentation) mammograms, and compare association of predicted VAS score with risk.

METHOD AND MATERIALS

Convolutional Neural Networks (CNNs) were trained using 67520 whole-image mammograms from 16968 women, each labelled with the average VAS score of two independent readers. The networks learned a mapping between mammographic appearance and mammographic density so that they can predict density for unseen images. To evaluate its use for risk assessment, we tested on case-control datasets of contralateral mammograms of screen detected cancers (SDC) and prior screening mammograms of women with cancers detected subsequently. Each cancer was matched to three controls on age, menopausal status, parity, HRT and BMI. The test datasets contained 366 cancers (SDC) and 338 (priors). Odds ratios between the top and bottom quintile were derived, and matched concordance indices were estimated. All images were acquired on GE Senographe systems, and none of the images from the case-control test sets were used in the training process.

RESULTS

For density estimates derived from raw images, odds ratios of cancer in the highest vs lowest quintile were 3.07 (95%CI: 1.97 - 4.77) for SDC and 3.52 (2.22 - 5.58) for priors, with matched concordance indices of 0.59 (0.55 - 0.64) and 0.61 (0.58 - 0.65) respectively. For processed images we obtained odds ratios of 3.22 (2.06 - 5.03) for SDC and 3.65 (2.27 - 5.88) for priors. Matched concordance indices were 0.58 (0.53 - 0.62) for SDC and 0.61 (0.57 - 0.65) for priors.

CONCLUSION

Our fully automated method demonstrated encouraging results on both raw and processed mammographic images, indicating that either image type could be used for screening stratification.

CLINICAL RELEVANCE/APPLICATION

Mammographic density is one of the most important risk factors for breast cancer. Our fully automated method could provide a pragmatic solution for population-based stratified screening.

SSK02-02 Breast Density Classification with Deep Convolutional Neural (DCN) Networks Utilizing 200,000 Screening Mammograms

Wednesday, Nov. 28 10:40AM - 10:50AM Room: E451B

Krzysztof J. Geras, New York City, NY (*Abstract Co-Author*) Nothing to Disclose Eric Kim, MD, New York, NY (*Presenter*) Nothing to Disclose Nan Wu, New York City, NY (*Abstract Co-Author*) Nothing to Disclose Yiqiu Shen, New York City, NY (*Abstract Co-Author*) Nothing to Disclose Jingyi Su, New York City, NY (*Abstract Co-Author*) Nothing to Disclose Sungheon Kim, PhD, New York, NY (*Abstract Co-Author*) Nothing to Disclose Stacey Wolfson, New York, NY (*Abstract Co-Author*) Nothing to Disclose Linda Moy, MD, New York, NY (*Abstract Co-Author*) Nothing to Disclose Kyunghyun Cho, New York City, NY (*Abstract Co-Author*) Nothing to Disclose

For information about this presentation, contact:

kime18@nyumc.org

PURPOSE

To develop a DCN network to reliably assess mammographic breast density

METHOD AND MATERIALS

In this retrospective study, we trained a multi-column DCN network on 200,000 digital screening mammograms performed at our institution from 2010-2016 to assess breast density. We extracted the textual reports associated with each exam to obtain the breast density as determined by the original interpreting radiologist. The algorithm was trained on 80% of the data sets, validated on a separate 10%, and tested on the remaining 10%. Once this convolutional neural network classifier was trained, we performed a reader study comparing our model to 3 radiologists. All readers independently evaluated the breast density in 100 mammograms in a randomized order. Breast density was assessed using the conventional BI-RADS categories: Class 0 - fatty, Class 1 - scattered fibroglandular densities, Class 2 - heterogeneously dense, and Class 3 - extremely dense. Performance of the model and the readers were assessed using the area under the ROC curve (AUC). Kappa score was used to assess for intra-observer and inter-observer variability.

RESULTS

Both the radiologists and our DCN model achieved a fair agreement (k = 0.34 - 0.51) with the labels in the reader study. The agreement between the predictions of our model and the labels in the data were higher (k = 0.65 - 0.72) compared to the interobserver agreement between the radiologists. There was higher agreement for the fatty and extremely dense breast tissue. Comparing our CNN model to an average of the radiologists, the CNN achieved AUC of 0.934 (class 0: 0.971, class 1: 0.859, class 2: 0.905 and class 3: 1.000) while the radiologists achieved an AUC of 0.892 (class 0: 0.960, class 1: 0.812, class 2: 0.807 and class 3: 0.990) (Figure 1).

CONCLUSION

The level of agreement between the trained classifier and the classes in the data was found to be similar to that between the radiologists and the classes in the data, as well as among the radiologists.

CLINICAL RELEVANCE/APPLICATION

The classifier provides quantitative, reproducible prediction of breast density, while there is often poor intra-reader and inter-reader correlation in the qualitative assessment of breast density.

SSK02-03 Improving Radiologists' Breast Cancer Detection with Mammography Using a Deep Learning-Based Computer System for Decision Support

Wednesday, Nov. 28 10:50AM - 11:00AM Room: E451B

Participants

Alejandro Rodriguez-Ruiz, Nijmegen, Netherlands (*Abstract Co-Author*) Nothing to Disclose Elizabeth A. Krupinski, PhD, Atlanta, GA (*Abstract Co-Author*) Nothing to Disclose Jan-Jurre Mordang, MSc, Nijmegen, Netherlands (*Abstract Co-Author*) Nothing to Disclose Kathy J. Schilling Colletta, MD, Boca Raton, FL (*Abstract Co-Author*) Nothing to Disclose Sylvia H. Heywang-Koebrunner, MD, Munich, Germany (*Abstract Co-Author*) Nothing to Disclose Ioannis Sechopoulos, PhD, Atlanta, GA (*Abstract Co-Author*) Research Grant, Siemens AG; Research Grant, Canon Medical Systems Corporation; Speakers Bureau, Siemens AG; Scientific Advisory Board, Fischer Medical Ritse M. Mann, MD, PhD, Nijmegen, Netherlands (*Presenter*) Researcher, Siemens AG; Researcher, Seno Medical Instruments, Inc; Researcher, Identification Solutions, Inc; Researcher, Micrima Limited; Researcher, Medtronic plc; Scientific Advisor, ScreenPoint Medical BV; Scientific Advisor, Transonic Imaging, Inc; Stockholder, Transonic Imaging, Inc

For information about this presentation, contact:

ritse.mann@radboudumc.nl

PURPOSE

To compare the breast cancer detection performance of radiologists reading mammography exams unaided versus reading using an interactive deep learning-based computer system for decision support (DS).

METHOD AND MATERIALS

A retrospective, fully-crossed (two sessions >4 weeks apart), multi-reader multi-case (MRMC) study was performed. 240 cases (100 cancers, 40 false positive recalls, 100 normals) were scored by 14 MQSA-qualified radiologists, once with and once without using DS. For each case, a forced BI-RADS® score and a level of suspicion (1-100) were provided. When reading with the DS system (Transpara, Screenpoint Medical, Nijmegen, The Netherlands), radiologists could activate the DS for a specific breast region by clicking on it and the system then displayed a cancer likelihood score (1-100). Additionally, traditional computer-aided detection was available to prompt calcification and soft tissue lesion markers. Area under the receiver operating characteristic curve (AUC), specificity and sensitivity, and reading time were compared using MRMC Analysis of Variance.

On average, with the DS system, the AUC increased significantly from 0.866 to 0.886 (P=0.0019) compared to unaided reading. Sensitivity increased from 83% to 86% (P=0.046), while specificity only slightly improved from 77% to 79% (P=0.061). Considering lesion type, AUC increased for soft tissue lesions (0.886 to 0.902, P=0.033), and calcifications (0.878 to 0.898, not significant, P=0.1021). Reading time per case was similar in both situations (unaided = 146 s, with DS = 149 s, P=0.147). As a stand-alone, the computer system had an equal detection performance (AUC=0.887) than the average of radiologists (P=0.333).

CONCLUSION

Radiologists significantly improved their cancer detection in mammography when using a deep learning-based computer system for decision support without taking more time.

CLINICAL RELEVANCE/APPLICATION

The use of decision support might prevent overlook and interpretation errors that are relatively common in the reading of mammography. The increase in performance when concurrently using DS does not lengthen radiologists reading time per case, as opposed to traditional computer-aided detection systems. The use of single-reading in combination with the computer system might achieve a performance similar to double human reading considering that the stand-alone performance of the system is similar to the average of radiologists.

Honored Educators

Presenters or authors on this event have been recognized as RSNA Honored Educators for participating in multiple qualifying educational activities. Honored Educators are invested in furthering the profession of radiology by delivering high-quality educational content in their field of study. Learn how you can become an honored educator by visiting the website at: https://www.rsna.org/Honored-Educator-Award/ Elizabeth A. Krupinski, PhD - 2017 Honored Educator

SSK02-04 Data-Driven Imaging Biomarker for Breast Cancer Screening in Mammography-Reader Study

Wednesday, Nov. 28 11:00AM - 11:10AM Room: E451B

Participants

Eun-Kyung Kim, MD, Seoul, Korea, Republic Of (*Abstract Co-Author*) Nothing to Disclose Hyo-Eun Kim, Seoul, Korea, Republic Of (*Abstract Co-Author*) Employee, Lunit Inc Hak Hee Kim, MD, Seoul, Korea, Republic Of (*Abstract Co-Author*) Nothing to Disclose Boo-Kyung Han, MD, PhD, Seoul, Korea, Republic Of (*Abstract Co-Author*) Nothing to Disclose Jung Yin Huh, MD, Seoul, Korea, Republic Of (*Presenter*) employee, Lunit Inc. Kyunghwa Han, PhD, Seoul, Korea, Republic Of (*Abstract Co-Author*) Nothing to Disclose

For information about this presentation, contact:

ekkim@yuhs.ac

PURPOSE

Previously, we demonstrated data-driven imaging biomarker in mammography (DIB-MMG; an imaging biomarker that is derived from large-scale mammography data by using deep learning technology) for detection of malignant lesions. Now, we assess the feasibility of DIB-MMG as a diagnosis-support-tool for radiologists.

METHOD AND MATERIALS

Total 96,191 exams of 4-view digital mammograms were retrospectively collected from two institutions. All cancer exams were proven by biopsy. Benign exams were proven by biopsy or at least 1 year of follow-up mammography, and normal exams were proven by at least 1 year of follow-up mammography. 90,637 exams of training data (16,086 cancer, 31,237 benign, and 43,314 normal exams) and 5,554 exams of test data (1,692 cancer, 2,780 benign, 1,082 normal cases) were used for developing the DIB-MMG. Sensitivity, specificity, and AUC of the final DIB-MMG on the test data were 82.6%, 93.3%, and 0.94, respectively. Total 120 exams of mammograms (38 cancer and 82 non-cancer exams) were independently collected for reader study, and five radiologists participated. For each exam, readers first read the exam without the help of DIB-MMG and Task-1) annotate the most suspicious lesion with DMIST 7-pt scores and Task-2) decide recall or not per breast. After reading of each exam, readers modify their decision based on the heat-map of DIB-MMG which denotes the likelihood of malignancy.

RESULTS

Per-breast standalone performance of DIB-MMG for 120 exams was 0.942 of AUC in Task-1, and 89.7% of sensitivity, 89.6% of specificity in Task-2. Average performance of five radiologists without DIB-MMG was 0.807 of AUC in Task-1, and 70.8% of sensitivity, 86.2% of specificity in Task-2. With DIB-MMG, the average performance was improved to 0.879 of AUC (p=0.024) in Task-1, and 79.5% of sensitivity, 86.5% of specificity in Task-2. Fig.1 shows exemplary DIB-MMG heat-maps.

CONCLUSION

This retrospective reader study showed the potential of DIB-MMG as a diagnosis support tool for radiologists in breast cancer screening. Further clinical validation with prospective study is needed.

CLINICAL RELEVANCE/APPLICATION

DIB-MMG is purely based on data-driven features from a large-scale mammography data instead of manually designed features of conventional computer-aided detection (CAD) algorithms. With further clinical validation, DIB-MMG can be practically used as a diagnosis support tool for radiologists in breast cancer screening.

SSK02-05 Generative Neural Network Inserting or Removing Cancer into Mammograms Fools Radiologists and Deep Learning Alike: Example of an Adversarial Attack

Wednesday, Nov. 28 11:10AM - 11:20AM Room: E451B

Participants Anton S. Becker, MD, Zurich, Switzerland (*Presenter*) Nothing to Disclose Lukas Jendele, Oberengstringen, Switzerland (*Abstract Co-Author*) Nothing to Disclose Ondrej Skopek, Oberengstringen, Switzerland (*Abstract Co-Author*) Nothing to Disclose Soleen Ghafoor, MD, Zurich, Switzerland (*Abstract Co-Author*) Nothing to Disclose Nicole Berger, MD, Zurich, Switzerland (*Abstract Co-Author*) Nothing to Disclose Magda Marcon, MD, Zurich, Switzerland (*Abstract Co-Author*) Nothing to Disclose Ender Konukoglu, Sophia Antipolis, France (*Abstract Co-Author*) Nothing to Disclose

For information about this presentation, contact:

anton@becker.md

PURPOSE

To investigate whether a cycle-consistent generative adversarial network (CycleGAN) can insert or remove cancer-specific features into mammographic images in a realistic fashion.

METHOD AND MATERIALS

From two publicly available datasets (BCDR and INbreast) 680 mammographic images from 334 patients were selected, 318 of which exhibited potentially cancerous masses, and 362 were healthy controls. We trained a CycleGAN, using two pairs of generator and discriminator networks to convert cancerous breast images to healthy and back, and vice versa for the controls, without the need for paired images. The network, implemented in TensorFlow, was trained for 40 epochs on an augmented dataset enlarged ten-fold by random rotation, scaling, and contrast perturbations. To investigate how realistic the images appear, we randomly selected 20 image pairs of original and generated images, and 10 single images of each category (60 images in total). The images were presented to three radiologists (5 and 3 years of experience, and PGY-5 resident) who rated them on a 5-point Likert-like scale and had to indicate whether the image was real or generated/modified. The readout was analysed with a receiver-operating-characteristics (ROC) analysis, performance was expressed as area under the ROC curve (AUC).

RESULTS

For the most experienced radiologist, the modifications introduced by CycleGAN reduced diagnostic performance, with the AUC dropping from 0.85 to 0.63 (p=0.06), respectively, while the two less experienced ones seemed unaffected at a lower baseline performance (AUC 0.75 vs. 0.77 and 0.67 vs. 0.69). None of the radiologists could reliably detect which images were real and which were modified by CycleGAN (AUC 0.50-0.66).

CONCLUSION

CycleGAN can inject or remove malignant features into mammographic images while retaining their realistic appearance. These artificial modifications may lead to false diagnoses.

CLINICAL RELEVANCE/APPLICATION

Modern adversarial attacks may go undetected by humans as well as deep learning algorithms, and could be used in cyber warfare. It is vital to secure healthcare devices and information systems against such attacks mediated by neural networks.

SSK02-06 Deep Learning for Detection of Breast Cancer and Negative Screening Exams Using an In-House Million Mammogram Dataset

Wednesday, Nov. 28 11:20AM - 11:30AM Room: E451B

Participants

Hari Trivedi, MD, San Francisco, CA (*Presenter*) Nothing to Disclose Peter Chang, MD, San Francisco, CA (*Abstract Co-Author*) Nothing to Disclose Dmytro Lituiev, San Francisco, CA (*Abstract Co-Author*) Nothing to Disclose April Liang, San Francisco, CA (*Abstract Co-Author*) Nothing to Disclose Maryam Panahiazar, San Francisco, CA (*Abstract Co-Author*) Nothing to Disclose Jae Ho Sohn, MD, San Francisco, CA (*Abstract Co-Author*) Nothing to Disclose Yunn-Yi Chen, MD, San Francisco, CA (*Abstract Co-Author*) Nothing to Disclose Benjamin L. Franc, MD, Sacramento, CA (*Abstract Co-Author*) Nothing to Disclose Bonnie N. Joe, MD, PhD, San Francisco, CA (*Abstract Co-Author*) Nothing to Disclose Dexter Hadley, San Francisco, CA (*Abstract Co-Author*) Nothing to Disclose

For information about this presentation, contact:

hari.trivedi@gmail.com

PURPOSE

Breast cancer is the second leading cause of cancer death in women in the US. Screening mammography is effective for early detection, however suffers from unnecessary recall imaging and biopsies. Deep learning shows promise in medical image recognition tasks, but requires large-scale, robustly-annotated datasets. We expand upon our previously described end-to-end process of constructing a million mammogram dataset using routine clinical data and present results of two preliminary deep learning models for cancer detection and the identification of true negative images.

METHOD AND MATERIALS

923,685 DICOM images and 37,730 free-text pathology reports were used to generate an in-house database labeled with groundtruth pathology results. The first deep learning model was created for cancer detection only in biopsy proven specimens - the most difficult subset of data as each image contained a suspicious finding. The model was comprised of two components: patch-based pre-training and end-to-end fine tuning. Training set size was 34,390 images (12,251 positive, 22,139 negative), and test set size was 6,778 images equally split. The second model was designed to have a high NPV for screening and diagnostic studies. An attention-based object detection network was used, with potential abnormalities identified by a region-proposal network and resolved by a separate head classifier network. The model was trained with 359,574 images (4,738 positive, 354,837 negative).

RESULTS

The first model achieved an AUC of 0.81, sensitivity of 0.764, and specificity of 0.797. The second model when tested on 100 positive and 100 negative cases achieved an AUC of 0.90, sensitivity of .866, and specificity of .873. If the test cases were

changed to a more clinically relevant distribution of 99% benign and 1% cancer, the AUC increased to 0.96.

CONCLUSION

We demonstrate the efficacy of deep learning for mammography in both cancer detection and the identification of negative studies. Future work includes enrichment of the dataset with further clinical data such as history of breast cancer, prior surgeries, and hormone replacement therapy. We also aim to improve model performance and efficiency through novel model architectures.

CLINICAL RELEVANCE/APPLICATION

We develop novel deep learning models for mammography using routine clinical data from a single institution with the potential to decrease recall imaging and unnecessary biopsies.

SSK02-07 Improved Cancer Detection using Artificial Intelligence: A Retrospective Evaluation of Missed Cancers on Mammography

Wednesday, Nov. 28 11:30AM - 11:40AM Room: E451B

Participants

Alyssa T. Watanabe, MD, Manhattan Beach, CA (*Presenter*) Consultant, CureMetrix, Inc Vivian Lim, MD, La Jolla, CA (*Abstract Co-Author*) Consultant, CureMetrix, Inc Jenna I. Liu, MD, La Jolla, CA (*Abstract Co-Author*) Consultant, Curemetrix, Inc Eric Weise, La Jolla, CA (*Abstract Co-Author*) Software developer, CureMetrix, Inc; Chi Yung Chim, La Jolla, CA (*Abstract Co-Author*) Researcher, CureMetrix, Inc William G. Bradley JR, MD, PhD, La Jolla, CA (*Abstract Co-Author*) Officer, CureMetrix, Inc Christopher E. Comstock, MD, New York, NY (*Abstract Co-Author*) Nothing to Disclose

For information about this presentation, contact:

alyssa90266@gmail.com

PURPOSE

To determine whether artificial intelligence-based (AI) software can be used to improve radiologists' sensitivity in breast cancer screening and detection.

METHOD AND MATERIALS

A set of 2-D Digital Mammograms originally interpreted with R2 ImageChecker CAD (Hologic, Sunnyvale, CA) and performed between October 2011 to March 2017 was collected from a community facility. Of the 317 cancer patients with available prior mammograms, 139 had retrospective findings, and 90 of those were deemed actionable. A blinded retrospective study was performed with a panel of seven radiologists comprised of false negative actionable mammograms obtained up to 5.8 years prior to diagnosis and 32 normal studies. Each radiologist viewed the cases without and then with benefit of cmAssist TM (CureMetrix, La Jolla, CA) AI based computer-aided detection (AI-CAD) flags and neuScore TM (quantitative AI-based probability for malignancy of flagged lesions, 1-100 scale). Reader decision making changes in true and false positive recalls with and without AI were analyzed.

RESULTS

All radiologists showed a significant improvement in their cancer detection rate (CDR) with the use of AI-CAD and neuScore (p =0.0069, C.I. = 95%). With the assistance of AI software, the sensitivity of less experienced general radiologists improved to a level higher than a fellowship-trained academic mammographer. The readers detected between 25% and 71% (mean 51%) of the early cancers without assistance. With AI software results,, overall reader CDR was 41% to 76% (mean 62%). Overall, there was less than 1% increase in the readers' false positive recalls with use of the AI software.

CONCLUSION

There was a statistically significant improvement in radiologists' sensitivity for cancer detection in this enriched data set of primarily false negative mammograms with the benefit of the AI-CAD with neuScore. The percentage increase in CDR for the radiologists in the reader panel, ranged from 6% to 64% (mean 27%) with the use of AI-CAD, with negligible increase in false positive recalls.

CLINICAL RELEVANCE/APPLICATION

This study shows a measurable, significant benefit for radiologists in mammography interpretation with the use of artificial intelligence (AI) based computer-aided detection software with quantitative scoring. The use of AI in clinical practice may potentially expedite workflow, enhance earlier detection of cancer, and reduce false negative mammograms.

SSK02-08 Data-Driven Imaging Biomarker for Breast Cancer Screening in Digital Breast Tomosynthesis

Wednesday, Nov. 28 11:40AM - 11:50AM Room: E451B

Participants

Sungwon Kim, MD, Seoul, Korea, Republic Of (*Presenter*) Nothing to Disclose Hyo-Eun Kim, Seoul, Korea, Republic Of (*Abstract Co-Author*) Employee, Lunit Inc Jin Chung, MD, Seoul, Korea, Republic Of (*Abstract Co-Author*) Nothing to Disclose Jee Eun Lee, MD, Seoul, Korea, Republic Of (*Abstract Co-Author*) Nothing to Disclose Minsung Kim, MD, Seoul, Korea, Republic Of (*Abstract Co-Author*) Nothing to Disclose Eun-Kyung Kim, MD, Seoul, Korea, Republic Of (*Abstract Co-Author*) Employee, Lunit Inc

For information about this presentation, contact:

dinbe@yuhs.ac

PURPOSE

To assess feasibility of a data-driven imaging biomarker in digital breast tomosynthesis (DIB-DBT) using the deep learning technology and evaluate its potential for detection of breast cancer.

METHOD AND MATERIALS

We retrospectively collected 49,577 exams of 4-view digital mammograms (MMG) and 1,196 exams of 4-view digital breast tomosynthesis images (DBT) from a single institution. We also collected 41 (10 cancer, 16 benign, 15 normal) exams of 4-view DBT retrospectively from another institution for external validation. 49,577 exams of MMG consists of 47,719 (5,599 cancer, 17,971 benign, and 24,149 normal) and independent 1,858 (619 cancer, 620 benign, 619 normal) exams of training and validation data, respectively. 1,196 exams of DBT consists of 996 (822 cancer, 40 benign, 134 normal) and independent 200 (120 cancer, 30 benign, 50 normal) exams of training and validation data, respectively. Previously, we assessed the feasibility of DIB-MMG as a screening tool for breast cancer detection in mammograms through external validation and pilot reader study. Thus, we exploit DIB-MMG for developing DIB-DBT in this study. Training of DIB-DBT consists of two stages - semi-supervised pre-training with partially-annotated large-scale MMG followed by fully-supervised fine-tuning with fully-annotated small-scale DBT. Residual network for image recognition is used as a baseline model. Diagnostic accuracy of DIB-DBT was assessed using receiver operating characteristic analysis.

RESULTS

Area under the curve (AUC) on the internal validation dataset of DIB-DBT with and without the pre-training stage of DIB-MMG was 0.9227 and 0.9081, respectively. AUC of the external validation dataset of DIB-DBT with and without the pre-training stage of DIB-MMG was 0.9710 and 0.9232, respectively.

CONCLUSION

This study showed the feasibility of DIB-DBT as a screening tool for breast cancer detection in DBT. This research also showed the potential of DIB-MMG as a base model for DIB-DBT. Further clinical validation of DIB-DBT is needed for using it as a reliable screening tool for breast cancer screening.

CLINICAL RELEVANCE/APPLICATION

With further clinical validation, DIB-DBT could be practically used as a second-reader to help radiologists detecting and diagnosing breast cancer in DBT efficiently.

SSK02-09 Improved Performance of Machine Learning-Based Analysis of Mammography by Using Digital Breast Tomosynthesis Versus 2D Mammography

Wednesday, Nov. 28 11:50AM - 12:00PM Room: E451B

Participants

Bill Lotter, Boston, MA (Abstract Co-Author) Officer, DeepHealth Inc

Jerrold L. Boxerman, MD, PhD, Providence, RI (Abstract Co-Author) Nothing to Disclose

A. Gregory Sorensen, MD, Belmont, MA (*Presenter*) Employee, DeepHealth, Inc; Board member, IMRIS Inc; Board member, Siemens AG; Board member, Fusion Healthcare Staffing; Board member, DFB Healthcare Acquisitions, Inc; Board member, inviCRO, LLC;

For information about this presentation, contact:

sorensen@deep.health

PURPOSE

Digital Breast Tomosynthesis (DBT) has been shown to be clinically superior to both full-field digital mammography and synthetic two-dimensional mammography (2D) for breast cancer detection. However, few studies to date have compared machine learning (ML) algorithmic performance in DBT versus 2D in large data sets. Technically, the much larger size of a DBT acquisition could actually be a hindrance for training convolutional neural networks (CNNs), for example via overfitting. Such technical issues could in turn imply impracticality of ML for DBT or a need for much larger training datasets. We sought to implement CNNs for both DBT and synthetic 2D X-ray mammograms and compare their performance.

METHOD AND MATERIALS

We compiled two separate datasets consisting of de-identified images and linked reports, collected from multiple mammography centers following an IRB-approved protocol. Data originated from equipment from the same manufacturer across all sites, and included presentation DBT and synthetic 2D images. We developed a novel CNN architecture and trained this model on the first dataset consisting of 22,000 DBT studies (323 cases of confirmed malignancy), where radiology reports and MQSA outcome data were used as estimates of ground truth. To simulate a more realistic evaluation scenario, the CNN was then tested on the second dataset collected from a different center. Using a test set of 1,750 screening DBT studies (94 confirmed cancers), receiver operating characteristic (ROC) curves and the corresponding area-under-the-curve (AUC) were calculated on both the full DBT study, and on just the synthetic 2D data alone.

RESULTS

AUC values for performance on the test dataset were: 2D: 0.894. DBT: 0.915. (p < 0.01 for difference between 2D and DBT on the full test dataset). At typical operating points (sensitivity 0.75 to 0.90) this corresponds to an average 19.6% relative decrease in model callback rates for the model (e.g., at sensitivity=0.8, from ~15% to ~11%).

CONCLUSION

ML can be applied successfully to DBT and results in improved performance over synthetic 2D mammography.

CLINICAL RELEVANCE/APPLICATION

Machine learning could play an important role in screening mammography, not only for traditional 2D mammography, but also when used with DBT; thus, ML is not in conflict with DBT but complementary and could further improve breast cancer screening performance.



SSK05

Science Session with Keynote: Chest (Artificial Intelligence/Deep Learning)

Wednesday, Nov. 28 10:30AM - 12:00PM Room: N227B



AMA PRA Category 1 Credits ™: 1.50 ARRT Category A+ Credit: 1.75

Participants

Bram Van Ginneken, PhD, Nijmegen, Netherlands (*Moderator*) Stockholder, Thirona BV; Co-founder, Thirona BV; Research Grant, Varian Medical Systems, Inc; Research Grant, Canon Medical Systems Corporation Carol C. Wu, MD, Bellaire, TX (*Moderator*) Author, Reed Elsevier

Sub-Events

SSK05-01 Chest Keynote Speaker: AI and Machine Learning in Thoracic Imaging

Participants

Bram Van Ginneken, PhD, Nijmegen, Netherlands (*Presenter*) Stockholder, Thirona BV; Co-founder, Thirona BV; Research Grant, Varian Medical Systems, Inc; Research Grant, Canon Medical Systems Corporation

SSK05-02 Application of Deep Learning for Risk Stratification of Pulmonary Nodules

Wednesday, Nov. 28 10:40AM - 10:50AM Room: N227B

Participants

Seyoun Park, Baltimore, MD (*Presenter*) Nothing to Disclose Linda C. Chu, MD, Baltimore, MD (*Abstract Co-Author*) Nothing to Disclose Cheng Ting Lin, MD, Baltimore, MD (*Abstract Co-Author*) Nothing to Disclose Alan Yuille, Baltimore, MD (*Abstract Co-Author*) Nothing to Disclose Elliot K. Fishman, MD, Baltimore, MD (*Abstract Co-Author*) Institutional Grant support, Siemens AG; Institutional Grant support, General Electric Company; Co-founder, HipGraphics, Inc

For information about this presentation, contact:

spark139@jhmi.edu

PURPOSE

The low dose CT (LDCT) screening criteria used in National Lung Screening Trial (NLST) has a 26.6% false positive rate at baseline. Even when updated more stringent Lung RADS criteria was retrospectively applied to the NLST data, the false positive rate remained at 12.8%. Deep learning, a form of artificial intelligence, has the potential to improve risk stratification of pulmonary nodules. The purpose of this study is compare the performance of deep learning vs. radiologists in the risk stratification of pulmonary nodules.

METHOD AND MATERIALS

264 patients with one solid nodule reported in NLST database up to 20mm (mean±standard deviation: 7.5±3.4mm) in size (223 benign, 41 malignant) were retrospectively selected from the NLST baseline LDCT (T0). All malignant nodules were confirmed pathologically and benign nodules were diagnosed based on pathology or clinical follow-up by NLST investigators. The nodules were semi-automatically segmented using our in-house software. 3D deep convolutional networks (CNN) was used for the deep learning classification of malignancy based on 64x64x64 input patch bounding intramodular and perinodular areas. 4-fold cross-validation was performed. Data augmentation by scaling and rotating was used to increase the number of training dataset. Two radiologists who were blinded to the diagnosis reviewed the cases independently and scored the nodules based on Lung RADS criteria. Scores 1 and 2 were considered negative and scores >= 3 were considered positive.

RESULTS

The selected cohort was 62.0±5.1 year-old-patients at T0 (150 male and 114 female). The average accuracy, sensitivity, and specificity of the review of radiologists were 0.67, 0.73, and 0.67, respectively. 4-fold cross validation result of deep learning was 0.88, 0.90, and 0.88 in the same terms of accuracy, sensitivity, and specificity. Especially, the false positive rate showed significant improvement from 0.33 to 0.12, which represents to reduce false positive cases from 73 to 27, using CNN.

CONCLUSION

Deep learning achieved improved sensitivity, specificity, and accuracy in risk stratification of pulmonary nodules compared with radiologists.

CLINICAL RELEVANCE/APPLICATION

Deep learning can improve the accuracy in risk stratification of pulmonary nodules compared with radiologists. This has the potential of achieving earlier cancer detection and reducing unnecessary work up in the lung screening population.

Honored Educators

Presenters or authors on this event have been recognized as RSNA Honored Educators for participating in multiple qualifying

educational activities. Honored Educators are invested in furthering the profession of radiology by delivering high-quality educational content in their field of study. Learn how you can become an honored educator by visiting the website at: https://www.rsna.org/Honored-Educator-Award/ Elliot K. Fishman, MD - 2012 Honored EducatorElliot K. Fishman, MD - 2014 Honored EducatorElliot K. Fishman, MD - 2016 Honored EducatorElliot K. Fishman, MD - 2018 Honored Educator

SSK05-03 Deep Learning with Convolutional Neural Network for the Differentiation of Pathologic Grades in Lung Adenocarcinomas

Wednesday, Nov. 28 10:50AM - 11:00AM Room: N227B

Participants

Hyun-Ju Lee, MD, PhD, Seoul, Korea, Republic Of (*Presenter*) Nothing to Disclose Young Jae Kim, PhD, Incheon, Korea, Republic Of (*Abstract Co-Author*) Nothing to Disclose Kwang Gi Kim, PhD, Incheon, Korea, Republic Of (*Abstract Co-Author*) Nothing to Disclose Ju G. Nam, MD, Seoul, Korea, Republic Of (*Abstract Co-Author*) Nothing to Disclose Young Joo Suh, MD, Seoul, Korea, Republic Of (*Abstract Co-Author*) Nothing to Disclose Heekyung Kim, Seoul, Korea, Republic Of (*Abstract Co-Author*) Nothing to Disclose Young Tae Kim, MD, PhD, Seoul, Korea, Republic Of (*Abstract Co-Author*) Nothing to Disclose Yoon Kyung Jeon, Seoul, Korea, Republic Of (*Abstract Co-Author*) Nothing to Disclose

For information about this presentation, contact:

lee.hyunju.rad@gmail.com

PURPOSE

To investigate the diagnostic performance of a deep learning method with a convolutional neural network (CNN) for the differentiation of pathologic grades in lung adenocarcinomas (ADs) manifesting as solitary lung nodules.

METHOD AND MATERIALS

This clinical retrospective study comprised preoperative CT image sets of lung ADs pathologically confirmed to be one of three grades (grade A, patterns with low metastatic potential [AIS, MIA, and lepidic-predominant]; grade B, patterns with intermediate metastatic potential [acinar and papillary]; and grade C, patterns with high metastatic potential [solid and micropapillary]). Supervised training was performed using 26,321 CT images (2390 sets) obtained between 2014 and 2016 (a total of 1066 image sets; 278, 718, and 70 nodules for grades A, B, and C, respectively; 609 enhanced and 457 non-enhanced). Image sets were augmented (rotated, parallel-shifted, strongly enlarged, and horizontal flipped images were generated from the original images) by a factor of 4 in images from grade A tumors and by a factor of 8 from grade C tumors. A CNN composed of 151 convolutional, two maximum pooling, and one fully connected layers was tested using independent 1268 image sets (762 enhanced and 506 non-enhanced) obtained between 2007 and 2013 (578 men and 690 women; mean age, 62.7 years ± 10.1; mean mass size, 23.5 mm ± 14.4; 400, 709, and 159 lung ADs of grades A, B, and C, respectively). Accuracy in categorizing lung ADs using the CNN model and the area under the ROC curve (AUC) for differentiating grades A vs. B+C, grade A vs. B, grade A vs. C, and grade B vs. C were calculated.

RESULTS

For the differentiation of grades A vs. B+C, diagnostic accuracy was 79.1% and AUC was 0.77 in the test data. For differentiating grades A vs. B, A vs. C, and B vs. C, diagnostic accuracies were 73.4%, 78.8%, 70.1% and AUCs were 0.77, 0.91, and 0.62, respectively.

CONCLUSION

Deep learning with CNN demonstrated high diagnostic performance in differentiating the pathologic grade of lung ADs.

CLINICAL RELEVANCE/APPLICATION

The CNN model can be useful in differentiating the pathologic grade of lung ADs, however, further study is warranted to correlate patients' prognoses with the output of CNN.

SSK05-04 Deep Machine Learning for Automatic Analysis of Chest X-Rays: Effect of Clinically Relevant Pathology Class Label Definition

Wednesday, Nov. 28 11:00AM - 11:10AM Room: N227B

Participants

Anas Ż. Abidin, MS, Rochester, NY (*Presenter*) Nothing to Disclose Adora M. D'Souza, MSc, Rochester, NY (*Abstract Co-Author*) Nothing to Disclose Axel Wismueller, MD, PhD, Rochester, NY (*Abstract Co-Author*) Nothing to Disclose

PURPOSE

To quantitatively analyze the effect of radiologically relevant pathology class label definition on deep machine learning results for automatic analysis of chest x-rays.

METHOD AND MATERIALS

With >100,000 frontal-view chest radiographs, the ChestX-ray14 data (Wang et al, 2017) is currently the largest publicly available annotated dataset for automatic chest x-ray analysis. Annotations consist of one or more of 14 thoracic pathology labels, e.g. Consolidation (C), Infiltration (I), Pneumonia (P) and 11 others. As radiologists cannot distinguish between C, I and P based on imaging findings alone, the stratification of these 'Opacity' entities into separate classes suggests a non-existent crispness of reported pathology class labels. To circumvent this key limitation of the ChestX-ray14 dataset and to investigate its effect on machine learning performance, we resampled data belonging to the 3 'Opacity' and 'No findings' classes, resulting in a 2-class classification problem with 63,000 chest x-rays. Images were resized to 10242 without preserving aspect ratio. Ensuring strict training/test (80%/20%) data separation, we fine-tuned a pre-trained ResNet-34 convolutional neural network with batch normalization, cross-entropy loss function, and last layer sigmoid activation. We also performed classification for all 14 individual pathology labels using the full dataset. Diagnostic accuracy was quantified using Area Under the receiver operating characteristics

RESULTS

For 'Opacity/No Findings' classification, we obtained AUC=0.78. This is close to the best performance obtained for original labels I, C, P with AUCs of 0.72, 0.81, 0.73, respectively. For the remaining 11 class labels, AUCs were comparable to, and for some labels, slightly better than the best published results of current state-of-the art methods (Rajpurkar et al 2017).

CONCLUSION

Our results suggest that radiologically relevant pathology label definition is important for training deep machine learning systems for automatic chest x-ray analysis, as it can influence their performance. Merging visually indistinguishable pathology classes can address a key limitation of the ChestX-ray14 data by alleviating the effect of 'structured noise'.

CLINICAL RELEVANCE/APPLICATION

It is critical that the datasets being used for training artificial intelligence recapitulate the characteristics of datasets encountered in a radiology setting as closely as possible.

SSK05-05 Evaluating the Use of a Deep Learning Algorithm for Radiology Quality Assurance in Out-Patient Chest X-Ray Reporting

Wednesday, Nov. 28 11:10AM - 11:20AM Room: N227B

Participants

Amit K. Sahu, MBBS, MD, New Delhi, India (Presenter) Nothing to Disclose Bharat Aggarwal, MBBS, MD, New Delhi, India (Abstract Co-Author) Nothing to Disclose Anandamoyee Dhar, New Delhi, India (Abstract Co-Author) Nothing to Disclose Gaurav Kapoor, MBBS, MD, Haryana, India (Abstract Co-Author) Nothing to Disclose Pooja Rao, MBBS, PhD, Mumbai, India (Abstract Co-Author) Employee, Qure.ai

For information about this presentation, contact:

drsahuamit@gmail.com

PURPOSE

To evaluate the accuracy of a deep learning algorithm - 1. To assist with screening of chest X-rays in the wellness check/primary care setting with predominantly normal X-rays 2. To help optimize the quality assurance (QA) process by selecting X-rays for review

METHOD AND MATERIALS

For this retrospective study, we used 3945 de-identified chest X-rays with the accompanying radiologist reports, randomly selected from the natural distribution of scans from adult patients attending OPD for a wellness check at 5 urban centers. Language processing algorithms were used to extract an initial ground truth of either 'normal' or 'abnormal' from the report impressions. A commercial deep learning-based chest X-ray screening system was then evaluated versus this ground truth. X-rays with a discordance between the original radiology report and the algorithm output were re-read by a panel of 3 radiologists. The majority opinion of the 3 radiologists was used as a new ground truth, to evaluate accuracy on this discordant set.

RESULTS

3274 of 3945 (82.9%) X-rays were normal, based on the original radiology report. Algorithm accuracy on the original dataset was 80%, with an AUC of 0.8, sensitivity of 0.63 and specificity of 0.83 on the detection of abnormal X-rays. Of the 789 discordant Xrays, 405were read by the panel of 3 radiologists. On this discordant dataset, the 3 radiologist-consensus agreed with the algorithm results in 64.9% of the cases, and with the original radiology report in the remaining 35.1%.

CONCLUSION

Among the discordant scans, the consensus ground truth was closer to the algorithm results than to the original report. Deep learning algorithms can effectively select chest X-rays for review during radiology quality control

CLINICAL RELEVANCE/APPLICATION

Artificial intelligence algorithms can be used for automated selection of chest X-rays for review during the radiology QA process, potentially increasing its effectiveness.

SSK05-06 Performance Validation of a Deep Learning-Based Automatic Detection Algorithm for Major Thoracic **Abnormalities on Chest Radiographs**

Wednesday, Nov. 28 11:20AM - 11:30AM Room: N227B

Participants

Eui Jin Hwang, Seoul, Korea, Republic Of (Presenter) Nothing to Disclose Sunggyun Park, Seoul, Korea, Republic Of (Abstract Co-Author) Employee, Lunit Inc So Young Choi, MD, Daejeon, Korea, Republic Of (Abstract Co-Author) Nothing to Disclose Jong Hyuk Lee, MD, Seoul, Korea, Republic Of (Abstract Co-Author) Nothing to Disclose Jin Mo Goo, MD, PhD, Seoul, Korea, Republic Of (Abstract Co-Author) Research Grant, Samsung Electronics Co, Ltd; Research Grant, Lunit Inc

Chang Min Park, MD, PhD, Seoul, Korea, Republic Of (Abstract Co-Author) Nothing to Disclose

For information about this presentation, contact:

ken921004@hotmail.com

PURPOSE

To evaluate the performance of a deep learning-based automatic detection (DLAD) algorithm for major thoracic abnormalities

including malignant pulmonary nodules/masses, tuberculosis, pneumonia, and pneumothorax on chest radiographs (CRs) in comparison with physicians.

METHOD AND MATERIALS

DLAD was developed using a 27-layer deep convolutional neural network. External validation of its diagnostic performance was conducted using 2 separate datasets from 2 institutions (normal: abnormal = 97:103 and 100:84). For comparison with physicians, an observer performance test was conducted using 1 of the datasets including 15 physicians (5 non-radiology physicians, 5 board-certified radiologists, 5 thoracic radiologists). All physicians reviewed each CR twice, without and with DLAD, and determined the presence of clinically significant thoracic abnormalities on a 5-point scale. Performance measurements were done using area under the receiver operating characteristic (ROC) curves for image-wise classification and area under the alternative free-response ROC curves for lesion-wise localization.

RESULTS

Image-wise classification performances of DLAD for abnormal CRs were 0.983 and 0.993 and lesion-wise localization performances were 0.974 and 0.985 on the two external validation datasets. Without DLAD, average classification performances of non-radiology physicians, board-certified radiologists, and thoracic radiologists were 0.813, 0.896, and 0.932, and average localization performances were 0.781, 0.870, and 0.907, respectively. DLAD demonstrated significantly higher performance in image-wise classification and lesion-wise localization compared with all reader groups (all Ps < 0.05). With DLAD, physicians' diagnostic performances were significantly improved in classification (0.904, 0.939, 0.958; all Ps <0.05) and localization (0.873, 0.919, 0.938; all Ps < 0.05) in all reader groups.

CONCLUSION

DLAD demonstrated excellent performance in image-wise classification and lesion-wise localization on CRs with major thoracic abnormalities, outperforming physicians, and enhancing the physician's diagnostic performance when used as a second reader.

CLINICAL RELEVANCE/APPLICATION

Our DLAD algorithm can accurately classify abnormal CRs and localize abnormal findings, and has the potential to improve diagnostic accuracy, patients' safety, and clinical workflow efficacy.

SSK05-07 Deep Learning-Based Automatic Detection Algorithm for the Detection of Major Thoracic Abnormalities on Chest Radiographs

Wednesday, Nov. 28 11:30AM - 11:40AM Room: N227B

Participants

Sunggyun Park, Seoul, Korea, Republic Of (*Presenter*) Employee, Lunit Inc Jaehong Aum, Seoul, Korea, Republic Of (*Abstract Co-Author*) Employee, Lunit Inc Chang Min Park, MD, PhD, Seoul, Korea, Republic Of (*Abstract Co-Author*) Nothing to Disclose Eui Jin Hwang, Seoul, Korea, Republic Of (*Abstract Co-Author*) Nothing to Disclose Jong Hyuk Lee, MD, Seoul, Korea, Republic Of (*Abstract Co-Author*) Nothing to Disclose Minsung Kim, MD, Seoul, Korea, Republic Of (*Abstract Co-Author*) Nothing to Disclose

For information about this presentation, contact:

sgpark@lunit.io

PURPOSE

To develop a deep learning-based automatic detection (DLAD) algorithm for major thoracic abnormalities including nodule/mass, tuberculosis (TB), pneumonia and pneumothorax on chest radiographs (CRs) using a large-scale CR dataset and evaluate its diagnostic performance.

METHOD AND MATERIALS

We collected a total of 89,832 CRs comprising 54,221 normal CRs and 35,641 abnormal CRs with major thoracic abnormalities including malignant pulmonary nodules/masses (n=13,925), pulmonary TB (n=6,798), pneumonia (n=6,903) and pneumothorax (n=8,015). Thereafter, all CRs were randomly split into three datasets; training dataset (n=84,072; 53,393 normal and 30,679 abnormal CRs), validation dataset (n=750; 300 normal and 450 abnormal CRs), and test dataset (n=750; 300 normal and 450 abnormal CRs). DLAD was designed using deep convolutional network consisting of 27 layers and 12 residual connections, and trained with 71,376 label-only CRs and 12,696 annotated CRs for which 15 thoracic radiologists marked the locations of the individual abnormalities. Diagnostic performance of the DLAD was investigated using receiver-operating characteristic (ROC) curve analysis for per-CR classification performance and jackknife alternative free-response receiver-operating characteristic (JAFROC) curve analysis for per-lesion detection performance. All CRs in the validation and test datasets were annotated by 5 out of 15 thoracic radiologists, and the final determination of the location of each abnormality was made by majority decision.

RESULTS

In the test dataset, DLAD showed an area under the ROC curve (AUC) of 0.9811 for per-CR classification performance and an area under the JAFROC curve of 0.9656 for per-lesion detection performance. The AUCs and JAFROCs of each disease category were 0.9674 and 0.9494 for malignant pulmonary nodule/mass, 0.9902 and 0.9742 for tuberculosis, 0.9854 and 0.9740 for pneumonia, and 0.9937 and 0.9800 for pneumothorax, respectively.

CONCLUSION

Our deep learning-based automatic detection algorithm demonstrated excellent, cutting-edge performances both in terms of differentiating normal and abnormal CRs and localizing individual abnormalities on CRs.

CLINICAL RELEVANCE/APPLICATION

DLAD can augment the diagnostic performance of radiologists both in terms of image-wise diagnosis and lesion-wise detection, thereby improving diagnostic accuracy, patients' safety, and work-flow efficacy.

"Change" versus "No-Change": Can Machine Learning Driven Algorithm Detect Stability or Change in Chest Radiographs?

Wednesday, Nov. 28 11:40AM - 11:50AM Room: N227B

Ramandeep Singh, MBBS, Boston, MA (*Presenter*) Nothing to Disclose Fatemeh Homayounieh, MD, Chelsea, MA (*Abstract Co-Author*) Nothing to Disclose Subba R. Digumarthy, MD, Boston, MA (*Abstract Co-Author*) Nothing to Disclose Chayanin Nitiwarangkul, MD, Boston, MA (*Abstract Co-Author*) Nothing to Disclose Atul Padole, MD, Boston, MA (*Abstract Co-Author*) Nothing to Disclose Mannudeep K. Kalra, MD, Boston, MA (*Abstract Co-Author*) Research Grant, Siemens AG; Research Grant, Canon Medical Systems Corporation John A. Patti, MD, Boston, MA (*Abstract Co-Author*) Nothing to Disclose Amita Sharma, MBBS, Boston, MA (*Abstract Co-Author*) Nothing to Disclose Manoj D. Tadepalli, BEng, Mumbai, India (*Abstract Co-Author*) Employee, Qure.ai Jo-Anne O. Shepard, MD, Boston, MA (*Abstract Co-Author*) Nothing to Disclose

PURPOSE

Chest radiograph is the most commonly performed imaging; changes, or lack thereof, of radiographic findings have tremendous implications on patient care. We compared accuracy of machine learning (ML) algorithm (Qure AI) and thoracic radiologists for assessing stability or change in findings over serial chest radiographs.

METHOD AND MATERIALS

We parsed the publicly available, de-identified, frontal-view chest radiographs from the NIH to identify 300 baseline and follow-up radiographs from 150 adult patients both with and without change in radiographic findings. Two thoracic radiologists reviewed all 300 radiographs to establish ground truth for radiographic findings [such as pleural effusions (EF), lung opacities (LO), hilar prominence (HP), and cardiomegaly (CM)]. All radiographs were processed with Qure AI ML to generate prediction scores and heat maps for each finding. Then, two different thoracic (test R1 and R2) radiologists independently recorded their findings, unaware of the ground truth and ML findings. Data were analyzed to determine accuracy and area under curve with free-choice receiver operating characteristics (FROC) analyses.

RESULTS

Respective percentage changes in findings on follow-up radiographs for EF, CM, HP and LO were 15% (21/138), 9% (13/150), 5% (8/150), 25% (33/132) for ground truth; 20% (28/138), 13% (20/150), 12% (18/150), 27% (36/132) for R1; 19% (26/138), 7% (11/150), 4.7% (7/150), 25% (33/132) for R2; and 25% (34/138), 23% (34/150), 23% (35/150), 40% (53/132) for ML. The AUC of ML algorithm for detecting lack of change in findings were 0.867 (EF), 0.904 (C), 0.872 (HP), 0.742 (LO). Accuracy of ML for detecting change in radiographic findings was also high with corresponding AUC of 0.804 (EF), 0.923 (C), 0.839 (HP), 0.758 (LO). Although both test radiologists had AUC similar to ML for stable radiographic findings, their AUC [0.867-0.878 (EF), 0.815-0.904 (CM), 0.635-0.872 (HP), 0.742-0.854 (LO) for change in findings were lower compared to corresponding AUC for ML.

CONCLUSION

ML algorithm can accurately predict stability and change in radiographic findings on follow up radiographs. Its accuracy varies across different types of findings, and is highest for cardiomegaly and lowest for lung opacities.

CLINICAL RELEVANCE/APPLICATION

ML can enable stratification of chest radiographs on basis of change or stability of findings, thus expediting interpretation of radiographs with important changes.

Honored Educators

Presenters or authors on this event have been recognized as RSNA Honored Educators for participating in multiple qualifying educational activities. Honored Educators are invested in furthering the profession of radiology by delivering high-quality educational content in their field of study. Learn how you can become an honored educator by visiting the website at: https://www.rsna.org/Honored-Educator-Award/ Subba R. Digumarthy, MD - 2013 Honored Educator

SSK05-09 Assessment of Endotracheal Tube Position on Chest Radiographs using Deep Learning

Wednesday, Nov. 28 11:50AM - 12:00PM Room: N227B

Participants

Paras Lakhani, MD, Philadelphia, PA (*Presenter*) Nothing to Disclose Adam E. Flanders, MD, Philadelphia, PA (*Abstract Co-Author*) Nothing to Disclose Baskaran Sundaram, MRCP, FRCR, Philadelphia, PA (*Abstract Co-Author*) Nothing to Disclose Maansi R. Parekh, MBBS, Philadelphia, PA (*Abstract Co-Author*) Nothing to Disclose Achala Donuru, MD, Philadelphia, PA (*Abstract Co-Author*) Nothing to Disclose Vijay M. Rao, MD, Philadelphia, PA (*Abstract Co-Author*) Nothing to Disclose Richard J. Gorniak, MD, Philadelphia, PA (*Abstract Co-Author*) Consultant, BioClinica, Inc; Consultant, Medtronic plc

For information about this presentation, contact:

paras.lakhani@jefferson.edu

PURPOSE

Assess the efficacy of deep learning in determining endotracheal tube (ETT) position on chest radiographs.

METHOD AND MATERIALS

23,079 de-identified frontal chest radiographs with an ETT were split into 12 categories, which included bronchial insertion, and distance from the carina at 1.0cm intervals (e.g. 0.0-0.9cm, 1.0-1.9cm...) and lastly >=10cm. Ground truth ETT position was determined by two board certified radiologists (original author and a second radiologist for QA confirmation). Images were split into

training (80%, 18467 images), validation (10%, 2306 images), and test (10%, 2306 images). The ETT was re-measured on 100 random images from the test data to assess inter-observer variability. The pretrained Inception V3 convolutional neural network was utilized to a) predict ETT distance from the carina in cm and b) categorize images as low ETT (< 2cm of carina), satisfactory (2-7cm above carina), or high (>= 7cm above carina). Image normalization and auto-cropping about the carina was performed prior to model training. Real-time data augmentation was employed, and an ensemble of 10 Inception V3 models was used in the final classification. Receiver operating characteristic (ROC), area-under-the-curves (AUC), sensitivity and specificity on test data were used to assess the models.

RESULTS

The predicted ETT distance from carina had a mean difference of 0.79cm (\pm 0.56) from the ground truth, and the two radiologists had a mean difference of 0.44cm (\pm 0.44). On the test data, the AUC was 0.97 (95%CI: 0.96-0.98) for differentiating ETT<2cm from carina from all others. The AUC was 0.96 (95%CI: 0.95-0.98) for differentiating high ETT>=7cm from all others. 4 bronchial insertions and ETT 0-0.9cm from carina were missed of 385 true positives (sensitivity: 99.0%). There were 86 false positives of 1921 true negative cases (specificity: 95.5%). However, threshold cases near a category were sometimes missed; for example, 43 cases of 1-1.9cm above carina were misclassified as >=2cm above carina, usually as 2-3cm above carina. Similarly, threshold cases of 6-6.9cm were predicted as 7-7.9cm above carina or vice-versa. The sensitivity of the model drops to 87.8% when including these threshold cases as misclassified.

CONCLUSION

Deep learning shows promise in assessing ETT position and predicts postion within 1cm in most cases.

CLINICAL RELEVANCE/APPLICATION

Automatic identification of ETT position may reduce time to identification of critical placement.



SSK18

Physics (CT: Image Quality)

Wednesday, Nov. 28 10:30AM - 12:00PM Room: E353C

AI CT PH SQ

AMA PRA Category 1 Credits ™: 1.50 ARRT Category A+ Credit: 1.75

FDA Discussions may include off-label uses.

Participants

Michael F. McNitt-Gray, PhD, Los Angeles, CA (*Moderator*) Institutional research agreement, Siemens AG; ; ; ; ; John M. Boone, PhD, Sacramento, CA (*Moderator*) Patent agreement, Isotropic Imaging Corporation Consultant, RadSite

Sub-Events

SSK18-01 Quantitative Impact of Denoising Strategies in Low-Dose CT

Participants

Juan Pablo Cruz Bastida, Madison, WI (*Presenter*) Nothing to Disclose Daniel Gomez-Cardona, PhD, Rochester , MN (*Abstract Co-Author*) Nothing to Disclose Ran Zhang, PhD, Madison, WI (*Abstract Co-Author*) Nothing to Disclose John W. Hayes, MS, Madison, WI (*Abstract Co-Author*) Nothing to Disclose Ke Li, PhD, Madison, WI (*Abstract Co-Author*) Nothing to Disclose Guang-Hong Chen, PhD, Madison, WI (*Abstract Co-Author*) Research funded, General Electric Company Research funded, Siemens AG

For information about this presentation, contact:

cruzbastida@wisc.edu

PURPOSE

CT number accuracy at low dose levels has been found to be strongly biased. It was demonstrated that the stochastic noise associated with photon detection is the root cause of inaccurate CT number. The purpose of this work is to investigate the impact of three different denoising strategies to alleviate CT number inaccuracy in FBP-based CT: image domain denoising, sinogram domain denoising and raw counts domain denoising.

METHOD AND MATERIALS

Data acquisition was performed in a benchtop CT system, which included a CdTe-based photon counting detector. A Catphan phantom, containing inserts of known composition, was scanned at 60 kV and two different CTDIw levels: 1.5 and 15 mGy. The acquired data was reconstructed using FBP with ramp filter. Locally adapted denoising diffusion filter was applied to the lowest dose data set, in image, sinogram and raw counts domain. The contrast of Teflon and LDPE inserts was measured in averaged images across repetitions. FBP reconstruction of the average raw counts at the highest dose was considered as reference.

RESULTS

Experimental results from in this study corroborate that CT number estimates are inaccurate at low dose levels. As a consequence, the contrast of inserts relative to the background is overestimated. Particularly, the contrast of the analyzed inserts is doubled in the lowest dose scans. After adapted denoising, only the strategy to perform denoise in the raw counts domain was successful in restoring the reference contrast values.

CONCLUSION

Results in this study suggest that locally adaptive denoising is an adequate methodology to preserve the quantitative accuracy of low dose CT when performed in the pre-log projection domain.

CLINICAL RELEVANCE/APPLICATION

Healthy tissue and disease characterization often rely on both absolute CT number and relative contrast, for example: liver and pancreatic steatosis, acute cerebral venous sinus thrombosis, etc. Dose reduction efforts in CT must be guided by both imaging performance and quantitative capabilities.

SSK18-02 Task-Based Image Quality Assessment of X-ray CT Using Convolutional Neural Networks

Wednesday, Nov. 28 10:40AM - 10:50AM Room: E353C

Participants

Felix K. Kopp, Munich, Germany (*Abstract Co-Author*) Nothing to Disclose Marco Catalano, Napoli, Italy (*Abstract Co-Author*) Nothing to Disclose Daniela Pfeiffer, MD, Munich, Germany (*Abstract Co-Author*) Nothing to Disclose Alexander A. Fingerle, MD, Munchen, Germany (*Abstract Co-Author*) Nothing to Disclose Ernst J. Rummeny, MD, Munich, Germany (*Abstract Co-Author*) Nothing to Disclose Peter B. Noel, PhD, Munich, Germany (*Presenter*) Nothing to Disclose

PURPOSE

The purpose of this study is the task-based image quality assessment of X-ray computed tomography.

METHOD AND MATERIALS

A phantom with contrast targets similar to lesions in a contrast enhanced liver (acrylic spheres, varying diameters, +30 HU) was repeatedly scanned with a computed tomography scanner. A board certified radiologist rated image patches containing the contrast targets with a confidence rating for the presence of the signal. Labeled image data were used to build several anthropomorphic model observers to predict the performance of the human observer: A neural network based on softmax regression (SR-MO) and a convolutional neural network (CNN-MO). Results were compared to a more traditional model observer, the channelized Hotelling observer (with Gabor channels and internal channel noise (CHOi)). The performance of the different model observers and the human observer were evaluated with a receiver operating characteristic curve analysis. The machine learning based model observers were trained with two different strategies: A) building a separate model for each lesion size; B) building one model that was applied to lesions of all sizes.

RESULTS

Machine learning based model observers as well as the CHOI and the human observer were highly correlated at each lesion size and dose level. With strategy A, Pearson's product-moment correlation coefficients r were 0.961 (95% confidence interval (CI): 0.863-0.989) for SR-MO and 0.974 (95% CI: 0.907-0.993) for CNN-MO. Mean absolute percentage differences (MAPD) between the model observer and the human observer were 1.1% for SR-MO and 1.0% for CNN-MO. With strategy B, r was 0.956 (95% CI: 0.845-0.988) for SR and 0.958 (95% CI: 0.854-0.989) for CNN. For CHOi, r was 0.971 (95% CI: 0.897-0.992). MAPD were 2.0% for SR-MO and 1.5% for CNN-MO. For the CHOi the MAPD was 1.9%.

CONCLUSION

Machine learning based model observers can accurately predict the performance of a human observer for all lesion sizes and dose levels in the evaluated signal detection task.

CLINICAL RELEVANCE/APPLICATION

Model observers are widely used in research regarding the development and optimization of medical imaging devices. Our results show that machine learning based model observers can accurately predict the performance of a human observer in a signal detection task for CT.

SSK18-03 DestreakNet: A Deep Convolutional Neural Network to Reduce Metal Streak Artifacts in CT Images

Wednesday, Nov. 28 10:50AM - 11:00AM Room: E353C

Participants

Lars Gjesteby, Troy, NY (*Presenter*) Nothing to Disclose Hongming Shan, Troy, NY (*Abstract Co-Author*) Research Grant, General Electric Company Qingsong Yang, Troy, NY (*Abstract Co-Author*) Nothing to Disclose Yan Xi, Shanghai, China (*Abstract Co-Author*) Employee, UEG Medical Imaging Yannan Jin, MSC, Erlangen, Germany (*Abstract Co-Author*) Employee, General Electric Company Bernhard Claus, PhD, Niskayuna, NY (*Abstract Co-Author*) Nothing to Disclose Bruno De Man, PhD, Niskayuna, NY (*Abstract Co-Author*) Employee, General Electric Company Ge Wang, PhD, troy, NY (*Abstract Co-Author*) Nothing to Disclose

For information about this presentation, contact:

ge-wang@ieee.org

PURPOSE

To design and train a deep convolutional neural network to reduce metal artifacts in CT images.

METHOD AND MATERIALS

Our network structure (DestreakNet) consists of two parallel streams, each with 20 residual units. In each residual unit, there are two convolution layers with batch normalization (BN) and rectified linear unit (ReLU) activation. The network is trained on the residual error between the input and output of the unit. The outputs of both streams are merged in the network's feature space, and then passed through nine more convolution layers to yield a final output. A mean squared error (MSE) and a perceptual loss function were both investigated for network optimization. All training, testing, and validation datasets were generated using CatSim, an industrial-grade CT simulator. Real data from the Visible Human Project were used to create voxelized phantoms of pelvic and spinal regions with and without metal implants. For initial correction, CT images were reconstructed using the state-of-the-art NMAR algorithm. The reconstructed images without metal were the ground truth and target of the network. From full-size images, approximately 150,000 patches of size 56x56 were extracted for training. Patches from the NMAR images were input to one network stream and patches from uncorrected CT images were input to the other to harness complimentary features simultaneously.

RESULTS

To validate the network performance, hip and spine images withheld from training were used. In a hip case, the image quality metrics including structural similarity index (SSIM) and peak signal-to-noise ratio (PSNR) were calculated for all images in reference to the artifact-free truth. The SSIM and PSNR were 0.2382 and 9.1830, respectively, for the initial uncorrected reconstruction image, 0.7014 and 18.8975 for the NMAR-corrected image, 0.8636 and 23.8582 for DestreakNet with MSE loss, and 0.8264 and 22.1685 for DestreakNet with perceptual loss.

CONCLUSION

Our network substantially reduced metal streak artifacts that remained in the CT image after initial correction by the NMAR algorithm.

CLINICAL RELEVANCE/APPLICATION

Our proposed data-driven metal artifact reduction method may provide sufficient image quality in radiation therapy planning, which requires accurate tumor characterization near implants for precise dose delivery.

SSK18-04 Patient-Specific Local Noise Power Spectrum Measurement via a Deep-Learning Generative Adversarial Network

Wednesday, Nov. 28 11:00AM - 11:10AM Room: E353C

Participants Chengzhu Zhang, BS, Madison, WI (*Presenter*) Nothing to Disclose Daniel Gomez-Cardona, PhD, Rochester , MN (*Abstract Co-Author*) Nothing to Disclose Yinsheng Li, BEng, Madison, WI (*Abstract Co-Author*) Nothing to Disclose Juan Montoya, Madison, WI (*Abstract Co-Author*) Nothing to Disclose Guang-Hong Chen, PhD, Madison, WI (*Abstract Co-Author*) Research funded, General Electric Company Research funded, Siemens AG

For information about this presentation, contact:

czhang553@wisc.edu

PURPOSE

With the increased use of low-dose CT techniques which are characterized for its highly shift-variant noise properties, the measurement of the noise power spectrum (NPS) has become challenging and time consuming since current solutions require multiple scans of a given clinical scenario. In this work, a deep-learning generative adversarial network (GAN) was developed to address this challenge and provide a fast and accurate way to measure patient-specific local NPS.

METHOD AND MATERIALS

GANs were utilized to learn a mapping from white noise input to output CT noise realizations with correct CT noise correlations from a single local uniform ROI. To achieve this, a two-stage training strategy was implemented. In the pre-training stage, repeated scans of a quality assurance phantom were performed to extract 1600 (64x64) local MBIR noise-only images used as labels to train the network. This network characterized the noise magnitude and correlation in labels and was able to generate 64x64 noise-only images with similar characteristics as the input. For the next stage, a single scan of an anthropomorphic phantom was used for fine-tuning, while repeated scans were used for validation. First, a 101x101 ROI was extracted from a single MBIR image, detrended, and augmented to obtain 128 (64x64) training labels and fine-tune the pre-trained GANs. To validate the GANgenerated noise images, their NPS was compared to the NPS from the physical ensemble of repeated scans in terms of overall RMSE, noise magnitude, and mean frequency across 30 trials. This patient-specific approach was applied to clinical data reconstructed with MBIR (same patient at two doses) to assess the estimated NPS in terms of noise magnitude and coarseness.

RESULTS

The overall RMSE between the GAN-generated NPS and the physical NPS was 0.83 HU2mm2. The mean percent discrepancy for their noise magnitude and mean frequency were 4.51% and 3.62%, respectively. The runtime for the fine-tuning stage was <100s and 1s to generate 250 noise images.

CONCLUSION

It was demonstrated that GANs can characterize CT noise in terms of magnitude and coarseness and generate multiple noise realizations with comparable characteristics from a single noise realization.

CLINICAL RELEVANCE/APPLICATION

A fast and accurate way to estimate patient-specific local NPS was provided and can be easily adapted to any given CT system. This is an essential step towards patient-specific image quality assessment.

SSK18-05 Multi-Kernel Synthesis for CT Images Using a Deep Convolutional Neural Network

Wednesday, Nov. 28 11:10AM - 11:20AM Room: E353C

Awards

Trainee Research Prize - Fellow

Participants Andrew Missert, PHD, Rochester, MN (*Presenter*) Nothing to Disclose Shuai Leng, PHD, Rochester, MN (*Abstract Co-Author*) License agreement, Bayer AG Lifeng Yu, PhD, Chicago, IL (*Abstract Co-Author*) Nothing to Disclose Cynthia H. McCollough, PhD, Rochester, MN (*Abstract Co-Author*) Research Grant, Siemens AG

For information about this presentation, contact:

Missert.Andrew@mayo.edu

PURPOSE

To produce a single synthetic image that combines the best qualities of images reconstructed with different kernels using a deep convolutional neural network (CNN).

METHOD AND MATERIALS

A CNN was trained from scratch to synthesize multiple input images, each produced with a different reconstruction kernel, into a single output image that exhibits improved image qualities (in terms of high sharpness and low noise levels) compared to each input individually. The CNN architecture was based on the ResNet design, and consisted of repeated blocks of residual units with a total of 32 convolutional layers. The CNN inputs consisted of three images produced by soft (B10), medium-sharp (B45), and sharp (B70) kernels that were stacked in the channel dimension. The CNN output was treated as a perturbation that was added to the sharp-kernel input, which reduced the required training time. The network was trained using supervised learning with both full-dose and simulated quarter-dose abdominal CT images. The simulated quarter-dose images obtained from different kernels were used as the

network input, and the corresponding full-dose images reconstructed with a sharp kernel were used as the ground truth to evaluate a mean-squared-error loss function. The network was trained on 500,000 example images of various sizes that were cropped from ten abdominal CT exams. After training, the performance was evaluated by comparing input and output images using a reserved set of full-dose abdominal, chest, and phantom CT scans that were not used in the network training.

RESULTS

The synthetic images improved the signal-to-noise ratio by 338% compared to the sharp kernel images, without observable blurring of sharp edges. No perceptible artificial texture was introduced that detracted from the natural appearance of the synthetic image. The algorithm was robust enough to be applied to multiple tissue types, including the bones, lungs, and liver.

CONCLUSION

An artificial neural network can be used to combine images from multiple reconstruction kernels into a single synthetic image that exhibits both low noise and a high degree of sharpness.

CLINICAL RELEVANCE/APPLICATION

CT Images from different reconstruction kernels can be merged using a neural network into a single image with superior qualities that can be used for reading multiple tissue types simultaneously.

SSK18-06 Correlation Between 2D Channelized Hoteling Observer in a Uniform Water Background and Human Observers in a Patient Liver Background for Low-Contrast Lesion Detection and Localization in CT

Wednesday, Nov. 28 11:20AM - 11:30AM Room: E353C

Participants

Hao Gong, PhD, Rochester,, MN (*Presenter*) Nothing to Disclose Lifeng Yu, PhD, Chicago, IL (*Abstract Co-Author*) Nothing to Disclose Shuai Leng, PHD, Rochester, MN (*Abstract Co-Author*) License agreement, Bayer AG Michael L. Wells, MD, Rochester, MN (*Abstract Co-Author*) Nothing to Disclose Joel G. Fletcher, MD, Rochester, MN (*Abstract Co-Author*) Grant, Siemens AG; Consultant, Medtronic plc; ; Cynthia H. McCollough, PhD, Rochester, MN (*Abstract Co-Author*) Research Grant, Siemens AG

For information about this presentation, contact:

Gong.Hao@mayo.edu

PURPOSE

To investigate the correlation between 2D channelized Hoteling observer (CHO) performance in a uniform water background (with single-slice viewing mode) and human observer (HO) performance in a patient liver background (with multi-slice scrolling viewing mode) for a low-contrast liver lesion detection and localization task when lesion location is uncertain.

METHOD AND MATERIALS

Seven routine dose abdominal patient scans (mean CTDIvol 12.6 mGy) were retrospectively collected. Patient scans at half and quarter of routine dose were simulated using a projection-based noise insertion tool. An abdomen-sized water phantom was repeatedly scanned (n = 10) on the same scanner. Lesion models generated from real metastatic liver lesions (size 7, 9 and 11 mm, and contrast 15, 20, and 25 HU) were inserted into both phantom and patient images using a projection-based method. CT images were created using filtered-back-projection (FBP) and iterative reconstruction (IR). Region-of-interests (ROIs) around lesions were extracted to generate trials for CHO and HO studies. Centers of the ROIs were shifted to randomly distribute lesion locations in the ROIs. A 2D CHO with 12 Gabor channels was applied to phantom images. Two subspecialized radiologists (10 and 25 years of experience) performed HO studies on patient images. For each trial, they localized lesions by scrolling through multiple slices. The performance of CHO and HO was compared across 12 experimental conditions with varying dose, lesion characteristics, and reconstruction types. Area under the receiver operating characteristic (ROC) curve and localization ROC curve were used as figure of merits for CHO and HO performance.

RESULTS

2D CHO performance in phantom images correlated well with HO performance in patient liver images (Pearson correlation coefficients 0.960 (p = 0.0023) and 0.984 (p = 0.0004) for detection and localization, respectively) for all conditions . No statistically significant difference was observed in Bland-Altman agreement analysis.

CONCLUSION

It is possible to use a simple single-slice viewing CHO and uniform water phantom to assess performance for realistic CT detection and localization tasks in patient liver backgrounds.

CLINICAL RELEVANCE/APPLICATION

Single-slice 2D CHO with Gabor channels provides a convenient tool to evaluate diagnostic performance and optimize abdominal CT scanning protocols.

Honored Educators

Presenters or authors on this event have been recognized as RSNA Honored Educators for participating in multiple qualifying educational activities. Honored Educators are invested in furthering the profession of radiology by delivering high-quality educational content in their field of study. Learn how you can become an honored educator by visiting the website at: https://www.rsna.org/Honored-Educator-Award/ Michael L. Wells, MD - 2017 Honored Educator

SSK18-07 Can Deep Learning Unseat Iterative Reconstruction for Low-Dose CT?

Wednesday, Nov. 28 11:30AM - 11:40AM Room: E353C

Participants Hongming Shan, Troy, NY (*Presenter*) Research Grant, General Electric Company Atul Padole, MD, Boston, MA (*Abstract Co-Author*) Nothing to Disclose Mannudeep K. Kalra, MD, Boston, MA (*Abstract Co-Author*) Research Grant, Siemens AG; Research Grant, Canon Medical Systems Corporation Uwe Kruger, Troy, NY (*Abstract Co-Author*) Nothing to Disclose Wenxiang Cong, Albany, NY (*Abstract Co-Author*) Nothing to Disclose Ge Wang, PhD, troy, NY (*Abstract Co-Author*) Nothing to Disclose

For information about this presentation, contact:

wangg6@rpi.edu

PURPOSE

Although widely applied in clinical practice, studies have reported that iterative reconstruction (IR) alters image appearance, and can adversely affect low contrast lesions. The purpose of this project is to systematically compare commercial/clinical iterative reconstructions by major vendors with FBP-reconstruction-based deep learning (FBP-DL) reconstruction for low-dose chest and abdomen CT exams.

METHOD AND MATERIALS

Our study included 80 low-dose chest and abdomen CT exams from three major CT vendors (de-identified). We created a neural network including 4 convolutional and 4 deconvolutional layers, each of the layers contains 32 filters except for the last layer with only 1 filter. For preserving image features, former feature-maps were reused at latter layers by three conveying-paths. The rectified linear unit was used for each layer. The network was optimized in the Wasserstein generative adversarial network framework with an additional perceptual loss. 128K normal- and low-dose FBP image patches from the MGH dataset were used in training our network. Image quality metrics including peak signal-to-noise ratio (PSNR) and structural similarity index (SSIM) were calculated for all the images in reference to the normal-dose FBP images. Also, a blinded reader study was designed to evaluate the image quality. Then, the Wilcoxon signed-rank test was used to compare FBP-DL with commercially available state-of-the-art IR techniques.

RESULTS

FBP-DL achieves a significantly better image quality and performance than commercially available IR images evaluated by PSNR and SSIM for all the selected vendors. Also, the reader study demonstrated that FBP-DL images had superior visibility of small and subtle structures with lower noise and less severe artifacts as compared to the IR counterparts. In addition to that, deep learning is computationally more efficient than IR.

CONCLUSION

The deep learning method has a great potential to outperform the commercial/clinical iterative reconstruction for low-dose CT. An integrated deep learning workflow from raw data to final images/radiomics is under active development.

CLINICAL RELEVANCE/APPLICATION

Emerging deep learning-based CT methods may provide a superior diagnostic performance in routine clinical applications.

SSK18-08 Reference-Based Image-Detail and Noise Texture Metrics for CT Image Quality Assessment

Wednesday, Nov. 28 11:40AM - 11:50AM Room: E353C

Participants

Sathish Ramani, Niskayuna, NY (*Abstract Co-Author*) Employee, General Electric Company Lin Fu, PhD, Niskayuan, NY (*Abstract Co-Author*) Employee, General Electric Company Bruno De Man, PhD, Niskayuna, NY (*Presenter*) Employee, General Electric Company

PURPOSE

Task-based image quality metrics are the gold-standard in evaluating and comparing the performance of imaging algorithms. Nevertheless, algorithm designers still benefit from lower-level more direct metrics reflecting the actual image presentation. Traditional noise and spatial resolution metrics are coming short for non-linear iterative reconstruction approaches. This work proposes quantitative metrics for separately assessing object-detail, artifact-level and noise texture based on a gold-standard reference.

METHOD AND MATERIALS

A phantom constructed from a freshly-cut turkey was scanned 117 times at 120 kV and 200 mA. FBP images were reconstructed and averaged over the scans to obtain a noise-free reference image Z, from which a noisy sinogram S was simulated. Model-Based Image Reconstruction (MBIR) images at varying regularization strengths, β , were reconstructed from S. For an MBIR-image M, the object-detail metric was computed as a normalized covariance between M and Z. Artifact metric was computed as the normalized energy of the difference between M and its geometric-projection along Z. Histogram and spectral density shapes of the residue R=M-Z, were used to assess noise texture.

RESULTS

With increasing β , noise decreased in M at the expense of loss of image features: the object-detail metric monotonically decreased correspondingly. Artifact metric exhibited a minimum and increased either way due to high noise at low β or loss of image features at high β . Histogram of R evolved from being broad with long tails (high noise at low β) to being narrow (nearly no noise at high β). The spectral density of R evolved from exhibiting high-frequency behavior (high noise at low β) to being predominantly low-frequency in nature (noise with long spatial correlation at low β).

CONCLUSION

The proposed metrics captured expected behavior of MBIR at varying strengths indicating their validity. These metrics can be helpful in judging preservation of image features and evaluation of artifact-level and noise texture for CT algorithm development and tuning.

CT iterative reconstruction was introduced a decade ago and is continuing to be improved. The proposed image quality evaluation methods are useful for algorithm designers to achieve the best possible tuning of CT algorithms before clinical deployment.

SSK18-09 Task Based Image Quality in Virtual Monoenergetic Images Across 3 Generations of Scanner Models

Wednesday, Nov. 28 11:50AM - 12:00PM Room: E353C

Participants

Jayasai R. Rajagopal, BA, Durham, NC (*Presenter*) Nothing to Disclose Yakun Zhang, MS, Durham, NC (*Abstract Co-Author*) Nothing to Disclose Juan Carlos Ramirez-Giraldo, PhD, St Louis, MO (*Abstract Co-Author*) Employee, Siemens AG Ehsan Samei, PhD, Durham, NC (*Abstract Co-Author*) Research Grant, General Electric Company; Research Grant, Siemens AG; Advisory Board, medInt Holdings, LLC; License agreement, 12 Sigma Technologies; License agreement, Gammex, Inc

For information about this presentation, contact:

yakun.zhang@duke.edu

PURPOSE

To use task-based metrics to assess the impact of patient size, beam spectra separation, and radiation exposure on image quality for virtual monoenergetic images (VMIs) across three scanner platforms.

METHOD AND MATERIALS

This study used a commercially available phantom with iodine, soft tissue and calcium inserts (Gammex Multi Energy CT phantom). The phantom was configured with additional fat rings simulating five different sizes (20, 30, 35, 40, and 50 cm diameter). All scans used radiation exposures of 4, 8, 16, and 24 mGy, and were repeated on three DECT platforms from one manufacturer (Siemens Force, Flash and Edge). VMIs were reconstructed at 50, 70 keV and 150 keV. Noise and image texture in terms of average frequency of the noise power spectra (Favg) and the contrast-dependent spatial resolution in terms of the 50% amplitude of the iodine-task transfer function (F50) were calculated. A task-specific detectability index (d') was calculated for iodine inserts using a 5 mm Gaussian circular disk as the task.

RESULTS

The Favg and F50 decreased with increasing phantom size. For 100/150Sn kV on Force scanner, Favg was 0.31, 0.30, 0.27, and 0.25 mm-1 for the 20, 30, 35, 40 cm sizes; F50 was 0.43, 0.43, 0.37, 0.32 mm-1, respectively. For the same phantom size, the Favg appeared to be insensitive to changes in acquisition spectra separations, but F50 increased with increasing spectra separation. Different keVs did not affect either Favg or F50, but affected the noise magnitude and contrast, and thus the detectability index. d' for the 15 mg/ml iodine insert had an average of 23% increase for all sizes and kV combinations when keV decreased from 70 to 50. At 70 keV, the larger spectra separation (80/150Sn kV) led to an increase in d' compared to less spectra separation (100/150Sn kV) at round 10% for the 20 and 30 cm phantoms, but only 3% higher d' for the 35 and 40 cm phantoms. For a fixed keV, image contrast, Favg, and F50 were relatively insensitive to changes in radiation exposure for sizes below 40cm.

CONCLUSION

The system behaved non-linearly for different phantom sizes and spectra separation. Task based metrics was able to capture the characteristics of the VMIs. Highest detectability was achieved with larger spectra separation and for smaller sizes.

CLINICAL RELEVANCE/APPLICATION

Highest iodine detectability for the VMIs was achieved with larger spectra separation and for smaller sizes.



ML41

Machine Learning Theater: The Curated Marketplace - A New Platform Approach: Presented by Blackford

Wednesday, Nov. 28 11:00AM - 11:20AM Room: Machine Learning Showcase North Hall

Program Information

The curated marketplace - A new platform approach for deploying medical imaging applications and AI algorithms. New imaging applications are streaming onto the market all the time, and it's hard to determine which will ultimately be most beneficial to the practice of healthcare. The limited bandwidth of a typical healthcare IT department, as well as limited financial resources, means that radiology departments are often forced to consider merely a subset of the clinical and productivity software applications they seek. Deploying more than one or two new software solutions a year is the limit for many radiology organizations as new software is costly and hard to get approved and deployed. There is a solution to this problem, and that is adopting a platform strategy instead of purchasing individual software applications from different vendors. A platform should offer access to a marketplace of applications that address the full range of needs of a radiology department and their referring physicians. Lately, platforms have been strongly associated with artificial intelligence (AI) applications and algorithms. A platform is a natural fit for AI, because the field is evolving rapidly, and these applications will continue to improve over time. But the benefits of a platform strategy are applicable to many other medical imaging applications and software add-ons beyond those involving AI. A standard marketplace may offer applications that are not validated by the platform provider. A curated marketplace takes the marketplace approach a step further, towards comprehensive vetting of the applications. The vetting process should cover regulatory clearances, software and hardware validation, technical and end-user support, interoperability, privacy and security issues. A curated marketplace should relieve the healthcare organization from the responsibility of the vetting process, saving time and money. This responsibility now lies with the platform provider.



ML42

Machine Learning Theater: AI-driven Mammography: Applying the Right Filter: Presented by Densitas, Inc.

Wednesday, Nov. 28 11:30AM - 11:50AM Room: Machine Learning Showcase North Hall

Participants

Ryan Duggan, Halifax, NS (*Presenter*) Nothing to Disclose Mohamed Abdolell, MSc, Halifax, NS (*Presenter*) Founder and CEO, Densitas Inc

PROGRAM INFORMATION

Densitas builds machine learning and AI solutions for breast screening that provide actionable information for radiologists and technologists to help improve existing workflows and quality, and lead to better care for patients.



ML43

Machine Learning Theater: From AI-powered Diagnostic Support Tools to Imaging Biomarkers: Aiming for Beyond Human-Level Accuracy: Presented by Lunit, Inc.

Wednesday, Nov. 28 12:00PM - 12:20PM Room: Machine Learning Showcase North Hall

Program Information

As stated in Lunit's company vision statement, 'Perfecting Intelligence. Transforming Medicine,' Lunit thrives to expand the boundaries of AI-driven capabilities for medical image analytics, specifically on chest, breast and cardiac imaging. Lunit's products that feature its state-of-the-art deep learning technology trained with large-scale high quality data will be introduced, inclduing results from its most recent clinical studies. Live demos for web-based Lunit INSIGHT will also be featured in the presentation.

Participants

Brandon Suh, CEO Lunit Inc; Seoul, Republic of Korea



AIS-WEA

Artificial Intelligence Wednesday Poster Discussions

Wednesday, Nov. 28 12:15PM - 12:45PM Room: AI Community, Learning Center

IN

Participants

Felipe C. Kitamura, MD, MSC, Sao Paulo, Brazil (Moderator) Developer, DASA

Sub-Events

AI146-ED-WEA1 (mD) Level by Means of 3D Deep Neural Network Convolution (NNC)

Station #1

Participants

Amin Zarshenas, MSc, Chicago, IL (Presenter) Nothing to Disclose

Yuji Zhao, MSc, Chicago, IL (Abstract Co-Author) Nothing to Disclose

Junchi Liu, MS, Chicago, IL (Abstract Co-Author) Nothing to Disclose

Toru Higaki, PhD, Hiroshima, Japan (Abstract Co-Author) Nothing to Disclose

Kazuo Awai, MD, Hiroshima, Japan (Abstract Co-Author) Research Grant, Canon Medical Systems Corporation; Research Grant,

Hitachi, Ltd; Research Grant, Fujitsu Limited; Research Grant, Bayer AG; Research Grant, DAIICHI SANKYO Group; Research Grant, Eisai Co, Ltd; Medical Advisory Board, General Electric Company; ;

Kenji Suzuki, PhD, Chicago, IL (*Abstract Co-Author*) Royalties, General Electric Company; Royalties, Hologic, Inc; Royalties, MEDIAN Technologies; Royalties, Riverain Technologies, LLC; Royalties, Canon Medical Systems Corporation; Royalties, Mitsubishi Corporation; Royalties, AlgoMedica, Inc

For information about this presentation, contact:

mzarshen@hawk.iit.edu

TEACHING POINTS

1) To understand the radiation dose issue with CT in lung cancer screening. 2) To learn the basic principles of NNC as a deep learning technique to reduce the radiation dose in chest CT. 3) To understand the performance and clinical utility of our radiation dose reduction technology for chest CT.

TABLE OF CONTENTS/OUTLINE

A. Radiation dose issue with CT in lung cancer screening B. Basic principles of NNC for converting micro-dose (mD) to higher-dose (HD) chest CT images to reduce radiation dose C. Radiation dose reduction, pre-clinical study: Anthropomorphic phantom image analysis D. Radiation dose reduction, clinical translation study: Clinical cases image analysis E. Quantitative evaluation: Image quality vs. radiation dose reduction F. Benefits and limitations of NNC for chest CT

AI013-EB A Deep Learning Approach for Identifying Imaging Biomarkers and Outcome Modeling in Chronic Obstructive Pulmonary Disease

All Day Room: AI Community, Learning Center

Participants

Tara A. Retson, MD, PhD, San Diego, CA (Presenter) Nothing to Disclose

Meet the Author: The authors of this poster will be available in person to discuss their project during these times: Wednesday November 28 12:15-12:45pm



LL31

Lunch and Learn: Breaking New Ground: Using AI at Scale Across a Global Imaging Network to Minimize Diagnostic Interpretation Risk: Presented by lifeIMAGE (invite-only)

Wednesday, Nov. 28 12:30PM - 1:30PM Room: S404AB

Participants

Donny Cheung, PhD, Senior Engineer, Google Cloud; Karim Galil, MD, Founder of Mendel.ai; Gabriel Brat, MD, Trauma Surgeon at Beth Israel Deaconess and Bioinformatics Professor at Harvard Medical School; Janak Joshi, CTO, Life Image; Ajay Kohli, MD, Radiology Resident Physician, AI Entrepreneur

Program Information

As healthcare shifts from volume to value, the need for analytics for medical imaging at scale has never been greater. Yet, the sheer velocity of data that's growing rapidly in silo'd environments presents an enormous challenge on data accuracy during the process of aggregating and normalizing information in a digestible way. Without this ability, interpreting providers, caregivers and patients cannot benefit from the advantages of artificial intelligence in improving evidence-based clinical decision making and reducing risk. lifeIMAGE and Google have been working closely to bring novel capabilities in the industry to service the discovery, interpretation and reproducibility of high quality comparative evidence for thousands of hospitals, whether in a care setting or academic research or in clinical R&D. During this lunch and learn session, a panel of clinical and technology experts will discuss and demonstrate the advancements that are shaping our industry through workflow integration to minimize risks for the patient and elevate the maturity of clinical decision making.



LL32

Lunch and Learn: How Artificial Intelligence is Changing Medical Imaging: Presented by Konica Minolta Healthcare (invite-only)

Wednesday, Nov. 28 12:30PM - 1:30PM Room: S403A

Program Information

In this educational session, participants will learn how advances in Artificial Intelligence and Deep Learning are fundamentally changing medical imaging to improve outcomes and increase productivity. Topics will include enhancing image quality at the point of capture, new tools to optimize workflow and clinical tools to improve detection and diagnosis.

RSVP Link

https://km-ai.cvent.com/c/express/b63aaab0-7cbd-4702-a500-1a2a6e07eaa3



LL33

Lunch and Learn: Thinking Faster, Safer, & Smarter: How You Can Use AI to improve MR and PET Imaging Efficiency, Patient Satisfaction, and Safety: Presented by Subtle Medical (invite-only)

Wednesday, Nov. 28 12:30PM - 1:30PM Room: S403B

Participants

Greg Zaharchuk, MD, PhD, Stanford, CA (*Presenter*) Research Grant, General Electric Company; Stockholder, Subtle Medical; Paul J. Chang, MD, Chicago, IL (*Presenter*) Co-founder, Koninklijke Philips NV; Researcher, Koninklijke Philips NV; Researcher, Bayer AG; Advisory Board, Bayer AG; Advisory Board, Aidoc Ltd; Advisory Board, EnvoyAI; Advisory Board, Inference Analytics Christopher P. Hess, MD, PhD, Mill Valley, CA (*Presenter*) Nothing to Disclose Michael N. Brant-Zawadzki, MD, Newport Beach, CA (*Presenter*) Nothing to Disclose

Program Information

With the AI technologies provided by Subtle Medical, medical imaging workflows will be significantly improved. Insights and feedback will be shared in this session by radiologists and executives from Stanford, UCSF, Hoag and University of Chicago hospitals on how they think about the impact of AI technologies.

RSVP

https://register.subtlemedical.com/rsna-lunch-and-learn?source=rsna-website



ML44

Machine Learning Theater: AI for Medical Image Diagnosis: Presented by LPixel, Inc.

Wednesday, Nov. 28 12:30PM - 12:50PM Room: Machine Learning Showcase North Hall

Participants

Yuki Shimahara, Bunkyo, Japan (*Presenter*) Nothing to Disclose Antoine Choppin, MS, Bunkyo-ku, Japan (*Presenter*) Nothing to Disclose

Program Information

LPixel is a spin-off venture from the University of Tokyo specializing in AI and life science image analysis. In this presentation, LPixel will introduce "EIRL," their latest medical diagnostic support technology designed to support radiologists enhance their diagnostic confidence. LPixel CEO, Yuki Shimahara, and Chief Engineer, Antoine Choppin will explain the progress of development from last year, and how this technology can help radiologists improve diagnostic accuracy and productivity in medical image reading. LPixel has implemented EIRL in the ongoing research and development of various areas of medical image diagnostics, such as brain MRI, chest CT and X-rays, breast MRI, endoscopy and pathology. EIRL's capabilities are further amplified with its ability to learn from a limited number of data with efficiency and accuracy, accommodate to images of varying quality, and integrate seamlessly with PACS.



RCC43

AI, Radiomics, Text Mining, and More: 2018's Key Advances in Imaging Informatics

Wednesday, Nov. 28 12:30PM - 2:00PM Room: S501ABC



AMA PRA Category 1 Credits ™: 1.50 ARRT Category A+ Credit: 1.75

Participants

Charles E. Kahn JR, MD, Philadelphia, PA (*Moderator*) Nothing to Disclose Charles E. Kahn JR, MD, Philadelphia, PA (*Presenter*) Nothing to Disclose William Hsu, PhD, Los Angeles, CA (*Presenter*) Research Grant, Siemens AG

For information about this presentation, contact:

ckahn@upenn.edu

LEARNING OBJECTIVES

1) Identify the year's most important advances in imaging informatics. 2) Describe the ways in which Artificial Intelligence (AI) and machine learning are impacting radiology. 3) Define how radiomics, radiogenomics, and 'big data' have added to our knowledge of radiology.

ABSTRACT

The field of imaging informatics continues to advance rapidly. Machine learning, a form of artificial intelligence (AI), has improved the ability to detect image features, make diagnoses, and assess prognosis from image data. Radiomics - which generates highdimensionality datasets from radiology images - provides insights to support precision medicine. Novel approaches have improved sharing of images and image-derived findings with patients and clinicians. Current research efforts go beyond pixel data to integrate imaging with other biomedical data, standardize imaging workflows, and improve the quality and utility of image-derived information in clinical practice. This session reviews key advances in imaging informatics research published this past year.

Honored Educators

Presenters or authors on this event have been recognized as RSNA Honored Educators for participating in multiple qualifying educational activities. Honored Educators are invested in furthering the profession of radiology by delivering high-quality educational content in their field of study. Learn how you can become an honored educator by visiting the website at: https://www.rsna.org/Honored-Educator-Award/ Charles E. Kahn JR, MD - 2012 Honored EducatorCharles E. Kahn JR, MD - 2018 Honored Educator



AIS-WEB

Artificial Intelligence Wednesday Poster Discussions

Wednesday, Nov. 28 12:45PM - 1:15PM Room: AI Community, Learning Center

IN

Participants

Felipe C. Kitamura, MD, MSC, Sao Paulo, Brazil (Moderator) Developer, DASA

Sub-Events

AI149-ED-WEB1 Quality Assurance for Crowdsource Annotation of the Chest X-ray 14 Dataset for the RSNA-STR Machine Learning Challenge: How We Did It

Station #1

Awards

Certificate of Merit

Participants

Carol C. Wu, MD, Bellaire, TX (*Presenter*) Author, Reed Elsevier Safwan Halabi, MD, Stanford, CA (*Abstract Co-Author*) Nothing to Disclose Luciano M. Prevedello, MD, MPH, Dublin, OH (*Abstract Co-Author*) Nothing to Disclose Marc D. Kohli, MD, San Francisco, CA (*Abstract Co-Author*) Nothing to Disclose Myrna C. Godoy, MD, PhD, Houston, TX (*Abstract Co-Author*) Research Grant, Siemens AG George L. Shih, MD, MS, New York, NY (*Abstract Co-Author*) Consultant, Image Safely, Inc; Stockholder, Image Safely, Inc; Consultant, MD.ai, Inc; Stockholder, MD.ai, Inc; Ritu R. Gill, MBBS, Boston, MA (*Abstract Co-Author*) Nothing to Disclose Anouk Stein, MD, Paradise Valley, AZ (*Abstract Co-Author*) Consultant, MD.ai, Inc; Stockholder, MD.ai, Inc

For information about this presentation, contact:

ccwu1@mdanderson.org

TEACHING POINTS

1. Review known inter-observer variabilities in the interpretation and annotation of chest radiographs and the implications for machine learning challenge 2. Describe the processes utilized to improve inter-observer consistency during crowdsource annotation 3. Provide lessons learned and methods to further refine quality assurance for crowdsouce annotation

TABLE OF CONTENTS/OUTLINE

A. Known inter-observer variability in: 1. clinical interpretation of chest radiograph due to lack of gold standard and variability of perception of overlapping findings 2. crowdsource annotations required for large dataset 3. general versus subspecialty chest radiologists B. Implications of 'noisy' annotation for machine learning C. Methods used to improve inter-observer consistency in annotation: 1. written instructions for annotation tasks 2. practice annotation dataset to detect possible sources of variabilities 3. group conference to formulate concensus for various scenarios D. Adjudication process 1. real-time feedback from subspecialty chest radiologist for difficult cases marked as 'Question' 2. adjudication by subspecialty radiologist of cases with discrepant labels/bounding boxes E. Lessons learned and potential refinements

AI011-EB Segmentation and Quantitative Assessment of Prognostic Features in Type B Aortic Dissection Using Machine Learning

All Day Room: AI Community, Learning Center

Participants

Lewis D. Hahn, MD, Stanford, CA (*Presenter*) Nothing to Disclose Gabriel Mistelbauer, Magdeburg, Germany (*Abstract Co-Author*) Nothing to Disclose Kai Higashigaito, MD, Stanford, CA (*Abstract Co-Author*) Nothing to Disclose Martin J. Willemink, MD,PhD, Menlo Park, CA (*Abstract Co-Author*) Speakers Bureau, Koninklijke Philips NV; Research Grant, Koninklijke Philips NV Anna M. Sailer, MD,PhD, West Hollywood, CA (*Abstract Co-Author*) Nothing to Disclose Michael Muelly, MD, Mountain View, CA (*Abstract Co-Author*) Employee, Google LLC; Partner, ClariPACS LLC Michael Fischbein, Stanford, CA (*Abstract Co-Author*) Nothing to Disclose Dominik Fleischmann, MD, Stanford, CA (*Abstract Co-Author*) Research Grant, Siemens AG Meet the Author: The authors of this poster will be available in person to discuss their project during these times: Wednesday November 28 12:45-1:15pm



ML46

Machine Learning Theater: AI Empowering Medical Data: Presented by Hangzhou YITU Healthcare Technology Co., Ltd

Wednesday, Nov. 28 1:30PM - 1:50PM Room: Machine Learning Showcase North Hall

Participants

Cathy Fang, PhD, MBA, Hangzhou, China (Presenter)

PROGRAM INFORMATION

Artificial Intelligence is considered to be the technology that will bring fundamental changes to the human world. Over the past few years, because of its world-leading technology and massive clinical data resources, China is leading the way by applying Ai technology to resolve actual healthcare pain points. YITU Healthcare, the leading AI healthcare company in China, is creating a new healthcare ecosystem with a full range of AI products and is helping humans to better understand and overcome diseases. Currently, YITU Healthcare has implemented its AI products in over 100 3A hospitals in China and covered multiple diseases such as lung cancer, breast cancer, leukemia, stroke, endocrine evaluation, etc. Those AI systems are widely used in clinical settings and the adoption rate for the AI-generated diagnosis reports by human doctors reaches over 92%. We are actively looking for strategic collaborations with healthcare players at both upstream and downstream of the value chain and advance AI development together and ultimately let the technology serve more patients world-wide.



RCA44

Advanced AI Tools for Radiologist-driven Mining of Imaging and Hospital-based Data Sets for Developing and Testing Hypothesis from Clinical Practice (Hands-on)

Wednesday, Nov. 28 2:30PM - 4:00PM Room: S401AB



AMA PRA Category 1 Credits ™: 1.50 ARRT Category A+ Credit: 0

FDA Discussions may include off-label uses.

Participants

Jaron Chong, MD, Montreal, QC (Moderator) Nothing to Disclose

Dimitris Mitsouras, PhD, Boston, MA (Moderator) Research Grant, Canon Medical Systems Corporation;

An Tang, MD, Montreal, QC (*Presenter*) Research Consultant, Imagia Cybernetics Inc; Speaker, Siemens AG; Speaker, Eli Lilly and Company

Leonid Chepelev, MD, PhD, Ottawa, ON (*Presenter*) Nothing to Disclose Adnan M. Sheikh, MD, Ottawa, ON (*Presenter*) Nothing to Disclose Betty Anne Schwarz, PhD, Ottawa, ON (*Presenter*) Nothing to Disclose

For information about this presentation, contact:

an.tang@umontreal.ca

dmitsouras@alum.mit.edu

LEARNING OBJECTIVES

1) Understand how to use NLP based tools in the clinical setting. 2) Interact with the AI to improve its training potential. 3) Assess those properties of data needed for optimized AI training. 4) Make conclusions regarding evidence for a biomarker in a particular data set.

ABSTRACT

This course fills a large unmet educational gap in hands-on learning using real clinical data set and active Deep Learning software. Hands-on actual clinical data will be accessed by clinical arenas that are well recognized by RSNA attendees and for which there is data and applications that will be available in a cloud-based format. The entirety of the program will run on RSNA computers already available for hands-on courses.



SSM02

Science Session with Keynote: Breast Imaging (Risk-Based Screening: Should We Do It?)

Wednesday, Nov. 28 3:00PM - 4:00PM Room: E350



AMA PRA Category 1 Credit ™: 1.00 ARRT Category A+ Credit: 1.00

Participants

Elizabeth A. Morris, MD, New York, NY (*Moderator*) Nothing to Disclose Daniel B. Kopans, MD, Waban, MA (*Moderator*) Royalties, Cook Group Incorporated; Research Consultant, Deep Health; Scientific Advisory Board, Dart, Inc

Sub-Events

SSM02-01 Breast Keynote Speaker: Risk Based Screening

Wednesday, Nov. 28 3:00PM - 3:10PM Room: E350

Participants Elizabeth A. Morris, MD, New York, NY (*Presenter*) Nothing to Disclose

SSM02-02 Risk-Based Screening Mammography for Women Age <40: Outcomes from the National Mammography Database

Wednesday, Nov. 28 3:10PM - 3:20PM Room: E350

Participants

Cindy S. Lee, MD, Garden City, NY (*Presenter*) Nothing to Disclose Heidi Ashih, PhD, Reston, VA (*Abstract Co-Author*) Nothing to Disclose Debapriya Sengupta, MBBS,MPH, Reston, VA (*Abstract Co-Author*) Nothing to Disclose Edward A. Sickles, MD, San Francisco, CA (*Abstract Co-Author*) Nothing to Disclose Margarita L. Zuley, MD, Pittsburgh, PA (*Abstract Co-Author*) Investigator, Hologic, Inc Etta D. Pisano, MD, Charleston, SC (*Abstract Co-Author*) Researcher, Freenome Holdings Inc; Researcher, Real Imaging Ltd; Researcher, Therapixel; Researcher, DeepHealth, Inc; Researcher, ToDos

For information about this presentation, contact:

Cindy.Lee3@nyumc.org

PURPOSE

There is insufficient large-scale evidence supporting screening mammography in women <40 years with risk factors. This study compares risk-based screening of women ages 30-39 versus women age 40-49 with no known risk factors, using screening mammography performance metrics from the National Mammography Database (NMD).

METHOD AND MATERIALS

This HIPAA compliant and IRB approved study analyzed data from 150 mammography facilities in 31 states in the NMD. The NMD collects clinical practice data including self-reported patient demographics, clinical findings, screening mammography interpretation and biopsy results. Patients were stratified by 5-year age intervals and specific risk factors for breast cancer: family history of breast cancer (any first degree relative regardless of age), personal history of breast cancer and breast density of heterogeneously or extremely dense (C or D). Prior mammography were identified by patient date of birth and facility-assigned identification number. Four performance metrics for screening mammography were calculated for each age and risk group: recall rate, cancer detection rate, and positive predictive values for biopsy recommended (PPV2) and biopsy performed (PPV3).

RESULTS

5,772,730 screening mammograms were performed between January 2008 and December 2015 in 2,647,315 women. Overall, mean cancer detection rate was 3.7 per 1000 (95% CI: 3.65-3.75), recall rate was 9.8% (9.8-9.8%), PPV2 was 20.1% (19.9-20.4%), and PPV3 was 28.2% (27.0-28.5%). Overall, women age 30-34 and 35-39 had similar cancer detection rates, recall rates and PPVs, with the presence of the three evaluated risk factors associated with significantly higher cancer detection rates. Moreover, compared to a population currently recommended for screening mammography in the USA (age 40-44 with no known risk factors), incidence screening (at least one prior screening examination) of women ages 30-39 with tthe three evaluated risk factors has similar cancer detection rates and recall rates.

CONCLUSION

Women ages 30-39 with 3 specific risk factors should benefit by starting screening at age 30 instead of the age 40 start recommended for average-risk women.

CLINICAL RELEVANCE/APPLICATION

Women

SSM02-03 A Deep-Learning Breast Cancer Risk Prediction Network: Trained on the Population-based Swedish CSAW Data

Wednesday, Nov. 28 3:20PM - 3:30PM Room: E350

Participants

Fredrik Strand, MD,PhD, Stockholm, Sweden (*Presenter*) Nothing to Disclose Yue Liu, Stockholm, Sweden (*Abstract Co-Author*) Nothing to Disclose Kevin Smith, Stockholm, Sweden (*Abstract Co-Author*) Nothing to Disclose Hossein Azizpour, Stockholm, Sweden (*Abstract Co-Author*) Nothing to Disclose Karin H. Dembrower, MD, Stockholm, Sweden (*Abstract Co-Author*) Nothing to Disclose Peter Lindholm, MD, PhD, Stockholm, Sweden (*Abstract Co-Author*) Nothing to Disclose

For information about this presentation, contact:

fredrik.strand@ki.se

PURPOSE

Almost half of breast cancer diagnoses among women attending mammographic screening are interval cancers or large screendetected cancers. To enable more effective individualized screening, accurate risk prediction is paramount. In this study, we examine how our trained deep learning network compares with mammographic density in risk prediction based on negative screening mammograms.

METHOD AND MATERIALS

The Swedish cohort of screen-age women (CSAW) contains over 500,000 women linked to the cancer registry and to an image database. Our deep learning network was trained on negative mammograms from incident cases from one uptake area 2008 to 2011. The test set consisted of cases from 2013 and 2014. In each set, we included a random sample of concurrent non-overlapping controls. The input was each negative mammogram downscaled as well as full-resolution central crops, age at mammography and selected DICOM parameters. The prediction output is called deep learning risk score (DLR). For comparison, mammographic density was calculated using the validated LIBRA software. Logistic regression models were fitted to examine odds ratios.

RESULTS

The training set consisted of 3167 negative mammograms from women with subsequent breast cancer and 125,683 mammograms from healthy women. The test set consisted of negative mammograms from 752 screening rounds of 326 women with subsequent breast cancer and 6728 rounds of 2065 healthy women. AUC was higher for DLR (0.63; 95%CI: 0.61 to 0.66) than for density (0.57; 95%CI: 0.54 to 0.60) and for age-adjusted density (0.58; 95%CI: 0.56 to 0.61). The proportion of cases were 10.1% in the top quintile and 2.5% in the bottom quintile of DLR. The top-to-bottom quintile odds ratio was 4.37 (95%CI: 3.01 to 6.45) and 1.69 (95%CI: 1.23 to 2.32) for DLR and age-adjusted density respectively.

CONCLUSION

We have demonstrated that it is possible to train a deep learning network on negative screening mammograms from subsequent breast cancer cases, and produce risk predictions with reasonable accuracy and ability to identify women at elevated risk.

CLINICAL RELEVANCE/APPLICATION

After external validation, our network may be used in individualizing breast cancer screening.

SSM02-04 Potential Role of Convolutional Neural Network based Algorithms in Patient Selection for DCIS Observation Trials

Wednesday, Nov. 28 3:30PM - 3:40PM Room: E350

Participants

Simukayi Mutasa, MD, New York, NY (*Presenter*) Nothing to Disclose Peter Chang, MD, San Francisco, CA (*Abstract Co-Author*) Nothing to Disclose Jenika Karcich, MD, New York, NY (*Abstract Co-Author*) Nothing to Disclose Eduardo Pascual Van Sant, BS, New York, NY (*Abstract Co-Author*) Nothing to Disclose Mary Q. Sun, MD, Manhasset, NY (*Abstract Co-Author*) Nothing to Disclose Michael Z. Liu, MS, New York, NY (*Abstract Co-Author*) Nothing to Disclose Sachin Jambawalikar, PhD, New York, NY (*Abstract Co-Author*) Nothing to Disclose Richard S. Ha, MD, New York, NY (*Abstract Co-Author*) Nothing to Disclose

For information about this presentation, contact:

s.mutasa@columbia.edu

PURPOSE

Minimizing over-diagnoses and treatment of Ductal Carcinoma in Situ (DCIS) has led to clinical trials of observing patients with DCIS instead of surgery. Despite careful selection for 'low risk' DCIS patients, there is evidence of occult invasive cancers in a significant number of these patients. We investigated the feasibility of utilizing convolutional neural networks (CNN) for predicting patients with pure DCIS versus DCIS with invasion using mammographic images.

METHOD AND MATERIALS

An IRB-approved retrospective study was performed. 246 unique images from 123 patients were used for our CNN algorithm. 164 images in 82 patients diagnosed with DCIS by stereotactic-guided biopsy of calcifications without any upgrade at the time of surgical excision (pure DCIS group). 82 images in 41 patients with mammographic calcifications yielding occult invasive carcinoma as the final upgraded diagnosis on surgery (occult invasive group). Two standard mammographic magnification views (CC and ML/LM) of the calcifications were used for analysis. Calcifications were segmented using an open source software platform 3D Slicer and resized to fit a 128x128 pixel bounding box. A 15 hidden layer topology based on residual convolutions was used to implement the

neural network. A class balanced holdout set with 40 patients was used for testing. 5-fold cross validation was utilized with cases randomly separated into a training set [80%] and validation set [20%].

RESULTS

The CNN algorithm for predicting patients with pure DCIS achieved an overall validation accuracy of 74.6% (95%CI, \pm 5) with area under the ROC curve of 0.71 (95% CI, \pm 0.04), specificity of 49.4% (95% CI, \pm 6%) and sensitivity of 91.6% (95% CI, \pm 5%).

CONCLUSION

It's feasible to apply a CNN to distinguish pure DCIS from DCIS with invasion using mammographic images. A larger dataset will likely improve our prediction model and could potentially be useful in appropriate patient selection for observation trials.

CLINICAL RELEVANCE/APPLICATION

Convolutional neural networks have demonstrated strong performance in various image classification tasks and may potentially be used in appropriate patient selection for DCIS observation trials.

SSM02-05 The Effect of Screening Modality and Race on BI-RADS Breast Density in a Large Urban Screening Cohort

Wednesday, Nov. 28 3:40PM - 3:50PM Room: E350

Participants

Aimilia Gastounioti, Philadelphia, PA (*Presenter*) Nothing to Disclose Anne Marie McCarthy, Boston, MA (*Abstract Co-Author*) Nothing to Disclose Lauren Pantalone, BS, Philadelphia, PA (*Abstract Co-Author*) Nothing to Disclose Marie Synnestvedt, Philadelphia, PA (*Abstract Co-Author*) Nothing to Disclose Despina Kontos, PhD, Philadelphia, PA (*Abstract Co-Author*) Nothing to Disclose Emily F. Conant, MD, Philadelphia, PA (*Abstract Co-Author*) Grant, Hologic, Inc; Consultant, Hologic, Inc; Grant, iCAD, Inc; Consultant, iCAD, Inc; Speaker, iiCME

For information about this presentation, contact:

aimilia.gastounioti@uphs.upenn.edu

PURPOSE

Increased breast density is an independent breast cancer risk factor and also limits the sensitivity and specificity of mammography. We investigated the effect of screening mammography modality and race on BI-RADS breast density assessments, accounting for age and body-mass index (BMI).

METHOD AND MATERIALS

We retrospectively analyzed data from 24,740 individual women (45% White, 55% Black) who underwent screening from September 2010 through February 2017 at our institution. 15,147 women (55%) had repeated screening studies (N = 60,774 studies). Over this time period, three screening modalities were used: digital mammography alone (DM; N = 8,936); digital breast tomosynthesis (DBT) with DM (DM/DBT, N = 30,786); and synthetic 2D with DBT (s2D/DBT, N = 21,052). BI-RADS density classifications ranging from lower (fatty or scattered) to higher (heterogeneous or extremely dense) density were extracted from screening reports. Random-effects ordered logistic regression (panel variable: individual woman) was performed to estimate the odds of being assigned to higher BI-RADS density by each modality, adjusted for race, age, BMI and radiologist. The interaction of modality and race on density was tested in the model, and analyses were stratified by race.

RESULTS

Women screened with DBT had significantly lower odds of high density compared to those screened with DM alone (DM/DBT vs. DM: OR = 0.62, p < .0001; s2D/DBT vs. DM: OR = 0.48, p < .0001). Lower odds of high density were also observed in s2D/DBT compared to DM/DBT (OR = 0.76, p < .0001). There was a significant interaction of modality and race on breast density (p = .0003). All differences by modality maintained statistical significance in analyses stratified by race, with lower ORs for black (DM/DBT vs. DM: OR = 0.61; s2D/DBT vs DM: OR = 0.40; s2D/DBT vs. DM/DBT: OR = 0.67) than for white women (DM/DBT vs. DM: OR = 0.65; s2D/DBT vs. DM: OR = 0.58; s2D/DBT vs. DM/DBT: OR = 0.89).

CONCLUSION

Screening mammography modality has a significant effect on BI-RADS density assessment with an overall trend of assigning lower density with DBT and s2D/DBT screening versus DM alone. Furthermore, this effect seems to be more prominent in black than in white women.

CLINICAL RELEVANCE/APPLICATION

Our findings have direct implications for personalized screening since breast density assignments, which often drive recommendations for supplemental screening, may vary greatly by modality and race.

SSM02-06 Breast Keynote Speaker: Risk Based Screening

Wednesday, Nov. 28 3:50PM - 4:00PM Room: E350

Participants

Daniel B. Kopans, MD, Waban, MA (*Presenter*) Royalties, Cook Group Incorporated; Research Consultant, Deep Health; Scientific Advisory Board, Dart, Inc



SSM03

Cardiac (Anatomy)

Wednesday, Nov. 28 3:00PM - 4:00PM Room: S102CD



AMA PRA Category 1 Credit ™: 1.00 ARRT Category A+ Credit: 1.00

Participants

Evan J. Zucker, MD, Stanford, CA (*Moderator*) Nothing to Disclose Karin E. Dill, MD, Worcester, MA (*Moderator*) Nothing to Disclose

Sub-Events

SSM03-01 The Automated Segmentation of the Left Ventricle Myocardium from Cardiac Computed Tomography using Deep Learning

Wednesday, Nov. 28 3:00PM - 3:10PM Room: S102CD

Participants

Hyun Jung Koo, MD, Seoul, Korea, Republic Of (*Presenter*) Nothing to Disclose Joon-Won Kang, MD, Seoul, Korea, Republic Of (*Abstract Co-Author*) Nothing to Disclose Ji-Yeon Ko, Seoul, Korea, Republic Of (*Abstract Co-Author*) Nothing to Disclose June-Goo Lee, PhD, Seoul, Korea, Republic Of (*Abstract Co-Author*) Nothing to Disclose Dong Hyun Yang, MD, Seoul, Korea, Republic Of (*Abstract Co-Author*) Nothing to Disclose

For information about this presentation, contact:

donghyun.yang@gmail.com

PURPOSE

Segmentation of the left ventricle myocardium of the heart is important to obtain information regarding myocardial wall thickening and functional analysis data. In this study, we performed deep learning analysis for the automated segmentation of the left ventricle of the heart in cardiac computed tomography (CT) data.

METHOD AND MATERIALS

To develop a fully automated deep learning algorithm using sementic segmentation methods based on fully convolution network, 50 subjects with coronary artery diseases were used as training set, and the approach is evaluated using a data set of 1000 subjects with coronary artery diseases present whole 3D volume images of the LV. Reference standard manual segmentation data generated by experienced cardiac radiologists. Cross validation was performed using randomly selected 5% cases from the training set. The comparison of quantitative measurement data between the manual and automatic segmentations was performed using dice similarity coefficient.

RESULTS

Overall, automated segmentation data were comparable to manual segmentation data. We obtained mean 88.3% (min 78.1% and max 96.5%) of dice similarity coefficient in whole LV myocardium. The sensitivity and specificity of automated segmentation in each segment (1-16 segments) were high (range: 85.5 - 99.9).

CONCLUSION

Using a large data set, we presented a deep learning based automatic segmentation of the left ventricle of the heart, and the results was comparable to manual segmentation data with high dice index.

CLINICAL RELEVANCE/APPLICATION

Automated LV segmentation can reduce time to obtain information regarding myocardial wall thickening and LV function, and might improve the reproducibility of clinical assessment.

SSM03-02 Microcirculation Dysfunction in Patients with End-Stage Renal Disease Undergoing Dialysis: Associated with Heart Failure in the Follow-Up

Wednesday, Nov. 28 3:10PM - 3:20PM Room: S102CD

Participants

Ying-Kun Guo, MD, Chengdu, China (*Presenter*) Nothing to Disclose Rong Xu, Chengdu, China (*Abstract Co-Author*) Nothing to Disclose Huayan Xu, Chengdu, China (*Abstract Co-Author*) Nothing to Disclose Zhigang Yang, MD, Chengdu, China (*Abstract Co-Author*) Nothing to Disclose

For information about this presentation, contact:

Xrongdoctor@163.com

PURPOSE

The dialysis treatment was used widely in the ESRD patients, but myocardial ischemia and the cardiovascular disease were the major cause of death in chronic kidney disease (CKD) patients. Our study aimed to quantitative evaluation of myocardial microcirculation dysfunction by rest CMR perfusion imaging in patients with ESRD undergoing dialysis, and to understand of the association between perfusion parameters and heart failure.

METHOD AND MATERIALS

In total, 67 ESRD patients with preserved EF (EF>=50%) and 22 healthy subjects underwent rest first-pass perfusion. The LV regional myocardial perfusion parameters were analyzed by a commercial soft included upslope, time to maximum signal intensity (TTM) and max signal intensity (Max SI). Continuous variables were compared using one-way analysis of variance (ANOVA). The association between perfusion parameters and the composite of CHF was assessed by Cox proportional hazards regression.

RESULTS

For the analysis, the Max SI of basal, mid- and apical segments were reduced in ESRD patients with preserved EF compared with normal controls (all P < 0.05). In contrast to the patients with preserved EF, the patients with impaired EF had lower upslope and longer TTM in the basal segment. Over a mean follow-up period of 12.5 months, 24 subjects developed heart failure. The TTM of Basal-, mid-, and apical- segments were inversely associated with risk of heart failure (per unit increment, HR:1.052, 95% CI: 1.010-1.095, HR:1.086, 95% CI: 1.033-1.143, and HR:1.084, 95% CI: 1.024-1.146, respectively) after multivariable adjustment by gender, age, BMI, dialysis time, hypertension, and diabetes.

CONCLUSION

In summary, the first-pass perfusion CMR parameters can early detect the regional myocardial microcirculation dysfunction in ESRD patients undergoing dialysis. The myocardial dysfunction can predictor the progression of heart failure.

CLINICAL RELEVANCE/APPLICATION

(dealing with first-pass perfusion CMR)CMR perfusion imaging with vasodilator can detect myocardial microcirculation dysfunction in ESRD patients undergoing dialysis.

SSM03-03 Differences in Cardiac MR-based Assessment of Myocardial 2D Strain between Subjects with Prediabetes, Diabetes, and Normal Controls in the General Population

Wednesday, Nov. 28 3:20PM - 3:30PM Room: S102CD

Participants

Tanja Zitzelsberger, MD, Tuebingen, Germany (*Presenter*) Nothing to Disclose Astrid Scholz, Tuebingen, Germany (*Abstract Co-Author*) Nothing to Disclose Susanne Rospleszcz, Munich, Germany (*Abstract Co-Author*) Nothing to Disclose Roberto Lorbeer, Greifswald, Germany (*Abstract Co-Author*) Nothing to Disclose Konstantin Nikolaou, MD, Tuebingen, Germany (*Abstract Co-Author*) Advisory Panel, Siemens AG; Speakers Bureau, Siemens AG; Speaker Bureau, Bayer AG Maximilian F. Reiser, MD, Munich, Germany (*Abstract Co-Author*) Nothing to Disclose Fabian Bamberg, MD, Tuebingen, Germany (*Abstract Co-Author*) Speakers Bureau, Bayer AG; Speakers Bureau, Siemens AG; Research Grant, Siemens AG

Christopher L. Schlett, MD, MPH, Heidelberg, Germany (Abstract Co-Author) Nothing to Disclose

PURPOSE

In the setting of diabetes mellitus, diabetic cardiomyopathy is associated with limited event-free survival but difficult to detect. However, cardiac MR based assessment of subtle alterations of left ventricular function using 2D cardiac strain analysis may represent an early marker of disease development. Thus, we determined differences in left ventricular strain between subjects with prediabetes, diabetes, and healthy controls in a sample from the general population.

METHOD AND MATERIALS

Subjects without prior history of stroke, coronary or peripheral artery disease were enrolled in a case-controlled study and underwent 3T whole body MRI. In all patients without history of hypertension, LGE and normal ejection fraction, radial, longitudinal and circumferential strain was measured on Cine SSFP imaging (TR: 29.97ms, TE: 1.46ms, ST: 8mm) using a semiautomatic segmentation algorithm (CVI42, Circle, Canada). Differences in strain rates were derived in multivariate linear regression analysis adjusting for age, gender, BMI, blood pressure, and smoking, HDL, LDL and TG.

RESULTS

Radial and circumferential strain analysis was performed in in total 347 subjects, of which 41 (11.8%) suffered from diabetes, 92 (26.5%) from pre-diabetes and 214 (61.7%) controls. Mean HbA1c of diabetic subjects was 6.5 ± 1 mmol/mol Hb. Pre-diabetic subjects showed a significantly higher systolic global and endocardial radial strain compared to controls (p=0.036 and p=0.011 respectively), whereas diabetic subjects didn't show any significant difference (p=1.00 and p=0.811). Similarly we detected significant lower systolic global and endocardial strain values in pre-diabetic subjects (p=0.044 and p=0.009), whereas diabetic subjects didn't show a significant difference (p=1.00 and p=0.580). Regarding diastolic radial and circumferential strain we didn't find any significant difference.

CONCLUSION

In our cohort of well-treated diabetic subjects we didn't find any changes in strain values whereas pre-diabetic subjects showed early changes. Therefore early and consequent treatment of diabetes seems to be cardioprotective.

CLINICAL RELEVANCE/APPLICATION

MR based Strain Imaging is able to detect early changes in cardic function in patients with prediabetes. As these changes are not seen in well treated diabetic patients consideration should be given to early antidiabetic therapy.

SSM03-04 Left Atrial Functional Impairment in Patients with Stroke: A Cardiovascular Magnetic Resonance

Study

Wednesday, Nov. 28 3:30PM - 3:40PM Room: S102CD

Participants

Wieland Staab, MD, Goettingen, Germany (*Presenter*) Nothing to Disclose Laura Wandelt, Goettingen, Germany (*Abstract Co-Author*) Nothing to Disclose Andreas Schuster, Goettingen, Germany (*Abstract Co-Author*) Nothing to Disclose Rolf Wachter, Goettingen, Germany (*Abstract Co-Author*) Nothing to Disclose Michael Steinmetz, Goettingen, Germany (*Abstract Co-Author*) Nothing to Disclose Christina Unterberg-Buchwald, Goettingen, Germany (*Abstract Co-Author*) Nothing to Disclose Joachim Lotz, MD, Gottingen, Germany (*Abstract Co-Author*) Nothing to Disclose Johannes T. Kowallick, Gottingen, Germany (*Abstract Co-Author*) Nothing to Disclose

For information about this presentation, contact:

wieland.staab@med.uni-goettingen.de

PURPOSE

In 25 % of patients with ischemic stroke, no etiologic factor can be identified. Asymptomatic paroxysmal atrial fibrillation (AF) is often suspected to be the cause of these cryptogenic strokes (CS). AF is frequently associated with left atrial (LA) structural and functional alterations. Accordingly, the aim of this study was to examine LA deformation in patients with CS using cardiovascular magnetic resonance myocardial feature tracking (CMR-FT).

METHOD AND MATERIALS

29 patients with the diagnosis of CS underwent CMR imaging. Based on the initial cranial computed tomography (cCT), the patient group was divided into patients with previous ischemic lesions (recurrent CS) and patients without (first-time CS). LA deformation was analyzed based on CMR-FT of standard cine 4- and 2-chamber views including LA reservoir function (peak total strain [s], peak positive SR [SRs]), LA conduit function (passive strain [e], peak early negative SR [SRe]) and LA booster pump function (active strain [a], late peak negative SR [SRa]). Moreover, the "time to s" and "time to SRs" were calculated and expressed as a percentage of the entire cardiac cycle.

RESULTS

Previous ischemic lesions were detected in 5 of 29 patients (17%). LA conduit strain was lower in patients with recurrent CS as compared to first-time CS (6.4 ± 1.1 % vs. 10.3 ± 3.3 %, respectively, p=0.005). Furthermore, "time to s" and "time to SRs" were prolonged in patients with recurrent CS (47 ± 6 % vs. 57 ± 8 %, p=0.007; and 19 ± 5 % vs. 30 ± 7 %, p=0.001, respectively). In multivariable regression models "time to s" and "time to SR" were independently associated with the presence of previous ischemic lesions (β =0.41, p=0.006 and β =0.51, p=0.015, respectively) after adjustment for traditional risk factors (age, gender, arterial hypertension, vascular disease and diabetes).

CONCLUSION

Prolonged time to peak LA reservoir strain and SR is associated with the presence of previous ischemic lesions in patients with CS. These findings propose advanced LA impairment as a distinct feature of CS which may be associated with unrecognized paroxysmal AF. Future research is warranted to confirm these findings alongside their prognostic implications in larger prospective clinical trials.

CLINICAL RELEVANCE/APPLICATION

Advanced LA impairment detected by cardiac magnetic resonance imaging may improve management of patients with or prior to CS.

SSM03-05 Machine Learning for Automated Image Quality Control and Segmentation of Large-Scale CMR Population Studies

Wednesday, Nov. 28 3:40PM - 3:50PM Room: S102CD

Participants

Wenjia Bai, DPhil, London, United Kingdom (*Abstract Co-Author*) Nothing to Disclose Giacomo Tarroni, London, United Kingdom (*Abstract Co-Author*) Nothing to Disclose Hideaki Suzuki, London, United Kingdom (*Abstract Co-Author*) Nothing to Disclose Ozan Oktay, PhD, London, United Kingdom (*Abstract Co-Author*) Nothing to Disclose Jo Schlemper, London, United Kingdom (*Abstract Co-Author*) Nothing to Disclose Paul M. Matthew, MD,DPhil, London, United Kingdom (*Abstract Co-Author*) Nothing to Disclose Daniel Rueckert, PhD, London, United Kingdom (*Presenter*) Nothing to Disclose

PURPOSE

UK Biobank is a large-scale prospective cohort study that follows the health of 500,000 subjects across the UK. Of all the subjects, 100,000 will undergo imaging scans including brain, heart and body scans. We propose a machine learning-based and automated pipeline for cardiac MR (CMR) image quality control and segmentation on this large-scale dataset.

METHOD AND MATERIALS

CMR images were obtained from the UK Biobank under Application Number *****. Short-axis and long-axis cine images were acquired using a Siemens 1.5T scanner with the balanced steady state free precession (bSSFP) sequence. For image quality control, hybrid random forests were trained to detect landmarks on long-axis images, specifically the apex and mitral valve, which were then compared to the space encompassed by short-axis image stacks for identifying incomplete heart coverage. For image segmentation, fully convolutional networks were trained to segment the left ventricle (LV) and right ventricle (RV) on short-axis images and the left atrium (LA) and right atrium (RA) on long-axis images. The segmentation accuracy was evaluated using the Dice metric and mean contour distance error.

RESULTS

The pipeline took ~1 second for image quality control and ~10 seconds for short-axis and long-axis image segmentation. Cases

with heart coverage deemed incomplete by visual examination were automatically identified with 88% sensitivity and 99% specificity on a random test set of 3,000 subjects. Regarding segmentation accuracy, the average Dice metric is 0.94 for LV cavity, 0.88 for LV myocardium, 0.90 for RV cavity, 0.93 for LA cavity (2-chamber view), 0.95 for LA cavity (4-chamber view) and 0.96 for RA cavity (4-chamber view), evaluated on a test set of 600 subjects. The average mean contour distance error is smaller than the in-plane pixel resolution of 1.8mm.

CONCLUSION

We have proposed a machine learning-based pipeline for CMR image quality control and segmentation, which is automated, fast and accurate.

CLINICAL RELEVANCE/APPLICATION

The pipeline will facilitate the analysis of large-scale CMR population studies such as the UK Biobank and enable automated extraction of clinically relevant phenotypes including the ventricular volumes and mass. Future work could evaluate its potential to add quantitative image-derived phenotypes as part of routine clinical practice.

SSM03-06 Cardiac Adaptation of Left Ventricular Volume and Mass during a Multistage Marathon Over 4486 Km

Wednesday, Nov. 28 3:50PM - 4:00PM Room: S102CD

Participants

Christopher Klenk, MD, Basel, Switzerland (*Presenter*) Nothing to Disclose Florian Sagmeister, MD, Ulm, Germany (*Abstract Co-Author*) Nothing to Disclose Thomas Nickel, Munich, Germany (*Abstract Co-Author*) Nothing to Disclose Meinrad J. Beer, MD, Ulm, Germany (*Abstract Co-Author*) Nothing to Disclose Arno Schmidt-Trucksass, Basel, Switzerland (*Abstract Co-Author*) Nothing to Disclose Uwe H. Schuetz, MD, Ulm, Germany (*Abstract Co-Author*) Nothing to Disclose

For information about this presentation, contact:

florian.sagmeister@uniklinik-ulm.de

PURPOSE

Long-term side effects of intense physical training and long-distance running has led to increasing concerns especially among athletes. However, the consequences on long-term endurance training on cardiac structure and function are not yet fully understood. The purpose of this study was to evaluate the effect of running a transcontinental, multistage ultramarathon of 4486km on 64 consecutive days on the heart.

METHOD AND MATERIALS

20 ultra-endurance athletes with a mean (standard deviation) age of 47.9 (10.4) years received a cardio MRI-scan at three time points (baseline, at ~2000km, ~3500km) during the multistage ultramarathon. Cardiovascular magnetic resonance (CMR) was performed on a portable 1.5 Tesla MRI unit (Magnetom Avanto[™] mobile MRI) which was installed on a specially hired truck. Left ventricular mass (LVM), end-diastolic volume (EDV), end-systolic volume (ESV) and myocardial strain was calculated from SSFP-cine gradient echo sequences using the commercially available software (Heart Deformation Analysis, HDA, Siemens, Erlangen, Germany). Cardiac MRI-parameters were indexed for body surface area (BSA). Ten runners were serially examined in follow-up scans eight months after the race.

RESULTS

Athletes ran at a mean running speed of 8.2 ± 1.2 km/h during the ultramarathon. Left ventricular mass increased significantly (p<0.001) over the course of the race while no significant changes were observed in end-diastolic volume, end-systolic volume as well as global radial, circumferential and longitudinal left ventricular strain. Results of follow-up scans showed a significant reduction in LVMi (p=0.004), left ventricular EDVi (p=0.015) and right ventricular EDVi (p=0.045). We did not observe any significant differences regarding myocardial strain during follow-up.

CONCLUSION

The observed structural cardiac alterations during a multistage ultra-endurance marathon indicates a physiological response to excessive cardiac volume load. The reduction in end-diastolic volumes during follow-up corresponds to the reduced endurance exercise volume within eight months after the multistage ultramarathon.

CLINICAL RELEVANCE/APPLICATION

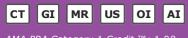
Extreme long-distance running leads to physiological cardiac adaptations without any detectable adverse cardiovascular remodeling in non-contrast enhanced cardiovascular magnetic resonance imaging.



SSM09

Gastrointestinal (Gallbladder and Bile Ducts)

Wednesday, Nov. 28 3:00PM - 4:00PM Room: S503AB



AMA PRA Category 1 Credit ™: 1.00 ARRT Category A+ Credit: 1.00

Participants

Alice W. Fung, MD, Portland, OR (*Moderator*) Nothing to Disclose Benjamin Wildman-Tobriner, MD, Durham, NC (*Moderator*) Nothing to Disclose

Sub-Events

SSM09-01 Apparent Diffusion Coefficient as a Potential Marker for Tumor Differentiation, Staging, and Long-Term Clinical Outcomes in Gallbladder Cancer

Wednesday, Nov. 28 3:00PM - 3:10PM Room: S503AB

Participants

Ji Hye Min, MD, PhD, Daejeon, Korea, Republic Of (*Presenter*) Nothing to Disclose Tae Wook Kang, MD, Seoul, Korea, Republic Of (*Abstract Co-Author*) Nothing to Disclose Seo-Youn Choi, MD, Bucheon, Korea, Republic Of (*Abstract Co-Author*) Nothing to Disclose Jeong Eun Lee, Daejeon, Korea, Republic Of (*Abstract Co-Author*) Nothing to Disclose Kyung-Sook Shin, MD, Taejon, Korea, Republic Of (*Abstract Co-Author*) Nothing to Disclose

For information about this presentation, contact:

minjh1123@gmail.com

PURPOSE

To evaluate the correlation between tumor differentiation or stage of gallbladder cancer (GBC) and the apparent diffusion coefficient (ADC), as well as to assess whether ADC value can predict long-term disease-free survival (DFS) after surgery.

METHOD AND MATERIALS

This retrospective study was approved by the Institutional Review Board and the requirement for informed consent was waived. Between March 2008 and June 2016, 79 patients who underwent magnetic resonance (MR) imaging with diffusion-weighted image and subsequent surgery for GBC were included in this study. Correlations between quantitative ADC values, and tumor differentiation or stage based on the American Joint Committee on Cancer (AJCC) were assessed using Spearman's correlation analysis. Prognostic factors for DFS were identified with multivariate Cox regression analysis using imaging and clinical characteristics.

RESULTS

All patients were classified as having well- (n = 18), moderately- (n = 35), or poorly-differentiated GBCs (n = 26). The ADC value of GBCs was significantly correlated with tumor differentiation and AJCC stage (p < 0.001 and p < 0.001, respectively). Sixty nine patients were followed up for 2.0-92.4 months (median, 23.5 months). On multivariate analysis, the significant prognostic factor for DFS was not tumor differentiation or AJCC stage, but a binary tumor ADC value (hazard ratio, 4.29, p = 0.009).

CONCLUSION

The ADC value of GBCs was significantly correlated with tumor differentiation as well as AJCC stage. In addition, it predicted long-term outcomes after surgery in patients with GBC.

CLINICAL RELEVANCE/APPLICATION

Tumor recurrence after curative surgical resection in patients with GBC could be predicted by using ADC values on diffusionweighted images preoperatively.

SSM09-02 Is the MR Contrast Agent Gadoxetate Disodium Suitable for CT Cholangiography?

Wednesday, Nov. 28 3:10PM - 3:20PM Room: S503AB

Participants

Samantha Dilger, PhD, Rochester, MN (*Presenter*) Nothing to Disclose Noelle Nelson, Rochester, MN (*Abstract Co-Author*) Nothing to Disclose Lifeng Yu, PhD, Chicago, IL (*Abstract Co-Author*) Nothing to Disclose Thomas J. Vrieze, RT, Rochester, MN (*Abstract Co-Author*) Nothing to Disclose Tammy A. Drees, Rochester, MN (*Abstract Co-Author*) Nothing to Disclose Sudhakar K. Venkatesh, MD, FRCR, Rochester, MN (*Abstract Co-Author*) Nothing to Disclose Jeff L. Fidler, MD, Rochester, MN (*Abstract Co-Author*) Nothing to Disclose Joel G. Fletcher, MD, Rochester, MN (*Abstract Co-Author*) Grant, Siemens AG; Consultant, Medtronic plc; ; Cynthia H. McCollough, PhD, Rochester, MN (*Abstract Co-Author*) Research Grant, Siemens AG

For information about this presentation, contact:

yu.lifeng@mayo.edu

PURPOSE

Gadoxetate disodium (Eovist®), a Gadolinium-based contrast agent, is primarily used in MR, with an FDA approved dose limit of 0.1 mL/kg. The purpose of this work is to determine whether low doses of gadoxetate disodium can be visualized for CT cholangiography using a phantom setup.

METHOD AND MATERIALS

Vials containing four concentrations of gadoxetate disodium (9.6, 4.8, 3.4, and 1.9mgGd/ml) were placed in a 35x26cm2 water phantom and imaged on two CT scanners: Siemens Somatom Flash and Force (Siemens Healthcare, Erlangen, Germany). These concentrations correspond to the dose limit for a 200, 100, 70, 40kg patient, respectively. Single-energy (SE) scans were acquired at 70, 80, 90, 100, 120, and 140kVp. Dual-energy (DE) scans were acquired at 90/150Sn (Force) and 100/150 (Flash) for two dose levels (13 and 23 mGy). Virtual monoenergetic images at 50keV were created (Mono+, Siemens). The mean intensity and standard deviation for each concentration of gadoxetate disodium and the water background were extracted from each image set. To determine whether the signal provided by gadoxetate disodium was sufficient for clinical imaging, the contrast, noise, and contrast-to-noise ratio (CNR) were compared to measurements acquired from 12 clinical CT cholangiography exams performed with iodine-containing iodipamide meglumine.

RESULTS

From the retrospective clinical cohort, mean contrast (± standard deviation) of 239±107HU and CNR of 12.8±4.2 were found in the bile duct relative to the liver. Comparing these metrics to the gadoxetate disodium samples, the highest concentration (9.6mgGd/ml) surpassed these thresholds at all energy levels. The 4.8mgGd/ml had sufficient CNR in the Force, but not in the Flash. The 3.4mgGd/ml had clinically relevant CNR at low kV of SE (<100kVp) and 50 keV of DE in the Force but was insufficient in the Flash. Images acquired by the Force had a lower noise level and greater CNR compared to the Flash. Similar trends were seen at both dose levels.

CONCLUSION

Gadoxetate disodium shows promise as a viable contrast agent for CT cholangiography, with CNR similar to those seen clinically with an iodine-based contrast agent. DE CT or low kV SE CT is helpful to enhance the signal.

CLINICAL RELEVANCE/APPLICATION

Gadoxetate disodium, a Gadolinium-based hepatobiliary contrast agent, shows promise as a CT cholangiography contrast agent with contrast-to-noise ratios similar to iodine contrast-enhanced CT.

Honored Educators

Presenters or authors on this event have been recognized as RSNA Honored Educators for participating in multiple qualifying educational activities. Honored Educators are invested in furthering the profession of radiology by delivering high-quality educational content in their field of study. Learn how you can become an honored educator by visiting the website at: https://www.rsna.org/Honored-Educator-Award/ Sudhakar K. Venkatesh, MD, FRCR - 2017 Honored Educator

SSM09-03 CT and Ultrasound for the Diagnosis of Cholecystitis in the Adult Emergency Department: A Comparison of Accuracy and Incremental Value Offered By Each Modality Over the Other

Wednesday, Nov. 28 3:20PM - 3:30PM Room: S503AB

Awards

Student Travel Stipend Award

Participants Kevin D. Hiatt, MD, Winston-Salem, NC (*Presenter*) Nothing to Disclose Jao J. Ou, MD,PhD, Winston-Salem, NC (*Abstract Co-Author*) Nothing to Disclose James Lovato, Winston-Salem, NC (*Abstract Co-Author*) Nothing to Disclose David D. Childs, MD, Clemmons, NC (*Abstract Co-Author*) Nothing to Disclose

PURPOSE

To compare the diagnostic accuracy and relative value of CT and ultrasound (US) in the workup of cholecystitis in adult emergency department (ED) patients.

METHOD AND MATERIALS

A retrospective chart review conducted over a 5 year period identified adult ED encounters for right upper quadrant pain where patients were evaluated with CT and/or US. Those with prior cholecystectomy, current pregnancy, and acute trauma were excluded. Imaging studies were assessed for the reported presence of gallstones, gallbladder distension, wall thickening, and pericholecystic fluid/inflammation. A positive suspicion for cholecystitis required at least two findings, or a positive sonographic Murphy's sign with at least one additional finding. Sensitivity, specificity, positive predictive value (PPV), and negative predictive value (NPV) were calculated for each modality based on linked clinical, surgical, and pathology data. When both US and CT were performed, the second modality was determined to add value if it correctly identified cholecystitis when the first study was incorrect or provided a non-gallbladder alternative diagnosis for acute abdominal pain. The second study was determined to detract value if it was incorrectly positive or negative for cholecystitis when the first study was correct.

RESULTS

3495 ED encounters were reviewed, with 2859 meeting inclusion criteria. 91% of patients had one or more imaging studies performed, with US performed in 81%, CT performed in 30%, and both US and CT performed in 20%. 559 patients went on to cholecystectomy with pathology results available for 540. For US and CT, respectively: sensitivity 48% and 53%, specificity 93% and 93%, PPV 65% and 58%, and NPV 88% and 92%. Only NPV represented a statistically significant difference. When performed after CT, US added value in 8% and detracted value in 6% of cases. When performed after US, CT added value in 35% and detracted value in 2% of cases.

CONCLUSION

In this patient cohort, imaging diagnosis of cholecystitis by CT was non-inferior to the more commonly utilized gold standard of US. There was also little added value for use of US after already obtaining a CT.

CLINICAL RELEVANCE/APPLICATION

CT performance in the diagnosis of cholecystitis is essentially equivalent to ultrasound and has an advantage in supplying additional information for adult ED patients presenting with right upper quadrant pain.

SSM09-04 Development and Validation of Deep Learning Based Clinical Decision Supporting System for the Diagnosis of Neoplastic Gallbladder Polyps Using High Resolution Ultrasonography: Preliminary Results

Wednesday, Nov. 28 3:30PM - 3:40PM Room: S503AB

Awards

Student Travel Stipend Award

Participants

Younbeom Jeong, MD, Seoul, Korea, Republic Of (*Presenter*) Nothing to Disclose Jung Hoon Kim, MD, Seoul, Korea, Republic Of (*Abstract Co-Author*) Nothing to Disclose Hee-Dong Chae, MD, Seoul, Korea, Republic Of (*Abstract Co-Author*) Nothing to Disclose Ijin Joo, MD, Seoul, Korea, Republic Of (*Abstract Co-Author*) Nothing to Disclose Jae Seok Bae, MD, Seoul, Korea, Republic Of (*Abstract Co-Author*) Nothing to Disclose Joon Koo Han, MD, Seoul, Korea, Republic Of (*Abstract Co-Author*) Nothing to Disclose

For information about this presentation, contact:

jhkim2008@gmail.com

PURPOSE

To investigate the added value of the deep learning based clinical decision supporting system for the differential diagnosis of neoplastic gallbladder (GB) polyps using high resolution ultrasonography (HRUS)

METHOD AND MATERIALS

We retrospectively collected 337 patients with GB polyps (>4 mm) proved by cholecystectomy. They were divided into training set (239 patients) and test set (98 patients) according to the time period. Based on pathology, all images of polyps (neoplastic: 1822 images in 137 patients, non-neoplastic: 2058 images in 200 patients) were manually cropped into a square box containing the polyp and labeled as either neoplastic or non-neoplastic. The binary classification convolutional neural network model was constructed by transfer learning based on Inception-v3 architecture. Using test set, two radiologists with different experience level, retrospectively graded the possibility of neoplastic polyp using a 5-point confident scale. After providing model's probability value on the test set for each patient, reviewers requested to re-evaluate the grade. Diagnostic performances were measured by ROC analysis and sensitivity, specificity, and accuracy were calculated.

RESULTS

For the diagnosis of neoplastic polyp, model itself provided AUC 0.920, sensitivity 82.1%, specificity 88.1%, accuracy 85.4% with optimal cut off >0.503 in training set and AUC 0.903, sensitivity 80.5%, specificity 85.3%, accuracy 82.8% with optimal cut off >0.726 in test set. On the first review, highly and less experienced reviewers showed AUC 0.944 and 0.775; sensitivity 88.6% and 71.4%; specificity 85.7% and 68.2%; accuracy 86.7% and 69.4%, respectively. On the second review with the supporting system, less experienced reviewer's AUC was improved from 0.775 to 0.859 (p=0.0513), whereas, highly experienced reviewer's AUC showed no significant change (0.944 to 0.940).

CONCLUSION

Our preliminary results suggest that deep learning based clinical decision supporting system for differential diagnosis of neoplastic GB polyp is helpful for improving diagnostic performance, especially in less experienced readers.

CLINICAL RELEVANCE/APPLICATION

Differential diagnosis of neoplastic GB polyp is important as it has a malignant potential. Our decision supporting system can improve the diagnostic performance of radiologists using HRUS.

SSM09-05 Differentiation Between Gallbladder Premalignant or Malignant Polyps and Cholesterol Polyps Using Contrast-Enhanced Ultrasound: Preliminary Study

Wednesday, Nov. 28 3:40PM - 3:50PM Room: S503AB

Participants

Jae Seok Bae, MD, Seoul, Korea, Republic Of (*Presenter*) Nothing to Disclose Se Hyung Kim, MD, Seoul, Korea, Republic Of (*Abstract Co-Author*) Nothing to Disclose Hyo-Jin Kang, MD, Seoul, Korea, Republic Of (*Abstract Co-Author*) Nothing to Disclose Ji Kon Ryu, Seoul, Korea, Republic Of (*Abstract Co-Author*) Nothing to Disclose Jin-Young Jang, Seoul, Korea, Republic Of (*Abstract Co-Author*) Nothing to Disclose Sang Hyub Lee, Seoul, Korea, Republic Of (*Abstract Co-Author*) Nothing to Disclose Woo Hyun Paik, Seoul, Korea, Republic Of (*Abstract Co-Author*) Nothing to Disclose Wooil Kwon, Seoul, Korea, Republic Of (*Abstract Co-Author*) Nothing to Disclose Jae Young Lee, MD,PhD, Seoul, Korea, Republic Of (*Abstract Co-Author*) Nothing to Disclose Joon Koo Han, MD, Seoul, Korea, Republic Of (*Abstract Co-Author*) Nothing to Disclose

PURPOSE

To differentiate between gallbladder (GB) premalignant or malignant polyps and cholesterol polyps using contrast-enhanced

ultrasound (CEUS).

METHOD AND MATERIALS

From September 2017 to March 2018, 20 patients with large GB polyps (>= 1 cm) who were scheduled to undergo cholecystectomy were prospectively enrolled. All patients underwent conventional US including color Doppler and CEUS prior to surgery. CEUS was performed using a LOGIQ E9 US scanner (GE Healthcare) after an injection of 2.5 ml of SonoVue® for 1 minute. After CEUS, perfusion US parameters including peak enhancement, mean transit time, fall time (FT), wash-in rate (WiR), and wash-out rate (WoR) were obtained using VueBox® software. Patients were separately classified into the cholesterol polyp group (n = 6) and premalignant or malignant polyp group (n = 14) according to the final histopathology. All US features and quantitative CEUS parameters between the two groups were compared using the Mann-Whitney U test. Diagnostic performances of the parameters were assessed using receiver operating characteristic (ROC) analysis.

RESULTS

Among US imaging features, there were significant differences in lesion size (2.20 cm for adenomatous polyps and 1.18 cm for cholesterol polyps) and internal homogeneity between the two groups (P<0.05); internal homogeneity was more commonly found in cholesterol polyps (5/6, 83%) than in malignant polyps (4/14, 28%). On quantitative analysis of CEUS parameters, FT and WoR demonstrated significant differences between the two groups (P<0.05), i.e., premalignant or malignant polyps showed significantly longer FT (12.74 sec) and smaller WoR (183.3 arbitrary units [a.u]) than cholesterol polyps (5.37 sec and 1068.3 a.u). On ROC analysis, an area under the curve (AUC) of 1.00, 100% (14/14) sensitivity, and 100% (4/4) specificity were demonstrated when the cut-off value was set at 9.62 sec for FT; and WoR yielded an AUC of 0.89, sensitivity of 100% (14/14), and a specificity of 75% (3/4) using a cut-off value of 784.4 a.u.

CONCLUSION

CEUS can be useful for the differentiation of premalignant or malignant GB polyps from cholesterol polyps >= 1 cm.

CLINICAL RELEVANCE/APPLICATION

CEUS can help distinguish premalignant or malignant GB polyps from cholesterol polyps >= 1 cm, thereby aiding in the selection of an optimal management option for large GB polyps.

SSM09-06 Fully Automated Detection of Primary Sclerosing Cholangitis (PSC) in 3D-MRCP Images Using Deep Learning

Wednesday, Nov. 28 3:50PM - 4:00PM Room: S503AB

Participants

Hinrich B. Winther, MD, Hannover, Germany (*Presenter*) Nothing to Disclose Van Dai Vo Chieu, MD, Hannover, Germany (*Abstract Co-Author*) Nothing to Disclose Christian Hundt, DIPLPHYS,PhD, Mainz, Germany (*Abstract Co-Author*) Nothing to Disclose Bertil Schmidt, Mainz, Germany (*Abstract Co-Author*) Nothing to Disclose Jens Vogel-Claussen, MD, Hannover, Germany (*Abstract Co-Author*) Nothing to Disclose Frank K. Wacker, MD, Hannover, Germany (*Abstract Co-Author*) Nothing to Disclose Kristina I. Ringe, MD, Hannover, Germany (*Abstract Co-Author*) Nothing to Disclose

PURPOSE

To automatically detect PSC-typical cholangiographic changes in 3D-MRCP images.

METHOD AND MATERIALS

428 patients (m = 274 / w = 154, age 42.5 \pm 18.5 years) who underwent liver MRI including 3D MRCP were included in this retrospective study. The study population consisted of 206 patients with confirmed PSC (based on clinical, typical cholangiographic and confirmatory histologic findings) and 222 patients in whom this diagnosis was excluded. The patients were randomized into a training (n = 386) and validation group (n = 42). For each individual case, 20 uniformly distributed axial MRCP rotations, covering a total of 180°, were calculated, followed by a maximum intensity projection (MIP). This resulted in a training record of 7720 and a validation record of 840 2D images. An Inception ResNet (Inception-v4 arXiv: 1602.07261) was trained, which was initialized with weights previously learned from ImageNet. Finally, we fine-tuned the entire network with a small learning rate of 10-5.

RESULTS

The mean absolute error (MAE) on the validation record was 30% and therefore insufficient. This value could be improved to 7.1% (3/42) by applying an ensemble strategy. For this purpose, the 20 related MRCP projections of each patient were binned and a majority vote was conducted. With this approach, sensitivity, specificity, positive predictive and negative predictive value for the detection of PSC-typical cholangiographic changes were 95.0%, 90.9%, 90.5%, and 95.2% respectively.

CONCLUSION

The results of this study demonstrate the feasibility of transfer learning to detect PSC-typical cholangiographic changes in 3D MRCP images with an MAE of ~7%. Further validation with more and multicentric data should be made, as experience shows that neural networks tend to overfit the characteristics of the dataset.

CLINICAL RELEVANCE/APPLICATION

Automatic detection of PSC typical changes at MRCP may improve early detection and aid in follow-up imaging, especially of subtle changes.



SSM22

Radiation Oncology (Genitourinary)

Wednesday, Nov. 28 3:00PM - 4:00PM Room: E261



AMA PRA Category 1 Credit ™: 1.00 ARRT Category A+ Credit: 1.00

Participants

Martin Colman, MD, Houston, TX (*Moderator*) Stockholder, Steward Health Care Edward Y. Kim, MD, Seattle, WA (*Moderator*) Nothing to Disclose

Sub-Events

SSM22-01 Deep Decision Forests of Radiomic Features for Automatic Contouring of Pelvic Anatomy for Prostate Radiotherapy

Wednesday, Nov. 28 3:00PM - 3:10PM Room: E261

Participants

Meghan W. Macomber, MD, Seattle, WA (*Abstract Co-Author*) Nothing to Disclose Mark H. Phillips, PhD, Seattle, WA (*Abstract Co-Author*) Nothing to Disclose Ivan Tarapov, MSc, Redmond, WA (*Abstract Co-Author*) Nothing to Disclose Rajesh Jena, MD, FRCR, Cambridge, United Kingdom (*Abstract Co-Author*) Royalties, Microsoft Corporation; Antonio Criminisi, PhD, Cambridge, United Kingdom (*Abstract Co-Author*) Employee, Microsoft Corporation Matthew J. Nyflot, PhD, Seattle, WA (*Presenter*) Nothing to Disclose

PURPOSE

Machine learning for image segmentation is a potentially innovative approach to improve efficiency and promote standardization for radiotherapy treatment planning. We evaluated a new model that uses deep decision forests of image features to contour pelvic anatomy on treatment planning CTs.

METHOD AND MATERIALS

We anonymized 193 prostate treatment planning CTs (acquired 2012-2016 at 1 UK and 2 US sites, GE and Toshiba scanners, 512x512 pixels inplane, 1.25 or 2.5 mm between slices). A deep decision forest (DF) was trained to contour prostate, bladder, rectum, femurs, and seminal vesicles on 94 images from Site 1. Testing was done on 99 separate scans (n=35, 34, and 25 from Site 1, 2, and 3). Similarity between DF contours and clinical (ground truth) contours was measured with Dice score (DSC) in the validation datasets. DF performance was compared to four commercial tools on a random subset of images (n=20). Additionally, interobserver variability (IOV) between three physicians' contours and ground truth was evaluated on 10 random images and compared to DF performance with Student's t-test.

RESULTS

Across all sites, DF agreement with ground truth was: bladder, DSC 0.94-0.97 [interquartile range (IQR) 0.92-0.98], prostate, DSC 0.75-0.76 [IQR 0.67-0.82], rectum: DSC 0.71-0.82 [IQR 0.63-0.87], femurs: DSC 0.96-0.97 [IQR 0.94-0.97], seminal vesicles: DSC 0.49-0.70 [IQR 0.31-0.79]. The results were similar across the three sites (e.g. median prostate DSC for each site was 0.76, 0.76, 0.75). In the commercial model comparison, DF had highest DSC for all organs, followed by the two model-based systems, with atlas-based systems having worst performance. For IOV data, variability between DF and ground truth was smaller than variability between raters for prostate (median DSC 0.87 vs 0.77, p=0.006) and femurs (median DSC 0.973 vs 0.968, p=0.002), and not significantly different for other contours (p>0.3).

CONCLUSION

Deep decision forests are effective at contouring pelvic anatomy for radiotherapy planning, with good performance relative to commercial programs, and agreement with ground truth was as similar as can be expected between human experts.

CLINICAL RELEVANCE/APPLICATION

Machine learning methods for automated treatment planning would be useful to improve clinical efficiency and increase standardization in radiation oncology.

SSM22-02 Nationwide Prostate Cancer Outcome Prediction Study of Permanent Iodine-125 Seed Implantation: Outcome Prediction Using Machine Learning Techniques with Cohort 1

Wednesday, Nov. 28 3:10PM - 3:20PM Room: E261

Participants

Taiki Magome, Tokyo, Japan (*Presenter*) Nothing to Disclose Katsumasa Nakamura, MD, PhD, Hamamatsu, Japan (*Abstract Co-Author*) Nothing to Disclose Takashi Kikuchi, Kobe, Japan (*Abstract Co-Author*) Nothing to Disclose Shinsuke Kojima, Kobe, Japan (*Abstract Co-Author*) Nothing to Disclose Kazuto Ito, Maebashi, Japan (*Abstract Co-Author*) Nothing to Disclose Atsunori Yorozu, MD, Tokyo, Japan (*Abstract Co-Author*) Nothing to Disclose Shiro Saito, Tokyo, Japan (*Abstract Co-Author*) Nothing to Disclose Masanori Fukushima, Kobe, Japan (*Abstract Co-Author*) Nothing to Disclose

PURPOSE

The nationwide Japanese Prostate Cancer Outcome Study of Permanent Iodine-125 Seed Implantation (J-POPS) is a big novel data with the fundamental aim of collecting clinical data as a prospective cohort study. The purpose of this study is to predict prostate cancer outcome after brachytherapy based on machine learning techniques using J-POPS big data.

METHOD AND MATERIALS

Among 72 hospitals performing brachytherapy in Japan, 46 (64 %) hospitals provided 2,339 cases of the J-POPS cohort 1. Patient/family background, TNM classification, serum PSA level, Gleason score, brachytherapy and external radiotherapy parameters, adverse event and outcome information, etc. were included in the survey items. Two types of dataset were used for the prediction; i.e., the large dataset including the majority of survey items, and limited dataset including only the survey items which are considered as relevant items with the outcome by radiation oncologists. In this study, four machine learning algorithms, i.e., logistic regression (LR), support vector machine (SVM), random forest (RF), and deep neural network (DNN) were tested. Outcome information including biochemical failure and rectal/urinary toxicity were predicted by the machine learning techniques. The prediction accuracy, defined as (true positive + true negative cases) / all cases, was evaluated by 10-fold cross-validation test.

RESULTS

The prediction accuracy with the large dataset was higher than that with the limited dataset in each machine learning algorithm. Although 5.2 percent of cases showed the biochemical failure, the highest accuracy of biochemical failure prediction with a large dataset and limited dataset was 0.938 and 0.892, respectively, for test data. The prediction model using RF had the highest accuracy.

CONCLUSION

Our results showed a potential to predict the outcome of prostate cancer patients with the big nationwide data including many survey items.

CLINICAL RELEVANCE/APPLICATION

Prostate cancer outcome after brachytherapy could be accurately predicted with big nationwide data.

SSM22-03 Dose to the Bladder Neck in MRI-guided High Dose-Rate Prostate Brachytherapy

Wednesday, Nov. 28 3:20PM - 3:30PM Room: E261

Participants

Noelia Sanmamed, MD, Toronto, ON (*Presenter*) Nothing to Disclose Peter Chung, Toronto, ON (*Abstract Co-Author*) Nothing to Disclose Sangeet Ghai, MD, Toronto, ON (*Abstract Co-Author*) Grant, InSightec Ltd Grant, Exact Imaging Inc Alejandro Berlin, Toronto, ON (*Abstract Co-Author*) Nothing to Disclose Jette Borg, PhD, Toronto, ON (*Abstract Co-Author*) Nothing to Disclose Bernadeth Lao, BSC, Toronto, ON (*Abstract Co-Author*) Nothing to Disclose Robert Weersink, Toronto, ON (*Abstract Co-Author*) Nothing to Disclose Anna Simeonov, Toronto, ON (*Abstract Co-Author*) Nothing to Disclose Alexandra Rink, PhD, Toronto, ON (*Abstract Co-Author*) Nothing to Disclose Cynthia Menard, MD, Montreal, QC (*Abstract Co-Author*) Nothing to Disclose Joelle Helou, Toronto, ON (*Abstract Co-Author*) Nothing to Disclose

PURPOSE

We aim to assess the impact of the dose to the bladder neck (BN) on physician and patient-reported GU toxicity after MRI-guided high dose-rate brachytherapy (HDR-BT) boost.

METHOD AND MATERIALS

Sixty-three patients were treated with a single 15-Gy MRI-guided HDR-BT implant followed by external beam radiotherapy. MRIbased treatment planning was used. The clinical target volume (CTV) was defined as the prostate and planning target volume was CTV + 2mm craniocaudal margin. BN was delineated in retrospect on T2-weighted images by a radiation oncologist (RO) and reviewed by an independent RO and a radiologist. Dosimetric parameters, acute (<=3 months) toxicity using CTCAE v.4 and healthrelated quality of life (HRQoL)using the expanded prostate index composite (EPIC) were collected prospectively. A minimally important difference (MID) was defined as a deterioration of HRQoL scores at 3 months compared to baseline >= 0.5 standard deviation of baseline score. Linear and logistic regression models were used to assess the impact of BN dose on GU toxicity and HRQoL. A p-value <=0.05 was considered statistically significant.

RESULTS

The median BN volume was 0.6 cc [interquartile range (IQR): 0.4-0.7]. Median maximum dose to the BN (BNDmax) and urethra (UDmax) was 24.9 Gy (IQR 18.8- 26.4) and 17 Gy (IQR 16.7- 17.7) respectively. Median dose to 2cc of the urethra was 52 Gy (IQR: 36-62). BNDmax was significantly associated with UDmax (p=0.027) and 7.7% of the total amount of variation in BNDmax was explained by the UDmax (R2=0.059, p=0.028). Grade 2+ GU toxicity was observed in 31% of patients. Among those, 4 patients had an acute urinary retention. No grade 4+ toxicity was reported. Furthermore 46% of patients reported a MID in EPIC urinary domain score at 3 months. None of the dosimetric parameters including BNDmax was associated with acute grade 2+ urinary toxicity or MID. However, 3 out of 4 patients with acute urinary retention had a BND max in the highest quartile; 26.4, 28.3 and 52.7 Gy (>175% of prescription dose).

CONCLUSION

MRI-based planning offers a unique opportunity to delineate and assess the dose to the BN. Although the predictive value of this parameter is yet to be determined in a larger population, it is worthwhile including BN contours and constraints into HDR-BT

treatment planning if an MRI-planning is available.

CLINICAL RELEVANCE/APPLICATION

Uncertainties exist regarding bladder neck definition.

SSM22-04 Machine Leaning Based Prediction of Prostate Cancer Recurrence After Radiotherapy with Radiosensitivity Related Proteins

Wednesday, Nov. 28 3:30PM - 3:40PM Room: E261

Participants

Takuya Mizutani, Tokyo, Japan (*Presenter*) Nothing to Disclose Taiki Magome, Tokyo, Japan (*Abstract Co-Author*) Nothing to Disclose Masanori Someya, MD,PhD, Hokkaido, Japan (*Abstract Co-Author*) Nothing to Disclose Tomokazu Hasegawa, Sapporo, Japan (*Abstract Co-Author*) Nothing to Disclose Koichi Sakata, Sapporo, Japan (*Abstract Co-Author*) Nothing to Disclose

For information about this presentation, contact:

mizutaku17@gmail.com

PURPOSE

There are several reports that the expression of proteins in tumors related to radiosensitivity could be used as biomarkers for the outcome prediction after radiotherapy. The purpose of this study was to predict local relapse of prostate cancer after radiotherapy using a machine learning methodology with the combination of conventional factors and the protein information related to radiosensitivity.

METHOD AND MATERIALS

A total of 100 patients with localized adenocarcinoma of the prostate who were treated from 2001 to 2010 were included in this study. Support vector machine (SVM) was used as a machine learning methodology to predict local relapse of prostate cancer. Candidate input features for the prediction included 16 clinical features (age, Gleason score, PSA level, etc.), 16 radiation dose features (mean dose, dose per fraction, etc.) and 3 protein information related to radiosensitivity (Ku70, Ku86, XRCC4). Effective features for prediction were determined by a sequential forward selection using Akaike's information criterion. The prediction performance of the models with or without protein information were compared by a leave-one-out cross-validation test. Accuracy, sensitivity, specificity and Matthew's correlation coefficient (MCC) were used as prediction performance metrics.

RESULTS

The prediction performance was improved by considering the radiosensitivity related protein information, e.g., accuracy of the models with and without the protein information was 0.78 and 0.69, respectively. Ku70 was the most selected feature in the proteins related to radiosensitivity.

CONCLUSION

Our result showed the potential to predict local relapse of prostate cancer with the combination of conventional factors and the protein information related to radiosensitivity. Accurate outcome prediction after radiotherapy could be useful for personalized optimal selection of treatment modalities of cancer.

CLINICAL RELEVANCE/APPLICATION

Accuracy of the machine learning model for outcome prediction after radiotherapy could be improved with the radiosensitivity related protein information.

SSM22-05 Prostate Cancer: Assessment of Toxicity of Focal Dose Escalation of Radiotherapy Guided by Multiparametric Magnetic Resonance Imaging

Wednesday, Nov. 28 3:40PM - 3:50PM Room: E261

Participants

Michael W. Schmuecking, Hamburg, Germany (*Presenter*) Nothing to Disclose Volker Brandes, Hamburg, Germany (*Abstract Co-Author*) Nothing to Disclose Arne Blechschmidt, MS, Hamburg, Germany (*Abstract Co-Author*) Nothing to Disclose Sarah Lomp, MS, Hamburg, Germany (*Abstract Co-Author*) Nothing to Disclose Imke Luetjens, MS, Hamburg, Germany (*Abstract Co-Author*) Nothing to Disclose Matthias Roethke, MD, Heidelberg, Germany (*Abstract Co-Author*) Nothing to Disclose

For information about this presentation, contact:

schmuecking@strahlentherapie-veritaskai.com

PURPOSE

To evaluate acute and late toxicity after moderately hypofractionated radiotherapy of prostate cancer with focal dose escalation guided by multiparametric magnetic resonance imaging (mpMRI) using intensity-modulated treatment planning and image-guided treatment (IGRT) delivery.

METHOD AND MATERIALS

58 patients (age 55-82y, cT2/cT3, initial PSA 3.3-16.4ng/ml, Gleason Score >3+4) were included into the study. Before implantation of three gold markers, each patient underwent mpMRI (T2-TSE, DCE, DWI) that detected a suspicious focal lesion (PIRADS 4+5) followed by image fusion with the radiation treatment planning CT. In total, a dose of 79.2Gy in 33 fractions (single dose 2.4Gy) were prescribed to PIRADS 4 and 5 intraprostatic lesions with a margin of 3mm (gross target volume + 3mm = planning target volume) delivered with a simultaneous integrated boost (SIB) by static field intensity-modulated radiotherapy (IMRT) or volumetric modulated arc therapy (VMAT). Further dose levels were 76.23Gy and 60.06Gy prescribed to the prostate and the

seminal vesicles, respectively. Patients with high risk prostate cancer received 46Gy to the pelvic lymphatics, lymph node metastases 60Gy in 25 fractions with SIB. Daily IGRT by cone-beam computed tomography (CBCT) in addition to gold markers. Acute and late gastrointestinal (GI) and genitourinary (GU) toxicity was evaluated using CTCAE v4.03.

RESULTS

Treatment was completed according to the treatment plan in all included patients. Acute GI and GU toxicity grade >=2 was observed in 13.8% and 39.6% of the patients, respectively, with 6.8% suffering from GU toxicity grade 3. Six weeks after treatment, the incidence of acute toxicity grade >=2 had decreased to 15.5%. With a median follow-up of 28 months, late GI and GU toxicity grade >=2 was seen in 1.7% and 8.6% of the patients, respectively. Three patients developed late toxicity grade 3 (GI n=2; GU n=1).

CONCLUSION

Moderately hypofractionated high-dose radiotherapy with further dose-escalation to mpMRI PIRADS 4 and 5 lesions resulted in acceptable rates of acute and late toxicity according to the current literature. Conformal IMRT / VMAT planning and accurate daily IGRT treatment delivery using goldmarker and CBCT may have contributed to these results.

CLINICAL RELEVANCE/APPLICATION

The use of mpMRI for focal dose escalation in patients with prostate cancer may enhance post-radiotherapeutic local control.

SSM22-06 Weekly Magnetic Resonance Imaging Using a Linear Accelerator Equipped with a 1.5 Tesla MRI (MR-Linac) Reveals Intra-Treatment Signal Variance in Regional Organs at Risk (OAR), An Exploratory Analysis

Wednesday, Nov. 28 3:50PM - 4:00PM Room: E261

Participants

Joshua Lorenz, Milwaukee, WI (*Presenter*) Nothing to Disclose Diane Schott, PhD, Milwaukee, WI (*Abstract Co-Author*) Nothing to Disclose Farshad Mostafaei, PhD, Milwaukee, WI (*Abstract Co-Author*) Nothing to Disclose Colleen A. Lawton, MD, Milwaukee, WI (*Abstract Co-Author*) Nothing to Disclose Manpreet Bedi, MD, Milwaukee, WI (*Abstract Co-Author*) Nothing to Disclose X. Allen Li, Milwaukee, WI (*Abstract Co-Author*) Nothing to Disclose Christopher J. Schultz, MD, Milwaukee, WI (*Abstract Co-Author*) Medical Advisory Board, Prism Clinical Imaging, Inc Eric Paulson, PHD, Milwaukee, WI (*Abstract Co-Author*) Nothing to Disclose William A. Hall, MD, Milwaukee, WI (*Abstract Co-Author*) Departmental research support, Elekta AB

PURPOSE

To investigate changes in quantitative signal variables of organs at risk (OAR) in serially obtained T2-weighted MR images, acquired on an MR-Linac, in patients being treated for prostate cancer.

METHOD AND MATERIALS

Four patients with prostate cancer undergoing treatment with radiation therapy (RT) were compiled from an ongoing prospective observational imaging trial using MR-Linac. All patients provided informed consent for weekly imaging; images were obtained between November 2017 and March 2018. Contiguous sections of rectal and bladder wall adjacent to the prostate were contoured and normalized to temporally corresponding regions of rectum and bladder removed from the planning target volume. Similarly, contiguous axial slices of Sartorius muscle outside of the regions of high dose RT exposure were also contoured as a normal control. The quantitative features considered included: max-to-mean ratio, kurtosis, mean, median, skewness, and standard deviation. A student's t-test was used to evaluate for statistically significant variance week-to-week.

RESULTS

Between weeks 1 and 2, significant variance in the mean and median signal values were seen in sections of rectal wall adjacent to the prostate (p=0.05, p=0.04). Bladder wall near the prostate also exhibited significant variance in the mean and median signal values between weeks 1 and 4 (p=0.05, p=0.04). No significant variance in signal values for the variables considered was observed in the Sartorius muscle control.

CONCLUSION

This is one of the earliest analyses examining quantitative signal value changes in regional organs (bladder and rectum), using an MR-Linac in patients being actively treated with RT for prostate cancer. Significant changes occurred after only 1 week of therapy in regional organs at risk during treatment with RT. Expanded data sets are needed to evaluate if these early changes correlate with clinical outcomes such as acute or late toxicity.

CLINICAL RELEVANCE/APPLICATION

Radiotherapy (RT) response assessment with a 1.5 Tesla MRI may allow for intra-treatment modification of RT plans to increase oncologic control and reduce toxicity. Increased understand of radiomic changes in OAR's will improve RT response assessment.



AI001-TH

RSNA Deep Learning Classroom: Presented by NVIDIA Deep Learning Institute

Thursday, Nov. 29 8:30AM - 4:00PM Room: AI Community, Learning Center

Program Information

Located in the Learning Center (Hall D), this classroom presented by NVIDIA will give meeting attendees a hands-on opportunity to engage with deep learning tools, write algorithms and improve their understanding of deep learning technology. "Attendees must bring a laptop capable of running the most recent version of Chrome."

Sub-Events

AI001-THA 3D Segmentation of Brain MR

Thursday, Nov. 29 8:30AM - 10:00AM Room: AI Community, Learning Center

Title and Abstract

3D Segmentation of Brain MR This session will focus on the use of deep learning methods for segmentation, with particular emphasis on 3D techniques (V-Nets) applied to the challenge of MR brain segmentation. While focused on this particular problem, the concepts should generalize to other organs and image types.

AI001-THB Multi-modal Classification

Thursday, Nov. 29 10:30AM - 12:00PM Room: AI Community, Learning Center

Title and Abstract

Multi-modal Classification This session will focus on multimodal classification. Classification is the recognition of an image or some portion of an image being of one type or another, such as 'tumor' or 'infection'. Multimodal classification means that there are more than 2 classes. While this is logically simple to understand, it presents some unique challenges that will be discussed.

AI001-THC Introduction to Deep Learning

Thursday, Nov. 29 12:30PM - 2:00PM Room: AI Community, Learning Center

Title and Abstract

Introduction to Deep Learning This class will focus on basic concepts of convolutional neural networks (CNNs), and walk the attendee through a working example. A popular training example is the MNIST data set which consists of hand-written digits. This course will use a data set we created, that we call 'MedNIST and consists of 1000 images each from 5 different categories: Chest X-ray, hand X-ray, Head CT, Chest CT, Abdomen CT, and Breast MRI. The task is to identify the image type. This will be used to train attendees on the basic principles and some pitfalls in training a CNN. The attendee will have the best experience if they are familiar with Python programming.

AI001-THD Data Science: Normalization, Annotation, Validation

Thursday, Nov. 29 2:30PM - 4:00PM Room: AI Community, Learning Center

Title and Abstract

Data Science: Normalization, Annotation, Validation This session will focus on preparation of the image and non-image data in order to obtain the best results from your deep learning system. It will include a discussion of different options for representing the data, how to normalize the data, particularly image data, the various options for image annotation and the benefits of each option. We will also discuss the 'after training' aspects of deep learning including validation and testing to ensure that the results are robust and reliable.



RC616

The Impact of Artificial Intelligence on Radiology Training and Practice Around the World (Sponsored by RSNA Committee of International Radiology Education)

Thursday, Nov. 29 8:30AM - 10:00AM Room: E350



AMA PRA Category 1 Credits ™: 1.50 ARRT Category A+ Credit: 1.75

LEARNING OBJECTIVES

1) Discuss how Artificial Intelligence (AI) will impact Radiology's role in global health. 2) Explain how AI is changing radiology training and practice in different parts of the world. 3) Identify radiology AI products that are ready and appropriate for implementation in low-resource environments. 4) Discuss how the CIRE might play a part in AI education.

ABSTRACT

Artificial intelligence (AI) will affect global health (global radiology) in myriad ways. In addition to AI for initial imaging evaluation in resource-limited environments, many AI products may be applicable to near-term implementation in these environments and may leap-frog traditional systems. AI will change not only the way in which radiology is practiced in global health but also how radiologists are trained and their roles within the healthcare system after residency.

Sub-Events

RC616A Introduction: The Potential for AI in Global Radiology and Training

Participants

Eliot L. Siegel, MD, Baltimore, MD (*Presenter*) Medical Advisory Board, Brightfield Technologies Medical Advisory Board, McCoy Board of Directors, Carestream Health, Inc Founder, MedPerception, LLC Board of Directors Clear Health Quality Institute Founder, Topoderm Founder, YYESIT, LLC Medical Advisory Board, Bayer AG Medical Advisory Board, Bracco Group Medical Advisory Board, Carestream Health, Inc Medical Advisory Board, Fovia, Inc Medical Advisory Board, McKesson Corporation Medical Advisory Board, Merge Healthcare Incorporated Medical Advisory Board, Microsoft Corporation Medical Advisory Board, Koninklijke Philips NV Medical Advisory Board, Toshiba Medical Systems Corporation Research Grant, Anatomical Travelogue, Inc Research Grant, Anthro Corp Research Grant, Barco nv Research Grant, Dell Inc Research Grant, Evolved Technologies Corporation Research Grant, General Electric Company Research Grant, Herman Miller, Inc Research Grant, Intel Corporation Research Grant, MModal IP LLC Research Grant, McKesson Corporation Research Grant, RedRick Technologies Inc Research Grant, Steelcase, Inc Research Grant, Virtual Radiology Research Grant, XYBIX Systems, Inc Research, TeraRecon, Inc Researcher, Bracco Group Researcher, Microsoft Corporation Speakers Bureau, Bayer AG Speakers Bureau, Siemens AG

For information about this presentation, contact:

esiegel@umaryland.edu

LEARNING OBJECTIVES

View learning objectives under main course title.

RC616B How Resident Training May Be Affected by AI

Participants David C. Gimarc, MD, Madison, WI (*Presenter*) Nothing to Disclose

LEARNING OBJECTIVES

View learning objectives under main course title.

RC616C Panel Discussion

Participants Nitin P. Ghonge, MD, New Delhi, India (*Presenter*) Nothing to Disclose Omolola M. Atalabi, MBBS, Ibadan, Nigeria (*Presenter*) Nothing to Disclose Claudio Silva, MD, Santiago, Chile (*Presenter*) Nothing to Disclose Jeong Min Lee, MD, Seoul, Korea, Republic Of (*Presenter*) Grant, Bayer AG Grant, General Electric Company Grant, Koninklijke Philips NV Grant, STARmed Co, Ltd Grant, RF Medical Co, Ltd Grant, Samsung Electronics Co, Ltd Grant, Guerbet SA

For information about this presentation, contact:

drnitinpghonge@gmail.com

csilvafa@alemana.cl

mojisola3t@hotmail.com

LEARNING OBJECTIVES

View learning objectives under main course title.

RC616D Near-term adoption of AI in Global Radiology: Barriers and Opportunities

Participants

Jeffrey B. Mendel, MD, West Newton, MA (Presenter) Advisor, McKesson Corporation

For information about this presentation, contact:

jmendel@pih.org

LEARNING OBJECTIVES

View learning objectives under main course title.

RC616E How CIRE Can Serve as a Locus for the Extension of AI Into Global Radiology Training

Participants Kristen K. DeStigter, MD, Burlington, VT (*Presenter*) Nothing to Disclose

LEARNING OBJECTIVES

View learning objectives under main course title.

RC616F Q&A

LEARNING OBJECTIVES

View learning objectives under main course title.



RC625

Mini-course: Radiation Safety for Patients and Staff - Emerging Advances in Patient Radiation Protection

Thursday, Nov. 29 8:30AM - 10:00AM Room: S105AB



AMA PRA Category 1 Credits ™: 1.50 ARRT Category A+ Credit: 1.75

FDA Discussions may include off-label uses.

Participants

Madan M. Rehani, PhD, Boston, MA (Coordinator) Nothing to Disclose

For information about this presentation, contact:

madan.rehani@gmail.com

Active Handout: Madan M. Rehani

http://abstract.rsna.org/uploads/2018/18001512/Rehani_RSNA_Quality _dose RC625.pdf

Sub-Events

RC625A Emerging Concepts of Integration of Image Quality, Radiation Dose, and Artificial Intelligence

Participants

Ehsan Samei, PhD, Durham, NC (*Presenter*) Research Grant, General Electric Company; Research Grant, Siemens AG; Advisory Board, medInt Holdings, LLC; License agreement, 12 Sigma Technologies; License agreement, Gammex, Inc

LEARNING OBJECTIVES

1) To understand how dose monitoring is but a component of the broad objective of quality and excellence in imaging. 2) To understand how dose and image quality need to be recognized together to enable optimized care. 3) To appreciate how artificial intelligence methods can be used to inform quality and safety monitoring and optimization.

RC625B Practical Aspects of Integration of Clinical Image Quality and Patient Dose Optimization

Participants

Madan M. Rehani, PhD, Boston, MA (Presenter) Nothing to Disclose

For information about this presentation, contact:

madan.rehani@gmail.com

LEARNING OBJECTIVES

1) Define strength and limitations of diagnostic reference levels (DRLs). 2) Describe criteria for image quality assessment. 3) Apply the concept of integration of image quality scoring with dose indices in CT imaging for the purpose of optimization.

Active Handout: Madan M. Rehani

http://abstract.rsna.org/uploads/2018/18001514/Rehani_RSNA_Quality _dose RC625B.pdf



RC653

Machine Learning and Artificial Intelligence: The Non-Interpretive Considerations

Thursday, Nov. 29 8:30AM - 10:00AM Room: E450A



AMA PRA Category 1 Credits ™: 1.50 ARRT Category A+ Credit: 1.75

FDA Discussions may include off-label uses.

Participants

Saurabh Jha, MD, Philadelphia, PA (Moderator) Speakers Bureau, Canon Medical Systems Corporation

For information about this presentation, contact:

saurabh.jha@uphs.upenn.edu

LEARNING OBJECTIVES

1) To appreciate the history of automation. 2) To understand the opposing economic factors in the adoption of artificial intelligence. 3) To understand what motivates entrepreneurs and venture capitalists to fund AI ventures. 4) To get an overview of how we can assess the quality of AI. 5) To appreciate the ethical and legal issues about AI.

ABSTRACT

This session will discuss the more non technical issues in artificial intelligence such as the economics, history, legal and ethical considerations, entrepreneurship and how we assess the product. The session intends to complement the more technical elements of artificial intelligence to give a rounded perspective about this emerging area.

Sub-Events

RC653A The Economics of Artificial Intelligence

Participants

Saurabh Jha, MD, Philadelphia, PA (Presenter) Speakers Bureau, Canon Medical Systems Corporation

For information about this presentation, contact:

saurabh.jha@uphs.upenn.edu

LEARNING OBJECTIVES

1) Understand the history of automation. 2) Is automation inevitable in radiology? 3) Review economic theory relevant to automation. 4) Critique the economic theory and empirical evidence which informs us about artificial intelligence.

ABSTRACT

Though artificial intelligence is a recent phenomenon, at least in terms of scale, automation and the replacement of labor by machines, is not new. There are broad economic and cultural principles. What are these principles? Can they be applied to radiology in general and healthcare in particular?

RC653B Entrepreneurship and Artificial Intelligence

Participants Ajay Kohli, MD, Philadelphia, PA (*Presenter*) Nothing to Disclose

For information about this presentation, contact:

ajay@ajaykohlimd.com

LEARNING OBJECTIVES

1) Start-ups, funding, exit strategies and more: to learn about what it means to be an entrepreneur in healthcare. 2) To understand what motivates venture capitalists and healthcare CEOs to invest in Artificial Intelligence start-up companies. 3) To understand some of the barriers faced by entrepreneurs, speficially those working on bringing in Artificial Intelligence in medical imaging. 4) To learn how to evaluate Artifical Intelligence applications from start-up companies.

RC653C How to Tell if My AI is Telling the Truth

Participants

Hugh Harvey, MBBS, London, United Kingdom (Presenter) Employee, Kheiron Medical

For information about this presentation, contact:

hugh@kheironmed.com

1) Learn an overview on how to assess an AI application. 2) Understand how training data selection, biases, disease prevalence, and statistics can alter medical device claims. 3) Learn about 'intended use' as per medical device regulations.

RC653D Ethical and Legal Aspects of Machine Learning

Participants

Falgun H. Chokshi, MD, Marietta, GA (Presenter) Nothing to Disclose

LEARNING OBJECTIVES

1) Discuss ethical ramifications of AI mediated imaging diagnosis versus detection. 2) Understand legal perspectives of AI's impact on Radiology as a speciality as they pertain to medical liability and risk. 3) Empathize with the patient's role and perspective in their care as AI augments radiologists' practices and workflow.



Novel Discoveries Using the NCI's Cancer Imaging Archive (TCIA) Public Data Sets

AI IN OI

Participants

Participants Janet F. Eary, MD, Bethesda, MD (*Moderator*) Nothing to Disclose Evis Sala, MD, PhD, Cambridge, United Kingdom (*Presenter*) Nothing to Disclose Andriy Fedorov, PhD, Boston, MA (*Presenter*) Research funded, Siemens AG Jayashree Kalpathy-Cramer, MS, PhD, Charlestown, MA (*Presenter*) Consultant, Infotech Software Solution Daniel L. Rubin, MD, MS, Stanford, CA (*Presenter*) Nothing to Disclose Aaron J. Grossberg, MD, PhD, Portland, OR (*Presenter*) Nothing to Disclose Jeffrey F. Williamson, PhD, St. Louis , MO (*Presenter*) Nothing to Disclose John B. Freymann, BS, Rockville, MD (*Presenter*) Nothing to Disclose

For information about this presentation, contact:

daniel.l.rubin@stanford.edu

john.freymann@nih.gov

arossber@ohsu.edu

andrey.fedorov@gmail.com

kalpathy@nmr.mgh.harvard.edu

janet.eary@nih.gov

LEARNING OBJECTIVES

1) Critically appraise The Cancer Imaging Archive (TCIA)/MD Anderson Cancer Center Head and Neck Squamous Cell Carcinoma (HNSCC) data set. 2) Identify solutions to challenges in sharing and curating RT DICOM data collections. 3) Describe novel discoveries made using the HNSCC data set. 4) Apply TCIA data sets to derive imaging-based predictors of oncologic outcome. 5) Recommend innovative research approaches using extant and future TCIA collections. 6) Discuss updates in enriching TCIA collections of images with results of their annotation and analysis. 7) Discuss the importance of standardization as applied to image-derived data representation for its reuse and harmonization across TCIA collections.

ABSTRACT

This didactic session will highlight popular data sets and major projects utilizing TCIA with presentations from leading researchers and data contributors. Attendees will hear presentations about the following projects and data sets: • The Applied Proteogenomics OrganizationaL Learning and Outcomes (APOLLO) network • Cancer Proteomics Turnor Analysis Consortium (CPTAC) • Crowds Cure Cancer • Quantitative Imaging Network (QIN) Prostate MRI • Quantitative Image Informatics for Cancer Research (QIICR) • Digital Database for Screening Mammography • Head and Neck Squamous Cell Carcinoma (HNSCC) • 4D-Lung

URL

https://na01.safelinks.protection.outlook.com/? url=https%3A%2F%2Fdicom4qi.readthedocs.io%2Fen%2Flatest%2Fresources%2Fdatasets%2F&data=02%7C01%7Ccricchio%40rsna.org%7Cb8fff403a6a34d30d3f408d651874712%7Cfb5fefcd7ca642 https://na01.safelinks.protection.outlook.com/?

url=https%3A%2F%2Fdicom4qi.readthedocs.io%2Fen%2Flatest%2Fresources%2Fsoftware%2F&data=02%7C01%7Ccricchio%40rsna.org%7Cb8fff403a6a34d30d3f408d651874712%7Cfb5fefcd7ca642 Honored Educators

Presenters or authors on this event have been recognized as RSNA Honored Educators for participating in multiple qualifying educational activities. Honored Educators are invested in furthering the profession of radiology by delivering high-quality educational content in their field of study. Learn how you can become an honored educator by visiting the website at: https://www.rsna.org/Honored-Educator-Award/ Evis Sala, MD, PhD - 2013 Honored EducatorEvis Sala, MD, PhD - 2017 Honored EducatorDaniel L. Rubin, MD, MS - 2012 Honored EducatorDaniel L. Rubin, MD, MS - 2013 Honored EducatorEvis Sala, MD, PhD - 2017 Honored EducatorDaniel L. Rubin, MD, MS - 2012 Honored EducatorDaniel L. Rubin, MD, MS - 2013 Honored EducatorEvis Sala, MD, PhD - 2017 Honored EducatorDaniel L. Rubin, MD, MS - 2012 Honored EducatorDaniel L. Rubin, MD, MS - 2013 Honored EducatorEvis Sala, MD, PhD - 2017 Honored EducatorDaniel L. Rubin, MD, MS - 2012 Honored EducatorDaniel L. Rubin, MD, MS - 2013 Honored EducatorEvis Sala, MD, PhD - 2017 Honored EducatorDaniel L. Rubin, MD, MS - 2012 Honored EducatorDaniel L. Rubin, MD, MS - 2013 Honored EducatorEvis Sala, MD, PhD - 2017 Honored EducatorDaniel L. Rubin, MD, MS - 2012 Honored EducatorDaniel L. Rubin, MD, MS - 2013 Honored Educator



SSQ01

Breast Imaging (Abbreviated MRI, Ultrafast Imaging and Artificial Intelligence)

Thursday, Nov. 29 10:30AM - 12:00PM Room: E450A



AMA PRA Category 1 Credits ™: 1.50 ARRT Category A+ Credit: 1.75

Participants

Christiane K. Kuhl, MD, Aachen, Germany (Moderator) Nothing to Disclose

Ritse M. Mann, MD, PhD, Nijmegen, Netherlands (*Moderator*) Researcher, Siemens AG; Researcher, Seno Medical Instruments, Inc; Researcher, Identification Solutions, Inc; Researcher, Micrima Limited; Researcher, Medtronic plc; Scientific Advisor, ScreenPoint Medical BV; Scientific Advisor, Transonic Imaging, Inc; Stockholder, Transonic Imaging, Inc

Sub-Events

SSQ01-01 Assessing the Accuracy of an Abbreviated Breast MRI Protocol Compared to a Full MRI Protocol in Women with a Personal History of Breast Cancer

Thursday, Nov. 29 10:30AM - 10:40AM Room: E450A

Participants

Jennifer Gillman, MD, Philadelphia, PA (*Abstract Co-Author*) Nothing to Disclose Emily F. Conant, MD, Philadelphia, PA (*Abstract Co-Author*) Grant, Hologic, Inc; Consultant, Hologic, Inc; Grant, iCAD, Inc; Consultant, iCAD, Inc; Speaker, iiCME Ari Borthakur, PhD,MBA, Philadelphia, PA (*Abstract Co-Author*) Nothing to Disclose Elizabeth S. McDonald, MD, Philadelphia, PA (*Presenter*) Nothing to Disclose Alice Chong, MD, Philadelphia, PA (*Abstract Co-Author*) Nothing to Disclose Susan Weinstein, MD, Philadelphia, PA (*Abstract Co-Author*) Nothing to Disclose

PURPOSE

Women with a personal history of breast cancer have an elevated lifetime risk for a second breast cancer. However, the current American Cancer Society guidelines do not recommend MRI screening in this population. Multiple studies have demonstrated that the sensitivity of Abbreviated breast MRI (AB-MRI) is similar to full diagnostic protocols (FDP-MRI). In this study, we retrospectively evaluate the use of surveillance AB-MRI in women with a personal history of breast cancer.

METHOD AND MATERIALS

An IRB approved and HIPAA compliant reader study was performed on 398 consecutive women with a personal history of breast cancer who underwent full protocol clinical breast MRIs from 9/13-12/15. There were 14 cancers detected (3.8%). An enriched reader study was performed consisting of 68 cases including the 14 cancer cases. Non-cancer cases had at least 1 year of follow-up. Interpretations from a limited image set simulating an AB-MR protocol (T2, pre, and post contrast) were compared with interpretations of the FDP-MRI clinical study.

RESULTS

The AB-MR interpretations were compared with those from the full, clinical protocol. The sensitivity (SN), specificity(SP), positive predictive value (PPV), and the negative predictive value (NPV) for the simulated AB-MR vs the FDP-MRI interpretations were: SN - 50% vs 71%, SP - 96% vs 77%, PPV- 74% vs 43%, NPV - 88% vs. 91%. The mean difference between reader 1 and reader 2 was 0.29 with 95% confidence interval: [-0.33, 0.90]. There were significantly fewer false positives with AB-MRI than FDP-MRI, but more false negatives were observed with AB-MRI.

CONCLUSION

Our preliminary results show higher specificity at the expense of sensitivity in our simulated AB-MRI reads compared to FDP-MRI in women with a history of breast cancer. Further evaluation is warranted.

CLINICAL RELEVANCE/APPLICATION

A simulated AB-MRI protocol resulted in fewer false positive exams than with a full, clinical MR protocol in women with a personal history of breast cancer, however, more research is needed.

sSQ01-02 Abbreviated Breast MRI : 'Ultrafast' DISCO Acquisition for Lesion Characterization

Thursday, Nov. 29 10:40AM - 10:50AM Room: E450A

Awards Student Travel Stipend Award

Participants Audrey Milon, MD, Paris, France (*Presenter*) Nothing to Disclose Isabelle Thomassin-Naggara, MD, Paris, France (*Abstract Co-Author*) Speakers Bureau, General Electric Company Julie Poujol, PhD, Vandoeuvre-les-Nancy, France (*Abstract Co-Author*) Nothing to Disclose Asma Bekhouche, Paris, France (*Abstract Co-Author*) Nothing to Disclose

Saskia Vande Perre, Paris, France (Abstract Co-Author) Nothing to Disclose

For information about this presentation, contact:

audrey.milon.am@gmail.com

PURPOSE

The purpose of our study was to evaluate the diagnostic performance of a dynamic acquisition over-sampling the first minute after contrast administration in an abbreviated dynamic-contrast-enhanced (DCE) breast-MRI.

METHOD AND MATERIALS

153 women were retrospectively consecutively included between July 2016 and March 2017, regardless of indication. All these women had a full breast- MRI protocol, including a DISCO ultrafast acquisition with 7 phases, and an enhanced lesion histologically proven (age= 55 (28-88)). Two readers analyzed 179 lesions (73 benign, 5 B3, 101 malignant lesions) with BIRADS classification for each protocol: an abbreviated protocol (T1-weighted, T2-wheigthed, DISCO, T1-fat suppressed VIBRANT 2mn after contrast administration) and a standard full protocol with late post-contrast phases. Then readers studied DISCO's early enhancement curve with the following semi-quantitative parameters: Wash-In Rate (WIR), Maximal Slope Increase (MSI), Enhancement Amplitude (EA), and Time of Half Rising (THS). Heterogeneity was also assessed using Standard Deviation (STD) at the different DISCO phases.

RESULTS

176/179 (98%) lesions were detected by the abbreviated protocol regarding to the full protocol : 122 mass and 57 non-mass-like enhancement or foci (medium size : 18mm). The 3 undetected lesions were benign. Malignant lesions showed a WIR, a MSI a EA higher, a THS shorter and were more heterogeneous at all DISCO phases than benign lesions (p<0.01). In the group of masses with benign morphology (n=42), THS was shorter for the malignant lesions (39.1 sec) than for the benign lesions (44.6 sec) (p=0.01).

CONCLUSION

Including an additional ultrafast-scan in an abbreviated breast-DCE-MRI protocol enables the early enhancement study that is useful for lesion characterization and is time efficient.

CLINICAL RELEVANCE/APPLICATION

DCE-abbreviated breast-MRI with ultrafast-scan is efficient for lesion detection and characterization; so might be considered as a screening tool in intermediate-risk women.

SSQ01-03 Ultrafast Breast DCE-MRI in the Evaluation of Tumor Size: Potential Utility in Moderate to Marked Background Parenchymal Enhancement

Thursday, Nov. 29 10:50AM - 11:00AM Room: E450A

Participants

Sooyeon Kim, MD, Seoul, Korea, Republic Of (*Presenter*) Nothing to Disclose Nariya Cho, MD, PhD, Seoul, Korea, Republic Of (*Abstract Co-Author*) Nothing to Disclose Rihyeon Kim, MD, Seoul, Korea, Republic Of (*Abstract Co-Author*) Nothing to Disclose Eun Sil Kim, Seoul, Korea, Republic Of (*Abstract Co-Author*) Nothing to Disclose Min Sun Bae, MD, New York, NY (*Abstract Co-Author*) Nothing to Disclose Su Hyun Lee, MD, PhD, Seoul, Korea, Republic Of (*Abstract Co-Author*) Nothing to Disclose Jung Min Chang, MD, Seoul, Korea, Republic Of (*Abstract Co-Author*) Nothing to Disclose Woo Kyung Moon, Seoul, Korea, Republic Of (*Abstract Co-Author*) Nothing to Disclose

For information about this presentation, contact:

river7774@gmail.com

PURPOSE

Ultrafast breast DCE-MRI allows imaging of early kinetics within the first 30 seconds after contrast injection, when the background parenchymal enhancement (BPE) is minimal. This study was performed to explore the clinical utility of ultrafast MRI focusing on tumor size evaluation according to the level of BPE.

METHOD AND MATERIALS

A total of 360 consecutive women (median age, 54 years; range, 26 - 82 years) with 361 tumors (49 DCIS and 312 invasive) who underwent both the ultrafast and conventional breast MRI before surgery were included. Ultrafast MR images were obtained using TWIST or 4D-TRAK sequence (temporal resolution, 4.5 sec; voxel size, $1.1 \times 1.1 \times 1.0$ mm3, TR/TE 4.1/1.3 ms). Then, conventional DCE-MR images were obtained using 3D FLASH sequence (temporal resolution, 90sec; voxel size, $0.8 \times 0.8 \times 1.0$ mm3, TR/TE 4.7/1.7 ms). Tumor size was independently measured on each scan, respectively. Agreement between tumor sizes on MRI and those on surgical histopathology was assessed using the intraclass correlation coefficient (ICC) analysis.

RESULTS

The ICC on ultrafast MRI was comparable to that on conventional MRI (ICC = 0.657 vs. 0.634, P =.598). For conventional MRI, the ICC was lower in women with moderate to marked BPE (ICC = 0.568) than in women with minimal to mild BPE (ICC = 0.650) with borderline significance (P =.080). However, no difference was found on ultrafast MRI (ICC = 0.625 for moderate to marked vs. 0.663 for minimal to mild BPE, P =.385). In women with moderate to marked BPE, the ICC was slightly higher on ultrafast MRI than that on conventional MRI, although the difference was not statistically significant (ICC = 0.625 vs. 0.568, P = .236). No difference was found for the ICC according to the age, menopausal status, family history, histologic type, ER positivity, HER2 positivity, and lesion type on MRI (mass vs. non-mass enhancement) (All P >.05).

CONCLUSION

In women with moderate to marked BPE, tumor size measurement might be more accurate on ultrafast MRI than on conventional MRI.

CLINICAL RELEVANCE/APPLICATION

In women with moderate to marked BPE, ultrafast MRI can be applied for more accurate evaluation of tumor extent.

SSQ01-04 Maximum Slope as a Kinetic Parameter Based on Ultrafast Dynamic Contrast-Enhanced MRI of the Breast Using K-Space Weighted Imaging Contrast

Thursday, Nov. 29 11:00AM - 11:10AM Room: E450A

Participants

Akane Ohashi, Kyoto-hu, Japan (*Presenter*) Nothing to Disclose Masako Y. Kataoka, MD, PhD, Kyoto, Japan (*Abstract Co-Author*) Nothing to Disclose Shotaro Kanao, MD, Kyoto, Japan (*Abstract Co-Author*) Nothing to Disclose Mami Iima, MD, PhD, Kyoto, Japan (*Abstract Co-Author*) Nothing to Disclose Makiko Kawai, MD, Kyoto, Japan (*Abstract Co-Author*) Nothing to Disclose Natsuko Onishi, MD, PhD, New York, NY (*Abstract Co-Author*) Nothing to Disclose Yuta Urushibata, Tokyo, Japan (*Abstract Co-Author*) Nothing to Disclose Katsutoshi Murata, Tokyo, Japan (*Abstract Co-Author*) Nothing to Disclose Elisabeth Weiland, Erlangen, Germany (*Abstract Co-Author*) Nothing to Disclose Kaori Togashi, MD, PhD, Kyoto, Japan (*Abstract Co-Author*) Nothing to Disclose Kaori Togashi, MD, PhD, Kyoto, Japan (*Abstract Co-Author*) Nothing to Disclose Kaori Togashi, MD, PhD, Kyoto, Japan (*Abstract Co-Author*) Research Grant, Bayer AG; Research Grant, DAIICHI SANKYO Group; Research Grant, Eisai Co, Ltd; Research Grant, FUJIFILM Holdings Corporation; Research Grant, Nihon Medi-Physics Co, Ltd; Research Grant, Canon Medical Systems Corporation

For information about this presentation, contact:

amaoh@kuhp.kyoto-u.ac.jp

PURPOSE

To investigate the diagnostic performance and inter-reader agreement of the maximum slope (MS) in breast malignant from benign lesions obtained by ultrafast dynamic contrast-enhanced magnetic resonance imaging (DCE MRI). Comparison with washout index (WI) was performed with the focus on discrepant cases.

METHOD AND MATERIALS

In total, 141 enhancing lesions (89 malignant, 52 benign) were included. Ultrafast DCE MRI sequences were acquired using a kspace-weighted imaging contrast (KWIC) sequence, obtained 0 to 1 min after gadolinium injection (3.75 s/frame; 16 frames) and followed by standard DCE MRI. The MS was calculated its percentage relative enhancement per second (%/s). The inter-reader agreement of MS values by two radiologists were evaluated using intra-class correlation coefficients (ICC). As a semi-quantitative parameter for conventional DCE MRI, washout index (WI: signal intensity [SI] delay - SI early) / SI pre × 100 (%) was calculated. The diagnostic performance (malignant/ benign differentiation) of the MS and WI was compared using ROC analysis.

RESULTS

Intra-class correlation coefficients (ICC) of the reading was 0.98 (95% confidence interval 0.97-0.99) for all, 0.96 (0.95-0.98) for malignant lesions and 0.99 (0.97-0.99) for benign lesions. The average MS was 25.4%/s (standard deviation: SD, 11.2 %/s) for malignant lesions and 11.8%/s (SD, 10.7 %/s) for benign lesions. The AUC of the MS (ICC: 0.98) was almost same as that of the WI (0.83 vs. 0.82, respectively; P = 0.80). Using the optimal cut-off points determined by the Youden index (>9.76% /s for the MS and <-23 % for the WI), MS tended to have higher sensitivity (92.1%) and specificity (65.4%) compared with WI (91.1% and 61.5%, respectively). False positive cases based on MS were FA (n=5) and intraductal papilloma (n=1), while false positive cases based on WI were fibrocystic change (n=6), intraductal papilloma (n=2) and flat epitherial atypia.

CONCLUSION

The overall diagnostic performance of MS in breast lesion was similar to the conventional kinetic parameter, with AUC of over 0.8. Excellent ICC was obtained. MS helped to reduce false positive in fibrocystic change, while FA tended to be false positive on MS.

CLINICAL RELEVANCE/APPLICATION

Our results suggest that maximum slope can be an alternative kinetic parameter to conventional kinetic curve, potentially shorten scan time, with excellent inter-reader agreement.

SSQ01-05 Combination of an Ultrafast TWIST VIBE Dixon Sequence Protocol and Diffusion-Weighted Imaging to a Highly Accurate Clinically Applicable Classification Tool for Suspicious Masses in Breast MRI

Thursday, Nov. 29 11:10AM - 11:20AM Room: E450A

Participants

Stephan Ellmann, MD, Erlangen, Germany (*Presenter*) Nothing to Disclose Sandra Peter, Erlangen, Germany (*Abstract Co-Author*) Nothing to Disclose Evelyn Wenkel, MD, Erlangen, Germany (*Abstract Co-Author*) Nothing to Disclose Elisabeth Weiland, Erlangen, Germany (*Abstract Co-Author*) Employee, Siemens AG Rolf Janka, MD, PhD, Erlangen, Germany (*Abstract Co-Author*) Nothing to Disclose Michael Uder, MD, Erlangen, Germany (*Abstract Co-Author*) Nothing to Disclose Bureau, Bayer AG Research Grant, Siemens AG

PURPOSE

To develop a statistical model for classification of suspicious masses in breast MRI when using TWIST VIBE Dixon (TVD) dynamic sequences in combination with diffusion-weighted imaging (DWI) and compare it to a model based on a combination of conventional dynamic contrast enhancement (DCE) and DWI. As ultrafast TVD sequences offer the potential to shorten breast MRI protocols, diagnostic accuracy might be hampered due to reduced kinetic information. A special focus of this study was thus to maintain high diagnostic accuracy in lesion classification.

METHOD AND MATERIALS

65 patients underwent clinically indicated breast MRI between 02/2014 and 04/2015, with 83 reported lesions (60 malignant, 23 benign). Inclusion criteria were suspicion of breast cancer or pre-therapeutic staging. Patients with non-mass-enhancements only were excluded. The protocol consisted of our institute's standard protocol complemented by an ultrafast TVD sequence. The apparent diffusion coefficient (ADC) and the peak enhancement of the TVD sequences were used to calculate a generalized linear model (GLM) for prediction of malignancy. A second model was calculated using ADC and the curve type derived from the conventional DCE sequence for the sake of comparison. Generalizability was ensured by applying leave-one-out cross validations. For easy application of the GLMs in clinical workflows, nomograms were created.

RESULTS

The GLM based on peak enhancement of the ultrafast TVD sequences and ADC performed comparably accurate to the model based on conventional DCE and ADC (Sensitivity 93.3% vs. 93.3%, specificity 91.3% vs. 87.0%, positive predictive value 96.6% vs. 94.9%, negative predictive value 84.0% vs. 83.3%; no significant differences).

CONCLUSION

This study presents a method to integrate ultrafast TVD sequences into a breast MRI protocol and reduce examination time while maintaining diagnostic accuracy. A GLM based on the combination of TVD-derived peak enhancement and ADC provides high diagnostic accuracy. The GLM can easily be applied in clinical routine using the supplied nomograms.

CLINICAL RELEVANCE/APPLICATION

One limiting factor hampering the comprehensive application of breast MRI is time. This study presents a breast MRI protocol with less than 5 minutes duration along with a classification scheme reaching high diagnostic accuracy. Use of this protocol could improve patient throughput and strenghten the role of breast MRI in screening.

SSQ01-06 Ultrafast Dynamic Contrast-Enhanced MRI for Detection of Invasive Components in Cases of Breast Ductal Carcinoma in Situ by Biopsy

Thursday, Nov. 29 11:20AM - 11:30AM Room: E450A

Participants

Naoko Mori, MD, PhD, Sendai, Japan (*Presenter*) Nothing to Disclose Hiroyuki Abe, MD, Chicago, IL (*Abstract Co-Author*) Nothing to Disclose Shunji Mugikura, MD, PhD, Sendai, Japan (*Abstract Co-Author*) Nothing to Disclose Kei Takase, MD, PhD, Sendai, Japan (*Abstract Co-Author*) Nothing to Disclose

For information about this presentation, contact:

naokomori7127@gmail.com

PURPOSE

To evaluate whether ultrafast dynamic contrast-enhanced (DCE) MRI could identify invasive components in cases with ductal carcinoma in situ (DCIS) diagnosed by percutaneous biopsy.

METHOD AND MATERIALS

Fifty-three consecutive women with 53 lesions diagnosed with DCIS by biopsy underwent IRB-approved ultrafast DCE-MRI including a pre- and 18 post-contrast ultrafast 3D bilateral scans using a 3T system. Ultrafast 3D bilateral scans were acquired with temporal resolution of 3 seconds per image. We evaluated the heterogeneity of enhancement in a target lesion using model-based analysis. Regions of interest (ROIs) were placed where the strongest and weakest signal increases were found in ultrafast DCE-MRI to obtain kinetic curves of maximum and minimum enhancement, respectively. The kinetic curve obtained from ultrafast DCE-MRI was analyzed using an empirical mathematical model: $\Delta S(t) = A^*(1-e-at)$. Where A is the upper limit of the signal intensity, a (min-1) is the rate of signal increase. The initial slope of the kinetic curve is given by 'A*a'. Amax, Amin, amax, amin, A*amax, and A*amin were obtained from ROIs for maximum and minimum enhancement, respectively. We obtained the following derivations for diagnostic parameters showing heterogeneity of enhancement: A difference=Amax - Amin; a difference= amax - amin; A*a difference= A*amax - A*amin.

RESULTS

Surgical specimens revealed 32 lesions with pure DCIS and the remaining 21 lesions with DCIS with invasive components (DCIS-IC). The A difference for DCIS-IC (132 ± 235) was significantly higher than that of pure DCIS (49 ± 34) (p = 0.013). No significant difference was found for a difference and A*a difference (p = 0.24 and 0.46, respectively). Receiver operating curve analysis revealed that the area under the curve of A difference was 0.70. The most effective threshold for A difference was 68, and the sensitivity, specificity, positive predictive value and negative predictive value were 62% (13/21), 72% (23/32), 59% (13/22), and 74% (23/31), respectively.

CONCLUSION

The A difference could suggest the presence of invasive components in cases with DCIS diagnosed by biopsy.

CLINICAL RELEVANCE/APPLICATION

The A difference showing the heterogeneity of enhancement of lesions in ultrafast DCE-MRI might suggest the presence of invasive components in cases of DCIS by biopsy.

SSQ01-07 Ultrafast Dynamic Contrast Enhanced Breast MRI in Differentiating between Subcentimeter Carcinomas and Benign Lesions: Quantitative versus Qualitative Assessments

Thursday, Nov. 29 11:30AM - 11:40AM Room: E450A

Participants

Natsuko Onishi, MD, PhD, New York, NY (*Presenter*) Nothing to Disclose Meredith Sadinski, PhD, New York, NY (*Abstract Co-Author*) Nothing to Disclose Peter Gibbs, BSC,PhD, New York, NY (*Abstract Co-Author*) Nothing to Disclose Katherine M. Gallagher, MD, Boston, MA (*Abstract Co-Author*) Nothing to Disclose Mary C. Hughes, MD, New York, NY (*Abstract Co-Author*) Nothing to Disclose Theodore M. Hunt, New York, NY (*Abstract Co-Author*) Nothing to Disclose Danny F. Martinez, BSC,MSc, New York, NY (*Abstract Co-Author*) Nothing to Disclose Amita Shukla-Dave, PhD, New York, NY (*Abstract Co-Author*) Nothing to Disclose Elizabeth A. Morris, MD, New York, NY (*Abstract Co-Author*) Nothing to Disclose Elizabeth J. Sutton, MD, New York, NY (*Abstract Co-Author*) Nothing to Disclose

For information about this presentation, contact:

natsucom1981@gmail.com

PURPOSE

Ultrafast dynamic contrast enhanced (UF-DCE) breast MRI, characterized by high temporal and spatial resolution, enables image acquisition at multiple time points starting simultaneously with the beginning of contrast injection. In a preliminary study comparing several quantitative parameters calculated from UF-DCE MRI, we determined bolus arrival time (BAT) and maximum slope (MS) were most useful in the differentiation between subcentimeter carcinomas and benign lesions. This study aims to compare the performance of these parameters with qualitative assessments of UF-DCE MRI.

METHOD AND MATERIALS

We identified female patients between February-October 2017 with a: 1) UF-DCE MRI as part of hybrid protocol with conventional DCE MRI performed with a 3.0T MRI with a 16-ch coil and 2) biopsy proven BI-RADS 4-6 lesion. UF-DCE MRI were acquired continuously 15 times during the approximately 60 sec (temporal resolution, 3.0-4.3 sec) starting simultaneously with the beginning of contrast injection. BAT and MS were computationally calculated based on 3D volumetric segmentation. Qualitative assessments were visually performed by a reader, identifying the time from scan start to the beginning of lesion enhancement (vBAT) and evaluating the degree of enhancement relative to background parenchymal enhancement (vE) by a 4-point grading scale from 'prominent' to 'indistinguishable'. Wilcoxon signed-rank test or Pearson's chi-squared test were used for the statistical analyses. P value <0.05 was considered satistically significant. The diagnostic performance was evaluated using areas under the receiver operating characteristic curve (AUC).

RESULTS

In total, 77 subcentimeter lesions (carcinomas, 33 [43%]; benign lesions, 44 [57%]) were analyzed. BAT, MS and vBAT presented significant difference between carcinomas and benign lesions (p=0.0004, p<.0001, p=0.0063), while vE did not (p=0.0607). AUCs of BAT (0.737) and MS (0.790) were higher than those of vBAT (0.683) and vE (0.605).

CONCLUSION

Quantitative assessments of UF-DCE MRI presented higher performance than qualitative assessments in differentiating between subcentimeter carcinomas and benign lesions.

CLINICAL RELEVANCE/APPLICATION

There is no standardized way to evaluate ultrafast DCE breast MRI. Although diagnostic utility of some quantitative parameters is known, little is known about the performance of qualitative assessment, especially for subcentimeter lesions.

SSQ01-08 Comparison of Machine Learning Based Measurement and Visual Assessment of Fibroglandular Tissue and Background Parenchymal Enhancement in Breast MR Imaging: A Preliminary Study

Thursday, Nov. 29 11:40AM - 11:50AM Room: E450A

Participants Heeyoung Chung, Seoul, Korea, Republic Of (*Presenter*) Nothing to Disclose Sung-Hun Kim, MD, Seoul, Korea, Republic Of (*Abstract Co-Author*) Nothing to Disclose Yoonho Nam, Seoul, Korea, Republic Of (*Abstract Co-Author*) Nothing to Disclose Ga-Eun Park, MD, Seoul, Korea, Republic Of (*Abstract Co-Author*) Nothing to Disclose

For information about this presentation, contact:

hoonhoony@naver.com

PURPOSE

To design and validate a machine learning model for the measurement of fibroglandular tissue (FGT) and background parenchymal enhancement (BPE) in breast MR imaging, and compare with estimation of radiologist according to BI-RADS categories.

METHOD AND MATERIALS

195 women (mean age, 54.9 years; range 30 - 86 years) who were diagnosed with invasive breast cancer and underwent preoperative breast MR, between January and December 2017 were enrolled in this study. Two radiologists independently assessed the categories of FGT and BPE of contralateral breast, using with axial precontrast, early dynamic contrast enhancement T1-weighted image, and subtraction image between them. In case of discordance, two radiologists reached consensus. Machine learning model was designed to measure the volume of whole breast, FGT and BPE, using nonnegative matrix factorization (NMF). In this study, 50 and 145 samples were assigned to train and valid, respectively. Areas under the receiver operating characteristic curve was used to assess model performance of predicting dense breast (FGT category c, d) and prominent BPE (BPE category c, d). Correlation between the visual assessment of radiologist and machine learning based measurement was assessed using Spearman correlation analysis.

RESULTS

With the machine learning model, AUC of prediction of dense breast were 0.971 (0.880-0.998) in training set and 0.902 (0.784-0.968) in validation set. AUC of prediction of prominent BPE were 0.959 (0.912-0.985) in training set and 0.819 (0.746-0.848) in validation set (P < .001). Correlation between machine learning based measurement and visual assessment by radiologist was r = 0.871 of FGT, and r = 0.523 of BPE, respectively (P < .001).

CONCLUSION

Machine learning model showed reliable predictive power for FGT and BPE assessment and close correlation with FGT assessment by radiologist.

CLINICAL RELEVANCE/APPLICATION

FGT and BPE are known as risk factors for breast cancer and are associated with poor prognosis. Machine learning can provide quantitative and objective information of FGT and BPE volume in breast MR imaging and can be helpful to predict patient's prognosis.

SSQ01-09 Deep Learning of Breast MRI Tumor Volume Improves Tumor Proliferation Marker Ki-67 Estimation

Thursday, Nov. 29 11:50AM - 12:00PM Room: E450A

Participants

Dooman Arefan, PhD, Pittsburgh, PA (*Presenter*) Nothing to Disclose Aly A. Mohamed, PhD, Pittsburgh, PA (*Abstract Co-Author*) Nothing to Disclose Hong Peng, MD, Xiangtan, China (*Abstract Co-Author*) Nothing to Disclose Wendie A. Berg, MD, PhD, Pittsburgh, PA (*Abstract Co-Author*) Nothing to Disclose Jules H. Sumkin, DO, Pittsburgh, PA (*Abstract Co-Author*) Research Grant, Hologic, Inc; Research Grant, General Electric Company Shandong Wu, PhD, MSc, Philadelphia, PA (*Abstract Co-Author*) Nothing to Disclose

For information about this presentation, contact:

wus3@upmc.edu

PURPOSE

Ki-67 is a commonly used immunohistochemistry marker for cellular proliferation in invasive tumors. A few recent studies showed some association between Ki-67 and DCE-MR imaging features. We performed an investigation to compare effects of a 3D deep learning approach versus conventional radiomic features in deriving breast DCE-MRI information to predict Ki-67 rate.

METHOD AND MATERIALS

In an IRB-approved retrospective study of 141 patients, we identified 141 breast DCE-MRI scans (2011-2016) at our institution. All patients have the Ki-67 proliferation rates measured that are further categorized into High vs Low category according to a clinically defined threshold of 14. Breast tumor volume were automatically segmented in 3D space from the first post-contrast breast MR sequence images. From the segmented 3D tumor volume, we extracted 30 common radiomic features, including morphological and contrast enhancement kinetic characteristics of the tumor volume; those features were fed to a logistic least absolute shrinkage and selection operator (LASSO) regression model to predict High vs Low Ki-67 categories. Also, a 3D convolutional neural network (CNN) deep learning model was used to perform the same prediction but directly using the original image of the segmented 3D tumor volume (i.e., here no any pre-defined imaging features extracted nor used). We performed 10-fold cross-validation for both logistic regression and deep learning model evaluation and used average AUC as the metric of model classification accuracy.

RESULTS

There are 102 and 39 patients in the High and Low Ki-67 category, respectively. The average of the Ki-67 was $28.05\% \pm 21.63$. The AUC of the logistic regression model was 0.74 (95% CI: 0.73-0.75) for 4 LASSO-selected top ranked radiomic features (1 morphological and 3 contrast-enhancement related), while the 3D deep learning model achieved an AUC of 0.80 (95% CI: 0.75-0.85).

CONCLUSION

In this study, the 3D CNN deep learning-based approach that automatically identifies and organizes hierarchical imaging features for predicting Ki-67 outperformed the LASSO regression model coupled with pre-defined radiomic features.

CLINICAL RELEVANCE/APPLICATION

Deep learning of breast DCE-MRI tumor volume using CNN models may improve interpretation on the association between radiological images and the immunohistochemistry tumor proliferation marker Ki-67.



ML51

Machine Learning Theater: Programming Clinical AI with Simulation: Presented by Riverain Technologies

Thursday, Nov. 29 11:00AM - 11:20AM Room: Machine Learning Showcase North Hall

Participants

Jason Knapp, Beavercreek, OH (Presenter) Employee, iCAD, Inc, Nashua, NH

PROGRAM INFORMATION

The increasing realization that AI will replace many aspects of conventional software development has been dubbed "software 2.0," where the software derives not from human programmers, but neural networks trained with large datasets. This paradigm shift is rapidly being applied to the medical imaging domain. The great diversity found in medical use cases, combined with challenges in acquiring adequate amounts of data to span those use cases with the necessary labels, presents unique challenges that lead to sub-optimal solutions, slower adoption and user disillusionment with fielded systems. In this talk, we present work that demonstrates how successful AI models can be built from simulated cases of disease. Along the way, we'll highlight the many advantages simulation has to offer and contrast these with the current approach to AI development in common use.



Machine Learning Theater: From Artificial Intelligence to Augmented Intelligence: The Role of Medical Imaging in Diagnosis: Presented by Shenzhen Imsight Medical Technology Co., Ltd

Thursday, Nov. 29 11:30AM - 11:50AM Room: Machine Learning Showcase North Hall

PROGRAM INFORMATION

In this presentation, Dr. Chen will show the advanced deep-learning techniques from Imsight and elaborate the results into clinical applications such as lung cancer diagnosis, liver tumor diagnosis and bone fracture detection, etc.



Machine Learning Theater: State-of-the-art Deep Learning for Breast Cancer Screening: Presented by Kheiron Medical Technologies

Thursday, Nov. 29 12:00PM - 12:20PM Room: Machine Learning Showcase North Hall

Participants

Tobias Rijken, London, United Kingdom (Presenter) Stockholder, Kheiron Medical Technologies Ltd

Program Information

Kheiron is at the cutting edge of deep learning technology for breast cancer screening. This session will cover our multi-site clinical trial, and how we have achieved state-of-the-art results using deep learning technology. In addition, we will discuss: - data processing at scale - deep learning infrastructures - the future of breast screening empowered by deep learning.



AIS-THA

Artificial Intelligence Thursday Poster Discussions

Thursday, Nov. 29 12:15PM - 12:45PM Room: AI Community, Learning Center

IN

Participants

Igor R. Dos Santos, MD, Sao Paulo, Brazil (Moderator) Nothing to Disclose

Sub-Events

AI230-SD- Support Vector Machine Model for Stratification of Liver Stiffness using Clinical Data

Station #1 Participants

Hailong Li, PhD, Cincinnati, OH (*Presenter*) Nothing to Disclose
Lili He, Cincinnati, OH (*Abstract Co-Author*) Nothing to Disclose
Thomas Maloney, Cincinnati, OH (*Abstract Co-Author*) Nothing to Disclose
Jonathan Dudley, Cincinnati, OH (*Abstract Co-Author*) Nothing to Disclose
Samuel L. Brady, PHD, Cincinnati, OH (*Abstract Co-Author*) Nothing to Disclose
Elanchezhian Somasundaram, Cincinnati, OH (*Abstract Co-Author*) Nothing to Disclose
Jonathan R. Dillman, MD, Cincinnati, OH (*Abstract Co-Author*) Research Grant, Siemens AG; Research Grant, Guerbet SA; Travel support, Koninklijke Philips NV; Research Grant, Canon Medical Systems Corporation; Research Grant, Bracco Group

For information about this presentation, contact:

Hailong.Li@cchmc.org

PURPOSE

To determine if a support vector machine (SVM) learning model can categorically classify MR elastography (MRE)-derived liver stiffness using clinical data from pediatric and young adult patients with chronic liver diseases.

METHOD AND MATERIALS

Clinical data. An IRB approved waiver of consent was obtained for this retrospective study. Clinical data (33 features) and MRE liver stiffness measurements from 362 chronic liver disease patients (mean age =14.2 yrs) were obtained. Clinical data were retrieved from our medical record system (Epic Systems Corporation; Verona, WI), including four domains: 1) demographics/vital signs (e.g., sex, age, weight, height, blood pressure); 2) medical history (e.g., diabetes mellitus [types I and II], non-alcoholic fatty liver disease [NAFLD], biliary atresia, Alagille syndrome, sclerosing cholangitis, cystic fibrosis, Fontan operation); 3) blood tests (e.g., bilirubin [total and direct], ALT, AST, GGT, albumin, platelet, APRI, FIB-4); and 4) MRI biomarkers (e.g., liver volume, liver proton density fat fraction) from imaging reports. MRE liver stiffness measurements were extracted from imaging reports. Patients were divided into two groups (<3 kPa=no/mild vs. >=3 kPa=moderate/severe liver stiffening). Machine learning model. Given clinical data and group label, the SVM model was trained to classify a given patient into either a no/mild or moderate/severe liver stiffness group (Figure (A)). Leave-one-out cross-validation was used. The performance was assessed using accuracy, sensitivity, specificity, and area under the receiver operating characteristic curve (AUC).

RESULTS

Classification results for our SVM model are shown in the Figure (B). Our model was able to correctly classify patients with an accuracy of 82%. This SVM model achieved an AUC of 0.85, with a sensitivity of 76% and a specificity of 86%. The most important features that contributed to stiffness classification are presented in the Figure (C).

CONCLUSION

Using only clinical data, an SVM model was able to stratify pediatric and young adult chronic liver disease patients into different liver stiffness groups. Future model improvements will include the incorporation of anatomic imaging features.

CLINICAL RELEVANCE/APPLICATION

Machine learning can use clinical data to categorically predict liver stiffness. Model refinements and incorporation of anatomic imaging features may soon decrease the need for MR elastography.

Honored Educators

Presenters or authors on this event have been recognized as RSNA Honored Educators for participating in multiple qualifying educational activities. Honored Educators are invested in furthering the profession of radiology by delivering high-quality educational content in their field of study. Learn how you can become an honored educator by visiting the website at: https://www.rsna.org/Honored-Educator-Award/ Jonathan R. Dillman, MD - 2016 Honored Educator

AI231-SD-THA2 Markerless Tumor Tracking for Hepatocellular Carcinoma Using Fluoroscopic Imaging with a Deep Neural Network

Station #2

Ryusuke Hirai, MENG, Kawasaki, Japan (*Presenter*) Employee, Toshiba Corporation Akiyuki Tanizawa, Kawasaki, Japan (*Abstract Co-Author*) Employee, Canon Medical Systems Corporation Yukinobu Sakata, Kawasaki, Japan (*Abstract Co-Author*) Employee, Toshiba Corporation Shinichiro Mori, Chiba, Japan (*Abstract Co-Author*) Nothing to Disclose

For information about this presentation, contact:

ryusuke.hirai@toshiba.co.jp

PURPOSE

To improve the treatment accuracy of particle-beam therapy by minimizing the effect of respiratory-induced target motion, it is necessary to directly capture tumor position during treatment. Several studies have investigated markerless lung tumor tracking by tumor image pattern learning. However, such pattern learning is limited to some extent by the low contrast of fluoroscopic images in the abdominal region. Here, we have developed a new tumor tracking method for liver cancer treatment by using fluoroscopic images with a deep neural network.

METHOD AND MATERIALS

Our method comprised a learning stage and a tracking stage. In the learning stage, we constructed the network using training datasets to estimate a tumor position map from the input image pattern. To prepare the training data, we used treatment planning four-dimensional computed tomography (4DCT). The tumor position on 4DCT was contoured in each phase by a certificated oncologist. To compile the training dataset, we sampled the tumor centroid and image pattern from digitally reconstructed radiographs from 4DCT. The intensity of the tumor position map for training was calculated using a 2D Gaussian kernel with mean of the tumor centroid and variance of *W*2/8, where *W* is the width or height of the map. In the tracking stage, we input the same position of the image pattern in the fluoroscopic image to the network to obtain the tumor position map. The centroid of tumor position was calculated using the map. The tumor position in 3D space could be derived using paired X-ray fluoroscopic images. Our method has been quantified using fluoroscopic image datasets from two cases of liver cancer. The tumor was tracked by our method and positional error was evaluated as the Euclidean distance between the calculated tumor position and the actual position input by a certificated oncologist.

RESULTS

Mean positional errors were 1.43 ± 0.39 mm and 1.87 ± 1.01 mm for the first and second cases, respectively. The calculation time was less than 24.4 ms/frame.

CONCLUSION

Our proposed algorithm achieved high accuracy and a short computation time, we expect that our method will be useful in improving gate treatment accuracy.

CLINICAL RELEVANCE/APPLICATION

Our proposed method required planning 4DCT at the learning stage only, and successfully tracked tumor position in real time without preventing treatment throughput.

AI232-SD-THA3 Morphological Classification of the Cortical Bone Layer Using Deep Learning in Panoramic Radiography

Station #3

Participants Wataru Nishiyama, DDS, Gifu, Japan (*Presenter*) Nothing to Disclose Yudai Yanashita, Gifu, Japan (*Abstract Co-Author*) Nothing to Disclose Chisako Muramatsu, PhD, Gifu, Japan (*Abstract Co-Author*) Nothing to Disclose Fujita Hiroshi, Gifu, Japan (*Abstract Co-Author*) Nothing to Disclose Akitoshi Katsumata, DDS, PhD, Mizuho, Japan (*Abstract Co-Author*) Nothing to Disclose

For information about this presentation, contact:

wataru@dent.asahi-u.ac.jp

PURPOSE

A rough inner surface of the mandible cortical bone layer is observed in patients with osteoporosis. Meta-analyses studies demonstrated that the mandibular cortical index (MCI) classification is useful to screen for osteoporosis. The MCI consists of normal cortex (Class 1), mildly to moderately eroded cortex (Class 2), and severely eroded cortex (Class 3). There are several previous studies regarding conventional machine learning or rule-based methods to automatically classify based on the MCI. To improve the accuracy of MCI classification, we applied the convolutional neural networks (CNN) method.

METHOD AND MATERIALS

An image database consisting of 205 panoramic radiography images, in which MCI classification was determined based on agreement among three experienced dental radiologists, was used to test the CNN method. The database consisted of 78, 67, and 60 cases of Class 1, Class 2, and Class 3, respectively. Bilateral regions of interest (ROIs) were set in the mental foramen region. Caffe was used as the deep learning framework.

RESULTS

A restrictive ROI setting in the cortical bone demonstrated higher classification accuracy than wider ROI settings including the teeth. The classification accuracy for separating the cases into the three classes was approximately 80%. Approximately 90% accuracy was observed for the differentiation between Class 1 and the other two classes, and between Class 3 and the other two classes.

CONCLUSION

In the present study, differentiation between Class 2 and the other two classes yielded the lowest accuracy. This was similar with the previously reported MCI classification using rule-based methods. In addition, the inter-observer agreement among several radiologists was low for diagnosing Class 2. These results suggest that the diagnostic criteria for Class 2, i.e., "the inner margin has resorption cavities with cortical residues one to three layers thick on one or both sides", should be revised.

CLINICAL RELEVANCE/APPLICATION

Morphological evaluation techniques for jaw bones are essential to screen both new osteoporosis patients and patients suspected of having medication-related osteonecrosis of the jaw. In addition, osteoporosis is important for dental implants and periodontitis treatment because their success largely depends on the quality and quantity of the bone.

AI150-ED- Emerging Approaches for Applying Artificial Intelligence in Neuroradiology

Station #4

Participants Jeffrey Rudie, MD, PhD, Philadelphia, PA (*Presenter*) Nothing to Disclose Andreas M. Rauschecker, MD,PhD, Philadelphia, PA (*Abstract Co-Author*) Nothing to Disclose R. Nick Bryan, MD, PhD, Austin, TX (*Abstract Co-Author*) Stockholder, Galileo CDS, Inc Officer, Galileo CDS, Inc James C. Gee, PhD, Philadelphia, PA (*Abstract Co-Author*) Nothing to Disclose Christos Davatzikos, PhD, Philadelphia, PA (*Abstract Co-Author*) Nothing to Disclose Suyash Mohan, MD, Philadelphia, PA (*Abstract Co-Author*) Grant, NovoCure Ltd; Grant, Galileo CDS, Inc

For information about this presentation, contact:

Jeff.Rudie@gmail.com

TEACHING POINTS

With the recent exponential growth of computational efficiency, artificial intelligence (AI) has become a hot topic in nearly all technology-related fields, including health care and radiology. Undoubtedly, radiological practice will substantially change as more AI technology is adopted into everyday use. In this exhibit, we will review various forms of artificial intelligence currently under development by our group in neuroradiology. We will (1) discuss relative advantages and disadvantages of different AI implementations and (2) highlight how targeted use of different methods for different purposes has the potential to significantly improve both the efficiency and quality of clinical practice in the near future.

TABLE OF CONTENTS/OUTLINE

1) Artificial Intelligence Methods - Bayesian Networks - Decision Trees - Support Vector Machines - Deep Learning/Convolutional Neural Networks 2) Automated Segmentation Methods - Deep Gray Nuclei and White Matter Lesion Segmentation - Brain Tumor Segmentation 3) Clinical Uses for AI in Neuroradiology - Neuro-oncologic Applications: Response Assessment, Molecular Subtypes and Prognostication - Differential Diagnosis Clinical Decision Support - Automated Draft Report Generation

AI015-EB Combining Genomic and Clinical/Dosimetric Variables to Predict Radiation Toxicity in Localized Prostate Cancer Patients Via Computational Genomics and Machine Learning

All Day Room: AI Community, Learning Center

Participants

John Kang, MD, PhD, Rochester, NY (Presenter) Nothing to Disclose

Robert Strawderman, DSc, Rochester, NY (Abstract Co-Author) Nothing to Disclose

Russell Schwartz, PhD, Pittsburgh, PA (*Abstract Co-Author*) Research Grant, University of Pittsburgh Medical Center Enterprises (UPMC-E)

Issam El Naga, PHD, Ann Arbor, MI (Abstract Co-Author) Scientific Advisory Board, Endectra, LLC

Thomas Mariani, PhD, Rochester, NY (Abstract Co-Author) Nothing to Disclose

Sarah L. Kerns, PhD, MPH, New York, NY (Abstract Co-Author) Nothing to Disclose

Meet the Author: The authors of this poster will be available in person to discuss their project during these times: Thursday November 29 12:15-12:45pm

Poster Information

Prostate cancer is the most common non-cutaneous cancer and third most deadly cancer in men in the United States. External beam radiotherapy is an effective treatment, but doses are set to limit the population-level incidence of significant toxicity to <5-10% of patients. Currently, there are no validated tools to predict an individual's risk of toxicity and patients are generally treated uniformly. In this project, we will apply machine learning and hypothesis testing to genomic, clinical and dosimetric data from randomized trials to create a predictor of an individual's toxicity. This tool will provide men with upfront information about their personal risk of toxicity to prostate radiotherapy in order to better inform their treatment decision making.



Machine Learning Theater: Towards Intelligent Healthcare: Presented by NVIDIA

Thursday, Nov. 29 12:30PM - 12:50PM Room: Machine Learning Showcase North Hall

Participants

Kimberly Powell, Vice President, Healthcare

Program Information

From self-driving cars to intelligent instruments, the unprecedented innovations made possible by AI are being applied to new health care initiatives and driving opportunities to deliver advances in medical diagnosis and treatment to improve access and outcomes.



RCA53

Leveraging Machine Learning Techniques and Predictive Analytics for Knowledge Discovery in Radiology (Hands-on)

Thursday, Nov. 29 12:30PM - 2:00PM Room: S401AB



AMA PRA Category 1 Credits ™: 1.50 ARRT Category A+ Credit: 1.75

Participants

Kevin Mader, DPhil,MSc, Basel, Switzerland (*Moderator*) Employee, 4Quant Ltd; Shareholder, 4Quant Ltd Kevin Mader, DPhil,MSc, Basel, Switzerland (*Presenter*) Employee, 4Quant Ltd; Shareholder, 4Quant Ltd Barbaros S. Erdal, PhD, Columbus, OH (*Presenter*) Nothing to Disclose Joshy Cyriac, Basel, Switzerland (*Presenter*) Nothing to Disclose

LEARNING OBJECTIVES

1) Review the basic principles of predictive analytics. 2) Be exposed to some of the existing validation methodologies to test predictive models. 3) Understand how to incorporate radiology data sources (PACS, RIS, etc) into predictive modeling. 4) Learn how to interpret results and make visualizations.

ABSTRACT

During this course, an introduction to machine learning and predictive analytics will be provided through hands on examples on imaging metadata (scan settings, configuration, timestamps, etc). Participants will use open source as well as freely available commercial platforms in order to achieve tasks such as image metadata and feature extraction, statistical analysis, building models, and validating them. Imaging samples will include datasets from a variety of modalities (CT, PET, MR) and scanners. The course will begin with a brief overview of important concepts and links to more detailed references. The concepts will then be directly applied in visual, easily understood workflows where the participants will see how the data are processed, features are selected, and models are built.



AIS-THB

Artificial Intelligence Thursday Poster Discussions

Thursday, Nov. 29 12:45PM - 1:15PM Room: AI Community, Learning Center

IN

Participants

Igor R. Dos Santos, MD, Sao Paulo, Brazil (Moderator) Nothing to Disclose

Sub-Events

AI234-SD- CT Image Enhancement for Lesion Segmentation Using Stacked Generative Adversarial Networks THB1

Station #1 Participants

Youbao Tang, PhD, Bethesda, MD (*Presenter*) Nothing to Disclose Jinzheng Cai, Gainesville, FL (*Abstract Co-Author*) Nothing to Disclose Le Lu, Bethesda, MD (*Abstract Co-Author*) Employee, NVIDIA Corporation Adam P. Harrison, PhD, Bethesda, MD (*Abstract Co-Author*) Nothing to Disclose Ke Yan, Bethesda, MD (*Abstract Co-Author*) Nothing to Disclose Jing Xiao, Shenzhen, China (*Abstract Co-Author*) Nothing to Disclose Lin Yang, Gainesville, FL (*Abstract Co-Author*) Nothing to Disclose Ronald M. Summers, MD, PhD, Bethesda, MD (*Abstract Co-Author*) Royalties, iCAD, Inc; Royalties, Koninklijke Philips NV; Royalties, ScanMed, LLC; Research support, Ping An Insurance Company of China, Ltd; Researcher, Carestream Health, Inc; Research support, NVIDIA Corporation; ; ; ;

For information about this presentation, contact:

youbao.tang@nih.gov

PURPOSE

Automated lesion segmentation from computed tomography (CT) is an important and challenging task in medical image analysis. As more and more elaborately designed segmentation methods are proposed, performance improvement may plateau. One hurdle is that CT images can exhibit high noise and low contrast, particularly in lower dosages. The collection of datasets more massive than currently available may provide the means to overcome this, but this eventuality is not guaranteed, particularly given the labor involved in manually annotating training images. We take a different tack, and instead leverage the massive amounts of data already residing in hospital PACS to develop a method to enhance CT images in a way that benefits lesion segmentation.

METHOD AND MATERIALS

A stacked generative adversarial networks (SGAN) approach is proposed for CT image enhancement (IE). Instead of directly performing IE, our SGAN decomposes IE into two sub-tasks, i.e., image denoising followed by enhancement. The first GAN reduces the noise in the CT image and the second GAN generates a higher resolution image with enhanced boundaries and high contrast. To make up for the absence of high quality CT images, we detail how to synthesize a large number of low- and high-quality natural images and use transfer learning with progressively larger amounts of CT images. We apply both the classic GrabCut method and the modern holistically nested network (HNN) to lesion segmentation, testing whether SGAN can yield improved lesion segmentation. The experiments are conducted on a large scale dataset containing 32,735 lesion images from 4,459 patients, where 1,000 lesions from 500 patients are manually segmented as a testing set.

RESULTS

The Dice scores of GrabCut/HNN are improved from 0.908/906 to 0.913/0.92 when using SGAN enhanced images. And compared with other enhanced approaches, using SGAN gets the best segmentation performance.

CONCLUSION

The results demonstrate that SGAN is effective in yielding improved lesion segmentation performance and SGAN enhancements alone can push GrabCut performance over HNN trained on original images, suggesting that focusing on dataset processing is a crucial research direction in medical imaging analysis.

CLINICAL RELEVANCE/APPLICATION

The SGAN enhanced images can provide auxiliary information to help radiologists for making decision and the improved segmentation performance can strengthen some CAD tasks, e.g. tumor growth evaluation.

AI151-ED-THB2 A Two-Stage Deep-Learning Scheme for Reducing Radiation Dose in Digital Breast Tomosynthesis (DBT)

Station #2

Participants Junchi Liu, MS, Chicago, IL (*Abstract Co-Author*) Nothing to Disclose Amin Zarshenas, MSc, Chicago, IL (*Abstract Co-Author*) Nothing to Disclose Syed Ammar Qadir, Chicago, IL (*Abstract Co-Author*) Nothing to Disclose Limin Yang, MD, PhD, Iowa City, IA (*Abstract Co-Author*) Nothing to Disclose Laurie L. Fajardo, MD, MBA, Park City, UT (*Abstract Co-Author*) Consultant, Hologic, Inc; Consultant, Siemens AG; Consultant, FUJIFILM Holdings Corporation;

Kenji Suzuki, PhD, Chicago, IL (*Presenter*) Royalties, General Electric Company; Royalties, Hologic, Inc; Royalties, MEDIAN Technologies; Royalties, Riverain Technologies, LLC; Royalties, Canon Medical Systems Corporation; Royalties, Mitsubishi Corporation; Royalties, AlgoMedica, Inc

For information about this presentation, contact:

jliu118@hawk.iit.edu

TEACHING POINTS

1) To understand the basic principles of our original neural network convolution (NNC) deep learning. 2) To understand our twostage deep-learning scheme based on two sequential NNC models for substantial reduction of radiation dose in DBT. 3) To demonstrate and compare the image quality of our "virtual" high-dose (VHD) images generated from lower-dose acquisitions to that of real clinical full-dose images in DBT. 4) To understand the clinical utility of our technology for reducing radiation dose in DBT.

TABLE OF CONTENTS/OUTLINE

A. Radiation dose issues with breast cancer screening in DBTB. Basic principles of NNC deep learning1) Patched-based neural network regression2) Processing of entire image in convolutional mannerC. NNC deep learning for dose reduction in DBT1) A two-stage deep-learning scheme consisting of two NNC models2) Training 1st NNC with raw projection images3) Training 2nd NNC with reconstructed DBT slicesD. Quantitative evaluation: Image quality vs. radiation dose reduction1) Evaluation of 51 non-training clinical cases2) 74% dose reduction rate of 1st NNC 3) 89% dose reduction rate of 2nd NNC 4) Processing time of 0.24 sec on a GPU for each studyE. Benefits and limitations of our radiation dose reduction technology for DBT

AI024-EC- Anatomical Borderline Structure Detection in Chest X-Ray by Deep Neural Networks

Custom Application Computer Demonstration

Participants Shinichi Fujimoto, MS,RT, Yoshida, Japan (*Presenter*) Nothing to Disclose Kenji Kondo, Tsukuba, Japan (*Abstract Co-Author*) Employee, Panasonic Corporation Harumi Itou, Yoshida, Japan (*Abstract Co-Author*) Nothing to Disclose Hirohiko Kimura, MD, PhD, Fukui, Japan (*Abstract Co-Author*) Nothing to Disclose Toshiki Adachi, RT, Yoshidagun, Japan (*Abstract Co-Author*) Nothing to Disclose Masakai Kiyono, Fukui, Japan (*Abstract Co-Author*) Employee, Panasonic Corporation Masato Tanaka, PhD, Yoshida, Japan (*Abstract Co-Author*) Nothing to Disclose Jun Ozawa, PhD, Tsukuba, Japan (*Abstract Co-Author*) Nothing to Disclose

For information about this presentation, contact:

sfuji@u-fukui.ac.jp

CONCLUSION

We implemented and evaluated an ABS detection algorithm for CXR. For normal cases, we showed good detection performance. For abnormal cases, borderlines of DA, LV, LD, and RLB could only be partially extracted. Our work supports further development of anomaly detection based on ABSs' changes due to disease.

FIGURE

http://abstract.rsna.org/uploads/2018/18006874/18006874_az5g.jpg

Background

Chest X-ray (CXR) is used for screening and diagnosis of many lung diseases. Conventional computer-aided diagnosis (CAD) methods for CXR involve analysis of predetermined target lesions; thus, those methods poorly manage unknown lesions. Hence, we are building a new CAD method to model normal local anatomical structures and their borderlines with the lung field [known as "anatomical borderline structures" (ABSs)] and to detect anomalies based on changes due to disease. Here, we implement and evaluate ABS detection in CXR as semantic segmentation tasks by deep neural networks.

Evaluation

We chose U-Net, a fully convolutional network, as ABS detection network, and selected the first thoracic vertebra (Th1), descending aorta (DA), left ventricle (LV), left diaphragm (LD), and dorsal portion of right lung base (RLB) as ABSs for detection. From CXR, each of five U-Nets outputs a region image of each respective ABS. A total of 627 normal cases were used to train five U-Nets; 70 normal and 143 abnormal cases were used for evaluation. For each normal CXR, mask images of the five ABSs were manually created, then used for training and evaluation. Detection accuracy for 70 normal cases was evaluated by Dice coefficient (DC). Average DC was 0.91 for Th1 (anatomical structure alone), and 0.71-0.81 for borderlines between anatomical structure (i.e., DA, LV, LD, or RLB) and the lung field. A total of 143 abnormal cases were visually evaluated. For example, in cases of pneumonia, partial to whole borderlines of DA, LV, LD, and RLB could not be extracted.

Discussion

Detection results for normal cases were sufficient for use in our CXR-CAD. For abnormal cases, partial to whole ABSs could not be extracted. Thus, we demonstrated the feasibility of our anomaly detection method for CXR. We continue work on detection of other ABSs and quantification of anomalies based on detection results.

AI012-EB Automated Liver Biometry and Fat Quantification in Non-alcoholic Fatty Liver Disease with Convolutional Neural Networks

All Day Room: AI Community, Learning Center

Participants

Kang Wang, MD, PhD, San Diego, CA (Presenter) Nothing to Disclose

Meet the Author: The authors of this poster will be available in person to discuss their project during these times: Thursday

November 29 12:45-1:15pm



Machine Learning Theater: SOPHiA Radiomics-Integration of Imaging, Genomic and Clinical Data to Support Decision Making in Oncology: Presented by SOPHIA GENETICS

Thursday, Nov. 29 1:00PM - 1:20PM Room: Machine Learning Showcase North Hall

Participants

Thierry Colin, PhD, Talence, France (Presenter) Nothing to Disclose

Program Information

Medical imaging techniques have a central role in the early detection of cancers. Radiomics is essential for determining the location and stage of tumors, for diagnosis and prognosis assessment, guiding therapeutic decisions and for assessing tumor response during and after treatment. It also supports interventional radiology acts (i.e. biopsies, thermo-ablations or embolization). Yet, this source of information, which is critical for the decision-making process, is not being used to its full potential. Radiomics is gaining importance in clinical cancer care. It has the potential to help oncologists take more precise and personalized clinical decisions. However, it faces many challenges such as (i) the complexity of extracting actionable information from imaging, genomic and clinical data; (ii) the limited number of cases, for some pathologies, that makes it difficult to apply classical machine learning based methodologies; and (iii) the fast evolution of cancer treatments that render the use of retrospective data useless. Therefore, the adoption of radiomics technologies by the medical community is so far limited. In this lecture, SOPHiA GENETICS will introduce SOPHiA Radiomics, its innovative decision-support technology combining imaging, genomic and clinical data to help oncologists monitor and treat their patients. Today, SOPHiA Radiomics is applied on lung cancer, gliomas and meningiomas.



Machine Learning Theater: DEEP:PHI, Medical Image AI Platform: Presented by DEEPNOID

Thursday, Nov. 29 1:30PM - 1:50PM Room: Machine Learning Showcase North Hall

Program Information

DEEP:PHI is the optimal AI-based medical image analysis platform. DEEP:PHI provides PACS, labeling tool, training function and reading function. DEEPNOID will present its AI solutions for detecting cerebral aneurysm, compression fracture and OPLL.



SPSH52

Hot Topic Session: Biomarker and Personalized Medicine in Lung Cancer Imaging

Thursday, Nov. 29 3:00PM - 4:00PM Room: E350



AMA PRA Category 1 Credit ™: 1.00 ARRT Category A+ Credit: 1.00

Participants

Patricia M. de Groot, MD, Houston, TX (Moderator) Nothing to Disclose

Sub-Events

SPSH52A Personalized Medicine and Lung Cancer Biomarkers: The Oncologist's Perspective

Participants

John V. Heymach, MD,PhD, Houston, TX (*Presenter*) Consultant, AstraZeneca PLC; Consultant, Boehringer Ingelheim GmbH; Consultant, Merck KGaA; Consultant, F. Hoffmann-La Roche Ltd; Consultant, Eli Lilly and Company; Consultant, Merck & Co, Inc; Consultant, Spectrum Dynamics Ltd; Consultant, Guardant; Consultant, Johnson & Johnson; Consultant, Novartis AG

LEARNING OBJECTIVES

1) Describe the goals and current state of personalized therapy for patients with non-small cell lung cancer. 2) Identify the lung cancer biomarkers now in clinical use as well as those in experimental trials. 3) Understand the barriers to optimal selection of individual patient therapy from the clinical and basic research perspective.

SPSH52B Imaging Biomarkers in Non-small Cell Lung Cancer

Participants Brett W. Carter, MD, Houston, TX (*Presenter*) Editor, Reed Elsevier;

For information about this presentation, contact:

bcarter2@mdanderson.org

LEARNING OBJECTIVES

1) Identify the imaging manifestations and patterns of disease associated with specific non-small cell lung cancer genetic mutations such as EGFR and KRAS and rearrangements such as ALK on computed tomography (CT) and FDG positron emission tomography (PET)/CT. 2) Describe the role of established response criteria and emerging and novel imaging techniques on the assessment of treatment response in non-small cell lung cancer. 2) Understand the continuously evolving impact of radiogenomics, defined as the linking of medical images with the genomic properties of neoplasms, in predicting the presence of specific genetic alterations, response to therapy, and survival of patients with non-small cell lung cancer.

Honored Educators

Presenters or authors on this event have been recognized as RSNA Honored Educators for participating in multiple qualifying educational activities. Honored Educators are invested in furthering the profession of radiology by delivering high-quality educational content in their field of study. Learn how you can become an honored educator by visiting the website at: https://www.rsna.org/Honored-Educator-Award/ Brett W. Carter, MD - 2015 Honored EducatorBrett W. Carter, MD - 2018 Honored Educator

SPSH52C Using Artificial Intelligence to Develop Non-invasive Biomarkers in Lung Cancer

Participants

Hugo Aerts, PhD, Boston, MA (Presenter) Stockholder, Sphera Inc

LEARNING OBJECTIVES

1) Learn about the motivation and methodology of AI technologies in lung cancer imaging. 2) Learn about scientific studies investigating the role of radiologic AI with other -omics data for precision medicine. 3) Learn about open-source informatics developments.



RC722

Machine Learning for Radiotherapy Applications

Thursday, Nov. 29 4:30PM - 6:00PM Room: N227B



AMA PRA Category 1 Credits ™: 1.50 ARRT Category A+ Credit: 1.75

Participants

Jayashree Kalpathy-Cramer, MS, PhD, Charlestown, MA (Moderator) Consultant, Infotech Software Solution

Sub-Events

RC722A Deep Learning for Image Segmentation, Analysis and Reconstruction

Participants

Jonas Teuwen, MSc, PhD, Nijmegen, Netherlands (Presenter) Nothing to Disclose

For information about this presentation, contact:

jonas.teuwen@radboudumc.nl

LEARNING OBJECTIVES

1) Learn about the types of clinical problems which are best suited for deep learning solutions. 2) Learn about the current state-ofthe-art deep learning technology in the analysis and segmentation of medical images, and learn about the advantages of reconstructing images using deep learning technology. 3) Being able to critically estimate the impact and assess the applicability of newly developed deep learning technology.

ABSTRACT

Deep learning has recently attracted much interest from the medical community, mainly due the successful application to problems which were previously considered to be purely within the human realm. The availability of an ever growing amount of medical images, and the increasing availability of affordable computation resources allows to apply deep learning technologies to many different problems. However, the scope of problems for which deep learning currently performs on par or outperforms humans is rather narrow. The required human and financial effort makes it important to be able to determine clinical problems where deep learning could bring an advantage. After this refresher course, you will be aware of the state-of-the-art in deep learning for image segmentation, analysis and reconstruction. You will be able to critically assess the impact and applicability of deep learning technology and be able to find future clinical opportunities.

RC722B Machine Learning Tumor Classification

Participants

Jayashree Kalpathy-Cramer, MS, PhD, Charlestown, MA (Presenter) Consultant, Infotech Software Solution

For information about this presentation, contact:

kalpathy@nmr.mgh.harvard.edu

LEARNING OBJECTIVES

1) Learn about applications of machine learning including radiomics and deep learning in classifiying tumor sub-types. 2) Learn about risk stratification using machine learning of MR and CT images. 3) Understand the challenges when applying machine learning to tumor analysis. 4) Review best practices for applying machine learning in cancer imaging.

ABSTRACT

Machine learning has shown great potential for a range of applications in oncology from diagnosis to therapy planning and response assessment. Large repositories of clinical and imaging data typicially available at most institutions can be be used to train and validate models. We will discuss the use of machine learning including radiomics and deep learning for the analysis of CT and MR imaging in a variety of cancer types for risk stratification, radiogenomics and response assessment..

RC722C Machine Learning for Automated Treatment Planning

Participants

Laurence E. Court, PhD, Houston, TX (Presenter) Nothing to Disclose



RC724

The Human Side of Artificial Intelligence

Thursday, Nov. 29 4:30PM - 6:00PM Room: E451B

AI

AMA PRA Category 1 Credits ™: 1.50 ARRT Category A+ Credit: 1.75

Participants

Richard B. Gunderman, MD, PhD, Indianapolis, IN (Moderator) Nothing to Disclose

LEARNING OBJECTIVES

1) Describe the respects in which, to be effective, artificial intelligence must serve human needs.

Sub-Events

RC724A Will We Trust AI?

Participants Saurabh Jha, MD, Philadelphia, PA (*Presenter*) Speakers Bureau, Canon Medical Systems Corporation

For information about this presentation, contact:

saurabh.jha@uphs.upenn.edu

LEARNING OBJECTIVES

1) Understand the epistemic controversies regarding artificial intelligence. 2) Do we attach an inordinate importance on 'how' and 'why'? 3) Appreciate the implications of the 'incompleteness theorem' in formal logic.

ABSTRACT

The incompleteness theorem, in formal logic, states that a system cannot vouch for its own validity. This begs a broader question how will we know if AI is speaking the truth? Will we be the machine's umpire or will the machine be our umpire? The answers to these questions have profound implications for the interaction between artificial intelligence and radiology

RC724B Voices of AI: Highlighting Perspective from the Radiology AI Journal Club

Participants

Judy W. Gichoya, MBChB, MS, Portland, OR (Presenter) Nothing to Disclose

For information about this presentation, contact:

jgichoya@iu.edu

RC724C How AI Can Go Ethically Awry

Participants Richard B. Gunderman, MD, PhD, Indianapolis, IN (*Presenter*) Nothing to Disclose

LEARNING OBJECTIVES

1) Describe the respects in which artificial intelligence must meet ethical as well as technical needs.

Honored Educators

Presenters or authors on this event have been recognized as RSNA Honored Educators for participating in multiple qualifying educational activities. Honored Educators are invested in furthering the profession of radiology by delivering high-quality educational content in their field of study. Learn how you can become an honored educator by visiting the website at: https://www.rsna.org/Honored-Educator-Award/ Richard B. Gunderman, MD, PhD - 2018 Honored Educator



RC753

Platforms and Infrastructures for Accelerated Discoveries in Machine Learning and Radiomics

Thursday, Nov. 29 4:30PM - 6:00PM Room: E451A



AMA PRA Category 1 Credits ™: 1.50 ARRT Category A+ Credit: 1.75

Participants

Katherine P. Andriole, PhD, Dedham, MA (*Moderator*) Research Grant, NVIDIA Corporation; Research Grant, General Electric Company; Research Grant, Nuance Communications, Inc; Advisory Board, McKinsey & Company, Inc

For information about this presentation, contact:

kandriole@bwh.harvard.edu

LEARNING OBJECTIVES

1) Understand the challenges involved in creating machine learning and radiomics experiments with standard clinical systems. 2) Review some of the tools that can bridge the gap between existing clinical systems and translational research in medical imaging. 3) Provide use case examples using open source tools.

ABSTRACT

Machine Learning and Radiomics promise to revolutionize the field of Radiology by allowing more quantification of medical images exposing previously "hidden" information within the imaging data. More recently, the combination machine learning techniques such as deep learning with radiomics, open new opportunities for researchers in this space. However, standard clinical systems are not suited for machine learning and radiomics experiments posing a significant challange for individuals together started. The pupose of this session is to review existing and custom developed infrastructures and platforms to bridge this gap.

Sub-Events

RC753A Overview of the R&D Process Pipeline for Machine Learning in Radiology

Participants

Mark H. Michalski, MD, Boston, MA (Presenter) Nothing to Disclose

LEARNING OBJECTIVES

1) Understand clinical data integration standards available to enable translational research in machine learning. 2) Gain introductory knowledge on enterprise data warehouses and understand how they can be used to augment machine learning systems. 3) Understand complexities associated with handling sensitive patient data.

RC753B Infrastructure and Software Platforms for Model Development, Training, Validation, and Clinical Integration

Participants

Neil Tenenholtz, PhD, Boston, MA (Presenter) Nothing to Disclose

For information about this presentation, contact:

ntenenholtz@partners.org

LEARNING OBJECTIVES

1) Identify cohorts for model development leveraging radiology reports and imaging metadata. 2) Rapidly annotate reports and imaging data on which machine learning models can be trained. 3) Build a pipeline for acquiring imaging data from a PACS for model development. 4) Train machine learning models on imaging data. 5) Validate machine learning models in the clinical workflow.

RC753C Machine Learning and Radiomics in Practice: Tools and Case Example

Participants

Daniel L. Rubin, MD, MS, Stanford, CA (Presenter) Nothing to Disclose

For information about this presentation, contact:

daniel.l.rubin@stanford.edu

LEARNING OBJECTIVES

1) To understand the role of image annotations in capuring essential information about images in radiomics. 2) To learn about tools, platforms, infrastructures, standards, and machine learning methods that can leverage medical images to better understand disease and enable decision support. 3) To see example use cases of radiomics and machine learning methods for accelerating research and improving clinical practice.

Honored Educators

Presenters or authors on this event have been recognized as RSNA Honored Educators for participating in multiple qualifying educational activities. Honored Educators are invested in furthering the profession of radiology by delivering high-quality educational content in their field of study. Learn how you can become an honored educator by visiting the website at: https://www.rsna.org/Honored-Educator-Award/ Daniel L. Rubin, MD, MS - 2012 Honored EducatorDaniel L. Rubin, MD, MS - 2013 Honored Educator



RSNA Deep Learning Classroom: Presented by NVIDIA Deep Learning Institute

Friday, Nov. 30 8:30AM - 12:00PM Room: AI Community, Learning Center

Program Information

Located in the Learning Center (Hall D), this classroom presented by NVIDIA will give meeting attendees a hands-on opportunity to engage with deep learning tools, write algorithms and improve their understanding of deep learning technology. "Attendees must bring a laptop capable of running the most recent version of Chrome."

Sub-Events

AI001-FRA Multi-modal Classification

Friday, Nov. 30 8:30AM - 10:00AM Room: AI Community, Learning Center

Title and Abstract

Multi-modal Classification This session will focus on multimodal classification. Classification is the recognition of an image or some portion of an image being of one type or another, such as 'tumor' or 'infection'. Multimodal classification means that there are more than 2 classes. While this is logically simple to understand, it presents some unique challenges that will be discussed.

AI001-FRB Advanced Data Augmentation Using GANs

Friday, Nov. 30 10:30AM - 12:00PM Room: AI Community, Learning Center

Title and Abstract

Advanced Data Augmentation Using GANs Getting 'large enough' data sets is a problem for most deep learning applications, and this is particularly true in medical imaging. Generative Adversarial Networks (GANs) are a deep learning technology in which a computer is trained to create images that look very 'real' even though they are completely synthetic. This may be one way to address the 'data shortage' problem in medicine.